

JOURNAL OF

## CHROMATOGRAPHY

INTERNATIONAL JOURNAL ON CHROMATOGRAPHY, ELECTROPHORESIS AND RELATED METHODS

EDITOR, Michael Lederer (Switzerland)

ASSOCIATE EDITOR, K. Macek (Prague)

## EDITORIAL BOARD

W. A. Aue (Halifax)  
 V. G. Berezkin (Moscow)  
 V. Betina (Bratislava)  
 A. Bevenue (Honolulu, HI)  
 P. Boulanger (Lille)  
 A. A. Boulton (Saskatoon)  
 G. P. Cartoni (Rome)  
 G. Duyckaerts (Liège)  
 L. Fishbein (Jefferson, AR)  
 A. Frigerio (Milan)  
 C. W. Gehrke (Columbia, MO)  
 E. Gil-Av (Rehovot)  
 G. Guiochon (Palaiseau)  
 I. M. Hais (Hradec Králové)  
 J. K. Haken (Kensington)  
 E. Heftmann (Berkeley, CA)  
 S. Hjertén (Uppsala)  
 E. C. Horning (Houston, TX)  
 Cs. Horváth (New Haven, CT)  
 J. F. K. Huber (Vienna)  
 A. T. James (Sharnbrook)  
 J. Janák (Brno)  
 E. sz. Kováts (Lausanne)  
 K. A. Kraus (Oak Ridge, TN)  
 E. Lederer (Gif-sur-Yvette)  
 A. Liberti (Rome)  
 H. M. McNair (Blacksburg, VA)  
 Y. Marcus (Jerusalem)  
 G. B. Marini-Bettolo (Rome)  
 Č. Michalec (Prague)  
 R. Neher (Basel)  
 G. Nickless (Bristol)  
 J. Novák (Brno)  
 N. A. Parris (Wilmington, DE)  
 P. G. Righetti (Milan)  
 O. Samuelson (Göteborg)  
 G.-M. Schwab (Munich)  
 G. Semenza (Zürich)  
 L. R. Snyder (Tarrytown, NY)  
 A. Zlatkis (Houston, TX)

## EDITORS, BIBLIOGRAPHY SECTION

K. Macek (Prague), J. Janák (Brno), Z. Deyl (Prague)

## COORD. EDITOR, DATA SECTION

J. Gasparič (Hradec Králové)

ELSEVIER SCIENTIFIC PUBLISHING COMPANY  
AMSTERDAM

## JOURNAL OF CHROMATOGRAPHY

**Scope.** The *Journal of Chromatography* publishes papers on all aspects of chromatography, electrophoresis and related methods. Contributions consist mainly of research papers dealing with chromatographic theory, instrumental development and their applications. The section *Biomedical Applications*, which is under separate editorship, deals with the following aspects: developments in and applications of chromatographic and electrophoretic techniques related to clinical diagnosis (including the publication of normal values); screening and profiling procedures with special reference to metabolic disorders; results from basic medical research with direct consequences in clinical practice; combinations of chromatographic and electrophoretic methods with other physicochemical techniques such as mass spectrometry. In *Chromatographic Reviews*, reviews on all aspects of chromatography, electrophoresis and related methods are published.

**Submission of Papers.** Papers in English, French and German may be submitted, in three copies. Manuscripts should be submitted to: The Editor of *Journal of Chromatography*, P.O. Box 681, 1000 AR Amsterdam, The Netherlands, or to: The Editor of *Journal of Chromatography, Biomedical Applications*, P.O. Box 681, 1000 AR Amsterdam, The Netherlands. Reviews are invited or proposed by letter to the Editors and will appear in *Chromatographic Reviews* or *Biomedical Applications*. An outline of the proposed review should first be forwarded to the Editors for preliminary discussion prior to preparation. Submission of an article is understood to imply that the article is original and unpublished and is not being considered for publication elsewhere. For copyright regulations, see below.

**Subscription Orders.** Subscription orders should be sent to: Elsevier Scientific Publishing Company, P.O. Box 211, 1000 AE Amsterdam, The Netherlands. The *Journal of Chromatography* and the *Biomedical Applications* section can be subscribed to separately.

**Publication.** The *Journal of Chromatography* (incl. *Biomedical Applications, Chromatographic Reviews* and *Cumulative Author and Subject Indexes*, Vols. 221-230, 231-240 and 241-250) has 25 volumes in 1982. The subscription prices for 1982 are:

J. *Chromatogr.* (incl. *Chromatogr. Rev.* and *Cum. Indexes*) + *Biomed. Appl.* (Vols. 227-251):

Dfl. 3625.00 plus Dfl. 500.00 (postage) total ca. US\$ 1650.00)

J. *Chromatogr.* (incl. *Chromatogr. Rev.* and *Cum. Indexes* Vols. 231-240 and 241-250) only (Vols. 234-251):

Dfl. 2826.00 plus Dfl. 360.00 (postage) (total ca. US\$ 1274.50)

*Biomed. Appl.* (incl. *Cum. Indexes* Vols. 221-230) only (Vols. 227-233):

Dfl. 1050.00 plus Dfl. 140.00 (postage) (total ca. US\$ 476.00).

journals are automatically sent by air mail to the U.S.A. and Canada at no extra costs, and to Japan, Australia and New Zealand with a small additional postal charge. Back volumes of the *Journal of Chromatography* (Vols. 1 through 226) are available at Dfl. 156.00 (plus postage). Claims for issues not received should be made within three months of publication of the issue. If not, they cannot be honoured free of charge. For customers in the U.S.A. and Canada wishing additional bibliographic information on this and other Elsevier journals, please contact Elsevier/North-Holland Inc., Journal Information Centre, 52 Vanderbilt Avenue, New York, NY 10017. Tel: (212) 867-9040.

**Abstracts/Contents Lists** published in Analytical Abstracts, Biochemical Abstracts, Biological Abstracts, Chemical Abstracts, Chemical Titles, Current Contents/Physical, Chemical & Earth Sciences, Current Contents/Life Sciences, Index Medicus, and Science Citation Index.

**See page 3 of cover** for Publication Schedule, Information for Authors, and information on the News Section and Advertisements.

© ELSEVIER SCIENTIFIC PUBLISHING COMPANY — 1982

All rights reserved. No part of this publication may be reproduced, stored in a retrieval system or transmitted in any form or by any means, electronic, mechanical, photocopying, recording or otherwise, without the prior written permission of the publisher, Elsevier Scientific Publishing Company, P.O. Box 330, 1000 AH Amsterdam, The Netherlands.

Submission of an article for publication implies the transfer of the copyright from the author(s) to the publisher and entails the authors' irrevocable and exclusive authorization of the publisher to collect any sums or considerations for copying or reproduction payable by third parties (as mentioned in article 17 paragraph 2 of the Dutch Copyright Act of 1912 and in the Royal Decree of June 20, 1974 (S. 351) pursuant to article 16 b of the Dutch Copyright Act of 1912) and/or to act in or out of Court in connection therewith.

**Special regulations for readers in the U.S.A.** This journal has been registered with the Copyright Clearance Center, Inc. Consent is given for copying of articles for personal or internal use, or for the personal use of specific clients. This consent is given on the condition that the copier pays through the Center the per-copy fee stated in the code on the first page of each article for copying beyond that permitted by Sections 107 or 108 of the U.S. Copyright Law. The appropriate fee should be forwarded with a copy of the first page of the article to the Copyright Clearance Center, Inc., 21 Congress Street, Salem, MA 01970, U.S.A. If no code appears in an article, the author has not given broad consent to copy and permission to copy must be obtained directly from the author. All articles published prior to 1980 may be copied for a per-copy fee of US\$ 2.25, also payable through the Center. This consent does not extend to other kinds of copying, such as for general distribution, resale, advertising and promotion purposes, or for creating new collective works. Special written permission must be obtained from the publisher for such copying.

**Special regulations for authors in the U.S.A.** Upon acceptance of an article by the journal, the author(s) will be asked to transfer copyright of the article to the publisher. This transfer will ensure the widest possible dissemination of information under the U.S. Copyright Law.

Printed in The Netherlands

## CONTENTS

(Abstracts/Contents Lists published in Analytical Abstracts, Biochemical Abstracts, Biological Abstracts, Chemical Abstracts, Chemical Titles, Current Contents/Physical, Chemical & Earth Sciences, Current Contents/Life Sciences, Index Medicus and Science Citation Index)

Non-radioactive electron-capture detector by A. Neukermans, W. Kruger and D. McManigill (Palo Alto, CA, U.S.A.) (Received June 22nd, 1981)	1
Electrochemical cell with effective volume less than 1 nl for liquid chromatography by K. Šlais and M. Krejčí (Brno, Czechoslovakia) (Received September 4th, 1981)	21
Investigation of N-alkylbenzamides by reversed-phase liquid chromatography. I. Isocratic elution characteristics of the C <sub>1</sub> -C <sub>5</sub> N-alkylbenzamides by M. J. M. Wells and C. R. Clark (Auburn University, AL, U.S.A.) (Received August 3rd, 1981)	31
Investigation of N-alkylbenzamides by reversed-phase liquid chromatography. II. Application of the solvophobic theory to the prediction of retention data for the C <sub>1</sub> -C <sub>5</sub> N-alkylbenzamides by M. J. M. Wells, C. R. Clark and R. M. Patterson (Auburn University, AL, U.S.A.) (Received May 7th, 1981)	43
Investigation of N-alkylbenzamides by reversed-phase liquid chromatography. III. Correlation of chromatographic parameters with molecular connectivity indices for the C <sub>1</sub> -C <sub>5</sub> N-alkylbenzamides by M. J. M. Wells, C. R. Clark and R. M. Patterson (Auburn University, AL, U.S.A.) (Received May 7th, 1981)	61
Gas chromatography and mass spectrometry of N-trifluoroacetyl <i>n</i> -butyl esters of alkylated tyrosines and lysines by M. Sakamoto, N. Tsuji, F. Nakyama and K.-I. Kajiyama (Tokyo, Japan) (Received August 10th, 1981)	75
Gas chromatographic resolution of optical isomers by diamide stationary phases, R'CONHCH(R'')CONHR'''. Effect of non-polar substituents (R'') at the $\alpha$ -carbon atom by S.-C. Chang, R. Charles and E. Gil-Av (Rehovot, Israel) (Received August 14th, 1981)	87
Studies on the thermodynamics of solution by gas chromatography. Solubility measurements of hydrocarbons in $\beta$ -alkoxypropionitriles by R. K. Kuchhal and K. L. Mallik (Dehradun, India) (Received August 10th, 1981)	109
Gaschromatographische Identifizierung niedrig siedender Substanzen mittels Retentionsindices und Rechnerhilfe von K.-J. Goebel (Bonn, B.R.D.) (Eingegangen am 13. August 1981)	119
Selektive Gruppentrennung von primären und sekundären biogenen Aminen mittels "reversed-phase" Hochleistungsflüssigkeitschromatographie mit [18]Krone-6 in der mobilen Phase von M. Wiechmann (Bayreuth, B.R.D.) (Eingegangen am 12. August 1981)	129
High-performance liquid chromatography and magnetic circular dichroism: a study of the "palladium(II)-thioether peptide" complexes by H. Lam-Thanh, S. Fermandjian and P. Fromageot (Gif-sur-Yvette, France) (Received August 21st, 1981)	139
Long-chain phenols. XXII. Compositional studies on Japanese Lac ( <i>Rhus vernicifera</i> ) by chromatography and mass spectrometry by J. H. P. Tyman and A. J. Matthews (Uxbridge, Great Britain) (Received August 14th, 1981)	149

(Continued overleaf)

Contents (continued)

Capillary column gas chromatographic-mass spectrometric-computer analysis of environmental spills by M. H. Carter (Athens, GA, U.S.A.) (Received July 20th, 1981)	165
Determination of nitrate in meat products and cheeses by gas-liquid chromatography with electron-capture detection by A. Tanaka, N. Nose and H. Iwasaki (Urama, Japan) (Received August 25th, 1981)	173
High-performance liquid chromatographic determination of nitrite in environmental samples by the use of hydralazine by H. Noda, M. Minemoto and T. Asahara (Kitakyushu, Japan) and A. Noda and S. Iguchi (Fukuoka, Japan) (Received August 11th, 1981)	187
High-performance liquid chromatographic separation and proton nuclear magnetic resonance identification of the 6-mono- <i>cis</i> and 6,6'-di- <i>cis</i> isomers of rhodoxanthin by G. Englert and M. Vecchi (Basle, Switzerland) (Received August 4th, 1981)	197
High-performance liquid chromatographic method for the determination of novobiocin by K. Tsuji, P. D. Rahn and M. P. Kane (Kalamazoo, MI, U.S.A.) (Received August 18th, 1981)	205
Improved high-performance liquid chromatographic method for simultaneous determination of neamine, neomycin B and neomycin C in neomycin sulphate by P. Helboe and S. Kryger (Brønshøj, Denmark) (Received September 1st, 1981)	215
Uronic acid analysis by high-performance liquid chromatography after methanolysis of glycosaminoglycans by A. Hjerpe (Huddinge, Sweden), C. A. Antonopoulos (Patras, Greece) and B. Classon, B. Engfeldt and M. Nurminen (Huddinge, Sweden) (Received August 18th, 1981)	221
Chromatography of cellodextrins and enzymatic hydrolysates of cellulose on ion-exchange derivatives of Spheron by Z. Hostomská-Chytilová, O. Mikeš and P. Vrátný (Prague, Czechoslovakia) and M. Smrž (Brno, Czechoslovakia) (Received September 1st, 1981)	229
Application of dye-ligand chromatography to the isolation of $\alpha$ -1-proteinase inhibitor and $\alpha$ -1-acid glycoprotein by G. Birkenmeier and G. Kopperschläger (Leipzig, G.D.R.) (Received August 11th, 1981)	237
Radioisotope assay for glutamine synthetase using thin-layer chromatography by S. L. Pahuja and T. W. Reid (New Haven, CT, U.S.A.) (Received August 6th, 1981)	249
Fluorodensitometric determination of trichothecene mycotoxins with nicotinamide and 2-acetylpyridine on a silica gel layer by A. Sano, Y. Asabe, S. Takitani and Y. Ueno (Tokyo, Japan) (Received August 17th, 1981)	257
<i>Notes</i>	
Dissociation of sulphonic acids sorbed onto a non-polar stationary phase by B. F. Nilsson and O. Samuelson (Göteborg, Sweden) (Received August 26th, 1981)	266
Gas chromatographic determination of methacrylamide and the other intermediates in reaction mixtures in the synthesis of methyl methacrylate from acetone cyanohydrin by J. Balák, M. Polievka, L. Uhlár and E. Čavojcová (Nováky, Czechoslovakia) (Received September 3rd, 1981)	269
Outer-sphere ligand exchange chromatography of nucleotides and related compounds on a modified polysaccharide gel by D. Corradini and M. Sinibaldi (Monterotondo Stazione, Italy) and A. Messina (Rome, Italy) (Received August 31st, 1981)	273
Thin-layer and gas chromatographic separation of ferrocene oxathiolanes and dithiolanes by L. Ogierman (Sosnicowice, Poland) and B. Czech (Katowice, Poland) (Received August 19th, 1981)	276
<i>Book Review</i>	
Pesticide analytical methodology (edited by J. Harvey, Jr. and G. Zweig), reviewed by W. A. Aue	280



# *Are these journals in your library?*

## **JOURNAL OF MOLECULAR STRUCTURE : THEOCHEM**

Applications of Theoretical Chemistry to Organic, Inorganic and Biological Problems

Editors: W.J. Orville-Thomas, *Salford, England* and I.G. Csizmadia, *Toronto, Canada*

THEOCHEM covers the application of theoretical methods to the study of molecular structure and associated molecular properties. Both chemical statics and chemical dynamics are involved; the structures of stable molecules, reaction intermediates and transition states are thus included in the scope. THEOCHEM is a section of the journal of Molecular Structure which is available separately.

1982 Vols. 85-87 ( in 12 issues )

Hfl. 555.00 including postage

ISSN 0166-1280

## **COLLOIDS AND SURFACES**

An International Journal Devoted to the Applications and Principles of Colloid and Interface Science

Editor-in-Chief: P. Somasundaran, *New York, NY, U.S.A.*

This journal is designed to encourage publication of original papers on basic colloid and surface science and, in particular, its application in engineering and applied science. In addition to research papers, the journal contains notes, brief communications, book reviews and announcements.

1982 Vols. 4-5 ( in 8 issues )

Hfl. 390.00 including postage

ISSN 0166-6622

# **ELSEVIER**

P.O. Box 211, 1000 AE Amsterdam, The Netherlands.

## **JOURNAL OF ANALYTICAL AND APPLIED PYROLYSIS**

Editor: H.L.C. Meuzelaar, *Salt Lake City, UT, U.S.A.* and H.-R. Schulten, *Bonn, F.R.G.*

Publishes qualitative and quantitative results related to: controlled thermal degradation and pyrolysis of technical and biological macromolecules; environmental, geochemical, biological and medical applications of analytical pyrolysis; basic studies in high temperature chemistry, reaction kinetics and pyrolysis mechanisms; pyrolysis investigations of energy related problems, fingerprinting of fossil and synthetic fuels, coal extraction and liquefaction products.

1982 Vol. 4 ( in 4 issues )

Hfl. 185.00 including postage

ISSN 0165-2370

## **TRENDS IN ANALYTICAL CHEMISTRY - TAC**

A new monthly magazine to highlight current trends and new developments in all areas of analytical chemistry for an interdisciplinary audience of analytical chemists and others using analytical methods. It consists primarily of short, broadly based review articles, written with the minimum technical 'jargon', and also contains editorials, feature articles, book reviews, letters to the editor, meeting reports and announcements of events in the field.

1982 12 issues

Hfl. 91.50 including postage

ISSN 0165-9936

*ask for a sample copy and see for yourself how these journals can help your research.*

# Electrodes of Conductive Metal Oxides

edited by SERGIO  
TRASATTI, *Laboratory of  
Electrochemistry, University  
of Milan, Italy.*

STUDIES IN PHYSICAL AND  
THEORETICAL CHEMISTRY  
11.

This two-part work provides a general unifying introduction plus a state-of-the-art review of the physicochemical properties and electrochemical behaviour of conductive oxide electrodes (DSA). The text has been divided into two volumes – Part A dealing mainly with structural and thermodynamic properties and Part B dealing with kinetic and electrocatalytic aspects. This division came about due to the large amount of material to be treated and also because, in a rapidly developing field, difficulties arise in collecting all relevant material at one given moment.

The editor approaches the subject from a multidisciplinary angle, for example, the electrochemical behaviour of oxide electrodes is presented and discussed in the context

of a variety of physico-chemical properties – electronic structure, nonstoichiometry, crystal structure, surface structure, morphology and adsorption properties. For the first time the different groups of oxides are treated together in order to emphasise their similarities and differences.

This major reference work is mainly directed to electrochemists and those working on catalysis. It will also be useful to those in the fields of materials science, physical chemistry, surface and colloid chemistry and in areas where oxide surfaces may play a major role as in chromatography and photochemistry.

CONTENTS: Chapters. 1. Electronic Band Structure of Oxides with Metallic or Semiconducting Characteristics (*J. M. Horig*). 2. Chemisorption and Catalysis on Metal Oxides (*A. Cimino and S. Carrà*). 3. Oxide Growth and Oxygen Evolution on Noble Metals (*L. D. Burke*). 4. Electrochemistry of Lead Dioxide (*J. P. Pohl and H. Rickert*). 5. Properties of Spinel-Type Oxide Electrodes (*M. R. Tarasevich and B. N. Efreimov*). 6. Physicochemical and Electrochemical Properties of Perovskite Oxides (*H. Tamura, Y. Yoneyama and Y. Matsumoto*). 7. Properties of Conductive Transition Metal Oxides with Rutile-Type Structure (*S. Trasatti and G. Lodi*). 8. Fundamental Properties of the Oxide/Aqueous Solution Interface (*D. N. Furlong, D. E. Yates and T. W. Healy*). 9. Reactions of Hydrogen and Organic Substances with and at Anodic Oxide Films at Electrodes (*B. E. Conway*). 10. Oxygen and Chlorine Evolution at Conductive Metallic Oxide Anodes (*S. Trasatti and G. Lodi*). 11. Technological Impact of Metallic Oxides as Anodes (*A. Nidola*).

**Part A:**  
**1980 xvi + 366 pages.**  
**US \$72.25/Dfl. 170.00.**  
**ISBN 0-444-41912-8.**

**Part B:**  
**1981 xiv + 336 pages.**  
**US \$72.25/Dfl. 170.00.**  
**ISBN 0-444-41988-8.**

# ELSEVIER



P.O. Box 211  
1000 AE Amsterdam  
The Netherlands

52 Vanderbilt Avenue,  
New York, N.Y. 10017

*The Dutch guildler price is definitive. US \$ prices are subject to exchange rate fluctuations.*

JOURNAL OF CHROMATOGRAPHY

VOL. 235 (1982)

# JOURNAL *of* CHROMATOGRAPHY

INTERNATIONAL JOURNAL ON CHROMATOGRAPHY,  
ELECTROPHORESIS AND RELATED METHODS

EDITOR

MICHAEL LEDERER (Switzerland)

ASSOCIATE EDITOR

K. MACEK (Prague)

EDITORIAL BOARD

W. A. Aue (Halifax), V. G. Berezkin (Moscow), V. Betina (Bratislava), A. Bevenue (Honolulu, HI), P. Boulanger (Lille), A. A. Boulton (Saskatoon), G. P. Cartoni (Rome), G. Duyckaerts (Liège), L. Fishbein (Jefferson, AR), A. Frigerio (Milan), C. W. Gehrke (Columbia, MO), E. Gil-Av (Rehovot), G. Guiochon (Palaiseau), I. M. Hais (Hradec Králové), J. K. Haken (Kensington), E. Heftmann (Berkeley, CA), S. Hjertén (Uppsala), E. C. Horning (Houston, TX), Cs. Horváth (New Haven, CT), J. F. K. Huber (Vienna), A. T. James (Sharnbrook), J. Janák (Brno), E. sz. Kováts (Lausanne), K. A. Kraus (Oak Ridge, TN), E. Lederer (Gif-sur-Yvette), A. Liberti (Rome), H. M. McNair (Blacksburg, VA), Y. Marcus (Jerusalem), G. B. Marini-Bettolo (Rome), Č. Michalec (Prague), R. Neher (Basel), G. Nickless (Bristol), J. Novák (Brno), N. A. Parris (Wilmington, DE), P. G. Righetti (Milan), O. Samuelson (Göteborg), G.-M. Schwab (Munich), G. Semenza (Zürich), L. R. Snyder (Tarrytown, NY), A. Zlatkis (Houston, TX)

EDITORS, BIBLIOGRAPHY SECTION

K. Macek (Prague), J. Janák (Brno), Z. Deyl (Prague)

COORDINATING EDITOR, DATA SECTION

J. Gasparič (Hradec Králové)



ELSEVIER SCIENTIFIC PUBLISHING COMPANY  
AMSTERDAM

---

*J. Chromatogr.*, Vol. 235 (1982)

© ELSEVIER SCIENTIFIC PUBLISHING COMPANY — 1982

All rights reserved. No part of this publication may be reproduced, stored in a retrieval system or transmitted in any form or by any means, electronic, mechanical, photocopying, recording or otherwise, without the prior written permission of the publisher, Elsevier Scientific Publishing Company, P.O. Box 330, 1000 AH Amsterdam, The Netherlands.

Submission of an article for publication implies the transfer of the copyright from the author(s) to the publisher and entails the authors' irrevocable and exclusive authorization of the publisher to collect any sums or considerations for copying or reproduction payable by third parties (as mentioned in article 17 paragraph 2 of the Dutch Copyright Act of 1912 and in the Royal Decree of June 20, 1974 (S. 351) pursuant to article 16 b of the Dutch Copyright Act of 1912) and/or to act in or out of Court in connection therewith.

**Special regulations for readers in the U.S.A.** This journal has been registered with the Copyright Clearance Center, Inc. Consent is given for copying of articles for personal or internal use, or for the personal use of specific clients. This consent is given on the condition that the copier pays through the Center the per-copy fee stated in the code on the first page of each article for copying beyond that permitted by Sections 107 or 108 of the U.S. Copyright Law. The appropriate fee should be forwarded with a copy of the first page of the article to the Copyright Clearance Center, Inc., 21 Congress Street, Salem, MA 01970, U.S.A. If no code appears in an article, the author has not given broad consent to copy and permission to copy must be obtained directly from the author. All articles published prior to 1980 may be copied for a per-copy fee of US\$ 2.25, also payable through the Center. This consent does not extend to other kinds of copying, such as for general distribution, resale, advertising and promotion purposes, or for creating new collective works. Special written permission must be obtained from the publisher for such copying.

**Special regulations for authors in the U.S.A.** Upon acceptance of an article by the journal, the author(s) will be asked to transfer copyright of the article to the publisher. This transfer will ensure the widest possible dissemination of information under the U.S. Copyright Law.

Printed in The Netherlands

CHROM. 14,325

## NON-RADIOACTIVE ELECTRON-CAPTURE DETECTOR

A. NEUKERMANS\*, W. KRUGER and D. McMANIGILL

*Hewlett-Packard, Palo Alto, CA 94304 (U.S.A.)*

(Received June 22nd, 1981)

---

### SUMMARY

A non-radioactive electron-capture detector is described which uses a thermionic emitter as a source of electrons. The use of this source allows a unique mode of operation which has greatly enhanced sensitivity, yet at the same time allows a large dynamic range. A signal-to-noise ratio of 180 to 1 has been obtained at the 1-pg level, together with a dynamic range of six orders of magnitude. It appears that with this method it is possible to detect femtogram quantities.

---

### INTRODUCTION

The electron-capture detector (ECD) has been in existence for almost twenty years. During that time it has evolved from a highly sensitive, yet extremely temperamental detector into a reliable laboratory instrument. During this period, the modes of operation of the detector have changed significantly, extending both the range and the sensitivity of the detector.

But the real principle has barely been changed since its inception, and due to the complexity of the reactions taking place, its operation is still relatively poorly understood. To quote Lovelock<sup>1</sup>, the inventor of this detector: "Perhaps because of the pressure to use the detector in the solution of practical and theoretical problems, it has barely changed since its inception. It is still a simple two-electrode ion-chamber with an internal radiation source, and there is no comprehensive theory of its response which explains numerically the signals it generates."

The radioactive source that is used is at the base of this deceiving physical simplicity, but chemical complexity. Typically, the sources used are  $\beta$ -emitters ranging in energy from 17 keV (max) for tritium ( $^3\text{H}$ ) to 230 keV for promethium ( $^{147}\text{Pm}$ ). As these energetic electrons thermalize by collisions with the molecules of the gas, they produce eventually near thermal electrons. These thermal electrons are used in the reaction with the electrophilic compounds as the cross-section for electron capture of most strong electrophores is maximum near zero energy. However in the process a host of other species such as positive ions, energetic radicals, etc., are created which may react with the electrons, the electrophilic compounds or the negative ions created by electron capture. The complexity of these reactions, coupled with the space charge present in the detector, gives rise to intractable problems<sup>2</sup>. Wentworth *et al.*<sup>3</sup>,

who were responsible for elucidating many of the phenomena taking place in the ECD, have recently reviewed in detail the shortcomings of the radioactive detector<sup>4</sup>. Briefly, these include: (1) contamination of the electron source by column bleed, necessitating frequent cleaning of the detector; (2) irreversible reactions between the source and the electrophilic compounds; (3) upper temperature limitations set by the use of the radioactive foils or platings; and (4) the sources involved require licensing by government agencies.

To these could be added the difficulties of producing small cell volumes. Since the primary  $\beta$  particles have significant energy, their range is substantial, and a large cell volume is required to avoid operation of the cell as a cross-section detector<sup>5</sup>, although newer designs are minimizing the extent of this problem<sup>6</sup>. It has therefore been apparent for a long time that an alternative source for electrons would be very desirable. Wentworth *et al.*<sup>4</sup> in their approach, produce the electrons by photoionization of additives to the effluent (such as triethylamine).

This technique suffers, however, also from a number of deficiencies. The electrons produced are still not truly thermal, as for good ionization efficiency, it is required that the difference between the ionization potential and the ionizing photon energy be at least a few electronvolts. Thermalization, in turn, requires the use of a quenching gas which is unfortunately highly absorbing to the ionizing photons. For this and a variety of other reasons, this approach is presently limited in sensitivity to 50 pg of carbon tetrachloride, a very strong electrophore.

Other approaches in the past have tried to use electrons produced from a gaseous discharge<sup>7</sup>, or photoelectrons provided by metallic photoemitters. It appears, however, somewhat unlikely that a discharge of sufficient stability can be produced to detect picogram quantities.

Similarly, it seems unlikely that a photocathode with sufficient current and with enough stability, unaffected by the effluent of the gas chromatograph, can be found.

Our approach has been to use a thermionic emitter, suitably protected by a guard gas. Thermionic emitters are usually associated with electron emission in vacuum, and their operation (except for some special cathodes such as the Philips cathode) is rapidly and irreversibly destroyed by the presence of small amounts of water or oxygen. In 1967, MacNair<sup>8</sup> developed the barium zirconate cathode, in particular for laser discharges, and it was found to operate suitably in oxidizing atmospheres at low pressure. Although the original current densities quoted by MacNair appear to be somewhat high<sup>9</sup>, the values required for operation as an electron-capture detector are rather minimal, so that the cathode can be operated at low temperature (650–750°C). We found that this cathode, when suitably protected, can also operate very adequately in the atmosphere of the gas chromatograph, with quite acceptable lifetimes. The cathode can be exposed to air and reused without any apparent damage.

It should be remembered that the atmosphere of the gas chromatograph is a rather demanding one. If 3  $\mu$ l of a typical solvent (*e.g.*, iso-octane or hexane) are injected at the commonly used flow-rates in chromatographic work, the cell will be filled with almost pure solvent vapor for several seconds. Pure metallic cathodes, such as rhenium or tungsten, working at elevated temperatures (1100–1200°C) oxidize very rapidly. If a suitable material is used to lower the work function, it is found that the

cathode is able to withstand immersion in the solvent vapor, but it takes several minutes for its emission to reach again the preimmersion level.

If the solvent problem could be circumvented, the thermionic emission itself is quite sensitive to the presence of electron capturing compounds, but the recovery constant is inadequately long for faithful detection of chromatographic peaks. In addition, efficient electron emission at atmospheric pressure in inert gases requires a strong electric field, since most of the emitted electrons are "reflected" to the filament by diffusion<sup>10</sup>. This large field is undesirable for efficient electron capture. However, if the filament is shrouded with a guard gas, these problems are all alleviated. The fact that a guard gas is used almost naturally divides the detector into two chambers, a guarded filament chamber used for the production of electrons, and a second chamber where a fraction of the previous electrons is used to react with the electrophores. This allows separate optimization of electron production in the first chamber and optimum conditions for electron capture in the second.

#### PRINCIPLE OF OPERATION

One implementation of a detector using a thermionic emitter is illustrated in Fig. 1. The detector consists of two concentric stainless-steel cylinders, an inner

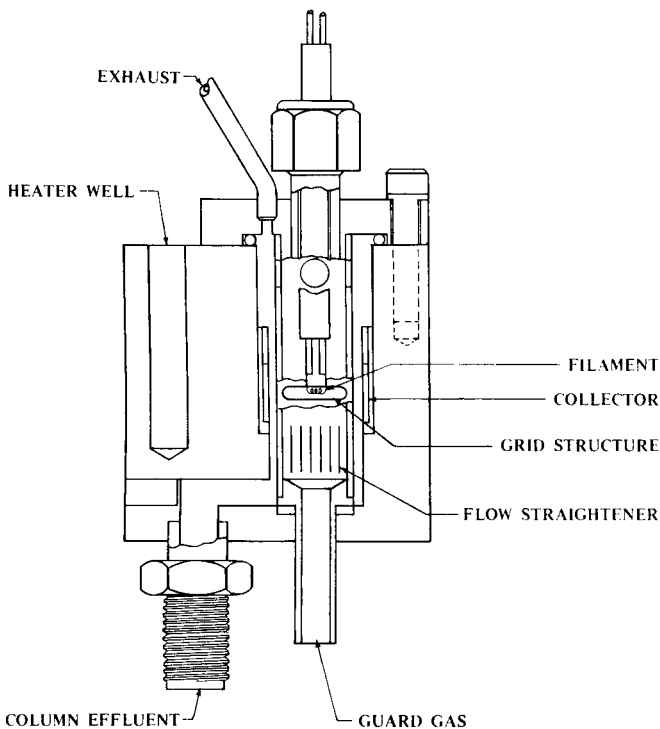


Fig. 1. Schematic illustration of a non-radioactive ECD. A direct heated thermionic cathode supplies electrons which are attracted towards a mesh-like anode. Electrons diffuse through the anode and are attracted with a small potential towards a collector. The column effluent flows in the outer cylinder and a guard gas flows in the inner cylinder. The guard gas prevents excessive penetration of the solvent in the filament chamber. The reaction chamber proper consists of the annulus between both cylinders, and its width is defined by the effective lateral spread of the electron cloud.



cylinder containing the thermionic source and through which the guard gas flows, and an outer one through which the chromatograph effluent flows. Separating the two chambers is a very fine metallic mesh (consisting of nickel or gold), of 80% transmission and about 12  $\mu\text{m}$  thick. The gas flows in both cylinders are colinear and, ideally, laminar and of equal velocity. For this purpose, operation of the detector is usually vertical, so that the thermal plume caused by the hot filament causes minimum disturbance in the outer chamber. Electrons emitted by the filament (which is biased negatively) are attracted toward the inner cylinder which is grounded, and which will be called the anode. Typically, although not necessarily, the electron source is kept at a variable potential by a servoloop to provide a constant current towards the inner cylinder. The current loop is set at a predetermined level, usually on the order of 10  $\mu\text{A}$ , and the voltage required to maintain this current under equilibrium conditions is on the order of 50 V (for a cylinder 12 mm in diameter).

Some of the electrons arriving at the anode pass through the open grid structure and diffuse through to the outer cylinder, which will be referred to as the collector. The potential difference between the collector, C, and the anode, A, is however kept quite small, and in fact operation is possible where the collector is slightly backbiased with respect to the anode.

The primary driving force for the electrons to reach the collector is therefore diffusion, not drift. Their own space charge sets up a field opposing their entry in the anode-collector region. The balance between the diffusion force, the space charge field and the applied field results in a current, typically three orders of magnitude smaller than the current in the inner diode. This region of the detector, which is the cell proper, operates therefore in what will be called a diffusion driven, space charge limited mode. As the effluent of the chromatograph flows through the cell, electrophores are converted into negative ions, through reaction with the electrons. Note that with this geometric arrangement, all of the gas flowing through the cell is exposed to the electrons, as the electron path completely traverses the effluent gas (although the effluent is not everywhere exposed to the same electron concentration).

The operation of the detector can now, in a simplified way, be understood as follows. After absorption of an electron by an electrophore, and its conversion into a negative ion, one may assume that another electron is prohibited from entering the cell region, because of the space charge limitation. This condition prevails as long as the ion remains in the cell. As there is only a very weak electric field present in the cell, and the mobility of the negative ion is some three orders of magnitude lower than the electron mobility, the ion is essentially removed by the gas flow, a process which may take a considerable fraction of a second. During the dwell time of the ion, an electron has been prevented from entering the cell. The replacement of an electron by an ionic specimen with largely reduced mobility, generally gives rise to a reduction in current. Since the electron transit time is on the order of a few microseconds, the single ions have effectively prevented the entrance of a large number of electrons so that a gain mechanism is taking place. The gain would be thought of as the ratio of the dwell time of the negative ion to the transit time of the electron, an operation somewhat similar to the gain process observed in photoconductors. It must be realized that this simple model does not hold everywhere, as the effect of a single ion may depend on its position in the cell, since the electron concentration, as will be seen, is highly variable in the cell. However, substantial gain has been measured in this cell.

From this simple outline, it is already possible to discern the advantages of a detector of this type. The electrons in the reaction cell proper are completely thermal (at the most experiencing the weak combination of their self-fields and the applied field). With this low electron energy value, the cross-section for desirable capture reactions with the strong electrophores is maximal, while the undesirable capture of weak electrophores such as oxygen, water and carbon dioxide have low cross-section (their maxima occur near 6.5 eV). The final electrons produced by the ionization shower of  $\beta$  particles have relatively large initial energies (estimated to be on the order of 0–6.5 eV (ref. 4) and therefore are more likely to react with the weakly capturing compounds.

No positive ions or energized radicals are formed in this process, as is the case in the radioactive source. The assimilated polymerization reactions taking place in the effluent, whose deposits eventually coat the radioactive foil are expected to be absent. Hence, frequent cleaning of the detector is not required. Positive ions emitted from the cathode (or the supporting platinum wire), a common phenomenon with most thermionic emitters, are restricted by the field in the inner cylinder from entering the cell proper. Negative ions formed in this region will either be swept out, or discharged on the walls. Overall, the chemistry is a lot cleaner, as there are, in principle, only three specimens present: electrons, electrophores, and negative ions.

The volume of the detector itself can be very small; the volume of the cell here is defined (in the configuration shown) as that section between the two cylinders exposed to electrons. Volumes as small as 50  $\mu\text{l}$  have been made and this represents by no means the lower limit. There is, however, a lower limit to the desirability of a small cell size, unless the flow is also reduced. The chemical reaction between the electrons on the electrophores



proceeds with a finite rate constant,  $k_1$ , and assuming a very low initial concentration of electrophores  $[AB]_0 \ll [e^-]$ , we have as a solution:

$$[AB] = [AB]_0 [1 - e^{-t/\tau}] \text{ where } \tau = 1/k_1 [e^-]$$

For most strong electrophores, the value of  $k_1$  is a few times  $10^{-7}$   $\text{cm}^3/\text{sec}$  (refs. 11 and 12), and if we assume an electron concentration of  $10^8$  per  $\text{cm}^3$ , the time constant,  $\tau$ , is around 0.03 sec. If the cell volume is so small that, at the flow-rate under consideration, the dwell time (cell volume/flow-rate) is much smaller than the above time constant, substantial reduction in response will occur.

This detector operates both with argon–methane and nitrogen, without any loss of sensitivity. Cleaning procedures are substantially simplified, and moreover, there is no temperature limit of operation. As another advantage may be listed that the choice of the cell material is vastly enlarged, when no preventive measures against radioactive leakage need to be taken. If necessary, the cell may be fabricated out of Pyrex or fused quartz with metal electrodes (platinum or gold) vacuum deposited in the appropriate places. Glass detectors made this way were found completely satisfactory, and in some ways, superior to stainless-steel detectors.

Note that with this detector there are no basic advantages for the pulse mode, as compared to the d.c. mode of operation. With the radioactive detector, the pulse mode has the advantage over the d.c. mode of operation that in the time between pulses, the electron concentration can build up to a maximum value (set by recombination) since no field is present. The use of the pulse mode is, in fact, dictated by the finite rate of electron production of the source. But with the thermionic emitter, there is no rate limitation of electron production.

If the cell were momentarily pulsed clean of electrons, the electron concentration would be re-established in a matter of microseconds to its previously undisturbed value. The inner chamber provides an almost infinite reservoir of electrons which can fill the cell proper in a very short time. For all practical purposes, the cell always operates in a d.c. mode of operation. There are various ways in which the signal can be retrieved from the detector, depending on whether the collector is operated under a constant voltage mode or under a constant current mode. These modes of operation will be described in more detail in the next section.

#### DESCRIPTION OF THE DETECTOR

Fig. 2 illustrates a cross-section of a detector operating on this principle. It consists of a solid block of stainless steel into which the inner cell is inserted. Column effluent and guard gas are brought in at the same temperature. A glass or ceramic flow straightener is inserted in the inner cell to provide laminar flow, to as good a degree as possible, as turbulent flow can significantly degrade the observed signal-to-noise ratios of the detector.

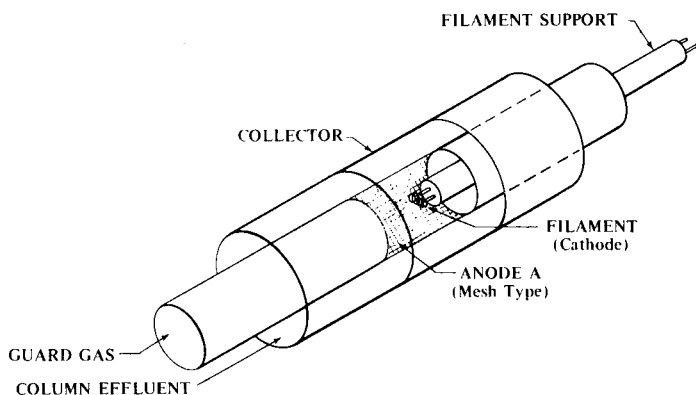


Fig. 2. Schematic illustration of a practical implementation of the non-radioactive ECD. The filament is oriented vertically, so that its thermal plume does not enter the reaction chamber. Provisions are taken so that the flow of both the guard gas and effluent are laminar in the detection chamber, so that a minimum of mixing takes place. All materials are stainless, or ceramic, with silicone rubber O-rings.

The thermionic filament consists of a 0.125 mm thick platinum wire, spirally wound with about ten turns to a length of about 3 mm, and cataphoretically coated with barium zirconate. The filament is heated by a small floating power supply; a few watts are typically all that is required to keep the filament at the required temperature. The outer diameter of the anode of the cell shown is about 14.8 mm, and the

## NON-RADIOACTIVE ECD

inner diameter of the collector 13 mm. The slit through which the electrons diffuse is about 1.3 mm, so that the effective cell volume is on the order of 50  $\mu\text{l}$ . The filament location is adjustable to provide optimum position for emission.

This detector was typically operated with a gas flow through the column of about 60 ml/min. The amount of guard gas required to protect the filament depends upon a number of parameters such as the amount of solvent injection, the diameter of the inner cylinder, and the desired (or acceptable) baseline recovery time.

Injections of 3–5  $\mu\text{l}$  tend to give relatively large penetration in the inner cylinder and require higher gas flow than the injection of 1–2  $\mu\text{l}$ . A large diameter is advantageous, but requires more gas flow if the same linear velocity is to be maintained. For minimum turbulence in the grid zone, it is desirable to have the flow velocities on both sides to be nearly equal, although a certain amount of mismatch can be tolerated. The overriding concern is, of course, an acceptable baseline recovery, before the arrival of the chromatographic peaks. The chromatographic conditions therefore determine to some degree the amount of guard gas required. Guard gas flows on the order of 1–3 ml/sec were typically used. No effect at all was seen on the peak heights when the guard flow was changed over a factor of five from 1 to 5 ml/sec. As stated above, a current loop, set at a predetermined level, keeps the cathode–anode current constant. As the solvent penetrates into the inner region, the voltage required to keep this current constant is generally increased, and may even drive the loop out of control. Small excursions of this control voltage are also noted during the passage of large sample quantities (nanogram or above). The current between the anode and the collector, which is primarily driven by diffusion (at least in equilibrium) can be collected with a constant voltage (typically a couple hundred millivolts) or may be set by another current loop. This secondary current is typically three orders of magnitude smaller than the primary current. For example, a common value for the setting of the primary loop is 10  $\mu\text{A}$ , *versus* 10 nA for the secondary loop. Control voltages required in the first loop would then be on the order of 40–50 V (depending on the filament condition and the type of gas used), and 100–200 mV for the cell loop.

In the constant-voltage mode of operation of the cell, the current excursion is measured by some electrometer, and generally speaking, the current decreases when the electrophores pass through the cell. In the constant-current mode of operation, an increase in the control voltage is typically needed to keep the current constant, and the incremental voltage is taken as the signal. The latter mode of operation has been used in the particular experiments described here. In this mode any shift in contact potential in the anode-collector region is automatically taken up simply as a shift in the standing voltage, but does not affect the signal amplitude.

In contrast with the constant-voltage mode, the measured value (voltage) tends to increase, rather than decrease with increasing injection of electrophores (*versus* decreasing current in the constant-voltage mode). As the sample size is increased, the voltage across the cell can always be increased to a value limited only by the design of the servoloop. However, as the voltage across the cell is increased, the cell ceases to operate in a diffusion controlled mode and becomes more and more field controlled. This means that as the sample quantity gets larger, the response factor automatically becomes lower, giving rise to a somewhat compressed range.

## THEORY OF OPERATION

Although a complete and rigorous theory has not yet been attempted, it is possible to describe approximations which give significant insights into the mode of operation. Consider Fig. 3 where the cell is schematically illustrated. A plane geometry has been assumed, since the radius of curvature of the cell is insignificant to the problem. The cylindrical problem is tractable, but offers no new insights into the solution.

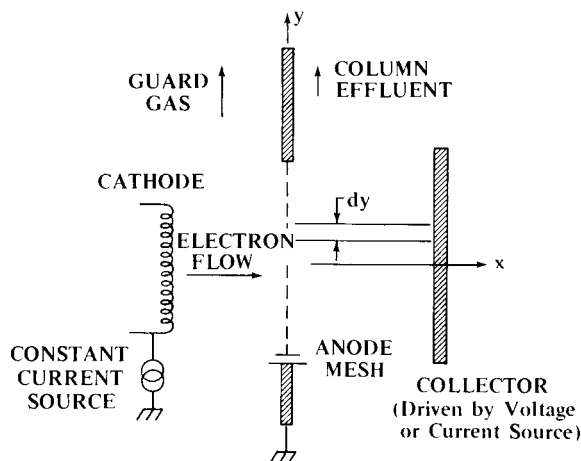


Fig. 3. Schematic illustration of the cell in planar geometry. The cathode current establishes an electron density  $N_e(0)$  at the anode, and due to the mesh-like structure of the latter, an equal electron density exists on the other side of the mesh. Diffusion, aided by a small field, drives the electrons towards the collector, which can be biased either in constant-current or constant-voltage mode.

The primary current from the thermionic filament to the anode establishes an equilibrium electron density at the grid, which can be estimated from the current in the first diode, since this current is dominated at all times by the field. It is assumed that this electron density,  $N_e(0)$ , is kept constant at all times, regardless of the concentration of electrophilics that are present. This assumption is an acceptable approximation, when the electrophilic concentration is small compared to  $N_e(0)$ . It is also assumed that the electron concentration on both sides of the grid is equal. Since the grid is both very open and very thin, this assumption will be always very nearly satisfied. If it were not, a large diffusion current would immediately establish equality. The ionization of an electron capturing compound entering the cell is a function of its rate constant,  $k_1$ , the electron concentration and the dwell time in the cell. Therefore, if a plug  $dy$  of electrophilic material moving along the  $y$  axis is assumed to enter the cell at  $y = 0$ , its ionization will be increasing with increasing  $y$  (and dwell time in the cell). In other terms, the ionization will have both a  $y$  dependence and, as will be seen, a strong  $x$  dependence. The  $y$  dependence is neglected in this approximate theory and replaced by an average ionization dwell time, taken to be half the time for the gas flow to sweep the cell volume.

Almost intuitively, it can be seen that the  $x$  dependence of the ionization will be very strong. From its initial value,  $N_e(0)$  at  $x = 0$ , the electron concentration will

decrease very rapidly with increasing  $x$ , giving rise to a strong diffusive flow. This flow is opposed by the field of the electron space charge. With increasing  $x$ , the space charge field gradually decreases and may change sign, while at the same time, the diffusion gradient decreases and may eventually become negligible.

The elution time for typical chromatographic peaks is much longer than any of the time constants involved, so we will assume that the concentration of unionized electrophilic material entering the cell is constant in time. A time varying peak can be reconstructed by calculating the responses for various static concentrations.

The behavior of the negative particle flow is given by the following equation

$$J = -D_e \cdot \frac{\partial N_e}{\partial x} - D_i \cdot \frac{\partial N_i}{\partial x} + V_e N_e + V_i N_i \quad (1)$$

where  $J$  is the total charged particle flow,  $D_e$ ,  $D_i$  are the electronic and ionic diffusion constants and  $N_e$ ,  $N_i$ ,  $V_e$ ,  $V_i$  are the electronic and ionic concentrations and velocities.

As the electric field,  $E$ , is quite small, and the cell is working under atmospheric pressure,  $p$ , the parameter  $E/p$  is very small so the velocities can be expressed in terms of their mobilities  $\mu_e$  and  $\mu_i$  as  $V_e = -\mu_e E$ ,  $V_i = -\mu_i E$ . Under equilibrium conditions, the particle flow is constant throughout the cell, or  $\partial J/\partial x = 0$ .

From Gauss' law:

$$\frac{\partial E}{\partial x} = - \frac{(N_e + N_i) e}{\epsilon_0} \quad (2)$$

where  $e$  is the electron charge,  $\epsilon_0$  the permittivity of the gas.

Furthermore, it is assumed that the ion concentration,  $N_i$ , is related to the incoming electrophore concentration ratio by

$$N_i(x) = N_{i0} \{1 - \exp[-N_e(x) k_1 t_1/2]\} \quad (3)$$

where  $N_e(x)$  is the local electron concentration,  $k_1$  the capturing rate constant and  $t_1$  the dwell time in the cell. The rate constant  $k_1$  for electron capture has been assumed in our calculations to be on the order of  $3 \times 10^{-7}$  cm<sup>3</sup>/sec, which is representative of strongly capturing compounds.

This set of equations is numerically solved by trial and error. Under constant-current conditions, the procedure is as follows: since the electron concentration  $N_e(0)$  is known at the boundary, the ion concentration is known there too. The electron gradient,  $\partial N_e/\partial x$ , is guessed at the boundary and the Taylor expansion of  $N_e$  and  $E$  can subsequently be calculated to the second order from eqns. 1 and 2. If the gradient  $\partial N_e/\partial x$  is not guessed right, it is found that the solution either diverges very rapidly, or gives rise to negative electron concentrations. Guessing the right electron derivative is a tedious process, and corresponds to determining the diffusion current at the grid. Since the diffusion current is there much larger than the total current (by typically two orders of magnitude), it is required that the derivative be known to high precision. An acceptable solution for  $N_e$  (and  $E$ ) is such that it neither diverges or yields negative  $N_e$  and matches smoothly with the solution  $J = N_e V_e$  at points far away from the grid, where diffusion has become negligible. (This requires the profile

$\partial N_e/\partial x$  to be convex at all times.) Although this procedure does not yield a unique solution, since these conditions can be met by a set of solutions, in practice it is found that the solution set is very narrowly bracketed, and does allow solutions to diverge only by a few per cent.

The above technique is used when the detector is operating in the constant-current mode. The voltage across the cell is found by integration of the field across the length of the cell. But if the detector is operating in the constant-voltage mode and the voltage found is not equal to the applied voltage, it is necessary to readjust the current value, reiterate the above procedure, integrate the electric field, compare with the applied voltage, readjust the current, etc.

The current-voltage characteristics of planar cells of various size in a nitrogen atmosphere, for different electron concentrations at the boundary are illustrated in Fig. 4. Note the very strong dependence of the current on the length of the cell. For comparison, the space charge limited current, as given by  $J = 9\mu_e V^2 \epsilon_0 / 8l^3$  has also been drawn, where  $\mu_e$  is the electron mobility in nitrogen and  $l$  the cell length. Due to the diffusion, the current always exceeds the space charge limited current, and moreover current is seen to flow for negative bias voltages, where repulsion of the electrons takes place. The cutoff voltage for current is on the order of 50–100 mV for most of the cells of interest.

The electron profile and the electric field across the cell are illustrated in Figs. 5 and 6, for electron fluxes of respectively 0 and  $1 \cdot 10^{11}/\text{cm}^2 \cdot \text{sec}$  (current densities of 0

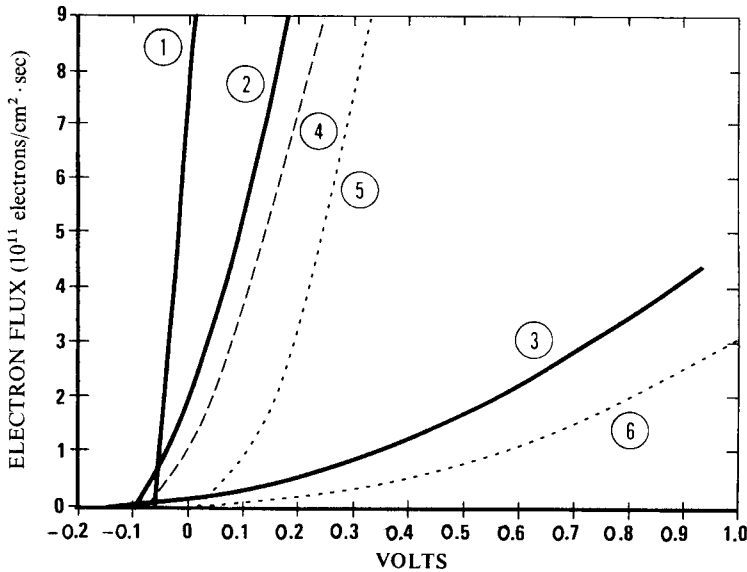


Fig. 4. Current-voltage characteristics of planar diodes, for various electron concentrations  $N_e(0)$  at the anode mesh and various anode-collector spacings,  $L$ . Note that because of the diffusive flow enhancement current can flow even with negative collector bias. With increasing anode-collector separation, the required voltage for a given current increases quite rapidly. The space charge limited current, neglecting diffusion is also illustrated for spacings of 1 and 3 mm. The ambient gas is assumed to be nitrogen. Curves: 1,  $N_e(0) = 2.8 \cdot 10^{14}$  electrons/ $\text{m}^3$ ,  $L = 0.5$  mm; 2,  $N_e(0) = 2.8 \cdot 10^{14}$  electrons/ $\text{m}^3$ ,  $L = 1$  mm; 3,  $N_e(0) = 2.8 \cdot 10^{14}$  electrons/ $\text{m}^3$ ,  $L = 3$  mm; 4,  $N_e(0) = 1 \cdot 10^{14}$  electrons/ $\text{m}^3$ ,  $L = 1$  mm; 5, space charge limited flow,  $L = 1$  mm; 6, space charge limited flow,  $L = 3$  mm.

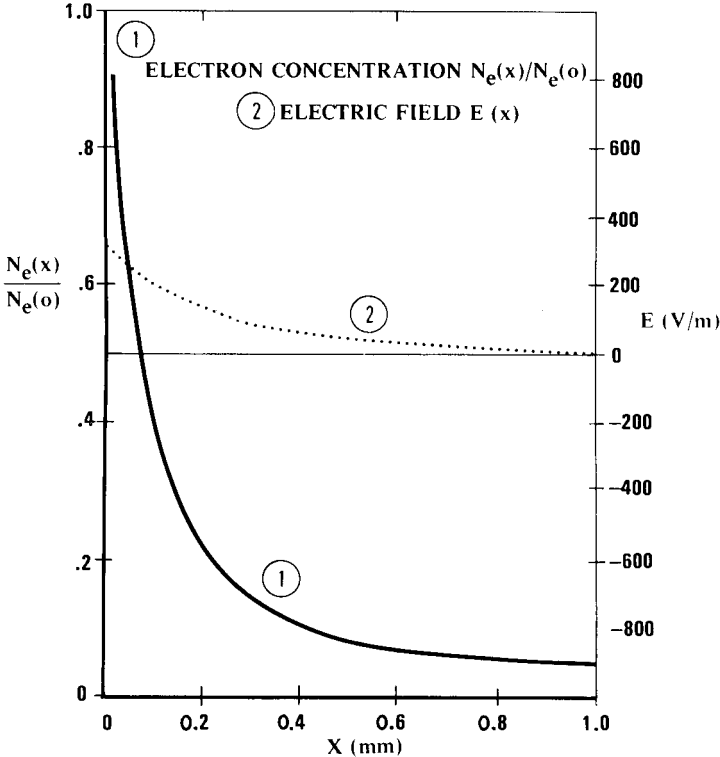


Fig. 5. Normalized electron profile  $N_e(x)/N_e(0)$  and electric field  $E$  across the detection chamber for zero current. The electron density at the anode  $N_e(0)$  is assumed to be  $10^8/\text{cm}^3$ . As the electrons enter the cell, the field opposes their entry; near the collector the diffusion gradient is zero, and so is the field. Nitrogen has been assumed for the carrier gas. Cell bias =  $-80$  mV.

and  $1.6 \cdot 10^{-8} \text{ A/cm}^2$ ). At zero total current, the diffusion and drift current obviously balance each other everywhere, and the electric field will always be positive, opposing the electron motion everywhere since the diffuse flow is always in the same direction.

As the current increases (Fig. 6), the electron concentration in the cell increases, as expected. The electric field is seen to change sign in the cell, opposing the entry of electrons at the grid, and pushing them towards the collector in the collector region. The nature of the current in the cell therefore changes gradually from predominantly a diffuse flow near the anode to drift flow near the collector.

The above characteristics have all assumed the absence of electron capturing compounds in the cell. When the electrophilics are introduced, the field and electron distribution are changed, due to the immobile space charge of the ions (Fig. 7). It has been assumed that the cell is operating under constant-current conditions, and an increase in bias voltage of about 25 mV has been necessary to maintain the same current as before the introduction of electrophores. The unionized electrophilic concentration is assumed to be distributed uniformly across the cell, and equal in magnitude to the electron concentration at the grid. A dwell time of 50 msec has been assumed. Note that the ion concentration is by no means uniform, and follows a



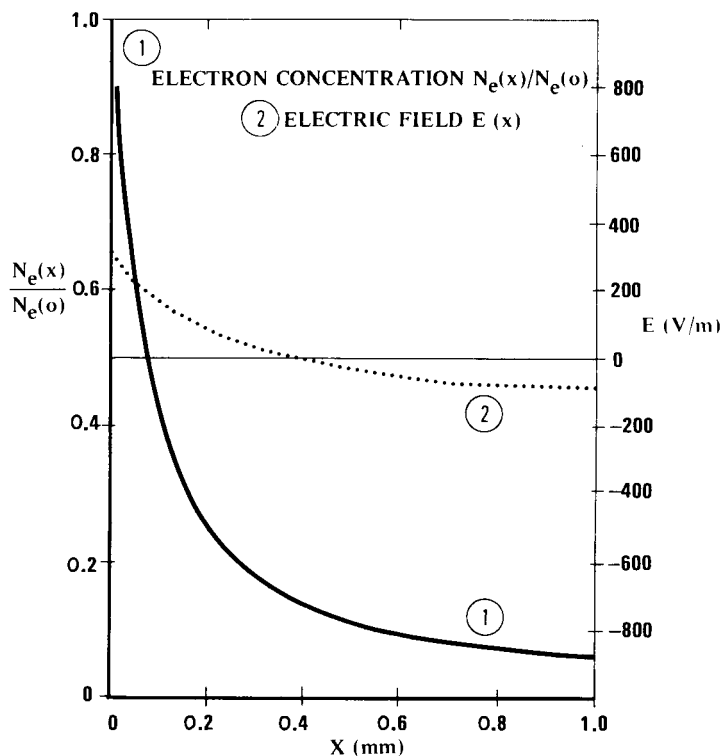


Fig. 6. Normalized electron profile and electric field across the detection chamber for an electron flux of  $5 \cdot 10^{11}/\text{cm}^2 \cdot \text{sec}$  ( $j = 8 \cdot 10^{-8} \text{ A}/\text{cm}^2$ ). The electron density at the anode is again  $10^8/\text{cm}^3$ . Note the increase in average electron density as compared with Fig. 5. Bias voltage is 130 mV. The electric field now changes sign in the cell, opposing the entrance of electrons at the anode, but aiding diffusion at the collector.

pattern similar to the electron concentration. Moreover, the ionization is far from complete. This is in contrast to the radioactive ECD, where for small concentrations, the ionization may approach 100%.

The response curve, namely the voltage across the cell necessary to keep the current constant, with varying concentrations of electrophilics, is illustrated in Fig. 8. The abscissa represents the electrophore concentration, normalized to the electron concentration at the grid. In this case, the response is nearly linear in the electrophore concentration. Fig. 9 illustrates a similar characteristic with the same equilibrium current, but taken under the condition of constant voltage ( $-4 \text{ mV}$ ). The ordinate now represents the cell current, normalized to the equilibrium value of the undisturbed cell and, as before, the abscissa represents the injected electrophilic compound concentration, normalized to the electron concentration at the grid. The current at first decreases linearly with the injected compound concentration, but becomes rather quickly supralinear.

One particular characteristic of the constant-voltage mode, according to this model, is that over a restricted range the normalized current-concentration characteristic is almost independent of the current value used as long as the cell voltage stays

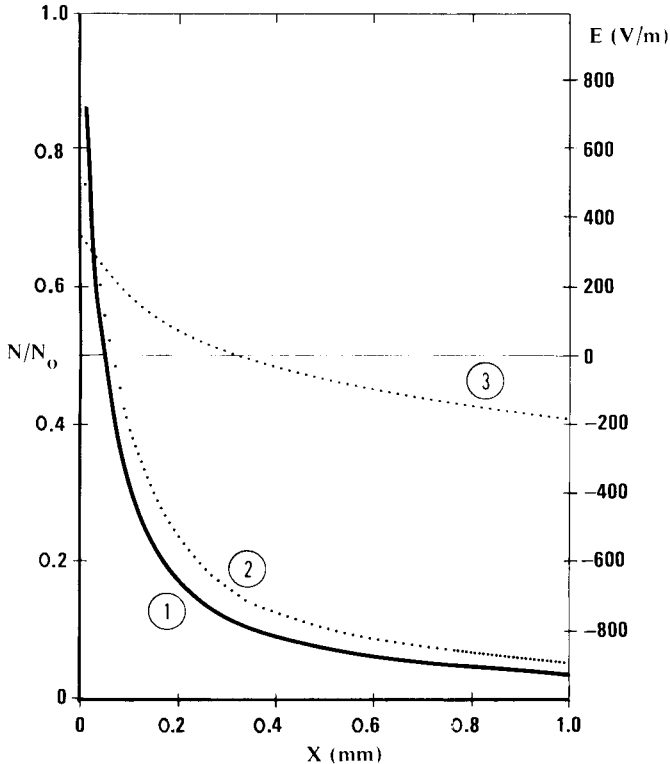


Fig. 7. Electron concentration  $N_e(x)/N_e(0)$  (1), ion concentration  $N_i(x)/N_i(0)$  (2) and electric field  $E_x$  (3) in a planar cell of length 1 mm, electron flux density of  $1 \cdot 10^{11}$  electrons/cm<sup>2</sup>·sec ( $j = 16$  nA/cm<sup>2</sup>). The electron concentration is normalized to the concentration at the grid, and similarly for the ion concentration, both of which are assumed to be  $10^8$ /cm<sup>3</sup>. To accommodate the ionic space charge, the collector voltage has to be raised from  $-4$  mV (in the absence of electrophilics) to 22 mV.

below 200 mV. Doubling the equilibrium current, which requires the voltage to be increased to 40 mV, gives rise to a very much identical characteristic (see Fig. 9).

All of the above characteristics were obtained with nitrogen as the carrier gas, and an electron mobility assumed to be  $1.35 \cdot 10^4$  cm<sup>2</sup>/Vsec (ref. 13). For argon-methane mixtures, (either 5% or 10% methane) the mobility and diffusion coefficient have been assumed to be three times larger<sup>14</sup>. The response of the same physical cell of Fig. 8, with identical electron concentration and operating at the same constant current, but using argon-methane as the carrier gas, is illustrated in Fig. 10.

The equilibrium value of the current can now be maintained with a reverse bias of almost 50 mV. Note however that the response is quite sluggish for low electrophilic concentrations. In fact, the response can even become inverted for low concentrations, that is introduction of an electron capturing compound will reduce the bias signal (under constant-current operation). This anomalous behavior is by no means peculiar to argon-methane mixtures, although it is somewhat more pronounced in them. It is characteristic of the cell behavior, when the operating conditions are

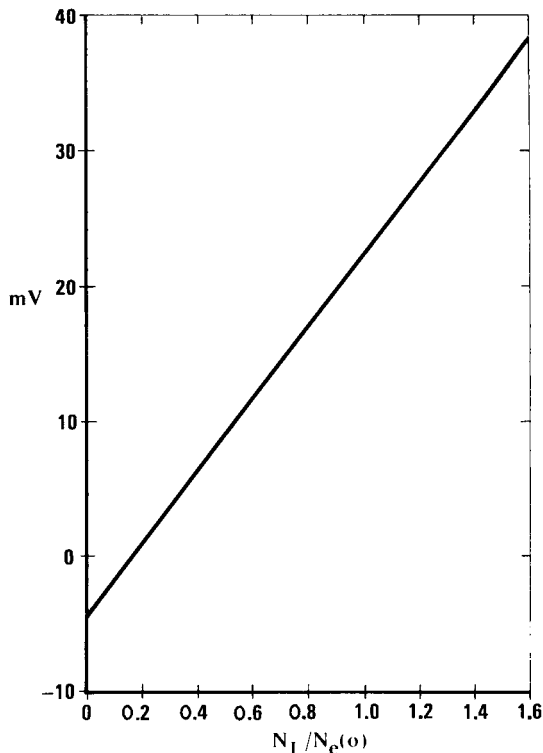


Fig.8. Calculated response curve for a planar detector operating in the constant-current mode. The conditions are the same as in Fig. 7: electron flux  $1 \cdot 10^{11}$  electrons/cm<sup>2</sup> · sec ( $j = 1.6 \times 10^{-8}$  A/cm<sup>2</sup>), electron concentration  $N_e(0) = 1 \cdot 10^8$ /cm<sup>3</sup>, cell length = 1 mm. Plotted is the voltage across the cell required to keep the current constant as a function of the unionized electrophilic concentration  $N_1$  flowing through the cell. The electrophilic concentration is normalized to  $N_e(0)$ , the electron concentration at the anode.

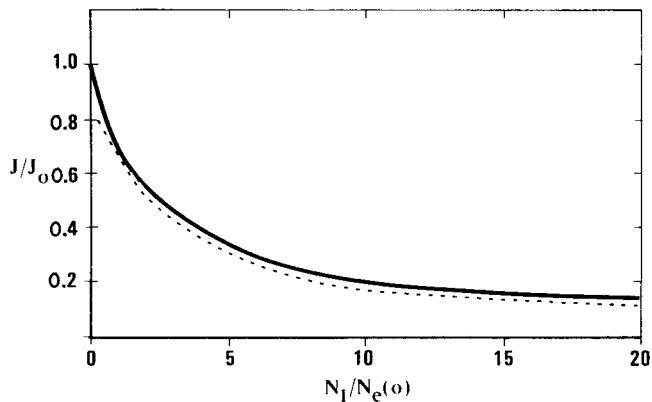


Fig. 9. Calculated response curve for a planar detector operating in the constant-voltage mode. The conditions are similar to Figs. 7 and 8: electron concentration at the anode  $N_e(0) = 1 \cdot 10^8$ /cm<sup>3</sup>, cell length 1 mm, cell-bias voltage  $-4$  mV. At rest, with no electrophilics present, the electron flux  $J_0$  is  $1 \cdot 10^{11}$  electrons/cm<sup>2</sup> · sec ( $j = 1.6 \cdot 10^{-8}$  A/cm<sup>2</sup>). Plotted is the variation of the normalized cell current,  $J/J_0$  as a function of the unionized electrophore concentration  $N_1$  normalized to  $N_e(0)$  introduced in the cell. The dotted line indicates the response curve, when the cell voltage is increased to 40 mV. The electron current at rest doubles, ( $J_0 = 2 \cdot 10^{11}$  electrons/cm<sup>2</sup> · sec) but the normalized graph of current *versus* electrophore concentration is very much identical.

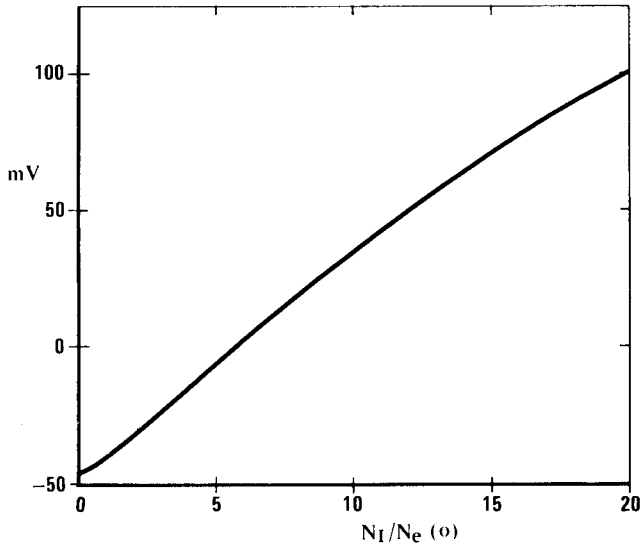


Fig. 10. Calculated response curve for a planar detector operating in the constant-current mode, but using argon-methane (5:95) as the carrier gas, instead of nitrogen. The cell length  $l$  is 1 mm, the electron density  $N_e(0) = 1 \cdot 10^8/\text{cm}^3$ , the constant electron flow  $J_0 = 1 \cdot 10^{11}$  electrons/ $\text{cm}^2 \cdot \text{sec}$  ( $j = 1.6 \cdot 10^{-8}$  A/ $\text{cm}^2$ ). Note the large negative bias voltage at rest, due to the increased electron diffusion and mobility, and the sluggish response for small electrophore concentrations.

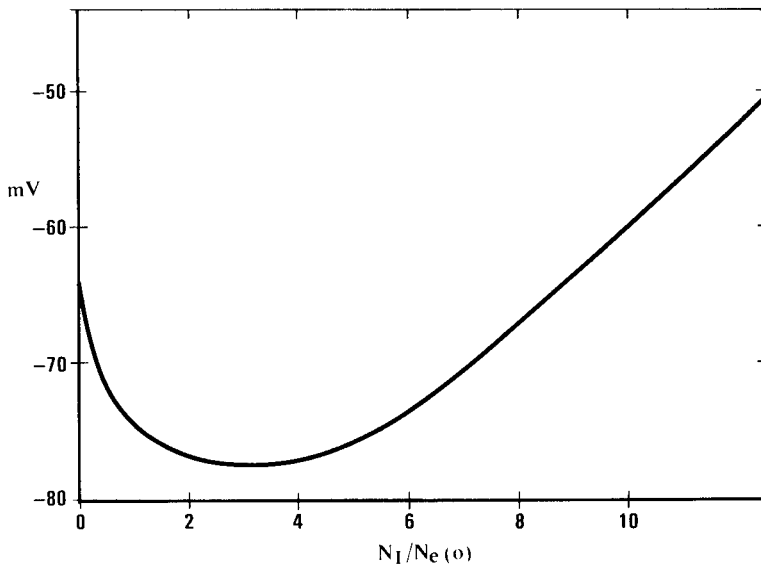


Fig. 11. Calculated response curve for a planar cell, operating in the constant-current mode, with nitrogen as the carrier gas, but with the current reduced by a factor of ten as compared to Fig. 8 ( $L = 1$  mm,  $N_0 = 10^8/\text{cm}^3$ ,  $J_0 = 1 \cdot 10^{10}$  electrons/ $\text{cm}^2 \cdot \text{sec}$ ,  $j = 1.8 \cdot 10^{-9}$  A/ $\text{cm}^2$ ). The response is now seen to be inverted at low electrophore concentrations. In this region, increasing concentrations of electron capturing compounds causes the cell voltage to decrease, rather than increase as is normally expected. This behavior is thought to be due to the predominance of diffusion under the conditions of low current.

chosen such that the cell is operating under reverse bias, which typically corresponds to small current values.

For example, Fig. 11 illustrates the calculated characteristic for the cell, operating under identical conditions as in Fig. 8, operating with nitrogen as the carrier gas, except that the current density has been reduced by a factor of ten. The bias voltage has now become quite strongly negative, at equilibrium, and becomes even more so when electrophores are introduced.

As stated, these inverted responses are found to occur only when the cell is strongly reversed biased. Clearly diffusion is the main driving force under those conditions, and it is perhaps not too surprising that if some electrons are removed (by conversion into ions), that the electron gradient is increased, and that therefore the diffusion current increases. However, as the ion concentration starts building up, the field effects eventually overpower the diffusion effects, and the response reverts to normal.

The effect also occurs in the constant-voltage mode, when a strong negative bias is imposed across the cell, such as to make the current quite small. This is illustrated in Fig. 12, where the current is seen to increase first with increasing electrophore concentrations, until it eventually decreases at higher concentrations.

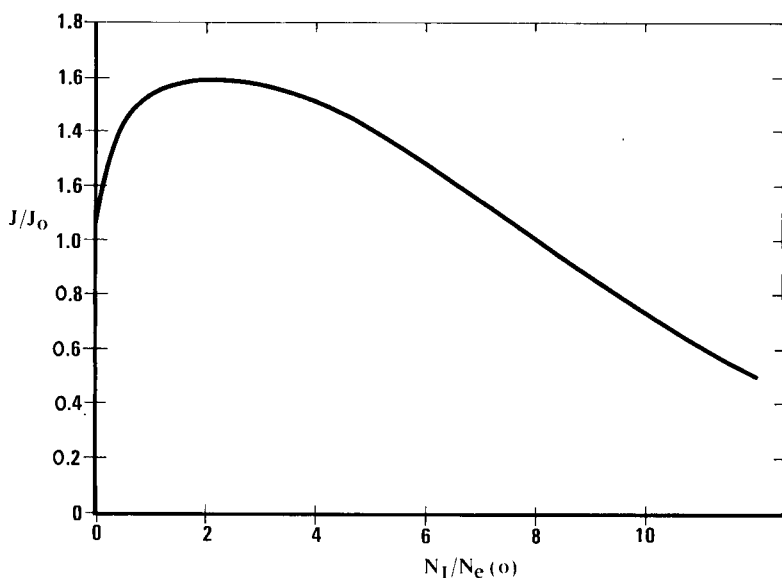


Fig. 12. Calculated response curve for a planar detector, using nitrogen operating under constant voltage with a strongly negative cell bias of  $-64$  mV [ $L = 10^{-3}$ ,  $N_e(0) = 10^8/\text{cm}^3$ , standing current  $J_0 = 1 \cdot 10^{10}$  electrons/ $\text{cm}^2 \cdot \text{sec}$ ]. Plotted is the cell current, normalized to  $J_0$ , as a function of the electrophore concentration in the cell [normalized to  $N_e(0)$ ]. The response is again anomalous, giving an increase in cell current with introduction of the electronegative compounds. At higher concentrations however, the response becomes normal, due to the increasing ionic space charge.

## RESULTS

A typical chromatogram, taken with a detector as illustrated in Fig. 2, is given in Fig. 13. A  $1\text{-}\mu\text{l}$  injection of isooctane was made containing 3  $\mu\text{g}$  of both lindane and

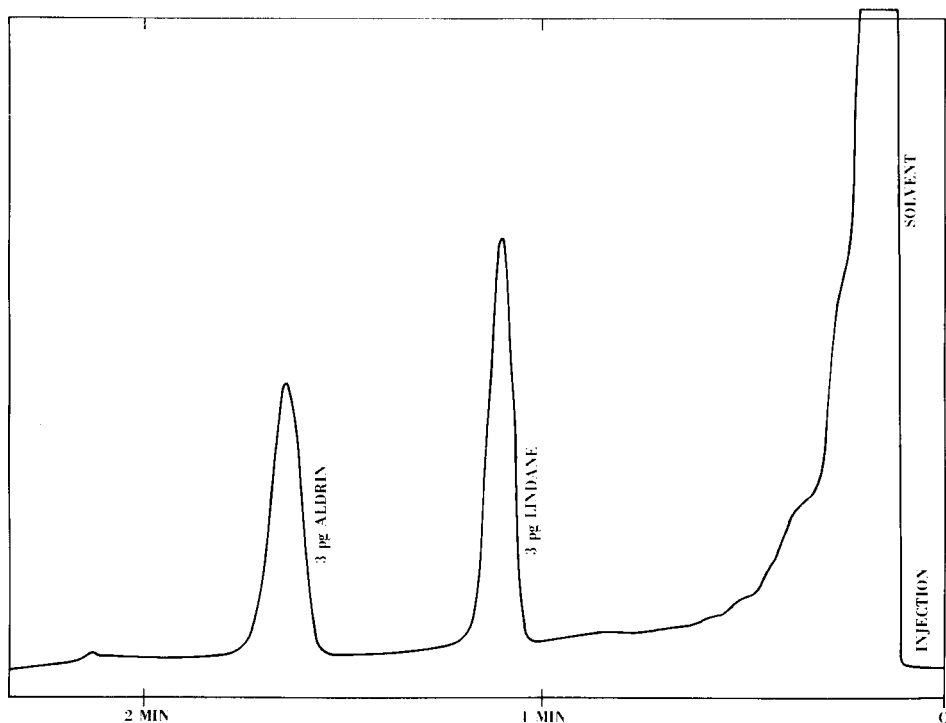


Fig. 13. Typical chromatogram obtained with the non-radioactive ECD for an injection of  $1 \mu\text{l}$  of iso-octane containing 3 pg of both lindane and aldrin. The chromatographic conditions were as follows: Hewlett-Packard Type 5710 chromatograph, 6-ft. Supelco column, Type E6806, column temperature  $220^\circ\text{C}$  (isothermal), injection port and detector temperature  $250^\circ\text{C}$ , nitrogen carrier gas flow 60 ml/min, nitrogen guard gas flow 120 ml/min. Horizontal scale: 15 divisions per min, vertical scale 100 mV. The detector was operated in the constant-current mode with a cathode-anode current of  $10 \mu\text{A}$  and an anode-collector current of 10 nA (bias voltage at rest 20 mV).

aldrin, on an HP 5710 chromatograph. A 6-ft. Supelco column, Type E6806, was used in these experiments, with nitrogen as a carrier gas at a flow-rate of 1 ml/sec, and with the guard gas flow set at 2 ml/sec. The column temperature was maintained at  $220^\circ\text{C}$ , and both the injection port and the detector were kept at  $250^\circ\text{C}$ . Ultra-high-purity carrier gases were used in all the experiments, together with vacuum tight fittings and large well baked out moisture traps and tubing, to provide the cleanest environment possible.

This chromatogram was taken in the constant-current mode with the cathode-anode current fixed at  $10 \mu\text{A}$ , and the anode-collector current maintained at 10 nA, at a bias of about 20 mV. Note the very distinct, noise-free signals, even at this low level of injection.

The response curve for lindane, from 1 pg to  $1 \mu\text{g}$ , is illustrated in Fig. 14. The incremental signal follows an almost  $\frac{2}{3}$  power law, although not exactly so. If the response were extrapolated with the same slope to lower injections, a signal-to-noise

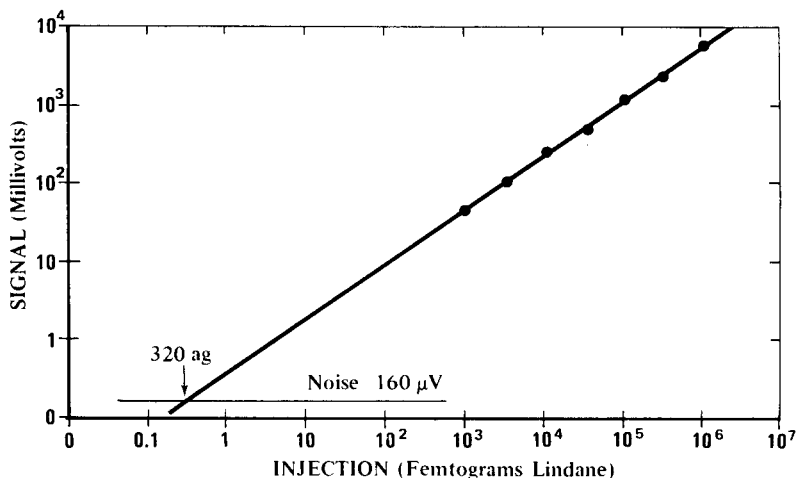


Fig. 14. Peak response curve of the ECD for lindane, measured under the same experimental conditions as Fig. 13. The response follows approximately a two thirds power law. If this response curve were to be extrapolated to the noise, the minimum detectable signal (signal-to-noise ratio = 2) would be 320 ag.

ratio of two (representing the minimum detectable signal) would be obtained at an injection of 320 ag ( $320 \cdot 10^{-18}$  g). It is, however, quite possible that the slope becomes more linear at lower levels; no subpicogram level injections have been attempted because of the difficulty of preparing correct dilutions at this level.

It is interesting to compare the experimental values with the estimates from the theory. Typically, a 1-pg injection of lindane will give a peak signal amplitude of about 30 mV. A total injection of 1 pg of lindane will, under the experimental conditions, give rise to a peak concentration of  $10^8$  atoms per  $\text{cm}^3$  in the detector. The average electron concentration on the anode is subject to some approximations, due to the difficulty of guessing the exact form of the current spreading from cathode to anode. Assuming cylindrical space charge flow, the best estimate is on the order of  $10^8$  electrons per  $\text{cm}^3$  at the anode (for  $10 \mu\text{A}$  of primary current). The ratio of the electrophilic to the electron concentration is therefore close to one, and since the experimental conditions are very close to those illustrated in Fig. 8, with  $N_i/N_e = 1$ , the expected signal is about 25 mV. The agreement is remarkable, and probably fortuitous, in view of the drastic approximations made in the numerical computation. The numerical model, however, does predict a linear concentration behavior in the picogram region, which is not born out by the experiments. On the other hand, it is interesting to note that the negative peaks predicted by the theory are indeed experimentally observed and precisely under those conditions, which indicated by the theory namely strong negative bias and low cell current.

At low injections (picogram) negative peaks are seen; at higher injections (20–30 pg), there is a negative precursor, followed by a positive peak, precisely as would be expected. Results for a similar, although not identical, detector operating in the constant-voltage mode, are illustrated in Fig. 15 again for lindane. Obviously, there will be a decrease in dynamic range if the sensitivity is increased, since the current can hardly be expected to drop below zero. The best observed experimental sensitivity

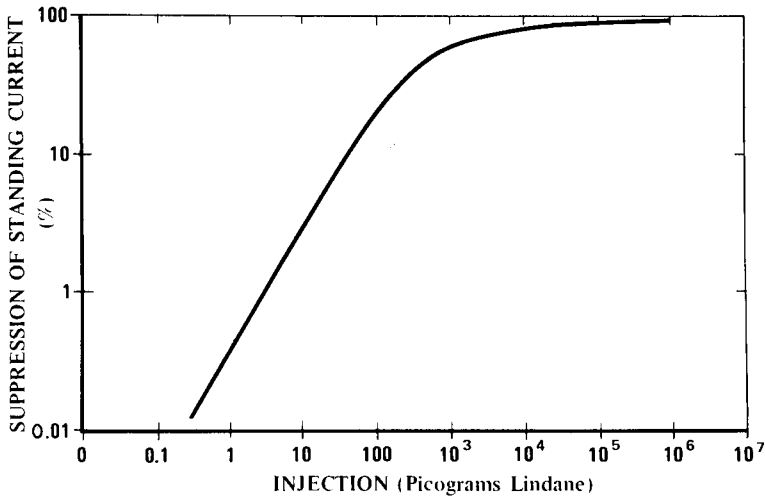


Fig. 15. Response curve for lindane, with the detector operating in the constant-voltage mode of operation. Bias voltage 200 mV, bias current at rest 8.1 nA. Plotted is the percentage suppression of the standing current, *versus* the total amount of lindane injected. The observed response, normalized to the standing current, is experimentally found to be largely independent of the standing current for small bias voltages, as predicted by theory.

was a current reduction of 65% at a 33-pg injection with a bias voltage of 200 mV. If the graph of Fig. 9 is taken to be representative, a 65% reduction in current would be obtained for a 4-pg injection, *versus* the 33 pg observed experimentally. The bias voltage was, however, 200 mV *versus* the  $-4$  mV obtained from the computation, indicating that probably substantial amounts of electrophores were present, even at equilibrium. The independence of the shape of the relative response curve was, however, experimentally verified.

When using the constant-current mode, a slight peak broadening, as yet unexplained, is generally observed at the 10-ng level.

Although only results with lindane and aldrin are represented, the detector was found to be sensitive to any of the common electron-capturing compounds such as Mirex, diazepam, anthraquinone, malathion, etc. Correlation between the observed response in a radioactive detector and this detector is very strong. A  $10\text{-}\mu\text{l}$  injection of room air containing  $1 \cdot 10^{-14}$  g/ $\mu\text{l}$  of carbon tetrachloride, gave signals about 30–40 times above the noise (the column temperature was at  $60^\circ\text{C}$  in this case, to provide for sufficient time separation between the air peak and the carbon tetrachloride).

The detector appears to tolerate overloads without prolonged noticeable ill-effects, and seems to require very little clean-up time after removal from the chromatograph. Detectors removed from the chromatograph, stored for a few days in a clean bench and remounted were found to be almost in complete equilibrium in a time span of 2–3 h, whereas a radioactive detector treated the same way, might require at least 1 day.



## CONCLUSION

A new type of ECD has been described which uses a thermionic source of electrons, rather than the usual radioactive source. This allows the use of a sensitive new mode of operation, due to the phenomenon of space charge amplification. It appears that femtogram quantities of capturing compounds may be detected with this detector. A one-dimensional theory of operation has been developed and shows agreement with the experimental results. In view of the simplicity of the reactions taking place, it is hoped that this detector will allow eventually a full theoretical understanding of its operation.

## REFERENCES

- 1 J. E. Lovelock, *J. Chromatogr.*, 99 (1974) 3.
- 2 W. A. Aue and S. Kapila, *J. Chromatogr. Sci.*, 2 (1973) 255.
- 3 W. E. Wentworth, E. Chen and J. E. Lovelock, *J. Phys. Chem.*, 70 (1966) 255.
- 4 W. E. Wentworth, A. Tishbee, C. F. Batten and A. Zlatkis, *J. Chromatogr.*, 112 (1975) 229-246.
- 5 J. E. Lovelock, *Anal. Chem.*, 35 (1963) 474.
- 6 P. L. Patterson, *J. Chromatogr.*, 134 (1977) 25-37.
- 7 M. Yamane, *J. Chromatogr.*, 9 (1962) 162.
- 8 D. MacNair, *Rev. Sci. Instrum.*, 38 (1967) 124.
- 9 C. Sherman, *Rev. Sci. Instrum.*, 45 (1974) 1165.
- 10 J. Loeb, *Basic Processes of Gaseous Electronics*, University of California Press, Berkeley, 1955.
- 11 J. J. Sullivan, *J. Chromatogr.*, 87 (1973) 9-16.
- 12 F. J. Davis, R. N. Compton and D. R. Nelson, *J. Chem. Phys.*, 59 (1973) 2324-2329.
- 13 L. G. Christophourou, *Atomic and Molecular Radiation Physics*, Wiley-Interscience, New York, 1971.
- 14 T. E. Bortner, G. S. Horst and W. G. Stone, *Rev. Sci. Instrum.*, 28 (1957) 103-108.

CHROM. 14,328

## ELECTROCHEMICAL CELL WITH EFFECTIVE VOLUME LESS THAN 1 nl FOR LIQUID CHROMATOGRAPHY

K. ŠLAIS and M. KREJČÍ\*

*Institute of Analytical Chemistry, Czechoslovak Academy of Sciences, 611 42 Brno (Czechoslovakia)*

(First received August 3rd, 1981; revised manuscript received September 4th, 1981)

### SUMMARY

The design and the application of an electrochemical detector with volume less than 1 nl is described. The detection limit is less than 0.1 pg. The application of the detector in combination with capillary columns in liquid chromatography yields good separation efficiencies within relatively short analysis times.

### INTRODUCTION

Recently it was derived theoretically<sup>1,2</sup> and verified experimentally<sup>3</sup> that the volume of the detection cell or the time constant of the detection restricts the use of capillary columns in liquid chromatography.

The volume of the detector cell,  $V_{\text{det}}$ , required should be less than half of the standard deviation,  $\sigma_V$  (ref. 1), of the peak of an unsorbed compound expressed in the terms of volumetric units

$$V_{\text{det}} \leq 1/2 \sigma_V = \pi d_c^2 L / 8 \sqrt{N} \quad (1)$$

where  $d_c$  is the column inner diameter,  $L$  is the column length and  $N$  is the number of theoretical plates. For mobile phase velocities higher than the velocity that would correspond to the minimal height equivalent to a theoretical plate,  $H$ ,  $N$  can be expressed as

$$N = \pi 24 D L / F_m \quad (2)$$

where  $D$  is the diffusion coefficient of the solute and  $F_m$  is the volumetric flow-rate of the mobile phase.

The demands imposed on the time constant of the detection,  $\tau_d$ , are also stringent. In order that the distortion of the signal is less than 5% it is necessary<sup>4</sup> that

$$\tau_d \leq 0.32 \sigma_t = 0.32 t_R / \sqrt{N} \quad (3)$$

where  $\sigma_t$  is the standard deviation of the peak of an unsorbed compound expressed in

terms of time units and  $t_R$  is the retention time of this peak. Strict technical requirements of the detection follow from eqns. 1–3. The advantages of capillary columns over packed columns can only be realized when the volume of the detector is less than 1 nl and the time constant of the detection is equal to a few tenths of a second.

Attempts at the miniaturization of the detection cell have been made for several years. So far the UV detector has been reduced to 50 nl<sup>5</sup> or to 100 nl<sup>6,7</sup>, the fluorometric detector to 53 nl<sup>8</sup> or 100 nl<sup>9</sup> and the electrochemical detector to 150 nl<sup>10</sup>. Very recently a UV detector with an effective volume of 6 nl<sup>11</sup> was reported, making it possible to measure concentrations of 1.5 ng/ $\mu$ l of benzene with a noise level of  $1.5 \cdot 10^{-5}$  a.u. These detectors permit operation without substantial distortion of the signal with capillary columns having inside diameters of 30–60  $\mu$ m<sup>5–9,11</sup>. The use of detectors based on the principle of flame ionization<sup>12</sup> permitted the application of columns with an inside diameter of 10  $\mu$ m<sup>3</sup>.

Liquid chromatography with electrochemical detection has become widespread<sup>13–15</sup>. The advantage of electrochemical detection is its sensitivity; thus, sensitivities higher than those of UV or fluorometric detection<sup>10</sup> can be obtained.

The present paper describes the design<sup>16</sup> and the application of an electrochemical cell with a volume of about 1 nl combined with capillary columns with inside diameters less than 20  $\mu$ m. The use of this combination permits analysis times comparable with those obtained in existing packed columns. At the same time the detection limit is less than 1 pg.

## EXPERIMENTAL

### *Electrochemical cell*

The construction of the electrochemical cell was based on “wall jet”<sup>17–19</sup> electrode, which was miniaturized so that very low flow-rates (*ca.* 1 nl/sec), usually used with capillary columns, could be applied. The design of the cell and its connection to a capillary column is shown in Fig. 1.

Into a stainless-steel capillary (0.8 mm O.D., 0.45 mm I.D.) was inserted a capillary of Simax glass (0.30 mm I.D.) into which a capillary of the same glass (0.25 mm O.D.) was freely inserted. A platinum wire (diameter 0.10 mm) was resin-bonded into the last capillary. The whole assembly was ground at one end perpendicularly to the axis of the capillary to form the auxiliary electrode, comprising a cross-section through the stainless-steel capillary, and the measuring electrode, comprising a cross-section through the platinum wire (Fig. 2). The annular space between the glass capillaries was filled with the mobile phase, thus providing a conducting bridge to a reference electrode. The other end of the capillary assembly was resin-bonded with the vessel for the reference electrode. A silver wire coated with silver chloride and immersed into a saturated solution of potassium chloride in water served as a reference electrode.

All of the measurements were carried out at a measuring electrode voltage of 0.8 V with respect to the reference electrode. The mobile phase enters the vessel with the reference electrode. Through this vessel the platinum wire of the measuring electrode, isolated from the surroundings by a glass capillary, also passed. The assembly was joined to the perpendicularly ground glass capillary column via a plastic tube with a suitable inside diameter such that the bearing surfaces were parallel and in close contact.

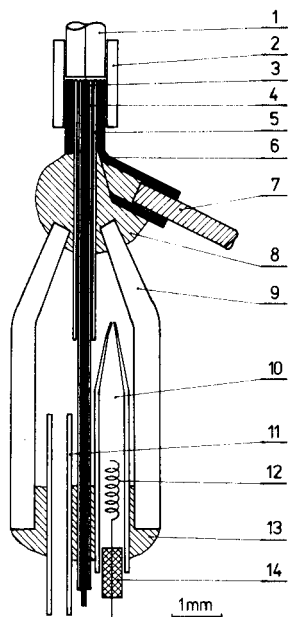


Fig. 1. The measuring electrode and its connection to the capillary column. 1 = Capillary column; 2 = PTFE tube; 3 = platinum wire (diameter 0.1 mm); 4, 5 = glass capillary; 6 = stainless-steel capillary; 7 = inlet wire for the auxiliary electrode; 8, 13 = epoxide resin; 9 = glass vessel for the reference electrode; 10 = reference electrode; 11 = output capillary; 12 = silver wire; 14 = rubber stopper.

As the surface area of the measuring electrode was less than  $0.01 \text{ mm}^2$  and the distance between the electrode and the exit of the capillary column was less than 0.1 mm, the volume of the space bounded by the capillary estuary and the reference electrode —“cell”— is less than 1 nl. The surface of the electrode can easily be cleaned by grinding the electrode assembly with a fine sharpening stone.

The electrochemical cell was connected to the electrical circuit as shown in Fig. 3. An alternative arrangement was also tested by omitting the reference electrode and connecting the corresponding amplifier into the circuit as a voltage follower. This variant gave no deterioration of the baseline or of the sensitivity.

#### *Sampling and the column*

A combination of a six-port valve and a splitter, Fig. 4, was used for the injection.

Glass capillary columns were drawn from glass tubes of suitable dimensions in the manner described earlier<sup>3,20</sup>. The previous work also describes the determination of the inside diameter of the columns prepared. A column coated with OV-101 silicone oil was used for reversed-phase chromatography. The procedure for stationary phase coating, and the properties of the columns prepared, will be described elsewhere<sup>21</sup>.

Distilled water, acidified with  $1 \cdot 10^{-3} \text{ M}$  perchloric acid, was used as a mobile phase for all of the measurements. This was pumped without any further treatment into the chromatograph with the aid of a high-pressure pump (Orlita, Giessen, G.F.R.) connected to a device for damping pressure pulses. A Kompensograph III

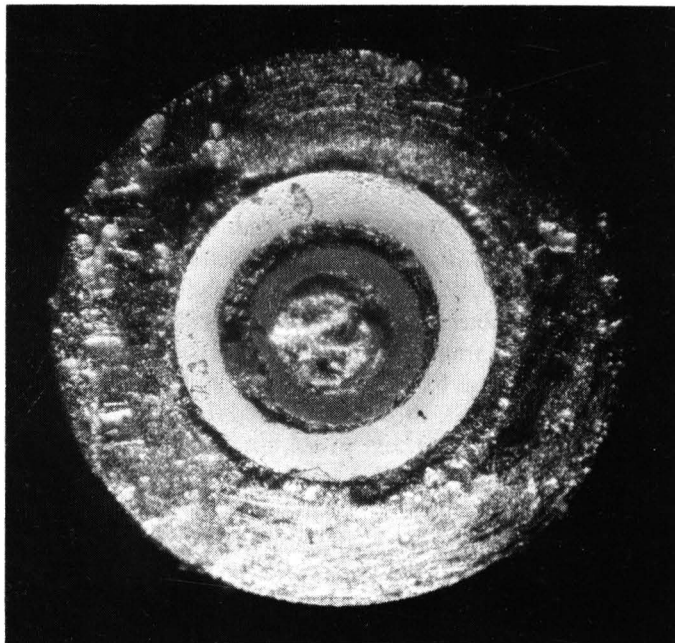


Fig. 2. Photograph of the measuring electrode.

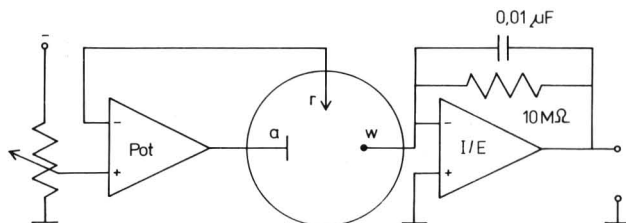


Fig. 3. Diagram of the electrical circuit used. The potentiostat (Pot) and current-to-voltage converter (I/E) are National Semiconductors JFET operational LF 356 N amplifiers. The time constant of the circuit is 0.1 sec. The auxiliary, working and reference electrodes are designated a, w and r, respectively.

recording millivoltmeter (Siemens, Karlsruhe, G.F.R.) with a time constant of 0.2 sec was used to record the chromatograms.

## RESULTS AND DISCUSSION

### *Character of the response*

A Sial glass capillary (1.2 m × 14.3 μm I.D.), corresponding to a column volume of 193 nl, was used to measure the character of the response. The solute was a solution of 10 mg/l hydroquinone in the mobile phase. The flow through the splitter was selected so that the volume sampled in the column from the sampling loop (volume 10 μl) was greater than the column volume. The splitting ratio was constant for all the mobile phase flow-rates.

The difference between the background current and the current corresponding

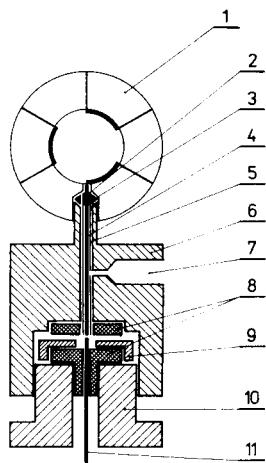


Fig. 4. Diagram of the six-port sampling valve and the splitter. 1 = Six-port valve; 2 = soldered; 3, 8 = PTFE sealing; 4 = stainless-steel capillary (0.2 mm I.D., 1.0 mm O.D.); 5 = stainless-steel tube (1.2 mm I.D., 2 mm O.D.); 6 = splitter body; 7 = splitter output; 9 = sealing holder; 10 = tightening screw; 11 = capillary column.

to the passage of the hydroquinone solution was then measured at various flow-rates of the mobile phase. Table I and Fig. 5 summarize the results obtained. It is obvious that for flow-rates greater than *ca.* 1 nl/sec the detector can be considered as a concentration detector, and is therefore suitable for the evaluation of chromatograms.

TABLE I

DEPENDENCE OF ELECTROCHEMICAL EFFICIENCY OF THE DETECTOR ON THE MOBILE PHASE FLOW-RATE

$t_R^0$ (sec)	$F_m$ (nl/sec)	Mass flow of hydroquinone (pg/sec)	Current for 100% coulometric yield (nA)	$I_d$ (nA)	Coulometric yield (%)
103	1.87	18.7	32.81	1.46	4.51
200	0.965	9.65	16.93	1.34	7.86
360	0.536	5.36	9.40	1.25	13.30
580	0.333	3.33	5.85	1.18	20.17
860	0.224	2.24	3.94	1.08	27.42
1300	0.148	1.48	2.59	0.78	30.16

The observed dependence does not correspond with the dependences of the diffusion current on the mobile phase flow-rate derived for wall-jet electrodes<sup>17,18</sup>:

$$I_d = f(F_m^{3/4}) \text{ or } I_d = f(F_m^{1/2})$$

These dependences were, however, derived for flow geometries rather different from that used in the present work.

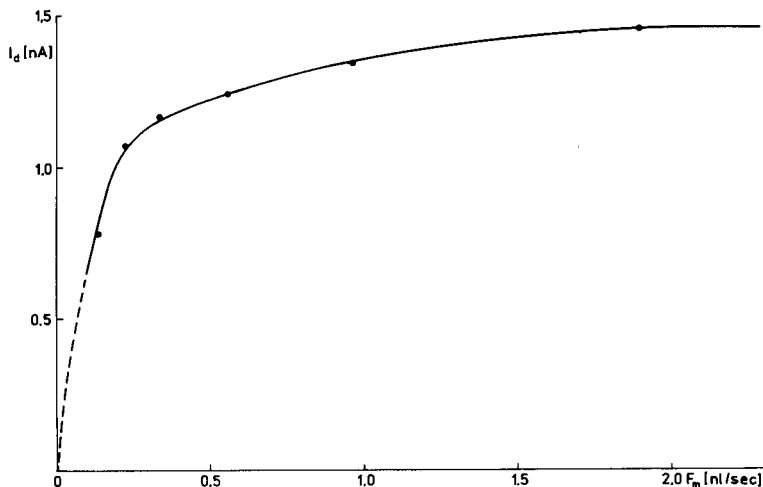


Fig. 5. Dependence of the response value of the amperometric detector,  $I_d$  on the mobile phase flow-rate,  $F_m$ . Solute: 10 mg hydroquinone per 1 l of the mobile phase.

The observed dependence has the exponential character of the relation derived for thin-layer electrode<sup>22</sup>

$$I_d = nFCF_m [1 - \exp(-Sh \cdot Dlb/2F_m d)] \quad (4)$$

where  $I_d$  is the diffusion current,  $Sh$  is Sherwood's number,  $l$ ,  $b$  and  $d$  are the length, width and height, respectively, of a thin-layer electrode,  $n$  is the number of electrons that participate in the electrode reaction,  $F$  is the Faraday constant and  $C$  is the solute concentration in the mobile phase. At high flow-rates, when the exponent  $(-Sh \cdot Dlb/2F_m d)$  is small in comparison with unity, the term in the square brackets can be approximated with a positive value of the exponent. Hence the diffusion current ceases to be a function of the flow-rate of the mobile phase and the detector response then has concentration character.

#### *Extra column peak broadening*

In order to estimate extra column peak broadening, the dependence of the height equivalent to a theoretical plate,  $H$ , on the linear velocity of the mobile phase was measured for the capillary used in the above measurement. The splitting ratio was adjusted to *ca.* 1:6000 and the injection was performed in such a manner that the sampling loop was inserted into the flow for only a fraction of a second. The dependence observed is shown in Fig. 6. It is obvious that for the range of mobile phase flow-rates studied, the value of  $H$  observed is approximately four times as high as would be predicted by theory. Hence, it follows that for the capillary used the broadening results chiefly from extra column contributions, *i.e.*, the extra column broadening,  $\sigma_{ex}^2 \approx 3\sigma_{col}^2$ . On the basis of eqns. 1 and 2, it can be calculated that, for the capillary used, the dependence of the broadening on the volumetric flow-rate of the mobile phase is expressed by the relationship

$$\sigma_{col}^2 = 0.412 \cdot F_m$$

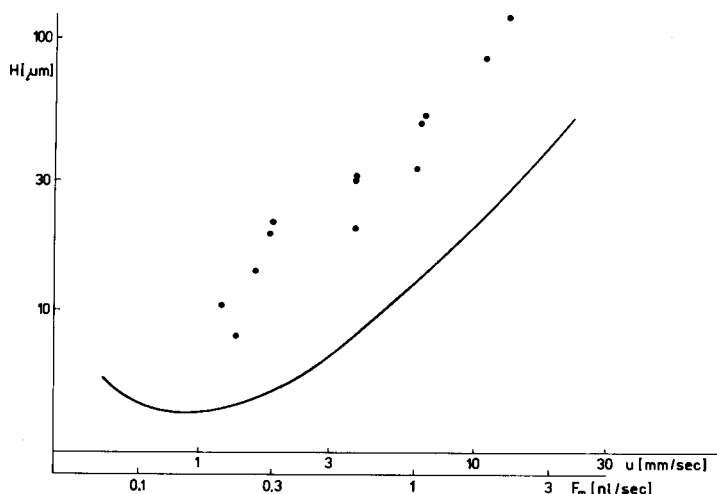


Fig. 6. Dependence of HETP on the linear velocity of the mobile phase. ●, Data measured experimentally with the use of the detector described; —, calculated dependence for a column of diameter  $14\ \mu\text{m}$  and diffusion coefficient  $D = 10^{-5}\ \text{cm}^2/\text{sec}$ .

where  $F_m$  is expressed in nl/sec and, as a result,  $\sigma_{\text{col}}^2$  is then obtained in  $\text{nl}^2$ . Hence the extra column broadening of the chromatographic system for the range of the mobile phase flow-rates used is as follows:

$$\sigma_{\text{ex}}^2 \approx 1.3 \cdot F_m$$

#### Detection limits

These were determined in the arrangement used above. An example of the chromatogram observed is shown in Fig. 7. Injection of the pure mobile phase does not provide any noticeable peak. From the measurements of the character of the detector response it can be calculated that the peak observed corresponds to 0.76 pg

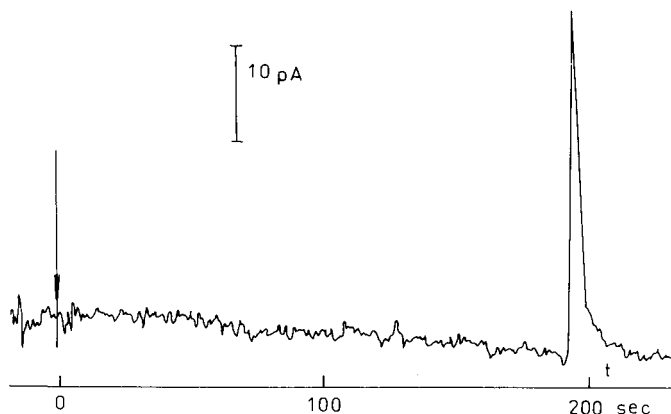


Fig. 7. An example of a chromatogram obtained with the capillary column ( $1.2\ \text{m} \times 14\ \mu\text{m}$  I.D.). Pressure: 1.0 MPa. The peak obtained corresponds to the injection of 0.76 pg hydroquinone.



of hydroquinone injected into the column. The noise observed is 1.5 pA peak-to-peak. Hence, the signal-to-noise ratio is equal to two and corresponds to the introduction of 0.05 pg hydroquinone into the column or to a concentration of 0.02 ppm at the peak maximum.

An example of the separation of phenols on the capillary column is shown in Fig. 8. The capillary column (2.8 m  $\times$  16  $\mu$ m I.D.) had a volume of 560 nl. On the basis of eqns. 1 and 2 it can be calculated for the elution of an unsorbed compound that the broadening is characterized by the relationship  $\sigma_{\text{col}}^2 = 1.5 \cdot F_m$ . Comparison of this result with the relationship characterizing extra column broadening indicates that for the elution of the unsorbed component the extra column broadening will lead to a *ca.* 85% increase in the value of  $H$ . At the linear velocity of the mobile phase used —7.2 mm/sec—  $H$  for the peak of the unsorbed compound was found to be 45  $\mu$ m, whereas the theory predicts 20  $\mu$ m. With respect to the extra column broadening estimated earlier,  $H$  should be 37  $\mu$ m. The discrepancy between this value and the value observed can be ascribed to indeterminacy of the value of the diffusion coefficient (estimated to be  $1 \cdot 10^{-5}$  cm<sup>2</sup>/sec) or to the error in the determination of the diameters of the capillary columns. Nevertheless, for sorbed compounds the extra column broadening is acceptably low for this type of separation, which makes it possible to take advantage of the separation capacity of the capillary column used.

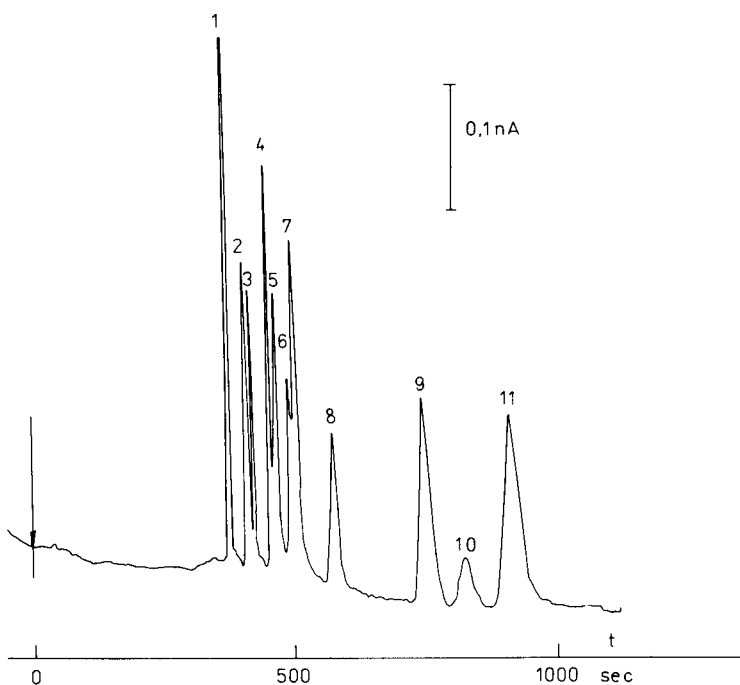


Fig. 8. Separation of phenols by capillary liquid chromatography. Peaks: 1 = hydroquinone ( $t_R$ ); 2 = 4-methylphenol; 3 = 2-methylphenol; 4 = 3,4-dimethylphenol; 5 = 3,5-dimethylphenol; 6 = 2,3-dimethylphenol; 7 = 2,4-dimethylphenol; 8 = 2,6-dimethylphenol; 9 = 2-methyl-4-ethylphenol; 10 = 2-isopropylphenol; 11 = 2,4,6-trimethylphenol. Mobile phase:  $10^{-3}$  M  $\text{HClO}_4$  in distilled water; flow-rate 1.7 nl/sec. Pressure: 2.5 MPa. Column: 2.8 m  $\times$  16  $\mu$ m I.D.; stationary phase OV-101. Flow through the splitter: 12  $\mu$ l/sec.

## CONCLUSIONS

A miniature amperometric detector has been designed which enables detection without substantial distortion of the effluent composition from capillary columns with diameters less than 20  $\mu\text{m}$  and with lengths less than 3 m. The electrochemical efficiency is comparable, at the mobile phase flow-rates used, with those of cells employed with packed columns. The small surface area of the measuring electrode results in a low noise (*ca.* <1.5 pA) with the minimal measuring space (volume less than 1 nl). These characteristics enable the detection of concentrations down to 0.02 ppm at the flow-rates employed which capillary columns.

The described combination of the capillary column with the amperometric detector makes it possible to achieve separations comparable with those obtained in high efficiency packed columns, in respect both of separation efficiency and speed of analysis, was demonstrated for the separation of eleven components within 15 min. The preparation of capillary columns with diameters less than 10  $\mu\text{m}$  will enable full use to be made of their advantages in liquid chromatography.

## REFERENCES

- 1 J. H. Knox and M. T. Gilbert, *J. Chromatogr.*, 186 (1979) 405.
- 2 J. H. Knox, *J. Chromatogr. Sci.*, 18 (1980) 453.
- 3 M. Krejčí, K. Tesařík, M. Rusek and J. Pajurek, *J. Chromatogr.*, 218 (1981) 167.
- 4 P. Kucera, *J. Chromatogr.*, 198 (1980) 93.
- 5 D. Ishii, T. Tsuda, K. Hibi, T. Takeuchi and T. Nakanishi, *J. High Resolut. Chromatogr. Chromatogr. Commun.*, 2 (1979) 371.
- 6 D. Ishii, K. Asai, K. Hibi, T. Jonokuchi and M. Nagaya, *J. Chromatogr.*, 144 (1977) 157.
- 7 T. Tsuda, K. Hibi, T. Nakanishi, T. Takeuchi and D. Ishii, *J. Chromatogr.*, 158 (1978) 227.
- 8 L. W. Hershberger, J. B. Callis and G. D. Christian, *Anal. Chem.*, 51 (1979) 1444.
- 9 Y. Hirata and M. Novotný, *J. Chromatogr.*, 186 (1979) 521.
- 10 Y. Hirata, P. T. Lin, M. Novotný and R. M. Wightman, *J. Chromatogr.*, 181 (1980) 287.
- 11 F. J. Yang, *J. High Resolut. Chromatogr. Chromatogr. Commun.*, 4 (1981) 83.
- 12 M. Krejčí, M. Rusek and K. Tesařík, *Collect. Czech. Chem. Commun.*, in press.
- 13 R. J. Rucki, *Talanta*, 27 (1980) 147.
- 14 E. Soczewinski, E. Zminkowska-Halliop and J. Matysik, *Wiad. Chem.*, 33 (1979) 775.
- 15 K. Štulík and V. Pacáková, *Chem. Listy*, 73 (1979) 795.
- 16 K. Šlais, *Czech. Pat. Appl.*, 5097-81, July 2, 1981.
- 17 J. Yamada and H. Matsuda, *J. Electroanal. Chem., Interfacial Electrochem.*, 44 (1973) 189.
- 18 H. Matsuda and J. Yamada, *J. Electroanal. Chem., Interfacial Electrochem.*, 30 (1971) 261.
- 19 B. Fleet and C. J. Little, *J. Chromatogr. Sci.*, 12 (1974) 747.
- 20 K. Tesařík and K. Šlais, *Technology of Preparation of Glass Capillary Columns with I.D. 2–30  $\mu\text{m}$* , Report VZ 68, Institute of Anal. Chemistry, Czech. Academy of Sciences, Brno, 1980.
- 21 M. Krejčí, K. Tesařík, K. Šlais and J. Pajurek, in preparation.
- 22 J. Lankelma and H. Poppe, *J. Chromatogr.*, 125 (1976) 375.

CHROM. 14,268

## INVESTIGATION OF N-ALKYLBENZAMIDES BY REVERSED-PHASE LIQUID CHROMATOGRAPHY

### I. ISOCRATIC ELUTION CHARACTERISTICS OF THE C<sub>1</sub>-C<sub>5</sub> N-ALKYLBENZAMIDES

MARTHA J. M. WELLS\* and C. RANDALL CLARK\*

*Division of Medicinal Chemistry, Department of Pharmacal Sciences, School of Pharmacy, Auburn University, Auburn University, AL 36849 (U.S.A.)*

(First received May 7th, 1981; revised manuscript received August 3rd, 1981)

---

#### SUMMARY

The reversed-phase liquid chromatographic retention of the C<sub>1</sub>-C<sub>5</sub> N-alkylbenzamides was investigated in aqueous-organic solvent mixtures. The log *k'* values for the amides were found to increase dramatically in mobile phases of low organic content. This non-linear relationship of log *k'* and mobile phase composition was observed on C<sub>18</sub> bonded-phase columns from different manufacturers. Attempts to measure retention data in pure water were successful only for the smaller molecules of the series. In general, the order of elution appears to parallel the carbon content of the N-alkyl group while increased branching decreases retention among isomeric amides.

---

#### INTRODUCTION

The effect of mobile phase composition on retention is the topic of a great deal of current research<sup>1-4</sup>. Most experimental results published to date show linear plots of the variation of log capacity factor (*k'*) with solvent composition in reversed-phase liquid chromatography. Using a C<sub>18</sub> column, Karger *et al.*<sup>1</sup> demonstrated a linear plot for log *k'* versus solvent composition over the entire range of a methanol-water system for *n*-hexanol and *n*-octanol. But comparable plots for the same solutes in acetonitrile-water mixtures deviated from linearity at high water and high acetonitrile mobile phase compositions. Snyder and co-workers<sup>2,3</sup> have proposed that eqn. 1 is valid over a wide range of *k'* and solvent compositions:

$$\log k' = \log k'_w - S\phi_B \quad (1)$$

---

\* Present address: USDA Forest Service, Southern Forest Experiment Station, George W. Andrews Forest Sciences Laboratory, Auburn University, AL 36849, U.S.A.

The relationship produces a linear plot where  $k'_w$  is the capacity factor for the solute in pure water under isocratic conditions,  $\varphi_B$  is the volume fraction of organic solvent B in the mobile phase, and  $S$  is related to the strength of pure organic solvent B. They imply that the curvature observed by Schoenmakers *et al.*<sup>4</sup> in similar plots might be due to experimental error.

In a recent study on the chromatographic behavior of selected barbiturates, alkaloids, and substituted alkyluracils on a  $C_{18}$  bonded-phase column in methanol-water mixtures, Jandera *et al.*<sup>5</sup> stated that the observed deviations from linearity could be tolerated for plots of  $\log k'$  vs. solvent composition. They calculated a capacity factor for solutes in pure water by fitting a straight line to the experimentally measured data points. Tanaka and Thornton<sup>6</sup> reported plots of  $\log k'$  vs. mole fraction of methanol-water solvent mixtures for a homologous series of straight chain aliphatic monocarboxylic acids on a  $C_{18}$  column. The plots demonstrated a slight curvature, with the curves appearing parallel over the range  $0.2 \leq k' \leq 25$ . Extrapolations to pure water were not attempted. Schoenmakers *et al.*<sup>4</sup> studied the retention of a variety of aromatic solutes in mixtures of methanol, ethanol, and *n*-propanol in water on a  $C_{18}$  column. Their work suggested that a quadratic rather than a linear function of the eluent composition was a better fit of  $\log k'$  vs. solvent composition plots

$$\ln k' = A\varphi^2 + B\varphi + C \quad (2)$$

where  $\varphi$  is the volume fraction of the less polar eluent. In this equation, the coefficient  $C$  represents the retention value for pure water ( $\varphi = 0$ ). Schoenmakers reports that upon recalculation of some literature data<sup>1,7,8</sup>, quadratic dependencies can be demonstrated that were not recognized by the authors. But even with a quadratic function, some discrepancies can be seen in Schoenmakers' results. For example, values for  $\ln k'$  of 8.55, 7.70, and 4.53 in pure water for diethyl *o*-phthalate are predicted from data measured in methanol-, ethanol-, and propanol-water mixtures, respectively.

The work described here reports the reversed-phase chromatographic properties of the  $C_1$ - $C_5$  *N*-alkylbenzamides and attempts to describe the effects of eluent composition on retention.

## EXPERIMENTAL

### *Apparatus*

The liquid chromatograph consisted of a Waters Model 6000A solvent pump, Model U6K injector, Model 440 ultraviolet (UV) absorbance detector, an Alltech Associates high-performance liquid chromatographic (HPLC) column water jacket, and a Hitachi recorder. UV absorbance spectra were determined on a Hitachi 60 or a Perkin-Elmer Model 200 spectrophotometer. Infrared (IR) spectra were determined using a Beckman Acculab 6. Refractive index (RI) measurements were determined on an Erma refractometer. Constant temperature in both the HPLC column water jacket and the refractometer was maintained by a Haake Model FE constant temperature circulator.

### *Reagents and chemicals*

All chemicals were of reagent grade quality or better and were used as purchased without further purification. Methylamine was obtained from Matheson, Coleman & Bell (Norwood, OH, U.S.A.), and 2-methylbutylamine from Pfaltz & Bauer (Stamford, CT, U.S.A.). Spectrophotometric grade methanol was obtained from Fisher Scientific (Fair Lawn, NJ, U.S.A.), spectrophotometric grade acetonitrile from Burdick & Jackson Labs. (Muskegon, MI, U.S.A.), and spectrophotometric grade carbon tetrachloride from J. T. Baker (Phillipsburg, NJ, U.S.A.). Sodium nitrate was obtained from Allied Chemicals (Morristown, NJ, U.S.A.). All other chemicals were purchased from Aldrich (Milwaukee, WI, U.S.A.). Doubly distilled water was further purified by pumping (Waters Model 6000 solvent pump) through a column (7 cm × 2.1 mm I.D.) dry packed with Whatman CO:PELL ODS (30–38  $\mu\text{m}$ ) prior to preparation of solvent mixtures.

### *Synthesis of amides*

A solution of the appropriate primary amine (0.03–0.07 mole) in 35 ml of tetrahydrofuran was mixed with 200 ml of a 20% (w/v) solution of potassium carbonate in a three-necked flask equipped with a magnetic stirrer, reflux condenser, addition funnel, and a heating mantle. A solution of benzoyl chloride (two-fold molar excess) in 35 ml of tetrahydrofuran was added dropwise. The resulting mixture was heated at 50°C for 3 h. The mixture was maintained at or above pH 8 during the reaction. The solution was cooled to room temperature and extracted with chloroform (3 × 100 ml). The extract was dried with magnesium sulfate and evaporated. The resulting residue was purified by recrystallization from light petroleum (b.p. 30–60°C)–benzene or by column chromatography on silica gel (40 mesh) using a light petroleum–diethyl ether step gradient.

### *Mobile phase characteristics*

The mobile phase solvent mixtures were prepared and allowed to equilibrate for at least 1 h before use. The specific gravity and refractive index were measured for each batch of HPLC solvent mixture (methanol–water or acetonitrile–water) as a means of quality control. The specific gravity of the mobile phase was determined by completely filling a 25-ml Kimax specific gravity bottle equipped with a thermometer, side arm and a side tube cap with vent. The bottle and contents were weighed ( $\pm 0.1$  mg) at 25°C. The refractometer was calibrated to a value of 1.3325 at 25°C using the purified water. Refractive index values of the mobile phase solutions were determined at 25°C.

### *Chromatographic procedures*

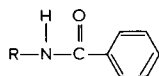
Two analytical HPLC columns were used in this study. A 25 cm × 4.60 mm I.D. Partisil ODS-2 (10  $\mu\text{m}$ ) column (1H3213) was purchased from Whatman (Clifton, NJ, U.S.A.), and a 15 cm × 4.60 mm I.D. Ultrasphere ODS (5  $\mu\text{m}$ ) column (UE795) was obtained from Altex Scientific (Berkeley, CA, U.S.A.). In operation, the columns were preceded by guard columns (7 cm × 2.1 mm I.D.) dry packed with Whatman CO:PELL ODS (30–38  $\mu\text{m}$ ). The guard column and analytical column were contained inside a column jacket and maintained at  $25.0 \pm 0.2^\circ\text{C}$  by circulating water from a constant temperature bath through the column jacket. The mobile

phase consisted of mixtures of water and methanol, or water and acetonitrile at a flow-rate of 1.5 ml/min. The column dead volume was taken as the elution volume for 0.5  $\mu$ l injection of an aqueous solution containing 0.3  $\mu$ g of sodium nitrate. The UV detector was operated at 254 nm and 0.005 a.u.f.s. Sufficiently dilute samples were prepared to give least detectable peaks (< 20% of scale). Capacity factors were calculated in the usual manner and based upon the average of at least two injections.

## RESULTS AND DISCUSSION

Reversed-phase liquid chromatography is a very effective tool for the separation of compounds differing only in the hydrocarbon portion of the molecule. In this report the isocratic elution characteristics of the C<sub>1</sub>–C<sub>5</sub> N-alkylbenzamides on C<sub>18</sub> bonded phases are evaluated. The amides were prepared from the appropriate primary amine and benzoyl chloride. The physical characteristics of these compounds are listed in Table I. The IR carbonyl absorption frequencies for the amides are very similar as are the values for the wavelength of maximum UV absorption indicating structural and electronic similarity in the "benzamide" portion of the molecules.

TABLE I  
PHYSICAL PROPERTIES OF BENZAMIDES



<i>R</i>		<i>m.p.</i> (°C)	$\lambda_{max}$ (nm)	Carbonyl stretch (cm <sup>-1</sup> )
Methyl	CH <sub>3</sub>	79– 82	225.5	1655
Ethyl	CH <sub>3</sub> CH <sub>2</sub>	68– 70	225.5	1652
<i>n</i> -Propyl	CH <sub>3</sub> CH <sub>2</sub> CH <sub>2</sub>	82– 84	225.5	1650
Isopropyl	(CH <sub>3</sub> ) <sub>2</sub> CH	98–103	225.2	1650
<i>n</i> -Butyl	CH <sub>3</sub> (CH <sub>2</sub> ) <sub>3</sub>	oil	225.5	1652
Isobutyl	(CH <sub>3</sub> ) <sub>2</sub> CHCH <sub>2</sub>	55– 58	225.2	1655
<i>sec.</i> -Butyl	CH <sub>3</sub> CH <sub>2</sub> CH(CH <sub>3</sub> )	68– 78	225.2	1648
<i>tert.</i> -Butyl	(CH <sub>3</sub> ) <sub>3</sub> C	132–135	224.5	1658
<i>n</i> -Pentyl	CH <sub>3</sub> (CH <sub>2</sub> ) <sub>4</sub>	31– 33	225.2	1650
<i>tert.</i> -Pentyl	CH <sub>3</sub> CH <sub>2</sub> C(CH <sub>3</sub> ) <sub>2</sub>	91– 93	224.0	1658
<i>sec.</i> -Pentyl	CH <sub>3</sub> CH <sub>2</sub> CH <sub>2</sub> CH(CH <sub>3</sub> )	73– 78	225.0	1650
Neopentyl	(CH <sub>3</sub> ) <sub>3</sub> CCH <sub>2</sub>	111–113	225.0	1658
Isopentyl	(CH <sub>3</sub> ) <sub>2</sub> CHCH <sub>2</sub> CH <sub>2</sub>	49– 53	225.5	1650
1-Ethylpropyl	(CH <sub>3</sub> CH <sub>2</sub> ) <sub>2</sub> CH	99–101	225.0	1652
1,2-Dimethylpropyl	(CH <sub>3</sub> ) <sub>2</sub> CHCH(CH <sub>3</sub> )	71– 75	225.0	1648
2-Methylbutyl	CH <sub>3</sub> CH <sub>2</sub> CH(CH <sub>3</sub> )CH <sub>2</sub>	oil	225.0	1655
Cyclopentyl	CH <sub>2</sub> CH <sub>2</sub> CH <sub>2</sub> CH <sub>2</sub> CH	157–160	226.0	1650

The logarithms of the experimentally measured values of the capacity factors ( $k'$ ) for the amides at various mobile phase compositions are plotted in Fig. 1–4. The figures present data from two different C<sub>18</sub> columns using acetonitrile–water and methanol–water eluents. Retention data were collected at a minimum of six different

compositions of water-organic mobile phase for each compound. Solvent compositions were chosen to give a wide range of  $k'$  values for each solute. A  $\log k'$  of 2.0 or greater was achieved for most solutes as the maximum degree of retention. The  $\log k'$  values achieved on the Ultrasphere column (15 cm) are, in general, smaller than those attained on the Partisil column (25 cm). Equivalent  $\log k'$  values from the two columns represent a substantially longer analysis time for the longer column. For example a  $\log k'$  of 2.0 on Partisil ODS-2 requires 2.13 h of analysis time and 1.46 h on Ultrasphere ODS. The void volume is smaller on the Ultrasphere column and the plate count is greater (25,700 plates per meter for Partisil ODS-2 and 48,600 plates per meter for Ultrasphere ODS based on measurements made in this lab when the columns were new).

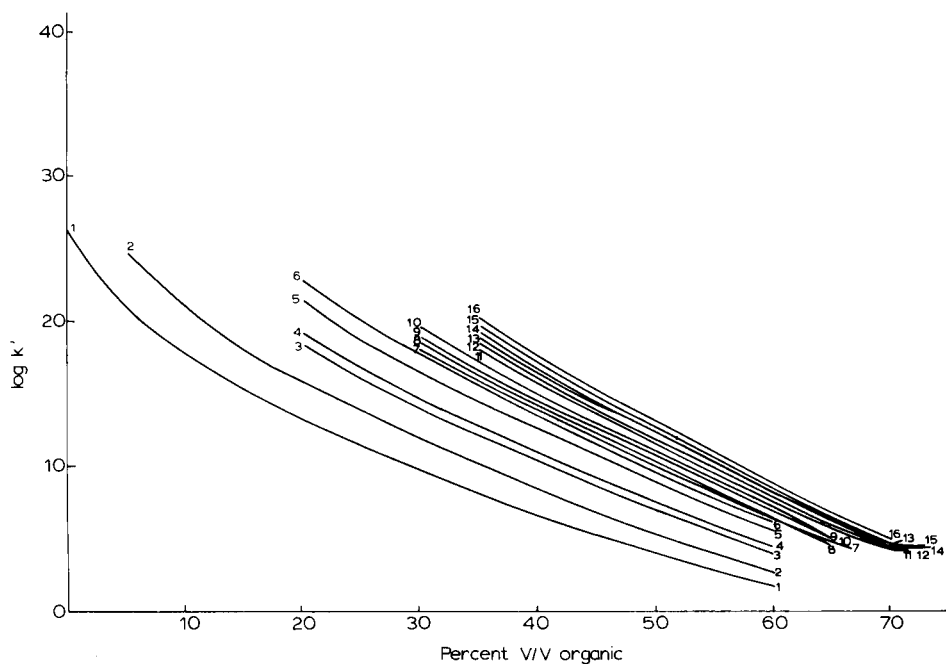


Fig. 1.  $\log k'$  versus solvent composition plots for N-alkylbenzamides on Partisil ODS-2 in methanol-water. Curves: 1, R = methyl; 2, R = ethyl; 3, R = isopropyl; 4, R = *n*-propyl; 5, R = *sec.*-butyl; 6, R = isobutyl; 7, R = *tert.*-butyl; 8, R = *n*-butyl; 9, R = 1-ethylpropyl; 10, R = 1,2-dimethylpropyl; 11, R = *sec.*-pentyl; 12, R = neopentyl; 13, R = *tert.*-pentyl; 14, R = 2-methylbutyl; 15, R = isopentyl; 16, R = *n*-pentyl. See general structure in Table I.

The effects of mobile phase composition on retention for the less retained members of the series are plotted in Figs. 5 and 6. Fig. 5 shows a plot of  $\log k'$  versus % (v/v) of the organic modifier for the compound N-methylbenzamide in acetonitrile and methanol-water solvent systems on the Partisil ODS-2 column. The open circles are for  $\log k'$  values which represent a  $k'$  less than 25. Plotting a straight line through the open circles in the form of eqn. 1 and extrapolation to a totally aqueous mobile phase, predicts the  $\log k'_w$  from acetonitrile-water data to be 1.605 ( $k'_w = 40.3$ ) with a correlation coefficient of  $-0.987$ . Similarly the  $\log k'_w$  is calculated to be 1.858 ( $k'_w =$

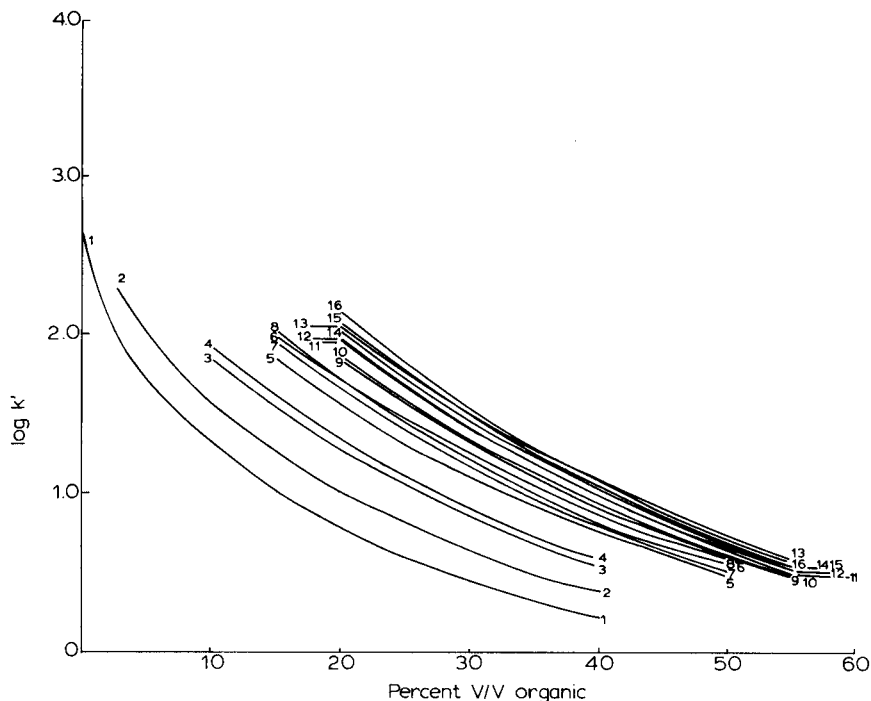


Fig. 2. Log  $k'$  versus solvent composition plots for N-alkylbenzamides on Partisil ODS-2 in acetonitrile-water. Curves: 1, R = methyl; 2, R = ethyl; 3, R = isopropyl; 4, R = *n*-propyl; 5, R = *sec*-butyl; 6, R = *tert*-butyl; 7, R = isobutyl; 8, R = *n*-butyl; 9, R = 1-ethylpropyl; 10, R = 1,2-dimethylpropyl; 11, R = neopentyl; 12, R = *sec*-pentyl; 13, R = *tert*-pentyl; 14, R = 2-methylbutyl; 15, R = isopentyl; 16, R = *n*-pentyl. See general structure in Table 1.

72.0) with a correlation coefficient of  $-0.996$  from methanol-water data. These lines should intersect at 0% organic modifier (100% water), yet the error between the calculated intercepts is very significant in terms of the capacity factor difference predicted in this example. The line was only extrapolated over a span of 10% in acetonitrile-water and 20% in methanol-water. Furthermore, the predicted values are vastly different from the actual measured value of  $\log k'_w = 2.608$  ( $k'_w = 405.5$ ). It was not possible to directly measure  $k'_w$  values for any of the higher homologs on this column since a  $\log k'$  of 2.608 represents an elution time of 8.6 h.

The shorter elution times obtained on the Ultrasphere ODS column permitted the evaluation of three of the amides in a pure water mobile phase. The curvilinear relationship of  $\log k'$  and solvent composition was also observed for N-methylbenzamide on this column (Fig. 6). Furthermore, the retention data for the N-ethyl- and -isopropylbenzamides produced similar results. Fig. 6 shows a plot of the experimentally determined data for the three earliest eluting amides. An extrapolated linear plot of  $k' < 25$  data predicts a  $\log k'_w$  of 1.542 ( $k'_w = 34.8$ ) from the methanol-water data points,  $r = -0.994$ , and 1.404 ( $k'_w = 25.4$ ),  $r = -0.982$ , from the acetonitrile-water data for N-methylbenzamide. The measured value of  $\log k'_w$  for this compound was 1.957 ( $k'_w = 90.6$ ). In this example the line was extrapolated over a range of 10% in methanol-water and only 5% in acetonitrile-water. The measured capacity factors



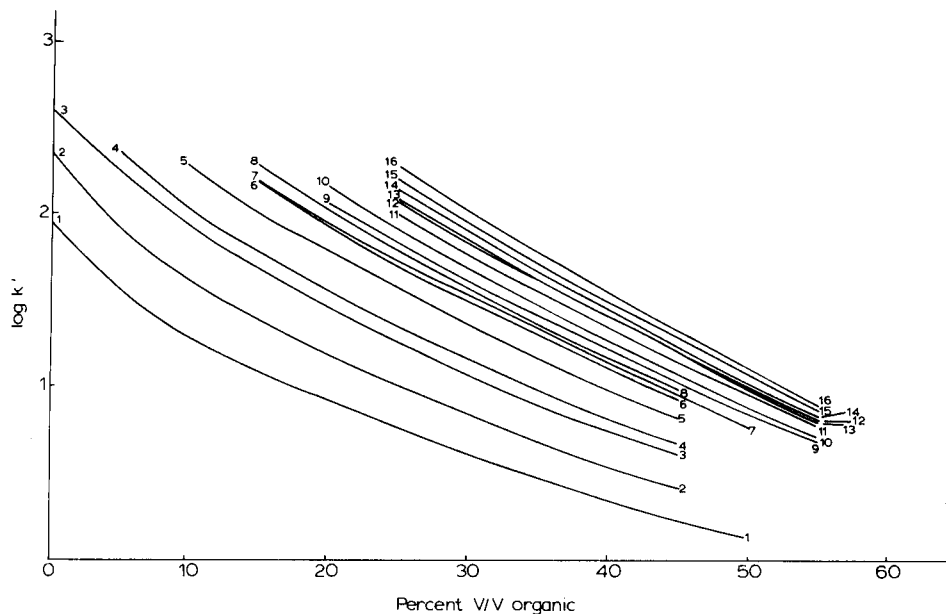


Fig. 3. Log  $k'$  versus solvent composition plots for N-alkylbenzamides on Ultrasphere ODS in methanol-water. Curves: 1, R = methyl; 2, R = ethyl; 3, R = isopropyl; 4, R = *n*-propyl; 5, R = *sec.*-butyl; 6, R = isobutyl; 7, R = *tert.*-butyl; 8, R = *n*-butyl; 9, R = 1-ethylpropyl; 10, R = 1,2-dimethylpropyl; 11, R = *sec.*-pentyl; 12, R = *tert.*-pentyl; 13, R = neopentyl; 14, R = 2-methylbutyl; 15, R = isopentyl; 16, R = *n*-pentyl. See general structure in Table I.

were observed to increase dramatically at low concentrations of organic modifier. This is particularly striking for N-methylbenzamide in acetonitrile-water (Table II). Linear extrapolation of the  $k' < 25$  data points for N-ethylbenzamide predicts a log  $k'_w$  of 1.862,  $r = -0.998$ , using the methanol-water data and 1.587,  $r = -0.987$  using the acetonitrile-water data. The measured data produced a log  $k'_w$  of 2.362 for N-ethylbenzamide. The same procedure predicted log  $k'_w = 2.092$ ,  $r = -0.998$  for N-isopropylbenzamide from the methanol-water data and 1.766,  $r = -0.993$ , from acetonitrile-water. Experimentally measured data gave a log  $k'_w$  of 2.601 for N-isopropylbenzamide.

Dolan *et al.*<sup>3</sup> outlined five points to consider when collecting data for the purpose of establishing the linearity or non-linearity of log  $k'$  vs. solvent composition plots. These are:

- (a) complete equilibration of column and mobile phase before collecting data
- (b) verification that  $k'$  is not a function of solute concentration, especially when  $k' < 5$
- (c) constancy of the temperature of the column and incoming mobile phase during collection of  $k'$  data
- (d) use of column packings that exhibit full coverage of the silica surface by the bonded phase
- (e) determination of the possible error in  $t_0$  and its effect on reported  $k'$  values

These are valid points and have been taken into consideration while measuring the data presented here. All measurements were made using very dilute solutions which

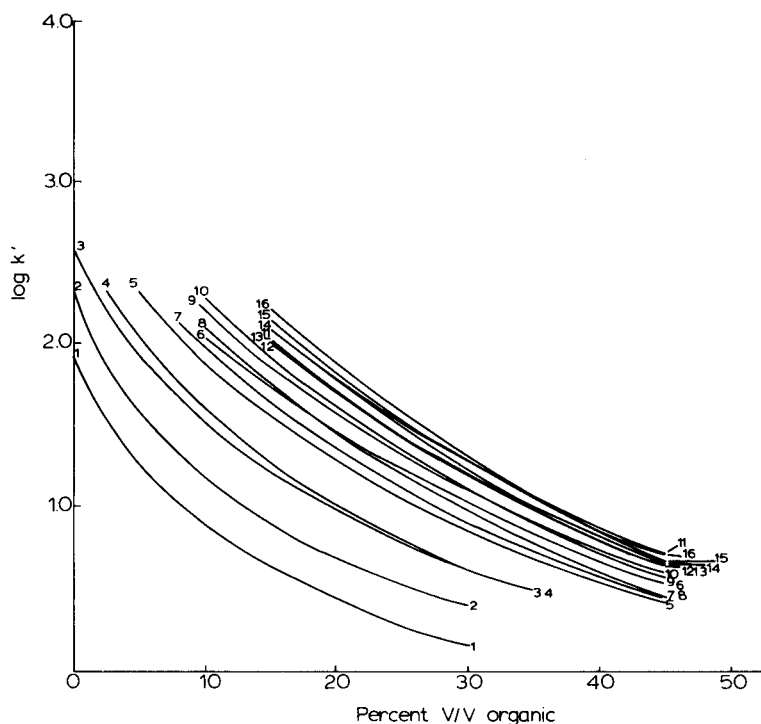


Fig. 4. Log  $k'$  versus solvent composition plots for N-alkylbenzamides on Ultrasphere ODS in acetonitrile-water. Curves: 1, R = methyl; 2, R = ethyl; 3, R = isopropyl; 4, R = *n*-propyl; 5, R = *sec.*-butyl; 6, R = *tert.*-butyl; 7, R = isobutyl; 8, R = *n*-butyl; 9, R = 1-ethylpropyl; 10, R = 1,2-dimethylpropyl; 11, R = *tert.*-pentyl; 12, R = *sec.*-pentyl; 13, R = neopentyl; 14, R = 2-methylbutyl; 15, R = isopentyl; 16, R = *n*-pentyl. See general structure in Table I.

gave peaks < 20% of full scale at 0.005 a.u.f.s. Because of the controversy surrounding the linearity vs. non-linearity of  $\log k'$  vs. organic modifier plots, the effect of concentration on the  $\log k'$  values measured at high concentrations of water in the mobile phase was investigated. On the Ultrasphere ODS column, the following percentage variations were found for N-methylbenzamide between the most dilute injection detectable and an injection representing 25 times that concentration: 0.9% variation at 10% methanol; 0.2% variation at 5% methanol; 0.1% variation at 2.5% acetonitrile; 2.2% variation at 0.5% acetonitrile (for 8.3 times the concentration); and 0.6% variation in pure water. If the values obtained at the higher concentration were plotted in Fig. 6 the difference made in the curve would hardly be noticeable. This information provides verification that the curvature observed in Fig. 5 and 6 does not result from concentration dependence. A measurement of the void volume was made for each chromatographic run using sodium nitrate without background electrolyte. This procedure actually determines the interstitial column volume<sup>9</sup> which is related to the true column void volume through a constant. Periodic measurements using sodium nitrate with background electrolyte (0.1 M phosphate buffer, pH 6.91) produced the true column void volume. The resulting void volume is higher than that measured without background electrolyte due to the electrochemical exclusion of

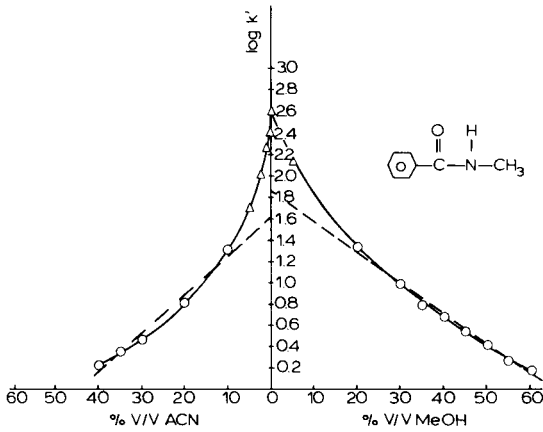


Fig. 5. Log  $k'$  versus solvent composition plots for N-methylbenzamide on Partisil ODS-2. ACN = Acetonitrile; MeOH = methanol.

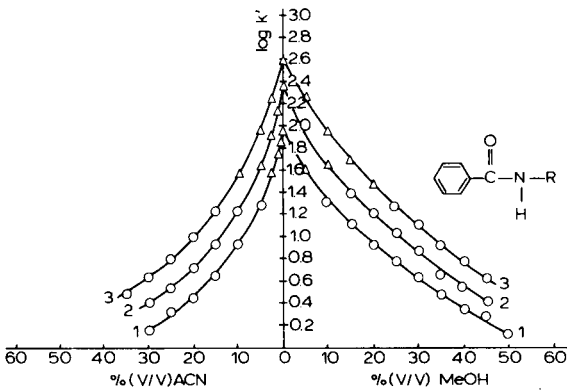


Fig. 6. Log  $k'$  versus solvent composition plots for N-alkylbenzamides on Ultrasphere ODS. Curves: 1, R = methyl; 2, R = ethyl; 3, R = isopropyl.

TABLE II

RETENTION DATA FOR N-METHYLBENZAMIDE IN LOW ACETONITRILE CONCENTRATIONS

Column	Acetonitrile (% v/v)	$k'$	$\log k'$	Retention time (h)
Partisil ODS-2	1.0	178.2	2.251	3.8
	0.5	251.2	2.400	5.3
	0.0	405.5	2.608	8.6
Ultrasphere ODS	1.0	55.1	1.741	0.8
	0.5	70.3	1.847	1.0
	0.0	90.6	1.957	1.3

sodium nitrate from the pore structure of the silica particle in the absence of background electrolyte<sup>10</sup>. Using either method for measuring the column void volume produces no more than a 3% variation in calculated  $k'$  values in the non-linear portion of the log  $k'$  vs. solvent composition plots and cannot account for the non-linearity of these plots. The similarities in the overall appearance of Figs. 5 and 6 is important to note. A linear model (eqn. 1) obviously does not suffice to explain the observed retention data, and efforts to improve this by using a quadratic model (eqn. 2) also proved futile.

The complete resolution of all sixteen benzamides studied was not obtained under isocratic conditions. The most efficient separation was obtained using the Ultrasphere ODS column with a methanol-water eluent (Fig. 7). Only peak 12 contained a mixture of two unresolved compounds, *N-tert.*-pentyl- and *N-neopentyl*benzamide. Solvent programming work was not attempted in this study. These results as well as Figs. 1-4 tend to point out relationships between structural features and elution order. In general, retention increases with the size of the *N*-alkyl group and chain branching reduces retention among isomers.

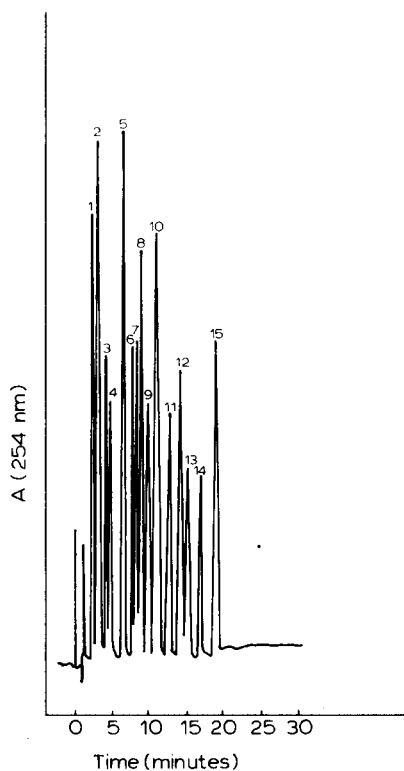


Fig. 7. Reversed-phase isocratic elution of the  $C_1$ - $C_5$  *N*-alkylbenzamides on Ultrasphere ODS in methanol-water (45:55). Peaks: 1, *R* = methyl; 2, *R* = ethyl; 3, *R* = isopropyl; 4, *R* = *n*-propyl; 5, *R* = *sec.*-butyl; 6, *R* = isobutyl; 7, *R* = *tert.*-butyl; 8, *R* = *n*-butyl; 9, *R* = 1-ethylpropyl; 10, *R* = 1,2-dimethylpropyl; 11, *R* = *sec.*-pentyl; 12, *R* = neopentyl and *R* = *tert.*-pentyl; 13, *R* = 2-methylbutyl; 14, *R* = isopentyl; 15, *R* = *n*-pentyl. See general structure in Table I.

## ACKNOWLEDGEMENT

We sincerely appreciate the support of the American Foundation for Pharmaceutical Education Silas M. Burroughs Memorial Fellowship for M.J.M.W.

## REFERENCES

- 1 B. L. Karger, J. R. Grant, A. Hartkopf and P. H. Weiner, *J. Chromatogr.*, 128 (1976) 65.
- 2 L. R. Snyder, J. W. Dolan and J. R. Gant, *J. Chromatogr.*, 165 (1979) 3.
- 3 J. W. Dolan, J. R. Gant and L. R. Snyder, *J. Chromatogr.*, 165 (1979) 31.
- 4 P. J. Schoenmakers, H. A. H. Billiet, R. Tijssen and L. de Galan, *J. Chromatogr.*, 149 (1978) 519.
- 5 P. Jandera, J. Churáček and L. Svoboda, *J. Chromatogr.*, 174 (1979) 35.
- 6 N. Tanaka and E. Thornton, *J. Amer. Chem. Soc.*, 99 (1977) 7300.
- 7 R. M. Carlson, R. E. Carlson and H. L. Kopperman, *J. Chromatogr.*, 107 (1975) 219.
- 8 G. Vigh and J. Inczédy, *J. Chromatogr.*, 129 (1976) 81.
- 9 M. J. M. Wells and C. R. Clark, *Anal. Chem.*, 53 (1981) 1341.
- 10 G. E. Berendsen, P. J. Schoenmakers, L. de Galan, G. Vigh, Z. Varga-Puchony and J. Inczédy, *J. Liquid Chromatogr.*, 3 (1980) 1669.

CHROM. 14,269

## INVESTIGATION OF N-ALKYLBENZAMIDES BY REVERSED-PHASE LIQUID CHROMATOGRAPHY

### II. APPLICATION OF THE SOLVOPHOBIC THEORY TO THE PREDICTION OF RETENTION DATA FOR THE C<sub>1</sub>-C<sub>5</sub> N-ALKYLBENZAMIDES

MARTHA J. M. WELLS\* and C. RANDALL CLARK\*

*Division of Medicinal Chemistry, Department of Pharmacal Sciences, School of Pharmacy, and Research Data Analysis, Auburn University, Auburn University, AL 36849 (U.S.A.)*

and

RICHARD M. PATTERSON

*Research Data Analysis, Auburn University, Auburn University, AL 36849 (U.S.A.)*

(Received May 7th, 1981)

---

#### SUMMARY

The relationship between capacity factor ( $k'$ ) and eluent composition for the C<sub>1</sub>-C<sub>5</sub> N-alkylbenzamides was not described adequately by either linear or quadratic equations. Using the chromatographic data determined in acetonitrile-water, the relationship between  $k'$  and eluent composition was described by the solvophobic theory. Regression coefficients obtained from the solvophobic equation were used to calculate the contact surface area of the solute-bonded ligand complex. The theory was used to calculate  $k'$  for each compound in a totally aqueous mobile phase. The results indicate that branched alkyl chains elute before their straight-chain analogues and among isomers the elution volume increases with the distance between the branching point and the amide nitrogen.

---

#### INTRODUCTION

The solvophobic theory, developed by Sinanoglu and Abdunur<sup>1</sup>, has been adapted for use in reversed-phase liquid chromatography (RPLC) by Horváth *et al.*<sup>2</sup>. According to this theory, the retention of a solute in RPLC is described by eqn. 1 when the mobile phase composition is varied while the temperature and flow-rate remain constant.

$$\ln k' = A + B\phi + C\gamma + D(\kappa^e - 1)V^{2/3}\gamma + E + \ln(RT/P_0V) \quad (1)$$

where

$$A = \phi - \frac{\Delta F_{\text{vdw, assoc}}}{RT} \quad (2)$$

\* Present address: USDA Forest Service, Southern Forest Experiment Station, George W. Andrews Forest Sciences Laboratory, Auburn University, AL 36849, U.S.A.

$$B = \frac{1}{RT} \frac{1 - \lambda \mu_s^2}{2\lambda v_s} NP \approx \frac{1}{4\pi\epsilon_0 RT} \frac{1 - \lambda \mu_s^2}{2\lambda v_s} \frac{N}{1 - (\alpha_s/v_s)} \quad (3)$$

with the approximation that  $\mathcal{D} \approx 1$

$$C = N\Delta A/RT \quad (4)$$

$$D = 4.836 N^{1/3}/RT \quad (5)$$

$$E = \Delta F_{\text{dw},s}/RT \quad (6)$$

See Appendix for a description of the variables and for a discussion of the derivation of this equation see ref. 2.

Eqn. 1 results from the hypothesis that the formation of a reversible solute-bonded ligand complex is governed by solvophobic effects, *i.e.* a hydrophobic effect when aqueous solvents are used. Studies concerning the nature of the hydrophobic effect have appeared in the literature since the early work of Traube<sup>3</sup> in 1891. According to Tanford<sup>4</sup>, a hydrophobic effect (hydrophobic effects, hydrophobic bonds, hydrophobic interactions are used synonymously in the literature) arises when any solute is dissolved in water. A hydrophobic bond has been defined<sup>5</sup> as one which forms when non-polar groups in an aqueous solvent associate, thereby decreasing the extent of interaction with surrounding water molecules, and liberating water originally bound by the solutes. In the past, the hydrophobic effect was believed to arise from the attraction of non-polar groups for each other<sup>6</sup>. While a like-attracts-like interaction certainly plays a role in this phenomenon, current opinion<sup>4</sup> views the strong forces between water molecules as primarily responsible for the hydrophobic effect. The detailed molecular structure of liquid water is complex and not well understood. Many of the unusual properties of water are the result of the isotropic network of hydrogen bonds linking individual molecules.

According to the solvophobic theory, interactions in RPLC between the hydrocarbonaceous ligand (bonded stationary phase) and non-polar solutes are not the result of attraction for each other. The formation of a solute-ligand complex reduces the total non-polar surface area and interaction with surrounding water molecules is thereby decreased. The hydrocarbonaceous stationary phase is therefore assumed to play a passive role toward solute retention. This is in contrast to the accepted view of bonded phases in gas chromatography in which the gaseous mobile phase is inactive, selectivity depending primarily upon the stationary phase<sup>7,8</sup>.

If the hydrophobic effect does indeed govern solute retention in RPLC, then the capacity factor may be viewed as a measure of relative hydrophobicity. The partition coefficient (usually expressed as  $\log P$ ) obtained from immiscible organic/water systems is probably the most commonly used index of hydrophobicity<sup>9</sup>. Various types of thin-layer chromatographic measurements have been made which use  $R_M$  as a measure of hydrophobicity<sup>5</sup>. The term  $R_M$  is the thermodynamic equivalent of the capacity factor ( $k'$ ). Both of these parameters have been correlated with biological activities and used to explain structure-activity relationships for improved drug design. The capacity factor determined in pure water ( $k'_w$ ) is the most desirable RPLC parameter for attempting to identify quantitative retention activity relationships (QRAR). The  $k'_w$  can only be obtained directly for a relatively small number of

solutes. Thus, some means of extrapolation of measurable  $k'$  data for a solute to the theoretical value in a mobile phase of water is necessary.

Recently, we described<sup>10</sup> the RPLC properties of the C<sub>1</sub>–C<sub>5</sub> N-alkylbenzamides. The  $k'$  values for these solutes were observed to vary in a curvilinear fashion with mobile phase composition and increase rapidly at low organic modifier concentration. Treatment of the water–organic  $k'$  data as a linear or quadratic relationship did not adequately predict  $k'_w$  values. This report describes the use of the solvophobic theory in an attempt to predict  $k'_w$  values.

## EXPERIMENTAL

The chromatographic data used in this study has been previously described<sup>10</sup>. Nuclear magnetic resonance (NMR) studies were performed on a Varian T-60A spectrometer with sample solutions prepared in carbon tetrachloride and tetramethylsilane as the internal standard. Multiple linear regression analyses and calculation of total molecular surface area were performed on an IBM 370/158, Computer Services, Auburn University. The programs used to calculate molecular surface area were obtained from G. L. Amidon, University of Wisconsin, Madison, WI, U.S.A.

## RESULTS AND DISCUSSION

### *Prediction of log $k'_w$ using the solvophobic theory*

Rearranging the terms in eqn. 1 produces the relationship in eqn. 7:

$$\ln k' - D(\kappa^e - 1)V^{2/3}\gamma - \ln(RT/P_0V) = (A + E) + B\mathcal{D} + C\gamma \quad (7)$$

The regression coefficients  $A$  and  $E$  were determined as the sum  $(A + E)$ . Coefficients  $A$ ,  $B$  and  $E$  are unitless and the units of  $C$  are  $\text{cm}^2 \text{l}^{-1}$ . The value of the regression coefficient  $D$  was calculated to be  $1.6693 \times 10^7 \text{ mole}^{2/3} \text{l}^{-1} \text{ atm}^{-1}$ . Data on density<sup>11,12</sup>, dielectric constant<sup>13,14</sup>, surface tension<sup>2</sup> and  $\kappa^e$  (ref. 2) for solvent mixtures were compiled from the literature and converted to % (v/v) of the organic modifier. Using these data, all terms except  $(A + E)$ ,  $B$  and  $C$  were calculated for each given solvent concentration at which a capacity factor was measured. This treatment leads to a series of  $n$  equations ( $n$  equals the number of experimentally determined data points) of the form in eqn. 8:

$$X = (A + E) + B\mathcal{D} + C\gamma \quad (8)$$

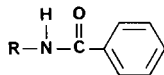
The regression coefficients of eqn. 8 were evaluated by means of the Statistical Analysis System procedure SYSREG (SAS Institute, Raleigh, NC, U.S.A.).

The calculated regression coefficients for the acetonitrile–water solvent system on the Partisil ODS-2 column are given in Table I while those for the Ultrasphere ODS column are presented in Table II. Thus far a description of the results obtained in methanol–water mixtures on either column by the application of the solvophobic theory has not been possible. The failure to predict reasonable solvophobic parameters in the aqueous methanol system may or may not be a failure of the model (eqn. 1) to account satisfactorily for all factors involved. Results of Melander *et al.*<sup>15</sup> demon-



TABLE I

SOLVOPHOBIC PARAMETERS OF SOME N-ALKYLBENZAMIDES ON PARTISIL ODS-2 IN ACETONITRILE-WATER



<i>R</i>	<i>B</i>	<i>C</i>	( <i>A</i> + <i>E</i> )	<i>r</i>
CH <sub>3</sub>	-327.77	206612152	303.394	0.9995
CH <sub>3</sub> CH <sub>2</sub>	-298.51	216131391	274.876	0.9994
CH <sub>3</sub> CH <sub>2</sub> CH <sub>2</sub>	-275.15	227673700	252.214	0.9999
(CH <sub>3</sub> ) <sub>2</sub> CH	-268.04	219825857	245.461	0.9999
CH <sub>3</sub> CH <sub>2</sub> CH(CH <sub>3</sub> )	-168.94	217293234	149.192	0.9990
(CH <sub>3</sub> ) <sub>2</sub> CHCH <sub>2</sub>	-154.07	222333721	134.589	0.9989
CH <sub>3</sub> (CH <sub>2</sub> ) <sub>3</sub>	-148.98	228127478	129.546	0.9992
(CH <sub>3</sub> ) <sub>3</sub> C	-146.49	214732624	127.651	0.9987
(CH <sub>3</sub> CH <sub>2</sub> ) <sub>2</sub> CH	-122.81	224850132	104.320	0.9961
(CH <sub>3</sub> ) <sub>2</sub> CHCH(CH <sub>3</sub> )	-111.86	225837894	93.644	0.9951
CH <sub>3</sub> CH <sub>2</sub> CH <sub>2</sub> CH(CH <sub>3</sub> )	-106.92	236073206	88.619	0.9968
CH <sub>3</sub> CH <sub>2</sub> CH(CH <sub>3</sub> )CH <sub>2</sub>	-105.66	243229778	87.232	0.9966
CH <sub>3</sub> CH <sub>2</sub> C(CH <sub>3</sub> ) <sub>2</sub>	-103.71	232045062	85.796	0.9964
(CH <sub>3</sub> ) <sub>3</sub> CCH <sub>2</sub>	-99.66	230498308	81.693	0.9956
(CH <sub>3</sub> ) <sub>2</sub> CHCH <sub>2</sub> CH <sub>2</sub>	-95.04	246301501	76.824	0.9971
CH <sub>3</sub> (CH <sub>2</sub> ) <sub>4</sub>	-85.07	250238960	67.069	0.9970
CH <sub>2</sub> CH <sub>2</sub> CH <sub>2</sub> CH <sub>2</sub> CH	-138.38	223124385	119.459	0.9953

TABLE II

SOLVOPHOBIC PARAMETERS OF SOME N-ALKYLBENZAMIDES ON ULTRASPHERE ODS IN ACETONITRILE-WATER

For general structure, see Table I.

<i>R</i>	<i>B</i>	<i>C</i>	( <i>A</i> + <i>E</i> )	<i>r</i>
CH <sub>3</sub>	-120.79	175914241	101.202	0.9992
CH <sub>3</sub> CH <sub>2</sub>	-135.46	186749400	115.728	0.9992
CH <sub>3</sub> CH <sub>2</sub> CH <sub>2</sub>	-194.62	206243456	173.633	0.9990
(CH <sub>3</sub> ) <sub>2</sub> CH	-222.02	201887060	200.541	0.9989
CH <sub>3</sub> CH <sub>2</sub> CH(CH <sub>3</sub> )	-247.25	220431346	225.178	0.9988
(CH <sub>3</sub> ) <sub>2</sub> CHCH <sub>2</sub>	-236.26	225520204	214.379	0.9974
CH <sub>3</sub> (CH <sub>2</sub> ) <sub>3</sub>	-203.53	227101260	182.433	0.9986
(CH <sub>3</sub> ) <sub>3</sub> C	-204.46	211786479	184.006	0.9983
(CH <sub>3</sub> CH <sub>2</sub> ) <sub>2</sub> CH	-162.51	218348621	142.932	0.9986
(CH <sub>3</sub> ) <sub>2</sub> CHCH(CH <sub>3</sub> )	-183.22	228066562	162.902	0.9983
CH <sub>3</sub> CH <sub>2</sub> CH <sub>2</sub> CH(CH <sub>3</sub> )	-142.03	226022173	122.859	0.9972
CH <sub>3</sub> CH <sub>2</sub> CH(CH <sub>3</sub> )CH <sub>2</sub>	-134.39	231268022	115.285	0.9972
CH <sub>3</sub> CH <sub>2</sub> C(CH <sub>3</sub> ) <sub>2</sub>	-130.83	218075199	112.398	0.9973
(CH <sub>3</sub> ) <sub>3</sub> CCH <sub>2</sub>	-159.92	231615578	140.145	0.9968
(CH <sub>3</sub> ) <sub>2</sub> CHCH <sub>2</sub> CH <sub>2</sub>	-120.68	234950318	101.832	0.9979
CH <sub>3</sub> (CH <sub>2</sub> ) <sub>4</sub>	-117.44	238603744	98.653	0.9976
CH <sub>2</sub> CH <sub>2</sub> CH <sub>2</sub> CH <sub>2</sub> CH	-202.09	224457477	181.194	0.9984

strated no difference in the mechanism of solute–ligand interaction in RPLC whether acetonitrile or methanol was used as the organic modifier. The failure thus far to mathematically describe the aqueous methanol data is being actively pursued.

The regression coefficients obtained from the acetonitrile–water data in Tables I and II were combined with the known solvent properties of an organic–water solvent system to estimate the value of  $X$  (from eqn. 8), and from  $X$  the values of the capacity factors of these solutes were determined at the desired solvent composition, including a totally aqueous mobile phase. Of the compounds investigated, the only capacity factors actually determined experimentally in pure water were 2.608 ( $\log k'_w$ ) for N-methylbenzamide on Partisil ODS-2 and 1.957 for N-methylbenzamide, 2.362

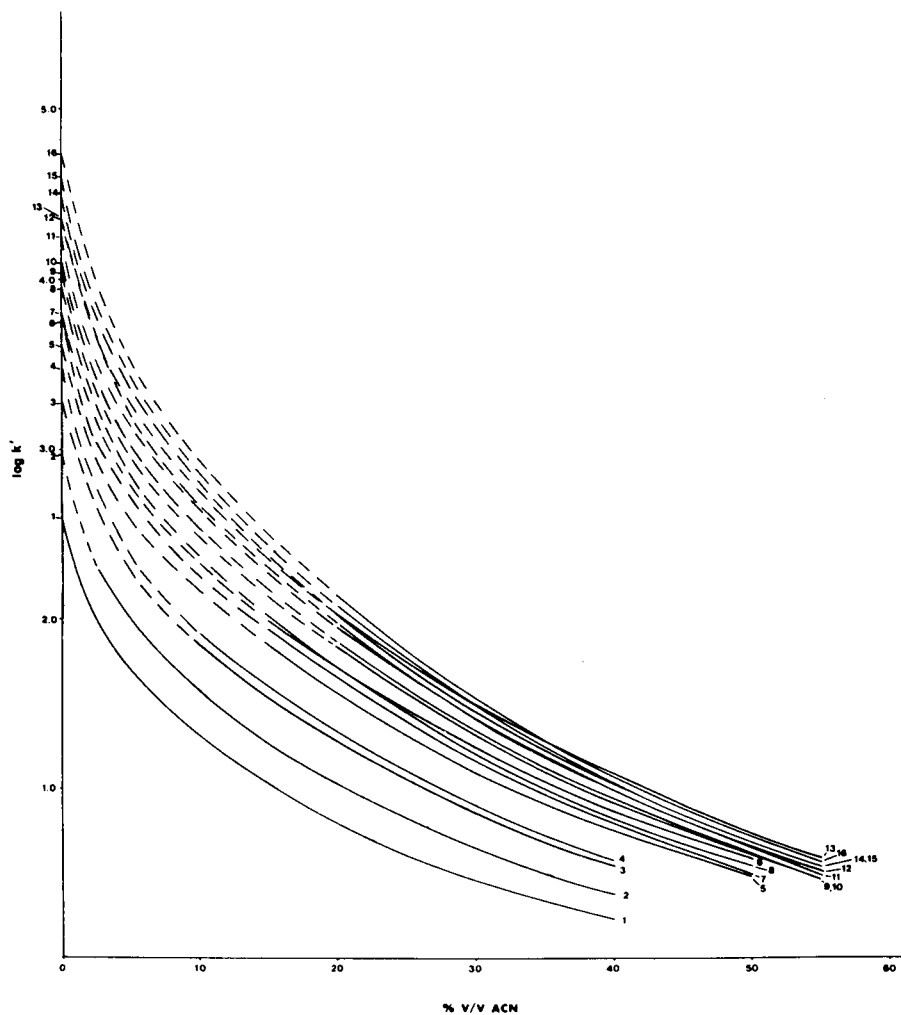


Fig. 1. Eluent composition (ACN = acetonitrile) versus  $\log k'$  plots for N-alkylbenzamides on Partisil ODS-2. Curves: 1, R = methyl; 2, R = ethyl; 3, R = isopropyl; 4, R = *n*-propyl; 5, R = *sec.*-butyl; 6, R = *tert.*-butyl; 7, R = isobutyl; 8, R = *n*-butyl; 9, R = 1-ethylpropyl; 10, R = 1,2-dimethylpropyl; 11, R = neopentyl; 12, R = *sec.*-pentyl; 13, R = *tert.*-pentyl; 14, R = 2-methylbutyl; 15, R = isopentyl; 16, R = *n*-pentyl. See general structure in Table I.

for N-ethylbenzamide, and 2.601 for N-isopropylbenzamide, on Ultrasphere ODS. The experimentally measured  $k'_w$  values were omitted from the regression analyses in order to test the ability to predict these values. The measured and calculated  $\log k'$  data are plotted as a function of mobile phase composition in Figs. 1 and 2. The  $\log k'$  data was calculated for each solute in 5% mobile phase composition increments from the last measured data point to 0% organic. At very low organic compositions a  $\log k'$  was calculated at each 2.5% change in solvent composition. The plots resulting from the calculated data show the same dramatic increase in slope at low organic mobile phase composition that was observed in the measured data<sup>10</sup>. Due to the complexity of the graphs, the data points have been omitted. In these figures the curves seem to vary in a regular fashion, except for the *tert.*-butyl and *tert.*-pentyl isomers.

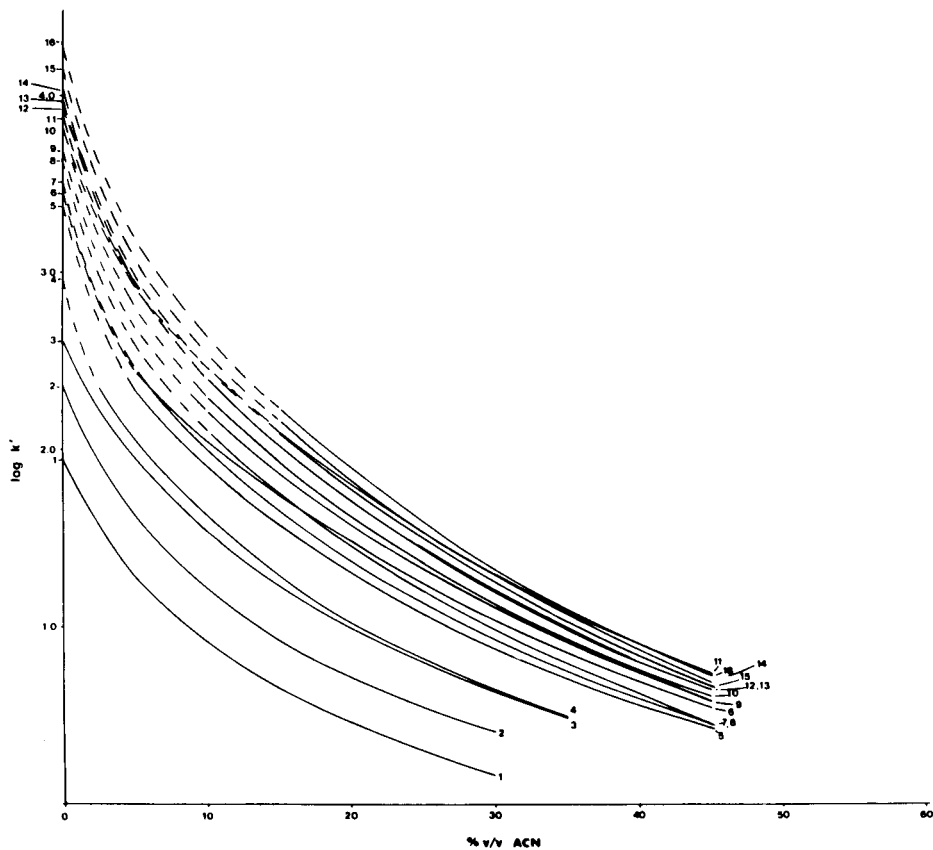


Fig. 2. Eluent composition versus  $\log k'$  plots for N-alkylbenzamides on Ultrasphere ODS. Curves: 1, R = methyl; 2, R = ethyl; 3, R = isopropyl; 4, R = propyl; 5, R = *sec.*-butyl; 6, R = *tert.*-butyl; 7, R = isobutyl; 8, R = *n*-butyl; 9, R = 1-ethylpropyl; 10, R = 1,2-dimethylpropyl; 11, R = *tert.*-pentyl; 12, R = *sec.*-pentyl; 13, R = neopentyl; 14, R = 2-methylbutyl; 15, R = isopentyl; 16, R = *n*-pentyl. See general structure in Table I.

The  $\log k'$  values predicted for 0% acetonitrile on both the Partisil ODS-2 and Ultrasphere ODS columns are listed in Table III. The order predicted for each column is nearly the same, differing only in exceptions denoted by an asterisk. In Fig.

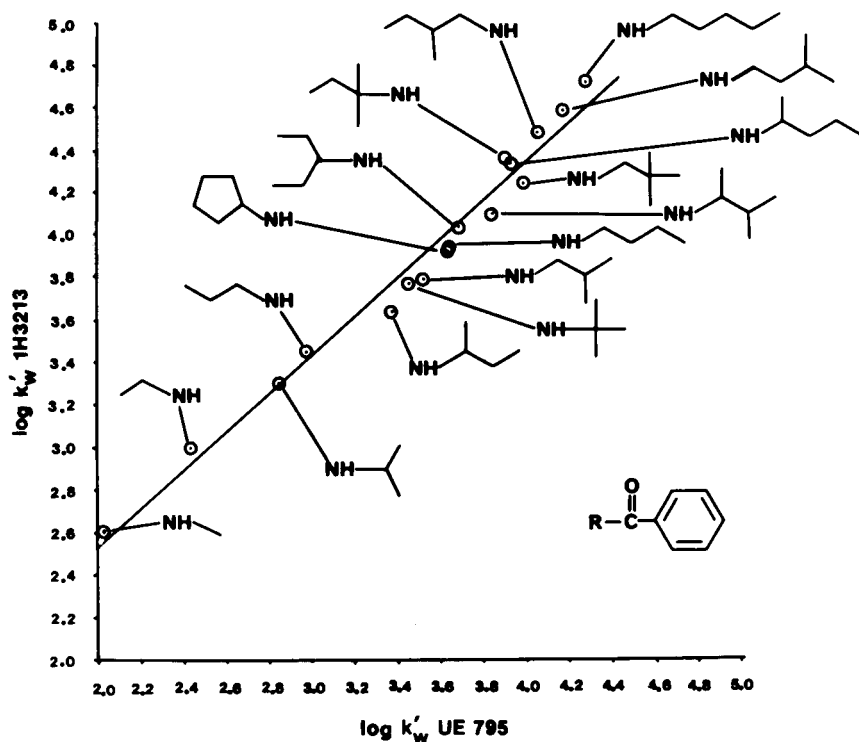
TABLE III

CALCULATED CAPACITY FACTORS AT 0% ACETONITRILE

For general structure, see Table I.

R	$\log k'_w$ (0% acetonitrile)	
	Partisil ODS-2	Ultrasphere ODS (UE795)
CH <sub>3</sub>	2.612	2.034
CH <sub>3</sub> CH <sub>2</sub>	2.987	2.427
(CH <sub>3</sub> ) <sub>2</sub> CH	3.305	2.850
CH <sub>3</sub> CH <sub>2</sub> CH <sub>2</sub>	3.452	2.972
CH <sub>3</sub> CH <sub>2</sub> CH(CH <sub>3</sub> )	3.638	3.373
(CH <sub>3</sub> ) <sub>3</sub> C	3.768	3.456
(CH <sub>3</sub> ) <sub>2</sub> CHCH <sub>2</sub>	3.786	3.522
CH <sub>3</sub> (CH <sub>2</sub> ) <sub>3</sub>	3.946	3.642
(CH <sub>3</sub> CH <sub>2</sub> ) <sub>2</sub> CH	4.039	3.692
(CH <sub>3</sub> ) <sub>2</sub> CHCH(CH <sub>3</sub> )	4.098	3.842
(CH <sub>3</sub> ) <sub>3</sub> CCH <sub>2</sub> *	4.248	3.995
CH <sub>3</sub> CH <sub>2</sub> CH <sub>2</sub> CH(CH <sub>3</sub> )*	4.337	3.937
CH <sub>3</sub> CH <sub>2</sub> C(CH <sub>3</sub> ) <sub>2</sub> *	4.353	3.920
CH <sub>3</sub> CH <sub>2</sub> CH(CH <sub>3</sub> )CH <sub>2</sub>	4.490	4.065
(CH <sub>3</sub> ) <sub>2</sub> CHCH <sub>2</sub> CH <sub>2</sub>	4.589	4.177
CH <sub>3</sub> (CH <sub>2</sub> ) <sub>4</sub>	4.722	4.289
CH <sub>2</sub> CH <sub>2</sub> CH <sub>2</sub> CH <sub>2</sub> CH	3.926	3.635

\* The predicted elution orders are the same on each column except for the compounds noted.

Fig. 3.  $\log k'_w$  versus  $\log k'_w$  plot for the C<sub>1</sub>-C<sub>5</sub> N-alkylbenzamides as measured on Partisil ODS-2 (IH3213) and Ultrasphere ODS (UE795) at 25 °C.

3, the  $\log k'_w$  values from the Partisil ODS-2 column are plotted against those obtained from the Ultrasphere ODS column, and the observed relationship is described by eqn. 9:

$$\begin{aligned} (\log k'_w \text{ Partisil ODS-2}) &= 0.906 (\log k'_w \text{ Ultrasphere ODS}) + 0.711 \\ r &= 0.988 \end{aligned} \quad (9)$$

There are some interesting patterns evident in the elution orders predicted for 0% acetonitrile. Branched compounds elute before their straight chain analogs, even though this is not always the case at higher concentrations of acetonitrile in the mobile phase. For those benzamides containing one single carbon branch, the compounds elute in the order of *sec.*-butyl < *isobutyl* and *sec.*-pentyl < 2-methylbutyl < *isopentyl*. In each instance, the compound having the branch on the carbon adjacent to the amide group is predicted to elute first, followed successively by compounds having the branch on the next carbon atom down the chain.

#### Analysis of solvophobic regression coefficients

The data reported in Tables I and II compare the values of  $B$  and  $(A + E)$  derived from the Partisil ODS-2 and Ultrasphere ODS columns, respectively. The benzamides in Table I are arranged in order of increasing values for the coefficient  $B$ , which correspond to decreasing values of  $(A + E)$ . The benzamides in Table II are arranged in the same order as those in Table I but the ordering of the values of  $B$  and

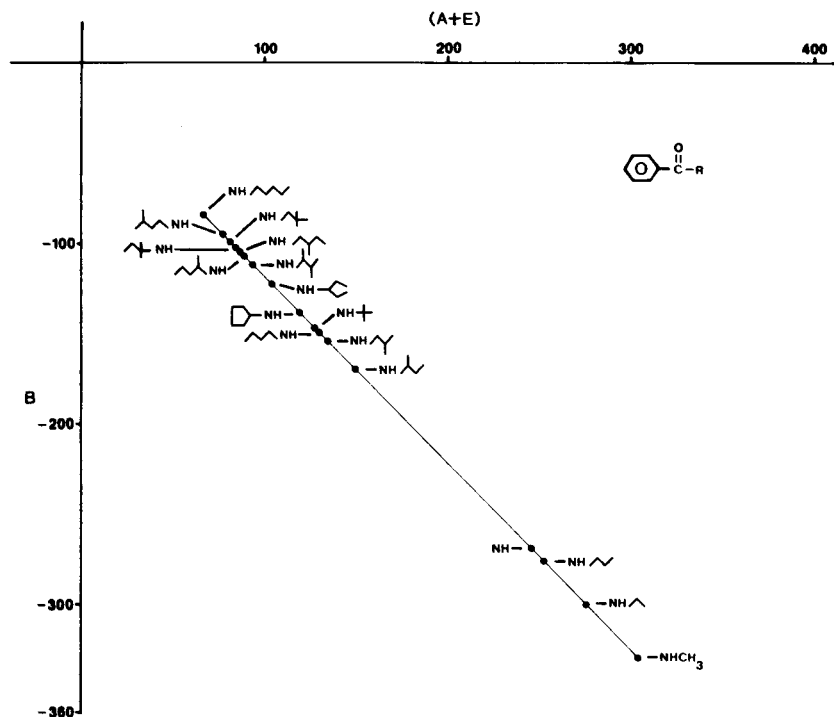


Fig. 4. Plot of the solvophobic parameters  $B$  versus  $(A + E)$  as derived from data obtained using Partisil ODS-2.

( $A + E$ ) are different. The regression coefficients  $A$ ,  $B$  and  $E$  were defined in eqns. 2, 3 and 6, respectively. The correlation between coefficients  $B$  and ( $A + E$ ) derived from the Partisil ODS-2 data is described by eqn. 10 and plotted in Fig. 4.

$$B = -1.028 (A + E) - 15.714 \quad r = -0.999 \quad (10)$$

For these compounds,  $B$  becomes less negative, and ( $A + E$ ) less positive from N-methylbenzamide to N-*n*-pentylbenzamide. Fig. 5 is a plot of  $B$  versus ( $A + E$ ) calculated from the data obtained on the Ultrasphere ODS column, and is described by eqn. 11:

$$B = -1.025 (A + E) - 16.270 \quad r = -0.999 \quad (11)$$

The similarity between eqns. 10 and 11 is remarkable, yet within each plot (Figs. 4 and 5) the individual compounds are not arranged in the same order. In Fig. 5, the methyl, ethyl, propyl and isopropyl derivatives appear in reverse order to that in Fig. 4. Other order changes among individual isomers can be noted. The coefficient  $B$  involves several solute properties which are all independent of the chromatographic system with the exception of  $\lambda$ . The  $\lambda$  term is the molecular volume of the solute-bonded ligand complex and is assumed to be a multiple of the molecular volume of the solute. This parameter varies from column to column with configurational differences in the bonded stationary phase. The coefficient  $A$  involves  $\varphi$  and  $\Delta F_{\text{vdw, assoc}}$

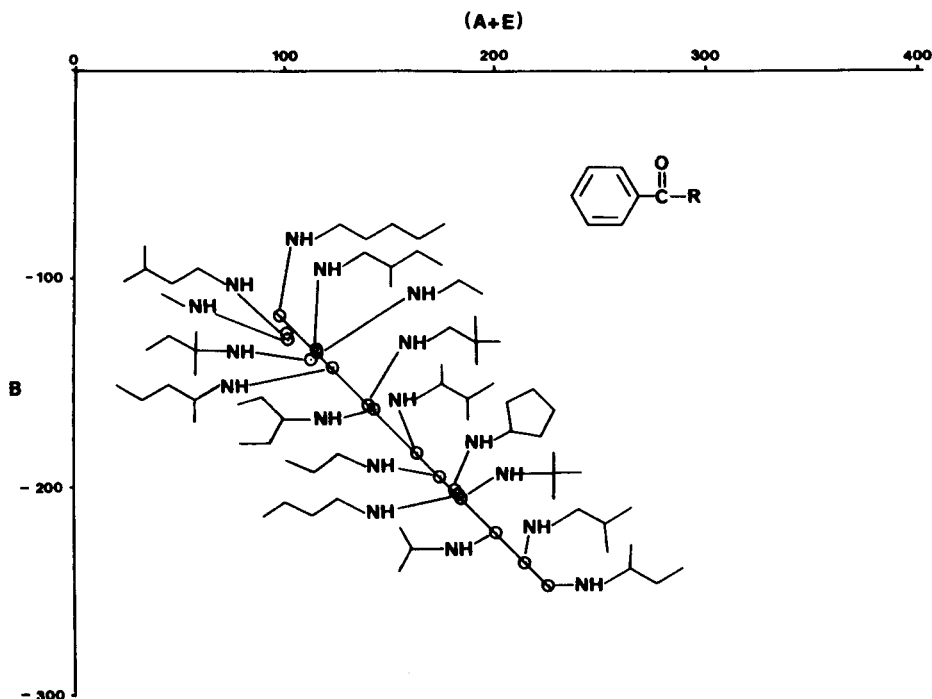


Fig. 5. Plot of the solvophobic parameters  $B$  versus ( $A + E$ ) as derived from data obtained using Ultrasphere ODS.

which are both expected to be dependent upon the individual column. Coefficient  $E$  is related to the interaction of solute and solvent, and, therefore, is independent of column properties. In spite of these variables, the fact that eqns. 10 and 11 are virtually identical suggests that some underlying factors in the chromatographic retention process are the same in these two columns. If the identical nature of these plots were simply a result of the solute properties being the same, one might expect the ordering of the compounds to be the same. The calculated regression parameters for the compound N-cyclopropylbenzamide have been included in Table I and II. Although it is not an isomer of the other  $C_5$  derivatives, the point  $((A + E), B)$  for the cyclopropyl derivative lies on the same line as the other compounds in both Figs. 4 and 5.

From eqn. 4, and the calculated values of regression coefficient  $C$  given in Tables I and II,  $\Delta A$ , the contact surface area of the associated solute-bonded ligand complex, can be evaluated. The values obtained for  $\Delta A$  are given in Table IV. The total surface area (TSA) for each solute was calculated in a manner totally independent of chromatographic measurements using standard bondlengths and bond angles<sup>16</sup> and compiled in Table IV. The purpose of comparing the solute-bonded ligand contact surface area to the total surface area is to attempt to lend credibility to the values predicted for  $\Delta A$ . The values for  $\Delta A$  appear reasonable as they are approximately equal to or less than one-half of the total molecular surface area. While for some solutes, the contact surface area calculated from the Ultrasphere ODS column is greater and in other cases  $\Delta A$  from the Partisil ODS-2 column is greater,

TABLE IV  
CONTACT SURFACE AREA AND TOTAL SURFACE AREA

For general structure, see Table I.

<i>R</i>	<i>Partisil ODS-2</i> $\Delta A$ ( $\text{\AA}^2$ ) <sup>*</sup>	<i>Ultrasphere ODS</i> ( <i>UE795</i> ) $\Delta A$ ( $\text{\AA}^2$ )	<i>TSA</i> ( $\text{\AA}^2$ ) <sup>**</sup>
CH <sub>3</sub>	83.9	71.4	165.0
CH <sub>3</sub> CH <sub>2</sub>	87.8	75.8	187.8
CH <sub>3</sub> CH <sub>2</sub> CH <sub>2</sub>	92.5	83.8	210.5
(CH <sub>3</sub> ) <sub>2</sub> CH	89.3	82.0	210.2
CH <sub>3</sub> CH <sub>2</sub> CH(CH <sub>3</sub> )	88.3	89.5	231.7
(CH <sub>3</sub> ) <sub>2</sub> CHCH <sub>2</sub>	90.3	91.6	227.7
CH <sub>3</sub> (CH <sub>2</sub> ) <sub>3</sub>	92.7	92.2	233.2
(CH <sub>3</sub> ) <sub>3</sub> C	87.2	86.0	226.4
(CH <sub>3</sub> CH <sub>2</sub> ) <sub>2</sub> CH	91.4	88.7	248.7
(CH <sub>3</sub> ) <sub>2</sub> CHCH(CH <sub>3</sub> )	91.8	92.6	246.2
CH <sub>3</sub> CH <sub>2</sub> CH <sub>2</sub> CH(CH <sub>3</sub> )	95.9	91.8	251.7
CH <sub>3</sub> CH <sub>2</sub> CH(CH <sub>3</sub> )CH <sub>2</sub>	98.8	93.9	250.3
CH <sub>3</sub> CH <sub>2</sub> C(CH <sub>3</sub> ) <sub>2</sub>	94.3	88.6	241.3
(CH <sub>3</sub> ) <sub>3</sub> CCH <sub>2</sub>	93.6	94.1	245.0
(CH <sub>3</sub> ) <sub>2</sub> CHCH <sub>2</sub> CH <sub>2</sub>	100.1	95.4	247.6
CH <sub>3</sub> (CH <sub>2</sub> ) <sub>4</sub>	101.7	96.9	255.9
CH <sub>2</sub> CH <sub>2</sub> CH <sub>2</sub> CH <sub>2</sub> CH	90.6	91.2	—

\* Contact surface area in square Angstroms.

\*\* Total surface area in square Angstroms.

overall, the values for  $\Delta A$  calculated from each of the two columns investigated are similar.

In Figs. 6 and 7,  $\log k'_w$  is plotted against the contact surface area in square angstroms ( $\text{\AA}^2$ ) as determined in acetonitrile-water. The plots demonstrate that compounds that have similar contact surface areas with the bonded ligand can also exhibit vastly differing capacity factors in water. Therefore, while the contact surface area between the solute and the hydrocarbonaceous stationary phase may contribute in part to determining retention in water, it is not the controlling factor. If one looks at only the four isomeric butylbenzamides in Fig. 6, a line of correlation  $r = 0.9996$  can be passed through the *sec.*-butyl, isobutyl, and *n*-butyl derivatives, omitting the

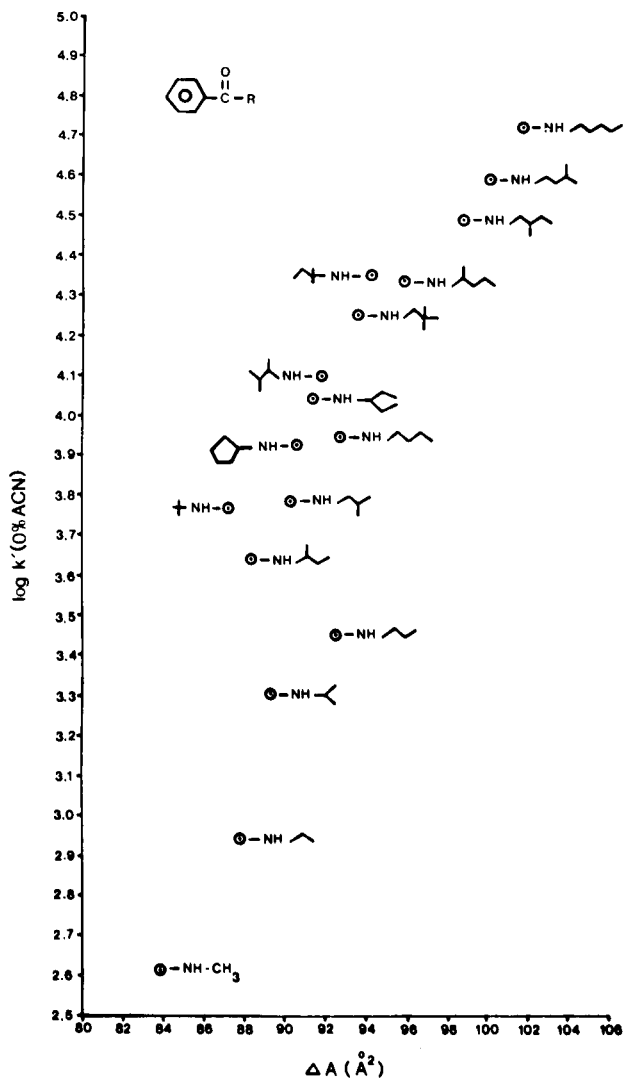


Fig. 6.  $\log k'_w$  versus solute-ligand contact surface area,  $\Delta A$ , determined from data obtained on Partisil ODS-2.



*tert.*-butyl derivative. Similarly, a line of correlation  $r = 0.9941$  can be drawn through the isomeric pentylbenzamides if the *tert.*-pentylbenzamide is excluded. If in each case, the excluded points are projected onto the line defined by the other isomeric benzamides, it can be seen that for these two compounds, the capacity factor in water is much greater than would be expected according to the contact surface area. This behavior of the *tert.*-butyl and *tert.*-pentyl derivatives is also observed to occur on the Ultrasphere ODS column (see Fig. 7).

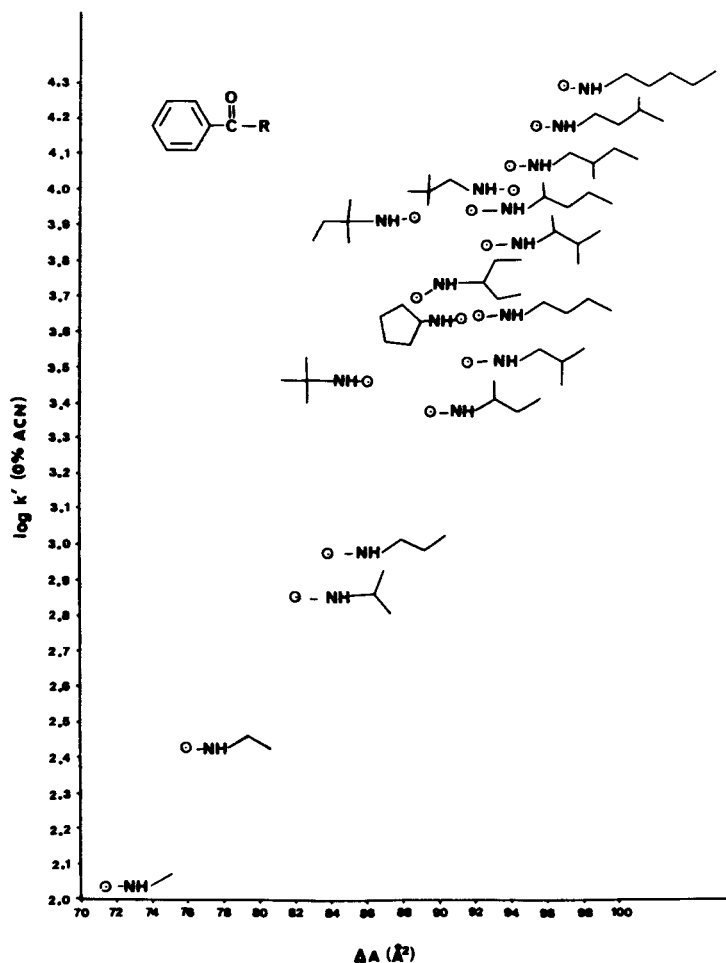


Fig. 7.  $\log k'_w$  versus solute-ligand contact surface area.  $\Delta A$ , determined from data obtained on Ultrasphere ODS.

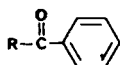
#### *Anomalous retention of the tertiary alkylbenzamides*

The unusual behavior of the two tertiary alkylbenzamides is also demonstrated in the overall profile of this series of compounds when the values for  $\log k'$  for these solutes are plotted versus the percent of the organic modifier in the mobile phase (Figs. 1 and 2). In these figures, the curves seem to vary in a regular fashion, except for the curves of the *tert.*-butyl and *tert.*-pentyl isomers which cross the curves of other

compounds. This is further pointed out by a closer look at the retention order of the compounds in various concentrations of acetonitrile-water listed in Table V. In each of the three cases presented in this table, where the order has been determined at 20% and at 40% acetonitrile and predicted at 0% acetonitrile, the elution order is the same if the *tert.*-butyl- and *tert.*-pentylbenzamides are again omitted. The *tert.*-pentylbenzamide changes from 13th to 14th to 15th in order of elution, while the *tert.*-butylbenzamide changes from 6th to tie for 7th and finally 8th in elution order as the percentage of the organic modifier increases. The elution orders at 0, 20 and 40% acetonitrile using the Ultrasphere ODS column are the same as those given in Table V for the Partisil ODS-2 column, except for the differences already noted (see Table III)

TABLE V

RETENTION ORDER OF THE C<sub>1</sub>-C<sub>5</sub> N-ALKYLBENZAMIDES AT 0, 20 AND 40% (v/v) ACETONITRILE-WATER ON PARTISIL ODS-2



Elution order	Acetonitrile (% v/v)		
	0	20	40
1			
2			
3			
4			
5			
6			
7			
8			
9			
10			
11			
12			
13			
14			
15			
16			

and for the elution of the *tert.*-pentylbenzamide after the *n*-pentyl derivative at 40% acetonitrile on the Ultrasphere ODS column. Therefore, both the *tert.*-butyl and *tert.*-pentyl solutes tend to elute after their straight-chain analogues as the percentage of acetonitrile in the mobile phase is increased.

When the structures of these two compounds are scrutinized, it appears that the factor they have in common is a quaternary carbon atom bonded to the amide nitrogen. Perhaps an explanation for this behavior concerns the energy required to place solutes back into the solvent after contact with the bonded ligand: (1) the structural bulkiness about this carbon atom should increase the energy required to prepare a solvent cavity of the proper shape and size, and (2) the arrangement about this carbon atom could obstruct the hydrogen bonding between the amide group and the solvent, thereby affecting the interaction energy between the solute and the solvent. The net result can be viewed as an increase in the contact time between the two solutes and the bonded phase and a concomitant increase in time of elution. A proton NMR study of hydrogen bonding effects in the butylbenzamides was conducted in an attempt to provide a means, independent of chromatography, to establish the validity of the above points.

Amide N-H groups produce somewhat broad NMR signals in the 5.0–8.5  $\delta$  region<sup>17</sup>. The position of resonance for amide protons is dependent upon concentration because these protons are involved in the formation of intermolecular hydrogen bonds (solute-solute and/or solute-solvent hydrogen bonds). The amide proton experiences a difference in magnetic shielding in the associated (hydrogen-bonded) and unassociated states. Dilution causes dissociation of solute-solute hydrogen bonds altering the populations of associated and unassociated states in non-hydrogen bonding solvents. Thus, the resonance frequency for amide protons is concentration dependent<sup>18</sup>.

The concentration dependence of the chemical shift of the amide proton in N-*n*-butyl-, N-isobutyl-, N-*sec.*-butyl- and N-*tert.*-butylbenzamide was investigated by proton NMR in carbon tetrachloride and is demonstrated in Fig. 8. The ordinate represents the  $\delta$  value of the amide proton in ppm relative to TMS, and the abscissa, the mole fraction of each benzamide in carbon tetrachloride. In such a non-hydrogen bonding solvent, the intermolecular interaction can be described by eqn. 12 and the equilibrium constant by eqn. 13:



$$K_{\text{eq}} = \frac{[\text{R-H} \cdots \text{R-H}]}{[\text{R-H}]^2} \quad (13)$$

Curve 1 in Fig. 8 represents the concentration dependencies of both the N-*n*-butyl- and the N-isobutylbenzamides; curve 2 is for N-*sec.*-butylbenzamide and curve 3 for N-*tert.*-butylbenzamide. Fewer data points are recorded for N-*tert.*-butylbenzamide due to its limited solubility in carbon tetrachloride compared to the other isomeric butylbenzamides. The relative displacement of the three curves at any given concentration can be attributed to the electron donating effects of the groups bonded to the carbon attached to the amide nitrogen atom. As the mole fraction of

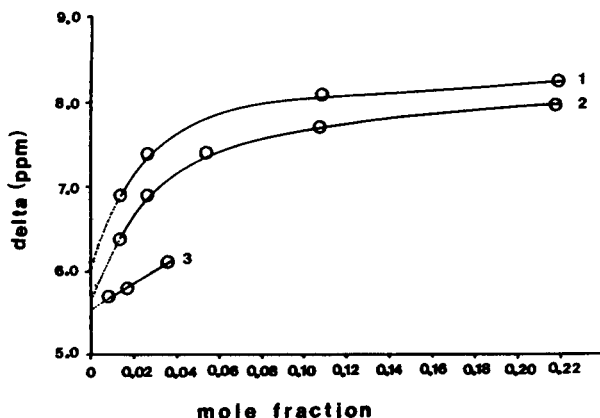


Fig. 8. Concentration versus NMR chemical shift for the N-H proton of the butylbenzamides. Curves: 1, N-*n*-butyl and N-isobutylbenzamide; 2, N-*sec.*-butylbenzamide; 3, N-*tert.*-butylbenzamide.

each benzamide in carbon tetrachloride is increased, the NMR signal of the amide proton is displaced to lower field due to an increase in the population of the associated state.

From these data,  $K_{eq}$  values of 4.4 for the N-*n*-butyl and N-isobutyl isomers, and 2.3 for the N-*sec.*-butyl derivative were calculated. The calculation of  $K_{eq}$  was based on the assumption that the  $\delta$  value obtained by extrapolation to zero concentration represents the completely non-hydrogen-bonded form, and that the  $\delta$  value obtained at high solute concentration represents the totally associated form. Due to the lack of data points at high concentration for N-*tert.*-butylbenzamide, calculation of the equilibrium constant for this compound was impossible. By qualitatively comparing the slopes of the plots in Fig. 8 at increasing dilutions, the tendency for the reaction in eqn. 12 to be displaced to the right (*i.e.*, toward dimerization) occurs in the following order: N-*n*-butyl-, N-isobutyl- > N-*sec.*-butyl- > N-*tert.*-butylbenzamide. It is reasonable to assume that this same trend occurs between a molecule of an individual isomer and a molecule of a hydrogen-bonding solvent used in chromatography. Steric crowding about the carbon adjacent to the amide nitrogen (due to the amount of substitution on this carbon) influences the ability of the forward reaction in eqn. 12 to occur. Therefore, the NMR data support the conclusions drawn chromatographically. Furthermore, the anomalous behavior of the tertiary alkylbenzamides was also observed chromatographically in methanol-water eluents. The behavior of *tert.*-butyl- and *tert.*-pentylbenzamide does not appear to result from solvent selectivity since it occurs in both aqueous methanol and acetonitrile solvents.

## CONCLUSIONS

The 16 isomeric  $C_1-C_5$  N-alkylbenzamides exhibit significant non-linearity of  $k'$  as a function of solvent composition in aqueous acetonitrile and methanol. The experimentally measured  $k'$  values were observed to increase dramatically at low concentrations of organic modifier. The relationship between  $k'$  and eluent composition for these compounds is not described by linear or quadratic equations. Using

the chromatographic data determined in acetonitrile–water, the relationship between  $k'$  and eluent composition was described by the solvophobic theory. Regression coefficients obtained from eqn. 1 were used to determine various fundamental chromatographic parameters. The calculated contact surface area of the solute-bonded ligand complex was found to be one-half or less of the total molecular surface area of the solute. Calculated  $k'_w$  data predicts that branched alkyl chains elute before their straight-chain analogues. In a compound with a single carbon branch, the elution volume increases with the distance between the methyl-branch and the amide nitrogen.

## APPENDIX

### Definition of Mathematical Variables

<i>Variables</i>	<i>Definition</i>
$A, B, C, D$ and $E$	Regression coefficients
$\mathcal{D} = 2(\epsilon - 1)/(2\epsilon + 1)$	$\mathcal{D}$ is a function of $\epsilon$ , the static dielectric constant of the solvent
$\gamma$	Surface tension of the solvent
$\kappa^e$	Microscopic cavity factor; curvature correction to convert the macroscopic surface tension to microscopic dimensions
$V$	Average mole volume of solvent
$R$	Gas law constant
$T$	Temperature in degrees Kelvin
$P_0$	Atmospheric pressure
$k' = (V_R - V_0)/V_0$	Chromatographic capacity factor
$V_R$	Retention volume
$V_0$	Column void volume
$\varphi$	Characteristic constant for a given column (logarithm of the phase ratio)
$N$	Avogadro's number
$\Delta F_{\text{vdw, assoc}}$	Free energy change for the interaction of solute and ligand in a hypothetical gas phase; assumed to occur by Van der Waals forces only
$\Delta F_{\text{vdw, s}}$	The Van der Waals component of the free energy change for the interaction of the solute with the solvent
$\lambda = v_{\text{SL}}/v_{\text{S}}$	The molecular volume of the complex, $v_{\text{SL}}$ , is assumed to be a multiple of the molecular volume of the solute, $v_{\text{S}}$
$\mu_{\text{s}}$	Static dipole moment of the solute
$P = \left[ 4\pi\epsilon_0 \left( 1 - \mathcal{D} \frac{\alpha_{\text{S}}}{v_{\text{S}}} \right) \right]^{-1}$	where $\epsilon_0$ is the permittivity constant, and $\alpha_{\text{S}}$ is the polarizability of the solute
$\Delta A$	Contact surface area of the solute ligand complex

## ACKNOWLEDGEMENT

We sincerely appreciate the support of the American Foundation for Pharmaceutical Education Silas M. Burroughs Memorial Fellowship for M. J. M. W.

## REFERENCES

- 1 O. Sinanoglu and S. Abdulnur, *Fed. Proc., Fed. Amer. Soc. Exp. Biol.*, 24 (1965) Part III:S-12.
- 2 Cs. Horváth, W. Melander and I. Molnár, *J. Chromatogr.*, 125 (1976) 129.
- 3 J. Traube, *Ann.*, 265 (1891) 27.
- 4 C. Tanford, *The Hydrophobic Effect: Formation of Micelles and Biological Membranes*, Wiley, New York, 1973.
- 5 E. Tomlinson, *J. Chromatogr.*, 113 (1975) 1.
- 6 J. W. McBain, *Colloid Science*, D. C. Heath and Co., Boston, MA, 1950.
- 7 J. J. Pesek and J. E. Daniels, *J. Chromatogr. Sci.*, 14 (1976) 288.
- 8 J. J. Pesek and J. A. Graham, *Anal. Chem.*, 49 (1977) 133.
- 9 C. Hansch and A. Leo, *Substituent Constants for Correlation Analysis in Chemistry and Biology*, Wiley, New York, 1979.
- 10 M. J. M. Wells and C. R. Clark, *J. Chromatogr.*, 235 (1982) 31.
- 11 J. Timmermans, *Physicochemical Constants of Binary Systems in Concentrated Solutions*, Vol. 4, Interscience, New York, 1960.
- 12 C. Carr and J. A. Riddick, *Ind. Eng. Chem.*, 43 (1951) 692.
- 13 G. Doheret and M. Morenas, *C. R. Acad. Sci., Ser. C.*, 264 (1967) 729.
- 14 G. Akerlof, *J. Amer. Chem. Soc.*, 54 (1932) 4125.
- 15 W. Melander, D. E. Campbell and Cs. Horváth, *J. Chromatogr.*, 158 (1978) 215.
- 16 J. A. Pople and D. L. Beveridge, *Approximate Molecular Orbital Theory*, McGraw-Hill, New York, 1970.
- 17 J. R. Dyer, *Applications of Absorption Spectroscopy of Organic Compounds*, Prentice-Hall, Englewood Cliffs, NJ, 1965.
- 18 J. A. Pople, W. G. Schneider and H. J. Bernstein, *High-resolution Nuclear Magnetic Resonance*, McGraw-Hill, New York, 1959.

CHROM. 14,270

## INVESTIGATION OF N-ALKYLBENZAMIDES BY REVERSED-PHASE LIQUID CHROMATOGRAPHY

### III. CORRELATION OF CHROMATOGRAPHIC PARAMETERS WITH MOLECULAR CONNECTIVITY INDICES FOR THE C<sub>1</sub>-C<sub>5</sub> N-ALKYLBENZAMIDES

MARTHA J. M. WELLS\* and C. RANDALL CLARK\*

*Division of Medicinal Chemistry, Department of Pharmacal Sciences, School of Pharmacy, Auburn University, Auburn University, AL 36849 (U.S.A.)*

and

RICHARD M. PATTERSON

*Research Data Analysis, Auburn University, Auburn University, AL 36849 (U.S.A.)*

(Received May 7th, 1981)

---

#### SUMMARY

Molecular connectivity indices were compared with measured and calculated reversed-phase liquid chromatographic retention data for the C<sub>1</sub>-C<sub>5</sub> N-alkylbenz-amides. Molecular connectivity is a topological index which encodes fundamental structural information about a molecule. The calculated indices are presented as bar-graph spectra and in tabular form. The various parameters of the solvophobic theory used to calculate log  $k'_w$  values for the amides were also compared to connectivity data. Highest correlations with  $k'$  were obtained for connectivity data which describes molecular bulk, branching, and site of branching in the hydrocarbon portion of the molecule.

---

#### INTRODUCTION

High-performance liquid chromatography (HPLC) is currently the most rapidly growing technique of the separation sciences<sup>1</sup>. Of all of the HPLC techniques, those involving reversed-phase application dominate the literature. Understanding of the retention process in reversed-phase liquid chromatography (RPLC) is growing, but much of the work published is still qualitative in nature and there is a need for increased quantitation of the obtained retention data.

One method of accounting for hydrophobic selectivity in RPLC is to correlate

---

\* Present Address: USDA Forest Service, Southern Forest Experiment Station, George W. Andrews Forest Sciences Laboratory, Auburn University, AL 36849, U.S.A.

retention values with a topological index which encodes structural information about the solute. Topological features of molecules can be quantitated by an easily computable set of molecular connectivity indices. These indices were first introduced by Randić<sup>2</sup>, and further developed by Kier and Hall<sup>3</sup>. The connectivity index,  $\chi$ , is a very fundamental parameter which reflects the shape and interatomic connections of a molecule. Many studies<sup>4-8</sup> have demonstrated that physicochemical and biological properties which depend upon the topology of a molecule may be related to the connectivity index.

Molecular connectivity calculations have been compared with gas-liquid chromatographic retention data<sup>9-11</sup>. The simple connectivity index as originally defined has been used by Karger *et al.*<sup>12</sup> and more recently by Colin and Guiochon<sup>13</sup> to evaluate hydrophobic effects in RPLC. The index has since been refined and expanded by Kier and Hall<sup>3</sup> to allow for differences in the identities of atoms and in bond orders<sup>14</sup>. In this study, relationships between predicted and measured chromatographic data and the expanded molecular connectivity indices will be pursued.

## EXPERIMENTAL

The chromatographic data used in this study has been previously reported<sup>15</sup> as has the application of the solvophobic theory to the chromatographic data<sup>16</sup>. Additionally, some data obtained using a 25 cm  $\times$  4.60 mm I.D. Partisil ODS (10  $\mu$ m) column purchased from Whatman (Clifton, NJ, U.S.A.) is also included in this study. Chromatographic procedures employed with this column were identical to those described previously<sup>15</sup> with the exception that the Partisil ODS column was operated at ambient temperature without a guard column.

## RESULTS AND DISCUSSION

The reversed-phase liquid chromatographic retention of the C<sub>1</sub>-C<sub>5</sub> N-alkylbenzamides has been investigated and the physical characteristics of these compounds described<sup>15</sup>. In Part II of this series<sup>16</sup> chromatographic parameters for the C<sub>1</sub>-C<sub>5</sub> N-alkylbenzamides were predicted by application of the solvophobic theory<sup>17-19</sup> to measured retention data. The purpose of this article is to associate the predicted parameters as well as the actually measured chromatographic capacity factors with structural features of the molecules.

Understanding of the structural meaning of connectivity indices is facilitated by bar graph spectra<sup>3</sup> of the  ${}^m\chi_t$  values for the C<sub>1</sub>-C<sub>5</sub> N-alkylbenzamides involved in this study (Fig. 1). The horizontal axes in Fig. 1 represent the order,  $m$ , and the vertical axes the magnitude of  ${}^m\chi_t$  values;  $t$  = type. These graphs can be visually compared to find trends in structure. A smooth falloff in the spectrum is observed for those compounds having long-chain portions. (Compare the methyl, ethyl, *n*-propyl, *n*-butyl, and *n*-pentyl derivatives.) The spectrum becomes more jagged (due to greater  ${}^2\chi$  values) with an increase in the amount of branching in the N-alkyl chain. The graphs of the *tert.*-butyl, *tert.*-pentyl, and neopentyl compounds have high  ${}^2\chi$  and  ${}^3\chi_c$  values and non-zero values of  ${}^4\chi_c$  due to the presence of carbon atoms assigned a  $\delta$  value of four (*i.e.*, a quaternary carbon).

The number of terms for each subgraph-type of molecular connectivity index



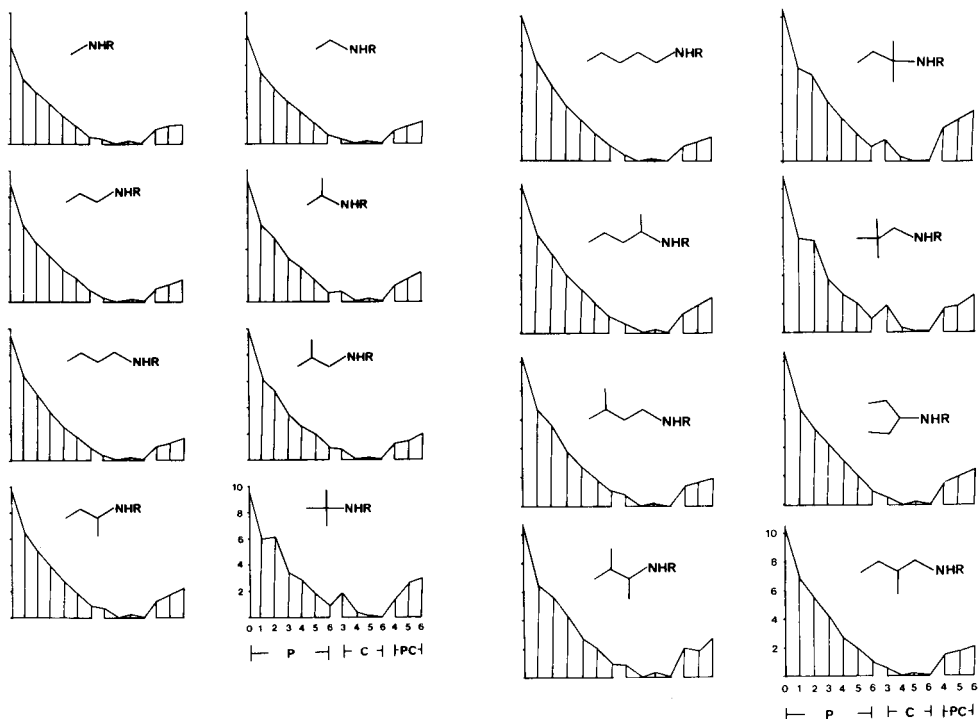


Fig. 1. Bar-graph spectra of the  $m\chi_l$  values for the  $C_1$ - $C_5$  N-alkylbenzamides: P = path; C = cluster; PC = path/cluster; R = benzoyl.

(path, P, cluster, C, and path/cluster, PC) is presented for the  $C_1$ - $C_5$  N-alkylbenzamides in Table I. The chain terms, CH (arising from an enclosed figure), were omitted since there are no 3rd, 4th, or 5th order chain terms possible for these compounds. Also, every compound has one 6th order chain term due to the presence of the aromatic ring.

By the use of the Statistical Analysis System procedure RSQUARE (SAS Institute, Raleigh, NC, U.S.A.) various parameters were screened against all possible two-variable combinations of the connectivity level ( $\chi$ ) and valence level ( $\chi^v$ ) indices, their inverses and their squares through sixth order. When the best combinations were selected, procedure SYSREG was used to evaluate the coefficients.

#### Comparison of $\log k'$ values with molecular connectivity indices

The method of predicting the  $\log k'_w$  values for 0% acetonitrile on both the Partisil ODS-2 and Ultrasphere ODS columns was discussed previously<sup>16</sup>. The molecular connectivity indices were regressed on the predicted  $\log k'_w$  values for the sixteen  $C_1$ - $C_5$  N-alkylbenzamides (Table IV, ref. 16), and the best two variable combinations chosen are given in eqns. 1 and 2:

Partisil ODS-2

$$\log k'_w = 0.070 (0.013) [{}^5\chi_{PC}]^2 + 20.930 (0.917) [{}^6\chi_P]^{-1} + 2.154 (0.082) \quad (1)$$

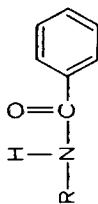
$$r = 0.9885$$

Ultrasphere ODS

$$\log k'_w = 0.834 (0.026) [{}^0\chi^v] + 0.326 (0.031) [{}^6\chi_{PC}^v]^{-1} - 3.991 (0.267) \quad (2)$$

$$r = 0.995$$

TABLE I  
NUMBER OF SUBGRAPH TERMS FOR PATH, CLUSTER, AND PATH/CLUSTER TYPES



R	1 $\chi$			2 $\chi$			3 $\chi$			4 $\chi$			5 $\chi$			6 $\chi$			Total				
	P	P	P	P	P	P	P	P	P	P	P	PC	C	P	P	PC	C	P	P	PC	C	P	PC
CH <sub>3</sub>	10	12	14	2	14	0	7	14	1	12	0	19	0	8	0	19	0	72	0	19	0	3	38
CH <sub>3</sub> CH <sub>2</sub>	11	13	15	2	16	0	7	16	1	13	0	22	0	10	0	22	0	81	0	22	0	3	42
CH <sub>3</sub> CH <sub>2</sub> CH <sub>2</sub>	12	14	16	2	17	0	7	18	1	13	0	23	0	12	0	23	0	89	0	23	0	3	43
(CH <sub>3</sub> ) <sub>2</sub> CH	12	15	16	3	18	0	8	18	1	16	0	28	0	12	0	28	0	91	0	28	0	4	52
CH <sub>3</sub> (CH <sub>2</sub> ) <sub>3</sub>	13	15	17	2	18	0	7	19	1	13	0	23	0	14	0	23	0	96	0	23	0	3	43
(CH <sub>3</sub> ) <sub>2</sub> CHCH <sub>2</sub>	13	16	17	3	18	0	8	20	1	14	0	26	0	14	0	26	0	98	0	26	0	4	48
CH <sub>3</sub> CH <sub>2</sub> CH(CH <sub>3</sub> )	13	16	18	3	19	0	9	20	1	17	0	31	0	14	0	31	0	100	0	31	0	4	57
(CH <sub>3</sub> ) <sub>3</sub> C	13	18	17	6	20	1	10	20	1	22	1	39	1	14	0	39	1	102	1	39	1	8	71
CH <sub>3</sub> (CH <sub>2</sub> ) <sub>4</sub>	14	16	18	2	19	0	7	20	1	13	0	23	0	15	0	23	0	102	0	23	0	3	43
CH <sub>3</sub> CH <sub>2</sub> C(CH <sub>3</sub> ) <sub>2</sub>	14	19	20	6	21	1	13	22	1	25	1	45	1	16	0	45	1	112	1	45	1	8	83
CH <sub>3</sub> CH <sub>2</sub> CH <sub>2</sub> CH(CH <sub>3</sub> )	14	17	19	3	21	0	9	21	1	18	0	32	0	16	0	32	0	108	0	32	0	4	59
(CH <sub>3</sub> ) <sub>3</sub> CCH <sub>2</sub>	14	19	18	6	19	1	10	22	1	17	1	32	1	16	0	32	1	108	1	32	1	8	59
(CH <sub>3</sub> ) <sub>2</sub> CHCH <sub>2</sub> CH <sub>2</sub>	14	17	18	3	19	0	8	20	1	14	0	24	0	16	0	24	0	104	0	24	0	4	46
(CH <sub>3</sub> CH <sub>2</sub> ) <sub>2</sub> CH	14	17	20	3	21	0	10	22	1	19	0	35	0	16	0	35	0	110	0	35	0	4	64
(CH <sub>3</sub> ) <sub>2</sub> CHCH(CH <sub>3</sub> )	14	18	20	4	20	0	12	22	2	19	0	37	0	16	0	37	0	110	0	37	0	6	68
CH <sub>3</sub> CH <sub>2</sub> CH(CH <sub>3</sub> )CH <sub>2</sub>	14	17	19	3	19	0	9	21	1	15	0	27	0	16	0	27	0	106	0	27	0	4	51

The numbers in parentheses in all equations are the standard error of the regression coefficients. The values of the chosen connectivity indices are given in Table II. The results (eqns. 1 and 2) should be compared and contrasted with the best regression equations obtained for the sixteen compounds at other solvent compositions and on other columns (eqns. 3–9; MeOH = methanol, ACN = acetonitrile):

## Partisil ODS

$$\log k'_{40\% \text{ MeOH}} = 0.024 (0.005) [\chi_{\text{PC}}^5]^2 + 6.879 (0.349) [\chi_{\text{P}}^6]^2 + 0.200 (0.031) \\ r = 0.9847 \quad (3)$$

## Partisil ODS-2

$$\log k'_{35\% \text{ MeOH}} = 0.053 (0.006) [\chi_{\text{PC}}^5]^2 + 12.625 (0.463) [\chi_{\text{P}}^6]^2 + 0.500 (0.041) \\ r = 0.9922 \quad (4)$$

$$\log k'_{55\% \text{ MeOH}} = 0.041 (0.004) [\chi_{\text{PC}}^5]^2 + 8.439 (0.303) [\chi_{\text{P}}^6]^2 + 0.055 (0.027) \\ r = 0.9927 \quad (5)$$

$$\log k'_{20\% \text{ ACN}} = 0.068 (0.006) [\chi_{\text{PC}}^5]^2 + 13.500 (0.416) [\chi_{\text{P}}^6]^2 + 0.490 (0.037) \\ r = 0.9946 \quad (6)$$

$$\log k'_{40\% \text{ ACN}} = 0.054 (0.004) [\chi_{\text{PC}}^5]^2 + 8.697 (0.304) [\chi_{\text{P}}^6]^2 + 0.001 (0.027) \\ r = 0.9935 \quad (7)$$

## Ultrasphere ODS

$$\log k'_{35\% \text{ MeOH}} = 0.056 (0.007) [\chi_{\text{PC}}^5]^2 + 13.334 (0.519) [\chi_{\text{P}}^6]^2 + 0.162 (0.046) \\ r = 0.9912 \quad (8)$$

$$\log k'_{20\% \text{ ACN}} = 0.077 (0.006) [\chi_{\text{PC}}^5]^2 + 14.520 (0.450) [\chi_{\text{P}}^6]^2 + 0.123 (0.040) \\ r = 0.9946 \quad (9)$$

The  $\log k'$  values predicted by eqns. 1–9 are listed in Tables III and IV. When a connectivity level ( $\chi$ ) value is chosen in a regression of this type, it implies that the nature of the atom itself is not important. However, if a valence level ( $\chi^v$ ) value is selected, the identity of the atom (carbon vs. oxygen vs. nitrogen, etc.) is important to correlation with a given property. In eqns. 1 and 3–9, the same connectivity parameters were chosen as the best descriptors of retention in these systems. This implies that the same structural features were important to the chromatographic retention process at various eluent compositions on these columns. However, at 0% acetonitrile on the Ultrasphere ODS column different structural parameters were selected. The most apparent anomalies in the predicted  $\log k'$  values (Tables III and IV) appear to be: (1) a consistently higher predicted value for the 1-ethylpropyl derivative, and (2) in all cases except one a reverse order of elution to that observed is predicted for the isopentyl and *n*-pentyl derivatives.

TABLE II  
SELECTED MOLECULAR CONNECTIVITY INDICES FOR THE C<sub>1</sub>-C<sub>5</sub> N-ALKYLBENZAMIDES

For general structure, see Table I.

R	0 <sub>γ</sub>	0 <sub>γ'</sub>	1 <sub>γ</sub>	2 <sub>γ'</sub>	5 <sub>γPC</sub>	6 <sub>γP</sub>	6 <sub>γPC</sub>	6 <sub>γ'PC</sub>
CH <sub>3</sub>	7.39734	5.79500	4.84253	1.94515	1.33925	0.13065	1.51603	0.27826
CH <sub>3</sub> CH <sub>2</sub>	8.10444	6.50210	5.34253	2.22547	1.37377	0.17548	1.68269	0.32036
CH <sub>3</sub> CH <sub>2</sub> CH <sub>2</sub>	8.81155	7.20921	5.84253	2.62192	1.32496	0.23039	1.70710	0.32504
(CH <sub>3</sub> ) <sub>2</sub> CH	8.97469	7.37235	5.69837	2.99418	1.79251	0.20654	2.14567	0.46531
CH <sub>3</sub> (CH <sub>2</sub> ) <sub>3</sub>	9.51866	7.91632	6.34253	2.97547	1.32496	0.28953	1.67258	0.31756
(CH <sub>3</sub> ) <sub>2</sub> CHCH <sub>2</sub>	9.68180	8.07945	6.19837	3.46989	1.47000	0.26843	2.00320	0.42466
CH <sub>3</sub> CH <sub>2</sub> CH(CH <sub>3</sub> )	9.68180	8.07945	6.23638	3.14878	1.81043	0.25137	2.33227	0.52879
(CH <sub>3</sub> ) <sub>3</sub> C	9.89734	8.29500	5.98898	4.07015	2.63726	0.23159	3.10821	0.78616
CH <sub>3</sub> (CH <sub>2</sub> ) <sub>4</sub>	10.22576	8.62342	6.84253	3.32903	1.32496	0.32852	1.67258	0.31756
(CH <sub>3</sub> ) <sub>2</sub> CHCH <sub>2</sub> CH <sub>2</sub>	10.38890	8.78656	6.69837	3.80444	1.52908	0.33098	1.77514	0.38642
CH <sub>3</sub> CH <sub>2</sub> CH(CH <sub>3</sub> )CH <sub>2</sub>	10.38890	8.78656	6.73638	3.58946	1.62530	0.31671	2.01586	0.46357
CH <sub>3</sub> CH <sub>2</sub> CH <sub>2</sub> CH(CH <sub>3</sub> )	10.38890	8.78656	6.73638	3.52920	1.96573	0.29966	2.34493	0.56771
(CH <sub>3</sub> CH <sub>2</sub> ) <sub>2</sub> CH	10.38890	8.78656	6.77438	3.52920	1.96673	0.29620	2.51089	0.61982
(CH <sub>3</sub> ) <sub>2</sub> CHCH(CH <sub>3</sub> )	10.55204	8.94970	6.60906	3.87217	1.98611	0.28243	2.83388	0.73751
(CH <sub>3</sub> ) <sub>3</sub> CCH <sub>2</sub>	10.60444	9.00210	6.48898	4.60936	1.97345	0.29911	2.60052	0.66814
CH <sub>3</sub> CH <sub>2</sub> C(CH <sub>3</sub> ) <sub>2</sub>	10.60444	9.00210	6.54964	4.05758	2.89302	0.27042	3.46418	0.94794

A subset (Table V) of the pertinent connectivity values from Table II illustrates the relationships observed. Branching increases the value of  ${}^5\chi_{PC}$  in the order: *n*-butyl < isobutyl < *sec.*-butyl < *tert.*-butyl. *sec.*-Butyl has a larger  ${}^5\chi_{PC}$  value than isobutyl because the branch occurs on the carbon atom attached to the amide nitrogen atom. The  ${}^6\chi_P^y$  values are decreased by branching in the same order to the increase of the  ${}^5\chi_{PC}$  indices.

*Comparison of solvophobic regression coefficients with molecular connectivity indices*

The solvophobic theory<sup>17-19</sup> was used in Part II<sup>16</sup> of this series to determine values for the chromatographic parameters *B*, (*A* + *E*), and *C*. The values obtained for (*A* + *E*) and *B* (Tables II and III, ref. 16) were screened against the molecular connectivity indices for the sixteen C<sub>1</sub>-C<sub>5</sub> N-alkylbenzamides and the results are given in eqns. 10 and 11 for the Partisil ODS-2 column and in eqns. 12 and 13 for the Ultrasphere ODS column:

Partisil ODS-2

$$B = 10.559 (1.572) [{}^6\chi_{PC}]^2 + 2653.980 (162.014) [{}^6\chi_P^y]^2 - 409.965 (14.350) \\ r = 0.9810 \quad (10)$$

$$(A + E) = -10.206 (1.525) [{}^6\chi_{PC}]^2 - 2584.280 (157.215) [{}^6\chi_P^y]^2 + 383.320 (13.925) \\ r = 0.9811 \quad (11)$$

Ultrasphere ODS

$$B = 101.329 (21.228) [{}^1\chi]^2 - 1195.480 (252.722) {}^1\chi + 3312.993 (746.060) \\ r = 0.8014 \quad (12)$$

$$(A + E) = -99.020 (20.660) [{}^1\chi]^2 + 1168.690 (245.974) {}^1\chi - 3256.500 (726.140) \\ r = 0.8022 \quad (13)$$

The best two-variable combination chosen for *B* and (*A* + *E*) was the same for each column. This is not unreasonable since a high degree of correlation between the variables *B* and (*A* + *E*) has already been established (see eqns. 10 and 11, ref. 16). The correlation between the connectivity indices and the values of *B* and (*A* + *E*) derived from the Ultrasphere ODS column is unexpectedly poor. Eqns. 10 and 11 involve a path/cluster term, which accounts for branching in these molecules, as well as a path term which is greater for those compounds that are less branched. However, the first-order connectivity level index (quadratic relationships of eqns. 12 and 13) is not usually considered to account best for molecular branching. The values of the molecular connectivity indices which appear in eqns. 10-13 are reported in Table II.

Table VI presents the calculated values for  ${}^6\chi_{PC}/{}^6\chi_P^y$  for the C<sub>1</sub>-C<sub>5</sub> N-alkylbenzamides. This ratio describes the relative amount of branched to unbranched portions in these compounds. In the straight-chain homologs the ratio decreases as the number of methylene groups increases. Not unexpectedly, the *tert.*-butyl- and *tert.*-pentylbenzamides have the largest values for the ratio.

TABLE III  
EXPERIMENTAL AND PREDICTED LOG  $k'$  VALUES OF SOME N-ALKYLBENZAMIDES ON PARTISIL ODS-2  
For general structure, see Table I.

R	0% ACN		20% ACN		40% ACN		35% MeOH		55% MeOH	
	log $k'$ ( <i>calc.</i> )*	log $k'$ ( <i>calc.</i> )**	log $k'$ ( <i>obs.</i> )	log $k'$ ( <i>calc.</i> )**	log $k'$ ( <i>obs.</i> )	log $k'$ ( <i>calc.</i> ) <sup>§</sup>	log $k'$ ( <i>obs.</i> )	log $k'$ ( <i>calc.</i> ) <sup>§§</sup>	log $k'$ ( <i>obs.</i> )	log $k'$ ( <i>calc.</i> ) <sup>§§§</sup>
CH <sub>3</sub>	2.612	2.637	0.804	0.842	0.228	0.246	0.805	0.810	0.268	0.272
CH <sub>3</sub> CH <sub>2</sub>	2.987	2.931	1.039	1.034	0.377	0.371	1.000	0.989	0.399	0.392
(CH <sub>2</sub> ) <sub>2</sub> CH	3.305	3.272	1.303	1.284	0.552	0.546	1.201	1.209	0.537	0.547
CH <sub>3</sub> CH <sub>2</sub> CH <sub>2</sub>	3.452	3.388	1.347	1.326	0.581	0.557	1.274	1.263	0.576	0.575
CH <sub>3</sub> CH <sub>2</sub> CH(CH <sub>3</sub> )	3.638	3.706	1.570	1.566	0.742	0.728	1.434	1.471	0.709	0.723
(CH <sub>2</sub> ) <sub>3</sub> C	3.768	3.763	1.718	1.687	0.874	0.843	1.569	1.546	0.813	0.793
(CH <sub>3</sub> ) <sub>2</sub> CHCH <sub>2</sub>	3.786	3.813	1.636	1.610	0.776	0.744	1.552	1.524	0.770	0.752
CH <sub>3</sub> (CH <sub>2</sub> ) <sub>3</sub>	3.946	4.031	1.717	1.741	0.818	0.825	1.638	1.651	0.826	0.834
(CH <sub>3</sub> CH <sub>2</sub> ) <sub>2</sub> CH	4.039	4.261	1.843	1.937	0.919	0.973	1.680	1.813	0.869	0.954
(CH <sub>3</sub> ) <sub>2</sub> CHCH(CH <sub>3</sub> )	4.098	4.100	1.880	1.835	0.944	0.908	1.743	1.716	0.906	0.890
(CH <sub>2</sub> ) <sub>3</sub> CCCH <sub>2</sub>	4.248	4.299	1.956	1.963	0.984	0.989	1.855	1.836	0.986	0.970
CH <sub>3</sub> CH <sub>2</sub> CH <sub>2</sub> CH(CH <sub>3</sub> )	4.337	4.304	1.974	1.965	0.984	0.991	1.816	1.838	0.954	0.971
CH <sub>3</sub> CH <sub>2</sub> C(CH <sub>3</sub> ) <sub>2</sub>	4.353	4.270	2.043	2.046	1.069	1.089	1.887	1.867	1.021	1.015
CH <sub>3</sub> CH <sub>2</sub> CH(CH <sub>3</sub> )CH <sub>2</sub>	4.490	4.438	2.028	2.024	1.014	1.016	1.924	1.906	1.014	1.010
(CH <sub>3</sub> ) <sub>2</sub> CHCH <sub>2</sub> CH <sub>2</sub>	4.589	4.610	2.076	2.128	1.034	1.080	1.978	2.007	1.053	1.075
CH <sub>3</sub> (CH <sub>2</sub> ) <sub>4</sub>	4.722	4.536	2.146	2.066	1.079	1.034	2.036	1.956	1.095	1.038

\* See ref. 16, Table III.

\*\* Eqn. 1.

\*\*\* Eqn. 6.

§ Eqn. 7.

§§ Eqn. 4.

§§§ Eqn. 5.

TABLE IV  
EXPERIMENTAL AND PREDICTED LOG  $k'$  VALUES OF SOME N-ALKYLBENZAMIDES  
For general structure, see Table I.

R	Partisil ODS		Ultrasphere ODS					
	40% MeOH		0% ACN		20% ACN		35% MeOH	
	log $k'$ (obs.)	log $k'$ (calc.)*	log $k'$ (calc.)**	log $k'$ (calc.)***	log $k'$ (obs.)	log $k'$ (calc.)§	log $k'$ (obs.)	log $k'$ (calc.)§§
CH <sub>3</sub>	0.382	0.360	2.034	2.014	0.458	0.509	0.479	0.490
CH <sub>3</sub> CH <sub>2</sub>	0.455	0.457	2.427	2.449	0.713	0.715	0.677	0.678
(CH <sub>3</sub> ) <sub>2</sub> CH	0.558	0.570	2.850	2.858	1.000	0.990	0.907	0.911
CH <sub>3</sub> CH <sub>2</sub> CH <sub>2</sub>	0.608	0.607	2.972	3.024	1.050	1.029	0.981	0.968
CH <sub>3</sub> CH <sub>2</sub> CH(CH <sub>3</sub> )	0.683	0.713	3.373	3.364	1.311	1.293	1.171	1.188
(CH <sub>3</sub> ) <sub>3</sub> C	0.762	0.736	3.456	3.342	1.485	1.437	1.320	1.267
(CH <sub>3</sub> ) <sub>2</sub> CHCH <sub>2</sub>	0.759	0.748	3.522	3.515	1.385	1.336	1.289	1.244
CH <sub>3</sub> (CH <sub>2</sub> ) <sub>3</sub>	0.813	0.819	3.642	3.638	1.456	1.475	1.360	1.378
(CH <sub>3</sub> CH <sub>2</sub> ) <sub>2</sub> CH	0.805	0.896	3.692	3.863	1.600	1.695	1.405	1.548
(CH <sub>3</sub> ) <sub>2</sub> CHCH(CH <sub>3</sub> )	0.841	0.843	3.842	3.915	1.635	1.585	1.475	1.446
(CH <sub>3</sub> ) <sub>3</sub> CCH <sub>2</sub>	0.928	0.909	3.995	4.005	1.724	1.722	1.617	1.573
CH <sub>3</sub> CH <sub>2</sub> CH <sub>2</sub> CH(CH <sub>3</sub> )	0.889	0.910	3.937	3.911	1.725	1.724	1.553	1.576
CH <sub>3</sub> CH <sub>2</sub> C(CH <sub>3</sub> ) <sub>2</sub>	0.924	0.904	3.920	3.860	1.809	1.829	1.610	1.606
CH <sub>3</sub> CH <sub>2</sub> CH(CH <sub>3</sub> )CH <sub>2</sub>	0.959	0.953	4.065	4.040	1.780	1.783	1.661	1.647
(CH <sub>3</sub> ) <sub>2</sub> CHCH <sub>2</sub> CH <sub>2</sub>	1.003	1.010	4.177	4.181	1.834	1.894	1.720	1.754
CH <sub>3</sub> (CH <sub>2</sub> ) <sub>4</sub>	1.057	0.984	4.289	4.228	1.894	1.825	1.785	1.699

\* Eqn. 3.

\*\* See ref. 16, Table III.

\*\*\* Eqn. 2.

§ Eqn. 9.

§§ Eqn. 8.

TABLE V

CONNECTIVITY DATA COMPARED TO LOG  $k'$  FOR THE BUTYLBENZAMIDES

For general structure, see Table I.

$R$	Partisil ODS-2 $\log k'$	${}^5\chi_{PC}$	${}^6\chi_P^v$
$\text{CH}_3(\text{CH}_2)_3$	3.946	1.32495	0.28953
$(\text{CH}_3)_2\text{CHCH}_2$	3.786	1.46999	0.26843
$\text{CH}_3\text{CH}_2\text{CH}(\text{CH}_3)$	3.638	1.81043	0.25137
$(\text{CH}_3)_3\text{C}$	3.768	2.63726	0.23159

The third regression coefficient derived through application of the solvophobic theory was the parameter  $C$ . The value of  $C$  was determined for the  $\text{C}_1$ - $\text{C}_5$  N-alkylbenzamides (Tables II and III, ref. 16) and used to evaluate  $\Delta A$ , the contact surface area of the associated solute-bonded ligand complex (Table V, ref. 16). Results of the best two-variable regression of connectivity indices on  $\Delta A$  (in  $\text{\AA}^2$ ) are given in eqns. 14 and 15:

Partisil ODS-2

$$\Delta A = 0.337 (0.039) [{}^0\chi]^2 + 36.429 (6.130) [{}^6\chi_{PC}]^{-1} + 42.878 (6.112)$$

$$r = 0.9220 \quad (14)$$

Ultrasphere ODS

$$\Delta A = -703.697 (36.660) [{}^0\chi]^{-1} + 24.030 (3.191) [{}^5\chi_{PC}]^{-1} + 147.197 (3.187)$$

$$r = 0.9835 \quad (15)$$

TABLE VI

COMPARISON OF BRANCHED TO UNBRANCHED PORTIONS IN THE  $\text{C}_1$ - $\text{C}_5$  N-ALKYLBENZAMIDES

For general structure, see Table I.

$R$	${}^6\chi_{PC}/{}^6\chi_P^v$
$\text{CH}_3$	11.604
$\text{CH}_3\text{CH}_2$	9.589
$\text{CH}_3\text{CH}_2\text{CH}_2$	7.410
$(\text{CH}_3)_2\text{CH}$	10.389
$\text{CH}_3(\text{CH}_2)_3$	5.777
$(\text{CH}_3)_2\text{CHCH}_2$	7.463
$\text{CH}_3\text{CH}_2\text{CH}(\text{CH}_3)$	9.278
$(\text{CH}_3)_3\text{C}$	13.421
$\text{CH}_3(\text{CH}_2)_4$	5.091
$(\text{CH}_3)_2\text{CHCH}_2\text{CH}_2$	5.363
$\text{CH}_3\text{CH}_2\text{CH}(\text{CH}_3)\text{CH}_2$	6.365
$\text{CH}_3\text{CH}_2\text{CH}_2\text{CH}(\text{CH}_3)$	7.825
$(\text{CH}_3\text{CH}_2)_2\text{CH}$	8.477
$(\text{CH}_3)_3\text{CCH}_2$	8.694
$(\text{CH}_3)_2\text{CHCH}(\text{CH}_3)$	10.034
$\text{CH}_3\text{CH}_2\text{C}(\text{CH}_3)_2$	12.810



The correlation of molecular connectivity with  $\Delta A$  was much better for the Ultra-sphere ODS column than for the Partisil ODS-2 column. Solute structure alone may not account for all of the variation in the contact surface area, since the solvent as well as the bonded ligand itself must play a part in determining the contact surface area between the solute and the ligand. Because the configurations of the two bonded phases may not be alike due to differences in bonding conditions, the fact is understandable that different connectivity indices were chosen to correlate with the contact surface area,  $\Delta A$ , on these two columns.

The molecular connectivity indices were also regressed on the calculated total molecular surface areas (TSA) for the C<sub>1</sub>-C<sub>5</sub> N-alkylbenzamides and the results are described by eqn. 16:

$$\text{TSA} = 37.212 (1.649)^{1\chi} - 58.877 (12.108) [{}^2\chi^v]^{-1} + 15.980 (13.620) \quad (16)$$

$$r = 0.9971$$

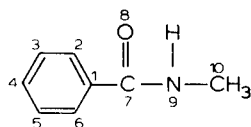
The  ${}^2\chi^v$  index does reflect some degree of branching because the value of the index increases with increases in the number of short branch points. The connectivity indices correlated with TSA are not the same as the indices chosen as the best variables for  $\Delta A$  on either column.

## CONCLUSIONS

A high degree of correlation was observed between molecular connectivity data and measured and calculated reversed-phase chromatographic retention data. The results suggest that bulk, branching, and site of hydrocarbon branching are the controlling factors in the retention of the C<sub>1</sub>-C<sub>5</sub> N-alkylbenzamides and molecular connectivity allows for the quantitation of these molecular features. The same connectivity indices were chosen upon regression of retention data obtained on different columns. Inconsistent correlations were observed between the solute-bonded ligand contact surface area and molecular connectivity indices.

## APPENDIX

### *Calculation of molecular connectivity indices*



I

The calculations of the molecular connectivity indices through sixth order for N-methylbenzamide, I, are outlined. The atoms of the molecular structure are referred to as vertices, and the bonds are called edges. Each non-hydrogen atom (ten in

this example) is assigned a vertex value ( $\delta$ ) equal to the number of non-hydrogen atoms connected to it, and a vertex valence value ( $\delta^v$ ) calculated by subtracting the number of hydrogen atoms attached to that atom from the number of valence electrons in the atom. These values are given in Table A1 for N-methylbenzamide.

TABLE A1  
VERTEX AND VERTEX VALENCE VALUES FOR N-METHYLBENZAMIDE

	<i>Atom number</i>									
	<i>1</i>	<i>2</i>	<i>3</i>	<i>4</i>	<i>5</i>	<i>6</i>	<i>7</i>	<i>8</i>	<i>9</i>	<i>10</i>
$\delta$	3	2	2	2	2	2	3	1	2	1
$\delta^v$	4	3	3	3	3	3	4	6	4	1

The vertex values,  $\delta$ , are used to calculate the connectivity level indices,  $\chi$ , in which the nature of the atom is not taken into consideration. These indices were expanded by allowing for differences in the identity of atoms and differences in bond order by introducing a valence level index,  $\chi^v$ , which is calculated by using the vertex valence values,  $\delta^v$ .

The molecular structure is broken down into parts called subgraphs. If a graph is taken as being composed of vertices alone (*i.e.*, no edges), the order of this index is zero order. The number of edges, or bonds, in a subgraph is the order of that subgraph and appears as the leftside superscript to the symbol,  $\chi$ , or  $\chi^v$ . There are four types of subgraphs which may be present in a molecule: paths, clusters, path/clusters, and chains which appear as the subscripts P, C, PC, and CH respectively. If no subscript appears it is understood to be a path index.

The actual number of subgraphs of each order,  $m$  (through sixth order), and type,  $t$ , present in N-methylbenzamide are listed in Table A2. The dashes in this table indicate that for a given order it is not possible to have a subgraph of that type in any molecule. Some of the representative subgraphs present in N-methylbenzamide are illustrated in Fig. A1.

TABLE A2  
NUMBER OF TERMS ( $t$ ) FOR ORDER ( $m$ ) OF  ${}^m\chi_t$  INDICES FOR N-METHYLBENZAMIDE

<i>Order</i>	<i>Type</i>			
	<i>Path</i>	<i>Cluster</i>	<i>Path cluster</i>	<i>Chain</i>
0	—	—	—	—
1	10	—	—	—
2	12	—	—	—
3	14	2	—	0
4	14	0	7	0
5	14	1	12	0
6	8	0	19	1

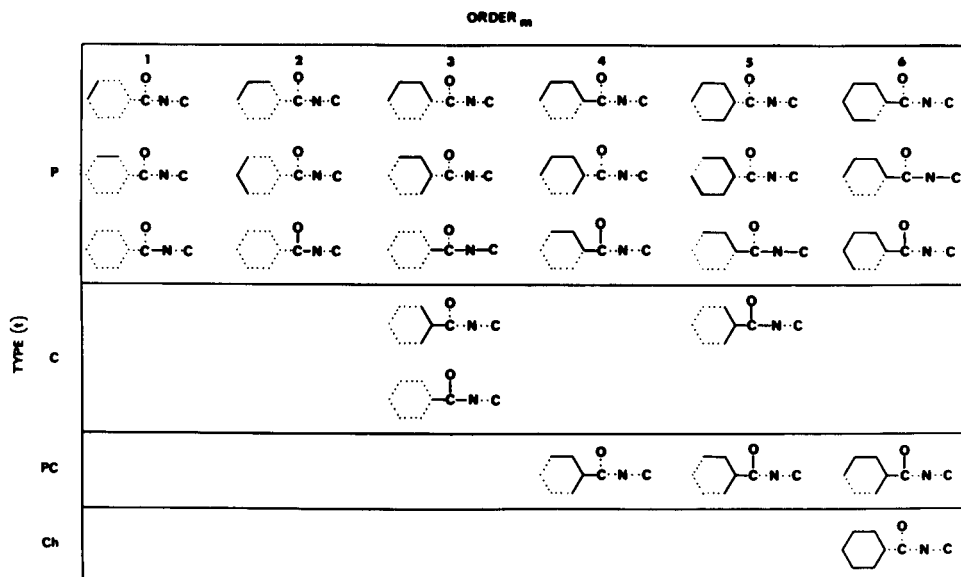


Fig. A1. Representative subgraphs (solid lines) of N-methylbenzamide.

Zero order indices are calculated by summing the reciprocal square roots of the vertex values,  $\delta$ , or of the vertex valence values,  $\delta^v$ . For subgraphs of order higher than zero, the reciprocal square root of the products of the  $\delta$  or  $\delta^v$  values assigned to the atoms participating in a bond or bonds is the value for that subgraph. All of the subgraph values are summed to give the  $\chi$  or  $\chi^v$  indices for the molecule. Molecular connectivity calculations were performed on the IBM 370/158, Computer Services, Auburn University. The program (CFUNC) used to calculate molecular connectivity indices was obtained from Dr. Lowell Hall (Eastern Nazarene College, Quincy, MA, U.S.A.). More detailed discussion of these calculations can be found in the literature<sup>3,14</sup>.

#### ACKNOWLEDGEMENT

We sincerely appreciate the support of the American Foundation for Pharmaceutical Education Silas M. Burroughs Memorial Fellowship for M.J.M.W.

#### REFERENCES

- 1 W. Worthy, *Chem. Eng. News*, 58 (33) (1980) 30.
- 2 M. Randic, *J. Amer. Chem. Soc.*, 97 (1975) 6609.
- 3 L. B. Kier and L. H. Hall, *Molecular Connectivity in Chemistry and Drug Research*, Academic Press, New York, 1976.
- 4 D. R. Henry and J. R. Block, *J. Med. Chem.*, 22 (1979) 465.
- 5 T. DiPaolo, L. B. Kier and L. H. Hall, *J. Pharm. Sci.*, 68 (1979) 39.
- 6 B. K. Evans, K. C. James and D. K. Luscombe, *J. Pharm. Sci.*, 68 (1979) 370.

- 7 R. A. Glennon, L. B. Kier and A. T. Shulgin, *J. Pharm. Sci.*, 68 (1979) 906.
- 8 L. B. Kier, *J. Pharm. Sci.*, 69 (1980) 1034.
- 9 Y. Michotte and D. L. Massart, *J. Pharm. Sci.*, 66 (1977) 1630.
- 10 J. S. Millership and A. D. Woolfson, *J. Pharm. Pharmacol.*, 30 (1978) 483.
- 11 L. B. Kier and L. H. Hall, *J. Pharm. Sci.*, 68 (1979) 120.
- 12 B. L. Karger, J. R. Gant, A. Hartkopf and P. H. Weiner, *J. Chromatogr.*, 128 (1976) 65.
- 13 H. Colin and G. Guiochon, *J. Chromatogr. Sci.*, 18 (1980) 54.
- 14 L. B. Kier and L. H. Hall, *J. Med. Chem.*, 20 (1977) 1631.
- 15 M. J. M. Wells and C. R. Clark, *J. Chromatogr.*, 235 (1982) 31.
- 16 M. J. M. Wells, C. R. Clark and R. M. Patterson, *J. Chromatogr.*, 235 (1982) 43.
- 17 O. Sinanoglu and S. Abdunur, *Fed. Proc. Fed. Amer. Soc. Exp. Biol.*, 24, No. 2, Part III (1965) S-12.
- 18 O. Sinanoglu, in B. Pullman (Editor), *Molecular Associations in Biology*, Academic Press, New York, 1968.
- 19 Cs. Horváth, W. Melander and I. Molnár, *J. Chromatogr.*, 125 (1976) 129.

CHROM. 14,279

## GAS CHROMATOGRAPHY AND MASS SPECTROMETRY OF N-TRIFLUOROACETYL *n*-BUTYL ESTERS OF ALKYLATED TYROSINES AND LYSINES

MUNENORI SAKAMOTO\*, NATSUKO TSUJI, FUMITAKA NAKAYAMA and KOH-ICHI KAJIYAMA

*Department of Textile and Polymeric Materials, Tokyo Institute of Technology, Meguro-ku, Tokyo (Japan)*  
(First received May 18th, 1981; revised manuscript received August 10th, 1981)

---

### SUMMARY

The gas chromatographic behaviour of three *O-n*-alkyltyrosines, four  $N^{\epsilon}$ -*n*-alkyllysines and three  $N^{\epsilon},N^{\epsilon}$ -di-*n*-alkyllysines was studied as their N-trifluoroacetyl *n*-butyl ester (BTFA) derivatives on columns of OV-17 and Dexsil 300 GC. The retention indices and some other retention parameters are discussed in relation to the chemical structures of the amino acids. Mass fragmentation patterns of the BTFA derivatives of these amino acids obtained by gas chromatography–mass spectrometry with electron impact ionization are also described.

---

### INTRODUCTION

Gehrke and co-workers<sup>1,2</sup> established a gas chromatographic (GC) method of analysis of protein amino acids as their N(O)-trifluoroacetyl *n*-butyl ester (BTFA) derivatives. Since then GC techniques have widely been used for the analysis of protein amino acids as well as unusual amino acids from various sources, after conversion into BTFA derivatives or other N(O)-trifluoroacetyl esters.

We have been engaged in the utilization of the GC method for the analysis of unusual amino acids present in the hydrolyzates of chemically modified proteins<sup>3–8</sup>. These amino acids originate from the chemical reactions of the reactive functional groups in the protein side chains. We are interested in finding a correlation between the GC retention characteristics and the chemical structures of the amino acids, in the expectation that, once established, this would be useful for the identification of unknown peaks in the chromatograms of complex amino acid mixtures such as the hydrolyzates of chemically modified proteins, when authentic samples are not available.

In a previous paper<sup>3</sup>, the GC characteristics of various S-substituted cysteines were studied as their BTFA derivatives. The present investigation concerns the GC characteristics of *O*-alkyltyrosines,  $N^{\epsilon}$ -alkyllysines and  $N^{\epsilon},N^{\epsilon}$ -dialkyllysines as their BTFA derivatives and the comparison with the GC characteristics of the BTFA derivatives of S-alkylcysteines. Cysteine, tyrosine and lysine residues in proteins are

susceptible to alkylation with various reagents. Lysine residues may be alkylated to give N<sup>ε</sup>-alkyllysine and/or N<sup>ε</sup>,N<sup>ε</sup>-dialkyllysine residues, depending on the reaction conditions employed. The alkyl-hetero atom bonds in the alkylated amino acid residues are more or less stable under the acid hydrolysis conditions, and the alkylated amino acids should be found in the hydrolyzates of alkylated proteins.

## EXPERIMENTAL

### *Amino acids*

O-Methyl-L-tyrosine<sup>9</sup>, O-ethyl-L-tyrosine hydrochloride<sup>10</sup> and O-*n*-propyl-L-tyrosine hydrochloride<sup>10</sup> were prepared from L-tyrosine. N<sup>ε</sup>-Methyl-L-lysine was a gift of Professor G. Ebert, University of Marburg/Lahn, G.F.R. N<sup>ε</sup>-Ethyl-DL-lysine<sup>11</sup> was obtained by the reaction of 5- $\delta$ -bromobutylhydantoin with ethylamine, followed by alkaline hydrolysis and was purified in the form of the hydrochloride, m.p. 210°C (decomp.). N<sup>ε</sup>-*n*-Propyl-DL-lysine, m.p. 205.5°C (decomp.), N<sup>ε</sup>-*n*-butyl-DL-lysine hydrobromide, m.p. 225°C (decomp.), and N<sup>ε</sup>,N<sup>ε</sup>-dimethyl-DL-lysine dioxalate, m.p. 143–144°C (decomp.), were prepared in a similar way. N<sup>ε</sup>,N<sup>ε</sup>-Diethyl-DL-lysine and N<sup>ε</sup>,N<sup>ε</sup>-di-*n*-propyl-DL-lysine were obtained as oils when the corresponding hydantoins were hydrolyzed. They could not be crystallized. Oily oxalates were used for conversion into BTFA derivatives.

Other amino acids used were as described previously<sup>3,4</sup>.

### *Reagents*

Ethyl acetate of guaranteed reagent grade (Wako, Tokyo, Japan) was purified according to Hurd and Strong<sup>12</sup>, and heptafluorobutyric anhydride of the same grade (Tokyo Chemical, Tokyo, Japan) was used without further purification. Other reagents used were as described previously<sup>3</sup>.

### *Derivatization*

The conversion of amino acids into their BTFA derivatives was carried out according to Kaiser *et al.*<sup>2</sup>. N(O)-Heptafluorobutyryl *n*-butyl esters (BHFB) were prepared by reaction of the *n*-butyl esters of the amino acid hydrochlorides<sup>2</sup> in a similar manner to the preparation of N(O)-heptafluorobutyryl isobutyl esters<sup>13</sup>. In both BTFA and BHFB preparations, the concentration of each amino acid in the final acylation mixture was *ca.* 0.25  $\mu\text{g}/\mu\text{l}$ .

### *Gas chromatography*

A Shimadzu Model GC-4BMPF dual-column gas chromatograph, equipped with hydrogen flame ionization detectors (FID) and a linear temperature programmer, was used. One of the two glass columns, 1 m  $\times$  0.3 cm I.D., was packed with 1.5% (w/w) OV-17 on acid-washed and heat-treated high-performance Chromosorb G (80–100 mesh), and the other with 1.5% (w/w) Dexsil 300 GC on the same quality Chromosorb G. Both column packings were purchased from Nihon Chromato (Tokyo, Japan). The carrier gas (N<sub>2</sub>) flow-rate was 70 ml/min. Other chromatographic conditions were as given previously<sup>3</sup>.

### *Gas chromatography-mass spectrometry (GC-MS)*

The GC-MS measurements were carried out on a Shimadzu-LKB Model GC-

MS 9000 gas chromatograph-mass spectrometer combined with a Shimadzu Model GC-MS PAC 300 on-line data processing system.

GC-MS retention indices were determined from the total ion current (TIC) chromatogram obtained at 20 eV with a glass column (1 m × 0.3 cm I.D.) packed with the same quality OV-17 packings used for GC. The temperature programme was the same as that used for the determination of GC retention indices. The flow-rate of the carrier gas (He) was 30 ml/min. In most cases, BTFA-amino acids were injected with appropriate pairs of even carbon-number *n*-paraffins, as in the case of the GC determination. Reproducibility of the retention times was generally good so that, in some cases, BTFA-amino acids and *n*-paraffins were injected separately in two successive chromatographic runs and the retention indices were calculated from the retention times thus determined separately.

Mass spectra were determined on the OV-17 column described above or on columns packed with other OV-17 packings: 2% (w/w) on Chromosorb W HP (80-100 mesh) and 2% (w/w) on Gas-Chrom Q (80-100 mesh), both purchased from Wako. They were obtained at 70 eV with an accelerating potential of 3.5 kV. The ion source was maintained at 290°C in most cases and the separator was kept at 280°C or at a temperature 10°C lower than the ion-source temperature. The column temperature was programmed at a rate of 5°C/min from 140°C to 210°C from 160°C to 210°C. The usual amount of sample injected was 1 µl.

## RESULTS AND DISCUSSION

The abbreviations of the amino acids used are listed in Table I. O-Alkyltyrosines, N<sup>ε</sup>-alkyllysines and N<sup>ε</sup>,N<sup>ε</sup>-dialkyllysines were synthesized in this laboratory, except for NML. OET, DEL and DPL could not be obtained in pure form; however,

TABLE I  
ABBREVIATIONS USED FOR AMINO ACIDS

<i>Class</i>	<i>No.</i>	<i>Name</i>	<i>Abbreviation</i>
(A) O-Alkyltyrosines	1	O-Methyltyrosine	OMT
	2	O-Ethyltyrosine	OET
	3	O- <i>n</i> -Propyltyrosine	OPT
(B) N <sup>ε</sup> -Alkyllysines	4	N <sup>ε</sup> -Methyllysine	NML
	5	N <sup>ε</sup> -Ethyllysine	NEL
	6	N <sup>ε</sup> - <i>n</i> -Propyllysine	NPL
	7	N <sup>ε</sup> - <i>n</i> -Butyllysine	NBL
(C) N <sup>ε</sup> ,N <sup>ε</sup> -Dialkyllysines	8	N <sup>ε</sup> ,N <sup>ε</sup> -Dimethyllysine	DML
	9	N <sup>ε</sup> ,N <sup>ε</sup> -Diethyllysine	DEL
	10	N <sup>ε</sup> ,N <sup>ε</sup> -Di- <i>n</i> -propyllysine	DPL
(D) S-Alkylcysteines	11	S-Methylcysteine	SMC
	12	S-Ethylcysteine	SEC
	13	S- <i>n</i> -Propylcysteine	SPC
	14	S- <i>n</i> -Butylcysteine	SBC
(E) Others	15	Cysteine	CySH
	16	Lysine	Lys
	17	Norleucine	Norleu
	18	Phenylalanine	Phe
	19	Tyrosine	Tyr

their GC peaks were clearly distinguished from the peaks of impurities, and the GC-MS analysis confirmed that the main chromatographic peaks observed were those of the expected amino acids.

### GC retention

The GC retention data of the BTFA-amino acids were recorded on two thermally stable liquid phases, OV-17 and Dexsil 300 GC, by the linear temperature programming method used previously<sup>3</sup>. The Kovát's retention indices,  $I^{14}$ , were determined as previously<sup>3</sup>, in order to investigate the correlation between the amino acid structure and the GC retention behaviour. The retention indices of BTFA derivatives of O-alkyltyrosines and N<sup>ε</sup>-alkyllysines were fairly reproducible. However, those of the BTFA derivatives of DML and DEL were significantly variable, especially on polar OV-17.

Table II lists the retention indices of BTFA-amino acids determined in this work as well as those reported earlier. The difference,  $\Delta I$ , between the two retention indices determined on the stationary phases of different polarity is also given. The  $\Delta I$  values of BTFA derivatives of three O-alkyltyrosines range between 116 and 142, larger than the  $\Delta I$  value of BTFA-Phe. The  $\Delta I$  values of BTFA derivatives of four N<sup>ε</sup>-alkyllysines range between 24 and 51, slightly smaller than those of BTFA derivatives of  $\alpha,\omega$ -diaminomonocarboxylic acids<sup>3</sup>.

Fig. 1 shows the good linear relationships between the retention index and the molecular weight for BTFA derivatives of O-alkyltyrosines and N<sup>ε</sup>-alkyllysines. It was assumed previously<sup>3</sup> that the retention index of a BTFA-amino acid was the sum

TABLE II  
RETENTION INDICES OF BTFA-AMINO ACIDS

Class	No.	Amino acid	Retention index, $I$				Ref.
			OV-17 by GC	OV-17 by GC-MS	Dexsil 300 GC by GC	Difference, $\Delta I$ , by GC	
(A)	1	OMT	2118	2118	1986	132	
	2	OET	2181	2164	2039	142	
	3	OPT	2246	2245	2130	116	
(B)	4	NML	2030	2055	1991	39	
	5	NEL	2103	2074	2052	51	
	6	NPL	2141	2115	2117	24	
	7	NBL	2217	2200	2190	27	
(C)	8	DML	1911	1930	1909	2	
	9	DEL	1952	2018	1932	20	
	10	DPL	2063	2046	2048	15	
(D)	11	SMC	1627	—	1530	97	3
	12	SEC	1680	—	1595	85	3
	13	SPC	1752	—	1670	82	3
	14	SBC	1835	—	1757	78	3
(E)	15	CySH	1499	—	1470	29	
	16	Lys	2000	2000	1930	70	3
	17	Norleu	1478	—	1452	26	3
	18	Phe	1852	—	1746	106	
	19	Tyr	1910	1907	1870	40	



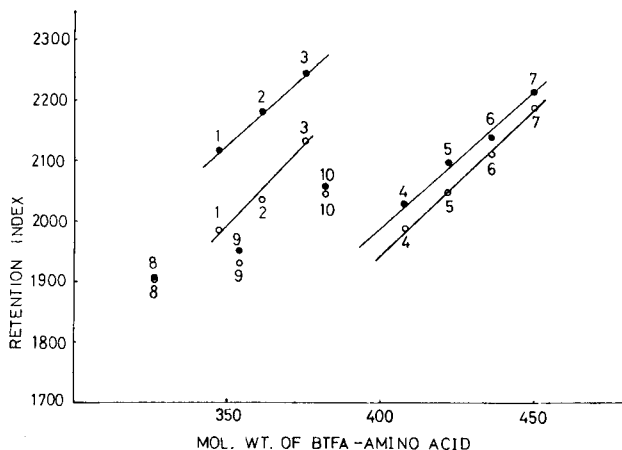


Fig. 1. Retention indices of BTFA derivatives of O-alkyltyrosines, N<sup>ε</sup>-alkyllysines and N<sup>ε</sup>,N<sup>ε</sup>-dialkyllysines on OV-17 (●) and Dexsil 300 GC (○) versus their molecular weights. Compounds are numbered as in Table I.

of the group retention indices,  $i$ , of the individual structural units, and an attempt was made to predict the retention indices of BTFA-amino acids from their chemical structures. From the plots of the retention indices versus molecular weights, group retention indices,  $i_C$ , of a methylene of the O- or N<sup>ε</sup>-alkyl groups and of a C<sub>4</sub>H<sub>9</sub>OCOCH(NHCOF<sub>3</sub>)CH<sub>2</sub>C<sub>6</sub>H<sub>4</sub>O-group,  $i_R$ , can be calculated (see Table III). The difference between  $i_R$  and the retention index of BTFA-Phe corresponds to the group retention index,  $i_O$ , of ether oxygen. The  $i_O$  values are about two thirds of the group retention indices of thioether sulphur<sup>3</sup> found for BTFA derivatives of S-substituted cysteines.

By definition, the retention indices of neighbouring members of *n*-paraffins differ by 100. The observed values of  $i_C$  are apparently lower than 100, as is the case for BTFA derivatives of S-alkylcysteines<sup>3</sup>. The values observed for BTFA derivatives of N<sup>ε</sup>-alkyllysines are much lower than the group retention indices of the methylene unit in BTFA-Lys (140 on either OV-17 or Dexsil 300 GC)<sup>3</sup>. From the plots of the retention indices versus molecular weights, the group retention index,  $i_R$ , of a

TABLE III  
GROUP RETENTION INDICES,  $i$

Class		OV-17	Dexsil 300 GC	Ref.
(A)	$i_C$	64	73	
	$i_R$	2053	1907	
	$i_O$	201	161	
(B)	$i_C$	63	67	
	$i_R$	1965	1915	
(D)	$i_{L\text{-NTFA}}$	487	463	
	$i_C$	77	81	3
	$i_S$	297	239	3

$C_4H_9OCOCH(NHCOCF_3)(CH_2)_4NCOCF_3$  group is obtained. Then, the difference between  $i_R$  and the retention index of BTFA-Norleu is assumed to be the group retention index,  $i_{L-NTF_3}$ , of a tertiary  $NCOCF_3$  group. The observed  $i_{L-NTF_3}$  values in Table III are larger than the group retention indices for a  $NHCOCF_3$  group observed for BTFA derivatives of  $\alpha,\omega$ -diaminomonocarboxylic acids<sup>3</sup>.

As stated earlier, the retention indices of BTFA derivatives of DML and DEL varied greatly with slight changes in the column conditions. The retention indices of these compounds (Table II) are the lowest of those determined on different occasions. The retention indices of BTFA derivatives of  $N^{\epsilon},N^{\epsilon}$ -dialkyllysines (Table II) increase with increasing molecular weight. It should be mentioned, however, that in another set of determinations the retention indices of BTFA-DML and BTFA-DEL were unusually high (2270 and 2200, respectively) on OV-17. The GC peak of BTFA-DML was broad with significant tailing. It seems that BTFA-DML with a tertiary amino group shielded by the small methyl group interacts most with the column packings in this particular case.

The GC-MS retention indices of BTFA derivatives of amino acids were determined from the total ion current (TIC) chromatograms on OV-17. The temperature programme and the column packings used were the same as those for GC, but the column size and the carrier gas flow-rate were different (see Experimental). The GC-MS retention indices were nearly equal to those determined by GC (see Table II). The shape of the peak of BTFA-DML in the TIC chromatogram was as

TABLE IV

DIFFERENCE,  $\Delta Me$ , BETWEEN EFFECTIVE AND ACTUAL MOLECULAR WEIGHTS OF BTFA-AMINO ACIDS

Class	No.	Amino acid	Mol. wt. of BTFA-amino acid	$\Delta Me$		Ref.
				OV-17	Dexsil 300 GC	
(A)	1	OMT	347.3	- 48.2	- 66.7	
	2	OET	361.4	- 53.5	- 73.4	
	3	OPT	375.4	- 58.4	- 74.6	
(B)	4	NML	408.3	-121.6	-127.0	
	5	NEL	422.4	-125.4	-132.6	
	6	NPL	436.4	-134.1	-137.5	
	7	NBL	450.4	-137.4	-141.2	
(C)	8	DML	326.4	- 56.3	- 56.6	
	9	DEL	354.4	- 78.6	- 81.4	
	10	DPL	382.5	- 91.1	- 93.2	
(D)	11	SMC	287.3	- 57.1	- 70.7	3
	12	SEC	301.3	- 63.7	- 75.6	3
	13	SPC	315.4	- 67.6	- 79.1	3
	14	SBC	329.4	- 69.9	- 80.9	3
(E)	15	CySH	369.3	-157.0	-161.1	
	16	Lys	394.3	-111.8	-121.6	3
	17	Norleu	283.3	- 74.0	- 77.6	3
	18	Phe	317.3	- 55.5	- 70.4	
	19	Tyr	429.3	-159.4	-165.0	

sharp as other BTFA-amino acids, and the observed retention index compared well with the lowest retention index observed by GC.

#### *ΔMe of Evans and Smith*

From Kováts' retention index, Evans and Smith<sup>15,16</sup> proposed another retention parameter,  $\Delta Me$ . Table IV gives the  $\Delta Me$  values of BTFA-amino acids calculated from their retention indices on OV-17 and Dexsil 300 GC. It was reported<sup>16,17</sup> that  $\Delta Me$  was virtually constant throughout a homologous series, except for a few initial homologues. The  $\Delta Me$  values of BTFA derivatives of O-alkyltyrosines range between  $-48$  and  $-58$  on OV-17 and  $-67$  and  $-75$  on Dexsil 300 GC. These values are in agreement with the  $\Delta Me$  values of BTFA-Phe and very close to the reported  $\Delta Me$  values of BTFA derivatives of monoaminomonocarboxylic acids<sup>3</sup>. Thus, ether oxygen has little influence on the  $\Delta Me$  value as in the case<sup>3</sup> of thioether sulphur.

In previous work<sup>3</sup> it was shown that the second  $CF_3CONH$  group in BTFA derivatives of  $\alpha,\omega$ -diaminomonocarboxylic acids has a significant effect on the  $\Delta Me$  value. The  $\Delta Me$  values of BTFA derivatives of  $N^\epsilon$ -alkyllysines are nearly equal to those of BTFA derivatives, of  $\alpha,\omega$ -diaminomonocarboxylic acids. The  $\Delta Me$  value of BTFA-DPL lies between those of BTFA derivatives of monoaminomonocarboxylic acids and  $\alpha,\omega$ -diaminomonocarboxylic acids. The absolute  $\Delta Me$  values of BTFA-DML are much lower than those of BTFA-DPL on both liquid phases.

Finally, retention indices of BTFA derivatives of O-alkyltyrosines,  $N^\epsilon$ -alkyllysines and S-alkylcysteines are compared (Table V). The retention index of an S-alkylcysteine and that of the corresponding  $N^\epsilon$ -alkyllysine differ on average by 339 and 450 on OV-17 and Dexsil 300 GC, respectively. The lysine derivative is eluted before the corresponding O-alkyltyrosine on OV-17, while the two are eluted at the same time on Dexsil 300 GC.  $N^\epsilon,N^\epsilon$ -Dialkyllysines have shorter retention times than the corresponding  $N^\epsilon$ -monoalkyllysines on both liquid phases.

Table V also shows the difference in the retention indices of BTFA derivatives of CySH, Lys and Tyr. The difference in the retention indices of BTFA-Lys and BTFA-Tyr is much different from that observed for the BTFA derivatives of  $N^\epsilon$ -

TABLE V

COMPARISON OF RETENTION INDICES OF BTFA DERIVATIVES OF O-ALKYLTYROSINES,  $N^\epsilon$ -ALKYLLYSINES AND S-ALKYLCYSTEINES

Retention indices:  $I_{AX}$  of a class (A) amino acid with an alkyl substituent, X;  $I_{BX}$  of a class (B) amino acid with an alkyl substituent, X;  $I_{DX}$  of a class (D) amino acid with an alkyl substituent, X.

Alkyl substituent, X	$I_{AX} - I_{BX}$		$I_{BX} - I_{DX}$		$I_{AX} - I_{DX}$	
	OV-17	Dexsil 300 GC	OV-17	Dexsil 300 GC	OV-17	Dexsil 300 GC
H*	-90	-60	501	460	411	400
CH <sub>3</sub>	88	-5	403	461	491	456
C <sub>2</sub> H <sub>5</sub>	78	-13	423	457	501	444
n-C <sub>3</sub> H <sub>7</sub>	105	13	389	447	494	460
n-C <sub>4</sub> H <sub>9</sub>	-	-	382	433	-	-

\* The actual substituent in the BTFA derivative is a  $CF_3CO$  group.

alkyllysines and O-alkyltyrosines. Similarly, the difference in retention indices of BTFA-CySH and BTFA-Tyr is also different from that of BTFA derivatives of S-alkylcysteines and O-alkyltyrosines. Thus, the contribution of the  $\text{CF}_3\text{CO}$  group to the retention index is dependent on the atom to which it is bound.

#### FID molar response

FID molar response is an additive property of the structural features, and the contribution of a structural unit to the molar response is usually expressed as the effective carbon number (ecn)<sup>17</sup>. The effective carbon number of a molecule (ECN) is a sum of the ecn values of the individual structural units. The ecn value of a carbon atom in an alkyl or an aryl group is 1.0 and that of an oxygen atom in ether is  $-1.0$ <sup>17</sup>. In previous work<sup>3</sup>, the ecn values of  $-\text{CO}_2-$  (ester) and  $-\text{NHCOCF}_3$  were estimated to be  $-0.5$  and  $-0.7$ , respectively, for BTFA-amino acids. The last value was assumed to be applicable to the trifluoroacetamide groups in BTFA derivatives of  $\text{N}^{\epsilon}$ -alkyllysines. By use of these values, the relative molar response (RMR) to BTFA-Glu was calculated.

The RMR values of BTFA derivatives of O-alkyltyrosines and  $\text{N}^{\epsilon}$ -alkyllysines available in pure form were determined on OV-17 and Dexsil 300 GC as described previously<sup>3</sup>. Table VI shows that the values observed on either column agree satisfactorily with each other, and the RMR values calculated from the ECN values compare well with the observed values. Considering the results of Islam and Darbre<sup>18</sup> and of Felt and Hušek<sup>19</sup> for different types of volatile derivatives of amino acids, it seems that the ecn values of perfluorocarboxamide groups are influenced by the FID apparatus used and by the operating conditions.

TABLE VI

FID MOLAR RESPONSES (RMR) OF BTFA-AMINO ACIDS RELATIVE TO BTFA-GLUTAMIC ACID

Class	No.	Amino acid	RMR calc.		RMR found	
			ECN	RMR	OV-17	Dexsil 300 GC
(A)	1	OMT	10.8	1.16	1.17	1.18
	3	OPT	12.8	1.38	1.26	1.31
(B)	4	NML	8.1	0.87	0.94	0.91
	5	NEL	9.1	0.98	0.99	1.05
	6	NPL	10.1	1.09	1.05	1.11
	7	NBL	11.1	1.19	1.14	1.27

#### Gas chromatography-mass spectrometry

The GC-MS of BTFA derivatives of 19 protein amino acids has been studied by Gelpi *et al.*<sup>20</sup> by electron impact ionization at 20 eV. Leimer *et al.*<sup>21</sup> reported the GC-MS of BTFA derivatives of 49 amino acids by electron impact ionization at 70 eV. In this work, the mass spectra of BTFA derivatives of O-alkyltyrosines,  $\text{N}^{\epsilon}$ -alkyllysines and  $\text{N}^{\epsilon}, \text{N}^{\epsilon}$ -dialkyllysines were taken at 70 eV. Some of the assignments made in this work for the fragment ions must be considered as tentative since no

TABLE VII

## MASS FRAGMENTATION PATTERNS OF BTFA DERIVATIVES OF O-ALKYLTYROSINES

r.a. = Relative abundance.

Ion	BTFA-Phe		BTFA-Tyr		BTFA-OMT		BTFA-OET		BTFA-OPT	
	m/z	r.a.	m/z	r.a.	m/z	r.a.	m/z	r.a.	m/z	r.a.
Molecular ion (M)	317	0.5	429	0.2	347	1	361	2	375	3
M - C <sub>4</sub> H <sub>9</sub> OCO	216	13	328	9	246	2	260	2	274	3
M - CF <sub>3</sub> CONH <sub>2</sub>	204	39	316	31	234	9	248	9	262	11
M - CF <sub>3</sub> CONH <sub>2</sub> - C <sub>4</sub> H <sub>8</sub>	148	80	260	93	178	5	192	4	206	2
M - CF <sub>3</sub> CONH <sub>2</sub> - C <sub>4</sub> H <sub>9</sub> O	131	15	243	13	161	2	175	1	189	0.4
M - C <sub>4</sub> H <sub>9</sub> OCO - CF <sub>3</sub> CO	119	10	231	5	149	1	163	1	177	0.4
M - C <sub>4</sub> H <sub>9</sub> OCO - CF <sub>3</sub> CONH <sub>2</sub>	103	18	215	7	133	3	147	2	161	0.3
M - C <sub>4</sub> H <sub>9</sub> OCOCHNHCOCF <sub>3</sub>	91	100	203	100	121	100	135	100	149	100
C <sub>2</sub> H <sub>2</sub> C <sub>6</sub> H <sub>4</sub> OH	-	-	119	2	119	1	119	3	119	6
CH <sub>2</sub> C <sub>6</sub> H <sub>4</sub> OH	-	-	107	4	107	1	107	48	107	95
CH <sub>2</sub> C <sub>6</sub> H <sub>5</sub>	91	100	91	4	91	2	91	4	91	5
C <sub>6</sub> H <sub>5</sub>	77	7	77	3	77	3	77	4	77	4

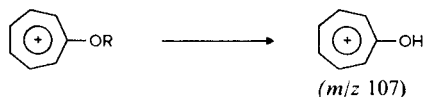
attempt was made to determine the elemental composition by high resolution measurements and there are several possible structures of different elemental compositions for some of the fragment ions. The ion formulae given in Tables VII-IX do not necessarily indicate the exact position of some of the hydrogen atoms and the charge designation is omitted for simplicity. The ions of  $m/z < 50$  are also omitted.

Table VII compares the mass fragmentation patterns of BTFA derivatives of Phe, Tyr and O-alkyltyrosines. The fragmentation patterns of the BTFA derivatives of the five aromatic amino acids are very similar. The most significant ions in the high  $m/z$  region are (M - CF<sub>3</sub>CONH<sub>2</sub>) ions. The base peaks are (M - C<sub>4</sub>H<sub>9</sub>OCOCHNHCOCF<sub>3</sub>) ions, which are actually stable tropylium ions:



X = H, OCOCF<sub>3</sub> or OR (R = alkyl group)

In the case of BTFA derivatives of O-alkyltyrosines, ions of  $m/z$  107 and 119 are formed. The relative abundance of the ion of  $m/z$  107 increases significantly with increasing carbon number of the O-alkyl group:



Characteristic ions for the BTFA derivatives of all the aromatic amino acids are CH<sub>2</sub>C<sub>6</sub>H<sub>5</sub> and C<sub>6</sub>H<sub>5</sub>, although their relative abundances are low.

The mass fragmentation patterns of BTFA-Phe and BTFA-Tyr given in Table VII are generally similar to those reported by Leimer *et al.*<sup>21</sup>. However, the fragmen-

TABLE VIII

MASS FRAGMENTATION PATTERNS OF BTFA DERIVATIVES OF N<sup>ε</sup>-ALKYLLYSINES

r.a. = Relative abundance.

Ion	BTFA-Lys		BTFA-NML		BTFA-NEL		BTFA-NPL		BTFA-NBL	
	<i>m/z</i>	<i>r.a.</i>	<i>m/z</i>	<i>r.a.</i>	<i>m/z</i>	<i>r.a.</i>	<i>m/z</i>	<i>r.a.</i>	<i>m/z</i>	<i>r.a.</i>
Molecular ion (M)	394	1	408	3	422	2	436	2	450	3
M - C <sub>4</sub> H <sub>9</sub> OH	320	5	334	41	348	17	362	38	376	14
M - CF <sub>3</sub> CO	297	—	331	6	325	6	339	13	353	6
M - C <sub>4</sub> H <sub>9</sub> OCO	293	5	307	23	321	11	335	24	349	12
M - CF <sub>3</sub> -C <sub>4</sub> H <sub>10</sub> OCO-H	195	2	209	10	223	6	237	9	251	4
(CF <sub>3</sub> CON)C <sub>8</sub> H <sub>17</sub>	—	—	—	—	—	—	—	—	224	23
(CF <sub>3</sub> CON)C <sub>7</sub> H <sub>15</sub>	—	—	—	—	—	—	210	41	210	9
(CF <sub>3</sub> CON)C <sub>6</sub> H <sub>13</sub>	—	—	—	—	196	22	196	19	196	2
(CF <sub>3</sub> CON)C <sub>5</sub> H <sub>11</sub>	182	1	182	20	182	11	182	3	182	50
(CF <sub>3</sub> CON)C <sub>5</sub> H <sub>9</sub>	180	100	180	56	180	41	180	86	180	57
(CF <sub>3</sub> CON)C <sub>4</sub> H <sub>9</sub>	168	4	168	10	168	3	168	100	168	4
(CF <sub>3</sub> CON)C <sub>3</sub> H <sub>7</sub>	154	1	154	4	154	100	154	5	154	2
(CF <sub>3</sub> CON)C <sub>3</sub> H <sub>5</sub>	152	4	152	9	152	9	152	13	152	8
(CF <sub>3</sub> CON)C <sub>2</sub> H <sub>5</sub>	140	3	140	100	140	7	140	35	140	100
(CF <sub>3</sub> CON)CH <sub>3</sub>	126	12	126	5	126	40	126	49	126	12
CF <sub>3</sub>	69	8	69	24	69	12	69	14	69	10
C <sub>4</sub> H <sub>9</sub>	57	12	57	18	57	18	57	27	57	41

tation pattern of BTFA-OMT in the table is much different from that reported previously<sup>21</sup>. The mass spectrum of BTFA-OMT did not change significantly when the ion-source temperature was lowered to 270°C and/or the amount of sample injected was reduced to one tenth\*. The mass spectrum of the N(O)-heptafluorobutyryl *n*-butyl ester (BHFB) derivative of OMT was taken and compared with that of BTFA-OMT. The two fragmentation patterns were very similar.

Table VIII compares the mass fragmentation patterns of BTFA derivatives of Lys and N<sup>ε</sup>-alkyllysines. The abundant ions in the high *m/z* region are (M -

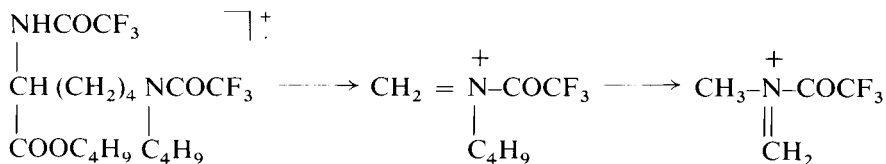
TABLE IX

MASS FRAGMENTATION PATTERNS OF BTFA DERIVATIVES OF N<sup>ε</sup>,N<sup>ε</sup>-DIALKYLlysINES*n* = 1 for DML, *n* = 2 for DEL and *n* = 3 for DPL. r.a. = Relative abundance.

Ion	BTFA-DML		BTFA-DEL		BTFA-DPL	
	<i>m/z</i>	<i>r.a.</i>	<i>m/z</i>	<i>r.a.</i>	<i>m/z</i>	<i>r.a.</i>
Molecular ion (M)	326	3	354	2	382	2
M - H	325	0.6	353	1	381	2
M - C <sub><i>n</i>-1</sub> H <sub>2<i>n</i>-1</sub>	325	0.6	339	8	353	100
M - C <sub>4</sub> H <sub>9</sub> OCO	225	5	253	5	281	10
(C <sub><i>n</i></sub> H <sub>2<i>n</i>+1</sub> ) <sub>2</sub> NCH <sub>2</sub>	58	100	86	100	114	98

\* In the case of BTFA derivatives of S-substituted cysteines such as S-β-aminoethylcysteine, the fragmentation patterns changed considerably on varying the ion-source temperature and the amount of sample injected<sup>22</sup>.

$C_4H_9OH$ ) and  $(M - C_4H_9OCO)$ . The ion of  $CF_3CONC_5H_9$  ( $m/z$  180) is formed abundantly for all the BTFA derivatives and is the base peak for BTFA-Lys. The ions of  $m/z$  126, 140, 154, 168 and 182 are found for all the BTFA derivatives of  $N^\epsilon$ -alkyllysines. There are isomeric structures for these ions except for that of  $m/z$  126. The ions of  $CF_3CON(C_nH_{2n+1})CH_2$  [ $n = 1$  for BTFA-NML ( $m/z$  140),  $n = 2$  for BTFA-NEL ( $m/z$  154),  $n = 3$  for BTFA-NPL ( $m/z$  168) and  $n = 4$  for BTFA-NBL ( $m/z$  182)] are formed abundantly for BTFA derivatives of  $N^\epsilon$ -alkyllysines and are base peaks except for BTFA-NBL. The base peak ion for BTFA-NBL is  $CF_3CON(CH_3)CH_2$  ( $m/z$  140) formed from  $CF_3CON(C_4H_9)CH_2$ :



The ions of  $CF_3CON(C_nH_{2n+1})(CH_2)_4$  ( $m/z$  182 for BTFA-NML,  $m/z$  196 for BTFA-NEL,  $m/z$  210 for BTFA-NPL and  $m/z$  224 for BTFA-NBL) are formed abundantly. Other significant ions for all the BTFA derivatives include  $C_5H_7$  ( $m/z$  67).

The mass fragmentation pattern of BTFA-Lys given in Table VIII is generally similar to that reported by Leimer *et al.*<sup>21</sup>, however, that of BTFA-NML is different from that reported by these authors. The mass fragmentation pattern of BHFB-NML was similar to that of BTFA-NML.

Table IX shows the mass fragmentation patterns of BTFA derivatives of  $N^\epsilon, N^\epsilon$ -dialkyllysines. The ions of  $(C_nH_{2n+1})NCH_2$ , where  $n = 1$  for BTFA-DML,  $n = 2$  for BTFA-DEL and  $n = 3$  for BTFA-DPL, are formed abundantly and are the base peaks except for BTFA-DPL, for which the ion of  $(M - C_2H_5)$  is the most abundantly formed. The mass fragmentation pattern of BHFB-DPL was very similar to that of BTFA-DPL.

## REFERENCES

- 1 C. W. Gehrke, D. Roach, R. M. Zumwalt, D. L. Stalling and L. L. Wall, *Quantitative Gas-Liquid Chromatography of Amino Acids in Proteins and Biological Substances*, Analytical Biochemistry Laboratories, Columbia, MO, 1968.
- 2 F. E. Kaiser, C. W. Gehrke, R. M. Zumwalt and K. C. Kuo, *J. Chromatogr.*, 94 (1974) 113.
- 3 M. Sakamoto, K.-I. Kajiyama and H. Tonami, *J. Chromatogr.*, 94 (1974) 189.
- 4 M. Sakamoto, K.-I. Kajiyama, T. Teshirogi and H. Tonami, *Text. Res. J.*, 45 (1975) 145.
- 5 M. Sakamoto, K.-I. Kajiyama, H. Shiozaki and Y. Tanaka, *Sen'i Gakkaishi*, 31 (1975) T-159.
- 6 M. Sakamoto, K.-I. Kajiyama, H. Shiozaki and Y. Tanaka, *Sen'i Gakkaishi*, 32 (1976) T-335.
- 7 M. Sakamoto, K.-I. Kajiyama, F. Nakayama, H. Shiozaki and Y. Tanaka, *Sen'i Gakkaishi*, 33 (1977) T-541.
- 8 M. Sakamoto, K.-I. Kajiyama, Y. Sato and F. Nakayama, *Proc. 5th Internat. Wool Text. Res. Conf., Aachen, 1976*, Vol. 5, p. 339.
- 9 L. D. Behr and H. T. Clarke, *J. Amer. Chem. Soc.*, 54 (1932) 1630.
- 10 H. M. Kissman, J. P. Joseph and B. R. Baker, *J. Med. Pharm. Chem.*, 2 (1960) 391.
- 11 L. M. Babineau and B. R. Berlinguet, *Can. J. Chem.*, 40 (1962) 1626.
- 12 C. H. Hurd and J. S. Strong, *Anal. Chem.*, 23 (1951) 542.
- 13 S. L. MacKenzie and D. Tenaschuk, *J. Chromatogr.*, 173 (1973) 53.
- 14 E. Kováts, *Helv. Chim. Acta*, 41 (1958) 1915.
- 15 M. B. Evans and J. F. Smith, *Nature (London)*, 190 (1961) 905.

- 16 M. B. Evans and J. F. Smith, *J. Chromatogr.*, 8 (1962) 303.
- 17 A. B. Littlewood, *Gas Chromatography*, Academic Press, New York, London, 2nd ed., 1970, p. 85.
- 18 A. Islam and A. Darbre, *J. Chromatogr.*, 71 (1972) 223.
- 19 V. Felt and P. Hušek, *J. Chromatogr.*, 197 (1980) 226.
- 20 E. Gelpi, W. A. Koenig, J. Gilbert and J. Oró, *J. Chromatogr. Sci.*, 7 (1969) 604.
- 21 K. R. Leimer, R. H. Rice and C. W. Gehrke, *J. Chromatogr.*, 141 (1977) 121.
- 22 M. Wakabayashi, *Master Thesis*, Tokyo Institute of Technology, Tokyo, 1981.



CHROM. 14,289

## GAS CHROMATOGRAPHIC RESOLUTION OF OPTICAL ISOMERS BY DIAMIDE STATIONARY PHASES, R'CONHCH(R'')CONHR'''

### EFFECT OF NON-POLAR SUBSTITUENTS (R'') AT THE $\alpha$ -CARBON ATOM

SHU-CHENG CHANG, R. CHARLES and E. GIL-AV\*

*Department of Organic Chemistry, The Weizmann Institute of Science, Rehovot (Israel)*

(Received August 14th, 1981)

---

#### SUMMARY

Four chiral diamide stationary phases of formula  $C_{11}H_{23}CONHCH(R'')CONH-tert.-C_4H_9$  derived from L-alanine (I,  $R'' = CH_3$ ), L-leucine [II,  $R'' = CH_2CH(CH_3)_2$ ], D-phenylglycine (III,  $R'' = C_6H_5$ ) and L-phenylalanine (IV,  $R'' = CH_2C_6H_5$ ) were synthesized in order to study the influence of  $R''$  on stereoselectivity in gas chromatography. N-TFA-isopropyl (TFA = trifluoroacetyl) esters of  $\alpha$ -,  $\beta$ - and  $\gamma$ -amino acids, N-TFA-O-acyl-2-aminoalkan-1-ols and N-TFA-amines were the solutes with which resolution was studied.

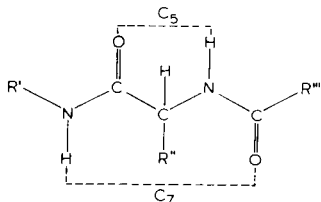
An increase in the size of  $R''$  from methyl (I) to isobutyl (II) leads throughout to larger resolution factors. Aromatic  $R''$  substituents (III, IV) can effect stereoselectivity both by their size and through specific interactions of the benzene ring with polar functions of solutes, compared with  $R'' =$  isobutyl (II), either an increase or a decrease in resolution factors may result. Methyl substitution in N-TFA esters of neutral  $\alpha$ -amino acids in the  $\beta$ - position leads to a decrease, and in the  $\gamma$ -position to an increase, respectively, in the stereoselectivity of the solutes on the stationary phases studied. The most useful are stationary phases II, which is suitable for all the above compounds except the  $\beta$ -amino acids, and IV, which is appropriate for the enantiomeric analysis of both  $\alpha$ - and  $\beta$ -amino acids.

---

#### INTRODUCTION

Diamide stationary phases of structure  $R'CONHCH(R'')CONHR'''$ , derived from optically active  $\alpha$ -amino acids, have been investigated in our laboratory for a number of years<sup>1,2</sup>. All compounds of this type prepared until recently were derived from valine ( $R'' = iso-C_3H_7$ ). The influence of variation of the  $R'$  and  $R'''$  substituents has been reported in several papers<sup>3-5</sup>. A recent modification of this approach is the incorporation of the valyl-*tert.*-butylamide moiety into a polymeric backbone<sup>6,7</sup>. All of these valine-derived stationary phases have been shown to have high stereoselectivity for various classes of optical isomers, and their use is becoming routine, particularly for the enantiomeric analysis of  $\alpha$ -amino acids.

We have proposed<sup>3-5</sup> that chiral recognition by the diamides involves diastereomeric association complexes in which the solute is hydrogen-bonded through the "C<sub>5</sub>" or "C<sub>7</sub>" side:



It was felt that the substituent at the asymmetric centre of the solvent molecule must, on the one hand, be sufficiently bulky in order to show stereoselective effects, but, on the other hand, it should not be so large as to make association with the solute difficult. The isopropyl group of valine seemed to be a good compromise.

However, having demonstrated the usefulness of the valine type of stationary phases, we have recently started to explore systematically the effect of the nature of the R'' group. The work appeared of interest for gaining a better understanding of the process of chiral recognition, and for improving and extending the procedures for the resolution of optical isomers by gas chromatography.

In this paper we report on four new diamide stationary phases, I-IV, where R' and R''' remain unchanged, being C<sub>11</sub>H<sub>23</sub> and *tert.*-butyl, respectively, and R'' is a non-polar aliphatic or aromatic substituent: I, (L-alanine phase)<sup>8</sup>, R'' = CH<sub>3</sub>; II, (L-leucine phase), R'' = *iso*-C<sub>4</sub>H<sub>9</sub>; III, (D-phenylglycine phase), R'' = C<sub>6</sub>H<sub>5</sub>; IV, (L-phenylalanine phase), R'' = C<sub>6</sub>H<sub>5</sub>CH<sub>2</sub>.

## EXPERIMENTAL

### *Derivatization of compounds chromatographed*

The N-TFA\*-isopropyl esters of the amino acids and the TFA derivatives of the other compounds were prepared as described previously<sup>9</sup>.

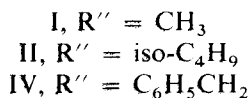
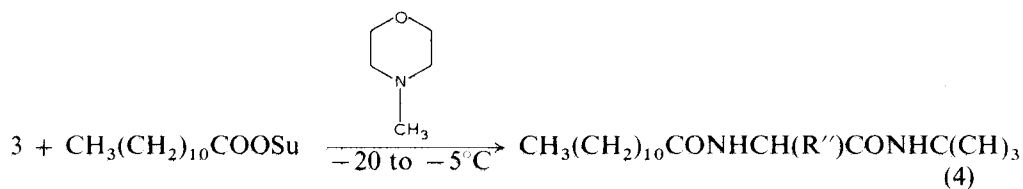
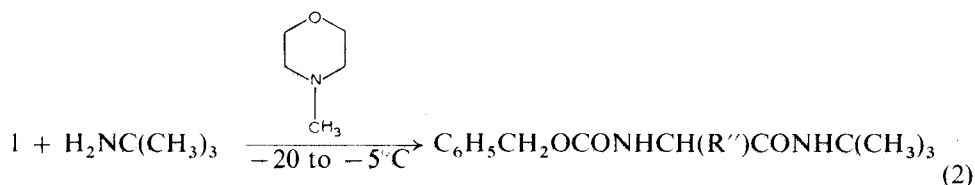
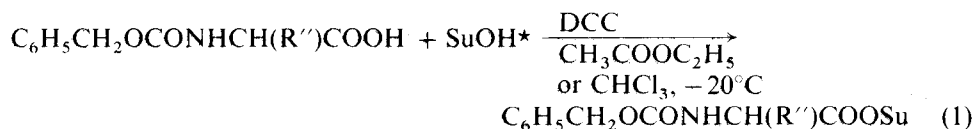
### *Synthesis of stationary phases*

The above-mentioned stationary phases were prepared by either Scheme A or Scheme B:

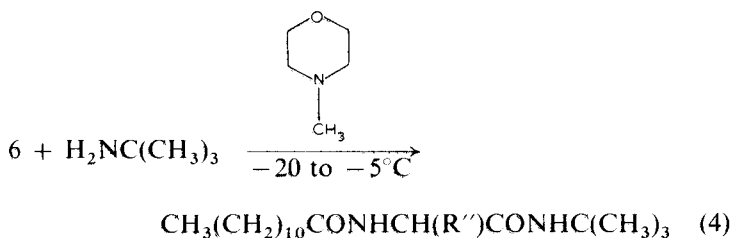
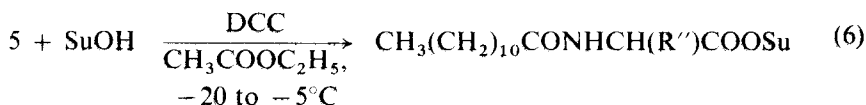
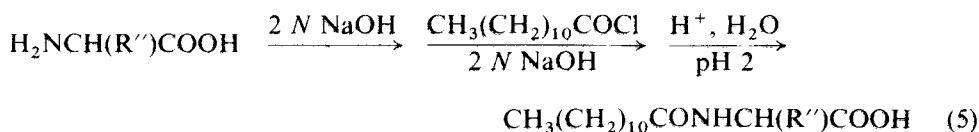
*N*-Carbobenzoxy-*tert.*-butylamides of  $\alpha$ -amino acids (2)<sup>4</sup>. A solution of N-carbobenzoxy- $\alpha$ -amino acid\*\* (0.01 mole) in dry ethyl acetate (70 ml) was cooled to -20°C and N-hydroxysuccinimide (0.011 mole) and dicyclohexylcarbodiimide (0.01 mole) were added, to obtain 1. The mixture was stirred overnight at 0°C, filtered and the filtrate cooled to -20°C. Then an ethyl acetate solution containing 0.01 mole each of *tert.*-butylamine and N-methylmorpholine was dropped in, and stirring at -20° to -5°C continued for 2 days. After filtration, the solvent was removed under reduced pressure, and the residue was dissolved in diethyl ether and washed succes-

\* TFA = trifluoroacetyl.

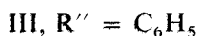
\*\* The derivatives of L-alanine and L-phenylalanine were kindly supplied by the Biophysics Dept. of the Weizmann Institute. The derivative of L-leucine was prepared by Dr. L. Wackerle in our laboratory.



Scheme A.



Scheme B.



\* SuOH = N-hydroxysuccinimide.

sively with water, 2% hydrochloric acid, water, 5% sodium hydrogen carbonate solution, water and saturated sodium chloride solution, and dried over anhydrous magnesium sulphate. The diethyl ether was removed under reduced pressure and the residue dried under high vacuum. The following *N*-carbobenzoxy-*tert*.-butylamides of  $\alpha$ -amino acids 2 were prepared. *L*-Leucine: m.p. 58.5–60°C; yield 98%. Elemental analysis: found: C, 68.18; H, 8.90; N, 8.80%; calculated for  $C_{18}H_{28}N_2O_3$ : C, 67.47; H, 8.81; N, 8.74%.  $[\alpha]_D^{24} - 29.1$  (*c* 5 in chloroform); optical purity, *ca.* 100%. *L*-Phenylalanine: m.p. 98–99°C; yield 98%. Elemental analysis: found: C, 71.35; H, 7.52; N, 8.02%; calculated for  $C_{21}H_{26}N_2O_3$ : C, 71.16; H, 7.39; N, 7.90%.  $[\alpha]_D^{24} + 10.4$  (*c* 5 in chloroform); optical purity, *ca.* 100%.

The *L*-alanine derivative was synthesized in the same way, but worked up to the final product 4 (I,  $R' = CH_3$ ) without isolating the intermediate 2.

*tert*.-Butylamides of  $\alpha$ -amino acids (3). Hydrogen was bubbled for 4 h at a low flow-rate through an alcoholic solution of 2 (0.01 mole) keeping in suspension 0.1 g of 10% palladium/charcoal. After the catalyst had been filtered off and the alcohol removed under reduced pressure, the *tert*.-butylamide of  $\alpha$ -amino acid 3 was obtained in quantitative yield.

*N*-Lauroyl-*tert*.-butylamides of  $\alpha$ -amino acids (4). A solution of 3 (0.01 mole) in dry ethyl acetate (70 ml) was cooled to  $-20^\circ C$ , stirred and the laurate of *N*-hydroxysuccinimide<sup>3</sup> (0.01 mole) added. *N*-Methylmorpholine (0.01 mole) was then dropped in and treatment continued as for 2.

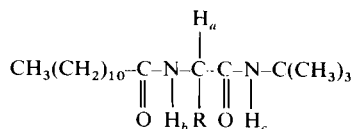
The crude product was further purified by chromatography on silica gel containing 6% of water, starting with *n*-hexane as eluent and increasing the polarity with ethyl acetate. Pure *N*-lauroyl-*L*-alanine-*tert*.-butylamide (I), *N*-lauroyl-*L*-leucine-*tert*.-butylamide (II) and *N*-lauroyl-*L*-phenylalanine-*tert*.-butylamide (IV) were thus obtained in yields of 43%, 60% and 54%, respectively. The properties of these stationary phases are summarized in Table I.

*N*-Lauroyl- $\alpha$ -amino acids (5). Condensation of lauroyl chloride with an  $\alpha$ -amino acid to give *N*-lauroyl- $\alpha$ -amino acid was carried out by the usual Schotten-Baumann procedure. The  $\alpha$ -amino acid (12.8 mmole) was dissolved in an ice-cold 2 *N* sodium hydroxide solution (7.1 ml), and 2 *N* sodium hydroxide solution (9.6 ml) and lauroyl chloride (15.4 mmole) were dropped in separately with vigorous stirring and cooling in an ice-bath. After addition of the reagents was complete, the mixture was stirred for a further 2 h at room temperature. The mixture was washed twice with diethyl ether, acidified to pH 2 with 6 *N* hydrochloric acid and extracted three times with ethyl acetate. The ethyl acetate extract was dried over anhydrous magnesium sulphate, the solvent removed under reduced pressure and the residue recrystallized from ethyl acetate. *N*-Lauroyl-*D*-phenylglycine was prepared by this method (m.p. 79.5–80.5°C; yield 43%). Elemental analysis: found: C, 72.01; H, 9.39; N, 4.11%; calculated for  $C_{20}H_{31}NO_3$ : C, 72.03; H, 9.37; N, 4.20%.  $[\alpha]_D^{24} - 14.6$  (*c* 1 in chloroform); optical purity, 93%.

#### *N*-Lauroyl-*D*-phenylglycine-*tert*.-butylamide (III)

For carrying out the reaction step 6  $\rightarrow$  4, *N*-lauroyl-*D*-phenylglycine (5 mmole) in dry ethyl acetate (50 ml) was cooled to  $-20^\circ C$ , *N*-hydroxysuccinimide (5.5 mmole) and dicyclohexyl carbodiimide (5 mmole) were added and the mixture was stirred overnight. After filtration to remove the dicyclohexylurea formed, the clear solution

TABLE I  
PROPERTIES OF THE DIAMIDE STATIONARY PHASES



Property	Stationary phase			
	<i>I</i> *, <i>R</i> = CH <sub>3</sub> (L-alanine)	<i>II</i> *, <i>R</i> = <i>i</i> -Bu (L-leucine)	<i>III</i> **, <i>R</i> = C <sub>6</sub> H <sub>5</sub> (D-phenyl- glycine)	<i>IV</i> *, <i>R</i> = C <sub>6</sub> H <sub>5</sub> CH <sub>2</sub> (L-phenyl- alanine)
Formula	C <sub>19</sub> H <sub>38</sub> N <sub>2</sub> O <sub>2</sub>	C <sub>22</sub> H <sub>44</sub> N <sub>2</sub> O <sub>2</sub>	C <sub>24</sub> H <sub>40</sub> N <sub>2</sub> O <sub>2</sub>	C <sub>25</sub> H <sub>42</sub> N <sub>2</sub> O <sub>2</sub>
%C Calcd.	69.99	71.68	74.18	74.58
Found	69.89	71.75	74.29	74.75
%H Calcd.	11.85	12.03	10.38	10.52
Found	11.73	12.07	10.43	10.52
%N Calcd.	8.58	7.60	7.22	6.96
Found	8.65	8.03	7.10	7.25
M.p. (°C)	87–88.5	Sticky, viscous oil	73–74	75–76
[α] <sub>D</sub> <sup>24</sup> (c 5% CHCl <sub>3</sub> )	–41.95	–49.6	–71.72	–0.3
Optical purity (%)***	98	≈ 100 <sup>§</sup>	81	≈ 100 <sup>§</sup>
<sup>1</sup> H NMR shift (ppm):				
H <sub>a</sub> (m)	4.40	4.39	5.54	4.50
H <sub>b</sub> (d)	6.26	6.69	7.08	6.63
H <sub>c</sub> (s)	6.22	6.45	6.31	5.39

\* Prepared by Scheme A.

\*\* Prepared by Scheme B.

\*\*\* See Experimental for details and accuracy of purity determination.

<sup>§</sup> Only one peak observed (see Experimental).

was cooled to –20°C and dry ethyl acetate, containing 5 mmole of each *tert*-butylamine and N-methylmorpholine, was added dropwise. The reaction and the work-up were then continued as above for 4 (scheme A). N-Lauroyl-D-phenylglycine-*tert*-butylamide (III) was prepared by this method in 54% yield; for the properties of the stationary phase, see Table I.

### Structures

NMR spectroscopy was used to check the structures of all products and intermediate compounds.

### Determination of optical purity of compounds

Hydrolysis and esterification were carried out in one step by refluxing 5 mg of

sample with a mixture of 2 ml of 6 *N* hydrochloric acid and 2 ml of 1.25 *N* hydrochloric acid in isopropanol in a sealed tube at 110°C for 4 h. The hydrochloric acid and isopropanol were removed under reduced pressure and the residue was converted into *N*-TFA-isopropyl esters.

The derivatives were gas chromatographed on a chiral diamide stationary phase and the optical purity was calculated from the areas of the peaks corresponding to the *D*- and *L*-enantiomers.

The accuracy of determination was, in general,  $\pm 1-2\%$ . Where only one peak was found, the optical purity was considered to be 99–100% as the limit of detection under the conditions used was  $\leq 0.5\%$ .

#### *Chromatographic conditions*

Stainless-steel capillary columns (100 ft.  $\times$  0.02 in. I.D.) were coated by the plug method with I and II (mounted in a Varian Series 2700 chromatograph) and 150 ft.  $\times$  0.02 in. I.D. columns were coated with III and IV (mounted in a Varian Series 1200 chromatograph). Both instruments were provided with a splitter and a flame-ionization detector. The injector temperature was 240°C and the detector temperature 240°C; the column temperatures used are indicated in the Tables. The helium flow-rate was 2.8–3 ml/min for all columns.

## RESULTS AND DISCUSSION

In this paper we deal with the resolution of *N*-TFA-isopropyl esters of  $\alpha$ -,  $\beta$ - and  $\gamma$ -amino acids, *N*-TFA-*O*-acyl-2-aminoalkan-1-ols and *N*-TFA-amines. The resolution of diamide solutes,  $\text{CF}_3\text{CONHCH(R)CONH-tert.-C}_4\text{H}_9$ , has been published previously<sup>10</sup>; work on the behaviour of other types of optically active compounds on stationary phases I–IV will be reported in a subsequent publication.

#### *Amino acid derivatives*

The data for the various types of amino acids resolved are listed in Table II.

*$\alpha$ -Amino acids.* The stereoselectivity for the  $\alpha$ -amino acid derivatives studied can be readily discussed with reference to the plots of the resolution factors on stationary phases I–IV (Fig. 1).

The order of emergence throughout is the *L*- after the *D*-isomer on the *L*-stationary phases. Further, both proline and aspartic acid have very low resolution coefficients\*. These results, already observed for the valine analogues<sup>2–5</sup>, show that the changes made thus far in the structure of the diamide solvents do not essentially affect the nature of the resolution mechanisms involved.

Of the four stationary phases synthesized, II and IV give the highest stereoselectivity, with only small differences in the *r* values on these two solvents for a given individual  $\alpha$ -amino acid. The data for II and IV are also close to those obtained on the *N*-lauroyl-*tert*-butylamide of valine (V), as can be seen in Table III. For the *D*-phenylglycine phase (III), it should be pointed out that its optical purity was not more

\* Proline and aspartic acid not only have very low *r* values, but also their resolution involves mechanisms different to that of the other  $\alpha$ -amino acids. Unless specifically mentioned, the following discussion does not relate to these two compounds.

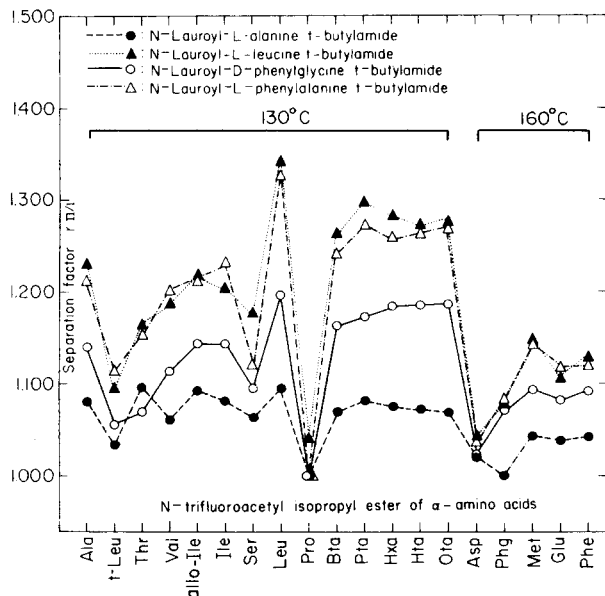


Fig. 1. Resolution factors of proteinic and non-proteinic amino acids on stationary phases I-IV.  $t = tert.$ ; for Bta, Pta, Hxa, Hta and Ota, see Table II.

than 81% and that the  $r$  values must be corrected<sup>4</sup> for proper comparison. However, even if the resolution factors are calculated for 100% purity (see figures in parentheses in Table II), the stereoselectivity in most instances is found to be lower than for II and IV.

A feature in which the aromatic stationary phases III and IV deviate from the aliphatic stationary phases I and II is the complete lack of chiral differentiation for proline; also, compared with II, they have a relatively lower resolution factor for serine.

The alanine stationary phase (I) has the lowest  $r$  values throughout, except for threonine on III. Further, the stereoselectivity is only slightly affected by variations of the nature of the substituent in the  $\alpha$ -position of the solutes; the spread of the data is relatively restricted (see the corresponding plot in Fig. 1). This pattern of behaviour can readily be rationalized with reference to the solvent-solute model proposed for explaining the chiral recognition, already discussed in previous papers for diamides and related optically active stationary phases<sup>2-4</sup> (Fig. 2).

If the  $R''$  group in the solvent is methyl, its radius of interaction is limited, and consequently the system is not greatly affected by the length of the chain and branching of the substituent at the asymmetric carbon of the solute, and essentially only the change in configuration is detected (Fig. 1, data for I at 130°C, except proline); on the other hand, sensitivity to the nature of the  $\alpha$ -substituent is observed when the  $R''$  group is larger, as in II-IV (and also in V)<sup>4,5</sup>.

It is of particular interest to examine the effect of branching in the aliphatic  $\alpha$ -amino acids. If  $\alpha$ -aminobutyric acid is taken as the reference solute, it is seen (Fig. 3) that the methyl substituents in the  $\gamma$ -position increase the resolution coefficient (leucine), whereas substitution in the  $\beta$ -position reduces the  $r$  values (alloisoleucine,

TABLE II

RESOLUTION OF  $\alpha$ -AMINO ACIDS ON DIAMIDE STATIONARY PHASES

For chromatographic conditions see Experimental.

Type of amino acid	<i>N</i> -TFA-isopropyl ester of	Stationary phase							
		<i>N</i> -Lauroyl-L-alanine- <i>tert</i> -butylamide (I)				<i>N</i> -Lauroyl-L-leucine- <i>tert</i> -butylamide (II)			
		Enantiomer	<i>r</i> * <sub>D</sub>	<i>r</i> * <sub>L</sub>	<i>T</i> (°C)	Enantiomer	<i>r</i> * <sub>D</sub>	<i>r</i> * <sub>L</sub>	<i>T</i> (°C)
Protein amino acids	Ala	D	5.94	1.091	120	D	—	—	—
		L	6.48	—	—	L	—	—	—
		D	5.00	1.080	130	D	12.80	1.231	130
		L	5.40	—	—	L	15.76	—	—
	Thr	D	10.00	1.120	120	D	8.46	1.163	150
		L	11.20	—	—	L	9.84	—	—
		D	6.90	1.096	130	D	20.12	1.175	130
		L	7.56	—	—	L	23.64	—	—
	Val	D	8.06	1.089	120	D	11.64	1.120	150
		L	8.76	—	—	L	13.04	—	—
		D	6.60	1.061	130	D	20.50	1.187	130
		L	7.00	—	—	L	24.34	—	—
	Gly	D	13.40	—	120	D	12.50	1.138	150
		L	10.70	—	130	L	14.22	—	—
		D	11.86	1.104	120	D	27.50	1.216	130
		L	13.10	—	—	L	33.44	—	—
	Allo-Ile	D	9.24	1.093	130	D	17.58	1.142	150
		L	10.10	—	—	L	20.08	—	—
		D	13.10	1.081	120	D	30.24	1.204	130
		L	14.16	—	—	L	36.40	—	—
	Ile	D	9.86	1.081	130	D	19.14	1.136	150
		L	10.66	—	—	L	21.74	—	—
		D	15.80	1.063	130	D	38.64	1.175	130
		L	16.80	—	—	L	45.40	—	—
Ser	D	19.60	1.110	120	D	38.80	1.342	130	
	L	21.76	—	—	L	52.06	—	—	
	D	15.70	1.095	130	D	24.30	1.216	150	
	L	17.20	—	—	L	29.54	—	—	
Leu	D	10.70	—	—	D	10.70	1.150	170	
	L	12.30	—	—	L	12.30	—	—	
	D	—	—	—	D	—	—	—	
	L	—	—	—	L	—	—	—	



*N-Lauroyl-D-phenylglycine-tert.-butylamide (III)**N-Lauroyl-L-phenylalanine-tert.-butylamide (IV)*

<i>Enantiomer</i>	<i>r*</i>	<i>r<sub>D</sub><sup>*</sup></i>	<i>T(°C)</i>	<i>Enantiomer</i>	<i>r*</i>	<i>r<sub>D</sub><sup>*</sup></i>	<i>T(°C)</i>
L	12.60	1.159	120	D	—	—	—
D	14.60			L	—	—	—
L	8.60	1.140	130	D	4.82	1.212	130
D	9.80	(1.175)		L	5.84		
—	—	—	—	—	—	—	—
—	—	—	—	—	—	—	—
L	11.60	1.069	130	D	7.16	1.154	130
D	12.40	(1.085)		L	8.26		
—	—	—	—	—	—	—	—
L	17.80	1.157	120	—	—	—	—
D	20.60			—	—	—	—
L	12.00	1.117	130	D	7.42	1.207	130
D	13.40	(1.146)		L	8.96		
—	—	—	—	—	—	—	—
—	—	—	—	—	—	—	—
—	19.20	—	130	—	9.94	—	130
L	25.80	1.171	120	—	—	—	—
D	30.20			—	—	—	—
L	17.20	1.144	130	D	10.70	1.215	130
D	19.68	(1.181)		L	13.00		
—	—	—	—	—	—	—	—
L	28.40	1.162	120	—	—	—	—
D	33.00			—	—	—	—
L	18.88	1.144	130	D	11.72	1.230	130
D	21.60	(1.181)		L	14.42		
—	—	—	—	—	—	—	—
L	22.08	1.096	130	D	14.24	1.126	130
D	24.20	(1.120)		L	16.04		
L	38.68	1.235	120	D	17.20	1.351	120
D	47.92			L	23.24		
L	25.20	1.198	130	D	15.64	1.326	130
D	30.20	(1.250)		L	20.74		
L	11.00	1.145	150	D	6.50	1.215	150
D	12.60			L	7.90		
—	—	—	—	D	5.00	1.176	160
—	—	—	—	L	5.88		
—	—	—	—	—	—	—	—

(Continued on p. 96)

TABLE II (continued)

Type of amino acid	<i>N</i> -TFA-isopropyl ester of	Stationary phase							
		<i>N</i> -Lauroyl-L-alanine- <i>tert.</i> -butylamide (I)				<i>N</i> -Lauroyl-L-leucine- <i>tert.</i> -butylamide (II)			
		Enantiomer	<i>r</i> <sup>*</sup>	<i>r</i> <sub>T</sub> <sup>†</sup>	<i>T</i> (°C)	Enantiomer	<i>r</i> <sup>*</sup>	<i>r</i> <sub>T</sub> <sup>†</sup>	<i>T</i> (°C)
Protein amino acids	Pro	D	20.46	1.036	120	—	—	—	—
		L	21.20			—	—	—	
		D	17.70	1.000	130	D	46.04	1.041	130
		L	17.70			L	47.92		
		—	—	—	—	D	29.02	1.036	150
		—	—	—	—	L	30.06		
	Asp	D	29.64	1.022	140	—	—	—	—
		L	30.30			—	—	—	
		—	—	—	—	—	—	—	—
		D	15.10	1.020	160	D	52.28	1.042	160
		L	15.30			L	54.46		
		—	—	—	—	D	41.08	1.035	170
	—	—	—	—	L	42.50			
	Met	D	51.12	1.063	140	—	—	—	—
		L	54.32			—	—	—	
		—	—	—	—	—	—	—	—
		D	24.90	1.044	160	D	81.76	1.145	160
		L	26.00			L	93.63		
		—	—	—	—	D	63.14	1.118	170
	—	—	—	—	L	70.56			
	Glu	—	—	—	—	D	30.84	1.065	200
		—	—	—	—	L	32.86		
		D	71.34	1.058	140	—	—	—	—
		L	75.48			—	—	—	
—		—	—	—	—	—	—	—	
D		34.80	1.040	160	D	114.14	1.110	160	
L	36.20	L			126.64				
—	—	—	—	D	87.70	1.090	170		
—	—	—	—	L	95.50				
Phe	—	—	—	—	D	61.14	1.089	180	
	—	—	—	—	L	66.64			
	—	—	—	—	D	40.28	1.072	200	
	—	—	—	—	L	43.20			
	D	76.64	1.069	140	—	—	—	—	
	L	81.94			—	—	—		
—	—	—	—	—	—	—	—		
D	39.00	1.044	160	D	118.06	1.131	160		
L	40.70			L	133.52				
—	—	—	—	D	90.06	1.105	170		
—	—	—	—	L	99.44				

*N-Lauroyl-D-phenylglycine-  
tert.-butylamide (III)**N-Lauroyl-L-phenyl-  
alanine-tert.-butylamide (IV)*

<i>Enantiomer</i>	<i>r*</i>	<i>r<sub>B</sub><sup>A</sup></i>	<i>T(°C)</i>	<i>Enantiomer</i>	<i>r*</i>	<i>r<sub>B</sub><sup>A</sup></i>	<i>T(°C)</i>
—	—	—	—	—	—	—	—
L	40.40	1.000	130	D	22.42	1.000	130
D	40.40			L	22.42		
—	—	—	—	—	—	—	—
—	—	—	—	—	—	—	—
L	36.80	1.033	150	—	—	—	—
D	38.00			—	—	—	—
L	26.00	1.023	160	D	26.86	1.038	160
D	26.60	(1.031)		L	27.88		
—	—	—	—	—	—	—	—
—	—	—	—	—	—	—	—
L	62.80	1.108	150	—	—	—	—
D	69.60			—	—	—	—
L	43.20	1.093	160	D	42.96	1.142	160
D	47.20	(1.116)		L	49.06		
—	—	—	—	—	—	—	—
—	—	—	—	—	—	—	—
—	—	—	—	—	—	—	—
L	87.60	1.096	150	—	—	—	—
D	96.00			—	—	—	—
L	59.80	1.082	160	D	58.14	1.118	160
D	63.60	(1.102)		L	64.98		
—	—	—	—	—	—	—	—
—	—	—	—	—	—	—	—
—	—	—	—	—	—	—	—
L	90.40	1.097	150	—	—	—	—
D	95.20			—	—	—	—
L	60.80	1.092	160	D	64.34	1.120	160
D	66.40	(1.115)		L	72.06		
—	—	—	—	—	—	—	—

(Continued on p. 98)

TABLE II (continued)

Type of amino acid	N-TFA-isopropyl ester of	Stationary phase								
		N-Lauroyl-L-alanine-tert.-butylamide (I)				N-Lauroyl-L-leucine-tert.-butylamide (II)				
		Enantiomer	$r^*$	$r_{L/D}^{**}$	$T(^{\circ}C)$	Enantiomer	$r^*$	$r_{L/D}^{**}$	$T(^{\circ}C)$	
Non-protein $\alpha$ -amino acids	$\alpha$ -Amino butyric acid (Bta)	D	8.46	1.116	120	—	—	—	—	
		L	9.44			—	—	—	—	
	$\alpha$ -Amino pentanoic acid (Pta)	D	8.60	1.070	130	D	11.00	1.264	130	
		L	9.20			L	13.90			
	$\alpha$ -Amino hexanoic acid (Hxa)	D	14.56	1.118	120	—	—	—	—	
		L	16.28			—	—	—	—	
		D	10.64			1.081	130	D	18.20	1.297
	L	11.50	L	23.60						
	$\alpha$ -Amino heptanoic acid (Hta)	D	24.64	1.102	120	—	—	—	—	
		L	27.14			—	—	—	—	
		D	17.40			1.075	130	D	30.90	1.282
	L	18.70	L	39.60						
	$\alpha$ -Amino octanoic acid (Ota)	D	42.88	1.090	120	—	—	—	—	
		L	46.74			—	—	—	—	
		D	29.70			1.071	130	D	53.60	1.272
	L	31.80	L	68.20						
	<i>t</i> -Leucine (t-Leu)	D	75.26	1.089	120	—	—	—	—	
		L	82.02			—	—	—	—	
		D	51.50			1.070	130	D	93.20	1.277
	L	55.10	L	119.00						
Phenylglycine (Phg)	D	8.30	1.060	120	—	—	—	—		
	L	8.80			—	—	—	—		
	D	5.90			1.034	130	D	12.70	1.095	130
L	6.10	L	13.90							
$\beta$ -Amino acids	$\beta$ -Amino butyric acid	D	37.08	1.018	140	—	—	—	—	
		L	37.74			—	—	—	—	
	$\beta$ -Amino- $\gamma$ -methyl-pentanoic acid	—	—	—	—	—	—	—	—	
		D	19.70	1.000	160	D	64.96	1.076	160	
	L	19.70	L			69.90				
	$\beta$ -Amino- $\delta$ -methyl-hexanoic acid	—	—	—	—	—	—	—	—	
		D	50.08	1.060	170	D	50.08	1.060	170	
	L	53.08	L			53.08				
	$\gamma$ -Amino acids	$\gamma$ -Amino valeric acid	D	21.88	1.028	130	D	21.88	1.028	130
			L	22.50			L	22.50		
$\gamma$ -Amino- $\delta$ -methyl-hexanoic acid		D	44.84	1.047	130	D	44.84	1.047	130	
		L	46.96			L	46.96			
$\gamma$ -Amino- $\epsilon$ -methyl-heptanoic acid		D	63.90	1.051	130	D	63.90	1.051	130	
		L	67.14			L	67.14			
$\gamma$ -Amino- $\delta$ -methyl-hexanoic acid	L	28.20	1.000	130	L	56.60	1.000	130		
	D	28.20			D	56.60				
$\gamma$ -Amino- $\epsilon$ -methyl-heptanoic acid	L	51.90	1.019	130	L	92.68	1.056	130		
	D	52.90			D	97.90				
$\gamma$ -Amino- $\delta$ -methyl-hexanoic acid	L	94.70	1.037	130	L	159.20	1.047	130		
	D	98.20			D	166.64				

\*  $r$  = corrected retention time (min).

\*\*  $r_{L/D}$  (for the L- stationary phases I, II and IV) and  $r_{D/L}$  (for the D- stationary phase III) = resolution factor = ratio of the corrected retention time of the second over that of the first emerging enantiomer, calculated with  $r$  values expressed to the second decimal place. For III (see Table I), figures in parentheses are corrected<sup>4</sup> for 100% optical purity.

<i>N-Lauroyl-D-phenylglycine-tert.-butylamide (III)</i>				<i>N-Lauroyl-L-phenylalanine-tert.-butylamide (IV)</i>			
Enantiomer	$r^*$	$r_{D,20}^{25}$	$T$ ( $^{\circ}\text{C}$ )	Enantiomer	$r^*$	$r_{D,20}^{25}$	$T$ ( $^{\circ}\text{C}$ )
—	—	—	—	D	7.92	1.263	120
L	11.00	1.164	130	L	10.00	1.242	130
D	12.80	(1.206)	—	D	7.36	1.347	120
—	—	—	—	L	9.14	1.274	130
L	18.60	1.172	130	D	13.84	1.289	120
D	21.80	(1.216)	—	L	18.64	1.257	130
—	—	—	—	D	12.04	1.286	120
L	29.00	1.186	130	L	15.34	1.266	130
D	34.40	(1.234)	—	D	25.08	1.274	120
—	—	—	—	L	32.32	1.286	120
L	49.60	1.187	130	D	20.70	1.274	120
D	58.80	(1.234)	—	L	26.02	1.272	130
—	—	—	—	D	43.92	—	—
L	85.20	1.188	130	L	56.48	—	—
D	101.20	(1.235)	—	D	34.68	—	—
—	—	—	—	L	43.92	—	—
L	11.00	1.055	130	D	75.76	—	—
D	11.60	(1.068)	—	L	96.52	—	—
—	—	—	—	D	59.58	—	—
L	47.20	1.089	150	L	75.76	—	—
D	51.40	—	—	—	—	—	—
L	33.00	1.073	160	D	33.16	1.084	160
D	35.40	(1.090)	—	L	35.96	—	—
—	—	—	—	—	—	—	—
L	21.80	1.046	130	D	13.52	1.050	120
D	22.80	—	—	L	14.60	1.152	120
L	40.00	1.075	130	D	29.00	1.120	120
D	43.00	—	—	L	33.40	—	—
L	56.80	1.063	130	D	41.40	—	—
D	60.40	—	—	L	46.40	—	—
No separation on III				No separation on IV			

TABLE III

COMPARISON OF RESOLUTION FACTORS ON THE N-LAUROYL-*tert*-BUTYLAMIDE STATIONARY PHASES DERIVED FROM D-VALINE (V), L-LEUCINE (II) AND L-PHENYLALANINE (IV) AT 130°C

For experimental conditions and definition of  $r_{L/D}$  see Table II.

$\alpha$ -Amino acid	Stationary phase		
	V*: $r_{D/L}$	II: $r_{L/D}$	IV: $r_{L/D}$
Ala	1.224	1.231	1.212
Val	1.172	1.187	1.207
Allo-Ile	1.188	1.216	1.215
Ile	1.175	1.204	1.230
Leu	1.288	1.342	1.326
$\alpha$ -Aminopentanoic acid	1.244	1.297	1.274
<i>t</i> -Leucine	1.094	1.095	1.114

\* The purest sample of V available (97.8% optical purity) was derived from D-valine. For this reason  $r_{D/L}$  and not  $r_{L/D}$  values are given; the data were remeasured under the same conditions and the same instrument as those employed for II and IV (Table II). The figures are corrected for 100% optical purity<sup>4</sup>. It should be mentioned that the resolution factors for V given in ref. 4 are too high, as those values were corrected using too low optical purities. It has been found since (see Experimental) that under the normal conditions of peptide hydrolysis the diamides are readily racemized.

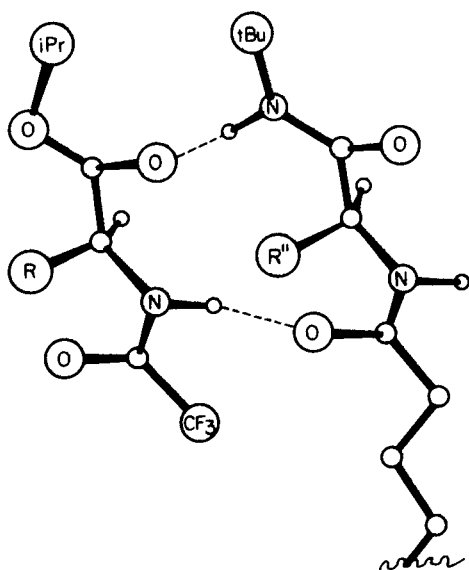


Fig. 2. Schematic representation of an L-solute-L-solvent interaction model (N-TFA-L-amino acid isopropyl ester-diamide stationary phase). iPr = Isopropyl; tBu = *tert*-butyl.

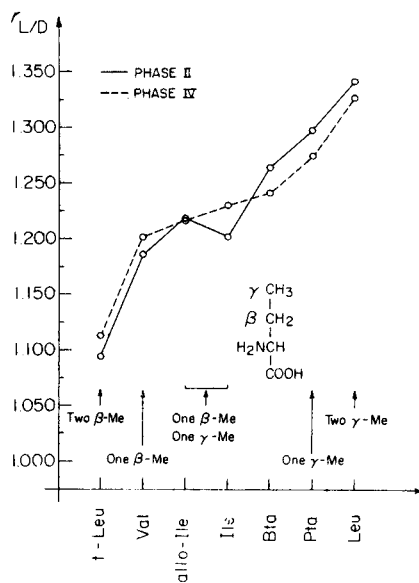


Fig. 3. Influence of  $\beta$ - and  $\gamma$ -methyl substitution on the resolution factor of some neutral  $\alpha$ -amino acids on diamides II and IV. Me = Methyl; Bta =  $\alpha$ -aminobutyric acid; Pta =  $\alpha$ -aminopentanoic acid.

isoleucine, valine). When two methyl groups are placed in the  $\beta$ -position, the resolution is very low indeed (*t*-leucine) with respect to the unsubstituted  $\alpha$ -aminobutyric acid.

This behaviour has already been observed and discussed previously<sup>11</sup> for the resolution of aliphatic amino acids on N-TFA-L-phenylalanine-L-leucine cyclohexyl ester. As it is assumed<sup>12</sup> that the mechanism of the resolution on the dipeptide stationary phases is similar to that on the diamides, the phenomena would appear to be related. It should be mentioned that examination of CPK\* models of L-solvent-L-solute pairs indicates that a  $\beta$ -substituent tends to interfere with a good fit of R'' with the corresponding alkyl group of the solute, whereas this is not the case for a  $\gamma$ -substituent. The resulting weakening or strengthening of the L-L solvent-solute associate should decrease ( $\beta$ -effect) or increase ( $\gamma$ -effect) the  $r_L$  values.

Possibly a better understanding of these effects might be achieved in the future through computation<sup>13</sup> of the minimal energies of the diastereomeric solvent-solute association complexes considered to be responsible for the chiral differentiation.

*Analytical considerations.* For the resolution of individual  $\alpha$ -amino acids, stationary phases II and IV are equivalent or even superior to the commonly used diamide materials derived from valine. Further, the increase in R'' permits a higher operating temperature to be used than on the respective N-acyl-*tert.*-butylamide derivative of valine (160–170°C for II and IV, compared with 140°C for V).

Considering peak overlap of neighbouring  $\alpha$ -amino acids, stationary phases II and IV (particularly II) give ready separations of all the isomers of alloisoleucine and isoleucine (Fig. 4), and stationary phases II and IV permit all components of coinjected N-TFA-isopropyl esters of ( $\pm$ )-phenylalanine and ( $\pm$ )-glutamic acid to be resolved completely (Fig. 5).

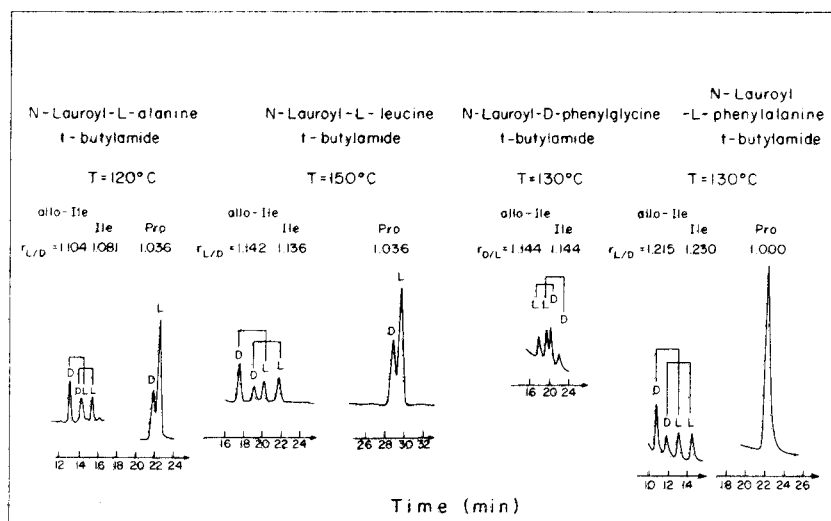


Fig. 4. Chromatogram of N-TFA-isopropyl esters of allo-Ile, Ile and Pro on capillary columns coated with I-IV.

\* Corey-Pauling-Koltun.

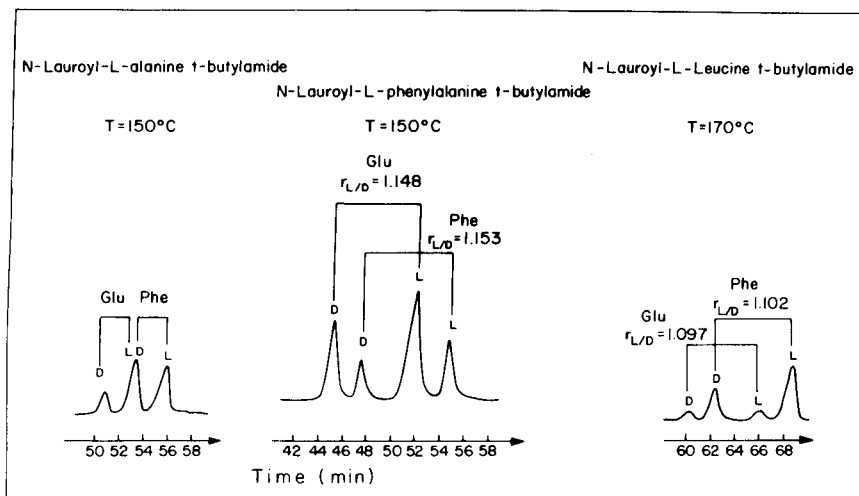


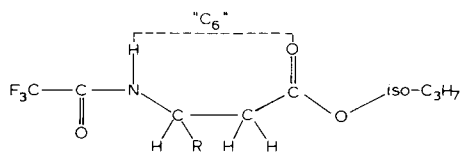
Fig. 5. Chromatogram of N-TFA-isopropyl esters of Glu and Phe on capillary columns coated with I, II and IV.

Stationary phases I and II (especially II) resolve proline reasonably well (Fig. 4) but, as already stated above, the aromatic stationary phases III and IV do not show chiral recognition for this secondary amino acid.

In a preceding paper<sup>10</sup>, the stereoselectivity observed in the chromatography of N-TFA-*tert.*-butylamides of  $\alpha$ -amino acids on stationary phases I-IV was reported, and the remarkable resolution of proline obtained through such derivatization was discussed.

In conclusion, II and IV are the most useful stationary phases for  $\alpha$ -amino acid analysis of the four diamides studied here. The phenylglycine stationary phase (III) is not expected to be very stable optically, owing to the presence of a benzylic carbon atom in its molecule. The main advantage of the alanine stationary phase (I) lies in its application to the resolution of  $\alpha,\alpha$ -dialkylamino acids<sup>8</sup>, which will be reported in a forthcoming publication.

*$\beta$ -Amino acids.* Placing the amino group in the  $\beta$ -position with respect to the carboxylic group imparts a " $C_6$ " moiety to these compounds, and strongly affects the nature of the stereoselective interaction with the diamides derived from  $\alpha$ -amino acids.



In agreement with previous work<sup>12</sup>, the  $\beta$ -amino acids listed in Table II gave considerably lower  $r$  values than those found for the  $\alpha$ -amino acids. The alanine stationary phase (I) does not show any chiral recognition for the derivatives examined, and II gives relatively low resolution factors (Table II) of the same magnitude and same order of emergence as on V<sup>12</sup>. On the other hand, the aromatic



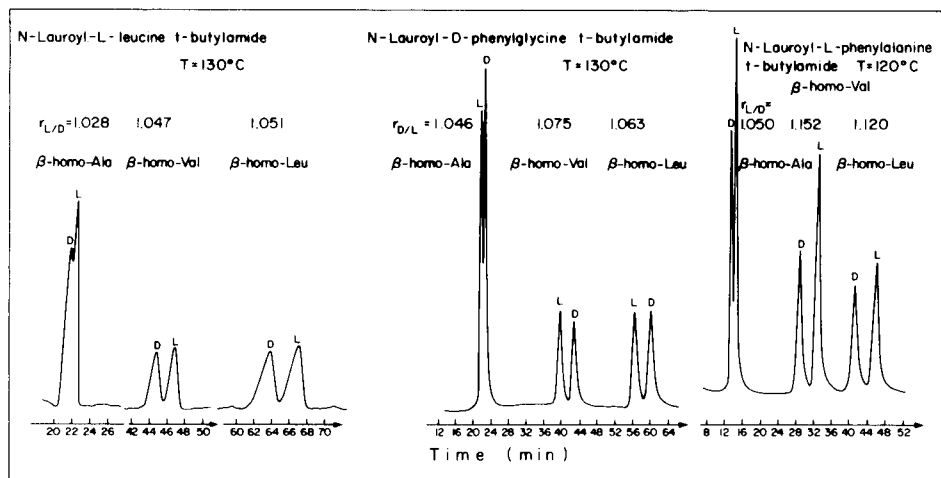
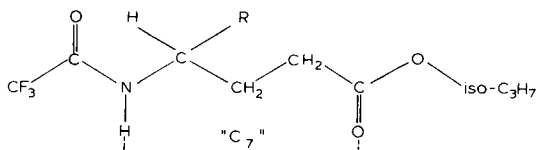


Fig. 6. Chromatogram of N-TFA-isopropyl esters of ( $\pm$ )- $\beta$ -amino acids on capillary columns coated with II–IV. The term "homo" signifies that a methylene group is inserted between the carboxylic group and the asymmetric carbon of the reference substance.

diamides III and IV are more stereoselective in their interaction with this class of compounds. This is true in particular for the phenylalanine stationary phase (IV), which is recommended for analytical applications (Fig. 6).

More data on the behaviour of  $\beta$ -amino acid derivatives will have to be collected before attempting to propose a mechanism for their chiral recognition.

*$\gamma$ -Amino acids.* The aliphatic stationary phases I and II were found to manifest chiral differentiation ( $r = 1.026$ – $1.056$ ) for the N-TFA-isopropyl esters of the branched  $\gamma$ -amino acids, but not for  $\gamma$ -aminovaleric acid (Table II). When a comparison is made with the resolution factors obtained on V and on N-lauroyl-L-valine-6-undecylamide (VI)<sup>12</sup>, taking into account the difference in column temperature (VI, 140°C) and optical purity (V, 75%; VI, 88%), it is found that I and II have lower stereoselectivity for the  $\gamma$ -amino acids resolved. The order of emergence is the same as for the valine stationary phase (V) ( $r_{L/D} < 1.00$ ). This latter finding is consistent with a common mechanism of resolution which is considered to involve hydrogen bonding between the " $C_7$ " side of the solutes and the " $C_5$ " side of the diamide stationary phases<sup>12</sup>.



On the other hand, in contrast to the results for the  $\beta$ -amino acids, the aromatic stationary phases III and IV did not show any stereoselectivity for the  $\gamma$ -amino acids examined (reduction of the temperature below 130°C did not change this result).

RESOLUTION OF N-TFA-O-ACYL DERIVATIVES OF 2-AMINO-ALKAN-1-OLS [RCH(NHCOCF<sub>3</sub>)CH<sub>2</sub>OCOR<sub>1</sub>] ON DIAMIDE STATIONARY PHASESSee Table II for chromatographic conditions and definition of  $r$  and  $r_{D,L}$ .

		Stationary phase												<i>T</i> / <i>C</i>				
		N-Lauroyl-L-valine-tert-butylamide (I)				N-Lauroyl-L-leucine-tert-butylamide (II)				N-Lauroyl-L-phenylalanine-tert-butylamide (III)								
		Acyl group (COR <sub>1</sub> )				Acyl group (COR <sub>1</sub> )				Acyl group (COR <sub>1</sub> )								
Enantiomer		Propionyl	Isobutyryl	Pivaloyl	Enantiomer		Propionyl	Isobutyryl	Pivaloyl	Enantiomer		Propionyl	Isobutyryl	Pivaloyl	<i>T</i> / <i>C</i>			
<i>r</i>	<i>r</i> <sub>D,L</sub>	<i>r</i>	<i>r</i> <sub>D,L</sub>	<i>r</i>	<i>r</i> <sub>D,L</sub>	<i>r</i>	<i>r</i> <sub>D,L</sub>	<i>r</i>	<i>r</i> <sub>D,L</sub>	<i>r</i>	<i>r</i> <sub>D,L</sub>	<i>r</i>	<i>r</i> <sub>D,L</sub>	<i>r</i>	<i>r</i> <sub>D,L</sub>	<i>r</i>	<i>r</i> <sub>D,L</sub>	
2-Amino-propan-1-ol	L	10.40	1.018	13.50	1.033	140	13.14	1.023	15.64	1.036	170	17.28	1.000	9.70	1.000	11.40	1.000	130
	D	11.60	1.030	13.90	1.050	140	13.44	1.031	16.12	1.036	170	17.90	1.000	9.70	1.000	11.40	1.000	130
2-Amino-butan-1-ol	L	14.36	1.033	16.84	1.065	140	19.22	1.043	22.66	1.070	170	24.44	1.000	19.12	1.000	19.66	1.035	130
	D	14.84	1.046	17.62	1.078	140	20.04	1.054	23.88	1.070	170	26.14	1.000	19.12	1.000	20.34	1.035	130
2-Amino-pentan-1-ol	L	21.68	1.045	25.34	1.062	140	28.56	1.052	33.26	1.063	170	35.30	1.000	31.20	1.000	32.10	1.041	130
	D	22.66	1.062	26.92	1.080	140	30.04	1.052	35.34	1.063	170	38.06	1.000	31.20	1.000	33.42	1.041	130
2-Amino-hexan-1-ol	L	34.26	1.052	39.68	1.067	140	43.48	1.052	49.92	1.059	170	53.24	1.000	29.44	1.000	30.60	1.038	150
	D	36.04	1.067	42.34	1.085	140	45.74	1.052	52.86	1.059	170	57.32	1.000	29.44	1.000	31.76	1.038	150
2-Amino-heptan-1-ol	L	36.40	1.045	40.92	1.058	150	67.98	1.052	79.28	1.065	170	83.84	1.000	49.60	1.014	60.24	1.052	150
	D	38.04	1.058	43.28	1.076	150	71.54	1.052	84.44	1.065	170	90.92	1.000	49.60	1.014	63.36	1.052	150
2-Amino-octan-1-ol	L	56.62	1.044	66.34	1.062	150	109.96	1.053	127.18	1.073	170	134.06	1.000	81.60	1.014	92.20	1.040	150
	D	59.12	1.066	70.48	1.078	150	115.70	1.053	136.52	1.073	170	145.30	1.000	81.60	1.014	95.84	1.040	150
2-Amino-3-methylbutan-1-ol	L	15.36	1.038	18.46	1.056	140	21.00	1.062	24.70	1.075	170	26.74	1.000	19.24	1.041	20.54	1.058	130
	D	15.94	1.056	19.50	1.069	140	22.30	1.062	26.54	1.075	170	29.02	1.000	19.24	1.041	21.72	1.058	130
2-Amino-4-methylpentan-1-ol	L	27.00	1.046	33.02	1.058	140	33.90	1.050	40.30	1.058	170	41.28	1.000	36.28	1.000	34.56	1.030	130
	D	28.24	1.066	34.92	1.081	140	35.60	1.050	42.64	1.058	170	44.70	1.000	36.28	1.000	35.60	1.030	130

### 2-Aminoalkan-1-ols

The N-TFA-O-acyl-2-aminoalkan-1-ols are considered to have a resolution mechanism similar to that of the above N-TFA esters of  $\gamma$ -amino acids<sup>1,2</sup>. In fact, on stationary phases I-IV the two classes of compounds show similar behaviour (Table IV), including, in particular, the order of emergence and a marked reduction in stereoselectivity by an R'' aryl substituent.

No chiral recognition occurred on the phenylglycine stationary phase (III) under any conditions tried, and none of the O-propionyl derivatives could be resolved in IV. For isobutyryl as the O-acyl group, only three of the compounds examined showed weak chiral differentiation on IV. Even the introduction of the usually very effective O-pivaloyl group led to no separation for 2-aminopropan-1-ol and very small *r* values for the other aminoalkanols.

On the other hand, far more efficient separation of the enantiomeric amino alkanols is possible on aliphatic stationary phases, paralleling the findings for the  $\gamma$ -amino acids. Not unexpectedly, the leucine stationary phase (II), with the larger R'' group, is superior to the alanine stationary phase (I). A comparison of chiral differentiation of the aminoalkanol derivatives on II and on the previously studied VI<sup>1,2</sup> cannot be readily made, as the respective *r* values were measured at column temperatures differing by 40°C. Stationary phase II is excellent for the enantiomeric analysis of aminoalkanols (see Fig. 7) and can also be readily operated at a temperature as high as 170°C.

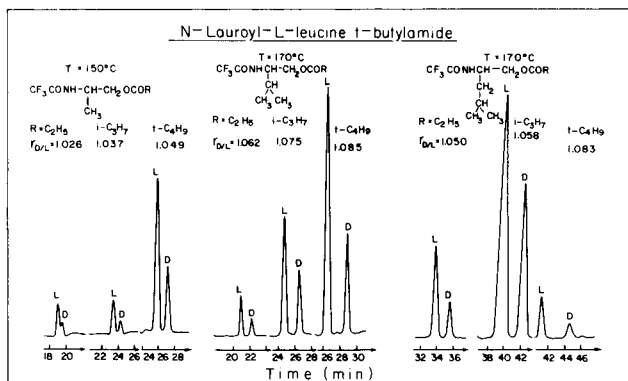


Fig. 7. Chromatogram of ( $\pm$ )-N-TFA-O-acyl-2-aminoalkan-1-ols on II.

### Amines

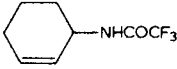
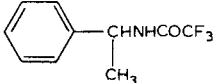
In a recent paper<sup>5</sup>, the chromatography of N-TFA-amines on the diamide N-docosanoyl-L-valine-2-(2-methyl)-*n*-heptadecylamide (VII) was discussed. It was pointed out that the pattern of solute-solvent hydrogen bonding and, hence, the mechanism of resolution for this class of stationary phase differs from that of amino acids and amino alcohol derivatives.

In this work it was found that the aliphatic, but not the aromatic, stationary phases have stereoselectivity for the amine derivatives; further, the aliphatic amines studied were resolved only on II, and not on I. Wherever separation of enantiomers was achieved, the order of emergence on the L-stationary phases was *S* after the *R* isomer, as on all other stationary phases permitting resolution of amines<sup>5,13-14</sup>.

TABLE V

RESOLUTION OF CHIRAL N-TFA-AMINES ON N-LAUROYL-L-ALANINE-*tert.*-BUTYL-AMIDE (I) AND N-LAUROYL-L-LEUCINE-*tert.*-BUTYLAMIDE (II)

For chromatographic conditions see Table II.

Compound	I			II		
	$r^*$ (min)	$r_{II/I}^{**}$	$T(^{\circ}\text{C})$	$r^*$ (min)	$r_{II/I}^{**}$	$T(^{\circ}\text{C})$
$n\text{-C}_5\text{H}_{11}\text{CHNHCOCF}_3$   CH <sub>3</sub>	}			R 14.04	Shoulder	140
				S 14.40		
$n\text{-C}_6\text{H}_{13}\text{CHNHCOCF}_3$   CH <sub>3</sub>	}			R 23.50	1.027	140
				S 24.14		
$n\text{-C}_7\text{H}_{15}\text{CHNHCOCF}_3$   CH <sub>3</sub>	} No separation on I			I 40.64	1.025	140
				II 41.64		
$n\text{-C}_8\text{H}_{17}\text{CHNHCOCF}_3$   CH <sub>3</sub>	}			I 71.74	1.023	140
				II 73.36		
$\text{C}_2\text{H}_5\text{CHCH}_2\text{CHNHCOCF}_3$         CH <sub>3</sub> CH <sub>3</sub>	}			I 12.66	1.040	150
				II 13.16		
	I 32.60	1.023	80			
	II 33.60					
	R 54.60	1.050	110	R 33.90	1.049	150
	S 57.36			S 35.56		

\* See Table II

\*\* See Table II.

Compared with the above valine stationary phase (VII), II shows a higher selectivity<sup>5</sup>. For instance, the aliphatic amines listed in Table V have  $r$  values at 140°C similar to those on VII<sup>5</sup> at 110°C, and peak resolution is improved (Fig. 8).

Remarkably, N-TFA-3-aminocyclohexene, which is difficult to resolve, separated to some extent into two peaks on the alanine stationary phase, as was also observed on VII<sup>5</sup>. On I at 80°C, the retention times of the peaks were 32.60 and 33.30 min, respectively ( $r_{II/I} = 1.023$ ;  $R_s = 0.25$ ); resolution on II was not possible under any of the conditions tried.

As reported previously<sup>5,13</sup>, the N-TFA derivative of  $\alpha$ -phenylethylamine is much better resolved than aliphatic amines. The difference between the leucine and alanine is also apparent in this instance. Whereas for II the resolution factor is 1.05 at 150°C, a similar  $r$  value can be obtained on I only at 110°C.

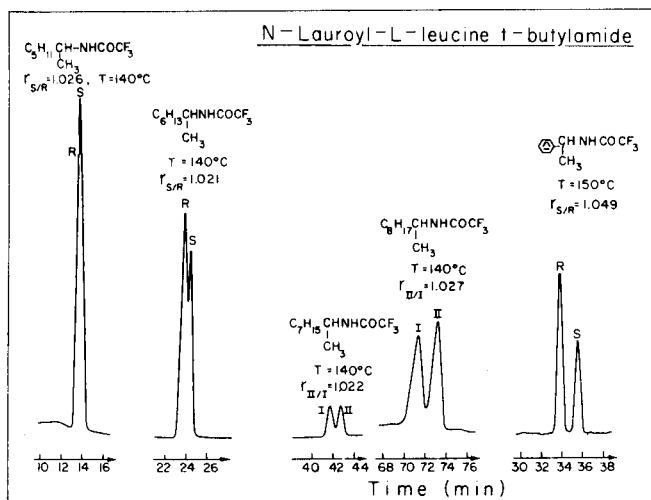


Fig. 8. Chromatogram of N-TFA-(±)amines on II.

On columns with a sufficient number of theoretical plates, II should be as useful for the enantiomeric analysis of amines (Fig. 8) as the stationary phases previously introduced for this purpose, *e.g.*, carbonylbis-(N-L-valine isopropyl ester)<sup>14</sup> and N-lauroyl-S- $\alpha$ -(1-naphthyl)ethylamine<sup>13</sup>.

*Aromatic R' groups.* Some comments can be made on the influence of the phenyl and the benzyl groups in III and IV, respectively, when substituted in the  $\alpha$ -position of the solvent molecule. As far as the resolution of derivatives of the  $\alpha$ -amino acids is concerned, the aromatic groups behave similarly to isobutyl (II), suggesting that their effect is essentially one of bulk. However, this parallelism with the isobutyl group breaks down for the other classes of solutes examined. Stationary phases III and IV are more selective with respect to derivatives of the  $\beta$ -amino acids. On the other hand, for  $\gamma$ -amino acids, aminoalkanols and amines, either no chiral recognition occurs or only very low resolution factors were observed (see N-TFA-O-pivaloylaminoalkanols, Table IV).

Stereoselective interactions between solutes and chiral solvents or supports, which seem to involve specifically an aromatic ring, have been observed in many instances. Thus, the interpretation of the resolution of aromatic amino acids on cellulose invokes absorption of the flat benzene residue as part of a "three-point" interaction model<sup>15</sup>. For various solutes it has been found that the gas chromatographic resolution of an aromatic compound is much more efficient than that of corresponding aliphatic or cycloaliphatic derivatives, as demonstrated, for example, by the amines listed in Table V. Also, the different stereoselective shifts of NMR signals of enantiomeric carbonyl-containing compounds in the presence of a chiral aromatic additive are assumed to be due to the formation of diastereomeric contact complexes with oriented donor-acceptor association between the carbonyl and benzene groups<sup>16</sup>. In the examples studied in this work, depending on the mechanism of resolution, additional associations with the benzene ring might have either a synergic effect or, on the contrary, interfere with the formation of the solute-solvent complex responsible for chiral recognition.

## ACKNOWLEDGEMENTS

We are indebted to the Stiftung Volkswagenwerk for partial support of this research. S.-C. C. thanks the Chung-Shan Institute of Science and Technology, Taiwan, Republic of China, for the grant of a scholarship.

## REFERENCES

- 1 E. Gil-Av and B. Feibush, *U.S. Pat.*, 3, 494, 105 (1970); *Jap. Pat.*, 567267.
- 2 B. Feibush, *Chem. Commun.*, (1971) 544.
- 3 R. Charles, U. Beitler, B. Feibush and E. Gil-Av, *J. Chromatogr.*, 112 (1975) 121.
- 4 U. Beitler and B. Feibush, *J. Chromatogr.*, 123 (1976) 149.
- 5 R. Charles and E. Gil-Av, *J. Chromatogr.*, 195 (1980) 317.
- 6 H. Frank, G. J. Nicholson and E. Bayer, *Angew. Chem.*, 90 (1978) 396.
- 7 T. Saeed, P. Sandra and M. Verzele, *J. Chromatogr.*, 186 (1979) 611.
- 8 Shu-Cheng Chang, R. Charles and E. Gil-Av, *Franco-Israeli Symposium on Chiral Structures, Milly-La Forêt, May 1979*.
- 9 E. Gil-Av, R. Charles-Sigler, G. Fischer and D. Nurok, *J. Gas Chromatogr.*, 4 (1966) 51.
- 10 S.-C. Chang, R. Charles and E. Gil-Av, *J. Chromatogr.*, 202 (1980) 247.
- 11 W. Parr, C. Yang, E. Bayer and E. Gil-Av, *J. Chromatogr. Sci.*, 8 (1970) 591.
- 12 B. Feibush, A. Balan, B. Altman and E. Gil-Av, *J. Chem. Soc., Perkin Trans. II*, (1979) 1230.
- 13 S. Weinstein, L. Leiserowitz and E. Gil-Av, *J. Amer. Chem. Soc.*, 102 (1980) 2768.
- 14 B. Feibush and E. Gil-Av, *J. Gas Chromatogr.*, 5 (1967) 257.
- 15 C. E. Dalglish, *J. Chem. Soc.*, (1952) 3940.
- 16 W. H. Pirkle and S. D. Beare, *J. Amer. Chem. Soc.*, 91 (1969) 5150.

CHROM. 14,299

## STUDIES ON THE THERMODYNAMICS OF SOLUTION BY GAS CHROMATOGRAPHY

### SOLUBILITY MEASUREMENTS OF HYDROCARBONS IN $\beta$ -ALKOXY-PROPIONITRILES

R. K. KUCHHAL\* and K. L. MALLIK\*

*Indian Institute of Petroleum, Dehradun (India)*

(First received May 21st, 1981; revised manuscript received August 10th, 1981)

---

#### SUMMARY

Gas chromatography was used to obtain activity coefficients at infinite dilution for twelve hydrocarbon solutes in five alkoxypropionitrile solvents at three temperatures, 30, 40 and 50°C. A comparative study of elution characteristics and thermodynamic parameters for the alkoxypropionitriles was made. The activity coefficient data were analysed in the light of the molecular structure of the solutes.

---

#### INTRODUCTION

Gas chromatography (GC) is an effective technique for studying the thermodynamics of non-electrolyte solutions<sup>1-7</sup>. The objective of this work was to obtain retention volumes for five  $\beta$ -alkoxypropionitriles (some of which are selective for C<sub>4</sub> isomer separation) and thus provide information bearing on theories of solution which might lead to a more quantitative approach to liquid phase selection and design. Propionitriles have long been known for their outstanding solvent characteristics for aromatics<sup>8,9</sup> and 1,3-butadiene<sup>10-15</sup>. Among the  $\beta$ -alkoxypropionitriles, the first member of the series,  $\beta$ -methoxypropionitrile, has already been established as superior to furfural for 1,3-butadiene extraction. Preliminary experimental data indicated<sup>15</sup> that  $\beta$ -ethoxypropionitrile may also be used as an extractant. In earlier detailed studies<sup>16-18</sup>, we reported that  $\beta$ -alkoxypropionitriles could be used as stationary phases for the analysis of lighter hydrocarbons, particularly for the resolution of difficult C<sub>4</sub> isomer pairs under appropriate conditions. So far, to our knowledge, no studies on the thermodynamics of solution have been reported for these  $\beta$ -alkoxypropionitriles. In this work, the thermodynamics of dilute solutions were investigated by determining activity coefficients.

---

\* Present address: Lubrizol India Ltd., Delstar, 9 A-S. Patkar Marg, Bombay, India.

## EXPERIMENTAL

The solvents  $\beta$ -methoxy- (MOPN),  $\beta$ -ethoxy- (EOPN),  $\beta$ -propoxy- (PrOPN),  $\beta$ -butoxy- (BOPN) and  $\beta$ -pentoxy- (POPN) propionitrile were synthesized by reaction of acrylonitrile with methyl, ethyl, *n*-propyl-, *n*-butyl and *n*-pentyl alcohol, respectively, according to Bruson and Riener<sup>19</sup>, the details of which have been described elsewhere<sup>20</sup>. The purity of the synthesized compounds was checked by gas chromatographic analysis and carbon and hydrogen determinations. The purity of each compound was found to be not less than 99.8%. The physical properties of the  $\beta$ -alkoxypropionitriles are reported in Table I.

TABLE I  
PHYSICAL PROPERTIES OF SOLVENTS

<i>Solvent</i>	<i>Mol. wt.</i>	<i>Boiling point (°C)</i>	<i>Density (<math>d_4^{20}</math>)</i>	<i>Refractive index (20°C)</i>
$\beta$ -Methoxypropionitrile	85.1	166	0.9328	1.4032
$\beta$ -Ethoxypropionitrile	99.1	58/10 mmHg	0.8940	1.4075
$\beta$ -Propoxypropionitrile	113.2	73.5/10 mmHg	0.8891	1.4131
$\beta$ -Butoxypropionitrile	127.2	98/20 mmHg	0.8810	1.4182
$\beta$ -Pentoxypropionitrile	141.2	117/18 mmHg	0.8794	1.4245

The solutes used were of analytical reagent grade from Philips Petroleum or BDH. In order to obtain a better comparison, the experimental conditions for all five solvents were kept almost identical. These solvents, used as typical GC stationary phases, were impregnated on a solid support, Chromosorb P (50–60 mesh). The stationary phase loading was maintained as high as 29% in order to prevent any significant solute adsorption at the gas–liquid interface. The coated support materials were packed in 2-m copper tubes (3 mm I.D.).

A Chrome-Alyzer-100 gas chromatograph equipped with a thermal conductivity detector was used. Hydrogen was used as the carrier gas. The size of the samples injected into the column ranged from 0.1 to 1.0  $\mu$ l for liquids and from 20 to 50  $\mu$ l for gaseous hydrocarbons.

Because of the low boiling points of the solvents, the columns were operated at low temperatures. MOPN and EOPN were studied at 30°C, PrOPN at 30 and 40°C and BOPN and POPN at 30, 40 and 50°C (all  $\pm 0.1^\circ\text{C}$ ). In order to minimize the depletion of solvents, a presaturator was used before the analytical column so that the carrier gas was saturated with the solvent, thus reducing the possibility of depletion of the stationary phase. While working with various volatile solvents in studies on the thermodynamics of solution during the last few years, we have found that the presaturator column helps to obtain consistent and accurate thermodynamic data<sup>20–23</sup>. The presaturator column (30 cm  $\times$  3 mm I.D.), packed with about 35% (w/w) of the desired solvent-coated support material, was located prior to the point of sample injection and manometer. Satisfactory functioning of the presaturator columns was reflected in the stability of the baseline, as no discernible changes were observed



throughout the brief experimental work. Moreover, the solvent loss, if any, was monitored by weighing the analytical column before and after each experimental run and making corrections accordingly.

The retention time ( $t'_R$ ) for each solute was measured from the air peak to solute peak maxima and the values used in calculations were averages of at least triplicate runs. The pressure difference was monitored with the help of a mercury manometer and was taken as the inlet pressure of the column. The outlet pressure was atmospheric at all times. The vapour pressures for hydrocarbon solutes were calculated from Antoine's equation constants<sup>24,25</sup>.

## RESULTS

Specific retention volumes ( $V'_g$ ) were determined for twelve hydrocarbons using the well known expression described by Littlewood *et al.*<sup>26</sup>. The  $V'_g$  data are reported in Table II.

Solute activity coefficients at infinite dilution in the liquid phase ( $\gamma_{2,p}^\infty$ ) were determined from the equation<sup>27-29</sup>

$$\gamma_{2,p}^\infty = \frac{1.704 \cdot 10^7}{M P_2 V'_g} \quad (1)$$

where  $M$  is the solvent molecular weight and  $P_2^\circ$  Torr is the vapour pressure of the pure saturated solute vapour. This equation has been discussed in detail elsewhere<sup>20,21</sup>.

Activity coefficients corrected for vapour phase imperfections,  $\gamma_{2,t}^\infty$ , are given by<sup>6,7</sup>

$$\ln \gamma_{2,t}^\infty = \ln \gamma_{2,p}^\infty - \frac{(\beta_{22} - v_2^\circ) p_2^\circ}{R T} + \frac{(2\beta_{12} - v_2^\circ) \bar{p}}{R T} \quad (2)$$

where  $v_2^\circ$  is the molar volume and  $\beta_{22}$  is the second virial coefficient for the pure solute at temperature  $T$ . In the last term,  $\beta_{12}$ ,  $v_2^\circ$  and  $\bar{p}$  are the cross second virial coefficient, the partial molar volume of the solute at infinite dilution and the mean column pressure, respectively. The  $\beta_{22}$  data for the solutes studied lie between  $-500$  and  $-1800$  cm<sup>3</sup>/mole in the temperature range 30–50°C, and the mixed virial coefficient ( $\beta_{12}$ ) data for the hydrogen–hydrocarbon system may be of either sign (values are of the order of  $-40$  to  $30$  cm<sup>3</sup>/mole<sup>30</sup>). More specifically, the  $\beta_{12}$  values with hydrogen as the carrier gas are towards the negative end and some cancellation occurs between the two gas-phase imperfection terms in eqn. 2. Hence, the activity coefficient at infinite dilution values were determined employing eqn. 1.

Table III gives the activity coefficient data for twelve hydrocarbons at infinite dilution. The values are the means of at least three experimental runs. No values are available in the literature for these solvents for comparison. The reliability of the method for the determination of  $\gamma_{2,p}^\infty$  has been demonstrated in earlier papers<sup>20-23</sup>, where comparisons were made of GC-derived  $\gamma_{2,p}^\infty$  values with those obtained either from the static method, vapour–liquid equilibria or from earlier reported GC data for a number of binary systems. In this study the reproducibility of  $\gamma_{2,p}^\infty$  was 2–3%.

TABLE II  
SPECIFIC RETENTION VOLUME IN  $\beta$ -ALKOXYPROPIONITRILES

Solute	MOPN,	EOPN,	Pi-OPN		BOPN		POPn		
	30°C	30°C	30°C	40°C	30°C	40°C	30°C	40°C	50°C
Isobutane	4.28	7.24	10.69	8.65	11.69	9.26	13.42	10.30	8.34
<i>n</i> -Butane	6.22	10.57	15.52	13.03	17.40	13.25	19.89	15.10	12.07
<i>n</i> -Pentane	15.24	28.03	43.00	32.03	49.88	37.12	57.50	41.32	31.93
<i>n</i> -Hexane	36.81	77.27	116.50	86.78	138.7	96.65	167.0	111.1	82.60
Isobutene	12.94	16.74	21.72	17.00	23.35	17.64	25.34	19.54	15.02
1-Butene	11.40	15.66	21.23	16.50	22.93	17.36	24.75	19.08	15.39
<i>trans</i> -2-Butene	14.14	19.88	25.58	20.25	28.67	21.42	30.38	23.67	17.80
<i>cis</i> -2-Butene	16.65	23.67	30.87	23.37	33.78	24.91	36.24	27.46	20.65
<i>trans</i> -2-Pentene	28.01	51.44	68.48	49.15	75.43	54.55	83.41	59.36	45.27
<i>cis</i> -2-Pentene	31.61	57.48	75.65	53.98	82.39	59.40	93.44	64.54	48.87
<i>trans</i> -2-Hexene	74.99	126.1	—	—	196.9	133.0	224.1	157.2	106.9
<i>cis</i> -2-Hexene	87.30	144.6	199.5	—	222.9	150.2	252.2	171.4	119.6

## DISCUSSION

With all the five stationary phases, it was possible to resolve saturated and unsaturated lower hydrocarbons in a relatively short time. The chromatograms of all of the compounds showed symmetrical peaks useful for analytical studies. The first member of the series, MOPN, separated a pair that is difficult to resolve, isobutene and butene-1.

Table II reveals that the  $\log V_g$  values are linearly related to the carbon number of the solutes at a particular temperature, and  $V_g$  increases systematically with increase in the carbon number of the alkyl chain attached to the  $\beta$ -alkoxypropionitrile solvents. Interestingly, this observation is in conformity with that of Langer *et al.*<sup>31</sup>.

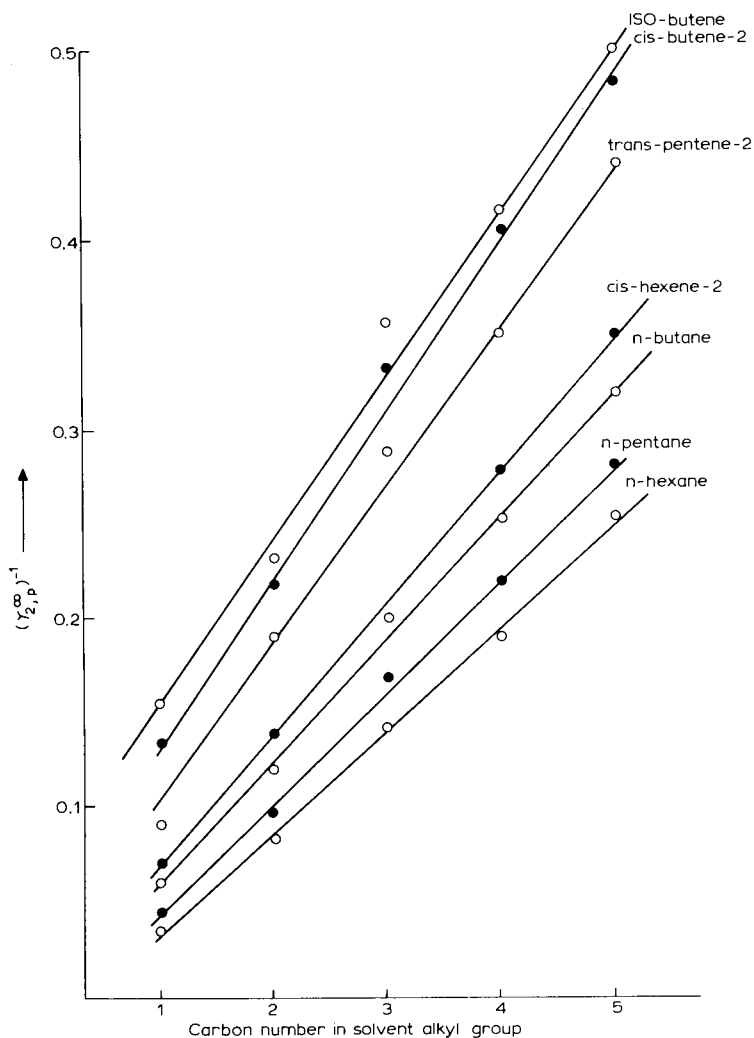


Fig. 1. Incremental relationship between solute activity coefficient and alkyl chain length of  $\beta$ -alkoxypropionitrile solvents.

TABLE III  
LIMITED ACTIVITY COEFFICIENT DATA FOR HYDROCARBONS IN  $\beta$ -ALKOXYPROPIONITRILES

Solute	MOPN, 30°C		EOPN, 30°C		PrOPN		BOPN		POPn	
	30°C	40°C	30°C	40°C	30°C	40°C	30°C	40°C	30°C	50°C
Isobutane	15.53	4.68	7.89	4.43	3.81	3.68	3.53	2.99	2.98	2.87
<i>n</i> -Butane	15.18	4.58	7.67	4.09	3.63	3.58	3.37	2.86	2.83	2.71
<i>n</i> -Pentane	21.33	5.69	9.96	5.43	4.34	4.17	4.06	3.41	3.37	3.17
<i>n</i> -Hexane	29.04	6.90	11.88	6.22	5.16	4.97	4.74	3.86	3.79	3.61
Isobutene	5.84	2.53	3.89	2.52	2.17	2.17	2.12	1.80	1.76	1.73
1-Butene	6.79	2.74	4.25	2.66	2.26	2.25	2.20	1.89	1.84	1.80
<i>trans</i> -2-Butene	6.42	3.87	3.87	2.54	2.12	2.13	2.04	1.78	1.74	1.75
<i>cis</i> -2-Butene	6.93	2.88	4.23	2.72	2.29	2.28	2.21	1.92	1.86	1.88
<i>trans</i> -2-Pentene	10.66	3.35	5.03	3.15	2.74	2.68	2.65	2.17	2.20	2.12
<i>cis</i> -2-Pentene	11.76	3.62	5.51	3.59	2.93	2.86	2.80	2.38	2.37	2.23
<i>trans</i> -2-Hexene	12.27	—	6.36	—	3.22	3.22	3.09	2.56	2.54	2.49
<i>cis</i> -2-Hexene	13.87	4.04	7.08	—	3.53	3.51	3.39	2.80	2.78	2.72

TABLE IV  
RELATIONSHIP BETWEEN SOLUTION PROPERTIES AND PHYSICAL PROPERTIES OF SOLUTES

Solute pair	Vapour pressure	Molar volume	Critical temperature	Electron polarizability ( $\alpha_e^2$ )	Activity coefficient ( $\gamma_{2,p}^*$ )	Chromatographic elution
<i>n</i> -Alkane to <i>n</i> -alkane ( <i>e.g.</i> , <i>n</i> -butane to <i>n</i> -pentane)	$n-C_5 < n-C_4$	$n-C_5 > n-C_4$	$n-C_5 > n-C_4$	$n-C_5 > n-C_4$	$n-C_5 > n-C_4$	$n-C_5 > n-C_4$
<i>n</i> -Alkane to branched-chain alkane ( <i>e.g.</i> , <i>n</i> -butane to isobutane)	$n-C_4 < i-C_4$	$n-C_4 < i-C_4$	$n-C_4 > i-C_4$	$n-C_4 > i-C_4$	$n-C_4 < i-C_4$	$n-C_4 > i-C_4$
<i>n</i> -Alkane to <i>n</i> -olefin ( <i>e.g.</i> , <i>n</i> -butane to 1-butene)	$n-C_4 < C_4^{-1}$	$n-C_4 > C_4^{-1}$	$n-C_4 > C_4^{-1}$	$n-C_4 < C_4^{-1}$	$n-C_4 > C_4^{-1}$	$n-C_4 < C_4^{-1}$
<i>n</i> -Olefin to branched-chain olefin (1-butene to isobutene)	$C_4^{-1} < i-C_4'$	$C_4^{-1} < i-C_4'$	$C_4^{-1} > i-C_4'$	$C_4^{-1} < i-C_4'$	$C_4^{-1} > i-C_4'$	$C_4^{-1} < i-C_4'$
<i>cis</i> -2-Alkene to <i>trans</i> -2-alkene ( <i>e.g.</i> , pentene-2)	$trans > cis$	$trans > cis$	$trans < cis$	$trans < cis$	$trans < cis$	$trans < cis$

The  $V_g^*$  values of ethylbenzene increase with increase in the alkyl chain length of di-*n*-alkylhalophthalate esters. The  $\gamma_{2,p}^\infty$  values for the solutes decrease from MOPN to POPN. A linear relationship exists between the inverse of the solute activity coefficient at infinite dilution and the carbon number of the alkyl group in the  $\beta$ -alkoxypropionitrile solvents, as indicated in Fig. 1. However, the logarithmic activity coefficients, as shown in Fig. 2, are directly related to the carbon number of the solutes. Both of these results indicate that the group contribution model of Pierotti and co-workers<sup>32-34</sup> can perhaps be employed.

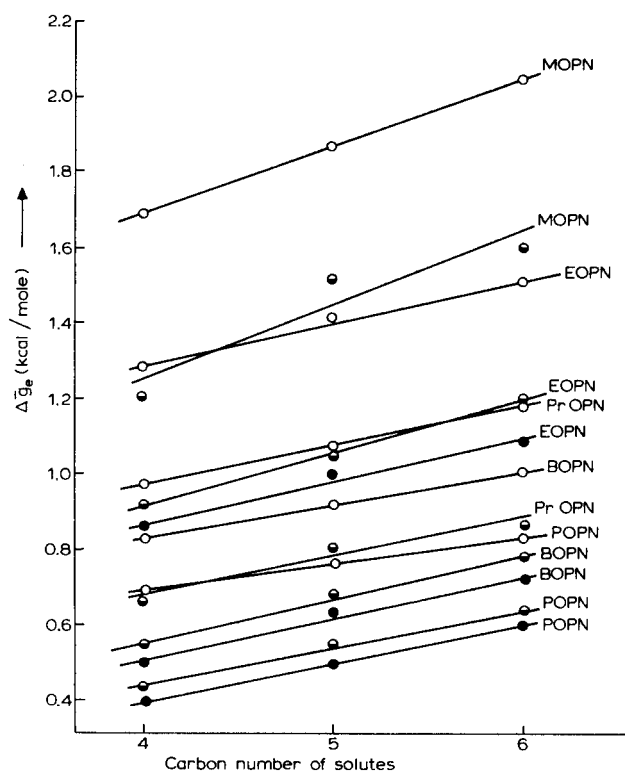


Fig. 2. Incremental relationship between excess free energy and molecular structure for solutes in  $\beta$ -alkoxypropionitrile solvents.  $\circ$ , *n*-Alkane;  $\bullet$ , *cis*-2-alkene;  $\bullet$ , *trans*-2-alkene.

Newman and Prausnitz<sup>35</sup> discussed the energetic effects in solution and classified them according to the chemical and physical forces operative in it. In the present system, it would be safer to assume that chemical forces are not very strong and the physical forces (dispersion and orientational) predominate. The physical interactions are best represented by electron polarizability. The electron polarizability per unit volume ( $\alpha_c^v$ ) can be obtained from the Clausius-Mosotti equation:

$$\alpha_c^v = \frac{n^2 - 1}{n^2 + 2} \cdot \frac{3}{4 \pi N} \cdot \frac{M}{\rho} \quad (3)$$

$\alpha_c^v$  was calculated from this equation for all solutes. Fig. 3 shows an interesting linear

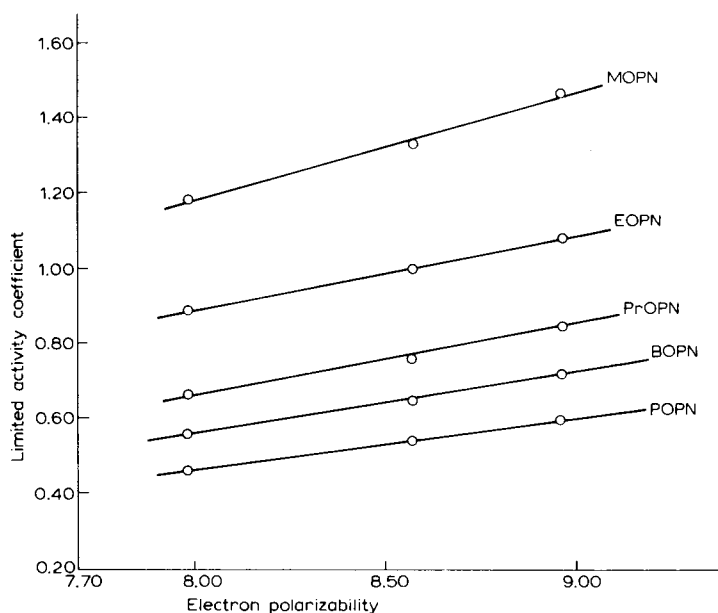


Fig. 3. Relationship between limited activity coefficient and electron polarizability of *n*-alkanes at 30°C.

relationship between  $\gamma_{2,p}^x$  and  $\alpha_c^v$  for *n*-alkane solutes at 30°C for all five solvents studied.

A comparison of the  $\gamma_{2,p}^x$  data for each *n*-alkane with those for the corresponding alkene indicates that the latter are strongly solvated in all five solvents owing to enhanced solute-solvent interactions (a dipole-induced dipole interaction between a strongly polar  $-C \equiv N^+$  group and a polarizable delocalized  $\pi$ -electron. Examination of the  $\gamma_{2,p}^x$  values for  $C_4$  olefins reveals that isobutene and *trans*-2-butene have preferential spatial arrangements compared with 1-butene and *cis*-2-butene, the interchange energy being minimized. In order to rationalize the solution properties of various isomers, it is worth considering solution properties in relation to some of the fundamental properties (additive as well as constitutive) of the solute. Table IV shows that  $\gamma_{2,p}^x$  values in general increase with the increase in molar volume and critical temperature and decrease with increase in the vapour pressure of the solutes. The data also indicate that the behaviour of two homologues (*n*-alkanes) is in accordance with their fundamental properties. For the pair *n*-butane-isobutane, it appears the molar volume predominates, isobutane has higher values of  $\gamma_{2,p}^x$  although the vapour pressure of isobutane is higher than that of *n*-butane. In a physical sense it seems that the higher molecular volume of isobutane molecules require a higher free energy to create a cavity in the solvent. Similarly, with two geometrical isomers *e.g.*, *cis*- and *trans*-2-alkenes, the *trans*-isomers have lower  $\gamma_{2,p}^x$  values, which reflects the fact that the *trans*-isomers have a favourable configuration for entering into solution. However, excluding vapour pressure, the electron polarizability and molar volume data of these olefins do not support this behaviour, because the  $\gamma_{2,p}^x$  values for *cis*-isomers should be lower than those of the *trans*-isomers, as the former have higher  $\alpha_c^v$  values and molar volumes. Interestingly, *cis*-2-alkenes are eluted later than the *trans*-isomers at all

temperatures in all five alkoxypropionitrile columns. In the absence of detailed data, it is difficult to explain this effect; however, perhaps when the alkyl groups are attached to the *syn*-position of an ethylenic double bond these bulky alkyl groups can hinder the approach of polar solvent molecules or *vice versa*, and thus reduce the interaction with polarizable  $\pi$ -bonds.

## REFERENCES

- 1 J. H. Purnell, *Ann. Phys. Rev.*, 18 (1967) 81.
- 2 R. Kobayashi, P. S. Chappellear and H. A. Deans, *Ind. Eng. Chem.*, 10 (1967) 64.
- 3 J. C. Giddings and K. L. Mallik, *Ind. Eng. Chem.*, 59, No. 4 (1967) 18.
- 4 C. L. Young, *Chromatogr. Rev.*, 14 (1968) 1.
- 5 K. L. Mallik, *An Introduction to Nonanalytical Applications of Gas Chromatography*, Peacock Press, New Delhi, 1976.
- 6 R. J. Laub and R. L. Pecsok, *Physicochemical Applications of Gas Chromatography*, Wiley-Interscience, New York, 1978.
- 7 J. R. Conder and C. L. Young, *Physicochemical Measurements by Gas Chromatography*, Wiley-Interscience, New York, 1979.
- 8 K. W. Saunders, *Ind. Eng. Chem.*, 43 (1951) 121.
- 9 E. C. Medcalf, A. G. Hill and G. N. Vriens, *Pet. Refiner*, 30 (1951) 97.
- 10 G. D. Davis and E. G. Makin, Jr., *U.S. Pat.*, 372109, March 5, 1968.
- 11 G. D. Davis, E. C. Mekin, Jr. and C. H. Middlebrooks, in R. F. Gould (Editor), *Refining Petroleum Chemicals*, American Chemical Society, Washington, DC, 1970, p. 215.
- 12 *Oil Gas J.*, 67, Oct. 20 (1969).
- 13 G. D. Davis and E. G. Makin, Jr., *Ind. Eng. Chem., Process Des. Develop.*, 8 (1969) 588.
- 14 B. S. Rawat, K. L. Mallik and I. B. Gulati, *J. Appl. Chem. Biotechnol.*, 22 (1972) 1001.
- 15 R. K. Kuchhal and K. L. Mallik, *J. Appl. Chem. Biotechnol.*, 26 (1976) 67.
- 16 R. K. Kuchhal and K. L. Mallik, *Chem. Ind. (London)*, (1972) 260; *Chromatographia*, 8 (1975) 639.
- 17 D. K. Banerjee, S. L. Chawla and K. L. Mallik, *Indian J. Technol.*, 13 (1975) 473.
- 18 R. K. Kuchhal and K. L. Mallik, *Indian J. Chem.*, 15B (1977) 478.
- 19 H. A. Bruson and J. W. J. Riener, *J. Amer. Chem. Soc.*, 65 (1943) 23.
- 20 R. K. Kuchhal, *PhD Thesis*, Meerut University, 1973.
- 21 R. K. Kuchhal and K. L. Mallik, *J. Chem. Eng. Data*, 17 (1972) 49.
- 22 R. K. Kuchhal, K. L. Mallik and P. L. Gupta, *Can. J. Chem.*, 55 (1977) 1273.
- 23 R. K. Kuchhal and K. L. Mallik, *Anal. Chem.*, 51 (1979) 392.
- 24 F. Rossini, *API Project 44, Selected Values of Physical and Thermodynamic Properties of Hydrocarbons and Related Compounds*, Carnegie Press, Pittsburgh, PA, 1953.
- 25 R. R. Driesbach, *Physical Properties of Chemical Compounds*, Advances in Chemistry Series, No. 15, 1955; No. 22, 1959, American Chemical Society, Washington, DC.
- 26 A. B. Littlewood, C. S. G. Phillips and D. T. Price, *J. Chem. Soc.*, (1955) 1480.
- 27 M. R. Hoare and J. H. Purnell, *Trans. Faraday Soc.*, 52 (1956) 222; *Research*, 8 (1955) 541.
- 28 D. E. Martire, in L. Fowler (Editor), *Gas Chromatography*, Academic Press, New York, 1963, p. 23.
- 29 D. E. Martire and L. Z. Pollara, *Advan. Chromatogr.*, 1 (1965) 335; *J. Chem. Eng. Data*, 10 (1965) 40.
- 30 D. H. Desty, A. Goldup, G. R. Luckhurst and W. T. Swanton, in M. Van Swaay (Editor), *Gas Chromatography 1962*, Butterworths, London, 1962, p. 67.
- 31 S. H. Langer, C. Zahn and G. Pantazoplos, *J. Chromatogr.*, 3 (1960) 154.
- 32 G. J. Pierotti, C. H. Deal, E. L. Derr and P. E. Porter, *J. Amer. Chem. Soc.*, 78 (1956) 2989.
- 33 G. J. Pierotti, C. H. Deal and E. L. Derr, *Ind. Eng. Chem.*, 51 (1959) 95.
- 34 C. H. Deal and E. L. Derr, *Applied Thermodynamics*, American Chemical Society, Washington, DC, 1968, p. 187.
- 35 R. D. Newman and J. M. Prausnitz, *J. Paint Technol.*, 45, No. 585 (1973) 33.

CHROM. 14,282

## GASCHROMATOGRAPHISCHE IDENTIFIZIERUNG NIEDRIG SIEDENDER SUBSTANZEN MITTELS RETENTIONSINDICES UND RECHNERHILFE

KARL-JOSEF GOEBEL

*Institut für Rechtsmedizin der Universität Bonn, Stiftsplatz 12, D-5300 Bonn (B.R.D.)*

(Eingegangen am 26. Juni 1981; geänderte Fassung eingegangen am 13. August 1981)

---

### SUMMARY

*Gas chromatographic identification of low boiling compounds by means of retention indices using a programmable pocket calculator*

For the rapid identification of volatile compounds in the forensic and clinic toxicological practice the retention indices were determined of 55 low boiling substances on Carbowax 1500 and Porapak Q. Based on a column efficiency characterized by the separation number  $TZ_{100}$  it is shown that most substances cannot unambiguously be identified using only one stationary phase, whereas the combination of both columns will allow to differentiate them with only few exceptions. The reproducibility of the index values within one laboratory and the prerequisites for the comparability between various laboratories are discussed.

---

### EINLEITUNG

Niedrig siedende Stoffe finden nicht nur in Industrie und Labor als Lösungsmittel und Extraktionsmittel, sondern auch im Haushalt als Verdünnungs- und Reinigungsmittel eine weite Verbreitung. Daher ist es nicht verwunderlich, dass sie eine grosse gewerbetoxikologische<sup>1-7</sup> und klinisch toxikologische Bedeutung erlangt haben<sup>8-11</sup>; neben den akzidentellen Intoxikationen sind hierbei auch die Fälle von Missbrauch (Schnüffeln)<sup>11-16</sup> sowie die Selbstvergiftungen<sup>8,11,17</sup> zu erwähnen. Die allgemeine Verfügbarkeit flüchtiger Substanzen stellt daher das toxikologische Labor immer wieder vor die Aufgabe, eine Identifizierung solcher Stoffe durchzuführen, um sie als Ursache für eine Intoxikation zu bestätigen oder aber auszuschliessen.

Die Methode der Wahl zur Bestimmung niedrig siedender Verbindungen ist zweifellos die Gaschromatographie, speziell die Dampfraumanalyse<sup>18,19</sup>. Die Identifizierung unbekannter Stoffe erreicht man hierbei i.a. durch Vergleich der gemessenen Retentionswerte mit selber erstellten oder der Literatur entnommenen Retentionsdaten. Voraussetzung hierfür ist jedoch, dass man hinreichend gut reproduzierbare Messergebnisse zur Verfügung hat, eine Forderung, die auch bei Benutzung von relativen Retentionszeiten nur unzulänglich erfüllt wird. Die Verwendbarkeit solcher



chromatographischer Daten aus der Literatur ist daher im wesentlichen beschränkt auf den Vergleich der Elutionsfolge der tabellierten Substanzen<sup>20</sup>. Dennoch sind die meisten publizierten Tabellen für niedrig siedende Stoffe nach relativen Retentionszeiten geordnet<sup>19,21-23</sup>. Während bereits zahlreiche Arzneimittel und Nichtarzneimittel mit Hilfe der —nach Kaiser<sup>24</sup>— “praktisch brauchbarsten Art qualifizierter Retentionsdaten”, dem Retentionsindex System nach Kováts, tabelliert wurden<sup>20,25-31</sup>, verwenden nur wenige Autoren Retentionsindices zur Katalogisierung flüchtiger Substanzen. Dabei wurden die Index-Werte entweder durch Umrechnen aus relativen Retentionszeiten oder mit Hilfe zweier, die zu messende Substanz einschliessender *n*-Alkane gewonnen<sup>32,33</sup>.

In der folgenden Arbeit sind die Retentionsindices von 55 flüchtigen Verbindungen auf zwei verschiedenen stationären Phasen aufgeführt. Zur Berechnung wurden statt zwei mindestens 4 bzw. 5 Standards verwendet und die erhaltenen Werte mit Hilfe eines programmierbaren Taschenrechners durch lineare Regression geglättet<sup>34,35</sup>. Hierdurch wurde eine deutlich bessere Reproduzierbarkeit mit geringen Standardabweichungen erreicht, die auch die Vergleichbarkeit von Retentionswerten zwischen verschiedenen Labors verbessert. Die Vergleichbarkeit und Austauschbarkeit von Analysendaten —eine Forderung, die angesichts einer stetig wachsenden Zahl toxikologisch relevanter Substanzen immer dringlicher erscheint— wird diskutiert.

## EXPERIMENTELLES

### Geräte

Zur Bestimmung der chromatographischen Daten wurde ein Doppelsäulengerät Modell 3400 der Firma Dani (Mailand, Italien) verwendet, versehen mit FID und ausgestattet mit Glassäulen von 2 m Länge und 3 mm I.D. Als Integrator diente der Chromatopac C-R1A (Shimadzu, Tokyo, Japan), als programmierbarer Taschenrechner das Modell HP-67 (Hewlett-Packard).

Die Probennahme erfolgte nach der “Head-space”-Methode, indem je nach 15% Carbowax 1500 auf Kieselgur, 60–100 mesh; Trägergas N<sub>2</sub>, 30 ml/min; Ofentemperatur 75°C. Stationäre Phase II: Porapak Q, 100–120 mesh; Trägergas N<sub>2</sub>, 30 ml/min; Ofentemperatur 200°C.

Die Probennahme erfolgte nach der “Head-space”-Methode, indem je nach Flüchtigkeit 1–2 Tropfen des zu messenden Lösungsmittels auf kleine Papierfilter gegeben und sofort in den üblichen Injektionsflaschen mit Septum und Bördelkappe verschlossen wurden.

Die Probenmengen wurden stets so bemessen, dass keine Überladung der Säule stattfand.

## ERGEBNISSE UND DISKUSSION

Zur Bestimmung der Retentionsindices (*I*) wurden zunächst die Retentionszeiten der *n*-Alkane C<sub>9</sub>–C<sub>13</sub> (Carbowax 1500) bzw. C<sub>5</sub>–C<sub>8</sub> (Porapak Q) mehrfach gemessen. Die Auswahl dieser beiden Reihen von *n*-Alkanen ergibt sich dadurch, dass einerseits die Nettoretentionszeit des Standards mit der niedrigsten C-Zahl wenigstens dreimal so gross wie die Totzeit sein sollte, da erst oberhalb dieses Bereiches eine

ausreichende Linearität der Retentionsindexbeziehung angenommen werden darf<sup>34</sup>. Andererseits wurde der Standard mit der höchsten C-Zahl so gewählt, dass seine Retentionszeit in der Nähe der schwerflüchtigsten Substanz lag. Zur Bestimmung der Totzeit wurde bei jeder Probennahme Methan (Stadtgas) mit in die Injektionsspritze aufgezogen.

An Hand der so gewonnenen Daten wurde mit Hilfe des programmierbaren Taschenrechners die Retentionsindex-Gerade bestimmt und ihr Verlauf durch lineare Regression geglättet. (Das als Standard-Zubehör zum Rechner gelieferte Programm "curve fittings" wurde für diesen Zweck entsprechend modifiziert.) Anschliessend konnten die jeweils gemessenen Brutto-Retentionszeiten der Lösungsmittel eingegeben und die zugehörigen *I*-werte nach *ca.* 1 sec, abgelesen werden. In Tabelle I sind die untersuchten Substanzen nach steigenden Index-Werten auf Carbowax 1500 geordnet. Tabelle II zeigt die in Tabelle I verwendeten Abkürzungen.

Es wurden jeweils mindestens 8–10 Messungen durchgeführt; dabei lagen die Standardabweichungen für die Indices unter einer Index-Einheit. Lediglich bei Stoffen mit sehr kurzer Retentionszeit (z.B. Diäthyläther und Diisopropyläther auf CW 1500, Methanol auf Porapak Q) waren Einzelmesswert-Differenzen von bis zu 8–9 Index-Einheiten zu beobachten, die Standardabweichungen lagen dementsprechend ungünstiger bei maximal 3–4 Einheiten. Andere Substanzen haben auf PPQ auch bei 200°C derart lange Retentionszeiten, dass sie nicht in die Tabelle aufgenommen wurden. Hierzu gehören Di-*n*-Butyläther, Nitromethan, Cyclohexanon und Brombenzol.

Methanol und Acetonitril zeigen zudem auf CW 1500 ein von allen anderen Substanzen abweichendes Verhalten: Der *I*-Wert beider Lösungsmittel ändert sich merklich mit der eingespritzten Menge; die Peaks zeigen dabei ein deutliches Tailing. Trägt man den *I*-Wert jeweils gegen den Logarithmus der Substanzmenge auf, so erhält man über mehrere Zehnerpotenzen eine fallende Gerade: Eine Erhöhung der Methanol-Konzentration um den Faktor 10 führt zu einer Erniedrigung des *I*-wertes um 4.7 Einheiten, beim Acetonitril zu einer solchen von 4.0 Einheiten. Dies ist bei der Auswertung von Chromatogrammen im Rahmen von Screening-Untersuchungen natürlich zu berücksichtigen. Der in Tabelle I angegebene Wert für diese beiden Lösungsmittel entspricht einer Säulenbelastung von *ca.* 1 ng, was in etwa der Nachweisgrenze beider Substanzen entspricht. Bei einer Stoffmenge von 1 µg würde der *I*-Wert von Methanol somit von 953 auf 939 erniedrigt, bei Acetonitril von 1045 auf 1033. Weiterhin sind in der Tabelle die möglichen Koinzidenzen angegeben. Zur Beurteilung solcher Koinzidenzen wurde die Trennzahl 100 (TZ<sub>100</sub>) herangezogen, die angibt, wieviele Peaks in einem *I*-Bereich von 100 Einheiten bzw. zwischen zwei aufeinander folgenden *n*-Alkanen getrennt werden können<sup>36</sup>. Die TZ<sub>100</sub>-Werte für die einzelnen Bereiche sind nach Gleichung 1 aus den Bruttoretentionszeiten und Halbwertsbreiten der zugehörigen *n*-Alkane leicht zu berechnen.

$$TZ_{100} = \frac{t_{ms(B)} - t_{ms(A)}}{b_{0.5(B)} + b_{0.5(A)}} - 1 \quad (1)$$

(A: *n*-Alkan mit *x* C-Atomen; B: *n*-Alkan mit *x* + 1 C-Atomen)

Damit lässt sich nun auch Gleichung 2 der Mindestabstand  $\Delta I$  zweier Signale bestimmen, der erforderlich ist, um eine 2.3 $\sigma$ -Trennung zu erhalten, bei der der Abstand der

TABELLE I  
RETENTIONSINDICES NIEDRIG SIEDENDER SUBSTANZEN

Substanz	Carbowax (CW)	Koinzidenzen	Porapak Q	Koinzidenzen
1 Diäthyläther	630	—	486	EtBr, EtFo, MeAc, Acetal, AliOH
2 Isooctan	676	iPr <sub>2</sub> O	744	C <sub>2</sub> Cl <sub>4</sub>
3 Diisopropyläther	679	iOct	624	CCl <sub>4</sub> , Bzl, MeCCl <sub>3</sub>
4 Acetaldehyd	723	—	330	—
5 Cyclohexan	735	—	639	MeCOiPr, CHCl:CCl <sub>2</sub> , Dioxan
6 Formaldehyd	754	—	284	MeOH
7 Äthylbromid	776	MeFo	484	Et <sub>2</sub> O, EtFo, MeAc, Acetal, AliOH
8 Ameisensäure- methylester	779	EtBr	369	—
9 Ameisensäure- äthylester	842	Aceton, MeAc	474	Et <sub>2</sub> O, EtBr, MeAc, CH <sub>2</sub> Cl <sub>2</sub> , Acetal, AliOH
10 Aceton	847	EtFo, MeAc	450	iPrOH
11 Essigsäure- methylester	850	EtFo, Aceton	477	Et <sub>2</sub> O, EtBr, EtFo, CH <sub>2</sub> Cl <sub>2</sub> , Acetal, AliOH
12 Tetrachlormethan	888	MeCCl <sub>3</sub> , EtI, THF	628	iPr <sub>2</sub> O, MeCCl <sub>3</sub> , Bzl, MeCOiPr, CHCl:CCl <sub>2</sub>
13 1.1.1-Trichloräthan	891	CCl <sub>4</sub> , EtI, THF	621	iPr <sub>2</sub> O, CCl <sub>4</sub> , Bzl
14 Äthyljodid	892	CCl <sub>4</sub> , MeCCl <sub>3</sub> , THF	586	(CH <sub>2</sub> Cl) <sub>2</sub> , iBuOH, GiMe
15 Tetrahydrofuran	895	CCl <sub>4</sub> , MeCCl <sub>3</sub> , EtI	570	EtAc, CHCl <sub>3</sub> , sBuOH
16 Essigsäureäthylester	906	Acetal	567	THF, MeCOEt, CHCl <sub>3</sub> , sBuOH
17 Acetaldehyddiäthylacetal	910	EtAc	485	Et <sub>2</sub> O, EtBr, EtFo, MeAc, AliOH
18 Äthylmethylester	930	CH <sub>2</sub> Cl <sub>2</sub> , tBuOH, (MeOH)	556	EtAc
19 Dichlormethan	933	MeCOEt, tBuOH, (MeOH)	472	EtFo, MeAc
20 <i>tert.</i> -Butanol	934	MeCOEt, CH <sub>2</sub> Cl <sub>2</sub> , (MeOH)	521	—
21 Methanol	953	(MeCOEt, CH <sub>2</sub> Cl <sub>2</sub> , tBuOH), MeCOiPr, iPrOH	281	HCHO
22 Benzol	959	MeOH, MeCOiPr, iPrOH	626	CCl <sub>4</sub> , CHCl:CCl <sub>2</sub> , iPr <sub>2</sub> O, MeCCl <sub>3</sub>
23 Methyl-isopropylketon	960	MeOH, Bzl, iPrOH	637	Cyhex, CCl <sub>4</sub> , CHCl:CCl <sub>2</sub>

24	Isopropanol	962	MeOH, Bzl, MeCOiPr, EtOH	458	Aceton
25	Äthanol	972	iPrOH, nBu <sub>2</sub> O	383	—
26	Di- <i>n</i> -Butyläther	976	EtOH	—	—
27	<i>n</i> -Propylacetat	994	CHCl <sub>3</sub> :CCl <sub>2</sub>	669	GlEt
28	Trichloräthylen	999	nPrAc	635	Cyhex, CCl <sub>4</sub> , Bzl, MeCOiPr
29	Chloroform	1026	C <sub>2</sub> Cl <sub>4</sub> , MeCOiBu, (MeCN)	568	THF, EtAc, sBuOH
30	Tetrachloräthylen	1030	CHCl <sub>3</sub> , MeCOiBu, (MeCN)	735	iOct, MeCOiBu, Tol
31	Methyl-isobutylketon	1034	CHCl <sub>3</sub> , C <sub>2</sub> Cl <sub>4</sub> , (MeCN)	727	C <sub>2</sub> Cl <sub>4</sub> , Tol
32	Acetonitril	1045	(CHCl <sub>3</sub> , C <sub>2</sub> Cl <sub>4</sub> , MeCOiBu)	425	—
33	Buttersäureäthylester	1054	Tol, sBuOH	760	nBuAc
34	Toluol	1054	EtBu, sBuOH	728	C <sub>2</sub> Cl <sub>4</sub> , MeCOiBu
35	sec.-Butanol	1057	EtBu, Tol	569	THF, EtAc, CHCl <sub>3</sub>
36	<i>n</i> -Propanol	1072	(CH <sub>2</sub> Cl) <sub>2</sub>	498	—
37	1,2-Dichloräthan	1076	nPrOH	596	EtI, iBuOH, GIMe
38	<i>n</i> -Butylacetat	1091	Dioxan	770	EtBu
39	Dioxan	1093	nBuAc	648	Cyhex
40	Isobutanol	1122	—	586	EtI, (CH <sub>2</sub> Cl) <sub>2</sub> , GIMe
41	Äthylbenzol	1136	pXyl	821	pXyl, mXyl
42	<i>p</i> -Xylol	1143	EtBzl, AlIOH, mXyl	827	EtBzl, mXyl
43	Allylalkohol	1145	pXyl, mXyl	486	Et <sub>2</sub> O, EtFo, MeAc, Acetal, EtBr
44	<i>m</i> -Xylol	1149	pXyl, AlIOH	827	EtBzl, pXyl
45	Nitromethan	1172	nBuOH	—	—
46	<i>n</i> -Butanol	1178	MeNO <sub>2</sub>	609	—
47	<i>o</i> -Xylol	1191	—	844	—
48	Chlorbenzol	1219	Pyridin, GIMe	786	—
49	Pyridin	1224	ClBzl, GIMe	690	iAmOH
50	Äthylenglykolmono-				
	methyliäther	1225	ClBzl, Pyridin	588	EtI, (CH <sub>2</sub> Cl) <sub>2</sub> , iBuOH
51	Isoamylalkohol	1240	—	697	Pyridin
52	Äthylenglykolmono-				
	äthyläther	1266	CH <sub>2</sub> Cl·CHCl <sub>2</sub>	671	nPrAc
53	1,1,2-Trichloräthan	1267	GlEt	713	—
54	Cyclohexanon	1310	—	—	—
55	Brombenzol	1338	—	—	—

TABELLE II

## ERKLÄRUNG DER IN TABELLE I VERWENDETEN ABKÜRZUNGEN

Abkürzung	Substanz	Abkürzung	Substanz
Acetal	Acetaldehyddiäthylacetal	Et <sub>2</sub> O	Diäthyläther
iAmOH	Isoamylalkohol	GlEt	Äthylenglykolmonoäthyläther
AlIOH	Allylalkohol	GlMe	Äthylenglykolmonomethyläther
BrBzl	Brombenzol	Me	Methyl-
nBuAc	<i>n</i> -Butylacetat	MeAc	Essigsäuremethylester
nBu <sub>2</sub> O	Di- <i>n</i> -Butyläther	MeCOiBu	Methylisobutylketon
iBuOH	Isobutanol	MeCOEt	Methyläthylketon
nBuOH	<i>n</i> -Butanol	MeFo	Ameisensäuremethylester
sBuOH	<i>sec.</i> -Butanol	MeCOiPr	Methylisopropylketon
tBuOH	<i>tert.</i> -Butanol	iOct	Isooctan
Bzl	Benzol	nPrAc	<i>n</i> -Propylacetat
ClBzl	Chlorbenzol	iPr <sub>2</sub> O	Diisopropyläther
Cyhex	Cyclohexan	iPrOH	Isopropanol
Cy'h'on	Cyclohexanon	nPrOH	<i>n</i> -Propanol
Et	Äthyl-	THF	Terahydrofuran
EtAc	Essigsäureäthylester	Tol	Toluol
EtBu	Buttersäureäthylester	Xyl	Xylol
EtFo	Ameisensäureäthylester		

Peakmaxima gerade ihrer mittleren Halbwertsbreite entspricht und eine störende, gegenseitige zeitliche Verfälschung der Peakspitzen noch zu vernachlässigen ist<sup>34</sup>.

$$\Delta I_{\min.} = 0.5 \frac{100}{TZ_{100} + 1} \quad (2)$$

In einer Übersicht in Tabelle III sind die *I*-Differenzen angegeben, die für eine Trennung zweier Substanzen in den jeweiligen *I*-Bereichen auf beiden stationären Phasen notwendig sind.

Aus dem Vergleich der Koinzidenzen der Tabelle I kann man ersehen, dass mit lediglich einer der beiden stationären Phasen nur wenige Substanzen eindeutig zu identifizieren sind, insbesondere, wenn Gemische vorliegen; durch Kombination beider Säulen hingegen sind bei nur mehr 5 Substanz-Paaren keine eindeutigen Zuordnungen möglich, falls Gemische vorliegen: Ameisensäureäthylester–Essigsäuremethylester, Tetrachlormethan–1,1,1-Trichloräthan, Tetrachloräthylen–Methylisobu-

TABELLE III

*ΔI*-WERTE FÜR EINE 2,3σ-TRENNUNG

<i>n</i> -Alkan-Bereich	CW 1500	<i>n</i> -Alkan-Bereich	Porapak Q
C <sub>7</sub> –C <sub>8</sub>	12	C <sub>4</sub> –C <sub>5</sub>	12
C <sub>8</sub> –C <sub>9</sub>	12	C <sub>5</sub> –C <sub>6</sub>	12
C <sub>9</sub> –C <sub>10</sub>	11	C <sub>6</sub> –C <sub>7</sub>	11
C <sub>10</sub> –C <sub>11</sub>	11	C <sub>7</sub> –C <sub>8</sub>	11
C <sub>11</sub> –C <sub>12</sub>	10		
C <sub>12</sub> –C <sub>13</sub>	9		

tylketon, Äthylbenzol-*p*-Xylol und *p*-Xylol-*m*-Xylol. Enthält die Probe jedoch nur jeweils eine der beiden Komponenten, so ist aufgrund der durch lineare Regression und Verwendung mehrerer Standards geringen Standardabweichung der Indices von meist weniger als 1 Einheit eine Differenzierung durchaus möglich.

Da sich die Retentionsindices von Acetonitril und Methanol auf Carbowax 1500 mit steigender Konzentration zu kleineren Werten hin verschieben, können hier zusätzliche Koinzidenzen auftreten (z.B. Acetonitril mit Methylisobutylketon und Tetrachloräthylen; Methanol mit *tert.*-Butanol und Dichlormethan). Eine Unterscheidung fällt jedoch nicht schwer, da die beiden genannten Lösungsmittel auf Carbowax durch tailing und *I*-Änderung bei wechselnden Probenmengen zu erkennen sind und zudem auf Porapak Q von den anderen in Frage kommenden Stoffen leicht getrennt werden können.

Es wurde auch der Frage nachgegangen, inwieweit die einmal gemessenen Indices über einen längeren Zeitraum konstant bleiben, da sich die Polarität der stationären Phase bei längerem Betrieb der Säule infolge Alterung ändern kann. Es stellte sich heraus, dass die Indices auf Porapak Q auch noch nach Monaten fast unverändert geblieben waren; bei Carbowax waren die Abweichungen geringfügig. Dies gilt zumindest bei Anwendung der "Head-space"-Technik; in welchem Ausmass ein direktes Auftragen flüssiger Proben (insbesondere biologischen Materials wie Serum, Urin etc.) neben einer starken Herabsetzung der Lebensdauer der Säule auch die Reproduzierbarkeit der Retentionsindices beeinträchtigt, wurde nicht untersucht.

Von grossem Interesse ist auch die Frage, inwieweit in der Literatur veröffentlichte *I*-Werte für das eigene Labor verwertbar sind. Rübel hat in diesem Zusammenhang die in verschiedenen Labors auf Carbowax 1500 ermittelten Indices verglichen, wobei z.T. auch relative Retentionszeiten in Retentionsindices umgerechnet wurden<sup>33</sup>. Es zeigt sich, dass die Differenzen z.T. erheblich waren (in manchen Fällen über 50 Index-Einheiten). Eine Erklärung liefert natürlich die Tatsache, dass *I*-Werte gegenüber gestellt wurden, die bei verschiedenen Temperaturen gemessen worden waren (60, 90°). In eigenen Untersuchungen konnte beobachtet werden, dass bei einer um 20°C niedrigeren Temperatur (55 statt 75°C) unter sonst gleichen Bedingungen Abweichungen bis zu 40 Index-Einheiten auftraten. Dies trifft hauptsächlich für die relativ unpolaren Substanzen (Benzol, Toluol, Xylol etc.) zu, bei den polaren Alkoholen ist der Temperatureinfluss jedoch gering. Genauer untersucht wurde dieses Phänomen von Martin<sup>37,38</sup> und Martire<sup>39</sup>, die eine Änderung gaschromatographischer Retentionswerte in Abhängigkeit von der Temperatur, insbesondere aber von der spezifischen Oberfläche des Trägermaterials und dem Verhältnis von stationärer Flüssigkeit zur Oberfläche des Trägers (der Belegungsdichte also) beobachteten und deuteten. Danach sind diese Abhängigkeiten an unpolaren Phasen gering und können auf eine Adsorption von Lösungsmitteln an aktiven Stellen des Trägermaterials zurückgeführt werden.

Damit nicht erklärbar sind jedoch die starken Änderungen bei Verwendung polarer Trennflüssigkeiten (wie z.B. Carbowax 1500<sup>40,41</sup>). Martin konnte zeigen, dass hierfür ein anderes Phänomen verantwortlich ist, nämlich die Adsorption an der Gas-Liquid Grenzfläche. Martire unterscheidet dabei noch zwei verschiedene Arten von Adsorption: Die eine tritt besonders stark in Erscheinung bei starken Polaritätsunterschieden zwischen Trennflüssigkeit und zu trennenden Komponenten (gegeben im Fall Carbowax 1500 und den als Standard verwendeten *n*-Alkanen!); die

andere ist von herausragender Bedeutung, wenn Dipol–Dipol Wechselwirkungen oder H-Brückenbindungen zwischen polarer stationärer Phase und den Molekülen der niedrig siedenden Lösungsmittel sehr stark werden (Methanol–Acetonitril!).

Wie notwendig eine genaue Spezifizierung der stationären Phase auch hinsichtlich des Trägermaterials ist, konnte auch in eigenen Versuchen beobachtet werden. Als zur Index-Messung an CW 1500 das Kieselgur durch dessen calcinierte und geglühte Form, das Chromosorb W NAW ersetzt wurde, ergaben sich starke Verschiebungen zu höheren *I*-Werten (teilweise über 50 Einheiten); in mehreren Fällen änderte sich auch die Elutionsfolge der Substanzen.

Für die Praxis ergibt sich daraus die Forderung, bei der Katalogisierung von Retentionsindices Art (Typ), mesh-Grösse und Vorbehandlung des Trägermaterials sowie dessen prozentuale Belegung mit stationärer Trennflüssigkeit genau anzugeben.

Ein weiterer Faktor, der beim Vergleich von *I*-Tabellen offensichtlich berücksichtigt werden muss, ist der Einfluss verschiedener Probenaufgabetechniken. So konnte Rübel<sup>33</sup> zeigen, dass die "Head-space"-Technik zu deutlich höheren Werten gegenüber der Injektion flüssiger Proben (Direkteinspritzungen von Serum, Harn etc.) führt. (Die Dampfdruckanalyse von Lösungen und die in dieser Arbeit beschriebene Papierfiltertechnik liefern die gleichen Resultate). Bei Berücksichtigung all dieser Parameter, die Differenzen in der Index-Messung hervorrufen können, bei Verwendung mehrerer Standards und bei Einsatz eines programmierbaren Rechners mit der Möglichkeit der linearen Regression sollte sich die Reproduzierbarkeit der Retentionsindices auch zwischen verschiedenen Labors weiter verbessern lassen.

#### ZUSAMMENFASSUNG

Zur schnellen Identifikation leicht flüchtiger Verbindungen in der forensisch- und klinisch-toxikologischen Praxis wurden die Retentions-Indices von 55 niedrig siedenden Substanzen auf Carbowax 1500 und Porapak Q gemessen. Die Berechnung erfolgte mit Hilfe eines programmierbaren Kleinrechners und unter Verwendung mehrerer Standards. Die Koinzidenzen wurden an Hand der Trennzahl 100 bestimmt. Dabei stellte sich heraus, dass eine eindeutige Identifizierung auf nur einer der beiden Phasen für die meisten Stoffe nicht möglich war, bei Kombination beider Säulen jedoch bis auf wenige Ausnahmen gelang. Die Reproduzierbarkeit der Index-Werte innerhalb eines Labors sowie die Voraussetzungen für die Vergleichbarkeit zwischen verschiedenen Labors werden diskutiert.

#### LITERATUR

- 1 R. Hoschek, *Arch. Toxicol.*, 14 (1953) 330.
- 2 W. Schollmeyer, *Arch. Toxicol.*, 18 (1960) 229.
- 3 J. Angerer, D. Szadkowski, A. Manz, R. Pett und G. Lehnert, *Int. Arch. Arbeitsmed.*, 31 (1973) 1.
- 4 J. Dequidt, D. Furon, F. Wattel, J. M. Haguenoer, Ph. Scherpereel, B. Gosselein und A. Ginestet, *J. Europ. Toxicol.*, 7 (1974) 91.
- 5 A. M. Thiess, E. Tress und I. Fleig, *Arbeitsmed. Sozialmed., Präy.-Med.*, 11 (1976) 36.
- 6 E. Kohn, *Kriminalistik*, 30 (1976) 506.
- 7 J. Angerer, *Int. Arch. Occup. Environ. Hlth.*, 42 (1979a) 25.
- 8 G. Uhl und P. Th. Haag, *Arch. Toxicol.*, 17 (1958) 197.
- 9 H. J. Gibitz und E. Plöchl, *Arch. Toxicol.*, 31 (1973) 13.
- 10 H. Bremer und D. Tiess, *Krimin. Forens.* 32 (1978) 45.

- 11 R. Bonnicksen und E. C. Maehly, *J. Forens. Sci.*, 11 (1966) 414.
- 12 G. Harrer, W. Kisser, P. Pilz, G. Sorgo und N. Wölkart, *Nervenarzt*, 44 (1973) 645.
- 13 A. Poklis, *J. Forens. Sci. Soc.*, 16 (1976) 43.
- 14 G. Sorgo, *Arch. Toxicol.*, 35 (1976) 295.
- 15 K. Nomiyama und H. Nomiyama, *Int. Arch. Occup. Environ. Hlth.*, 41 (1978) 55.
- 16 H. v. Lüpke, J. Gerchow und K. Schmidt, *Z. Rechtsmed.*, 81 (1978) 55.
- 17 V. Lachnit, *Wien Med. Wschr.*, 99 (1949) 338.
- 18 G. Machata, *Blutalkohol*, 4 (1967) 252.
- 19 G. Hauck, J. Janzen und H. P. Terfloth, *Blutalkohol*, 7 (1970) 252.
- 20 H. Berninger, R. Grünagel, S. Mall und M. R. Möller, *Beitr. Gerichtl. Med.*, 33 (1975) 185.
- 21 G. Weyrich, G. Hauck und V. Zimmer, *Med. Welt*, 18 (1967) 119.
- 22 D. Henschler (Herausgeber), *Analysen in biologischem Material*, Band 2, Teil 2, Verlag Chemie, Weinheim, 1978.
- 23 P. Dellert und G. Machata, *Angewandte Chromatographie*, Application No. 31, Bodenseewerk Perkin-Elmer, Überlingen, 1977.
- 24 R. Kaiser, *Chromatographia*, 3 (1970) 134.
- 25 L. Kazyak und R. Permisohn, *J. Forens. Sci.*, 15 (1970) 346.
- 26 B. Finkle, E. J. Cherry und D. M. Taylor, *J. Chromatogr. Sci.*, 9 (1971) 393.
- 27 B. Caddy, F. Fish und D. Scott, *Chromatographia*, 6 (1973) 293.
- 28 A. C. Moffat, A. H. Stead und K. W. Smalldon, *J. Chromatogr.*, 90 (1974) 19.
- 29 A. C. Moffat, *J. Chromatogr.*, 113 (1975) 69.
- 30 H. Schütz und V. Westenberger, *J. Chromatogr.*, 169 (1979) 409.
- 31 J. D. Ramsey, T. D. Lee, M. D. Osselton und A. C. Moffat, *J. Chromatogr.*, 184 (1980) 185.
- 32 E. Kováts, *Helv. Chim. Acta*, 41 (1958) 1915.
- 33 F. R. Rübel, *Dissertation*, Saarbrücken 1980.
- 34 R. E. Kaiser, *Chromatographia*, 7 (1974) 251.
- 35 G. Machata, *Z. Rechtsmed.*, 79 (1977) 193.
- 36 R. E. Kaiser, *Chromatographia*, 9 (1976) 337.
- 37 R. L. Martin, *Anal. Chem.*, 33 (1961) 347.
- 38 R. L. Martin, *Anal. Chem.*, 35 (1963) 116.
- 39 D. E. Martire, *Anal. Chem.*, 38 (1966) 244.
- 40 F. Riedo und E.sz. Kováts, *J. Chromatogr.*, 186 (1979) 47.
- 41 D. F. Fritz, A. Sahil und E.sz. Kováts, *J. Chromatogr.*, 186 (1979) 63.



CHROM. 14,293

## SELEKTIVE GRUPPENTRENNUNG VON PRIMÄREN UND SEKUNDÄREN BIOGENEN AMINEN MITTELS "REVERSED-PHASE" HOCHLEISTUNGSFLÜSSIGKEITSCROMATOGRAPHIE MIT [18]KRONE-6 IN DER MOBILEN PHASE

MANFRED WIECHMANN

*Universität Bayreuth, Lehrstuhl für Tierphysiologie, Postfach 3008, D-8580 Bayreuth (B.R.D.)*  
(Eingegangen am 12. August 1981)

---

### SUMMARY

*Selective group separation of primary and secondary biogenic amines by reversed-phase high-performance liquid chromatography with 18-crown-6 in the mobile phase*

A high-performance liquid chromatographic procedure is described for the selective group separation of primary and secondary biogenic amines. The procedure is based on the selective formation of complexes of primary amines with 18-crown-6 and the high affinity of the ammonium–18-crown-6 complexes on the hydrophobic phase in the two-phase system reversed phase/0.01 *N* hydrochloric acid–18-crown-6. It is shown that the degree of the group separation is dependent on the characteristics of the reversed phase and on the concentration of the crown ether.

---

### EINLEITUNG

Die Chromatographie von nativen biogenen Aminen, insbesondere von Noradrenalin und Adrenalin, mittels der Hochleistungsflüssigkeitschromatographie (HPLC) wurde wiederholt beschrieben<sup>1–32</sup>. Die einzelnen Verfahren unterscheiden sich im wesentlichen dadurch, dass verschiedene Phasen (Ionenaustauscher, Kieselgel, "Reversed-Phase", "Reversed-Phase"/Ionenpaar) in Kombination mit mehreren Messverfahren (UV-Spektroskopie<sup>3,4,6</sup>, Fluorometrie<sup>1,2,7–16,18–20</sup>, Elektrochemische Detektion<sup>17,21–32</sup>) angewandt wurden. Dabei handelte es sich immer um eine chromatographische Trennung der verschiedenen biogenen Amine untereinander. Eine selektive chromatographische Gruppentrennung von primären und sekundären biogenen Aminen wurde unseres Wissens bisher nicht mitgeteilt.

In dieser Arbeit wird die selektive Gruppentrennung der sekundären biogenen Amine Adrenalin, Metanephrin, *p*-Synephrin, *m*-Synephrin, Epinin und N-Methylserotonin von den entsprechenden N-demethylierten primären biogenen Aminen Noradrenalin, Normetanephrin, *p*-Octopamin, *m*-Octopamin, Dopamin und Serotonin an einer Reversed-Phase-Säule mit [18]Krone-6\* im wässrigen Eluenten demon-

---

\* Beim Arbeiten mit [18]Krone-6 ist besondere Sorgfalt geboten, da die Substanz sehr toxisch ist<sup>70</sup>.

striert. Diese Trennung beruht darauf, dass die relativen Retentionszeiten der primären und sekundären Amine zueinander durch [18]Krone-6 extrem verändert werden. Während normalerweise die polareren primären Amine vor den entsprechenden N-Methyl-Verbindungen eluiert werden, haben in Gegenwart von [18]Krone-6 im Eluenten die sekundären Amine die kürzeren Retentionszeiten.

Die starke Retardierung der primären biogenen Amine beruht auf der hohen Affinität eines [18]Krone-6-aminhydrochlorid-Komplexes zur Reversed-Phase, der sich ausschliesslich mit den primären und nicht mit den sekundären biogenen Aminhydrochloriden bildet. Die erhöhte Retention der primären Amine ist abhängig von der Lipophilie der Reversed-Phase und von der Konzentration des [18]Krone-6 im Eluenten. Entsprechend kann die Qualität der Gruppentrennung an den unterschiedlichsten analytischen Problemen gezielt orientiert werden.

## MATERIAL UND METHODEN

### Geräte

Das HPLC System bestand aus einer Altex-Pumpe (Modell 110 A), gekoppelt mit einem Pulsationsdämpfer (Altex, Modell 110-40), einem Einlassventil (Rheodyne Modell 71020) mit 100  $\mu$ l Probenschleife, einer Stahlchromatographiefertigsäule (Länge: 250 mm, I.D.: 4,6 mm, gefüllt mit RP-2- (10  $\mu$ m, Nr. 103.07.15) bzw. mit RP-8-Material (7  $\mu$ m, Nr. 103.07.13) (H. Knauer, Oberursel, B.R.D.) und einem Aminco-Bowman (SPF)-Fluorometer (J4-8960E) in Verbindung mit dem Mikrophotometer J10-222 A (American Instrument).

Die native Fluoreszenz der biogenen Amine wurde in einer 25- $\mu$ l Durchflussküvette (Nr. 176.70, Hellma, Mühlheim/Baden, B.R.D.) bei 285 nm (Anregung) und 325 nm (Emission) gemessen. Chromatographiert wurde bei Raumtemperatur (20–25°C). Die Fließgeschwindigkeit des Eluenten ist bei den Abbildungen angegeben. Zur Aufzeichnung der Chromatogramme diente ein Linearkompensationsschreiber (Modell 385, Abimed, Düsseldorf, B.R.D.) und zur Bestimmung der Retentionszeiten ein Integrator (Modell 3380 A, Hewlett-Packard). Der Papiervorschub betrug 0.5 cm/min.

### Chemikalien

Alle biogenen Amine wurden kommerziell erworben. Serotoninsulfat stammte von E. Merck (Darmstadt, B.R.D.), *m*-Synephrin (L- $\beta$ -3-(Hydroxyphenyl)- $\beta$ -hydroxyäthylmethylamin), *m*-Octopamin (L- $\beta$ -3-(Hydroxyphenyl)- $\beta$ -hydroxyäthylamin), N-Methylserotonin von Serva (Heidelberg, B.R.D.), und Adrenalin, Noradrenalinhydrochlorid, Dopaminhydrochlorid, Epinin (N-Methyldopamin)hydrochlorid, 3-O-Methyldopamin (3-Methoxytyramin)hydrochlorid, *p*-Synephrin, *p*-Octopaminhydrochlorid, Normetanephrinhydrochlorid, Metanephrinhydrochlorid von Sigma (St. Louis, MO, U.S.A.).

Für die Chromatographie und zum Lösen der Substanzen wurde deionisiertes Wasser (Milli-Q; Millipore, Neu-Isenburg, B.R.D.) verwendet. Als Basiseluent diente 0.01 N Salzsäure (Titrisol, E. Merck); [18]Krone-6 stammte von Fluka (Buchs, Schweiz).

Das für die Lösungen der Amine und den Eluenten benötigte Wasser wurde 1 h am Wasserstrahlpumpenvakuum, die Lösungen vor Gebrauch im Ultraschallbad (Modell 58.000, H. Knauer) entgast.

## ERGEBNISSE UND DISKUSSION

Seit der grundlegenden Arbeit über die Komplexierung von Metallionen mit Kronenethern von Pedersen<sup>33</sup>, und deren Einführung in die Phasentransfer-Katalyse (PTC) in verschiedene Bereiche der präparativen organischen Chemie zwischen 1972 und 1974 durch einige Arbeitsgruppen<sup>34–39</sup>, hat die PTC eine stürmische Entwicklung genommen. Einige zusammenfassende Darstellungen informieren hierüber<sup>40–48</sup>. In die Chromatographie wurden die Kronenether von Blasius und Mitarbeiter<sup>49–52</sup> sowie Cram und Mitarbeiter<sup>53–55</sup> eingeführt. Sie benutzen covalent an Kieselgel<sup>52,55</sup>, Ionenaustauscher<sup>49,52</sup> oder Polystyrolharze<sup>54</sup> gebundene Kronenether zur flüssigkeitschromatographischen Trennung von Alkali-, Erdalkali- und anderen Metallionen<sup>49–52</sup>, zur Trennung einfacher alkylsubstituierter und strukturisomerer Ammoniumionen<sup>49</sup>, zur Trennung verschiedener organischer Verbindungen (Halogenbenzole, Vitamine, Penicilline, Heterocyklen und Digitalisglykosiden)<sup>50</sup> sowie zur Trennung der Enantiomere von racemischen  $\alpha$ -Aminosäuren<sup>51,53–55</sup> und  $\alpha$ -Phenyläthylaminsalzen<sup>55</sup> in organischen Lösungsmitteln.

Bei der Trennung der Enantiomere in die optisch reinen Isomere wirken die covalent fixierten optisch aktiven Kronenether als chirale Molekülrezeptoren. Diese sogenannten abiotischen Rezeptoren sind als Modellsubstanzen zur Untersuchung des Erkennungsvermögens biologischer Rezeptoren bedeutungsvoll. Neuere Übersichten geben hierüber Auskunft<sup>56,57</sup>.

Über die Verwendung monomerer Kronenether in organischen Lösungsmittelgemischen als Elutionsmittel in der Ionenaustauscherchromatographie<sup>58</sup> oder an Kieselgel<sup>53</sup> wurde gleichfalls berichtet. Horváth *et al.*<sup>59</sup> sowie Brugman und Kraak<sup>60</sup> erweiterten den Anwendungsbereich für monomere Kronenether in der Flüssigkeitschromatographie. Sie chromatographierten Kronenetheralkaliumkomplexe in Methanol an Reversed-Phase-Säulen<sup>59</sup> oder benutzten Kronenetherkaliumkomplexe zur Komplexierung der Anionen  $R-SO_3^-$  (Lit. 60). Dadurch ist die Löslichkeit von Nitro- und Halogenbenzolsulfonsäuren in Methylenchlorid–Methanol-Gemischen für die Chromatographie an Kieselgel erhöht worden. Kürzlich berichteten Nakagawa *et al.*<sup>61</sup> über das Retentionsverhalten von aromatischen primären Aminoverbindungen an einer Reversed-Phase-Säule mit wässrigem Methanol–Kronenether-Gemischen als mobiler Phase. In Abhängigkeit von der Kronenetherkonzentration ermittelten sie für isomere Aminobenzoessäuren, Benzoessäureamide, isomere Toluidine und einige  $\alpha$ -Aminocarbonsäuren (Phenylalanin, Tyrosin, Tryptophan) die Kapazitätsfaktoren.

In dieser Arbeit berichten wir erstmals über die Komplexierung von primären biogenen Aminhydrochloriden und [18]Krone-6 aus rein wässriger Lösung in dem Zweiphasensystem Reversed-Phase/0,01 N Salzsäure–[18]Krone-6 und über die Anwendung dieses Systems zur selektiven chromatographischen Gruppentrennung von primären und sekundären biogenen Aminen.

Bereits Pedersen<sup>33</sup> zeigte, dass einfache primäre Alkylaminhydrochloride in Methanol mit Dibenzo-[18]Krone-6 zu komplexieren sind, während die Hydrochloride des cyclischen sekundären Amins Morpholin und der tertiären Amine Tetramethylamin, N-Methylmorpholin und 1,4-Diazabicyclo(2.2.2.)octan keine Komplexe mit dem verwendeten Kronenether bilden. Die Messungen von Izatt *et al.*<sup>62</sup> stehen der Allgemeingültigkeit dieser Ergebnisse entgegen. Sie bestimmten die Stabilitätskonstanten von [18]Krone-6–ammoniumkomplexen und fanden, dass diese von Kom-

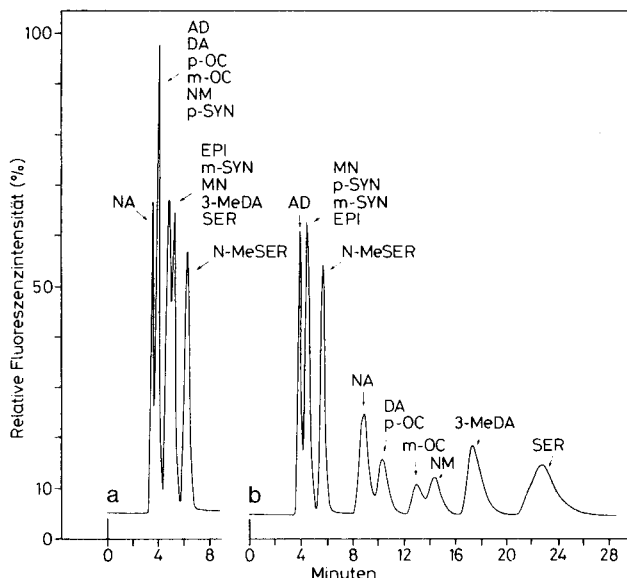


Fig. 1. Chromatogramme eines Standardgemisches von primären und sekundären Aminen; NA = Noradrenalin, AD = Adrenalin, NM = Normetanephrin, MN = Metanephrin, *p*-OC = *p*-Octopamin, *p*-SYN = *p*-Synephrin, *m*-OC = *m*-Octopamin, *m*-SYN = *m*-Synephrin, DA = Dopamin, 3-MeDA = 3-O-Methyldopamin, EPI = Epinin, SER = Serotonin, N-MeSER = N-Methylserotonin. Je 1 nMol/100  $\mu$ l Applikationslösung an einer RP-2-Säule. (a) Elutionsdiagramm mit 0.01 *N* Salzsäure. (b) Elutionsdiagramm mit 0.01 *N* Salzsäure-[18]Krone-6 (5 g/l). Die Säule wurde 4 h äquilibriert. Die Fließgeschwindigkeit betrug bei der Äquilibrierung und bei der Chromatographie 1.0 ml/min. Weitere Einzelheiten siehe Material und Methoden.

plexen mit sekundären Aminen (Pyrrolidinhydrojodid, Dimethylaminhydrojodid) in absolutem Methanol gegenüber Komplexen mit primären Alkylaminhydrojodiden (Methyl-, Äthyl-, Propyl- und *tert.*-Butyl-) um *ca.* 1 bis 2 Größenordnungen kleiner sind.

Aus dem Vergleich der Chromatogramme in Fig. 1 ergibt sich, dass in dem Zweiphasensystem Reversed-Phase/rein wässrige Lösung die selektive Komplexbildung von [18]Krone-6 mit primären Aminhydrochloriden im Sinne Pedersens gilt. Fig. 1a zeigt, dass die Retentionszeiten der verschiedenen Amine mit ihrer Polarität korreliert sind, wenn sie an einer RP-2-Säule mit 0.01 *N* Salzsäure als Eluenten chromatographiert werden. In Gegenwart von [18]Krone-6 im Eluenten zeigt die Gruppe der primären Amine gegenüber der Gruppe der sekundären Amine ein extrem verändertes Retentionsverhalten (Fig. 1b). Die sekundären Amine Adrenalin, Metanephrin, *p*-Synephrin, *m*-Synephrin, Epinin und N-Methylserotonin werden generell etwas schneller eluiert. Wir führen dies auf den —gegenüber 0.01 *N* Salzsäure— stärkeren Eluenten 0.01 *N* Salzsäure-[18]Krone-6 zurück. Die primären Amine Noradrenalin, Normetanephrin, *p*-Octopamin, *m*-Octopamin, Dopamin und Serotonin —die jeweils N-demethylierten Substanzen der verwendeten sekundären Amine— sowie 3-O-Methyldopamin, haben dagegen eine wesentlich verlängerte Retentionszeit, die aus der Komplexbildung des primären Aminalsches mit dem Kronenether resultiert. Für eine Komplexbildung der sekundären Amine ergibt sich aus dem Retentionsverhalten

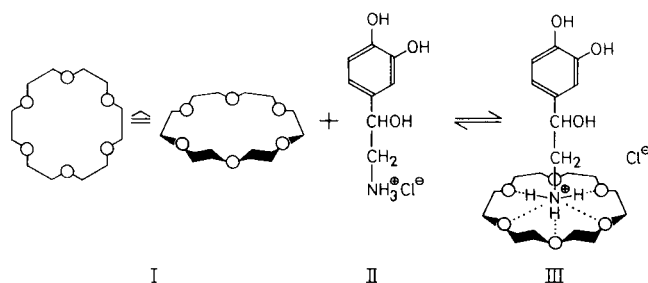


Fig. 2. Komplexbildung zwischen [18]Krone-6 und Noradrenalinhydrochlorid. Die Strukturen des [18]-Krone-6 (I) und des mit Noradrenalinhydrochlorid (II) gebildeten [18]Krone-6-noradrenalinhydrochlorid-Komplexes (III) sind idealisiert (vergl. hierzu Lit. 64, 65). Die punktierten Linien illustrieren die elektrostatischen Anziehungskräfte zwischen Aminkation und Sauerstoffatomen des Kronenethers —eine Krafflinie ist durch die  $-\text{CH}_2-\text{N}$ -Bindung in der Zeichnung verdeckt— sowie die drei Wasserstoffbrückenbindungen im Komplex.

dieser Substanzklasse kein Hinweis, und dies trotz der Tatsache, dass die stationäre Phase bei der Chromatographie gegenüber dem von Izatt *et al.*<sup>62</sup> verwendeten absoluten Methanol eine wesentlich stärkere Lipophilität aufweist.

In Fig. 2 ist die idealisierte Struktur des [18]Krone-6-noradrenalin-Komplexes als Beispiel für die Kronenetherkomplexe der biogenen primären Amine wiedergegeben. Die Struktur entspricht den Vorstellungen von Pedersen<sup>33</sup>, Cram<sup>57</sup>, Kyba *et al.*<sup>63</sup> und Timko *et al.*<sup>64</sup> vom Aufbau der Kronenetherammoniumkomplexe und deren Bestätigung durch die Bestimmung der Kristallstruktur des [18]Krone-6-ammoniumhydrobromids durch Nagano *et al.*<sup>65</sup>. Innerhalb des 1:1-Komplexes steht das komplexierte Aminhydrochlorid senkrecht auf dem annähernd plan liegenden Kronenether, wobei die  $\text{NH}_3^+$ -Gruppe des Amins über dem Zentrum der Kronenverbindung fixiert ist. Als punktierte Linien sind die elektrostatischen Anziehungskräfte eingezeichnet, die sich aufgrund der Dipol-Dipol- und Ionen-Dipol-Wechselwirkungen zwischen den Wasserstoffatomen der  $\text{NH}_3^+$ -Gruppe sowie dem Aminkation und den einsamen Elektronenpaaren der Sauerstoffatome des Kronenethers ausbilden. Sie bedingen die Stabilität des Komplexes und halten das Aminkation in seiner Position. Das Volumen der  $\text{NH}_3^+$ -Gruppe ist zu gross —Ionenradius von  $\text{NH}_4^+$  (im Kristall) = 2.86 Å (Lit. 40)— um die Kronenetherhöhle vollständig auszufüllen, die im [18]Krone-6-ammoniumhydrobromid einen Durchmesser von 2.84 Å besitzt<sup>65</sup>. Entsprechend steht das Aminkation in diesem Komplex 1.00 Å über dem plan ausgerichteten Polyätherring, der im komplexierten Zustand weitgehend symmetrisch ist<sup>65</sup>. Weitere Einzelheiten über die Kristallstrukturen von Kronenetherkomplexen sind einer diesem Thema gewidmeten Zusammenfassung zu entnehmen<sup>66</sup>.

Die Stabilität derartiger Kronenetherkationenkomplexe hängt allgemein ausser vom Verhältnis des Kationenvolumens zum Durchmesser des Kronenetherhohlraumes auch wesentlich von der Solvationsstärke des verwendeten Lösungsmittels ab. Aus diesem Grunde ist in wässrigen Lösungen das in Fig. 2 dargestellte Gleichgewicht, in dem die Dissoziation der Salze und des Komplexionspaares nicht berücksichtigt wurde, weitgehend nach links verschoben. Dies erklärt sich aus dem Bestreben des Aminkations, eine Hydrathülle auszubilden —ein Prozess, der der Komplexbildung wegen der grossen Volumenzunahme der  $\text{NH}_3^+$ -Gruppe entgegensteht.

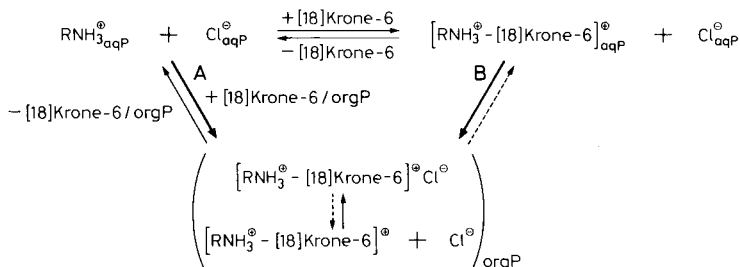


Fig. 3. Schematische Darstellung verschiedener Gleichgewichte in dem Zweiphasensystem Reversed-Phase/0.01 *N* Salzsäure-[18]Krone-6. Die Komplexbildung aus dem Gleichgewicht in der wässrigen Phase (aqP). Über den Weg A verläuft die direkte Komplexierung des protoniertenamins "in" der stationären organischen Phase (orgP), während über den Weg B der direkte Phasentransfer des [18]Krone-6-ammoniumkomplexes erfolgt. "Innerhalb" der stationären Phase ist die Dissoziation des Komplexes weitgehend zurückgedrängt.

Die Stabilitätskonstanten der [18]Krone-6-ammoniumkomplexe, die ein Maß für die Komplexbildung in Lösung darstellen, sind entsprechend in wässriger Lösung sehr klein. Sie wurden von Izatt<sup>67</sup> für den [18]Krone-6-methylammoniumkomplex ( $K_s$  ([18]Krone-6/MeNH<sub>3</sub><sup>+</sup>) in Wasser  $\leq 5$ ) und von Behr *et al.*<sup>68</sup> für den Ammoniumkomplex mit einem tetrasubstituierten Kronenether ( $K_s$  ([18]Krone-6(-CON(CH<sub>3</sub>)<sub>2</sub>)<sub>4</sub>/NH<sub>4</sub><sup>+</sup> in Wasser  $< 5$ ) gemessen. Wurde Methanol als Lösungsmittel benutzt, das gegenüber Wasser eine wesentlich geringere Solvationsstärke besitzt, erhöhen sich die Stabilitätskonstanten der Kronenetherkomplexe um mehrere Zehnerpotenzen<sup>40</sup>. Zu einer weiteren Zunahme der Stabilitätskonstanten kommt es in Abhängigkeit von der Polaritätsabnahme des Lösungsmittels. Über die hieraus erwachsenden analytischen Möglichkeiten, mit unpolaren organischen Lösungsmitteln (Chloroform, Benzol etc.) Kronenethermetallkationenkomplexe aus wässrigen Lösungen zu extrahieren, gab Kolthoff<sup>69</sup> eine zusammenfassende Darstellung.

Für die Komplexierung der primären biogenen Amine in dem Zweiphasensystem Reversed-phase/0.01 *N* Salzsäure-[18]Krone-6 nehmen wir mehrere Reaktionswege an (Fig. 3). Danach erfolgt über den Weg A die Komplexbildung mit dem vollständig dissoziierten protonierten Amin direkt "in" der mit [18]Krone-6 äquilibrierten Reversed-Phase über das Gleichgewicht im Zweiphasensystem. Gleichzeitig wird dem Gleichgewicht im Eluenten, durch den Phasentransport des Komplexes "in" die Reversed-Phase über Weg B, ständig der [18]Krone-6-ammoniumkomplex entzogen, weil der Komplex wegen der starken Abschirmung der polaren Ammoniumgruppe des biogenen Amins durch die lipophilen Äthylenbrücken des Kronenethers eine hohe Affinität zu der lipophilen stationären Phase besitzt.

Fig. 4 zeigt, in welcher Zeit eine RP-8-Säule in Abhängigkeit von der Konzentration des Kronenethers mit dem Eluenten 0.01 *N* Salzsäure-[18]Krone-6 äquilibriert ist. Diese Zeit ist mit *ca.* 4 h für eine Kronenetherkonzentration von 20 mg/l relativ lang; sie verkürzt sich auf *ca.* 1.5 h bei einer Konzentration von 500 mg [18]Krone-6/l. Beim Vergleich der Fig. 1b und 4 ist der Einfluss zu erkennen, den die Art der Reversed-Phase auf die Retentionszeit der Kronenetherammoniumkomplexe hat. Denn für eine Erhöhung der Retentionszeit des Noradrenalins auf *ca.* 8.5 min wurden für die RP-2-Phase 5 g [18]Krone-6/l benötigt. Den gleichen Effekt er-

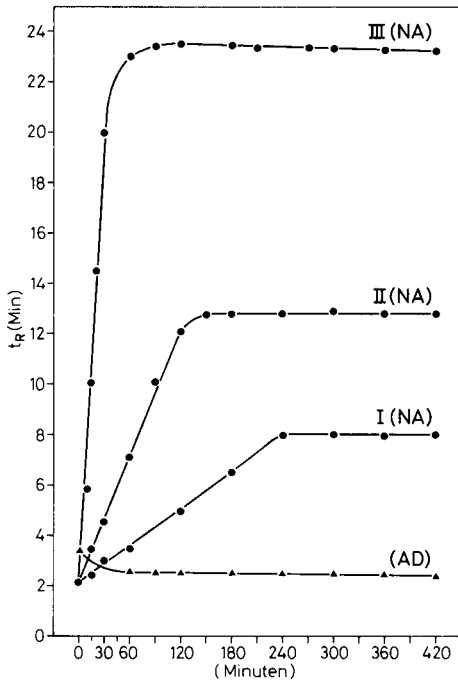


Fig. 4. Äquilibration einer RP-8-Säule in Abhängigkeit von verschiedenen [18]Krone-6-Konzentrationen in 0.01 N Salzsäure. Testamine: Adrenalin (AD) und Noradrenalin (NA). [18]Krone-6 = 20 mg/l (I), 100 mg/l (II), 500 mg/l (III). Für Adrenalin ist der Kurvenverlauf für die getesteten Kronenetherkonzentrationen angenähert identisch, weshalb aus Gründen einer besseren Übersichtlichkeit nur Werte für die höchste Konzentration eingezeichnet wurden. Die Fließgeschwindigkeit betrug 2.0 ml/min. Weitere Einzelheiten siehe Material und Methoden.

zielt man an einer RP-8-Phase mit 100 mg [18]Krone-6/l.

Darüberhinaus verdeutlicht Fig. 4, in welchem Ausmass die Trennung von primären und sekundären Aminen gesteuert werden kann. Denn Adrenalin zeigt als Vertreter der sekundären Amine erwartungsgemäss auch an einer RP-8-Säule nur eine geringe Verkürzung der Retentionszeit. Noradrenalin wird dagegen mit steigender Konzentration von [18]Krone-6 in 0.01 N Salzsäure im untersuchten Bereich immer langsamer eluiert.

#### ZUSAMMENFASSUNG

Es wird die selektive Gruppentrennung von primären und sekundären biogenen Aminen mittels HPLC in dem Zweiphasensystem Reversed-Phase/0.01 N Salzsäure-[18]Krone-6 beschrieben. Es handelt sich um ein Verfahren, dass in der Analytik und der organischen Chemie allgemein anwendbar ist, denn die Vortrennung in Gruppen vereinfacht die Analyse komplexer Amingemische im Bereich der Biologie und der Medizin wesentlich. Für die präparative organische Chemie eröffnet das Verfahren die Möglichkeit, Reaktionsprodukte und Ausgangsverbindungen bei N-Alkylierungen von primären Aminoverbindungen einfach, schnell und sehr effektiv zu trennen.

DANK

Die Arbeit wurde durch die Deutsche Forschungsgemeinschaft durch Sachmittelfinanzierung gefördert. Für die Anfertigung der Zeichnungen sei Herrn Söllner, Universität Bayreuth, gedankt.

## LITERATUR

- 1 K. Mori, *Jap. J. Ind. Health*, 12 (1974) 171.
- 2 K. Mori, *Jap. J. Ind. Health*, 17 (1975) 170.
- 3 J. H. Knox und A. Pryde, *J. Chromatogr.*, 112 (1975) 171.
- 4 J. H. Knox und J. Jurand, *J. Chromatogr.*, 125 (1976) 89.
- 5 I. Molnar und Cs. Horváth, *Clin. Chem.*, 22 (1976) 1497.
- 6 Cs. Horváth, W. Melander, I. Molnar und P. Molnar, *Anal. Chem.* 49 (1977) 2295.
- 7 J. P. Crombeen, J. C. Kraak und H. Poppe, *J. Chromatogr.*, 167 (1978) 219.
- 8 G. Schwedt, *Z. Anal. Chem.*, 293 (1978) 40.
- 9 G. Schwedt, *Angew. Chem.*, 91 (1979) 192.
- 10 Y. Yui, M. Kimura, Y. Itokawa und Ch. Kawai, *J. Chromatogr.*, 177 (1979) 376.
- 11 Y. Yui, Y. Itokawa und Ch. Kawai, *Anal. Biochem.*, 108 (1980) 11.
- 12 G. P. Jackman, V. J. Carson, A. Bobik und H. Skews, *J. Chromatogr.*, 182 (1980) 277.
- 13 N. Nimura, K. Ishida und T. Kinoshita, *J. Chromatogr.*, 221 (1980) 249.
- 14 T. Seki, *J. Chromatogr.*, 207 (1981) 286.
- 15 K. Imai, M. Tsukamoto und Z. Tamura, *J. Chromatogr.*, 137 (1977) 357.
- 16 K.-I. Okamoto, Y. Ishida und K. Asai, *J. Chromatogr.*, 167 (1978) 205.
- 17 C. R. Freed und P. A. Asmus, *J. Neurochem.*, 32 (1979) 163.
- 18 A. J. Cross und M. H. Joseph, *Life Sci.*, 28 (1981) 499.
- 19 T. Flatmark, S. Wahlström-Jacobsen und J. Haavik, *Anal. Biochem.*, 107 (1980) 71.
- 20 G. M. Anderson und J. G. Young, *Life Sci.*, 28 (1981) 507.
- 21 C. Refshage, P. T. Kissinger, R. Dreiling, L. Blank, R. Freeman und R. N. Adams, *Life Sci.*, 14 (1974) 311.
- 22 P. T. Kissinger, R. M. Roggins, R. L. Alcorn und D. L. Rau, *Biochem. Med.*, 13 (1975) 299.
- 23 M. Rigglin und P. T. Kissinger, *Anal. Chem.* 49 (1977) 2109.
- 24 L. R. Hegstrand und B. Eichelman, *J. Chromatogr.*, 222 (1981) 107.
- 25 Th. P. Moyer und Nai-Siang Jiang, *J. Chromatogr.*, 153 (1978) 365.
- 26 J. Wagner, M. Palfreyman und M. Zraika, *J. Chromatogr.*, 164 (1979) 41.
- 27 J. F. Reinhard, jr., M. A. Moskowitz, A. F. Sved und J. D. Fernstrom, *Life Sci.*, 27 (1980) 905.
- 28 P. Kissinger, B. S. Craig und R. E. Shoup, *Life Sci.*, 28 (1981) 455.
- 29 D. S. Goldstein, G. Feuerstein, J. L. Izzo, Jr., I. J. Kopin und H. R. Keiser, *Life Sci.*, 28 (1981) 467.
- 30 I. N. Mefford, *J. Neurosci. Meth.*, 3 (1981) 207.
- 31 K. Rahman, T. Nagatsu und T. Koto, *Life Sci.*, 28 (1981) 485.
- 32 E. Watson, *Life Sci.*, 28 (1981) 493.
- 33 C. J. Pedersen, *J. Amer. Chem. Soc.*, 86 (1967) 7017.
- 34 D. J. Sam und H. E. Simmons, *J. Amer. Chem. Soc.*, 94 (1972) 4024.
- 35 H. D. Durst, *Tetrahedron Lett.*, (1974) 2421.
- 36 D. Landini, F. Montanari und F. M. Piris, *J. Chem. Soc., Chem. Commun.*, (1974) 879.
- 37 M. Makosza und M. Ludwikow, *Angew. Chem.*, 86 (1974) 744.
- 38 C. L. Liotto und H. P. Harris, *J. Amer. Chem. Soc.*, 96 (1974) 2250.
- 39 D. T. Sepp, K. V. Scherrer und W. P. Weber, *Tetrahedron Lett.*, (1974) 2983.
- 40 C. J. Pedersen und H. K. Frensdorff, *Angew. Chem.*, 84 (1972) 16.
- 41 E. V. Demlow, *Angew. Chem.*, 86 (1974) 187 und 89 (1977) 521.
- 42 S. L. Regen, *Angew. Chem.*, 91 (1979) 464.
- 43 F. Vögtle und E. Weber, *Angew. Chem.*, 91 (1979) 813.
- 44 F. Vögtle und E. Weber, in S. Patai (Herausgeber), *The Chemistry of Ethers, Crown Ethers, Hydroxyl Groups and their Sulphur Analogues*, Suppl. E. Part 1, Wiley, Chichester, New York, Brisbane, Toronto, 1980, p. 59.
- 45 W. P. Weber und G. W. Gokel, *Phase-Transfer Catalysis in Organic Synthesis*, Springer, Berlin, 1977.



- 46 G. W. Gokel und W. P. Weber, *J. Chem. Educ.*, 55 (1978) 350, 430.
- 47 C. M. Starks und C. Liotta, *Phase-Transfer Catalysis: Principles and Techniques*, Academic Press, New York, 1978.
- 48 M. Makosza, in A. F. Scott (Herausgeber), *Survey of Progress in Chemistry, Vol. IX*, Academic Press, New York, 1979.
- 49 E. Blasius, W. Adrian, K.-P. Janzen und G. Klautke, *J. Chromatogr.*, 96 (1974) 89.
- 50 E. Blasius, K.-P. Janzen, H. Luxenburger, V. B. Nguyen, H. Klotz und J. Stockemer, *J. Chromatogr.*, 167 (1978) 307.
- 51 E. Blasius, K.-P. Janzen, W. Adrian, G. Klautke, R. Lorscheider, P.-G. Maurer, V. B. Nguyen, T. Nguyen-Tien, G. Scholten und J. Stockemer, *Z. Anal. Chem.* 284 (1977) 337.
- 52 E. Blasius, K.-P. Janzen, W. Klein, H. Klotz, V. B. Nguyen, T. Nguyen-Tien, R. Pfeiffer, G. Scholten, H. Simon, H. Stockemer und A. Toussaint, *J. Chromatogr.*, 201 (1980) 147.
- 53 L. R. Sousa, D. H. Hoffman, L. Kaplan und D. J. Cram, *J. Amer. Chem. Soc.*, 96 (1974) 7100.
- 54 G. Dotsevi, Y. Sogah und D. J. Cram, *J. Amer. Chem. Soc.*, 98 (1976) 3038.
- 55 L. R. Sousa, G. D. Y. Sogah, D. H. Hoffman und D. J. Cram, *J. Amer. Chem. Soc.*, 100 (1978) 4569.
- 56 R. C. Hayward, *Nachr. Chem., Techn. Labor.*, 25 (1977) 15.
- 57 D. J. Cram und J. M. Cram, *Science*, 183 (1974) 803.
- 58 W. H. Delphin und E. P. Horwitz, *Anal. Chem.* 50 (1978) 84.
- 59 Cs. Horváth, W. Melander und A. Nahum, *J. Chromatogr.*, 186 (1979) 371.
- 60 W. J. T. Brugman und J. C. Kraak, *J. Chromatogr.*, 205 (1981) 170.
- 61 T. Nakagawa, H. Mizunuma, A. Shibukawa und T. Uno, *J. Chromatogr.*, 211 (1981) 1.
- 62 R. M. Izatt, N. E. Izatt, B. E. Rossiter und J. J. Christensen, *Science*, 199 (1978) 994.
- 63 E. P. Kyba, K. Koga, L. R. Sousa, M. G. Siegel und D. J. Cram, *J. Amer. Chem. Soc.*, 95 (1973) 2692.
- 64 J. M. Timko, R. C. Helgeson, M. Newcomb, G. W. Gokel und D. J. Cram, *J. Amer. Chem. Soc.*, 96 (1974) 7097.
- 65 O. Nagano, A. Kobayashi und Y. Sasaki, *Bull. Chem. Soc. Jap.*, 51 (1978) 790.
- 66 I. Goldberg in S. Patai (Herausgeber), *The Chemistry of Functional Groups, Suppl. E, Part 1*, Wiley, Chichester, New York, Brisbane, Toronto, 1980, p. 175.
- 67 R. M. Izatt; persönliche Mitteilung an J. M. Lehn, zitiert in Lit. 68.
- 68 J.-P. Behr, J.-M. Lehn und P. Vierling, *J. Chem. Soc., Chem. Commun.*, (1976) 621.
- 69 I. M. Kolthoff, *Anal. Chem.* 51 (1979) 1R.
- 70 D. A. Laidler und J. F. Stoddart, in S. Patai (Herausgeber), *The Chemistry of Functional Groups, Suppl. E, Part 1*, Wiley, Chichester, New York, Brisbane, Toronto, 1980, p. 51.

CHROM. 14,307

## HIGH-PERFORMANCE LIQUID CHROMATOGRAPHY AND MAGNETIC CIRCULAR DICHROISM: A STUDY OF THE "PALLADIUM(II)-THIOETHER PEPTIDE" COMPLEXES\*

HUNG LAM-THANH\*, SERGE FERMANDJIAN and PIERRE FROMAGEOT

*Service de Biochimie, Département de Biologie, Centre d'Études Nucléaires de Saclay, F-91191 Gif-sur-Yvette Cédex (France)*

(First received May 12th, 1981; revised manuscript received August 21st, 1981)

---

### SUMMARY

By using ion-pair reversed-phase chromatography with cetyltrimethylammonium or trioctylmethylammonium as the counter ion, two classes of Pd(II) complexes with completely different properties were distinguished, depending on whether the thioether group is inside a linear moiety (L-methionine and related peptides, S-ethyl-L-cysteine) or intracyclic (L-thiazolidine-4-carboxylic acid and related peptides). The retention times clearly indicate that in the complexes these ligands interact differently with the metal through their sulphur atom. Fixation of the palladium(II)-S-ethyl-L-cysteine complex on the stationary phase is useful for the characterization of D- and L-methionine. Magnetic circular dichroism studies indicated the existence of a charge-transfer band arising from the interaction of the metal with the ligand, the intensity of which varies as a function of the chemical structure of the ligand, either cyclic or linear, and its sequence. There is a good correlation between the intensity of the charge-transfer band and the retention time of the complexes.

---

### INTRODUCTION

Complexes of palladium(II) and platinum(II) possess antiviral properties which have been extensively studied<sup>1</sup>. Our laboratory has been primarily interested in the optical, *e.g.*, circular dichroism, properties of the complexes of palladium(II) with disulphide and thioether groups of amino acids and peptides<sup>2,3</sup> and in their chromatographic properties. This work briefly describes some correlated high-performance liquid chromatographic (HPLC) and magnetic circular dichroism (MCD) results obtained with complexes of palladium(II) with two types of thioether groups in peptides: linear thioethers (L-methionine and L-methionyl peptides) and cyclic thioethers (L-thiazolidine-4-carboxylic acid and related dipeptides). Additional results suggest

---

\* Presented at the *5th International Symposium on Column Liquid Chromatography, Avignon, May 11–15, 1981*. The majority of the papers presented at this symposium have been published in *J. Chromatogr.*, Vol. 218 (1981).

that fixation of the palladium(II)–S-ethyl-L-cysteine complex on the stationary phase should allow the characterization of D- and L-methionine.

## EXPERIMENTAL

The materials and methods of detection have been described earlier<sup>4</sup>. Measurements were carried out at room temperature.

L-Methionine (Sigma), D-methionine (Protein Research Foundation), D,L-methionine (Prolabo), L-methionyl-L-alanine · 0.5H<sub>2</sub>O, L-alanyl-L-methionine, L-methionyl-L-methionyl-L-alanine (Schwarz/Mann), L-thiazolidine-4-carboxylic acid (Fluka), S-ethyl-L-cysteine (Calbiochem) and L-proline (Sigma) were used without further purification. Glycyl-L-proline, cycloglycyl-L-proline, glycyl-L-thiazolidine-4-carboxylic acid and cycloglycyl-L-thiazolidine-4-carboxylic acid were synthesized and purified according to conventional methods.

The column for the characterization of D,L-methionine was prepared as follows: a  $\mu$ Bondapak C<sub>18</sub> (10  $\mu$ m) stainless-steel column (30 cm × 4 mm I.D.) was equilibrated with the mobile phase [2 mM cetyltrimethylammonium bromide (CTAB) in methanol–water (40:60), pH adjusted to 3 by with orthophosphoric acid. The preformed stoichiometry palladium(II)–S-ethyl-L-cysteine complex (up to 20  $\mu$ M in 2 ml at pH 2.3) was injected into the column where it was fully retained; washing with 120 ml of mobile phase did not lead to any detectable absorbance at 380 nm (Fig. 3). For the elution of the complex, 10 mM trichloroacetic acid as mobile phase is needed. Binding of this complex to the C<sub>18</sub> stationary phase is assumed to be homogeneous on the basis of previous findings by Davankov *et al.*<sup>5</sup> and our laboratory<sup>4</sup>. Whereas free PdCl<sub>4</sub><sup>2-</sup> ions in the mobile phase may attack steel columns and tubes, the palladium(II) complexes do not<sup>4</sup>. We checked this fact by searching for iron in the eluate by atomic-absorption spectroscopy. No iron at concentrations above 0.1  $\mu$ g/ml was detectable. The column in which the reversed phase is converted into a chiral phase is now ready for the characterization of D,L-methionine.

MCD measurements were performed on a modified Jouan-Roussel (II) dichrograph in which the magnetic field of 66,600 gauss was produced in a supra coil<sup>6</sup>. The magnetic molar ellipticity ( $\theta$ )<sub>M</sub>, expressed in degrees · cm<sup>2</sup> · dmol<sup>-1</sup> · gauss<sup>-1</sup>, was calculated from the difference between the ellipticity in the presence and absence of the magnetic field and normalized to 1 gauss.

Titrisol solutions from Merck (Darmstadt, G.F.R.) were used as buffers in which amino acids and peptides were diluted to 1 mM.

## RESULTS AND DISCUSSION

We have reported previously<sup>4</sup> that optimal separation of L-methionine, L-methionyl-L-alanine and L-alanyl-L-methionine complexed with Pd(II) is obtained on a stainless-steel column according to a dynamic ion-exchange mechanism. Such a separation has also been achieved with a polyethylene  $\mu$ Bondapak C<sub>18</sub> (RCSS; Waters) column (Figs. 1 and 2), where the retention times are about double those obtained on stainless-steel columns. Such effects can be explained by differences in both the number of theoretical plates and the volume of the stationary phase. Whereas we might expect a retention time for L-methionyl-L-methionyl-L-alanine of at most twice that of L-methionine, it is found that 10 mM trichloroacetic acid is

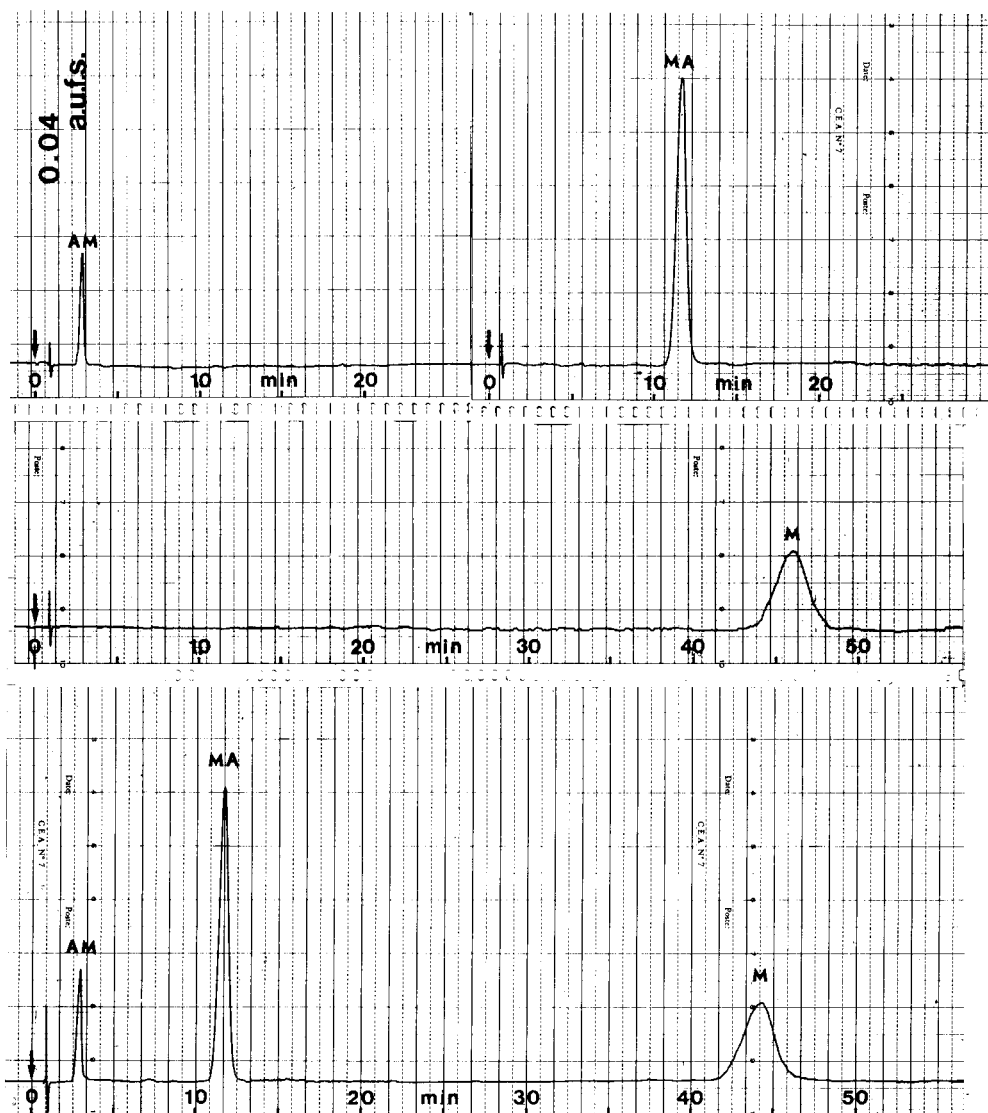


Fig. 1. Ion-pair separation by reversed-phase chromatography of L-methionine (M), L-methionyl-L-alanine (MA) and L-alanyl-L-methionine complexes with  $\text{PdCl}_4^{2-}$  or Pd(II). RCSS polyethylene  $\mu\text{Bondapak C}_{18}$  column; flow-rate, 4 ml/min; temperature, 20°C; eluent, methanol-water (40:60)-2 mM CTAB; pH, adjusted to 3 with orthophosphoric acid. Absorbance units full-scale (a.u.f.s.) at 380 nm, 0.040. Volume of complexes injected, 10  $\mu\text{l}$  or 0.1  $\mu\text{mol}$ . Top, complexes analysed separately; bottom, mixture of three complexes.

needed to elute the palladium(II)-L-methionyl-L-methionyl-L-alanine complex (Fig. 3). An additional interaction of the tripeptide carboxylate group ( $\text{p}K = 2.35$ ) according to the mechanism of dynamic ion exchange might occur again in this instance. On the other hand, the retention time of S-ethyl-L-cysteine is much longer than that of its chemical isomer L-methionine, and again 10 mM trichloroacetate is needed for its

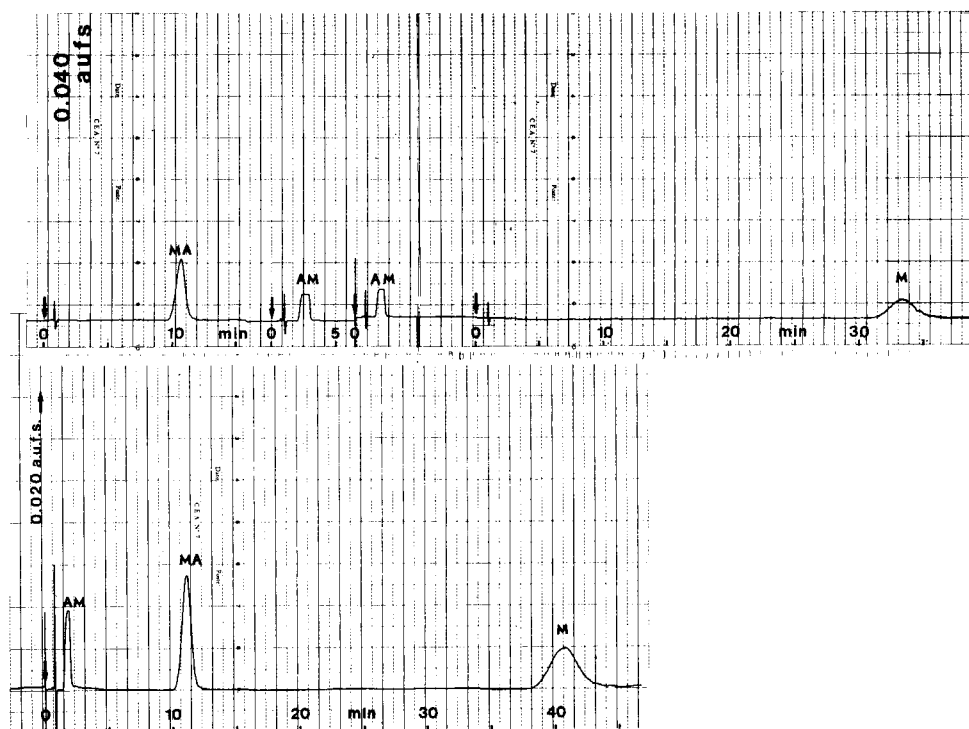


Fig. 2. Ion-pair separation by reversed-phase chromatography of L-methionine (M), L-methionyl-L-alanine (MA) and L-alanyl-L-methionine complexes with  $\text{PdCl}_2^{2-}$  or Pd(II). Experimental conditions as in Fig. 1 except that the counter ion used was triethylmethylammonium (Adogen 464).

elution (Fig. 3). This difference might result from two conjugate effects: (i) the uncomplexed carboxylate group [the  $\text{p}K_{\text{COOH}}$  value of S-ethyl-L-cysteine is lower (2.03)<sup>7</sup> than that of L-methionine (2.28)<sup>8</sup>] interacting with the stationary phase through an ion pairing mechanism, and (ii) the stability of the chelate ring in the two complexes: a five membered ring is observed in the S-methyl-L-cysteine–palladium(II) crystal, and a six membered ring in the L-methionine–palladium(II) crystal<sup>9,10</sup>.

#### *Cyclic thioether derivatives*

Palladium(II) complexes of L-thiazolidine-4-carboxylic acid, glycyl-L-thiazolidine-4-carboxylic acid and cycloglycyl-L-thiazolidine-4-carboxylic acid were chromatographed by ion-pair formation with CTAB in the mobile phase as with the linear thioethers (Fig. 3). Comparison of the retention times of L-thiazolidine-4-carboxylic acid (3 min) and L-proline (1.5 min) suggests that ionic and sulphur–palladium(II) interactions contribute together to the effects observed for the sulphur-containing compound. As CD experiments<sup>11</sup> indicate that the carboxylate group is not involved in the complex with palladium(II), this group undoubtedly contributes to the ionic interaction with the quaternary ammonium of the counter ion. On the other hand, the sulphur–metal interaction in this soft metal ion–soft base system<sup>12</sup> would explain the differences observed between L-proline and L-thiazolidine-4-

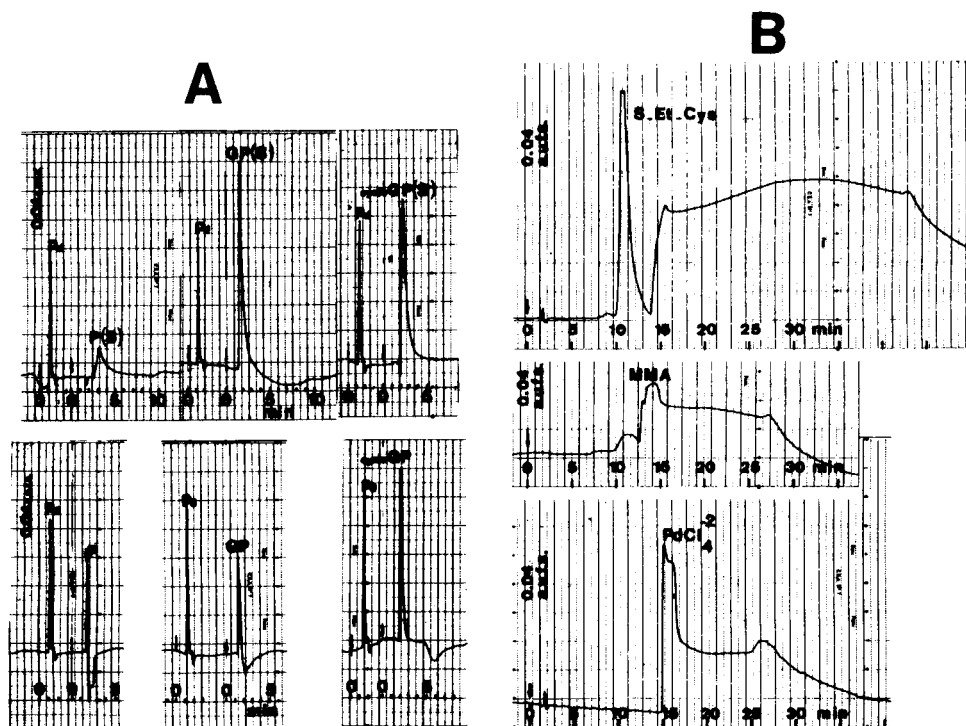


Fig. 3. (A) Ion-pair separation by reversed-phase chromatography of cyclic thioethers complexed with  $\text{PdCl}_4^{2-}$  or Pd(II). P(S), L-thiazolidine-4-carboxylic acid; GP(S), glycyl-L-thiazolidine-4-carboxylic acid; cycloGP(S), cycloglycyl-L-thiazolidine-4-carboxylic acid. L-Proline (P), glycyl-L-proline (GP) and cycloglycyl-L-proline (cycloGP) complexed with Pd(II) were chromatographed as controls. Complexing was performed at pH 2 with amino acid- or peptide-Pd(II) = 1:1 at a concentration of  $10^{-3}$  M. Amount of each complex injected, 100 nmol. Stainless-steel column,  $\mu$ Bondapak  $\text{C}_{18}$ ; flow-rate, 2 ml/min; temperature, 20°C; eluent, methanol-water (40:60)-2 mM CTAB; pH, adjusted to 3 with orthophosphoric acid. A.u.f.s. at 210 nm, 0.04. (B) Ion-pair separation by reversed-phase chromatography of S-ethyl-L-cysteine (S-Et-Cys) and L-methionyl-L-methionyl-L-alanine (MMA) complexed by palladium(II). Experimental conditions as in A. After injection of the complex elution was performed with methanol-water (40:60)-2 mM CTAB (pH 3) for 30 min (*i.e.*, the elution time of L-methionine). The start of the elution shown corresponds to the use of 10 mM trichloroacetate (pH 3). Sodium tetrachloropalladate ( $\text{PdCl}_4^{2-}$ ) was also eluted with 10 mM trichloroacetate (pH 3) as a control. A.u.f.s. at 380 nm, 0.04.

carboxylic acid. The retention times of glycyl-L-thiazolidine-4-carboxylic acid and the cycloglycyl-L-thiazolidine-4-carboxylic acid complex lie between 1.5 and 2.0 min. The peak widths of sulphur-containing dipeptides are larger than those of non-sulphur-containing compounds. This probably results from a better diffusion of thioether compounds in the stationary phase.

As the S-ethyl-L-cysteine-palladium(II) complex is completely retained on the  $\mu$ Bondapak  $\text{C}_{18}$  stationary phase under the conditions described in Fig. 3, we examined the possibility of using this new chiral support for the resolution of D,L-methionine. The stationary phase is prepared by immobilization of the chiral ligand on the solid support to create a specific solute-sorbent interaction for resolution of racemates of underivatized amino acids<sup>13-16</sup>. The system works under the conditions

given above unless the mobile phase is 10 mM trichloroacetate (TCA). Fig. 4 shows that D-methionine has a shorter retention time than L-methionine when the two compounds are chromatographed separately, in agreement with the results obtained by Lefebvre *et al.*<sup>15</sup> and Foucault *et al.*<sup>16</sup>. The retention time of D,L-methionine (24.4 min), however, lies between those of D-methionine (23.2 min) and L-methionine (27.6 min). This phenomenon could be explained by the concomitant resolution of the D- and L-peaks and the formation of a bis-ligand complex [D-Pd(II)-L] as suggested by Vicol *et al.*<sup>17</sup>. The role of palladium(II), uncomplexed to S-ethyl-L-cysteine but ion paired to the stationary phase, is emphasized by the strong absorbance of methionine

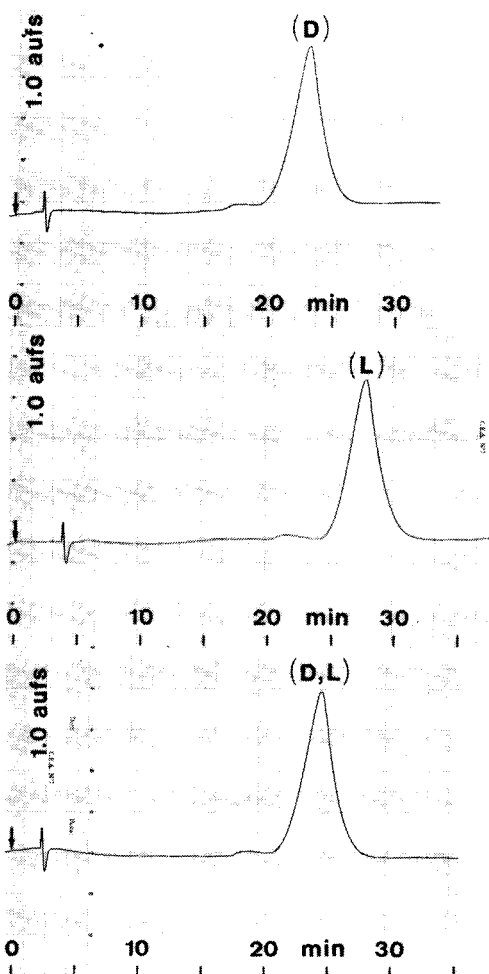


Fig. 4. Elution patterns of L-, D- and D,L-methionine from S-ethyl-L-cysteine (S-Et-Cys)-Pd(II) chiral phase. The complex is bound to the  $\mu$ Bondapak C<sub>18</sub> column (experimental conditions as in the text): Top, D-methionine (0.2  $\mu$ M); middle, L-methionine (0.2  $\mu$ M); bottom, racemate (0.2  $\mu$ M). Mobile phase: methanol-water (40:60)-2 mM CTAB; pH, adjusted to 3 with orthophosphoric acid. Flow-rate, 2 ml/min. a.u.f.s. at 210 nm, 1.0.

(0.4 absorbance unit at 210 nm for 0.2  $\mu\text{M}$  injected) which is, of course, eluted in a palladium(II)-bound form as previously observed<sup>4</sup>.

To understand better the behaviour of the thioether group in the various complexes with palladium(II), we examined the charge-transfer transition by MCD. Fig. 5 shows the Faraday effect obtained at acidic pH where the most intense effects are observed. Looking at the signals around 230 nm, which have previously been assigned to the interaction of the metal with the sulphur atom from the L-cysteine-palladium(II) complex<sup>2,3</sup>, we find differences according to the type of compound examined, either cyclic or linear. These can be explained by the properties of the  $p$  orbital of the sulphur atom: the bond angle of the S atom ( $R_1-S-R_2$ ) is  $92.5^\circ$  in the cyclic compound and appears strained compared with the value of  $100^\circ$  found in the linear compounds. Also, the shape and size of the chelates may influence the MCD properties. More specifically, for linear compounds, we find that intensities vary from one compound to another as a function of chemical structure. For instance, the magnetic ellipticity of L-methionyl-L-alanine is higher than that of L-alanyl-L-methionine, a feature which can be related to the difference in the distance existing between the donors S and  $\text{NH}_2$  in the two compounds. We also find that the magnetic ellipticity in L-methionyl-L-methionyl-L-alanine (containing two L-methionyl residues) is about twice as strong as that in L-methionyl-L-alanine (not shown). S-Ethyl-L-cysteine, a chemical isomer of L-methionine, is an apparent exception: the Faraday effect is twice that found for L-methionine. The weaker interaction between palladium(II) and the thioether sulphur of methionine compared with S-ethyl-L-cysteine might be a consequence of the atomic coordinates: the Pd-S distance and the N-Pd-S bond angle are 2.230 Å and  $86.8^\circ$ , respectively, in the S-methyl-L-cysteine-palladium(II) complex<sup>10</sup> compared with 2.265 Å and  $96.9^\circ$  in the L-methionine-palladium(II) com-

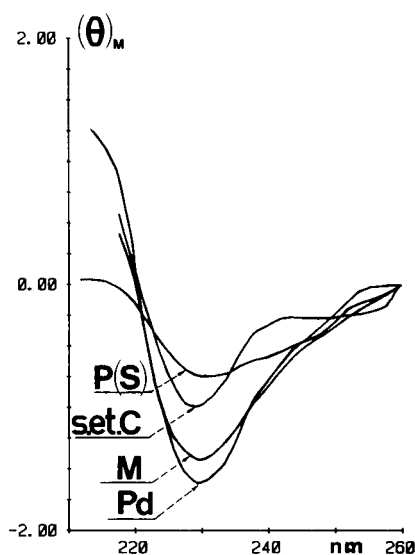


Fig. 5. MCD spectra of three thioether amino acids complexed by palladium(II) in citrate buffer at pH 2. The spectrum of sodium tetrachloropalladate ( $\text{PdCl}_4^{2-}$ ) was recorded as a control. Amino acid-palladium(II), 1:1 at a concentration of  $10^{-3}$  M. P(S) = L-thiazolidine-4-carboxylic acid; S-et-C = S-ethyl-L-cysteine; M = L-methionine.



plex<sup>9</sup>. In addition, the size of the chelate rings is different in the two complexes, as S-methyl-L-cysteine–palladium(II) is stabilized through a five-membered ring<sup>10</sup> and L-methionine–palladium(II) through a six-membered ring<sup>9</sup>. Hence the strain and the sum (or resultant) of the dielectric and magnetic dipoles are larger in the S-ethyl-L-cysteine (or S-methyl-L-cysteine) complex.

In conclusion, the palladium(II) complexes of linear and cyclic thioethers show distinctly different chromatographic and MCD properties. Retention times indicate that ligands interact with the palladium(II)-bound stationary phase through a variety of forces. A good parallelism is observed between the intensity of the charge-transfer band (MCD) of the complexes and the retention time: the larger the magnetic ellipticity, the longer is the retention time (Fig. 6).

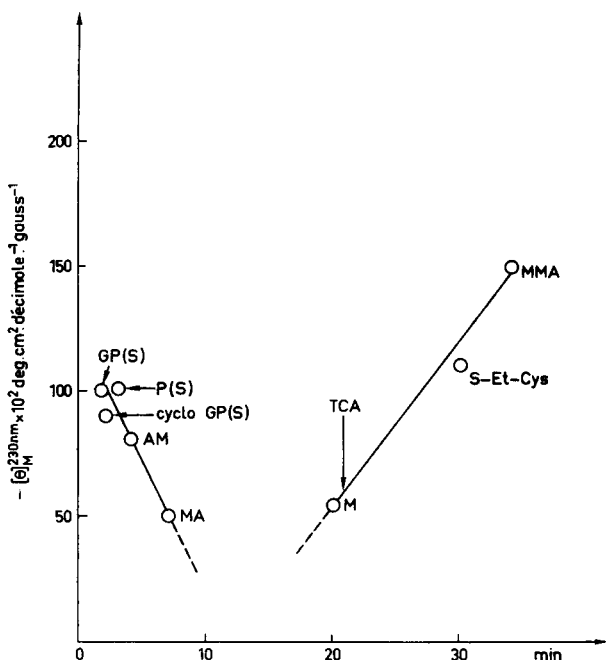


Fig. 6. Magnetic ellipticities  $[\theta]_M$  plotted versus retention times (min) obtained in reversed-phase chromatography for the thioether–palladium(II) complexes. Trichloroacetate (TCA), 10 mM, pH 3.

Finally, the chiral support obtained by fixation of the S-ethyl-L-cysteine complex to  $\mu$ Bondapak C<sub>18</sub> columns seem promising for the resolution of underivatized amino acid racemates.

#### REFERENCES

- 1 A. B. Bikhazi, S. M. Aghazanian and H. A. Tayim, *J. Pharm. Sci.*, 66 (1977) 1515.
- 2 H. Lam-Thanh and S. Femandjian, *J. Chim. Phys., Phys. Chim. Biol.*, 74 (1977) 361.
- 3 H. Lam-Thanh, K. Lintner, M. Monnot, F. Piriou and S. Femandjian, *J. Chim. Phys., Phys. Chim. Biol.*, 75 (1978) 755.
- 4 H. Lam-Thanh, S. Femandjian and P. Fromageot, *J. Liquid Chromatogr.*, 4 (1981) 681.

- 5 V. A. Davankov, A. S. Bochkov, A. A. Kurganov, P. Roumeliotis and K. K. Unger, *Chromatographia*, 13 (1980) 677.
- 6 R. Blondet, D. Rappanello and C. Schneider, *Proceedings of the 3rd International Cryogenic Engineering Conference, Berlin*, ILIFFE Science & Technology Publ., 1970, p. 238.
- 7 S. Ratner and H. T. Clarke, *J. Amer. Chem. Soc.*, 59 (1937) 200.
- 8 J. P. Greenstein and M. Winitz, in J. P. Greenstein and M. Winitz (Editors), *Chemistry of the Amino Acids*, Vol. 1, Wiley, New York, 1961, p. 435.
- 9 R. C. Warren, J. F. McConnell and N. C. Stephenson, *Acta Crystallogr., Sect. B*, 26 (1970) 1402.
- 10 L. P. Battaglia, A. B. Corradi, C. G. Palmieri, M. Nardelli and M. E. V. Tani, *Acta Crystallogr., Sect. B*, 29 (1973) 762.
- 11 H. Lam-Thanh, M. Juy, C. Schneider, S. Fermandjian and P. Fromageot, *J. Chim. Phys., Phys. Chim. Biol.*, (1981) in press.
- 12 R. B. Martin, in H. Sigel (Editor), *Metal Ions in Biological Systems*, Vol. 9, Marcel Dekker, New York, 1979, pp. 1-39.
- 13 V. A. Davankov and S. V. Rogozhin, *J. Chromatogr.*, 60 (1971) 280.
- 14 V. A. Davankov, S. V. Rogozhin, A. V. Semechkin and T. P. Sachkova, *J. Chromatogr.*, 82 (1973) 359.
- 15 B. Lefebvre, R. Audebert and C. Quiviron, *Israel J. Chem.*, 15 (1977) 69.
- 16 A. Foucault, M. Caude and L. Oliveros, *J. Chromatogr.*, 185 (1979) 345.
- 17 O. Vicol, N. Hurduc and I. A. Schneider, *J. Inorg. Nucl. Chem.*, 41 (1979) 309.

CHROM. 14,286

## LONG-CHAIN PHENOLS

### XXII\*. COMPOSITIONAL STUDIES ON JAPANESE LAC (*RHUS VERNICIFERA*) BY CHROMATOGRAPHY AND MASS SPECTROMETRY

J. H. P. TYMAN\* and A. J. MATTHEWS

*School of Chemistry, Brunel University, Uxbridge, Middlesex UB8 3PH (Great Britain)*

(First received July 28th, 1981; revised manuscript received August 14th, 1981)

---

#### SUMMARY

Preparative thin-layer (TLC) and column chromatography of Japanese Lac and the hydrogenated material have been used for compositional analysis by gravimetry and the isolation of certain polar minor components. From this examination the composition was approximately 62% urushiol, 18% other monomeric/dimeric components and 20% polymeric material. By gas-liquid chromatography (GLC) of methylated or bistrimethylsilylated Japanese Lac on 2% PEGA, four unsaturated constituents the 8-monoene (19%), 8,11-diene (9%), 8,11,14-triene (6%), which is a new constituent not previously detected and the 8,11,13-triene (62%) in addition to the saturated constituent (4%) were shown to be present. The results for the two derivatives have not been corrected for different response factors of the constituents but are in good agreement. GLC-mass spectroscopy of bistrimethylsilylated Japanese Lac on 2% PEGA as stationary phase confirmed the nature of the unsaturated constituents, and on E-301 indicated the presence of C<sub>17</sub> homologous urushiol and a minor polar component each comprising four constituents. Mass spectroscopy was used to determine the unsaturated composition and the semi-corrected results indicate a close similarity to those found by GLC. Bis(trimethylsilyl)urushiol is more volatile than the dimethyl derivative only on a polar stationary phase (PEGA). The dimethyl ether is more polar than the monomethyl ether (2-methoxyl-6-pentadecylphenol) by TLC but the reverse holds in GLC.

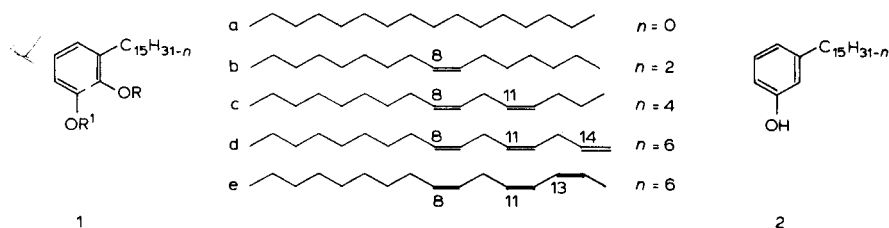
In the minor components a more polar material has been shown to be nuclear hydroxyurushiol while one of the less polar materials appears to be a diphenyl derivative isomeric with a previously described substance isolated from oxidised Japanese Lac. A mechanism for their formation is proposed.

---

#### INTRODUCTION

The quantitative composition of the major constituents and the identity of certain minor materials in Japanese Lac, *Rhus vernicifera* have been investigated.

\* Part XXI, J. H. P. Tyman, V. Tychopoulos and B. A. Colenutt, *J. Chromatogr.*, 213 (1981) 287.



Although this work is not yet complete it is desirable to describe the results, briefly referred to in a preliminary communication<sup>1</sup>, in view of a recent account<sup>2</sup> of an analysis of urushiol diacetate by high-performance liquid chromatography (HPLC).

The heterogeneous nature of urushiol and its partial structural determination was originally investigated by Majima<sup>3</sup> although the column chromatographic separation of methylated urushiol constituents of Japanese Lac and of *Rhus toxicodendron* was first effected by Dawson and co-workers<sup>4,5</sup> and followed by structural studies which showed the former to comprise four materials (1,  $R = R^1 = H$ ; a, b, c, e) and the latter three similar materials (a, b, c) and a fourth (d). The detailed chemistry has been reviewed<sup>6</sup>.

The increasing utilisation of Japanese Lac and interest in the biosynthesis of urushiol<sup>7</sup> makes it of interest to have quantitative information on the component phenols and the unsaturated constituents present. No gas-liquid chromatographic (GLC), mass spectroscopic (MS) or GLC-MS studies on the phenols have previously been carried out.

As found possible for the constituents of the component phenols of *Anacardium occidentale*<sup>8</sup>, the unsaturated composition of the urushiol constituents has been quantitatively determined by MS and confirmed by GLC on the dimethyl and bis(trimethylsilyl) ethers.

In addition to a small proportion of the less polar material cardanol<sup>7</sup> ( $2; n = 0, 2, 4, 6$ ) several substances more polar than urushiol have been found and partially identified, one probably a diphenyl compound isomeric with an earlier described material<sup>9</sup> and the other a nuclear hydroxy urushiol, the *o*-quinone of which has been postulated as an intermediate in certain photochemical transformations<sup>10</sup>.

In the methylated and hydrogenated derivatives of urushiol, striking differences<sup>11</sup> in polarity have been found between the monomethyl (1,  $R = H, R^1 = CH_3$ ) and the dimethyl ether series (1,  $R = R^1 = CH_3$ ) and the former\* appears to be a type of "hindered" phenol.

Our GLC work on the determination of relative molar response values of the constituents of urushiol and on HPLC analysis will be described in a subsequent paper.

## EXPERIMENTAL

### Materials

Japanese Lac was obtained through the help of Dr. M. Sato, National Industrial Research Institute, Sendai, Japan, and the Japanese Trade Centre, London.

\* For steric reasons the methyl group has been assigned to the 1-position, the  $C_{15}$  chain being in the 3-position.

Cashew nut-shell liquid (natural) used as a reference material was obtained<sup>12</sup> from Mozambique cashew nuts.

Hydrogenations were carried out in a Parr apparatus with Japanese Lac (5.2455 g) in ethyl acetate (48 cm<sup>3</sup>) with 10% palladium-carbon (0.5215 g) at 15 p.s.i., and also in a glass apparatus at atmospheric pressure. They were monitored by <sup>1</sup>H nuclear magnetic resonance (NMR) and argentation thin-layer chromatography (TLC). Methylations were carried out under nitrogen on Japanese Lac (1.000 g) in refluxing benzene (27 cm<sup>3</sup>) containing anhydrous potassium carbonate and dimethyl sulphate (4.00 g) or by the phase transfer method<sup>7</sup>. Silylations were effected in warm anhydrous pyridine solutions with bis(trimethylsilyl)acetamide or bis(trimethylsilyl)trifluoroacetamide in five molar proportion.

#### *TLC*

TLC was carried out on silica gel G (Merck Type 60) with self-prepared microscope slides, analytical plates (10 × 8 cm, and 20 × 10 cm) with a 0.25-mm layer, and preparative plates (20 × 20 cm) with a 1-mm layer. Spots and bands were visualised with 0.1% ethanolic Rhodamine 6G. Silver nitrate plates (15% silver nitrate) were self-prepared by aqueous slurring<sup>13</sup> and bands were visualised with 0.1% ethanolic dichlorofluorescein. All TLC sample applications (10% urushiol in chloroform) were made in a nitrogen-box which was also used for removal of solvent after development/visualisation. Bands were eluted overnight under nitrogen with diethyl ether, whereby selective removal of the organic material but not the fluorescein indicator occurred, the suspensions were filtered and the filtrate then concentrated. All evaporations were carried out below 60°C and samples brought back to atmospheric pressure under nitrogen.

#### *Column chromatography*

Column chromatography was effected with silica gel (MFC) in a glass column (21 × 1.25 in.) equipped with a silica disc of zero porosity and outlet tap fitted with a PTFE key. The column was wrapped with tin foil to exclude light. Japanese Lac (2.5682 g) was applied directly to the column and fractions were monitored by TLC and GLC as indicated in the results and discussion section.

#### *GLC and GLC-MS*

GLC was conducted generally with a Pye 104 dual column chromatograph equipped with a flame ionisation detector and a Vitatron recorder. Peak areas were measured by accurate triangulation and the results expressed were the average of at least six determinations. Glass columns (5 ft. ×  $\frac{3}{16}$  in.) with nitrogen at a flow-rate 45 cm<sup>3</sup>/min and 20 p.s.i. were used containing acid-washed and silanised diatomite C with 3% SE-30 and (for unsaturated constituents) diatomite M (80–100 mesh) with 2% polyethyleneglycol adipate (PEGA).

GLC-MS was effected by the Physico-Chemical Measurements Unit (PCMU) (Aldermarston and Harwell, Great Britain) with a Pye 104 and 2% E-301 as stationary phase at 230°C with helium as carrier gas (40 cm<sup>3</sup>/min). For the silylated unsaturated constituents, 2% PEGA on diatomite C at 185°C was used under similar gas flow conditions. Subsequently the low resolution D31 service was used by PCMU (Harwell) with a 6-ft. column coated with 3% OV-1 with helium (30 cm<sup>3</sup>/min) and temperature programming from 200 to 250°C, the mass spectrometry being carried out at 70 eV with a resolution of 1000 and the ion source at 200°C.

TABLE I

TLC SEPARATION OF JAPANESE LAC AND HYDROGENATED JAPANESE LAC IN DIFFERENT SOLVENTS

<i>Material</i>	<i>Solvent</i>	<i>R<sub>F</sub> values and observations</i>
Natural	Chloroform	No migration beyond $R_F$ 0.1
Natural	Benzene	No migration beyond $R_F$ 0.1
Natural	Acetone	All components, $R_F$ 0.8–0.9
Natural	Chloroform–ethyl acetate (19:1)	Separation: $R_F$ 0.49 (1, urushiol); 0.23 (2); 0.09 (3); 0.0 (4 and 5)
Natural	Chloroform–ethyl acetate (90:10)	Good separation: $R_F$ 0.65 (1, urushiol); 0.46 (2); 0.25 (3); 0.1 (4); 0.0 (5)
Hydrogenated urushiol	Chloroform–ethyl acetate (90:10)	Good separation, sharper bands, with less tailing

Mass spectrometry for analytical purposes was carried out on an MS 902 instrument by a repeated scanning procedure<sup>8</sup> with direct sample insertion, through the courtesy of Mr. D. Carter, School of Pharmacy, London, and more recently by the PCMU (Harwell) low resolution D11 service (with the VG ZAB system). Accurate mass measurements were made with the D21 service.

<sup>1</sup>H NMR spectra were determined on a Varian T60 instrument with tetramethylsilane as internal standard. Infrared spectra were obtained with a Unicam SP200 instrument. Elemental analyses were carried out by Mr. G. Crouch, School of Pharmacy, London, and by Butterworth Analytical Services (Teddington, Great Britain).

## RESULTS AND DISCUSSION

Most separatory techniques were used in conjunction or with spectroscopic identification of materials, but it is convenient to discuss the former individually.

### TLC

Solvents, chloroform, benzene, acetone, chloroform–ethyl acetate (95:5, 90:10 and 80:20) were used for the analytical TLC examination of Japanese Lac and the results are summarised in Table I. Generally chloroform–ethyl acetate (90:10) gave the best separation and the bands with  $R_F$  values 0.65 (urushiol), 0.46 and 0.25 appear to approximately correspond with those observed<sup>9</sup>, in a different solvent, namely 0.5 (urushiol), 0.37 and 0.20 for a mildly oxidised Japanese Lac. Our MS results on the material from the two bands below urushiol have led us to different conclusions from the latter authors concerning their identity as discussed subsequently. A small band  $R_F$  0.75, in chloroform–ethyl acetate (90:10), has been identified as cardanol<sup>7</sup>.

Preparative TLC was used to estimate the composition and to isolate new components for structural determination. Following an initial experiment which indicated gravimetrically 61.2% urushiol to be present, four preparative separations on Japanese Lac (2.040 g) carried out with chloroform–ethyl acetate (90:10) indicated urushiol (61.9%), 3.3% of less polar material (cardanol), fraction 3 (4.7%), fraction 4 (3.0%) and fraction 5 together with polymeric material (27.1%) to be present. The streaking and manipulative problem in recovering materials sensitive to oxidation led

TABLE II

VARIATION IN  $R_F$  VALUE (TLC) OF URUSHIOL MONO- AND DIMETHYL ETHERS WITH PERCENTAGE OF CHLOROFORM IN CHLOROFORM-LIGHT PETROLEUM (B.P. 40-60°C)

Urushiol compound	Chloroform-light petroleum (b.p. 40-60°C)				
	0:100	20:80	40:60	60:40	100:0
Monomethyl ether	0.11	0.29	0.38	0.60	0.70
Dimethyl ether	0.06	0.17	0.24	0.48	0.65

us to use hydrogenated Japanese Lac. Hydrogenation was monitored by  $^1\text{H}$  NMR examination and was continued until olefinic absorption ( $\delta$ ,  $\text{CCl}_4$ , 5.1-6.2) and methylenic absorption in proximity to double bonds ( $\delta$ , 1.69-2.9) had disappeared\*. Although less streaking was encountered, accurate analyses, particularly of smaller % components, were rendered difficult due to variations in the delineation of bands observable at the visualisation stage with level of solvent impregnation. TLC on this material revealed the main components present and was useful for the isolation of the more polar material such as fraction 3 (2.05-4.70%), fraction 4 (3.0-6.1%), fraction 5 (8.2-8.6%) and baseline polymeric material (18.7-24.8%).

Methylation of hydrogenated phenolic lipids has been useful analytically<sup>14</sup> and was expected as well in the present work to both aid volatilisation and stabilisation of Japanese Lac. Methylated and methylated/hydrogenated Japanese Lac were examined by TLC in the solvent system, chloroform-light petroleum (b.p. 60-80°C) and the variation in  $R_F$  values with solvent composition of the two main bands, an upper purple and a lower yellow zone, are shown in Table II.  $^1\text{H}$  NMR and MS examination of the preparatively separated bands indicated that the purple band consisted of urushiol monomethyl ether (1,  $n = 0$ ,  $R = \text{H}$ ,  $R^1 = \text{CH}_3$ ) and the yellow band was the dimethyl ether (1,  $n = 0$ ,  $R = R^1 = \text{CH}_3$ ), the parent molecular ions having  $m/e$  values 334 and 348 respectively.

The phenolic methyl ether is evidently a hindered phenol similar in TLC behaviour<sup>11</sup> to 2,6-di-*tert.*-butyl-4-methylphenol and a number of similar compounds in relation to the corresponding dimethyl ethers all of which had greater polarity. By GLC the monomethyl ethers were more polar than the dimethyl ethers as discussed subsequently. Methylation either of Japanese Lac or the hydrogenated material did not enable fractions 3, 4, 5 and the baseline component to be more easily characterised although it was useful for the quantitative analysis of the unsaturated constituents by GLC.

#### Column chromatography of Japanese Lac

Column chromatography of Japanese Lac on silica gel (MFC) was conducted with chloroform initially and then with chloroform-ethyl acetate as shown in Table III. Twenty-two fractions were collected and monitored by analytical TLC. Although the method was useful for obtaining larger quantities of minor components its pro-

\* The  $^1\text{H}$  NMR absorption of unsaturated constituents of urushiol in connection with synthetic studies will be described elsewhere in full.

TABLE III  
COLUMN CHROMATOGRAPHIC SEPARATION OF JAPANESE LAC

EA = Ethyl acetate; C = chloroform.

<i>Fraction no.</i>	<i>Solvent</i>	<i>Wt. (g)*</i>	<i>R<sub>F</sub> (TLC) in chloroform-ethyl acetate (90:10)</i>
1	Chloroform	0.1160 ( 4.5)	0.75 (Cardanol and non-polar material)
2-12	C-EA (95:5)	1.4525 (58)	0.65 (Urushiol)
13-15	C-EA (90:10)	0.1969 (8)	0.46 <i>cf.</i> , Fraction 3
16-18	C-EA (85:15)	0.3156 (12)	0.25 <i>cf.</i> , Fraction 4
19-22	C-EA (80:20 to 75:25)	0.1068 (4)	Baseline <i>cf.</i> , Fraction 5 and baseline material.
(residue on column)		(13.5)	

\* Percentages are given in parentheses.

tracted nature resulted in some deterioration of fractions, a feature observed by others<sup>15</sup>, and only an approximate estimate of composition could be obtained. Methylated Japanese Lac was considerably more stable in column chromatographic conditions. By column chromatography of methylated Japanese Lac the phenolic mono-methyl ether (purple fraction) and the dimethyl ether (yellow fraction) were effectively separated, the former being eluted first thus confirming its less polar character in adsorption conditions. The extensive range of fractions collected was monitored by analytical TLC and by GLC upon the stationary phase SE-30 and small differences both in  $R_F$  values and retention times suggested that some fractionation of the unsaturated constituents of the mono- and dimethyl ethers was taking place in column adsorption chromatographic experiments.

#### *GLC of Japanese Lac and its hydrogenated and methylated products*

GLC examination of Japanese Lac on the stationary phase 3% SE-30 at 220°C showed a series of peaks, at first thought to be due to the bands found in TLC analysis, at the (uncorrected) retention times of 6.4 min (trace %), 9.0 min (trace %), 10.8 min (5.8%), 14.2 min (26.7%), 17.2 min (57.3%), 21.0 min (10.2%) and 28.6 min (trace %). The main urushiol band from preparative TLC gave a similar chromatogram while the lower bands referred to as fractions 3, 4 and 5 were substantially non-volatile. Similar results were shown by the fractions from column chromatography. The succession of peaks was clearly due to the partial resolution of urushiol into its unsaturated constituents since hydrogenated urushiol exhibited only one peak. Subsequently this partial resolution, which does not take place with cardanol or cardol upon 3% SE-30<sup>16</sup> and is largely due to the triene constituent having 8,11,13- rather than 8,11,14-unsaturation, was confirmed later by GLC-MS on the bis(trimethylsilyl)ether. The uncertain level of separation of the first peak comprising the saturated and monoene constituents from the second consisting of the diene and triene constituents and the tailing encountered precluded quantitative analysis of the phenols. Methylations of Japanese Lac afforded products with symmetrical peaks but



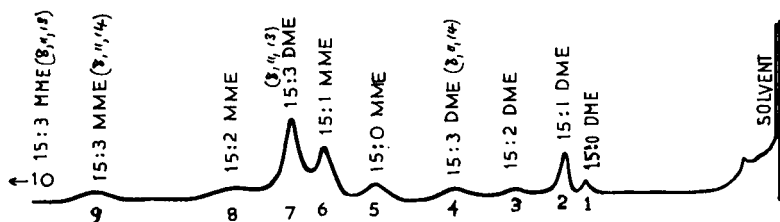


Fig. 1. GLC of methylated urushiol on 2% PEGA at 200°C. DME = Dimethyl ether; MME = monomethyl ether.

still showing resolution not only of the unsaturated constituents but also of mono- and dimethyl ethers. GLC monitoring of fractions from the column chromatographic separation of methylated Japanese Lac again confirmed these findings. Hydrogenated and methylated Japanese Lac by GLC analysis on 3% SE-30 at 220°C gave peaks at the uncorrected retention times of 9.7 min (1.9%), 13.5 min [64.7%, (15:0)-urushiol dimethyl ether], 15.2 min [27.7%, (15:0)-urushiol monomethyl ether] and 22.6 min [5.7%, (17:0)-urushiol dimethyl ether]. The identity of the two main bands was confirmed from the GLC retention times of the purple band (monomethyl ether) and yellow band (dimethyl ether), separated by preparative TLC, both of which gave single GLC peaks.

By GLC the monomethyl ether is more polar than the dimethyl ether while the reverse holds for TLC. Quantitative analysis could only be achieved by complete resolution of the unsaturated constituents for which 2% PEGA<sup>17</sup> appeared to be a more suitable stationary than 3% SE-30. Methylated Japanese Lac, the methylated urushiol band from preparative TLC and the hydrogenated and methylated mono- and dimethyl ethers were examined on 2% PEGA at 200°C and the retention times observed have been summarised in Table IV. Five peaks were observed in each group as seen in Fig. 1, the fourth and fifth peaks being due from MS studies to the isomeric 8,11,14- and 8,11,13-trienes respectively. Prolonged methylation resulted in a diminution of the series of peaks due to the monomethyl ether and a corresponding increase in those of the dimethyl ether as seen in the GLC trace (Fig. 2). The relative retentions<sup>17</sup> of the (15:0), (15:1), (15:2) and (15:3) constituents of cardanol methyl ether were similar to those for the first four peaks in each group. The greater retention of the major peak due to the 8,11,13-triene was in conformity with data for conjugated compared with non-conjugated dienes<sup>18</sup> and the retention time of the 8,11,14-triene was in agreement with that observed for the triene constituent of *Rhus toxic-*

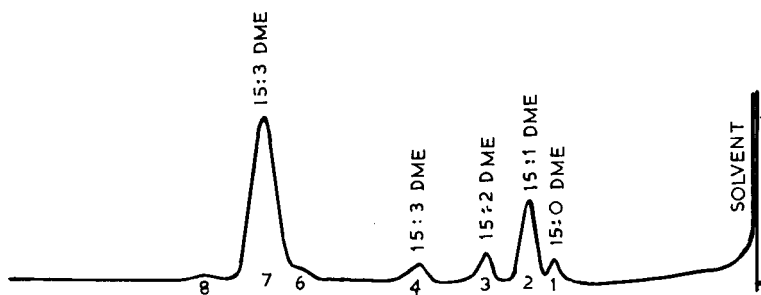


Fig. 2. GLC of methylated Japanese Lacquer (prolonged reaction) on 2% PEGA at 200°C.

TABLE IV  
RETENTION DISTANCES (RD) (mm), TIMES (RT) (min) AND RELATIVE RETENTIONS (RR) OF CONSTITUENTS OF METHYLATED AND TRIMETHYLATED URUSHIOL BY GLC ON 2% PEGA AT 200°C

Parameter	Dimethyl ether and bis-trimethylsilyl ether		Monomethyl ether								
	(15:0)	(15:1)	(15:2)	(15:3)	(15:0)	(15:1)	(15:2)	(15:3)			
				8, 11, 14				8, 11, 14, 8, 11, 13			
Methylated urushiol	RD	52.7 ± 0.80	58.50 ± 0.90	70.2 ± 0.70	87.8 ± 1.00	128.0 ± 1.73	108.5 ± 0.70	120.0 ± 1.40	144.5 ± 0.70	183.0	271.0
	RT*	10.54	11.70	14.04	17.56	25.60	21.7	24	28.9	36.6	54.2
(Methylated band 2 from preparative TLC)	RR	1.00	1.11	1.33	1.67	2.43	2.06 (1.00)	2.28 (1.11)	2.74 (1.33)	3.47 (1.68)	5.15 (2.49)
Methylated hydrogenated urushiol	RD	54.0**	-	-	-	-	109	-	-	-	-
Trimethylsilylated urushiol	RD	62.8 ± 1.02	68.4 ± 0.83	78.3 ± 0.15	95.5 ± 1.01	138.9 ± 0.30					
	RT***	6.28	6.84	7.83	9.55	13.89					
	RR §	0.59 (1.00)	0.65 (1.10)	0.74 (1.25)	0.91 (1.54)	1.32 (2.24)					

\* Chart speed 5 mm/min.

\*\* The retention distance of (15:0) urushiol was 302.3 mm, but the unsaturated constituents of the dihydric phenol had impracticably long retentions.

\*\*\* Chart speed 10 mm/min.

§ Relative to (15:0) urushiol dimethyl ether (= 1). Values in parentheses are relative to bis-trimethylsilylurushiol.

TABLE V  
COMPOSITION (%) OF UNSATURATED CONSTITUENTS OF URUSHIOL ETHERS BY GLC  
ON 2% PEGA

Parameter	Constituent			
	(15:0) Saturated	(15:1) Monoene	(15:2) Diene	(15:3) 8, 11, 14-Triene
<i>Dimethyl ether</i>				(15:3) 8, 11, 13-Triene
Mol. wt.	348	346	344	342
GLC peak no. (Fig. 2)	1	2	3	4
Normalised compn. (%) (from peak area)	4.93 ± 0.19	18.45 ± 0.17	8.85 ± 0.16	5.78 ± 0.15
				62.00 ± 0.37
<i>Bis(trimethylsilyl) ether</i>				
Mol. wt.	464	462	460	458
GLC peak no. (Fig. 3)	E	A	B	C
Normalised compn. (%) (from peak area)	3.83 ± 0.25	19.44 ± 0.82	8.79 ± 0.37	5.79 ± 0.27
				62.13 ± 0.98

*dendron*<sup>7,19</sup>. Mass spectral and GLC-MS examination has confirmed these observations as described in the next section. The co-occurrence of a minor proportion of the 8,11,14-triene with the 8,11,13-triene is both of biosynthetic interest and because previous analyses by column chromatography<sup>4,5</sup> have not detected its presence.

Following a number of GLC analyses, summarised in Table V, a semi-quantitative\* determination of the % composition of the unsaturated constituents was possible. Methylation although useful for spectral characterisation was not ideal for volatilisation purposes since it was a substantially incomplete process and the elution of the monomethyl series of peaks prolonged the procedure. Remarkably, complete trimethylsilylation was found to be relatively easily achieved by interaction of urushiol in warm pyridine solution with bis(trimethylsilyl)acetamide. The retention times of the bis(trimethylsilyl) derivatives of the constituents of urushiol on 2% PEGA at 200°C are given in Table IV, and a chromatogram shown in Fig. 3 obtained at 185°C for GLC-MS purposes. The compositional results of semi-quantitative analysis are shown in Table V and the results are in good agreement with those for the dimethyl ether series and indicate the presence of 62% of the 8,11,13-triene, 6% of the 8,11,14-triene, 9% of the 8,11-diene, 19% of the 8-monoene and 4% of the saturated constituent.

TABLE VI

% COMPOSITION OF UNSATURATED CONSTITUENTS OF URUSHIOL BY MASS SPECTROMETRY

Parameter	Urushiol constituent			
	(15:0) Saturated	(15:1) Monoene	(15:2) Diene	(15:3) 8, 11, 13- and 8, 11, 14-Trienes
Uncorrected normalised composition (from peak height)	8.53 ± 0.97	19.34 ± 1.69	10.11 ± 0.40	62.02 ± 2.59
(P + 2) peak, % of P	2.63	2.63	2.63	2.63
Normalised composition, semi-corrected	8.22	19.54	8.96	63.55

On PEGA as stationary phase urushiol bis(trimethylsilyl) ethers were more volatile than dimethyl ethers while on SE-30 the reverse applied. The relative retentions on the latter of (15:0)-urushiol bis(trimethylsilyl) ether, (15:0)-cardanol trimethylsilyl ether, (15:0)-urushiol dimethyl ether and (15:0)-urushiol monomethyl ether were 1.725, 1.00, 1.00, 1.15 respectively.

Our work on the determination of relative response factors of the unsaturated constituents is as yet incomplete. Argentation analytical TLC with the solvent, chloroform-ethyl acetate-formic acid (80:20:2) indicated the presence of five unsaturated

\* The analysis is termed semi-quantitative since response factors for the unsaturated constituents were not available to correct the results. The magnitude of the correction is considered to be small however.

TABLE VII

COMPOSITION OF TRIMETHYLSILYLATED JAPANESE LAC BY GLC-MS ON NON-POLAR E-301

No.	Rel. peak height (GLC)	Uncorrected composition (%), normalised*											
		<i>C</i> <sub>15</sub> Urushiol				<i>C</i> <sub>17</sub> Urushiol				<i>C</i> <sub>15</sub> Hydroxyurushiol			
		MW 458 (15:3)	460 (15:2)	462 (15:1)	464 (15:0)	486 (17:3)	488 (17:2)	490 (17:1)	492 (17:0)	546	548	550	552**
1	0.97	16.9	20.2	54.7	9.2								
2	2.35	7.8	22.3	59.7	10.4								
3	1.20	4.4	18.6	44.2	32.8								
4	0.56	37.7	20.1	18.8	23.4								
5	3.32	80.9	15.3	3.4	0.4								
6	1.14	72.5	19.3	7.7	0.5								
7	0.03					17.2	59.0	16.9	6.9				
8	0.06					13.1	29.5	59.0	10.8				
9	0.04					8.8	14.6	38.4	10.1	3.9	12.5	8.7	3.0
10	0.14					9.5	11.7	17.2	4.7	28.1	19.3	7.5	2.0
11	0.27									43.6	41.4	13.2	1.8
12	0.15									42.8	37.8	16.1	3.3

\* Calculated from peak heights in the mass spectrum.

\*\* Earlier determinations had indicated this group of peaks as having peaks in the range 548–554.

materials, in agreement with the GLC results described. Preparative separations however were unsatisfactory because of the instability of urushiol. Currently work is proceeding on the argentation TLC separation of the bis(trimethylsilyl) ethers which are readily converted to the parent phenol, rather than by column chromatography of the dibenzyl ether and reductive chemical removal of the protective group<sup>20</sup>. Our more recent analytical-scale results<sup>21</sup> suggest that preparative HPLC would be a more convenient separatory procedure for obtaining the saturated, monoene, diene and triene constituents.

We have examined the conversion of urushiol to its diacetate in pyridine solution with acetic anhydride and found it to be an inferior procedure to the formation of ether derivatives. Molecular distillation of Japanese Lac, acetylation of the distillate with acetic anhydride containing sulphuric acid followed by HPLC analysis of the diacetate has revealed a complex mixture<sup>2</sup>, which may be partly ascribable to the acidic conditions of derivative formation. These can result in rearrangement, isomerisation and polymerisation of cashew phenols<sup>6</sup>. Our GLC results on bis(trimethylsilyl) derivatives have not indicated the presence of fully conjugated material at longer retention than the 8,11,13-triene although such peaks would be broad and, if minor materials, would be difficult to observe at long retentions.

#### MS and GLC-MS

The unsaturated composition of Japanese Lac by the direct insertion technique, as for the cashew phenols<sup>8</sup>, has been determined by mass spectroscopy. The normalised results from peak height measurements for the saturated, monoene, diene and triene (8,11,13 and 8,11,14) constituents are summarised in Table VI, the peak heights of the diene, monoene and saturated having been corrected for the (P + 2)

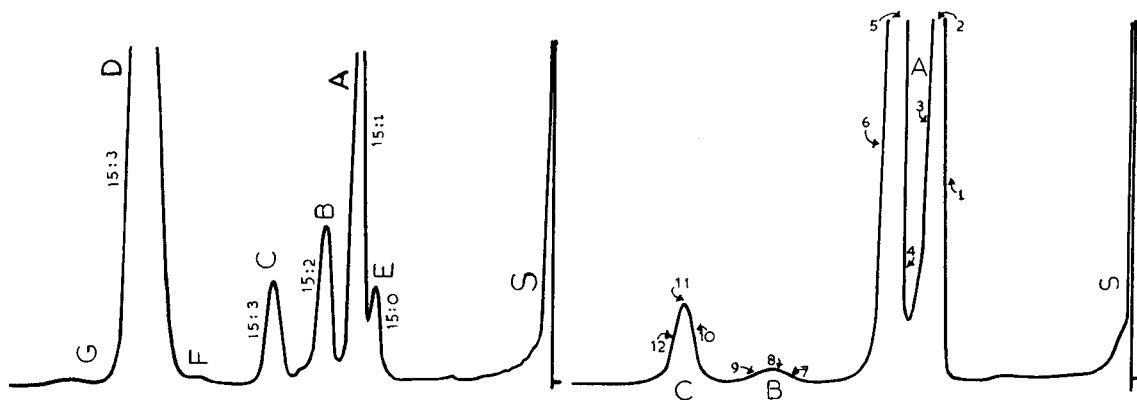


Fig. 3. GLC-MS of urushiol bis(trimethylsilyl) ether on 2% PEGA at 185°C.

Fig. 4. GLC-MS of Japanese Lacquer trimethylsilylated on 2% E-301 at 230°C.

peak contribution of the triene, diene and monoene respectively<sup>8</sup>, but without allowance for the small difference in response factors to be expected for the unsaturated constituents. Moderately good agreement is shown with the results of GLC analysis (Tables IV and V). Methylation prior to MS did not appear necessary since the phenolic unsaturated constituents were sufficiently volatile. The unsaturated composition obtained from peak heights for the dimethyl and monomethyl ethers of the triene, diene, monoene and saturated constituents although reproducible, was different from that derived from the phenols suggesting that response factors may be intrinsically more important for the methyl derivatives, since the same sample examined by GLC gave results in agreement with those from MS on the phenols\*. The unsaturated composition of C<sub>17</sub> urushiol (bis-homourushiol) was also found from the series of peaks at 342, 344, 346, 348 for its triene, diene, monoene and saturated constituents respectively. Mass spectroscopy of methylated hydrogenated Japanese Lac was convenient for determining, by the repeated scanning procedure, the proportion of monomethyl and dimethyl ethers from the peak heights of the molecular ions at *m/e* 334 and *m/e* 348.

GLC-MS was used to identify the major long retention 8,11,13-triene constituent and certain minor components of greater polarity than urushiol. The % compositional results in terms of the normalised peak heights with the non-polar stationary phase E-301 which gives separations similar to SE-30 are shown in Table VII for the chromatogram of bistrimethylsilylated Japanese Lac represented by Fig. 4. Scans 1-6 show the results of the partial separation which takes place into a first peak for the saturated and monoene constituents (MW 464, 462) and a second peak for the diene and triene constituents (MW 460, 458). Scans 7 and 8 are for the C<sub>17</sub> urushiol constituent (MW 486, 488, 490, 492) and scans 9-12 evidence of a minor component existing as four constituents (MW 546, 548, 550, 552) all of which were 88 mass units greater than their urushiol counterparts.

GLC-MS of the bistrimethylsilylated Japanese Lac on the semi-polar 2% PEGA at 185°C (Fig. 3) shows the peaks A, B, C, D referred to in Table VIII

\* Our results on the MS of the dimethyl ether of urushiol show some agreement with those in a brief communication<sup>22</sup> on methylated Japanese Lac of uncertain origin, and which were not corrected in any way.

TABLE VIII

COMPOSITION OF TRIMETHYLSILYLATED JAPANESE LAC BY GLC-MS ON SEMI-POLAR PEGA

Scan no.	Peak	Rel. peak height	Uncorrected composition (%), normalised*			
			MW 458 (15:3)	460 (15:2)	462 (15:1)	464 (15:0)
1	A	2.49		1.4	66.3	32.3
2	A			1.4	79.5	19.1
3	B	1.00		54.1	35.6	10.4
4	C	0.74	28.9	26.6	33.1	11.4
5	D	4.87	65.6	18.4	11.3	4.7
6	D		61.5	20.8	13.4	4.3

\* Some carry over from successive scans was encountered giving in each case a higher background of the preceding constituent than expected for % (P + 2).

with major masses corresponding to the 8-monoene, 8,11-diene, 8,11,14-triene and 8,11,13-triene constituents respectively, confirming that the major material is trienoid. E represents the saturated constituent and F, G appear to represent traces of monotrimethylsilylated constituents.

From the peak height in the gas chromatogram at the particular scan number (1-6) in Table VIII an approximate composition can be calculated based on  $\Sigma$  (peak height<sub>GLC</sub> × peak height<sub>MS</sub>) for each constituent and final normalisation, the results of which show a measure of agreement with those in Tables V and VI.

#### Minor components of Japanese Lac

The minor components of Japanese Lac were most readily seen by TLC. By GLC-MS of the bistrimethylsilylated natural product only one minor component (*m/e* 546-552) was revealed. It seemed probable that the remaining minor materials had masses above this and since GLC was negative, MS on the trimethylsilyl derivatives of the fractions having  $R_f$  values 0.46, 0.25, 0.1, obtained by preparative TLC was investigated. The findings have been summarised in Table IX.

The main urushiol band ( $R_f$  0.65) trimethylsilylated gave as expected from Table VII principal masses in the range 458-464 and 486-492. Material of  $R_f$  0.46 contained some of the preceding masses and higher constituents with *m/e* 914-922 suggesting the presence of dimeric material. Bands with  $R_f$  0.25 and 0.1 in addition to containing trimethylsilylated urushiol revealed *m/e* 546-552 corresponding to those masses found in GLC-MS examination on E-301. Different levels of side-chain unsaturation were clearly present and with the objective of obtaining the more stable saturated form and also of preventing reversion of dimeric type substances to the monomer\*, hydrogenated Japanese Lac was used for the isolation of the minor materials.

MS examination of the trimethylsilylated materials gave single peaks with prominent molecular ions. The more polar material ( $R_f$  0.25) indicated a molecular

\* Diels-Alder adducts (*cf.*, 8) undergo this reversion.

TABLE IX

MOLECULAR IONS OF PRINCIPAL COMPONENTS FROM PREPARATIVE TLC SEPARATIONS BY MS

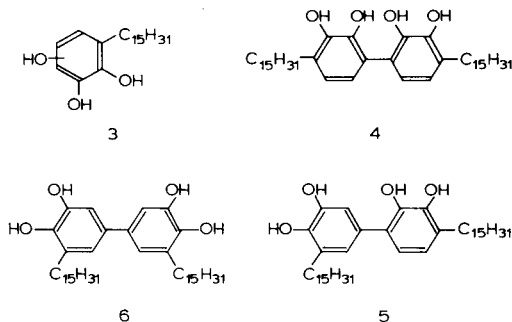
Fraction no. ( $R_F$ ) <sup>*</sup>	Masses of molecular ions of trimethylsilylated material	
	Unhydrogenated fraction	Hydrogenated fraction
(1) (0.75)	—	304, $C_{21}H_{36}O$ (15:0)-cardanol <sup>**</sup>
(2) Main urushiol band (0.65)	458, 460, 462, 464, ( $C_{15}$ side chain) 486, 488, 490, 492 ( $C_{17}$ side chain)	464, $C_{27}H_{52}O_2Si_2$ 492, $C_{29}H_{56}O_2Si_2$
(3) (0.46)	914–926 (and 458–464)	926, $C_{54}H_{102}O_4Si_4$
(4) (0.25)	546–582 (and 458–464)	552, $C_{30}H_{60}O_3Si_3$ ; 926 (small)
(5) (0.1)	546–552 (and 458–464)	552, $C_{30}H_{60}O_3Si_3$
(6) Baseline (0)	458, 460, 462, 464 (small)	348, $C_{21}H_{34}O_2$

\* Solvent, chloroform–ethyl acetate (90:10).

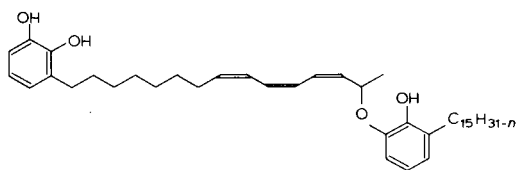
\*\* Ref. 7.

ion  $m/e$  552 and the molecular weight by accurate mass measurement was 552.3858 ( $C_{30}H_{60}O_3Si_3$  requires 552.3850). The  $^1H$  NMR spectrum, in particular the ratio of aromatic to benzylic protons, the polarity, the similar unsaturation to that of urushiol and the molecular weight [88 mass units more than for bis(trimethylsilyl)urushiol] suggest that this component is an hydroxyurushiol (3) in the tris(trimethylsilyl)ated form. From limited spectral evidence compound 3 appears to be 2,3,5-trihydroxy- rather than 1,3,4-trihydroxy-substituted but further work is required with model compounds to substantiate this. Although this compound has not been isolated previously from Japanese Lac its transient formation in the photochemical decomposition of dilute solutions of Japanese Lac has been postulated<sup>10</sup>. The less polar component ( $R_F$  0.46) exhibited a molecular ion at  $m/e$  926 in which region accurate mass measurement was not possible. Its structure is most probably 4 or 5, in the form of the tetrakis (trimethylsilyl) derivative, rather than 6 which has been described as a product of oxidised Japanese Lac<sup>23</sup> having  $R_F$  0.2. Our own spectral work is incomplete at the present and we have reservations on this group of diphenyls pending the preparation of certain reference compounds. A greater  $R_F$  value and reduced polarity would be expected for the sterically hindered structures 4 and 5 in comparison with 6. For the pairs of compounds, 2,2',4,4',6,6'- and 3,3',4,4',5,5'-hexachlorodiphenyl, 2,2',4,4'-tetra-chloro- and 4,4'-dichlorodiphenyl, the  $R_F$  values reported<sup>24</sup> support this.

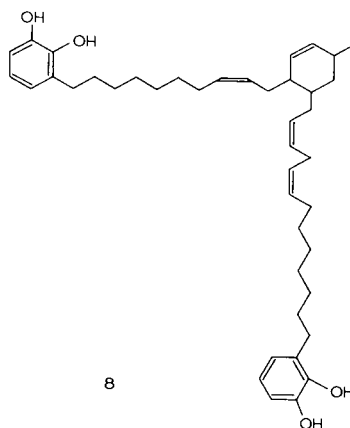
Structures such as 7 have been postulated<sup>9</sup> as minor components of oxidised







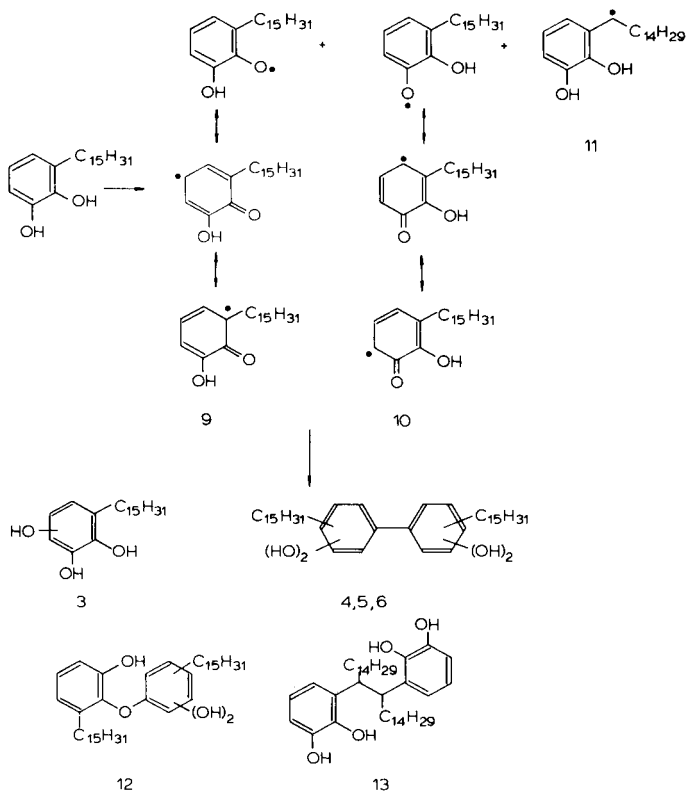
7



8

Japanese Lac on the basis of model reactions. Trimethylsilylation of the fully saturated material (7,  $n = 0$ ) would afford a derivative with  $m/e$  854, a mass not observed however in our work as a major peak. A Diels-Alder type product such as 8, reminiscent of kitol from vitamin A<sup>25,26</sup>, after saturation and trimethylsilylation would give a mass at  $m/e$  924. It would be expected to be chromatographically similar to urushiol itself but our experiments have not revealed its presence.

It seems likely that minor materials arise from a common precursor of a reac-



tive intermediate type which can then yield diverse products. An ionic mechanism has been proposed<sup>10</sup> to explain the ethoxylation of urushiol in dilute ethanol solution in the presence of light and moisture. In hexane, carbon tetrachloride and chloroform solutions of urushiol were observed to be stable. The conditions in our work of preparative TLC and the subsequent processing of separated bands under essentially anhydrous conditions and in the absence of light are therefore unlikely to have contributed to the formation of minor materials. Their origin must lie with Lac in its natural state and at the extraction stage.

A scheme proceeding by a radical participation is shown involving attack at either oxygen of saturated urushiol to give the resonant radicals 9, 10 or to a less extent at benzylic carbon to give 11 which could then by the action of water or by coupling reactions lead to the observed products (3) and others (4, 5, 6) believed to be present. In the natural product the side-chain allylic methylene system would be likely to be involved also and it is clear that other modes of reaction such as the formation of 12 and 13 could occur. A radical such as 9 would be more sterically stabilised<sup>27</sup> than 10 as well as through the contribution of a tertiary C radical and thus the formation of 2,3,5-trihydroxypentadecylbenzene would appear to be favoured. From preparative TLC it is clear that many minor polar products are present in urushiol and a more complex oxidative situation is apparent than has perhaps hitherto been appreciated.

#### REFERENCES

- 1 J. H. P. Tyman and A. J. Matthews, *Quantitative Compositional Studies on Urushiol*, contribution to the 26th IUPAC Congress, Tokyo, 1977.
- 2 Y. Yamauchi, R. Oshima and J. Kumanotani, *J. Chromatogr.*, 198 (1980) 49.
- 3 R. Majima, *Chem. Ber.*, 55B (1922) 172.
- 4 S. V. Sunthakar and C. R. Dawson, *J. Amer. Chem. Soc.*, 76 (1954) 5070.
- 5 W. F. Symes and C. R. Dawson, *J. Amer. Chem. Soc.*, 76 (1954) 2957.
- 6 J. H. P. Tyman, *Quart. Rev., Chem. Soc.*, 8 (1979) 499.
- 7 S. K. Lam and J. H. P. Tyman, *J. Chem. Soc., Perkin Trans. I*, (1981) 1942.
- 8 J. H. P. Tyman, *J. Chromatogr.*, 136 (1977) 289.
- 9 T. Kato and J. Kumanotani, *J. Polym. Sci., Part A-1*, 7 (1969) 1455.
- 10 A. V. Balint, J. H. Dawson and C. R. Dawson, *Anal. Biochem.*, 66 (1975) 340.
- 11 A. J. Matthews and J. H. P. Tyman, *Chem. Ind. (London)*, (1977) 740.
- 12 J. H. P. Tyman, *J. Chem. Soc., Perkin Trans. I*, (1973) 1693.
- 13 J. H. P. Tyman and N. Jacobs, *J. Chromatogr.*, 54 (1971) 83.
- 14 J. H. P. Tyman, *Anal. Chem.*, 48 (1976) 30.
- 15 R. G. Khurana and C. R. Dawson, *U.S. Pat.*, 3,819,726 (25 June 1974).
- 16 J. H. P. Tyman, *J. Chromatogr.*, 111 (1975) 277.
- 17 J. H. P. Tyman, *J. Chromatogr.*, 111 (1975) 285.
- 18 *Gas Chromatographic Data Compilation*, Special Technical Publication No. DS 25A, American Society for Testing Materials, 1962.
- 19 J. H. P. Tyman and C. H. Khor, *Chem. Ind. (London)*, (1974) 526.
- 20 B. Loev and C. R. Dawson, *J. Org. Chem.*, 24 (1959) 980.
- 21 V. Tychopoulos and J. H. P. Tyman, unpublished results.
- 22 M. Sato and S. Syogi, *Nippon Kagaku Zasshi*, 89 (1968) 814.
- 23 T. Kato and J. Kumanotani, *Bull. Chem. Soc. Jap.*, 42 (1969) 2375.
- 24 L. Fishbein, *J. Chromatogr.*, 68 (1972) 345.
- 25 B. V. Burger, C. F. Garbers, K. Pachler, R. Bonnett and B. C. L. Weedon, *Chem. Commun.*, (1965) 588.
- 26 J. H. P. Tyman, *J. Chromatogr.*, 156 (1978) 255.
- 27 G. Scott, *Chem. Ind. (London)*, (1963) 271.

CHROM 14,280

## CAPILLARY COLUMN GAS CHROMATOGRAPHIC-MASS SPECTROMETRIC-COMPUTER ANALYSIS OF ENVIRONMENTAL SPILLS

MIKE H. CARTER

*U.S. Environmental Protection Agency, Environmental Research Laboratory, College Station Road, Athens, GA 30605 (U.S.A.)*

(Received July 20th, 1981)

---

### SUMMARY

Two samples taken from the sites of environmental spills were analyzed by computerized gas chromatography-mass spectrometry utilizing packed and capillary chromatographic columns.

An oil spill sample was compared with a sample from a possible source by examining specific ion profiles from both. A sample from a spill involving an industrial discharge was examined for the presence of specific types of compounds by examining characteristic ion profiles.

The capillary columns provided greatly improved chromatographic separations compared to packed columns.

---

### INTRODUCTION

Packed column gas chromatograms have been useful in the matching of oil spills and oil samples from suspect sources; however, it has not always been possible to differentiate samples of similar oil types. Capillary column gas chromatography (GC) of complex hydrocarbon mixtures has been shown by Grob and Grob<sup>1</sup> to provide greater resolution than packed column GC. Previous work in this laboratory<sup>2</sup> has shown the ability of computerized GC-mass spectrometry (MS) to serve as retrospective specific GC detectors in detecting low level components of complex mixtures.

The present work was undertaken to determine the utility of capillary column GC combined with computer-controlled low-resolution MS in matching suspects with spills. Two environmental spills that had previously been analyzed utilizing packed GC columns were selected as candidates for this examination.

### EXPERIMENTAL\*

The GC-MS-computer system utilized was a Finnigan 9500 GC, 3200 EI/CI

\* Mention of commercial products does not constitute endorsement or recommendation for use by the Environmental Protection Agency.

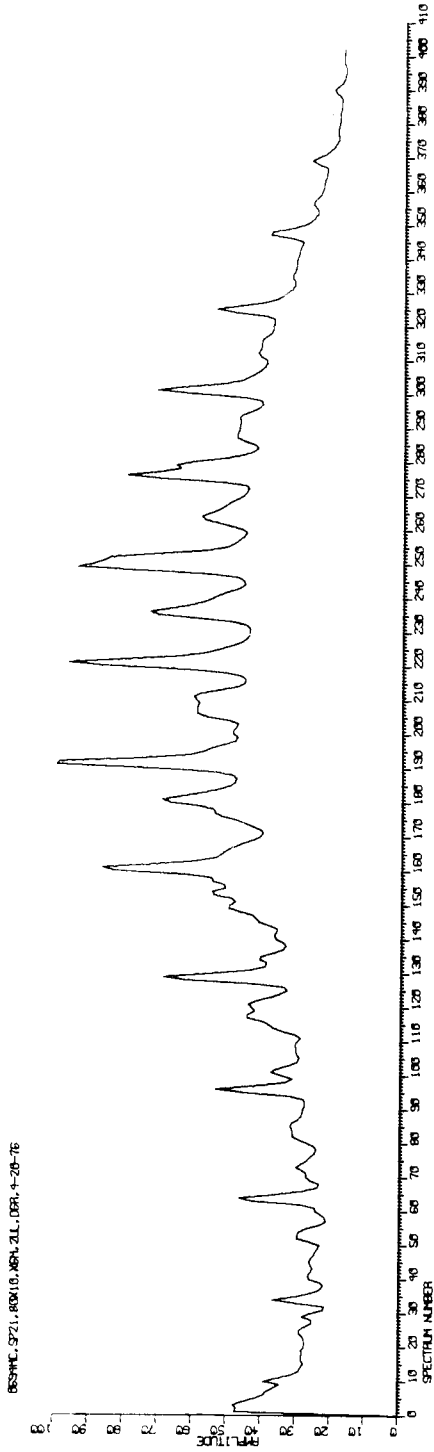


Fig. 1. TICP of an oil spill analyzed on a packed column with E1-MS.

chemical ionization (CI) mass spectrometer interfaced to a System Industries System 150 data system. The gas chromatograph was equipped with a Grob type injector<sup>1</sup> and was interfaced to the mass spectrometer with a 45-cm platinum capillary coaxial inside a 0.3175 cm O.D., glass-lined stainless-steel tube. (The use of noble metal interfaces can lead to chromatographic problems in certain circumstances<sup>3</sup>; however, the liquid phases utilized and the type compounds examined in this work do not appear to be affected.) The CI reagent gas was introduced into the ion source through the stainless-steel tube surrounding the platinum capillary. A 34-m glass capillary column coated with SE-30 fabricated at the Athens Laboratory and a 33-m glass support-coated open tubular (SCOT) column with OV-17 liquid phase supplied by Scientific Glass Engineering (Austin, TX, U.S.A.) were used in the study.

The system used for packed column analysis was a Finnigan 1015 gas chromatograph-mass spectrometer interfaced to a System 150 data system. The column used was a 250 cm × 2 mm I.D. glass column packed with 3% Supelco SP-2100 on Supelcoport (80-100 mesh). The gas chromatograph to mass spectrometer interface was a glass jet separator.

For the oil spill samples, the capillary column system was run in CI mode with methane as the reagent gas and helium as the carrier gas. The CI mode was selected because it gives better molecular weight information than electron impact (EI) for aliphatic hydrocarbons; the  $M - 1^+$  ion in CI is stronger than the  $M^+$  in EI. Indicated source pressure was 800  $\mu\text{m}$ ; scan range was  $m/z$  66-420 with an integration time of 4 msec per mass and a settling time of 2.3 msec per mass. A 1.5- $\mu\text{l}$  injection was made with the septum wash valve of the Grob injector closed and the column oven at ambient temperature (approximately 25°C). The valve was opened 30 sec after injection and left open. The oven was heated rapidly to 50°C one minute after injection and programmed to 230°C at a rate of 4°C/min; the injection port pressure was 30 p.s.i.g.

The MS data acquisition parameters resulted in the acquisition of mass spectra at the rate of approximately one spectrum every 2.2 sec. Because the GC peaks were approximately 9 sec wide at the beginning of the GC run, this scan rate was not fast enough to utilize all the resolution offered by the helium carrier and tuning the source at low pressure. The scan range was from  $m/z$  41 to 430 with an integration time of 4 msec per mass and a settling time of 2.3 msec per mass. Spectra were acquired at the rate of approximately 24 per minute. The GC program and injection procedure was the same as with the oil spill samples.

## RESULTS

### *Oil spill*

An MS total ion current profile (TICP) of an oil spill sample obtained on a packed column in the EI mode by the Surveillance and Analysis Division of EPA Region IV is shown in Fig. 1. This oil spill sample and a sample from a possible source were then run on the capillary system in order to obtain fingerprints having more points of comparison than the packed column analysis. Fig. 2 shows the TICPs in the CI mode of the spill and the possible source.

The spectra acquired on the packed column system were scanned at a slower rate because the chromatographic peaks were wider. The total analysis times were

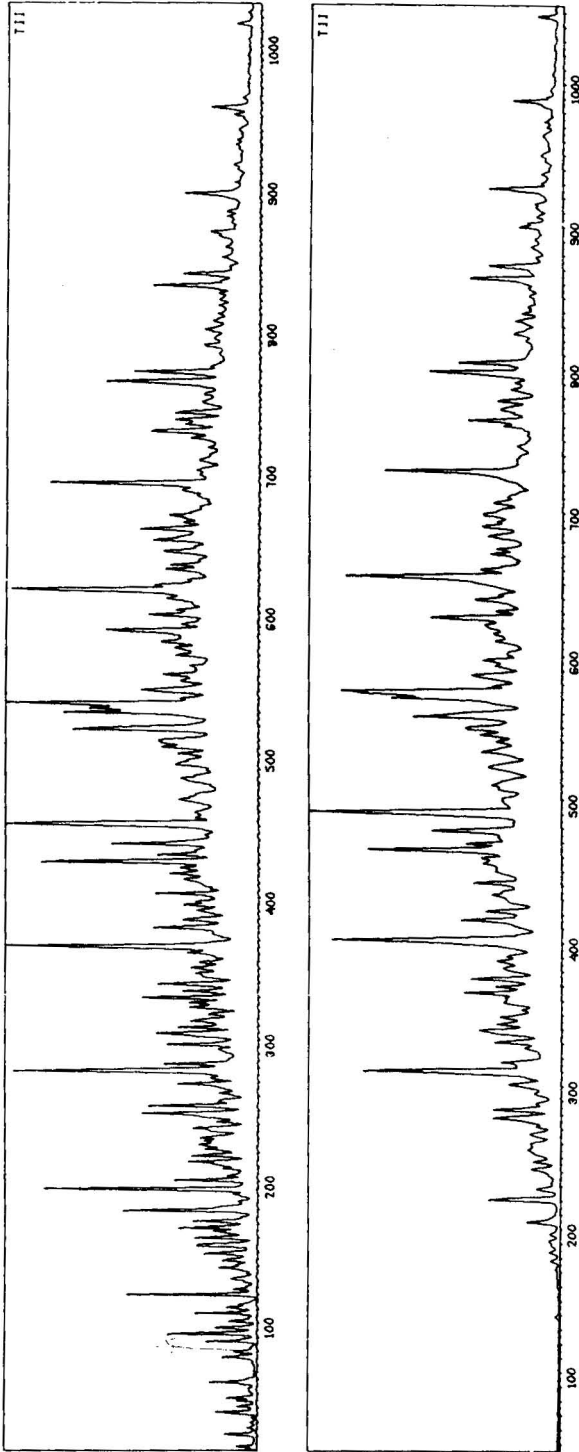


Fig. 2. TICPs of an oil spill (bottom) and a possible source analyzed on a capillary column with CI-MS.

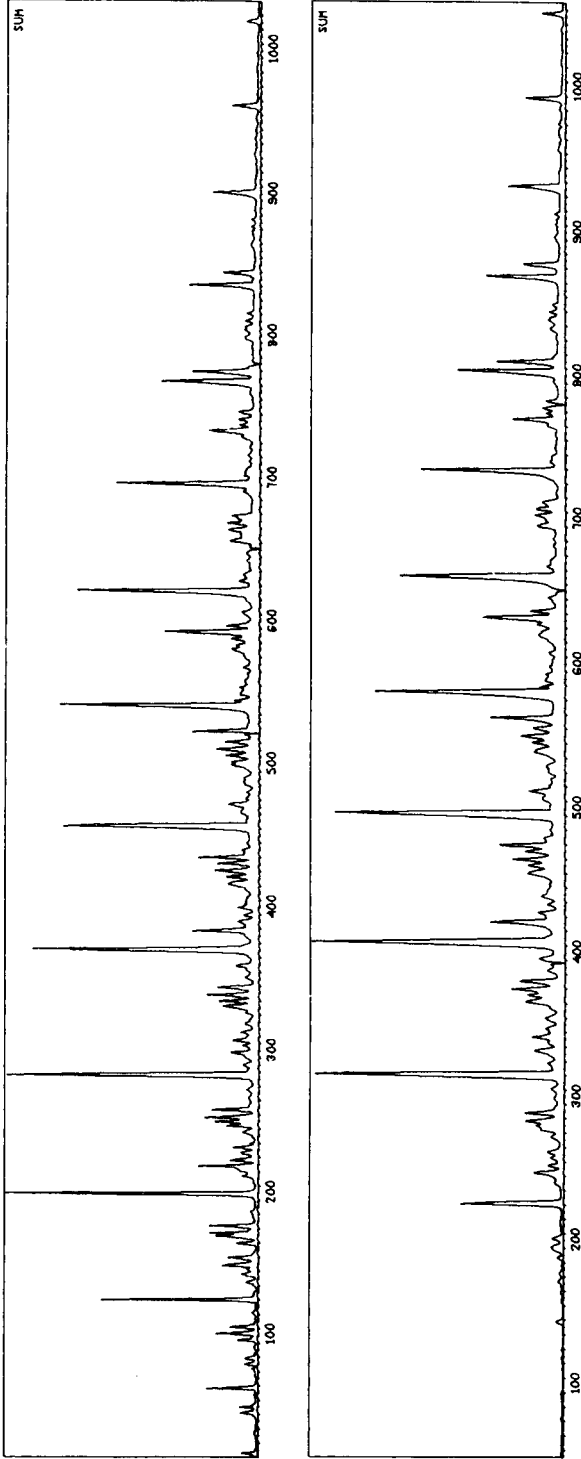


Fig. 3. Summation of  $m/z$  71 and 85 for an oil spill (bottom) and a possible source analyzed on a capillary column with CI-MS.

comparable in all three TICPs. A comparison of the TICPs in Fig. 1 and 2 shows that the capillary column resolved many more peaks than the packed column.

The traces in Fig. 2 have many similarities. The one major difference—the lack of chromatographic peaks before spectrum number 160 in the spill sample—was attributed to weathering and evaporation losses. The large number of peaks in these two TICPs made visual comparison rather difficult, so extracted ion current profiles (EICPs) of masses characteristic of certain classes of compounds were plotted. EICPs are plots of the intensity of individual masses by spectrum number. Peaks indicate compounds that may be members of the class of interest. If the intensities of two or more characteristic ions are summed and plotted by spectrum number, peaks are more likely to indicate compounds of the class of interest than are single ion peaks.

Fig. 3 shows profiles generated by summing the intensities of  $m/z$  71 and 85. These masses are characteristic of the methane CI spectra of aliphatic hydrocarbons<sup>4</sup>. Compared with Fig. 2, the specificity of the profiles is increased, the number of peaks is reduced, and comparison of the spill with the possible source is simplified.

Similarly, Fig. 4 shows a portion of the profiles generated by summing the intensities of  $m/z$  129, 143, and 157. These masses are characteristic of the methane CI spectra of naphthalene, methylnaphthalene, and dimethyl- or ethylnaphthalene<sup>5</sup>. These profiles provide a further basis of comparison.

#### *Industrial spill*

The second spill analyzed was an industrial discharge involving chlorinated compounds in addition to hydrocarbons. The TICP of the spill and an EICP for  $m/z$

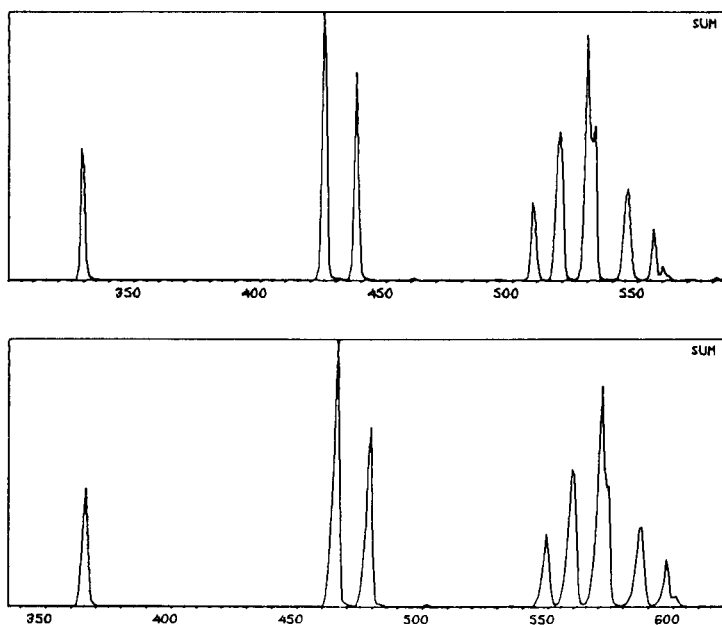


Fig. 4. Summation of  $m/z$  129, 143, and 157 for an oil spill (bottom) and a possible source analyzed on a capillary column with CI-MS.



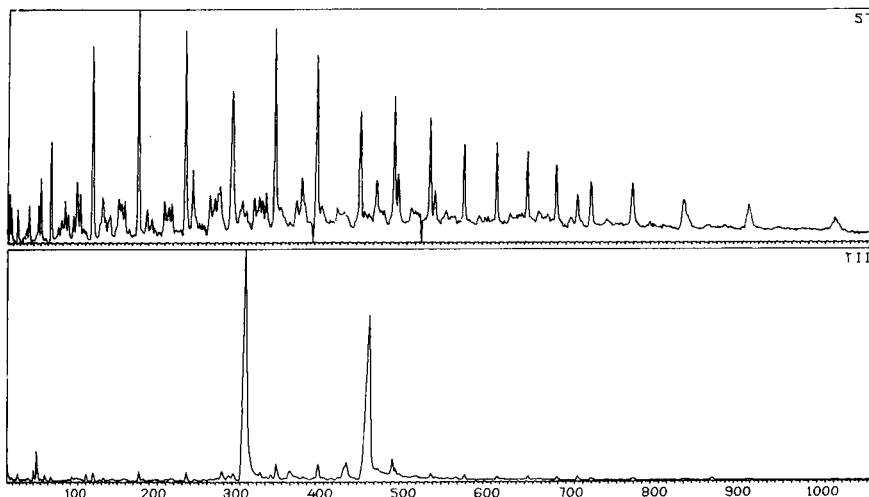


Fig. 5. TICP and EICP for  $m/z$  57 for an industrial spill and analyzed on a capillary column with EI-MS.

57 are shown in Fig. 5. The large chromatographic peaks at spectrum numbers 310 and 450 in the TICP reflect the presence of chlorinated compounds at much higher concentrations than the other components in the sample.

Since the TICP is dominated by two large chromatographic peaks, other characteristics of the sample are not apparent. The ion at  $m/z$  57 is characteristic of the EI mass spectra of aliphatic hydrocarbons<sup>6</sup>; therefore, that EICP was obtained to

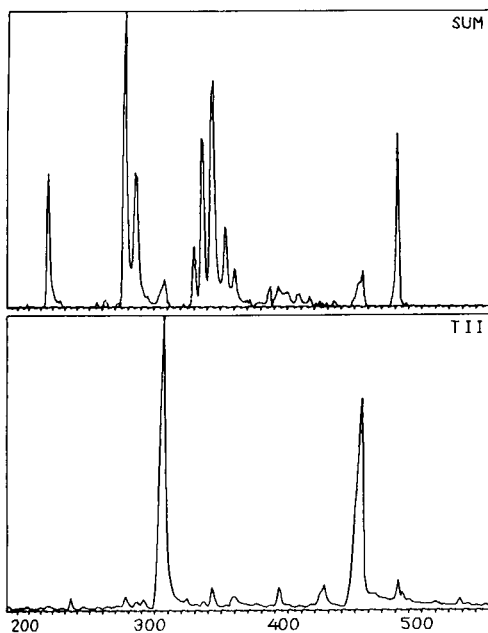


Fig. 6. TICP and summation of  $m/z$  128, 142, and 156 for industrial spill analyzed on a capillary column with EI-MS.

check for the presence of petroleum products. The mass spectra of the chlorinated compounds have no significant intensity at  $m/z$  51, so there is minimal response to them in this trace. The  $m/z$  57 profile in Fig. 5, therefore, suggests the presence of oil, which is not evident in the TICP.

Similarly, Fig. 6 shows a comparison of a portion of the TICP to the same portion of the profile as a result of the summation of  $m/z$  128, 142, and 156. These masses are characteristic of the EI mass spectra of naphthalene, methylnaphthalene, and dimethyl- or ethylnaphthalene<sup>7</sup>. These components are indistinguishable in the TICP, but clearly defined in the summation profile and further suggest the presence of oil in the sample.

## CONCLUSIONS

These examples illustrate the power of computerized MS as a detector in capillary column gas chromatography. From stored data, characteristic profiles can be generated for the comparison of different samples or the examination of individual samples to identify specific classes of compounds. Mass spectra of each chromatographic peak are available for more exact identification of the peak, and archival storage of the data permits future examination if additional information is required.

## ACKNOWLEDGEMENTS

The author wishes to thank the Laboratory Services Branch of the EPA Region IV Surveillance and Analysis Division for providing the samples used in this work. The late Ronald G. Webb of the Athens Environmental Research Laboratory contributed a capillary column and many helpful suggestions.

## REFERENCES

- 1 K. Grob and G. Grob, *Chromatographia*, 5 (1972) 3.
- 2 J. M. McGuire, A. L. Alford and M. H. Carter, *Organic Pollutant Identification Utilizing Mass Spectrometry: EPA Research Report EPA-R2-73-234*, Environmental Protection Agency, Athens, GA, 1973.
- 3 K. Grob, *Chromatographia*, 9 (1976) 509.
- 4 B. Munson, *Anal. Chem.*, 43 (1971) 32A.
- 5 B. Munson, *Anal. Chem.*, 43 (1971) 34A.
- 6 F. McLafferty, *Interpretation of Mass Spectra*, W. A. Benjamin, Reading, MA, 2nd ed., 1973, p. 264.
- 7 F. McLafferty, *Interpretation of Mass Spectra*, W. A. Benjamin, Reading, MA, 2nd ed., 1973, p. 262.

CHROM. 14,319

## DETERMINATION OF NITRATE IN MEAT PRODUCTS AND CHEESES BY GAS-LIQUID CHROMATOGRAPHY WITH ELECTRON-CAPTURE DETECTION

AKIO TANAKA\*, NORIHIDE NOSE and HISAO IWASAKI

*Saitama Institute of Public Health, Kamiokubo-Higashi, 639-1, Urawa, Saitama (Japan)*

(Received August 25th, 1981)

---

### SUMMARY

A simple, sensitive and practical method for the determination of nitrate in various meat products and cheeses is described. The method is based on the nitration of 2-*sec.*-butylphenol in *ca.* 57% sulphuric acid to form 4-nitro-2-*sec.*-butylphenol. After nitration, the toluene extract is re-extracted with an alkaline solution and subsequently analysed by gas-liquid chromatography with an electron-capture detector (GLC-ECD) using a column of OV-17 on Chromosorb W HP after pentafluorobenzoylation and extraction with *n*-hexane. The nitrate concentration is calculated from the peak height. Amounts of 0.05–1.0  $\mu\text{g}$  of nitrate can be determined. The detection limit for nitrate is 0.006  $\mu\text{g}/\text{ml}$ . The procedure for determining nitrate in meat products and cheeses involves direct analysis by GLC-ECD without clean-up; the detection limit is 0.07 ppm and the recovery from meat products and cheeses ranged from 96.8 to 99.0% at the 5 ppm level and from 94.7 to 98.6% at the 10 ppm level. The nitrated compound of 2-*sec.*-butylphenol was identified as 4-nitro-2-*sec.*-butylphenol by thin-layer chromatography and nuclear magnetic resonance spectroscopy and the final pentafluorobenzoylated product was confirmed by combined gas chromatography-mass spectrometry.

---

### INTRODUCTION

Nitrogen plays an important biological role in living organisms and nitrate is one of the principle nutrients for aquatic life. In recent years, increasing concern has been focused on the formation of carcinogenic nitrosoamines from various nitrogen oxides<sup>1,2</sup>. The development of rapid, sensitive and accurate methods for the determination of trace amounts of nitrate in environmental samples is therefore of interest. Current methods for the determination of nitrate-nitrogen include reduction to ammonia followed by titration or spectrophotometry<sup>3,4</sup>, chemical or biochemical reduction to nitrate and its diazotization with a variety of reagents<sup>5–8</sup>, nitration of organic reagents and determination of the nitration product<sup>9–11</sup>, ultraviolet spectrometry<sup>12,13</sup>, polarography<sup>14</sup> and ion-selective electrodes<sup>15,16</sup>. The highly sensitive method<sup>5,6,8</sup> based on copperized cadmium for reducing nitrate to nitrite and then

diazotization of sulphanilamide is precise but time consuming and cadmium is highly toxic. Spectrophotometric methods<sup>17,18</sup> are also time consuming because of the need for a distillation stage after nitration.

Recently, the determination of nitrate by gas-liquid chromatography (GLC) has been described. Brief studies of nitration with nitrate and benzene<sup>19</sup> or 2,4-xylene<sup>20</sup> in the presence of 80% sulphuric acid using an electron-capture detector (ECD) have been made; the procedure is complex and vigorous reaction conditions are required. Tanner *et al.*<sup>21</sup> applied an ECD to 4-nitro-2,3,5,6-tetrafluoroanisole after nitration of 2,3,5,6-tetrafluoroanisole, Tan<sup>22</sup> studied the determination of nitrate as nitrobenzene after reaction with 1,3,5-trimethoxybenzene with a multiple ion detector. These methods were not suitable for routine use because of the many interferences and the conditions required. However, we found that 4-nitro-2-*sec.*-butylphenol can be prepared quantitatively by reaction of nitrate and 2-*sec.*-butylphenol in acidic medium, followed by GLC-ECD after reaction with pentafluorobenzoyl chloride (PFB-Cl) in a weak alkaline solution. The detection limit was 0.006  $\mu\text{g}$  of nitrate-nitrogen.

Nitrate in meat products and cheeses was extracted with an alkaline solution. This GLC method is a simple and highly sensitive and practical means of determining nitrate in various meat products and cheeses. The recovery of nitrate added to meat products and cheeses was satisfactory.

## EXPERIMENTAL

### *Reagents and apparatus*

Potassium nitrate was dried at 110°C for 4 h under vacuum immediately before use. A stock nitrate solution was prepared by dissolving 0.718 g of potassium nitrate in 1000 ml of distilled water to give a concentration of 1  $\mu\text{g}/\text{ml}$  of nitrate-nitrogen. 2-*sec.*-Butylphenol (Tokyo Kasei Kogyo, Tokyo, Japan) was of a special high grade and used without further purification; a 5% (w/v) solution was prepared by dissolving 5.0 g in 100 ml of ethanol. Pentafluorobenzoyl chloride (Aldrich, Milwaukee, WI, U.S.A.) was of a special high grade and was used without further purification.

The internal standard solution for GLC was prepared by dissolving 1.0  $\mu\text{g}$  of *p,p'*-dichlorophenyldichloroethylene (DDE) in 1 ml of *n*-hexane. Deproteinizing solution (12%, w/v) was prepared by dissolving 12 g of zinc sulphate in 100 ml of distilled water. Silver sulphate solution (5%, w/v) was prepared by dissolving 5 g of silver sulphate in 100 ml of distilled water. All water was triply distilled and deionized. The column packing materials for GLC, *viz.*, Chromosorb W HP, SE-30, OV-101, OV-17, OV-225, QF-1 and XE-60, were of high purity and were obtained from Nihon Chromato (Tokyo, Japan). All other reagents and solvents were of high purity and were obtained from Wako (Osaka, Japan).

For identification of the pentafluorobenzoylated product of 4-nitro-2-*sec.*-butylphenol, a Shimadzu LKB-9000 combined gas chromatograph-mass spectrometer was used. For GLC, a glass tube (1.5 m  $\times$  3 mm I.D.) packed with OV-17 on Chromosorb W HP (80-100 mesh) was used; the helium flow-rate was 30 ml/min and the column temperature 210°C. The conditions for mass spectrometry (MS) were as follows: separator temperature, 260°C; ion source temperature, 290°C; trap current, 60  $\mu\text{A}$ ; electron energy, 70 eV; and accelerating potential, 3.5 keV. Nuclear magnetic

resonance (NMR) spectra were measured at 60 Hz with a Varian EM-60 spectrometer.

#### *Preparation of pentafluorobenzoyl ester of 4-nitro-2-sec.-butylphenol*

A suitably diluted solution of nitrate was placed in a test-tube (about 20 × 2.0 cm I.D.) and made up accurately to 4 ml with distilled water, then 1 ml of 5% silver sulphate solution, 7 ml of sulphuric acid (gently) and 0.1 ml of 5% 2-sec.-butylphenol solution were added. After reaction at room temperature with occasional shaking for 15 min, the reaction mixture was transferred into a 50-ml separating funnel and 10 ml of toluene were added. The mixture was shaken for 5 min and the toluene layer was separated and washed twice with 10 ml of distilled water. The toluene layer was re-extracted with 10 ml of 5% sodium carbonate solution, the alkaline solution was transferred into a 50-ml separating funnel and 20  $\mu$ l of PFB-Cl were added. The mixture was shaken for 1 min and allowed to stand for 5 min, then extracted with 10 ml of *n*-hexane, separated and dried with 1 g of anhydrous sodium sulphate. After addition of 1 ml of internal standard solution, a 1- $\mu$ l volume of the solution was injected into the gas chromatograph.

#### *Gas-liquid chromatography*

A Shimadzu GC-4BM gas chromatograph with an ECD was used for all analyses. The column was a glass tube (1.5 m × 3 mm I.D.) packed with 5% OV-17 on Chromosorb W HP (80–100 mesh) and was conditioned at 210°C; the detector and injector temperature were 300°C. The flow-rate of the carrier gas (nitrogen) was 75 ml/min and the electrometer range was  $10^2$  M $\Omega$  × 0.16 V.

#### *Calibration graph*

A series of standard nitrate solutions were prepared by dilution of the stock solution. Aliquots were placed into a test-tube to give amounts of 0.05, 0.1, 0.25, 0.5, 0.75 and 1.0  $\mu$ g of NO<sub>3</sub>-N. According to the procedure described above, 10 ml of toluene extracts were obtained in each instance, and then re-extracted with sodium carbonate solution. After pentafluorobenzoylation by addition of PFB-Cl and subsequent reaction and extraction, a 1- $\mu$ l aliquots of the mixture (11 ml) was injected into the GLC column with the internal standard solution as in the described procedure. As shown in Fig. 1, the retention time of the PFB derivative relative to that of DDE was 0.64. The peak-height ratio of the PFB derivative of DDE was plotted against the amount of NO<sub>3</sub>-N analysed; a typical calibration graph is shown in Fig. 2.

#### *Preparation of meat products and cheese extracts and their determinations*

To 10 g of finely ground sample in a 100-ml flask fitted with a ground-glass stopper were added 70 ml of hot water (70–80°C) and 2.5 ml of 1 N sodium hydroxide solution. After occasional shaking in a water-bath at 80°C for 30 min, addition of 5 ml of 12% zinc sulphate solution and cooling to room temperature, the extracted solution was filtered and diluted accurately to 100 ml with distilled water. A 1-ml volume of the filtrate was placed in a test-tube and 1 ml of 5% silver sulphate solution, 3 ml of distilled water and (gently) 7 ml of sulphuric acid were added, followed by 0.1 ml of 2-sec.-butylphenol solution. The mixture was allowed to react as described above and analysed by GLC under the described conditions. The con-

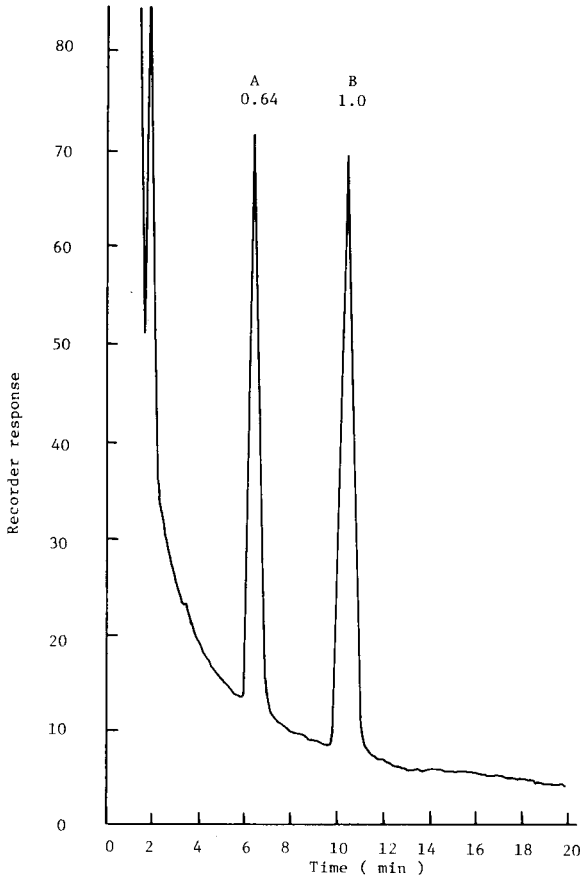


Fig. 1. Gas chromatogram of pentafluorobenzoylated extract of a standard reaction mixture (A) to which nitrate-nitrogen ( $0.05 \mu\text{g}$ ) was added, with retention time relative to that of the internal standard (B). The pentafluoro derivative was obtained according to the described procedure. Sample size:  $1 \mu\text{l}$ .

tents of nitrate in meat products and cheeses were determined from the peak height relative to that of the internal standard on the gas chromatograms and comparison with a calibration graph.

## RESULTS AND DISCUSSION

### *Standard assay*

As shown in Fig. 2, the calibration graph was rectilinear for 0.013–0.25 of  $\text{NO}_3\text{-N}$  per ml of reaction mixture. The average relative standard deviation of five determinations was 3.4% for 0.05 and 0.10 of  $\text{NO}_3\text{-N}$  and 4.5% for 0.25  $\mu\text{g}$ , and the reproducibility was considered satisfactory.

### *Conditions for nitration of 2-sec.-butylphenol*

The influence of sulphuric acid concentration on the nitration of 2-sec.-

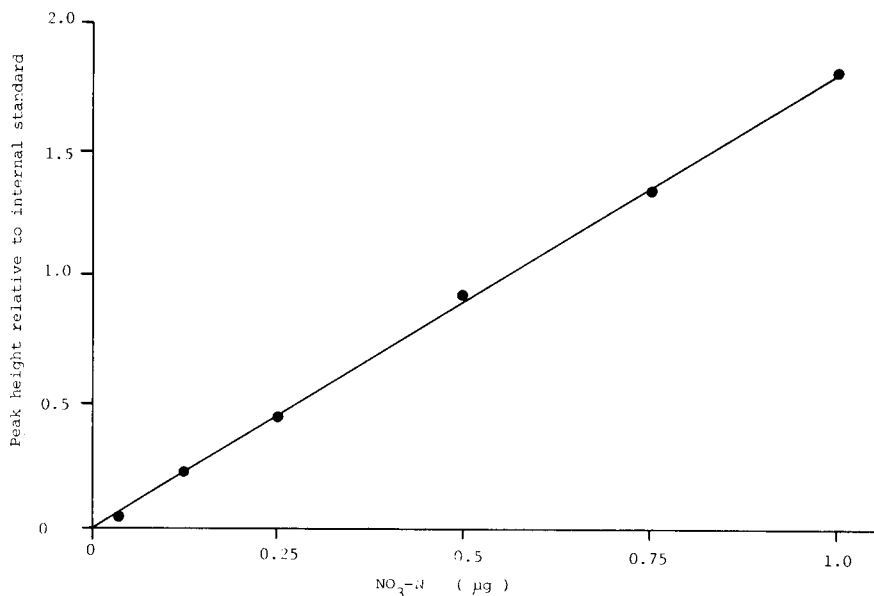


Fig. 2. Calibration graph for nitrate-nitrogen in the reaction mixture. The nitration and pentafluorobenzoylation and the subsequent GLC analysis were performed according to the described procedures. Sample size: 1  $\mu$ l. Column temperature: 210°C. Nitrogen flow-rate: 75 ml/min.

butylphenol with nitrate to form the nitrated compound was studied by mixing 1.0  $\mu$ g of NO<sub>3</sub>-N, 0.1 ml of 5% 2-*sec.*-butylphenol solution, 50 mg of silver sulphate and 12 ml of sulphuric acid of various concentration for 15 min at room temperature. The results are shown in Fig. 3. In the sulphuric acid concentration range 55–75%, a constant peak height was obtained, but above a concentration of 80% the nitration yield of 2-*sec.*-butylphenol decreased. The use of a high concentration of sulphuric acid is dangerous and inconvenient for practical analyses. In our procedure, if 7 ml of sulphuric acid are added, the concentration of sulphuric acid is about 57.2%. If we assume that 1 mol of 2-*sec.*-butylphenol reacts with 1 mol of potassium nitrate, then 10.7  $\mu$ g of 2-*sec.*-butylphenol are required for 7.2  $\mu$ g of potassium nitrate (1.0  $\mu$ g of NO<sub>3</sub>-N). The relative yields of the nitro compound for various amounts of 2-*sec.*-butylphenol added to 7.2  $\mu$ g of potassium nitrate in a total of 5 ml of solution were 95.8% for 0.5 mg of 2-*sec.*-butylphenol, 99.5% for 1 mg and 100% for 3, 5, 10, 15, 20 and 25 mg at room temperature with a reaction time of 15 min. To some extent, therefore, addition of 2-*sec.*-butylphenol in excess gave reasonable results, and in practice 0.1 ml of 5% reagent solution was added.

The optimal reaction time was investigated by mixing 1.0  $\mu$ g of NO<sub>3</sub>-N, 0.1 ml of 5% 2-*sec.*-butylphenol and 7 ml of sulphuric acid. After reaction, the mixture was analysed by GLC according to the described procedure. The production of the nitro derivative of 2-*sec.*-butylphenol with time is shown in Fig. 4. A reaction time of at least 5 min at room temperature is required, and in practice 15 min was used.

The production of the nitro compound at several temperatures was studied by mixing 1.0  $\mu$ g of NO<sub>3</sub>-N and 0.1 ml of 5% 2-*sec.*-butylphenol in a total volume of 5

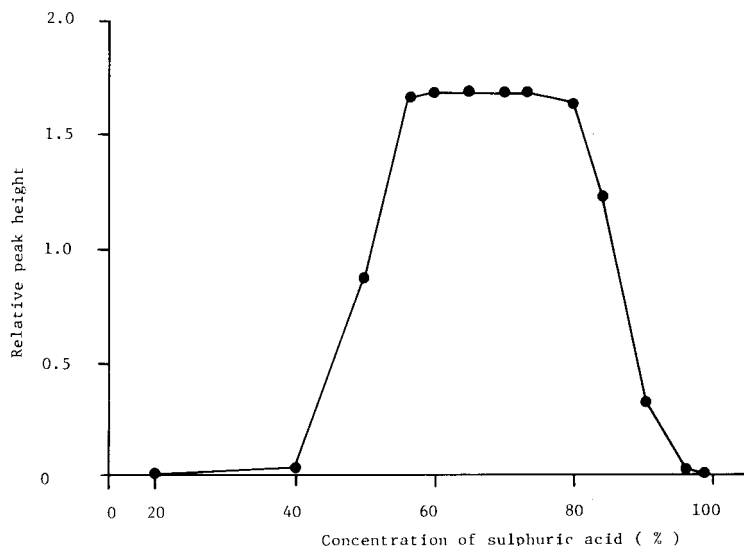


Fig. 3. Optimal concentration of sulphuric acid for the nitration of 2-*sec.*-butylphenol. To 1.0  $\mu$ g of nitrate-nitrogen were added 0.1 ml of 5% 2-*sec.*-butylphenol solution, 50 mg of silver sulphate and 12 ml of various concentrations of sulphuric acid with reaction at room temperature for 15 min. The product was analysed by GLC according to the described procedure.

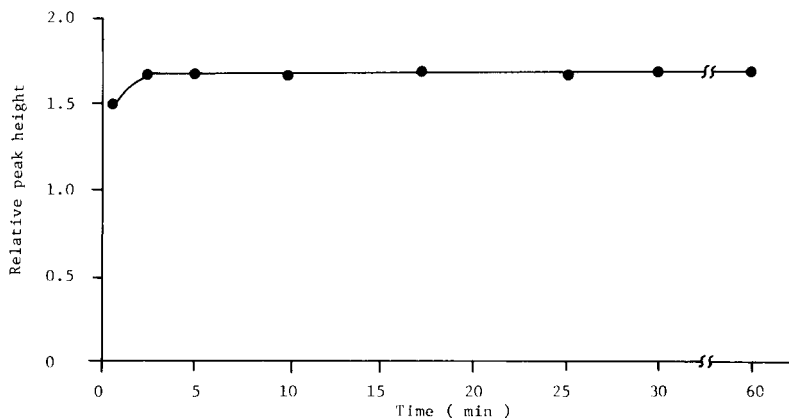


Fig. 4. Effect of reaction time on the nitration of 2-*sec.*-butylphenol. To 1.0  $\mu$ g of nitrate-nitrogen were added 0.1 ml of 5% 2-*sec.*-butylphenol solution and 1 ml of 5% silver sulphate solution in a total volume of 5 ml, followed by 7 ml of sulphuric acid. The mixture was reacted with occasional shaking at room temperature. After nitration, the pentafluorobenzoylated extract was analysed by GLC according to the described procedure.

ml, followed by 7 ml of sulphuric acid. After reaction the mixture was analysed by GLC according to the described procedure. The relative yields obtained after reaction for 15 min were 100% at 0, 10, 40 and 60°C, 99.6% at 80°C and 94.0% at 100°C. Therefore, the reaction was performed at room temperature.



*Pentafluorobenzoylation of the nitro compound of 2-sec.-butylphenol*

Phenol benzoates are formed by the Schotten–Baumann reaction from the phenol and benzoyl chloride in the presence of an alkaline medium. The influence of sodium carbonate concentration on the reaction of the nitro derivative of 2-sec.-butylphenol with PFB-Cl to form the phenol benzoate was studied by mixing 20  $\mu\text{l}$  of PFB-Cl, and the results are shown in Fig. 5. In the range 2.0–7.0%, a constant relative peak height is obtained, but above 7.5% the formation of phenol benzoate gradually decreased. On the other hand, other alkaline solutions such as sodium hydroxide and potassium hydroxide did not give symmetrical peaks on the chromatogram and sodium hydrogen carbonate did not form the phenol benzoate. Therefore, in practice 10 ml of 5% sodium carbonate solution is used. The optimal amount of PFB-Cl for the formation of phenol benzoate was investigated after proceeding to the nitration stage as described above using 1.0  $\mu\text{g}$  of  $\text{NO}_3\text{-N}$ . The relative yields obtained after 5 min were 92.8% for 1  $\mu\text{l}$  and 100% for 5, 10, 50 and 100  $\mu\text{l}$ . Hence the use of 20  $\mu\text{l}$  of PFB-Cl was adopted. On the other hand, the reaction proceeds fairly rapidly and when 20  $\mu\text{l}$  of PFB-Cl were added to 10 ml of 5% sodium carbonate solution after nitration with the described procedure using 1.0  $\mu\text{g}$  of  $\text{NO}_3\text{-N}$ , the yield of the phenol benzoate reached 100% within 5 min.

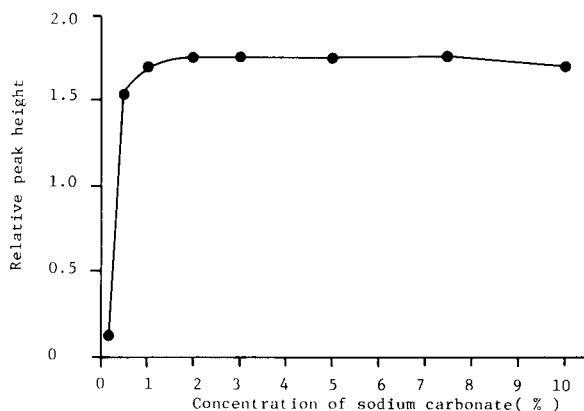


Fig. 5. Effect of sodium carbonate concentration on the pentafluorobenzoylation of nitrated 2-sec.-butylphenol. Reaction at room temperature for 5 min. Sample size for GLC: 1  $\mu\text{l}$ .

*Extraction*

Various solvents were tried for the extraction of the nitrated derivative of 2-sec.-butylphenol and its PFB derivative, as shown in Table I. When benzene, toluene, xylene, chloroform, dichloromethane and carbon tetrachloride were used for the nitrated derivative of 2-sec.-butylphenol, the extraction yields were high, but with *n*-hexane it was low. Toluene was selected for the extraction of the nitrated derivative of 2-sec.-butylphenol because it did not cause co-extraction from the meat products and cheese and did not form an emulsion with water; *n*-hexane was used for the extraction of the PFB derivative for the same reason.

TABLE I

OPTIMAL SOLVENT FOR EXTRACTION OF NITRATED 2-*sec.*-BUTYLPHENOL (A) AND ITS PENTAFLUOROBENZOYL DERIVATIVE (B)

Reaction and GLC conditions as in the described procedure. The reaction mixture contained 5% 2-*sec.*-butylphenol (0.1 ml) and nitrate-nitrogen (1.0  $\mu\text{g}$ ).

Solvent	Relative peak height (%)	
	Compound A	Compound B
Benzene	100	100
Toluene	100	100
Xylene	99.5	100
Chloroform	99.3	100
Dichloromethane	93.1	100
Carbon tetrachloride	93.1	100
<i>n</i> -Hexane	48.0	100

*Interferences*

Potassium nitrate can be extracted from meat products and cheese with an alkaline solution. To investigate the effect of preservatives such as sorbic acid, benzoic acid, butylhydroxyanisole, butylhydroxytoluene, dehydroacetic acid and sodium nitrite on the determination, 1.0- $\mu\text{g}$  portions of  $\text{NO}_3\text{-N}$  were added to 50–100  $\mu\text{g}$  of various preservatives, and each mixture was analysed by GLC after the nitration and pentafluorobenzoylation stages as described procedure. As shown in Table II, none of them had much effect on the determination. On the other hand, the interference from nitrite can be prevented by using sulphamic acid if large amounts of nitrite are present, as reported by many investigators<sup>9-11,17,18,20,22</sup> (Table II). Therefore, a further clean-up stage is not needed. The influence of various amounts of chloride ions as another possible interferent was studied by mixing 1.0  $\mu\text{g}$  of  $\text{NO}_3\text{-N}$  with the same reaction conditions as in the described procedure. As shown in Table III, chloride decreased the recovery of  $\text{NO}_3\text{-N}$ , as reported by many investigators<sup>9-11,17,18,20-22</sup>. However, this is also prevented by addition of silver sulphate solution (Table III). Therefore, in practice 1 ml of 5% silver sulphate solution is used. On the other hand, an addition of silver sulphate in the range 2.5–100 mg did not affect the recovery of  $\text{NO}_3\text{-N}$ . As shown in Fig. 6, the pentafluorobenzoylated extract obtained from various meat products and cheese gave gas chromatograms with good peak characteristics.

*Gas chromatographic sensitivity*

Columns containing 5% (w/w) of SE-30, DC-200, QF-1, OV-17, OV-101, OV-225 and XE-60 on Chromosorb W HP were tested. Except with OV-225, the columns showed the peak of the PFB derivative of the nitrated compound of 2-*sec.*-butylphenol; particularly good peak characteristics and sensitivity were achieved with OV-17 under the conditions described above. A high temperature and a short column were preferable for the GLC of the PFB derivative of the nitrated derivative of 2-*sec.*-butylphenol. At 200°C, a 1.5-m column containing OV-17 on Chromosorb W HP gave a good gas chromatogram, the retention time of the PFB derivative of the

TABLE II

## INFLUENCE OF FOOD ADDITIVES ON RECOVERY OF NITRATE-NITROGEN

Each amount of food additive was added to a mixture of 1.0  $\mu\text{g}$  of  $\text{NO}_3\text{-N}$ , 1 ml of 5% silver sulphate solution and 0.1 ml of 5% 2-*sec.*-butylphenol solution. Reaction and GLC conditions as in the described procedure.

<i>Additive</i>	<i>Amount added (<math>\mu\text{g}</math>)</i>	<i>Recovery of <math>\text{NO}_3\text{-N}</math> (%)</i>
Sorbic acid	50	100
	100	100
Benzoic acid	50	100
	100	99.8
Dehydroacetic acid	50	100
	100	99.7
Butyl <i>p</i> -hydroxybenzoate	50	100
	100	99.4
Butylhydroxyanisole	50	100
	100	98.9
Butylhydroxytoluene	50	100
	100	99.3
Sodium nitrite	50	98.8
	100	93.5

TABLE III

## INFLUENCE OF CHLORIDE IONS ON RECOVERY OF NITRATE-NITROGEN

Each amount of chloride ion was added to a mixture of 1.0  $\mu\text{g}$  nitrate-nitrogen and 0.1 ml of 5% 2-*sec.*-butylphenol solution. Reaction and GLC conditions as in the described procedure.

<i>Chloride ion added (mg)</i>	<i>Recovery (%)*</i>
0	100
0.5	90.3 (100)
1.0	84.2 (100)
3.0	60.5 (100)
5.0	56.3 (100)
10.0	52.8 (100)
20.0	34.4 ( 63.7)
30.0	7.2 ( 16.7)

\* Values in parentheses are recoveries after addition of 1 ml of 5% silver sulphate solution.

nitrated derivative of 2-*sec.*-butylphenol relative to that of the internal standard being 0.64. After pentafluorobenzoylation, the *n*-hexane phase extracted according to the described procedure should be injected into the gas chromatograph as soon as possible; with refrigeration, the sample was stable for at least 12 h, but after 24 h the content of the PFB derivative decreased to 90%.

*Application and recoveries*

Nitrate added to 10-g samples of pork sausage, fish sausage, meat ham, salami sausage, pollack roe, corned beef (canned) and cheese, chopped and then ground with

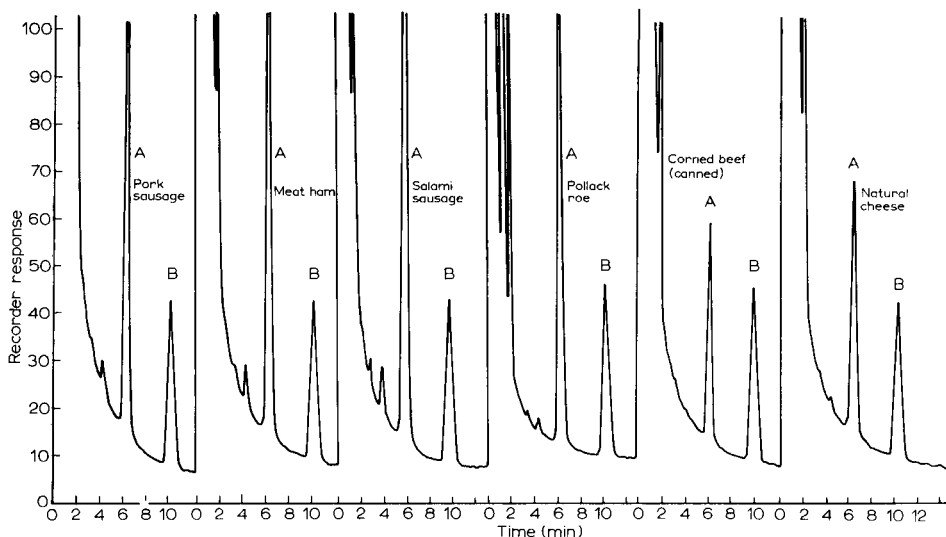


Fig. 6. Gas chromatograms of pentafluorobenzoylated extracts of various meat products and cheeses. Sample size: 1  $\mu$ l. Peaks: A, pentafluorobenzoyl ester of 4-nitro-2-sec.-butylphenol; B, DDE.

a porcelain pestle and mortar, was determined by the proposed method. The recoveries of 5 and 10 ppm of nitrate-nitrogen, given in Table IV, ranged from 96.8 to 99.0% for 5 ppm and from 94.7 to 98.6% for 10 ppm. The detection limit was 0.07 ppm.

#### Identification of the nitrated compound of 2-sec.-butylphenol and its PFB derivative

To obtain the nitrated derivative of 2-sec.-butylphenol, 0.51 g of potassium nitrate and 0.75 g of 2-sec.-butylphenol (molar ratio 1:1) were added to 10 ml of *ca.* 57% sulphuric acid and the mixture was allowed to stand with occasional shaking for 15 min at room temperature; when the reaction was complete, the mixture was extracted with toluene. After washing with distilled water and drying with 0.1 g of

TABLE IV

PERCENTAGE RECOVERIES OF NITRATE ADDED TO VARIOUS MEAT PRODUCTS AND CHEESES AT THE 5 AND 10 ppm LEVELS

Each result is the average of four determinations.

Sample	Amount of nitrate-nitrogen added ( $\mu$ g)	
	50	100
Pork sausage	98.4	97.6
Fish sausage	96.8	98.3
Meat ham	98.4	98.2
Salami sausage	98.9	97.4
Pollack roe	97.8	96.4
Corned beef (canned)	97.1	95.9
Natural cheese	99.3	98.6
Processed cheese	96.8	94.7

anhydrous sodium sulphate, the toluene extract was evaporated to dryness. The residue was dissolved in 1 ml of acetone and portions of the acetone solution were spotted on a thin-layer plate (20 × 20 cm) pre-coated with a 0.3-mm layer of silica gel (Merck, Darmstadt, G.F.R.). Development was carried out with *n*-hexane in an equilibrated tank; the  $R_f$  values of the two yellowish bands were 0.21 and 0.98. The

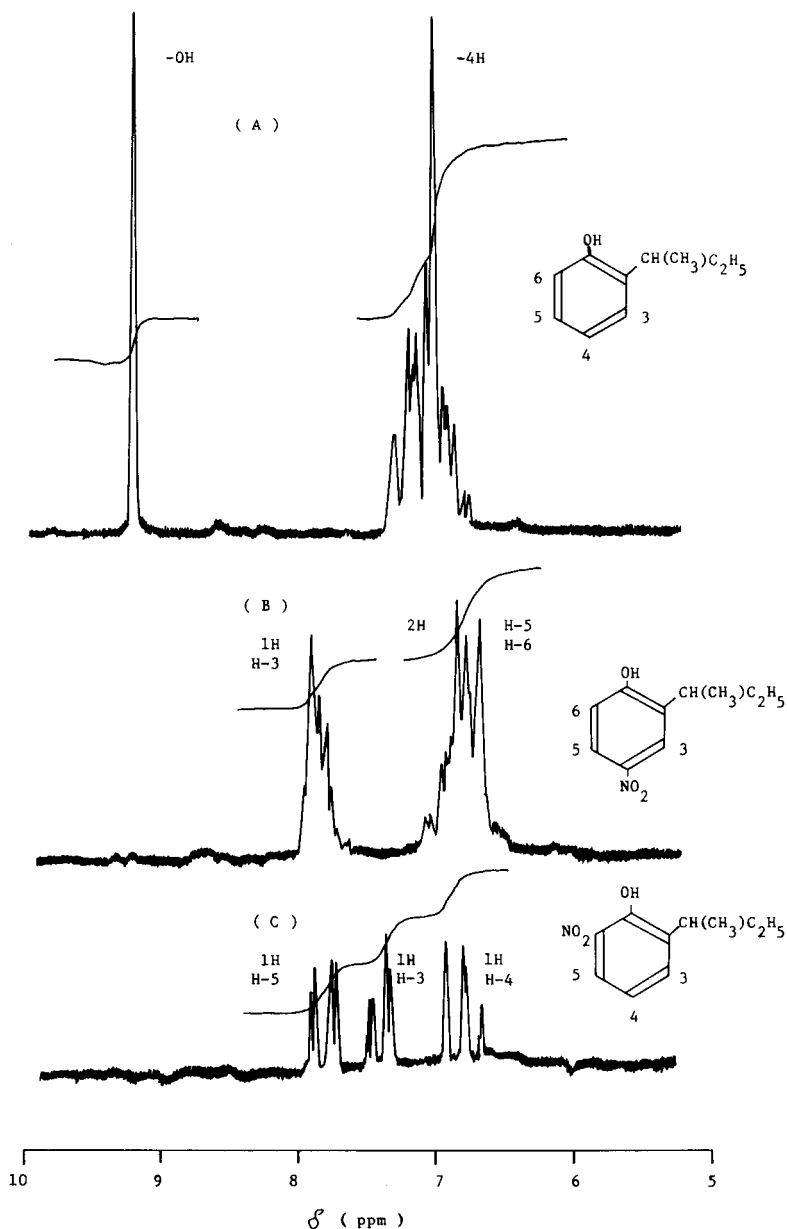


Fig. 7. NMR spectra of 2-sec-butylphenol (A), 4-nitro-2-sec-butylphenol (B) and 6-nitro-2-sec-butylphenol (C) in dimethyl sulphoxide at 60 Hz.

spots were removed from the plate and dissolved in methanol, then filtered to separate the sample substances from silica gel. The filtrates were evaporated to dryness with a stream of dry nitrogen at room temperature and the residues were dissolved in 5 ml of dimethyl sulphoxide in order to identify the nitrated derivatives of 2-*sec.*-butylphenol by NMR spectroscopy. In the NMR spectrum of 2-*sec.*-butylphenol, signals appear at  $\delta = 9.0$  (singlet peak; 1 H), which is indicative of a phenol group, and at  $\delta = 6.5\text{--}7.2$  (multiplet; 4 H), which is indicative of an aromatic compound. As shown in Fig. 7, in the NMR spectrum of the nitrated compound ( $R_F = 0.21$ ), signals appear at  $\delta = 6.6\text{--}6.9$  (multiplet; 2 H), which is indicative of the C-5 and C-6 protons, and at  $\delta = 7.7\text{--}8.0$  (singlet; 1 H), which is indicative of the C-3 proton; this suggests the replacement of the C-4 proton by a nitro group. On the other hand, in the NMR spectrum of the nitrated compound ( $R_F = 0.98$ ), signals appear at  $\delta = 6.65\text{--}6.98$  (triplet; 1 H),  $\delta = 7.32\text{--}7.58$  (doublet; 1 H) and  $\delta = 7.72\text{--}7.94$  (doublet; 1 H), which are indicative of C-4, C-3 and C-5 protons, respectively. This suggests the replacement of the C-6 proton by a nitro group (Fig. 7). Therefore, from these NMR spectra, we concluded that the product with  $R_F = 0.21$  was 4-nitro-2-*sec.*-butylphenol and that with  $R_F = 0.98$  was 6-nitro-2-*sec.*-butylphenol.

The two products were subjected to gas chromatography after pentafluorobenzoylation according to the described procedure. These PFB derivatives gave single peaks on the gas chromatogram with retention times of 0.64 ( $R_F = 0.21$ ) and 0.61 ( $R_F = 0.98$ ) relative to the internal standard. Although the peak obtained from the TLC band with  $R_F = 0.21$  was in agreement with Fig. 1, the other product ( $R_F = 0.98$ ) was not. In order to determine whether the PFB derivative of 4-nitro-2-*sec.*-butylphenol decomposed during the GLC process, the identity of the product was confirmed by GLC-MS. The mass spectrum of 2-*sec.*-butylphenol exhibited ion peaks at  $m/e$  150 ( $M^+$ ), 149 ( $M^+ - H$ ), 132 ( $M^+ - H_2O$ ), 122 ( $M^+ - CO$ ) and 121 ( $M^+ - CHO$ ). The fragmentation pattern of the PFB derivative of 4-nitro-2-*sec.*-butylphenol is shown in Fig. 8, with peaks at  $m/e$  389 ( $M^+$ ), 194 ( $C_6F_5CO$ ) (a), 166 (a - CO) (b), 150 (b - NO) and 120 (b -  $NO_2$ ). The parent peak ( $m/e$  150) for 2-*sec.*-butylphenol and that at  $m/e$  389 for the PFB derivative of 4-nitro-2-*sec.*-butylphenol correspond to the molecular weight of each compound. The shift of the peaks from  $m/e$  150 to 121 for 2-*sec.*-butylphenol could be attributed to a characteristic phenol degradation

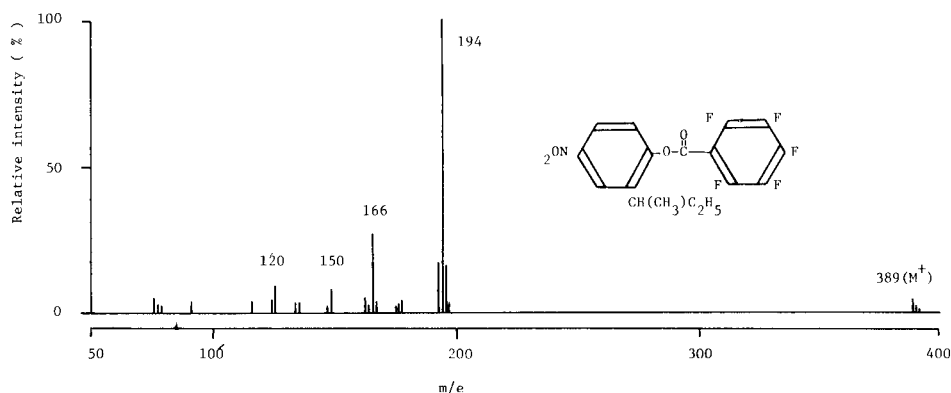


Fig. 8. Mass spectrum of pentafluorobenzoyl ester of 4-nitro-2-*sec.*-butylphenol.

compound. On the other hand, the shift of the peaks from  $m/e$  389 to 194 for the PFB derivative could be attributed to initial degradation of the PFB group, and the subsequent shift from  $m/e$  166 to 120 could be ascribed to the loss of a nitro group.

From this series of experiments, it was concluded that the PFB derivative of nitrated 2-*sec.*-butylphenol was the pentafluorobenzoyl ester of 4-nitro-2-*sec.*-butylphenol.

#### ACKNOWLEDGEMENT

We thank Mrs. Eri Inamura for her help in carrying out the NMR studies.

#### REFERENCES

- 1 W. Likinsky and S. S. Epstein, *Nature (London)*, 225 (1970) 21.
- 2 D. Shapley, *Science*, 191 (1976) 268.
- 3 J. M. Bremmer and R. R. Kenny, *Anal. Chim. Acta*, 32 (1956) 485.
- 4 J. Keary and P. M. A. Menage, *Analyst (London)*, 95 (1970) 379.
- 5 E. D. Wood, F. A. J. Armstrong and F. A. Richards, *J. Mar. Biol. Assoc. U.K.*, 47 (1967) 23.
- 6 A. Henriksen and A. R. Selmer-Olsen, *Analyst (London)*, 95 (1970) 514.
- 7 A. L. McNamarra, G. B. Meeker, P. D. Shaw and R. H. Hageman, *J. Agr. Food. Chem.*, 19 (1971) 22.
- 8 W. Horwitz (Editor), *Official Methods of Analysis of the AOAC*, Association of Official Analytical Chemists, Washington, DC, 1975, 12th ed., p. 421.
- 9 C. M. Johnson and A. Ulrich, *Anal. Chem.*, 22 (1950) 1256.
- 10 A. C. Holler and R. V. Huch, *Anal. Chem.*, 21 (1949) 1385.
- 11 D. A. Cataldo, M. Haroon, L. E. Schrader and V. L. Youngs, *Commun. Soil Sci. Plant Anal.*, 6, No. 1 (1975) 81.
- 12 E. Goldman and R. Jacobs, *J. Amer. Water Works Assoc.*, Feb. (1961) 187.
- 13 A. L. Clarke and A. C. Jennings, *J. Agr. Food Chem.*, 13 (1965) 174.
- 14 G. W. Skyring, B. J. Carey and V. S. D. Skerman, *Soil Sci.*, 91 (1961) 388.
- 15 D. R. Kenny, B. H. Byrnes and J. J. Genson, *Analyst (London)*, 95 (1970) 383.
- 16 P. J. Milham, A. S. Awad, R. E. Paul and J. H. Bull, *Analyst (London)*, 95 (1970) 751.
- 17 R. R. Elton-Bott, *Anal. Chim. Acta*, 90 (1977) 215.
- 18 G. Norwitz and H. Gordon, *Anal. Chim. Acta*, 89 (1977) 177.
- 19 W. S. Wu and W. S. Peter, *J. Ass. Offic. Anal. Chem.*, 60 (1977) 1137.
- 20 M. Toyoda, H. Suzuki, Y. Ito and M. Iwaida, *J. Ass. Offic. Anal. Chem.*, 61 (1978) 508.
- 21 R. L. Tanner, R. Fajer and J. Gaffney, *Anal. Chem.*, 51 (1975) 865.
- 22 Y. L. Tan, *J. Chromatogr.*, 140 (1977) 41.

CHROM. 14,284

## HIGH-PERFORMANCE LIQUID CHROMATOGRAPHIC DETERMINATION OF NITRITE IN ENVIRONMENTAL SAMPLES BY THE USE OF HYDRALAZINE

HIROSHI NODA\*, MASAO MINEMOTO and TOSHIO ASAHARA

*Department of Hospital Pharmacy, School of Medicine, University of Occupational and Environmental Health, Japan (Sangyo Ikadaigaku), 1-1 Iseigaoka, Yahatanishi-ku, Kitakyushu 807 (Japan)*

and

ATSUKO NODA and SADA O IGUCHI

*Faculty of Pharmaceutical Sciences, Kyushu University, 3-1-1 Maidashi, Higashi-ku, Fukuoka 812 (Japan)*

(Received August 11th, 1981)

---

### SUMMARY

A high-performance liquid chromatographic (HPLC) procedure with UV and fluorometric detectors has been developed for the determination of nitrite by use of hydralazine. Hydralazine reacts with nitrite ion under acidic conditions at 37°C to form tetrazolo[5,1-*a*]phthalazine (Tetra-P) almost quantitatively. Without extraction, the determination of Tetra-P by reversed-phase HPLC was simple, specific, sensitive and reliable over the range 0.001-0.10 ppm of nitrite nitrogen. This procedure using hydralazine is one of the most useful methods for routine analysis of nitrites in foods, biological fluids and ambient waters.

---

### INTRODUCTION

In previous papers<sup>1-3</sup> we reported that hydralazine (1-hydrazinophthalazine, HP), an effective depressor of hypertension, was transformed in human saliva to an acetylated product, 3-methyl-*s*-triazolo[3,4-*a*]phthalazine (MTP), together with a formylated one, *s*-triazolo[3,4-*a*]phthalazine (Tri-P). On the other hand, we also found that HP was nitrosated very easily to give tetrazolo[5,1-*a*]phthalazine (Tetra-P) under acidic conditions with nitrite ion, which is contained in human saliva. The Tetra-P formation from HP and sodium nitrite *in vitro* was very rapid in acidic buffer solutions (pH 1.1, 2.1 and 3.0) at 37°C<sup>1-3</sup>, suggesting that appropriate choice of conditions might afford Tetra-P quantitatively in preference to MTP and Tri-P. Therefore, we developed a sensitive, accurate and reliable high-performance liquid chromatographic (HPLC) method which employs HP for the determination of nitrite ion in aqueous solutions; a part of this work has already been reported<sup>4</sup>.

For nitrite analysis, colorimetric methods using sulphanilic acid<sup>5</sup> or sulphanilamide<sup>6</sup> have generally been used. Recently, gas chromatographic (GC) methods using *o*-phenylenediamine<sup>7,8</sup> or aromatic primary amines for the Sandmeyer reaction<sup>9,10</sup>,



and HPLC of nitrite ion itself without any derivatization<sup>11-13</sup>, were reported. The colorimetric methods possess a lack of specificity which is crucially important for microanalysis because the sample is often turbid and slightly coloured. The GC methods generally require complex pre-treatments, and the methods using HPLC for nitrite itself have unsatisfactory detection limits.

In this paper we describe the usefulness of the HPLC method developed by us<sup>4</sup> for the determination of nitrite ion in environmental samples, namely in biological fluids, foods and ambient waters. We have succeeded in the detection of Tetra-P excreted in urine from a patient treated with HP, as has been reported in detail elsewhere<sup>14</sup>.

## EXPERIMENTAL

### *Chemicals*

Reagent grade HP-HCl was purchased from Tokyo Chemical and reagent grade sodium nitrite from Wako. Tetra-P, MTP and Tri-P were prepared by known methods<sup>15</sup>. Other chemicals used were of reagent grade.

### *Apparatus and HPLC conditions*

The liquid chromatograph (Toyo Soda, Tokyo, Japan) was equipped with an HLC-803A system, UV detector (UV-8), fluorometric (FL) detector (FS-970) and TSK GEL LS-410 ODS column (15 cm × 4 mm I.D.). The mobile phase (pH *ca.* 4.5) was 20% acetonitrile in 0.05 M KH<sub>2</sub>PO<sub>4</sub>. The solvent was degassed by ultrasonication before use. The flow-rate was 1.0 ml/min. The column eluate was monitored at 228 nm by the UV detector (0.02 a.u.f.s.), and at 228 nm (excitation) and above 340 nm or 370 nm (emission) by the FL detector (1.0 μA f.s.). The intensities were recorded by means of a two-pen recorder (Rikadenki Kogyo) and a Chromatopak C-RIA chromatography integrator (Shimadzu Seisakusho).

### *Sample preparation*

A 200-ml solution of the food extracts was prepared from 10 g of food samples according to the procedure described in ref. 6. A 5-ml sample solution was prepared from 0.5 ml of human saliva or rat plasma according to the method of Shechter *et al.*<sup>16</sup>.

Ambient waters were passed through a filter-paper, if necessary.

### *Standard nitrite solution*

Dried sodium nitrite (197 mg) was dissolved in distilled water followed by dilution to 200 ml (the stock solution). A 2.0-ml volume of this stock solution was diluted with water to 200 ml, from which 5.0 ml were transferred to a 100-ml volumetric flask and diluted to volume with water (the work solution). The work solution was prepared just before the experiment. A 1-ml volume of the standard work solution contains 0.1 μg nitrite nitrogen (NO<sub>2</sub><sup>-</sup>-N) or 0.328 μg nitrite ion (NO<sub>2</sub><sup>-</sup>).

### *Determination of nitrite*

A 200-μl volume of HP-HCl dissolved in 1 N HCl (1 mg/ml) was added to 2.0 ml of the nitrite sample solution, the concentration of which was less than 0.10 ppm

$\text{NO}_2^-$ -N. After adjusting the pH to about 1.1, the mixture was incubated at  $37^\circ\text{C}$  for 30 min. A methanolic solution ( $100\ \mu\text{l}$ ) of phenobarbital (PB) ( $200\ \mu\text{g}/\text{ml}$ ) was added to the reaction mixture as an internal standard (IS), and  $20\text{-}\mu\text{l}$  aliquots were injected directly for HPLC.

### Calculations

The concentrations of the sample solutions were determined by interpolation from a calibration curve, which was constructed by plotting the peak area ratios of Tetra-P to PB (IS) versus the concentrations of  $\text{NO}_2^-$ -N ( $0.001\text{--}0.10\ \text{ppm}$ ).

## RESULTS AND DISCUSSION

### Tetra-P formation from HP and nitrite

In previous papers <sup>1-4</sup>, we reported that HP reacts with nitrite under acidic conditions at  $37^\circ\text{C}$  to form Tetra-P almost quantitatively. We now describe this reaction in more detail.

*Effect of HP-HCl concentration.* The effect of the HP-HCl concentration was examined in the range of  $0.04\text{--}5.0\ \text{mg}/\text{ml}$  using a  $0.06\ \text{ppm}$  nitrite-nitrogen solution (Fig. 1). The yields of Tetra-P were constant at HP-HCl concentrations above  $0.2\ \text{mg}/\text{ml}$  in the aqueous solutions. At concentrations above  $5.0\ \text{mg}/\text{ml}$  HP-HCl, broad tailing of the peaks due to the presence of the excess of HP-HCl made it difficult to determine the amounts of Tetra-P. Therefore,  $1.0\ \text{mg}/\text{ml}$  HP-HCl was employed for subsequent experiments.

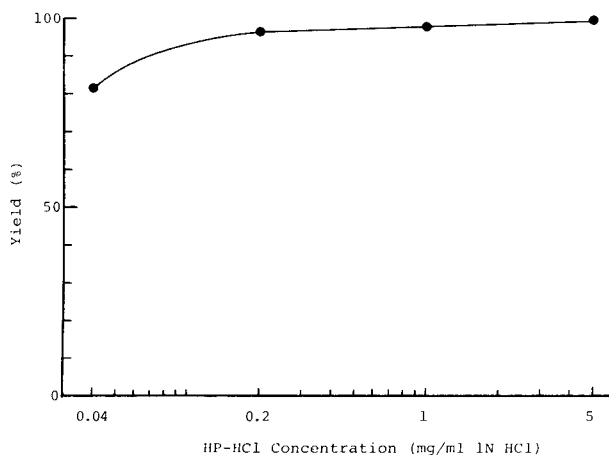


Fig. 1. Effect of HP-HCl concentration on the formation of Tetra-P. A  $200\text{-}\mu\text{l}$  portion of HP-HCl dissolved in  $1\ \text{N}$  HCl was added to  $2.0\ \text{ml}$  of the nitrite aqueous solution ( $0.06\ \text{ppm}$   $\text{NO}_2^-$ -N), and the mixture was incubated at  $37^\circ\text{C}$  for 30 min.

*Effect of pH.* The effect of pH was examined over the pH range  $1.0\text{--}5.0$  (Fig. 2). The test solutions were prepared as follows. Each  $200\text{-}\mu\text{l}$  portion of HP-HCl aqueous solution ( $1\ \text{mg}/\text{ml}$ ) was added to  $2\text{-ml}$  aliquots of  $0.06\ \text{ppm}$   $\text{NO}_2^-$ -N solution, which was prepared by mixing nitrite with  $0.05\ \text{M}$  phosphate buffer solutions (pH  $1.5\text{--}5.0$ ),

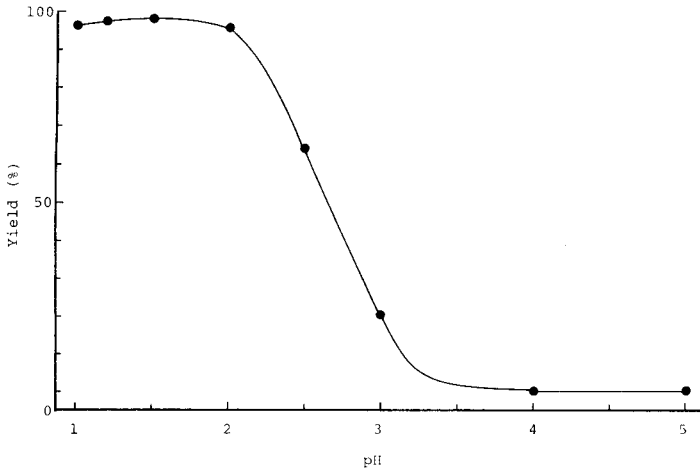


Fig. 2. Effect of pH of the reaction mixture on the formation of Tetra-P. A 200- $\mu$ l portion of HP-HCl aqueous solution (1 mg/ml) was added to 2.0 ml of the nitrite buffer solution (0.06 ppm  $\text{NO}_2^-$ -N), and the mixture was incubated at 37°C for 30 min.

0.1 N HCl or 0.25 N HCl. Constant yields of Tetra-P were obtained in the range of pH 1.0–2.0. Therefore, pH *ca.* 1.1 was adopted.

*Effects of temperature and time.* The effect of temperature was investigated in the range of 0–50°C. The rates and amounts of Tetra-P formation are dependent on the reaction temperature and the time (Fig. 3). When the reactants were incubated at 37°C or 50°C, a maximal yield was reached after about 15 min in each case. At room temperature (22°C), yields of Tetra-P of higher than 90% were detected after about 45 min. When the determination was performed on extracts from foods and biological fluids, the formation of undesirable by-products, MTP and Tri-P, increased with increasing temperature and time. Therefore, a procedure at 37°C for 30 min was

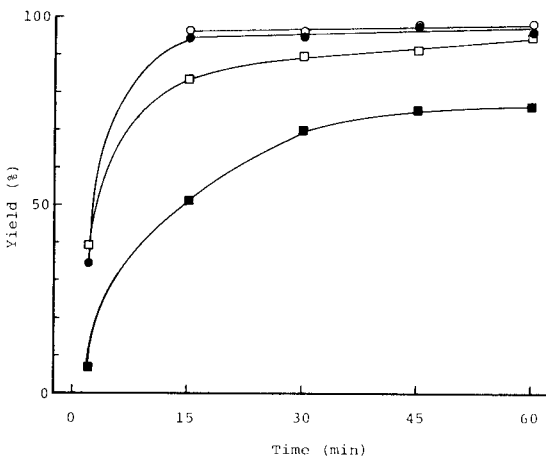


Fig. 3. Time course of Tetra-P formation at 50°C (O), 37°C (●), room temperature (22°C) (□) and in an ice-bath (■).

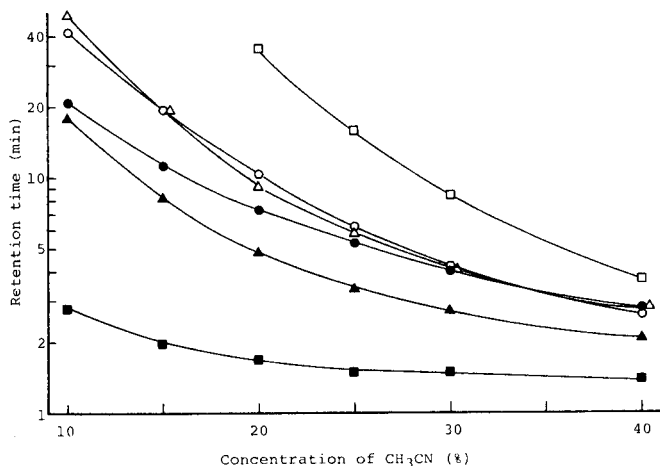


Fig. 4. Effect of acetonitrile concentration on the retention times of PHT (□), PB (○), Tetra-P (●), HP (■), MTP (△) and Tri-P (▲), respectively. HPLC conditions: column, TSK-GEL LS-410 ODS, 15 cm × 4 mm I.D.; mobile phase, 10–40% acetonitrile in 0.05 M KH<sub>2</sub>PO<sub>4</sub>; flow-rate, 1.0 ml/min.

adopted in the subsequent experiments. In order to prevent further side reactions, the reaction mixture was stored in an ice-bath until required for HPLC.

#### *Effects of mobile phase-pH and acetonitrile concentration on the separation and detection of Tetra-P*

A reversed-phase column packed with TSK GEL LS-410 ODS was used. Increasing the concentration of acetonitrile in phosphate buffer solution shortened the retention time of Tetra-P. When the concentration was greater than 25%, however, it became difficult to separate Tetra-P from the two by-products, MTP and Tri-P (Fig. 4).

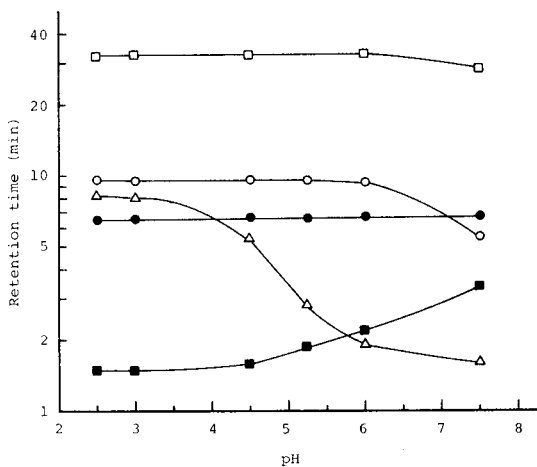


Fig. 5. Effect of mobile phase pH on the retention times of PHT (□), PB (○), Tetra-P (●), HP (■) and sorbic acid (△). HPLC conditions: column, TSK-GEL LS-410 ODS, 15 cm × 4 mm I.D.; mobile phase, 20% acetonitrile in 0.05 M phosphate buffer (pH 2.5–7.5); flow-rate, 1.0 ml/min.

In the range of pH 2.5–7.5 in the mobile phase, the retention time of Tetra-P is constant, but below pH 3.0 a large peak due to sorbic acid, a food preservative, overlaps that of Tetra-P (Fig. 5). A satisfactory result was obtained when the reaction mixture was eluted with 20% acetonitrile in phosphate buffer (pH 4.5–5.25).

PB was adopted as IS instead of phenytoin (PHT), used in our previous work<sup>4</sup>, because the retention time of PHT was too long under the elution conditions.

The UV absorption spectrum of Tetra-P in 0.05 M  $\text{KH}_2\text{PO}_4$  is given in Fig. 6. UV and FL monitoring of Tetra-P was not only very sensitive but also effective for the identification of Tetra-P, MTP and Tri-P. The detection limits of Tetra-P by UV and FL detection were 0.25 and 0.06 ppb  $\text{NO}_2^-$ -N in aqueous solution (signal-to-noise ratio = 5).

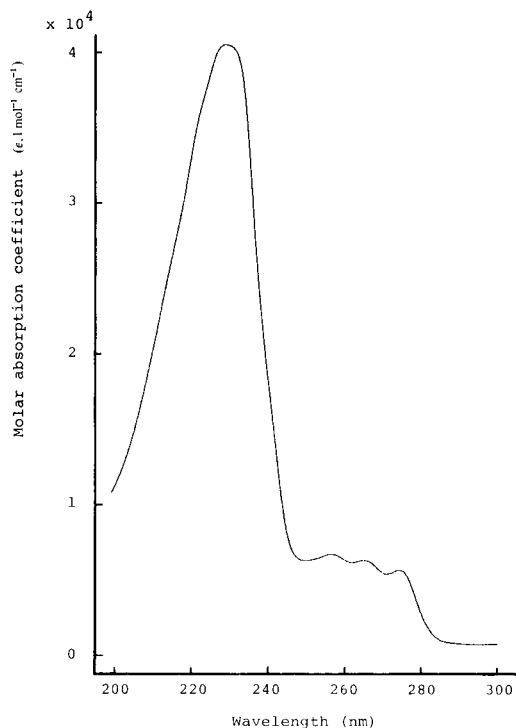


Fig. 6. UV spectrum of Tetra-P in 0.05 M  $\text{KH}_2\text{PO}_4$ .

Fig. 7 shows HPLC chromatograms of a mixture of authentic samples of Tetra-P, MTP and Tri-P, and of the reaction mixtures in water and in fish sausage extract.

#### Calibration curve

A linear relationship between the peak area ratio of Tetra-P to PB and the concentrations of nitrite-nitrogen was obtained (Fig. 8). The reproducibility of the method was examined by analyzing samples whose concentrations of  $\text{NO}_2^-$ -N were 0.001, 0.01 and 0.10 ppm ( $N = 5$ ). The corresponding coefficients of variation were 15.8, 4.2 and 0.9%, respectively.

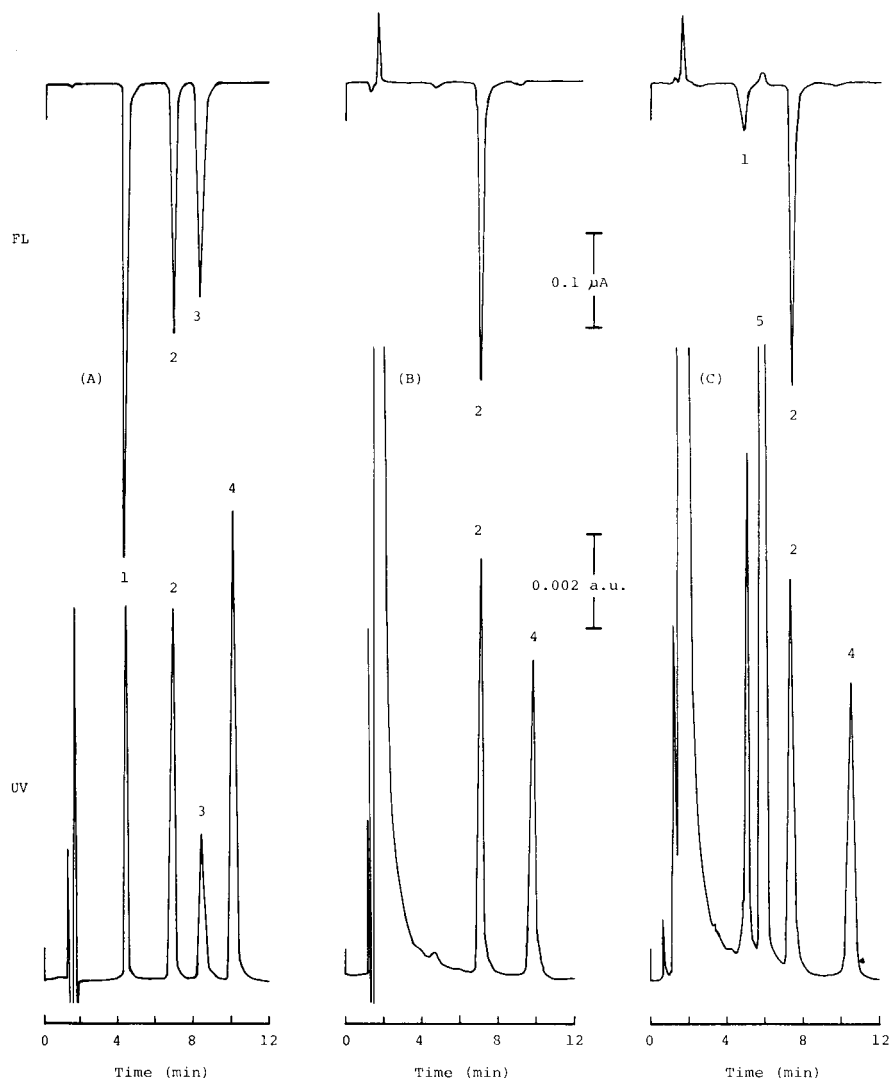


Fig. 7. HPLC chromatograms of authentic samples (A), and of the reaction mixture of HP-HCl and nitrite in water (B) or in fish sausage extract (C), each being spiked with 0.06 ppm  $\text{NO}_2^-$ -N before the reaction. Peaks: 1 = Tri-P; 2 = Tetra-P; 3 = MTP; 4 = PB (internal standard); 5 = sorbic acid. HPLC conditions: column, TSK-GEL LS-410 ODS, 15 cm  $\times$  4 mm I.D.; mobile phase, 20% acetonitrile in 0.05 M  $\text{KH}_2\text{PO}_4$ ; flow-rate, 1.0 ml/min. Detection, UV 228 nm, 0.02 a.u.f.s. (bottom); fluorescence, excitation = 228 nm, emission  $>$ 370 nm, 1.0  $\mu\text{A}$  f.s. (top).

#### *Application to the determination of environmental nitrites*

The results of the determinations of nitrites in foods, biological fluids and river-water are given in Table I. The recoveries were calculated from the yields of Tetra-P based on the addition of an extra 0.06 ppm  $\text{NO}_2^-$ -N to each sample solution. The fish sausage extract contained very small amounts of nitrite although it was coloured pink. In such a case, this HPLC method is very favourable for microanalysis as regards specificity and reliability.

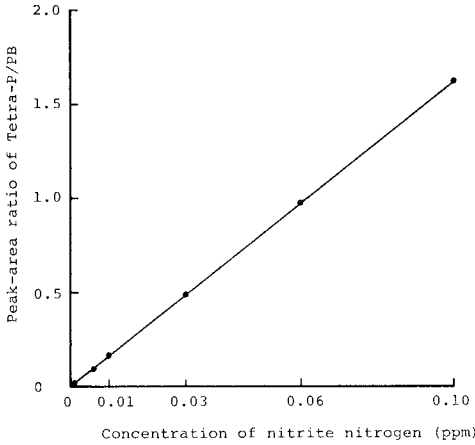


Fig. 8. Calibration curve for nitrite. Details as in the text.

After we had reported a brief summary of our method<sup>4</sup>, an alternative procedure which was based on the same reaction but using GC was described by Tanaka and co-workers<sup>17-19</sup>. Their method gave very satisfactory results, that is, very high recoveries of nitrites in foods, milk and blood, and excellent detection limits (0.02 ppm, GC-FID; 0.3-4.0 ppb, GC-ECD). The sensitivity of the GC-ECD method is comparable to that of our method. However, the GC method requires more complex pre-treatments —extraction, drying, evaporation and alumina column chromato-

TABLE I  
ANALYTICAL RESULTS OBTAINED BY THE PROPOSED METHOD

Sample	$NO_2^-$ -N added (ppm)	Found ppm	ppm		Mean (ppm)	Recovery (%)
			ppm	ppm		
Fish sausage*	0	0.02	0.02	0.02	0.02	
	1.2	1.20	1.17	1.17	1.18	97
Fish ham*	0	0.41	0.40	0.40	0.40	
	1.2	1.48	1.46	1.47	1.47	89
Wiener*	0	1.44	1.23	1.32	1.33	
	1.2	2.43	2.39	2.39	2.40	89
Tomato*	0	0.02	0.02	0.04	0.03	
	1.2	1.00	1.00	0.99	1.00	81
Spinach*	0	0.08	0.06	0.08	0.07	
	1.2	1.06	1.13	1.05	1.08	84
Saliva (human)**	0	1.55	1.56	1.57	1.56	
	0.6	2.15	2.15	2.15	2.15	98
Plasma (rat)**	0	0.02	0.01	0.01	0.01	
	0.6	0.60	0.59	0.60	0.60	98
River-water	0	0.004	0.004	0.004	0.004	
	0.06	0.065	0.065	0.066	0.065	102

\* A 200-ml sample solution was prepared from 10 g of a sample.

\*\* A 5-ml sample solution was prepared from 0.5 ml of a sample.

graphy as clean-up— all of which is unnecessary in our HPLC procedure. The most striking characteristics of the HPLC method are the high sensitivity and the simple procedure. In conclusion, the described method is considered to be one of the most useful methods for routine analysis of nitrites in environmental samples.

## REFERENCES

- 1 A. Noda, K. Matsuyama, S.-H. Yen, N. Otsuji, S. Iguchi and H. Noda, *Chem. Pharm. Bull.*, 27 (1979) 1938.
- 2 A. Noda, K. Matsuyama, S.-H. Yen, K. Sogabe, Y. Aso, S. Iguchi and H. Noda, *Chem. Pharm. Bull.*, 27 (1979) 2820.
- 3 H. Noda, A. Noda, K. Matsuyama, S.-H. Yen and S. Iguchi, *J. UOEH (Sangyo Ikadaigaku Zasshi)*, 1 (1979) 339.
- 4 H. Noda, M. Minemoto, A. Noda, K. Matsuyama, S. Iguchi and T. Kohinata, *Chem. Pharm. Bull.*, 28 (1980) 2541.
- 5 C. D. Usher and G. M. Telling, *J. Sci. Food Agric.*, 2 (1975) 1793.
- 6 *Standard Method of Analysis for Hygienic Chemists, with Commentary, 1980*, Pharmaceutical Society of Japan, Kanehara, Tokyo, 1980, pp. 69, 311.
- 7 M. Akiba, K. Toei and Y. Shimoishi, *Bunseki Kagaku (Jap. Anal.)*, 22 (1973) 924.
- 8 M. Ishizaki, N. Oyamada, S. Ueno, F. Kataoka, R. Murakami and K. Katsumura, *J. Food Hyg. Soc. Jap.*, 17 (1976) 428.
- 9 K. Funazo, M. Tanaka and T. Shono, *Chem. Lett.*, (1979) 309.
- 10 T. Chikamoto, S. Nagata and T. Maitani, *J. Food Hyg. Soc. Jap.*, 22 (1981) 113.
- 11 A. Takahashi, *Bunseki Kagaku (Jap. Anal.)*, 29 (1980) 508.
- 12 H. Terada, T. Ishihara and Y. Sakabe, *Eisei Kagaku*, 26 (1980) 136.
- 13 J. R. Thayer and R. C. Huffaker, *Anal. Biochem.*, 102 (1980) 110.
- 14 A. Noda, H. Noda, M. Minemoto, K. Zaitzu, Y. Ohkura and S. Iguchi, *Chem. Pharm. Bull.*, 29 (1981) 2683.
- 15 K. D. Haegle, H. B. Skrdlant, N. W. Robie, D. Lalka and J. L. McNay, Jr., *J. Chromatogr.*, 126 (1976) 517.
- 16 H. Shechter, N. Gruener and H. I. Shuval, *Anal. Chim. Acta*, 60 (1972) 93.
- 17 A. Tanaka, N. Nose and A. Watanabe, *J. Food Hyg. Soc. Jap.*, 22 (1981) 14.
- 18 A. Tanaka, N. Nose, F. Yamada, S. Saito and A. Watanabe, *J. Chromatogr.*, 206 (1981) 531.
- 19 A. Tanaka, N. Nose, S. Saito, H. Masaki and A. Watanabe, *Bunseki Kagaku (Jap. Anal.)*, 30 (1981) 269.



CHROM. 14,275

## HIGH-PERFORMANCE LIQUID CHROMATOGRAPHIC SEPARATION AND PROTON NUCLEAR MAGNETIC RESONANCE IDENTIFICATION OF THE 6-MONO-*cis* AND 6,6'-DI-*cis* ISOMERS OF RHODOXANTHIN

GERHARD ENGLERT\* and MAX VECCHI

Central Research Units, F. Hoffmann-La Roche & Co., Ltd., 4002 Basle (Switzerland)

(Received August 4th, 1981)

---

### SUMMARY

The separation by high-performance liquid chromatography of the all-*trans*, the 6-mono-*cis* and the 6,6'-di-*cis*-isomers from synthetic samples of rhodoxanthin is described. The structures of the *cis* isomers are deduced by  $^1\text{H}$  nuclear magnetic resonance (NMR) at 400 MHz, including several homonuclear Overhauser  $^1\text{H}$  NMR experiments and, in part, by  $^{13}\text{C}$  NMR at 100 MHz.

---

### INTRODUCTION

Rhodoxanthin, a natural  $\text{C}_{40}$  carotenoid with the retro diketone structure 1a (Fig. 1) constitutes the main pigment of the red fruit of the yew and also occurs in the fungus *Epicoccum nigrum* and in some bird feathers<sup>1</sup>. As with other related compounds having retro and substituted retro end groups, there has long been some doubt as to whether these compounds should be formulated as all-*trans* according to 1a or as di-*cis* as in 1c<sup>1</sup>. For rhodoxanthin, Mayer *et al.*<sup>2</sup> tentatively favoured the all-*trans* structure on the basis of  $^1\text{H}$  nuclear magnetic resonance (NMR). By homonuclear Overhauser  $^1\text{H}$  NMR experiments it was eventually conclusively shown<sup>3</sup> that rhodoxanthin, eschscholtzanthin [all-*trans* (3*S*, 3'*S*)-4',5'-didehydro-4,5'-retro- $\beta,\beta$ -carotene-3,3'-diol] and other related retro compounds in fact possess the all-*trans* structure.

It was also found that the  $^1\text{H}$  NMR spectra of such compounds frequently indicated the presence of at least one other minor isomer as was revealed by additional signals in the spectra<sup>4</sup>. This can be explained by the fact that these compounds are often not very stable. Thus, in chloroform solutions as used for the NMR measurements a slow isomerization takes place. A full spectroscopic characterization and hence an elucidation of the structure of these by-products was, however, impossible due to the superposition of the much stronger signals of the major all-*trans* component.

In this paper we report the high-performance liquid chromatographic (HPLC) separation and the NMR identification of two isomers of rhodoxanthin, namely the 6-mono-*cis* and the 6,6'-di-*cis* compounds.

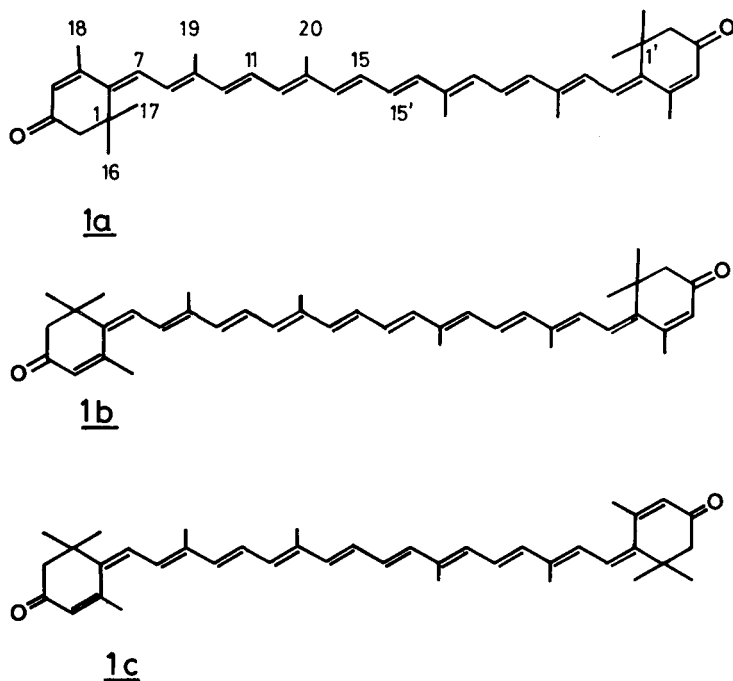


Fig. 1. Chemical structures of rhodoxanthin (1a) and its 6-*cis* (1b) and 6,6'-di-*cis* (1c) isomers.

## EXPERIMENTAL

### *Rhodoxanthin*

Crystalline samples were kindly provided by Drs. R. Marbet and R. Zell of our company. The synthesis was previously described<sup>2</sup>. In order to increase the concentration of the isomers, 1 g of 1a (95% pure) was dissolved in 50 ml chloroform and 0.1 ml triethylamine was added. The solution was refluxed while stirring for 18 h. After crystallization of *ca.* 100 mg of pure 1a the remaining mother-liquor was used for the separation of the *cis* isomers.

### *Stability*

The stability of the three chromatographic fractions dissolved in deuteriochloroform was checked by comparing their HPLC chromatograms before and after running the <sup>1</sup>H NMR spectra. It was found that the all-*trans* isomer is significantly isomerized, mainly to the mono-*cis* compound. Thus, a sample of 1a with an initial purity of better than 95% was found after 16 h in C<sup>2</sup>HCl<sub>3</sub> to consist of 46% 1a, 41% 1b and 13% 1c. The two *cis* isomers, however, were relatively stable. A sample of 1c originally of 95% purity was later found to contain *ca.* 15% 1b and 1.5% 1a. Similarly, a sample of 1b of 95% purity contained 11% 1c and 12% 1a after several hours in C<sup>2</sup>HCl<sub>3</sub>.

### *Chromatography*

All analytical work was performed with an HPLC unit consisting of an Altex

100 solvent delivery system, septum injection port (Perkin-Elmer) and UV/VIS detector LCD-725 (Kontron). The separation columns (500 × 3.2 mm I.D.) were home-made. Spherisorb S 5-CN (mean particle diameter 5 μm) purchased from Phase Separations was used as column packing. The mobile phase consisted of *n*-hexane–isopropyl acetate–acetone (76:17:7). The flow-rate was kept at 1 ml/min. For the collection of the three chromatographic fractions the same mobile phase but a semi-preparative column (600 × 7.7 mm) and a flow-rate of 3 ml/min were used. UV–visible spectra from 290 to 600 nm were recorded with a Variscan spectrophotometer using the stopped-flow technique.

### NMR

All spectra were measured on a Bruker WM-400 FT spectrometer with an ASPECT 2000 computer (32 K data) and disk unit. The <sup>1</sup>H NMR spectra at 400 MHz were run in 0.6 ml C<sup>2</sup>HCl<sub>3</sub> (100% <sup>2</sup>H) for sample amounts of *ca.* 0.5 mg (1a and 1b) and *ca.* 0.1 mg (1c). The <sup>13</sup>C NMR spectra were obtained at 100.6 MHz in C<sup>2</sup>HCl<sub>3</sub>. The assignments given below for 1a and, in part, for 1b are mainly based on the spectra of a mixture of 1a and 1b (*ca.* 75% and 25%; *ca.* 30 mg in 0.6 ml) which were run with several increasing concentrations of the shift reagent Yb(dpm)<sub>3</sub> purchased from Stohler Isotope Chemicals (dpm = dipivaloylmethane). This method gave in most cases unambiguous assignments as was previously shown for other carotenoids<sup>5</sup>.

#### <sup>13</sup>C NMR data

*All-trans 1a* (31 mg in 0.6 ml C<sup>2</sup>HCl<sub>3</sub>, 13°C). 198.95, C(3); 154.74, C(5); 142.70, C(6); 141.32, C(9); 138.04, C(10); 137.68, C(14); 137.51, C(13); 132.56, C(12); 129.85, C(15); 128.32, C(8); 128.15, C(7); 126.93, C(11); 126.05, C(4); 54.37, C(2); 38.56, C(1); 29.87, C(16,17); 22.31, C(18); 12.91, C(20); 12.41, C(19).

*6-cis 1b* (1.4 mg in 0.24 ml C<sup>2</sup>HCl<sub>3</sub>, 6°C). 199.25 and 198.97, C(3) and C(3'); 155.48, C(5); 154.99, C(5'); 143.80, C(6); 142.44, C(6'); 141.40, C(9'); 139.58, C(9); further peaks at 138.37, 137.92 (2 ×), 137.68, 137.51 and 137.48 due to C(10,10'), C(13,13') and C(14,14'); 132.56, C(12'); 132.43, C(12); 129.82 and 129.56, C(15,15'); 128.86, 128.75, 128.24, C(4'), C(7'), C(8) and C(8'); 126.91, 126.40, 125.91 and 125.48, C(11), C(11'), C(4) and C(7); 54.22, C(2'); 52.44, C(2); 41.26, C(1); 38.44, C(1'); 29.80, C(16',17'); 28.30, C(16,17); 25.46, C(18); 22.40, C(18'); 12.90, C(20,20'); 12.42, C(19,19').

*6,6-Di-cis 1c* (4 mg in 0.22 ml C<sup>2</sup>HCl<sub>3</sub>, 13°C). 198.99, C(3); 155.46, C(5); 143.83, C(6); 139.58, C(9); 137.87, 137.54 and 137.05, C(10), C(13) and C(14); 132.47, C(12); 129.60, C(15); 128.83 and 128.79, C(4) and C(8); 126.40, C(11); 125.48, C(7); 52.50, C(2); 41.26, C(1); 28.30, C(16,17); 25.42, C(18); 12.88, C(20); 12.42, C(19).

## RESULTS AND DISCUSSION

### HPLC Separation

The chromatographic separation was accomplished by using a chemically bonded nitrile phase on silica gel as the stationary phase and *n*-hexane–isopropyl acetate–acetone (76:17:7) as the mobile phase. As is seen from Fig. 2 a complete separation of the *all-trans* and the two other isomers was achieved.

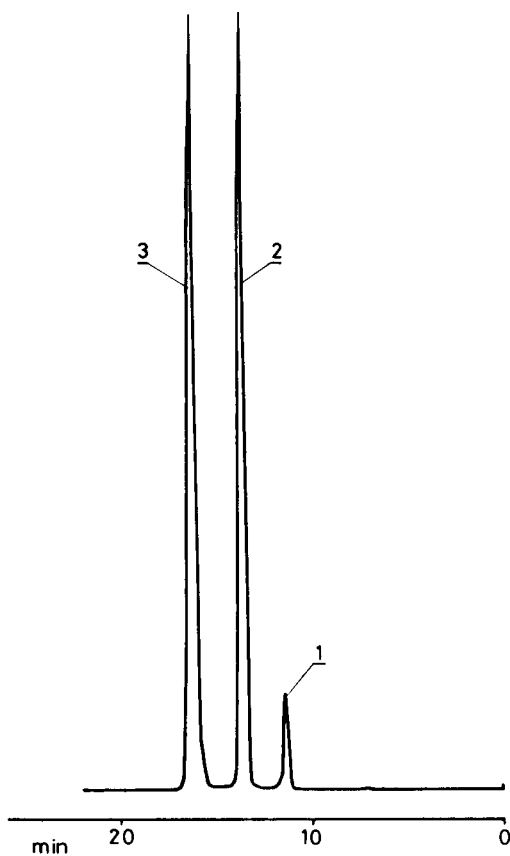


Fig. 2. Analytical high-performance liquid chromatogram of a mixture of 1a (peak 3), 1b (peak 2) and 1c (peak 1).

### Identification

The 400-MHz  $^1\text{H}$  NMR spectra including several homonuclear Overhauser experiments of the three chromatographic fractions (see Tables I and II) made possible the assignment of the isomeric structures all-*trans* (1a) to peak 3, of 6-*mono-cis* (1b) to peak 2 and 6,6'-*di-cis* (1c) to peak 1 as will readily be seen from the following arguments.

Thus, the  $^1\text{H}$  NMR data of peak 3 were identical with those of all-*trans* rhodoxanthin<sup>3</sup>. The previous Overhauser experiments were fully confirmed by application of the improved technique of Overhauser difference spectroscopy. In addition to the signal being irradiated, in the difference spectrum (free induction decay with irradiation on-resonance minus off-resonance) only those signals appear which have altered intensities caused by the nuclear Overhauser effect<sup>6</sup>. This technique is especially useful in cases like this where many of the signals overlap. As previously, the relevant result for 1a (peak 3) was the observation of an enhancement of the intensity of the signal of the protons at C(8,8') of 14% upon irradiation of the protons at C(16,17,17',16') (1.387 ppm, 12 H), showing their close spatial proximity and hence

TABLE I

400-MHz  $^1\text{H}$  NMR DATA ( $\text{C}^2\text{HCl}_3$ , CHEMICAL SHIFTS IN ppm, COUPLING CONSTANTS IN Hz IN PARENTHESES) OF RHODOXANTHIN (1a) AND ITS 6-*cis* (1b) AND 6,6'-DI-*cis* ISOMERS (1c)

n.o. = Not observed (due to superimposed signals).

Protons	All- <i>trans</i> (1a)	6- <i>cis</i> (1b)	6,6'-di- <i>cis</i> (1c)
H <sub>3</sub> C(16,17)	1.387	1.251	1.251
H <sub>3</sub> C(16',17')		1.386	
H-C(2)	2.395	2.340	2.341
H-C(2')		2.394	
H-C(4)	5.936	≈ 5.937	5.940
H-C(4')		≈ 5.937	
H-C(7)	6.904 (12.7)	6.667 (12.2)	6.668 (11.9)
H-C(7')		6.903 (12.3)	
H-C(8)	6.802 (n.o.)	6.551 (12.2)	6.551 (12)
H-C(8')		6.800 (n.o.)	
H-C(10)	6.462 (≈ 15)	6.404 (≈ 14.5)	6.402 (≈ 15)
H-C(10')		6.456 (14.5)	
H-C(11)	6.785 (14.5, 12)	6.739 (15, 11.5)	6.739 (14.5, 11.5)
H-C(11')		6.781 (n.o.)	
H-C(12)	6.260 (11.5)	6.242 (11.7)	6.238 (10.9)
H-C(12')		6.255 (11.7)	
H-C(14,14')	≈ 6.43*	≈ 6.43*	≈ 6.43*
H-C(15,15')			
H <sub>3</sub> C(18)	2.155 (≈ 1)	2.304 (1.2)	2.305
H <sub>3</sub> C(18')		2.154 (≈ 1)	
H <sub>3</sub> C(19)	2.029	2.016	2.017
H <sub>3</sub> C(19')		2.029	
H <sub>3</sub> C(20)	1.995	1.987	1.985
H <sub>3</sub> C(20')		1.993	

\* Centre of gravity of the corresponding AA'BB'-type spectrum.

$\Delta^{6,6'}$  *trans*. In this context it is worth mentioning that the differentiation between the two doublets of protons at C(7,7') and C(8,8') (AB-type spectrum) is possible by the observation of an additional broadening of the latter doublet by coupling to the methyl protons at C(19,19').  $\Delta^{8,8'}$  *trans* follows from the observed effect on the protons at C(7,7') upon irradiation of the methyl protons at C(19,19'). In the same experiment the enhancement of the protons at C(11, 11') is unexpectedly small. However,  $\Delta^{10,10'}$  *trans* clearly follows from the observed coupling constants  $J_{10,11} = J_{10',11'}$  of ca. 15 Hz. In another experiment, namely saturation of the signal at 1.995 ppm [protons at C(20,20')], the full AA'BB'-multiplet of the strongly coupled protons at C(14,15,15',14') is enhanced. Although  $\Delta^{14,14'}$  *trans* could not be derived from these experiments this will be assumed to be the case for 1a, 1b and 1c. For all three compounds the 100-MHz  $^{13}\text{C}$  NMR spectra gave additional evidence for  $\Delta^{8,8'}$  and  $\Delta^{12,12'}$  *trans* from the chemical shifts of C(19,19') and C(20,20'), as is shown in the Experimental section.

TABLE II  
400-MHz  $^1\text{H}$  NUCLEAR OVERHAUSER RESULTS FOR RHODOXANTHIN AND ITS TWO *cis* ISOMERS

Compound	Irrad. signals	Enhancements	Conclusion
1a all- <i>trans</i>	1.387 ppm	$\text{H}_3\text{C}(16,17)$	$\Delta^{6,6'}$ <i>trans</i>
		$\text{H}_3\text{C}(16',17')$	
	2.395 ppm	$\text{H}-\text{C}(2,2')$	$\text{H}-\text{C}(2,2') \approx 6\%$ ; $\text{H}-\text{C}(8,8') \approx 14\%$
		$\text{H}-\text{C}(7,7')$	$\text{H}-\text{C}(7,7') \approx 2\%$ ; $\text{H}-\text{C}(4,4') \approx 2\%$
	2.155 ppm	$\text{H}_3\text{C}(18,18')$	$\text{H}_3\text{C}(16,16',17,17') \approx 2\%$ ; $\text{H}-\text{C}(4,4') \approx 2\%$
	2.029 ppm	$\text{H}_3\text{C}(19,19')$	$\text{H}-\text{C}(4,4') \approx 25\%$ ; $\text{H}-\text{C}(7,7') \approx 8\%$
1b 6- <i>cis</i>	1.995 ppm	$\text{H}_3\text{C}(20,20')$	$\Delta^{6,6'}$ <i>trans</i> $\Delta^{8,8'}$ <i>trans</i>
			$\text{H}-\text{C}(7,7') \approx 7\%$ ; $\text{H}-\text{C}(11,11') \approx 4\%$
			$\text{H}-\text{C}(11,11') \approx 2\%^*$ ; $\text{H}-\text{C}(14,15,15',14') > 0^{**}$
	1.251 ppm	$\text{H}_3\text{C}(16,17)$	$\Delta^6$ <i>cis</i>
	1.386 ppm	$\text{H}_3\text{C}(16',17')$	$\Delta^6$ <i>trans</i>
	2.394 ppm	$\text{H}-\text{C}(2')$	$\text{H}-\text{C}(7) \approx 13\%$ ; $\text{H}-\text{C}(4) \approx 3\%$ ; $\text{H}-\text{C}(2) \approx 8\%$
1c di- <i>cis</i>	2.340 ppm	$\text{H}-\text{C}(2)$	$\Delta^6$ <i>cis</i>
	2.304 ppm	$\text{H}_3\text{C}(18)$	$\Delta^6$ <i>trans</i>
	2.154 ppm	$\text{H}_3\text{C}(18')$	
			$\text{H}-\text{C}(4) \approx 3\%$ ; $\text{H}_3\text{C}(16,17) \approx 1\%$
			$\text{H}-\text{C}(4) \approx 24\%$ ; $\text{H}-\text{C}(8) \approx 8\%$
			$\text{H}-\text{C}(4) \approx 26\%$ ; $\text{H}-\text{C}(7) \approx 9\%$
1c di- <i>cis</i>	1.251 ppm	$\text{H}_3\text{C}(16,17,16',17')$	$\Delta^{6,6'}$ <i>cis</i>
	2.341 ppm	$\text{H}-\text{C}(2,2')$	
	2.305 ppm	$\text{H}_3\text{C}(18,18')$	$\Delta^{6,6'}$ <i>cis</i>

\* Enhancement unexpectedly small.

\*\* The full AA'BB'-multiplet of the four strongly coupled protons is enhanced ca. 4% per proton.

The  $^1\text{H}$  NMR of peak 1 exhibited the same number of signals, indicating the same symmetry as 1a. Despite the small amount of sample available, several Overhauser experiments (of reduced signal-to-noise ratio) were performed which provided support for  $\Delta^{6,6'}$  *cis* (see Table II).

The number of signals in the  $^1\text{H}$  NMR of fraction 2 pointed to the lower symmetry of the molecule. The fact that the spectrum can be fully interpreted to a good approximation by a superposition of the individual spectra of fractions 3 and 1 is seen by inspection of the data of Table I. This result is quite reasonable since the influence of an end group with either  $\Delta^6$  *cis* or *trans* on the chemical shifts of the "in-chain" olefinic protons is expected to become small near the centre of the molecule.

## CONCLUSIONS

By HPLC a full separation of the two major geometrical isomers from all-*trans* rhodoxanthin was successfully achieved. With the aid of the  $^1\text{H}$  NMR spectrum, even that obtained at 400 MHz, it is practically impossible to measure quantitatively the concentration of all three components since the chemical shifts of either end group are not sufficiently influenced by the configuration of the other end of the molecule. This might explain why for retro- and substituted retro-compounds the presence of only one isomer besides the all-*trans* (1a) was discussed in the literature<sup>3,4</sup>.

## ACKNOWLEDGEMENTS

We are indebted to Drs. R. Marbet and R. Zell for providing the samples. We also gratefully acknowledge the technical assistance of Mr. E. Glinz.

## REFERENCES

- 1 B. C. L. Weedon, in O. Isler (Editor), *Carotenoids*, Birkhäuser, Basle, 1971, Ch. II, p. 37.
- 2 H. Mayer, M. Montavon, R. Rüegg and O. Isler, *Helv. Chim. Acta*, 50 (1967) 1606.
- 3 G. Andrewes, G. Englert, G. Borch, H. H. Strain and S. Liaaen-Jensen, *Phytochemistry*, 18 (1979) 303.
- 4 W. Vetter, G. Englert, N. Rigassi and U. Schwieter, in O. Isler (Editor), *Carotenoids*, Birkhäuser, Basle, 1971, Ch. IV, pp. 189-266.
- 5 G. Englert, *Helv. Chim. Acta*, 58 (1975) 2367.
- 6 G. Englert, *Helv. Chim. Acta*, 62 (1979) 1497.

CHROM. 14,300

## HIGH-PERFORMANCE LIQUID CHROMATOGRAPHIC METHOD FOR THE DETERMINATION OF NOVOBIOCIN

KIYOSHI TSUJI\*, PAUL D. RAHN and MICHAEL P. KANE

Control Analytical Research and Development, The Upjohn Company, Kalamazoo, MI 49001 (U.S.A.)

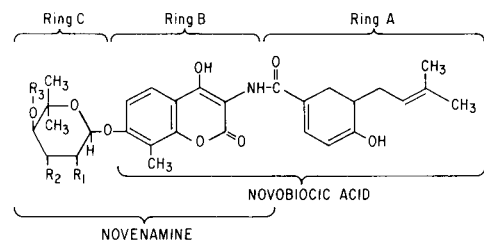
(Received August 18th, 1981)

### SUMMARY

A stability-indicating normal-phase high-performance liquid chromatographic (HPLC) method for the assay of novobiocin has been developed. The method uses a silica column with a mobile phase composed of butyl chloride-tetrahydrofuran-methanol-acetic acid (88:5:4:3). The amount of acetic acid in the mobile phase significantly influences the resolution of novobiocin and desmethyldescarbamylnovobiocin peaks. Isonovobiocin and degradation compounds of novobiocin have been separated. The standard curve for the quantification of novobiocin was linear in the range of 0.2-0.6 mg novobiocin per ml and the relative standard deviation of the assay was less than 1%. Excellent correlation was obtained between the HPLC and microbiological assay methods. The method was used to assay novobiocin in mastitis products.

### INTRODUCTION

Novobiocin (Fig. 1) is an aminocyclitol antibiotic produced by *Streptomyces niveus* or related microorganisms. The official assay method for the potency determi-



	R <sub>1</sub>	R <sub>2</sub>	R <sub>3</sub>
NOVOBIOCIN	OH	OCONH <sub>2</sub>	CH <sub>3</sub>
ISONOVOBIOCIN	OCONH <sub>2</sub>	OH	CH <sub>3</sub>
DESCARBAMYLNOVOBIOCIN	OH	OH	CH <sub>3</sub>
DESMETHYLDESCARBAMYLNOVOBIOCIN	OH	OH	H
DIHYDRONOVOBIOCIN (REDUCTION OF ISOPENT-2-ENYL SIDE CHAIN TO ISOPENTYL)			

Fig. 1. Structure of novobiocin.



nation of novobiocin by the Food and Drug Administration is a cylinder cup agar diffusion assay using *Staphylococcus epidermidis* ATCC 12228 as the test microorganism<sup>1</sup>. Since isomers and degradation products of novobiocin are reported as being microbiologically inactive<sup>2-4</sup>, the microbiological assay method is a stability-indicating assay method. The microbiological assay method, however, is not a precise method for quantification and is influenced by varieties of factors<sup>5</sup>. The method is also incapable of detecting and quantifying degradation compounds and process impurities.

Several chemical assay methods are available for the determination of novobiocin<sup>6-13</sup>; those listed in refs. 8 and 9 are stability-indicating assay methods. A gas-liquid chromatographic (GLC) method, based on the acetylation of novobiocin and chromatography using an OV-17 column, is also available<sup>14</sup>. Although the precision of the GLC method is excellent (relative standard deviation, R.S.D. = 0.3%), the method cleaves either the glycosidic or the amide bond, depending upon the derivatization method used. The method, moreover, is incapable of differentiating isonovobiocin from novobiocin.

A high-performance liquid chromatographic (HPLC) method for the determination of novobiocin has been reported<sup>4</sup>. Excellent separation of isomers and degradation compounds was obtained. However, the HCP column used was not stable and the column performance deteriorated rapidly upon use. This paper reports the development of a normal-phase HPLC method for separation and quantification of novobiocin, its isomers and degradation compounds.

## EXPERIMENTAL

### *Instruments*

An LDC M19-60066-022 high pressure mini-pump (Laboratory Data Control, Riviera Beach, FL, U.S.A.) was used to pump the mobile phase at a flow-rate of about 1 ml/min. Analysis was performed using a silica column (Cat. No. SI-5A, Brownlee LiChrosorb SI-100, 5  $\mu$ m, 250  $\times$  4.6 mm I.D.; Rheodyne, Berkeley, CA, U.S.A.) at room temperature. A 20- $\mu$ l sample containing about 0.1 mg/ml of novobiocin acid was injected quantitatively onto the column using a Rheodyne M70-10, 20- $\mu$ l loop injector or Waters intelligent Sample Processor (WISP, Model 710B; Waters Assoc., Milford, MA, U.S.A.). The column effluent was monitored either at 340 nm using an LDC Spectromonitor I variable-wavelength detector or at 254 nm using an LDC UV III monitor fixed-wavelength detector with an attenuation setting of 0.032 a.u.f.s.

### *Reagents*

Butyl chloride, tetrahydrofuran, and methanol were all UV grade, distilled in glass, obtained from Burdick & Jackson Labs. (Muskegon, MI, U.S.A.). Acetic acid was AR grade obtained from Mallinckrodt (Paris, KY, U.S.A.).

### *Mobile phase*

The mobile phase used was butyl chloride (50% water saturated)-tetrahydrofuran-methanol-acetic acid (88:5:4:3). Fifty percent water-saturated butyl chloride was prepared by mixing one volume of water-saturated butyl chloride with an equal volume of butyl chloride.

### *Novobiocin reference standard solution*

USP novobiocin acid reference standard was dried for 4 h at 100°C under vacuum (< 5 mmHg). Approximately 10 mg of the dried and cooled reference standard were accurately weighed into a 100-ml volumetric flask. The novobiocin acid was dissolved by adding 10 ml tetrahydrofuran, and the solution was diluted with the mobile phase and sonicated to aid dissolution. The tetrahydrofuran used contained 0.3 mg prednisone per ml, an internal standard suitable for monitoring at 254 nm.

### *Sample preparation*

*Novobiocin powder.* Approximately 12–14 mg of sodium or calcium novobiocin were accurately weighed “as is” into a 100-ml volumetric flask. A 10-ml volume of tetrahydrofuran was added and the solution diluted to volume with the mobile phase.

*Peanut oil based veterinary mastitis products.* Each plasket (a unique syringe and needle assembly made entirely of polyethylene) was vigorously shaken with two glass beads for 30 min on a platform reciprocating shaker to obtain a uniform suspension. The contents of each plasket were expelled into a 100-ml volumetric flask. The syringe was weighed before and after to obtain sample weight. A 10-ml volume of tetrahydrofuran was added to the flask and the solution was diluted to volume with mobile phase. This solution was sonicated and shaken on a platform reciprocating shaker at high speed for 5 min. An aliquot was centrifuged in a disposable vial for 5 min at 2000 g. A portion of the clear supernatant was then used for analysis. Novobiocin samples thus prepared are stable up to 1 week at room temperature.

### *Calculations*

The amount of novobiocin in the mastitis product can be calculated by

$$\text{Novobiocin (mg per 10 ml)} = \frac{A_{\text{smp}}}{A_{\text{std}}} \times \frac{C_{\text{std}}}{W_{\text{smp}}} \times F \times V \times S \times 10$$

where  $A_{\text{smp}}$  and  $A_{\text{std}}$  are the peak areas of novobiocin in the sample and the reference standard,  $C_{\text{std}}$  is the concentration (mg/ml) of the novobiocin reference standard solution,  $W_{\text{smp}}$  is the weight (mg) of sample,  $F$  is the assigned purity of the reference standard,  $V$  is the volume of the sample solution (100 ml),  $S$  is the specific gravity of the sample, and 10 is a factor to express the result on a 10-ml basis.

## RESULTS AND DISCUSSION

### *Chromatographic separation of impurities and degradation compounds*

Commercially available novobiocin contains, in addition to novobiocin, small amounts of isonovobiocin, descarbamylnovobiocin, desmethyl Descarbamylnovobiocin, novenammine, novobiocic acid, and rings A, B, and C (Fig. 1). Since efforts to develop an HPLC method using a reversed-phase column to separate isonovobiocin from novobiocin failed, a normal-phase HPLC method for the assay of novobiocin was developed to separate the isomers. Isonovobiocin was reported to have no antimicrobial activity<sup>3</sup>. The HPLC method described in this report is capable of differentiating and quantifying novobiocin and its isomers and degradation products. Authentic samples of these isomer and degradation compounds, available at

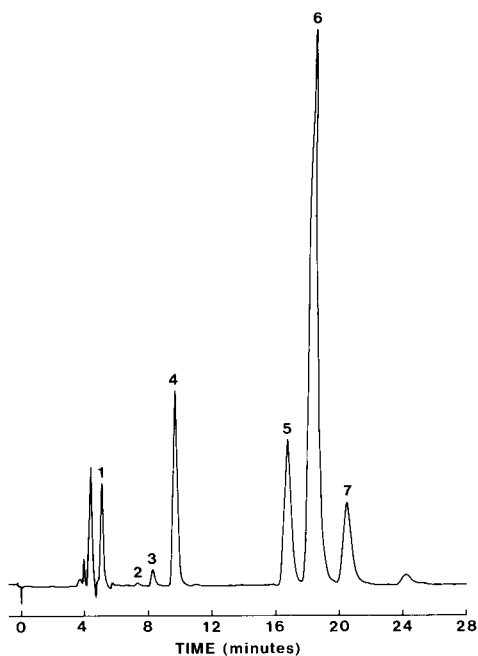


Fig. 2. HPLC Separation of novobiocin from its isomers and degradation compounds. Peaks: 1 = ring B; 2 = novobiocic acid; 3 = ring A amide; 4 = descarbamylnovobiocin; 5 = isonovobiocin; 6 = novobiocin; 7 = desmethyldescarbamylnovobiocin.

The Upjohn Company, were spiked into a solution of sodium novobiocin bulk powder and identified on the chromatogram on the basis of relative retention. A chromatogram indicating the separation of various degradation products can be seen in Fig. 2. The relative retention of these isomer and degradation compounds are presented in their order of elution in Table I. Among the components of the mobile phase, acetic acid significantly influenced the resolution of novobiocin and desmethyl-descarbamylnovobiocin peaks. An increase of acetic acid from 1.0% to 3.0% changed the peak resolution from 0.41 to 1.44.

Unless specifically derivatized, the ring C cannot be detected when monitored by an UV spectrophotometer. Detection of the ring A and/or novobiocic acid should be indicative of the ring C formation. Under the chromatographic conditions used,

TABLE I

RELATIVE RETENTION OF NOVOBIOCIN AND IMPURITIES

<i>Compound</i>	<i>Relative retention</i>
Ring B	0.20
Ring A acid	0.27
Novobiocic acid	0.44
Ring A amide	0.48
Descarbamylnovobiocin	0.53
Isonovobiocin	0.91
Novobiocin	1.00
Desmethyldescarbamylnovobiocin	1.10

novenammine does not elute from the column. Formation of novenammine should coincide with that of the ring A; the latter can be monitored by HPLC (Table I, Fig. 2). Fig. 3 is a typical chromatogram of a production lot of sodium novobiocin indicating the presence of isomers and impurities.

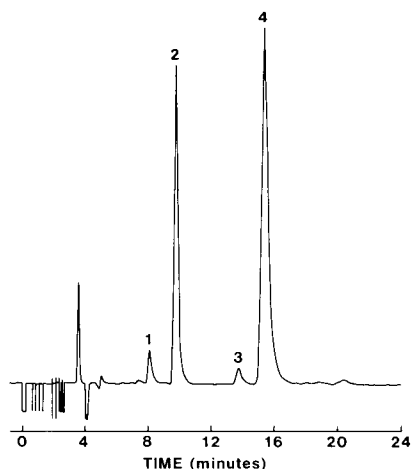


Fig. 3. HPLC chromatogram of sodium novobiocin with prednisone as the internal standard. Peaks: 1 = descarbamylnovobiocin; 2 = internal standard; 3 = isonovobiocin; 4 = novobiocin.

#### *Assay of novobiocin bulk drug*

Prednisone was selected as the internal standard suitable for monitoring at 254 nm. As shown in Fig. 3, prednisone elutes after descarbamylnovobiocin but well ahead of isonovobiocin. The impurities and degradation compounds in novobiocin do not interfere with prednisone.

A standard curve for the assay of novobiocin was constructed using a Novobiocin Acid Reference Standard between the range of 0.2 to 0.6 mg/ml. The standard curve is linear (correlation coefficient of 0.99998) with a linear regression of  $y = 361x + 1.04$ . A small bias observed at the  $y$  intercept when  $x = 0$  can be considered as well within error of the assay.

The effect of the use of the internal standard on the precision of the assay was evaluated from the R.S.D. obtained by analyzing six individually weighed samples of sodium novobiocin powder and diluting in a solution containing the internal standard. As shown in Table II, the R.S.D. of the assay, calculated without the use of the internal standard, was 0.93%. The R.S.D. of 1.62% was obtained when the internal standard calculation format was used. This apparent increase in the R.S.D. of the assay by the internal standard calculation method can be explained by the design of the method, which requires use of the peak area ratio of the two peaks, novobiocin and prednisone, for calculation. Therefore, the assay variance become additive due to the two independent variables. The potency of the novobiocin powder did not differ significantly whether or not the internal standard was used for calculation. The potency was 809  $\mu\text{g}/\text{mg}$  and 811  $\mu\text{g}/\text{mg}$  with and without the use of the internal standard, respectively (Table II).

The sensitivity of the assay is approximately 40 ng novobiocin per column injected. The novobiocin sample prepared in the mobile phase is stable for approxi-

TABLE II

EFFECT OF THE INTERNAL STANDARD ON PRECISION OF THE HPLC ASSAY FOR NOVOBIOCIN POWDER

Sample no.	Weight of novobiocin (mg/100 ml)	Peak area		Ratio	
		Novobiocin	Internal standard	No internal std. Novo peak area/wt.	With internal std. Novo/wt./int. std.
1	10.03	18,369	9736	1831.4	0.1881
2	10.24	18,419	9876	1798.8	0.1821
3	10.32	18,710	9837	1813.0	0.1843
4	9.98	18,298	10112	1833.5	0.1813
5	10.04	18,141	9865	1806.9	0.1832
6	10.19	18,265	9989	1792.5	0.1794
				R.S.D. 0.93%	1.62%
				Potency 811 µg/mg	809 µg/mg

mately 1 week when tightly capped and stored at room temperature (peak height of novobiocin: initial, 46.6; 1 week later, 46.5). No decrease in the novobiocin peak nor appearance of degradation peaks was noted.

#### Correlation between HPLC and microbiological assay methods

Novobiocin is normally quantified by the microbiological cylinder cup agar diffusion method using *Staphylococcus epidermidis* ATCC 1228<sup>1</sup>. This method, however, is incapable of detecting and quantifying the presence of minor degradation products and impurities, which are microbiologically inactive. Several lots of commercially available novobiocin powder were assayed using the HPLC method and the results were compared with those of the microbiological assay method (Table III).

TABLE III

COMPARISON OF HPLC AND MICROBIOLOGICAL ASSAY METHODS FOR ANALYSIS OF NOVOBIOCIN

Lot no.	Potency (µg/mg)	
	HPLC	Microbioassay
1	810	831
2	885	862
3	865	903
4	844	886
5	861	855
6	856	870
7	871	863
8	829	823
9	809	807
10	801	793
11	809	781

Analysis of the data indicated that there is no statistically significant difference between the HPLC and the microbiological assay data.

In order to evaluate further the correlation between the HPLC and the microbiological assay methods, sodium novobiocin was intentionally degraded by acid, base, and  $^{60}\text{Co}$  treatments. These degraded samples were analyzed by HPLC and by the microbiological assay methods. HPLC data indicated that acid treatment degraded novobiocin and formed at least five peaks, one of which has a relative retention identical to novobiocin acid. A mild base hydrolysis formed a substantial quantity of descarbamylnovobiocin with a lesser amount of novobiocin acid. Isenovobiocin was relatively stable to the treatment. Stronger base treatment caused complete degradation of the novobiocin peak and degradation of descarbamylnovobiocin with substantial increase of ring A.

Potencies of these degraded samples were calculated from the residual quantities of novobiocin detected by HPLC and the values were compared with those of the microbiological assay method (Table IV). In general, agreement between the two assay methods are good for base degraded samples. The higher HPLC potency obtained on the acid degraded sample may be attributed to incomplete separation of the novobiocin peak from one of the degradation peaks, and to the low quantity of novobiocin, which was outside the linear portion of the standard curve for the microbiological assay method.

TABLE IV

ASSAY OF INTENTIONALLY DEGRADED NOVOBIOCIN SAMPLES

<i>Treatment</i>	<i>Potency (<math>\mu\text{g}/\text{mg}</math>)</i>	
	<i>HPLC</i>	<i>Microbiological</i>
Control	811, 809	879, 816, 758 767, 907, 859 ( $\bar{x}$ = 831)
Acid with heat	18	2.5, 1.8
Mild base	14	18, 12
Strong base with heat	0	0.05, 0.04

Novobiocin powder was submitted to Isomedix, Inc. (Morton Grove, IL, U.S.A.) for  $^{60}\text{Co}$ -irradiation at various doses up to 5.87 Mrad. These samples were analyzed by the HPLC and the microbiological methods (Table V) and the results indicated excellent correlation between the HPLC and the microbiological assay methods.

The results of these studies confirm the published reports that the isomers and degradation compounds of novobiocin are microbiologically inactive<sup>2-4</sup>. Thus, the HPLC method for the determination of novobiocin provides not only a potency value which correlates well with the microbiological assay method, but also provides opportunity to detect and quantify the degradation compounds and impurities present.

#### *Identification of a degradation compound*

Upon examination of chromatograms of irradiated and non-irradiated sodium

TABLE V  
ANALYSIS OF  $^{60}\text{Co}$ -IRRADIATED SODIUM NOVOBIOCIN POWDER

Irradiation dose (Mrad)	Potency ( $\mu\text{g}/\text{mg}$ )	
	HPLC	Microbiological
0	815	816
0.6	784	754
1.76	758	757
2.85	746	697
3.45	736	722
4.78	720	690
5.87	724	728

novobiocin powder, it became evident that one peak (peak No. 2) which was originally present in bulk powder increased upon irradiation (Fig. 4). Dry heat treatment of the bulk powder also formed this peak (Fig. 4). The relative chromatographic retention of this peak (RT, 0.48) is close but not identical to that of novobiocic acid (RT, 0.44) (Table I); moreover, this peak lacks absorptivity at 340 nm. Novobiocic acid absorbs strongly at 340 nm.

In order to identify the peak, sodium novobiocin was refluxed for 30 min in ethyl acetate to enrich the compound. Alternatively, the compound was enriched by two-phase extraction using water and ethyl acetate. The compound is extremely solu-

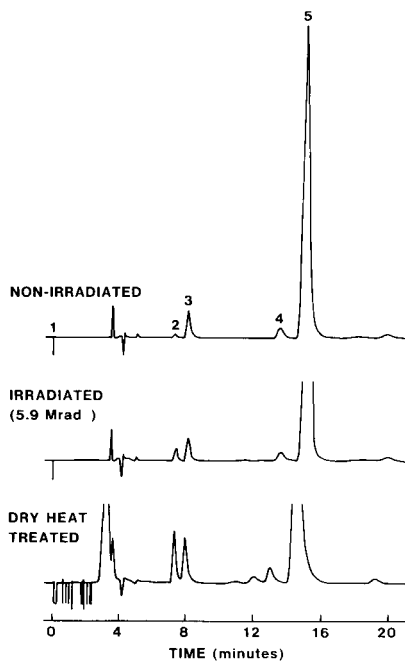
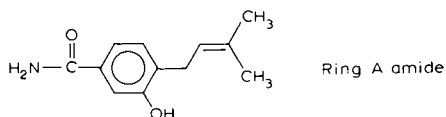


Fig. 4. HPLC chromatograms of novobiocin indicating increase in the Ring A amide by  $^{60}\text{Co}$ -irradiation or dry heat treatment. Peaks: 2 = ring A amide; 3 = descarbamylnovobiocin; 4 = isonovobiocin; 5 = novobiocin (1 = injection point).

ble in ethyl acetate while sodium novobiocin is soluble in water. The enriched sample was purified by semi-preparative scale HPLC. The purified sample was freeze-dried and analyzed by high-resolution ring mass spectrometry. The mass spectrum (Fig. 5) identified the compound as the ring A amide (mol.wt. found, 205.1087; theory for  $C_{12}H_{15}N_1O_2$ , 205.1103):



The mass fragmentation pattern also confirmed this identification.

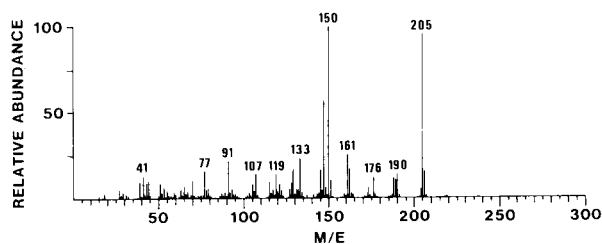


Fig. 5. Mass spectrum of Ring A amide.

#### *Analysis of mastitis product*

When the HPLC procedure was applied to analyze novobiocin in a peanut oil based mastitis product containing prednisolone, the steroid was inadequately separated from novobiocin for precise quantification. Efforts to improve separation by the modification of chromatographic conditions were not successful. Use of ion-exchange resins and solvent extraction methods were also examined without success. Interference from prednisolone was eliminated by monitoring column effluent at 340

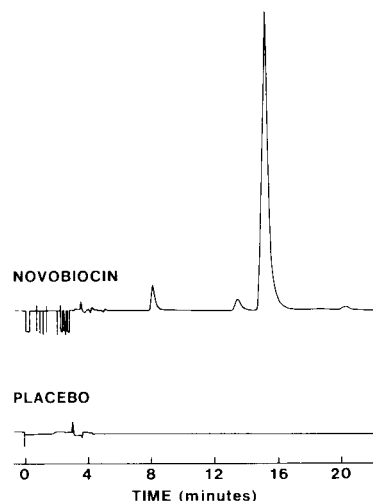


Fig. 6. HPLC chromatograms of novobiocin in peanut oil-based mastitis product and of placebo.



nm. Novobiocin has a maximum absorbance at 340 nm while prednisolone has a maximum at 254 nm and no absorbance at 340 nm.

HPLC chromatograms of novobiocin in mastitis product and of the placebo are shown in Fig. 6. A suitable internal standard to monitor the column effluent at 340 nm is being investigated. Prednisone, however, may satisfactorily be used as the internal standard if a rapid scanning spectromonitor is used to monitor at both 254 nm and 340 nm. The sensitivity of the assay is approximately 10 ng novobiocin per injection when monitored at 340 nm. This is approximately a four-fold increase in sensitivity when compared to monitoring at 254 nm.

The average recovery of novobiocin when spiked at 70–120% of the label was 100.8% with a relative standard deviation of 0.6% (Table VI).

TABLE VI

## RECOVERY OF SODIUM NOVOBIOCIN SPIKED IN PLACEBO OF A MASTITIS PRODUCT

<i>Sodium novobiocin</i> (percent label)	<i>Weight added</i> (mg/10 ml)	<i>Weight recovered</i> (mg/10 ml)	<i>Recovery (%)</i>
67.6	80.44	80.72	100.4
68.1	81.04	81.47	100.5
76.7	91.26	91.14	99.9
76.5	91.02	91.88	100.9
84.4	100.52	100.44	99.9
85.2	101.47	102.29	100.8
92.6	110.21	111.60	101.3
92.6	110.24	110.85	100.6
100.8	120.03	121.27	101.0
101.0	120.19	121.27	100.9
120.7	143.7	146.3	101.8
121.0	144.1	146.6	101.7
			Average 100.8%
			R.S.D. 0.60%

## ACKNOWLEDGEMENT

Acknowledgement is made to L. Baczynskyj for mass spectrometric analysis.

## REFERENCES

- 1 *Code of Federal Regulations*, Title 21, 436.103. Food and Drug, U.S. Government Printing Office, Washington, DC, 1980.
- 2 L. V. Birlova and D. M. Trakhlenberg, *Antibiotiki (Moscow)*, 11 (1966) 395.
- 3 J. W. Hinman, E. L. Caron and H. Hoeksema, *J. Amer. Chem. Soc.*, 79 (1957) 5321.
- 4 K. Tsuji and J. H. Robertson, *J. Chromatogr.*, 94 (1974) 245.
- 5 A. Morris, A. D. Russel and I. L. Thomas, *Experientia*, 23 (1967) 244.
- 6 A. Angelov, *Farmatsiya (Sofia)*, 18 (1968) 37.
- 7 F. A. Bacher, G. V. Downing and J. S. Wood, *Anal. Chem.*, 30 (1958) 1993.
- 8 A. A. Forist, S. Theal and W. A. Struck, *Anal. Chem.*, 31 (1959) 100.
- 9 T. Ikewawa, F. Iwai, E. Akita and H. Umezawa, *J. Antibiot., Ser. A*, 16 (1963) 56.
- 10 J. W. Lightbrown and P. De Rossi, *Analyst (London)*, 90 (1965) 89.
- 11 R. Rangone and C. Ambrosio, *Farmaco Ed. Parct.*, 26 (1971) 237.
- 12 P. Sensi, G. G. Gallo and L. Chiesa, *Anal. Chem.*, 29 (1957) 1611.
- 13 R. M. Smith, J. J. Perry, G. C. Prescott, J. L. Johnson and I. H. Ford, *Antibiotic Ann.*, (1958) 43.
- 14 K. Tsuji, in K. Tsuji (Editor), *GLC and HPLC Determination of Therapeutic Agents*, Marcel Dekker, New York, 1978, p. 793.

CHROM. 14,316

## IMPROVED HIGH-PERFORMANCE LIQUID CHROMATOGRAPHIC METHOD FOR SIMULTANEOUS DETERMINATION OF NEAMINE, NEOMYCIN B AND NEOMYCIN C IN NEOMYCIN SULPHATE

PER HELBOE and SONJA KRYGER\*

*National Board of Health, Drug Standardization Laboratory, 378 Frederikssundsvej, DK-2700 Brønshøj (Denmark)*

(Received September 1st, 1981)

---

### SUMMARY

A fast and reliable isocratic high-performance liquid chromatographic method suitable for simultaneous determination of the main component and impurities in neomycin sulphate is elaborated. Neomycin B and the related substances are separated as their 2,4-dinitrophenyl derivatives on a Zorbax SIL column using 1,2-dichloroethane–heptane–methanol–water–diethylamine (790:150:55:3.6:1.5) as the eluent. The method is compared to the commonly used microbiological method for quantitating neomycin.

---

### INTRODUCTION

Pharmacopoeias, even modern ones, contain specifications for purity and assay of neomycin sulphate that are based on a combination of various chromatographic tests for related substances, including thin-layer chromatography (TLC) and ion-exchange column chromatography, and a microbiological assay<sup>1,2</sup>. These procedures are time consuming and as far as the microbiological assay is concerned, not very precise. The speed of analysis using the ion-exchange method may be increased by automation and refractive index (RI) detection<sup>3</sup>, but due to poor column performance the method is still unsuitable for the detection of impurities present in low concentrations, *i.e.*, neamine. Recently Tsuji *et al.*<sup>4</sup> described a high-performance liquid chromatographic (HPLC) method to separate neomycin B and C and neamine as their 2,4-dinitrophenyl (DNP) derivatives. The method did not, however, allow simultaneous determination by isocratic elution of these components, but two slightly different isocratic systems or, alternatively, a gradient system were used.

The major feature of an HPLC method suitable for pharmacopoeial control of neomycin sulphate would be that an isocratic method should allow simultaneous determination of the contents of neomycin B and C and those of related substances, *i.e.*, neamine. The present paper describes a method which meets these demands.

## EXPERIMENTAL

*Chemicals*

All reagents were of analytical grade from E. Merck (Darmstadt, G.F.R.). Samples of neomycin sulphate of pharmacopoeial grade were investigated. Neamine hydrochloride was the European Pharmacopoeia Chemical Reference Substance. Pure neomycin B sulphate and enriched neomycin C sulphate (containing 95% of neomycin C and 5% of neomycin B) were supplied by H. Lundbeck (Copenhagen, Denmark). The 1st International Reference Preparation for neomycin B was used as the reference material in quantitations.

*Chromatography*

The liquid chromatograph used consisted of a Kontron Model 410 LC pump, a Cecil 2012 spectrophotometer detector operated at 350 nm and a Rheodyne Model 7120 injection valve with a 20- $\mu$ l loop. Chromatograms were recorded on a Kipp and Zonen Model BD-8 recorder, and peak areas were measured and processed by means of a Hewlett-Packard Model A laboratory data system.

A prepacked silica column, Zorbax SIL (250  $\times$  4.6 mm) (DuPont, Hitchin, Great Britain), was used. The eluent was 1,2-dichloroethane–heptane–methanol–water–diethylamine (790:150:55:3.6:1.5).

*Derivatization*

The derivatization reagent was prepared by dissolving 0.5 ml of 2,4-dinitrofluorobenzene (DNFB) in 25 ml methanol. It was freshly prepared daily. A 0.02 M borate buffer (pH 9.0) was prepared by dissolving 4.02 g of anhydrous sodium borate in 1000 ml water.

A 500- $\mu$ l volume of test or standard solution (1 mg/ml) of neomycin sulphate in 0.02 M borate buffer (pH 9.0) was placed in a 25-ml volumetric flask, 1.5 ml of DNFB were added and the mixture was heated in a water-bath at 60°C for 60 min. After cooling, 15 ml of 1,2-dichloroethane were added and the mixture was shaken in a mechanical shaker for 5 min. 1,2-Dichloroethane was added until the lower phase reached the 25-ml mark, and following centrifugation 20  $\mu$ l of the lower phase were injected.

## RESULTS AND DISCUSSION

*Derivatization*

Preliminary investigations were carried out using the procedure proposed by Tsuji *et al.*<sup>4</sup>, *i.e.*, heating a mixture of neomycin and DNFB solution in an oil-bath at 100°C. Problems were encountered, however, through the formation of insoluble lumps which adhered to the walls of the flask when mixing with eluent. This might be due to evaporation of water from the reaction mixture; no difficulties occurred when performing the derivatization at lower temperatures. Fig. 1 shows the formation of the derivatives of neomycin B and C and neamine as a function of reaction time at 60°C, and it appears that the derivatization is complete within about 1 h.

*Chromatography*

The eluent mixture prescribed by Tsuji *et al.*<sup>4</sup> was found to be unsuitable as the

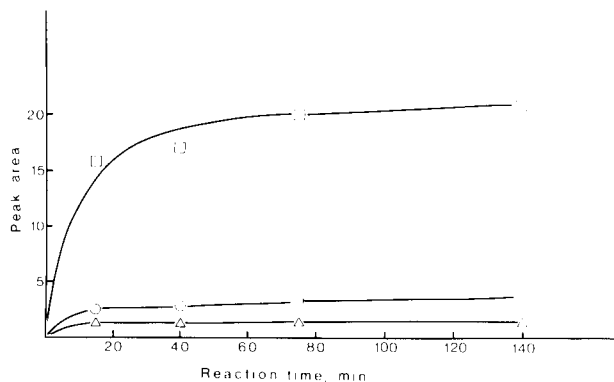


Fig. 1. Peak area (in arbitrary units) plotted as a function of reaction time. For conditions see Experimental.  $\Delta$ , Neomine;  $\circ$ , neomycin C;  $\square$ , neomycin B.

basis for an isocratic system for the separation of neamine and neomycin B and C within a reasonable time, even when changing the ratio between the components. More promising results were obtained when using mixtures of 1,2-dichloroethane, methanol, water and diethylamine; such mixtures had previously proven valuable for several separations, and are a modification of a system originally proposed by Hansen and Madsen<sup>5</sup>.

The main problem in optimizing the eluent composition appeared to be that small amounts of impurities originating from neomycin and from the reagents disturbed the peak corresponding to neamine. Extraction of the derivatization mixture with pure 1,2-dichloroethane rather than with the eluent gave an obvious improvement in the shape of the neamine peak and in its separation from disturbing peaks. This is probably due to the fact that the eluent which contains an appreciable amount of methanol is able to extract some water from the reaction mixture, thereby leading to a change in polarity relative to the eluent proper and consequently to solvent induced anomalies in the peak shapes. Furthermore, it was found that the addition of heptane to the eluent also improved the separation.

Fig. 2a–d shows the results of further investigations into the influence of the eluent composition on the retention of the compounds of interest. The influence of the concentrations of water and methanol are evident, but also the concentrations of heptane and diethylamine are of importance for the separation of the neamine peak from other impurity peaks and from a small, negative solvent peak. The optimal composition of the eluent was found to be 1,2-dichloroethane–heptane–methanol–water–diethylamine (790:150:55:3.6:1.5). Fig. 3 shows a chromatogram of a neomycin sample and a chromatogram exhibiting the peaks resulting from the reagents. The peak identities in Fig. 3a were established by chromatographing derivatized samples of pure neamine and neomycin B and a sample of enriched neomycin C.

#### *Linearity and precision*

For the quantitative evaluation of the chromatograms the method of external standardization was used, with the International Reference Preparation for neomycin B as the external standard. The linearity of the method, including the derivatization procedure and the detector response, was checked by analyzing samples in concentra-

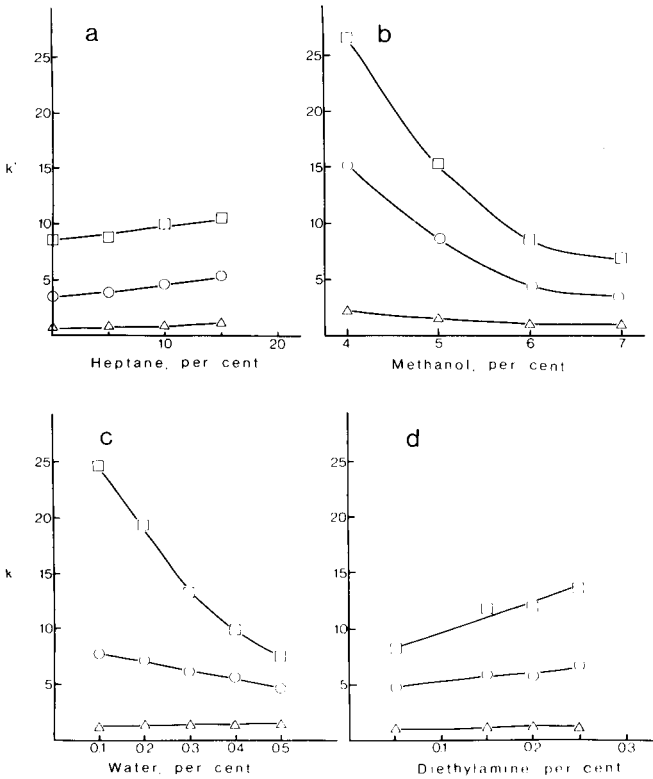


Fig. 2. Influence of the concentrations of the eluent components on retention.  $\Delta$ , Neamine;  $\circ$ , neomycin C;  $\square$ , neomycin B.

tions up to 1 mg/ml of neomycin B, 0.15 mg/ml of neomycin C and 0.03 mg/ml of neamine, respectively. Plots of detector responses against the concentrations gave straight lines through the origin for all three compounds, thus establishing the linearity of the method in the concentration range of interest.

The precision of the method was examined by analyzing ten solutions, made from ten individual weighings of one sample of neomycin sulphate, and the results are shown in Table I. It appears that the relative standard deviation is fairly small for the two main components neomycin B and C, whereas it is larger for neamine which is present in only small amounts. The limit for neamine stated in pharmacopoeias is usually 1 or 2%.

#### *Chromatographic versus microbiological assay*

Quantitation of neomycin sulphate by both chromatographic and microbiological methods is complicated by the fact that both neomycin B and C exhibit an antimicrobial effect, but not to the same extent.

In the microbiological assay the potency ratio varies with the microorganism used and with the experimental conditions<sup>6</sup>, which means that the most reliable results are obtained when the same B/C ratio is present in the test and the reference material.

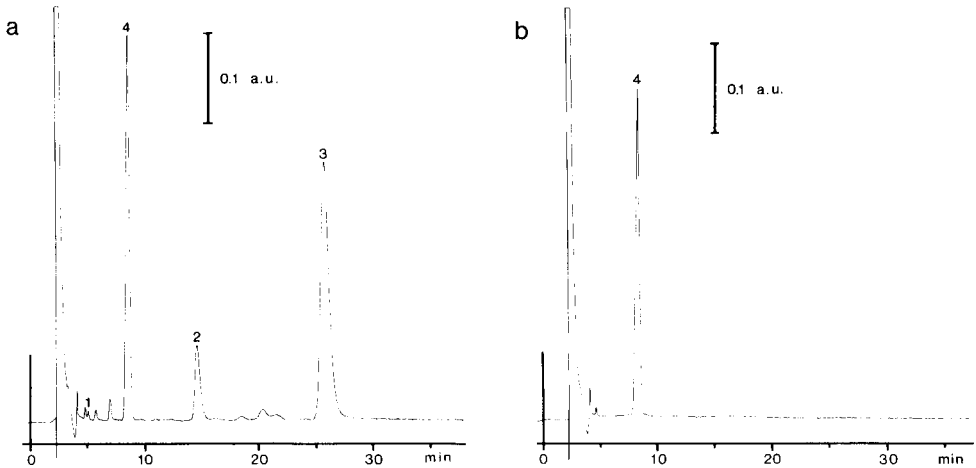


Fig. 3. Separation of components from a derivatized sample of neomycin sulphate (a) and components originating from the reagents (b). Support: Zorbax SIL. Eluent: 1,2-dichloroethane–heptane–methanol–water–diethylamine (790:150:55:3.6:1.5). Solvent velocity: 1.5 mm/sec. Pressure: 7 MPa. Detection wavelength: 350 nm. Peaks: 1 = neamine; 2 = neomycin C; 3 = neomycin B; 4 = 2,4-dinitrophenol.

When using the International Reference Preparation for neomycin as the external standard in the chromatographic assay, in order to be able to compare the results with the microbiological assay, it is necessary to know its exact content of neomycin C (*ca.* 10%) as well as the relative antimicrobial activity of neomycin B and C. By assaying an enriched neomycin C sample (containing 95% of neomycin C and 5% of neomycin B) using the microbiological method<sup>1</sup> it was found that neomycin C exhibits one third of the potency of neomycin B. The chromatographic standardization against the International Reference Preparation for neomycin, however, is still complicated owing to the fact that the standard is a mixture. Hence the standardization against the International Reference Preparation for neomycin B, which contains no neomycin C, was found more convenient.

In Table II the results of determinations using the two different methods are shown. It appears that after correcting for the difference in the potency of neomycin B and C the HPLC method and the microbiological method show concordant results.

TABLE I  
PRECISION OF THE HPLC METHOD

Means and relative standard deviations were determined by derivatizing and analyzing ten individually prepared solutions of the same sample of neomycin sulphate. Each solution was chromatographed in triplicate.

Compound	$\bar{x}_{10}$ (%)	$s_r$ (%)
Neamine	0.43	11.0
Neomycin C	15.6	4.0
Neomycin B	84.0	2.9

TABLE II  
COMPARISON OF THE HPLC AND MICROBIOLOGICAL METHODS

In both methods the 1st International Reference Preparation for neomycin B was used as the reference material.

Sample	Potency (in % of neomycin B standard)				
	HPLC			Microbiological	
	B	C	B + 1/3C	Potency	Fiducial lim.
1	95	10.7	99	95	90-110
2	108	1	108	101	92-109
3	80.8	15	86	84	90-111

#### CONCLUSION

An isocratic HPLC method has been elaborated for the simultaneous determination of active ingredients and impurities in neomycin sulphate. The method is deemed suitable for pharmacopoeial purposes, and could replace the various chromatographic methods for determination of neamine and neomycin C commonly used and also the microbiological assay.

#### ACKNOWLEDGEMENTS

We thank Birgitte Kristensen for preliminary chromatographic investigations. Eva Sandberg for the microbiological determinations and Lizzi Olsen and Ilse Jørgensen for technical assistance during the chromatographic determinations. H. Lundbeck and Co. Ltd. is thanked for gifts of neomycin B and enriched neomycin C.

#### REFERENCES

- 1 *European Pharmacopoeia*, Vol. II, Maisonneuve, Sainte Ruffine, 1971, p. 308.
- 2 *British Pharmacopoeia 1980*, HMS, London, 1980, p. 203.
- 3 W. Decoster, P. Claes and H. Vanderhaeghe, *J. Chromatogr.*, 211 (1981) 223.
- 4 K. Tsuji, J. F. Goetz, W. VanMeter and K. A. Gusciora, *J. Chromatogr.*, 175 (1979) 141.
- 5 S. H. Hansen and J. H. Madsen, *Arch. Pharm. Chem., Sci. Ed.*, 5 (1977) 157.
- 6 T. Sokolski, C. G. Chidester and D. G. Kaiser, *J. Pharm. Sci.*, 53 (1964) 726.

CHROM. 14,290

## URONIC ACID ANALYSIS BY HIGH-PERFORMANCE LIQUID CHROMATOGRAPHY AFTER METHANOLYSIS OF GLYCOSAMINOGLYCANS

A. HJERPE\*

*Department of Pathology II, Karolinska Institutet, F2-42, Huddinge University Hospital, S-141 86 Huddinge (Sweden)*

C. A. ANTONOPOULOS

*Laboratory of Organic Chemistry, University of Patras, Patras (Greece)*

and

B. CLASSON\*, B. ENGFELDT and M. NURMINEN

*Department of Pathology II, Karolinska Institutet, F2-42, Huddinge University Hospital, S-141 86 Huddinge (Sweden)*

(First received August 3rd, 1981; revised manuscript received August 18th, 1981)

---

### SUMMARY

Two high-performance liquid chromatographic applications for the study of glucuronic and iduronic acid in glycosaminoglycans are presented. In the simplest form these uronic acids are separated on a reversed-phase column as their 1-methylglycoside-6-methyl esters, *i.e.*, the form in which they are recovered after methanolysis. The sensitivity for glucuronic acid is somewhat increased if the polysaccharide is deaminated prior to methanolysis, the subsequent separation being performed on a weak ion-exchange column. To allow this separation, however, an extra preparative step is necessary, consisting of alkaline hydrolysis of the ester bonds. Using these separations, the conditions for methanolysis were studied. Optimal release of uronic acids was achieved after 30–50 h of methanolysis using 1 *M* dry HCl in methanol at 100°C.

---

### INTRODUCTION

The identification of dermatan sulphate in glycosaminoglycan preparations requires the determination of iduronic acid and glucuronic acid. Enzymatic reactions<sup>1</sup>, paper chromatography<sup>2</sup>, gas chromatography<sup>3</sup> and ion-exchange chromatography<sup>4</sup> have been used to determine the amounts of these uronic acids.

One problem common to all the chromatographic procedures is the depolymerization reactions by which the uronic acids are liberated. One way to perform this disintegration is to hydrolyze the polysaccharides using sulphuric acid<sup>4</sup>, formic acid<sup>3</sup> or ion-exchange resins in hydrochloric acid<sup>5</sup>. Since the uronic acids in water are less

---

\* Present address: Department of Organic Chemistry, University of Stockholm, Stockholm, Sweden.



stable at low pH, methanolysis has been used as an alternative<sup>6,7</sup>. By this procedure the uronic acids are obtained as their 1-methylglycoside-6-methyl esters, and problems with mutarotation reactions during the chromatographic procedure are thereby eliminated. Furthermore, it has been claimed that the recovery of glucuronic acid as well as iduronic acid is higher when compared to the hydrolytic procedures.

The ion-exchange systems used to separate the uronic acids, involve chromatography on strong ion-exchange resins, and the times required are in the order of 1.5–6 h. High-performance liquid chromatography (HPLC) on weak ion-exchange resins has proved to be useful for the separation of isomeric anionic disaccharides<sup>8</sup>, the separation being completed within 20 min. In order to obtain a simple and more sensitive determination of iduronic acid and glucuronic acid in glycosaminoglycans we tried various HPLC separations of the methanolysate products. Since such a separation by ion-exchange chromatography requires the removal of the 6-methyl esters, the separation of intact esters in reversed-phase systems was primarily studied. Using this determination of uronic acids, we could also study the conditions for the methanolysis.

#### MATERIALS AND METHODS

Chondroitin sulphate (CS) was prepared from bovine nasal cartilage as described by Antonopoulos *et al.*<sup>9</sup>. Different dermatan sulphate preparations with different iduronic/glucuronic acid ratios, as well as a pure iduronic acid preparation, were gifts from Dr. Anders Malmström, Lund. Commercially available dermatan sulphate, prepared from porcine skin (Sigma), was also used. All other chemicals used were of analytical grade. To evaluate the methanolysis and chromatographic procedures, various chondroitin sulphate–dermatan sulphate mixtures were used. The iduronic/glucuronic acid ratios of these mixtures were estimated enzymatically<sup>1</sup>, measuring the amount of 4,5-unsaturated uronic acids<sup>10</sup> liberated by chondroitinase ABC and AC, or by <sup>1</sup>H nuclear magnetic resonance (NMR) spectral analysis, comparing the resonance peaks of the anomeric uronic acid protons.

Methanolysis was performed in sealed Pyrex glass tubes using 0.5 M or 1 M dry HCl in methanol. The reaction was tested at different temperatures (80–120°C) and at different time intervals (6–100 h). The effect of deacetylation and deamination<sup>7,11</sup> prior to methanolysis was also studied. In order to remove irrelevant decomposition products, the dried methanolysates were dissolved in a small volume of methanol and added to an ion-exchange column (20 × 3 mm I.D.) of Dowex 50-X8, on which 20 × 3 mm I.D. of AG 1-X8 is layered. This column was then washed with 2.0 ml methanol; the pooled eluate containing virtually all uronic acid-6-ester which was subsequently desiccated. This preparative step is, however, not necessary for the subsequent HPLC separation when pure polysaccharide preparations are to be studied. Preparations intended for ion-exchange chromatography were thus prepared and subsequently dissolved in 1% ammonia in water, thereby hydrolyzing the ester bonds at 100°C for 3 h. After desiccation these preparations were ready for the ion-exchange HPLC procedure.

The materials to be chromatographed were dissolved in eluent and particulate materials were removed by centrifugation at 10,000 g for 5 min. The materials were subsequently added to the column via a loop injector. Reversed-phase chromatogra-

phy of non-hydrolyzed methanolyzates was performed using either a ODS-Hypersil column (250 × 4.6 mm I.D.) (Shandon, Southern Products, Great Britain) or a Supelcosil RC 18 column (150 × 4.6 mm I.D.) (Supelco, Switzerland) with a ODS-Hypersil precolumn (50 × 4.6 mm I.D.). These columns were eluted with 5% methanol which was pumped at 0.5 ml/min in an Optilab 931 chromatograph equipped with a high sensitivity refractive index (RI) detector (15-mm cell) at just above room temperature, or by connecting the column to a Technicon AutoAnalyzer II system designed for the carbazole reaction<sup>12</sup>. When using RI detection the dimethyl ester of DL-tartaric acid was found to be a suitable internal standard, eluting shortly after the main glucuronic acid peak.

Ion-exchange chromatography of hydrolyzed methanolyzates was performed on an APS-Hypersil column (250 × 4.6 mm I.D.) (Shandon). The column was eluted with 0.02 M sodium acetate, pH adjusted to 3.4 with acetic acid. The eluate was pumped at 0.7 ml/min and monitored with the same high-sensitivity RI detector as above.

## RESULTS AND DISCUSSION

As shown in Fig. 1 the material is eluted from the reversed-phase column within seven column volumes, *i.e.*, within 20 min. With shorter methanolysis times a minor peak may be recorded at 23 min. Recovery experiments indicate that no carbazole reactive material is retained on the column after this period. With the RI-detector used, separate peaks containing 0.5 µg can be determined within a 95% confidence interval. When the AutoAnalyzer II was used as detector (Fig. 1d-f), the sensitivity was about the same, but the resolution of the chromatogram was considerably reduced.

The treatment of free glucuronic acid with 1 M HCl in methanol gives a product which can be separated into at least four different carbazole reactive peaks (Fig. 1d). The first of these is eluted with the front, similar to free uronic acids. A second peak is eluted at capacity factor,  $k' = 1$  (6.6 min). This is the region where glucuronolactone and 1-methylglycosides of hexoses are eluted, while methanol is recovered immediately prior to this peak (a negative peak in Fig. 1a-c) and while the 1-methylglycoside of xylose is eluted slightly later (7.5 min). It may well be that the anhydrous "methanolytic" conditions would also yield a lactone, which is eluted with this second peak. The third and fourth carbazole reactive peaks are eluted at  $k' = 3.5$  and 4.5 (13.8 and 16.4 min). From the chromatographic behaviour we suggest that these peaks consist of 1-methylglycoside-6-methyl esters in their  $\beta$ - and  $\alpha$ -anomeric configurations respectively.

CS methanolyzates give a pattern similar to "methanolyzed" glucuronic acid (Fig. 1b and e) with two retarded peaks. When dermatan sulphate methanolyzates are chromatographed at least four additional and probably iduronic acid derived peaks occur (Fig. 1c and f). The appearance of several iduronic acid derivatives after methanolysis is in accordance with earlier findings<sup>7</sup>. The major iduronic acid peak is eluted at  $k' = 2.9$  (11.4 min). This peak and the main glucuronic acid derivative (16.4 min) are both recorded without interference from other uronic acid derivatives.

A further increased sensitivity of the uronic acid determination could be obtained by ion-exchange chromatography (Fig. 2). This determination is, however,

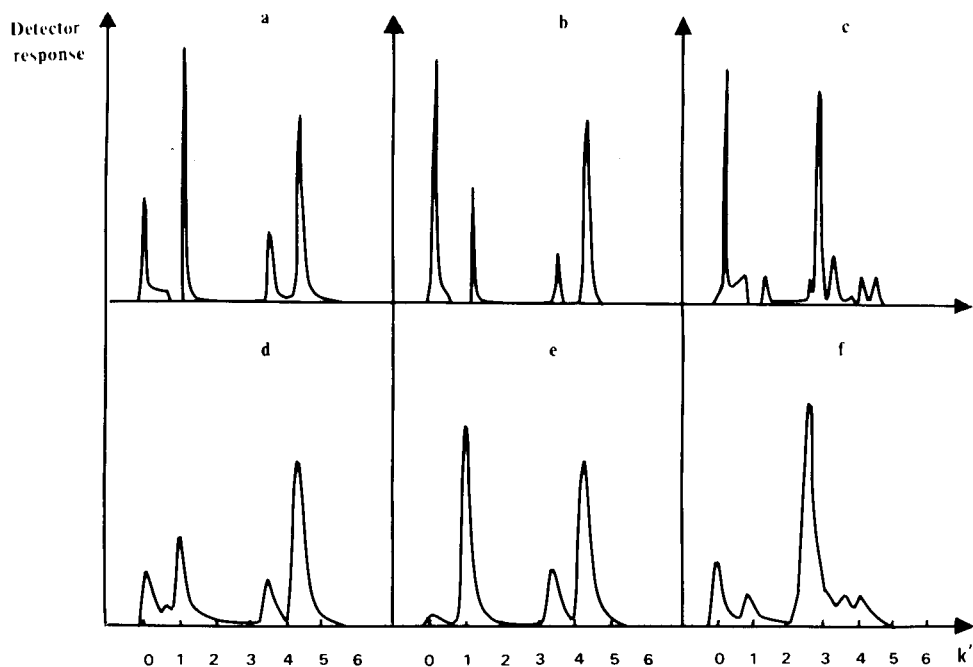


Fig. 1. Chromatography of methanolyzate products on ODS-Hypersil® using RI detection (a-c) or automatic carbazole reaction (d-f) to record the eluate. a, d, Glucuronic acid kept under methanolytic conditions; b, e, chondroitin sulphate and c, f, dermatan sulphate.

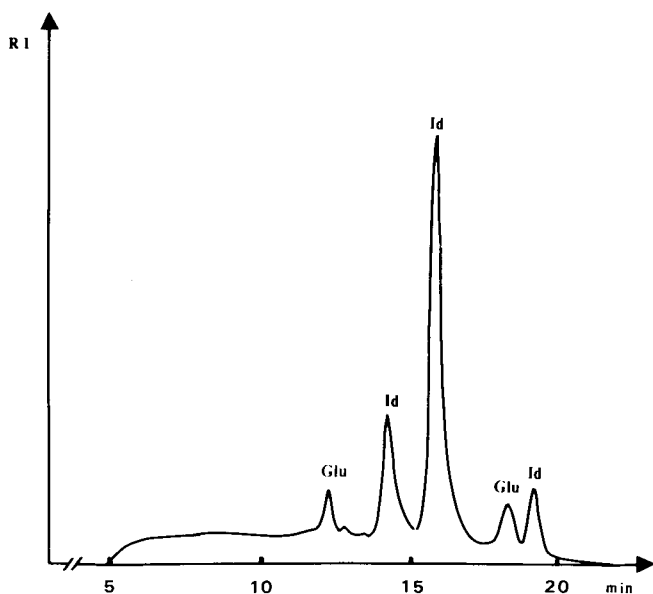


Fig. 2. Chromatography of hydrolyzed dermatan sulphate methanolyzate on APS-Hypersil® using RI detection. Id = Iduronic acid; Glu = glucuronic acid.

somewhat more laborious, since it requires the hydrolysis of the ester bonds. Recovery experiments indicated a virtually complete uronic acid recovery from this hydrolysis, when it was performed with 1%  $\text{NH}_3$  as described above. In the ion-exchange chromatogram two glucuronic acid and three iduronic acid derived peaks can be distinguished. Here the main iduronic acid peak is obtained at 16 min and the main glucuronic acid peak at 18.5 min. The pH interval used is just above the  $pK$  values of the studied uronic acids. This pH was experimentally found to give optimal separation of the peaks, and even minor pH deviations caused confluence of the peak materials.

In order to optimize the release of these main peak materials, the conditions for the methanolysis procedure were studied (Fig. 3). When the lower HCl concentration (0.5  $M$  instead of 1  $M$ ) was used the disintegration was slower and with similar maximal recovery of the uronic acid derivatives. With 1  $M$  HCl, maximal iduronic acid recovery was obtained after methanolysis for 6 h, while the glucuronic acid derivative, on the other hand, was not released at the same rate, the maximum being obtained after 18 h. Except for methanolysis at 120°C, longer reaction times did not significantly alter the recovery. The temperatures tested (80°C, 100°C and 120°C) only gave slightly varying results. The iduronic/glucuronic acid ratios obtained from 30–50 h of methanolysis were virtually independent of temperature variations within the interval studied. When the sum of the carbazole reactive peaks was measured, using an external glucuronic acid standard, the total recovery from chondroitin sulphate was 33% and from dermatan sulphate 64% of the expected values. Half of these total recovery figures corresponded to main peak materials.

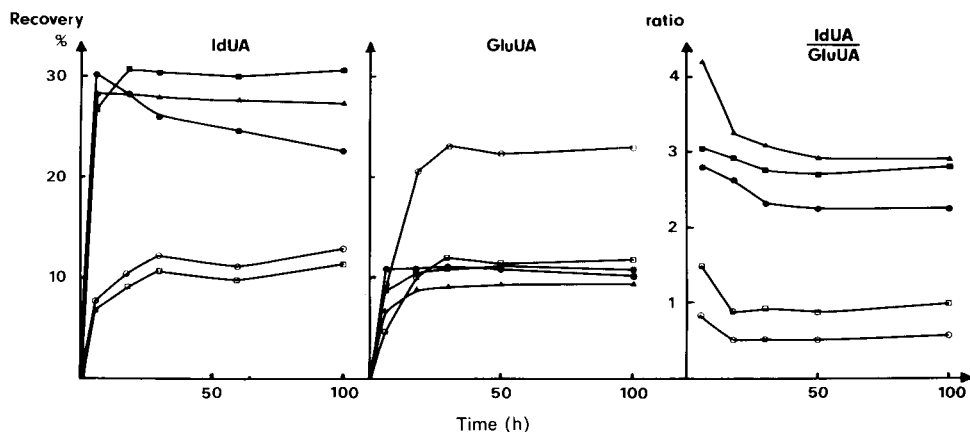


Fig. 3. Recoveries from the methanolysis of iduronic acid (IdUA) main peak material and glucuronic acid (GluUA) main peak material, as well as the obtained ratios between these recoveries. The methanolyses were performed on glycosaminoglycans using 1  $M$  HCl in dry methanol at 80°C ( $\blacktriangle$ ), 100°C ( $\blacksquare$ ) and 120°C ( $\bullet$ ), as well as on deacetylated deaminated preparations at 80°C ( $\square$ ) and 100°C ( $\circ$ ), the time for methanolysis varying from 6 to 100 h.

These recoveries are somewhat lower than those given by Inoue and Miyawaki<sup>7</sup>. The obtained values may, however, be artificially low, as indicated by comparing the carbazole and RI results. The first way of detecting uronic acids gives their molar amounts, while the second is more related to the total mass of the peak

material. The obtained RI/carbazole ratios are higher than can be explained by the molecular weight increase corresponding to two methyl groups. Furthermore, the expected lower carbazole reactivity for iduronic acid derivatives is not observed. One explanation for these findings may be that the derived uronic acids possess lower reactivity in the carbazole reaction, the decrease being somewhat more pronounced with the glucuronic acid derivative. If this is true the reported recoveries are artificially low.

The lower recovery of glucuronic acid after methanolysis alone has been shown by Inoue and Miyawaki<sup>7</sup> to be due to the higher resistance of the glucuronidic linkage compared with the iduronidic linkage. These authors also demonstrated that higher glucuronic acid recovery was obtained after deacetylation and deamination of the glycosaminoglycans prior to methanolysis. After 30–50 h of methanolysis the deacetylated and deaminated sample showed similar recoveries of glucuronic acid main peak material and a considerable decrease in iduronic acid main peak material compared to the non-deacetylated sample (Fig. 3). When the deaminated materials were hydrolyzed and chromatographed on the ion-exchange column, glucuronic acid recoveries considerably increased, which is in accordance with earlier results<sup>7</sup>. The time curve also indicates a pattern of different resistance to methanolysis for these deaminated glycosaminoglycans. While the glucuronic acid derivative shows maximum values after 18 h of methanolysis, the full release of iduronic acid is not obtained until after 50 h. It thus seems as if the deamination procedure somehow decreases the rate by which iduronic acid is released. This effect has not yet been further studied.

Fig. 4 shows the linear recoveries of glucuronic acid and iduronic acid from the different chondroitin sulphate–dermatan sulphate preparations. The deviations from the indicated lines may well be due to errors in the enzymatic determinations rather than in the HPLC procedure. The correct uronic acid ratio in a glycosaminoglycan preparation may therefore be calculated by relating the results to a standard prepara-

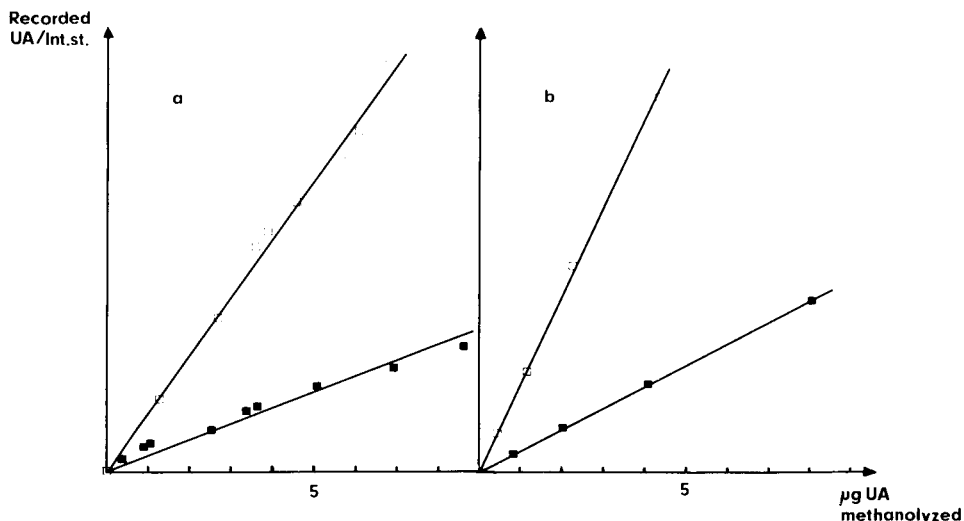


Fig. 4. Standard curves obtained for chondroitin sulphate–dermatan sulphate preparations with iduronic acid/glucuronic acid ratios determined enzymatically (a) and by <sup>1</sup>H NMR analysis (b). ■, Glucuronic acid; □, iduronic acid. Note the better correlation in the last case.

tion of known uronic acid composition. Duplicate determinations require 40–80  $\mu\text{g}$  or more of the polysaccharide preparation (corresponding to 10–20  $\mu\text{g}$  uronic acid, *cf.*, Fig. 4). The sensitivity can be increased by the deamination procedure and subsequent ion-exchange HPLC, especially when the glycosaminoglycan in question has a low glucuronic acid content. One reason for the improved sensitivity may be that the alkaline hydrolysis not only splits the methyl ester bonds, but also the lactone bonds formed during methanolysis. A higher recovery within the main peaks would thus ensue.

According to these results the uronic acid composition in chondroitin sulphate–dermatan sulphate preparations can be analyzed according to the following scheme. The dried glycosaminoglycan preparation is methanolized in sealed ampoules using 1 *M* dry HCl in methanol for 30–50 h at 100°C. The samples are subsequently dried, and purified with the use of a small Dowex 50-X8/AG 1-X8 mixed ion-exchange column. With the dimethyl ester of DL-tartaric acid as internal standard and comparing the chromatograms with known chondroitin sulphate and dermatan sulphate preparations, the iduronic acid and glucuronic acid contents are directly determined by reversed-phase chromatography. With lower amounts of glycosaminoglycans, it is preferable to deacylate and deaminate the polysaccharides prior to methanolysis. After methanolysis the materials are desiccated and subsequently hydrolyzed with 1%  $\text{NH}_3$  in water. The resulting products are lyophilized again and subjected to ion-exchange chromatography.

#### ACKNOWLEDGEMENTS

This study has been supported by a grant from the Swedish Medical Research Council, No. B81-12X-05943-01 and from the funds of the Karolinska Institute. The authors are indebted to Ms. I.-L. Wallgren for typing the manuscript and to Ms. K. Ormstad for linguistic advice.

#### REFERENCES

- 1 H. Saito, T. Yamagata and S. Suzuki, *J. Biol. Chem.*, 243 (1968) 1536–1542.
- 2 B. Radhakrishnamurthy and G. S. Berenson, *Arch. Biochem. Biophys.*, 101 (1963) 360–362.
- 3 B. Radhakrishnamurthy, E. R. Dalferes, Jr. and G. S. Berenson, *Anal. Biochem.*, 24 (1968) 397–408.
- 4 L. Å. Fransson, L. Rodén and M. L. Spach, *Anal. Biochem.*, 21 (1968) 317–330.
- 5 M. J. Spiro, *Anal. Biochem.*, 82 (1977) 348–352.
- 6 J. R. Clamp, T. Bhatti and R. E. Chambers, *Methods Biochem. Anal.*, 19 (1971) 229–344.
- 7 S. Inoue and M. Miyawaki, *Anal. Biochem.*, 65 (1975) 164–174.
- 8 A. Hjerpe, C. A. Antonopoulos and B. Engfeldt, *J. Chromatogr.*, 171 (1979) 339–344.
- 9 C. A. Antonopoulos, S. Gardell, J. A. Szirmai and E. R. de Tyssonsk, *Biochim. Biophys. Acta*, 83 (1964) 1–19.
- 10 V. C. Hascall, R. L. Riolo, J. Hayward, Jr. and C. C. Reynolds, *J. Biol. Chem.*, 247 (1972) 4521–4528.
- 11 D. Lagunoff and G. Warren, *Arch. Biochem. Biophys.*, 99 (1962) 396–400.
- 12 A. Hjerpe, C. A. Antonopoulos and B. Engfeldt, *Scand. J. Clin. Lab. Invest.*, 39 (1979) 491–494.

CHROM. 14,315

## CHROMATOGRAPHY OF CELLODEXTRINS AND ENZYMATIC HYDROLYSATES OF CELLULOSE ON ION-EXCHANGE DERIVATIVES OF SPHERON

Z. HOSTOMSKÁ-CHYTILOVÁ and O. MIKEŠ\*

*Institute of Organic Chemistry and Biochemistry, Czechoslovak Academy of Sciences, 166 10 Prague 6 (Czechoslovakia)*

P. VRÁTNÝ

*Institute of Agriculture, 160 21 Prague 6 (Czechoslovakia)*

and

M. SMRŽ

*Research Institute of Pure Chemicals, Lachema, 621 33 Brno (Czechoslovakia)*

(Received September 1st, 1981)

---

### SUMMARY

Cellodextrins (cellohexaose to cellobiose) and glucose were separated on derivatives of Spheron®. The optimum conditions found (TEAE-Spheron 1000; 0.025 *M* sodium borate, pH 7.5 or 8.0) are suitable for the chromatography of cellodextrins prepared from acid hydrolysates of cellulose. The same conditions can be used for the separation of the enzymatic hydrolysates of cellulose. At higher buffer concentrations (0.1–0.35 *M*) and at higher pH (8.5–8.8) lower sugars can be chromatographed together with cellodextrins. The enzymatic hydrolysate of cellulose, prepared by means of cellulases from *Trichoderma viride*, was most conveniently chromatographed on DEAE-Spheron 300 in 0.25 *M* sodium borate, pH 7.5, when the separation of glucose and cellobiose was achieved. For simultaneous detection of glucose, cellobiose and further cellodextrins, a two-column system was developed, composed of DEAE-Spheron and TEAE-Spheron.

---

### INTRODUCTION

By use of enzymatic methods or partial acid hydrolysis, cellulose can be split into cellodextrins. These are linear oligomers consisting of two to seven glucose units linked by  $\beta$ -1,4-glucoside bonds. The final product of their hydrolysis is glucose. Study of the quantitative course of the enzymatic hydrolysis and of the catalytic effect of individual enzymes led to the development of numerous techniques for the separation of the hydrolysis products, one of which is liquid chromatography on various types of ion exchangers.

The separation of cellodextrins may be achieved on cation exchangers in various forms by elution with water<sup>1</sup> or aqueous solutions of organic solvents<sup>2</sup>, or on

anion exchangers eluted with borate buffers<sup>3</sup>. Anion-exchange derivatives of Spheron have already been used for the chromatography of monosaccharides<sup>4</sup> and of mixtures of mono- and oligo-saccharides<sup>5</sup>.

In this paper the liquid chromatography of sugars and their borate complexes on Spheron derivatives has been investigated for the separation of cellodextrins, for the study of the course of their hydrolysis and as a method for monitoring the enzymatic hydrolysis of cellulose.

## EXPERIMENTAL

### Materials

Medium basic anion exchangers DEAE-Spheron 300 (capacity 0.6 mequiv./g and 2.2 mequiv./g) were laboratory products<sup>6</sup> (particle size 20–40  $\mu\text{m}$ ). A partly quaternized derivative (*cf.*, Type 2, capacity 2.2 mequiv./g; ref. 7) was prepared from DEAE-Spheron 300 (particle size 20–40  $\mu\text{m}$ ). This derivative had half of the total number of diethylaminoethyl groups quaternized. Fully quaternized TEAE-Spheron 1000 (capacity 1.4 mequiv./g, particle size 25–40  $\mu\text{m}$ ; and 2 mequiv./g, 13–18  $\mu\text{m}$ ) and sulphonated S-Spheron cation exchanger (1.42 mequiv./g, 13–18  $\mu\text{m}$ ) were experimental laboratory products from Lachema (Brno, Czechoslovakia).

Cellohexaose, cellopentaose, cellotetraose, cellotriose and cellobiose\* were prepared in the pure form according to Miller *et al.*<sup>8</sup>. Monosaccharides and all other analytical grade chemicals used were commercial products of Lachema.

The crude preparation of cellulases was prepared from a liquid cultivation medium of *Trichoderma viride* (Research Institute of the Food Industry, Prague, Czechoslovakia) by desalting on Bio-Gel P-6 and freeze-drying.

### Methods

Chromatography was carried out on a sugar analyzer 71 000 (Developmental Workshops of the Czechoslovak Academy of Sciences) described in ref. 4. The preparation of buffers, solutions of saccharides, detection reagent and the adjustment of ion exchangers has also been described<sup>4</sup>. 100- $\mu\text{l}$  Samples, containing mostly 30  $\mu\text{g}$  of individual saccharides, were injected.

*Enzymatic hydrolysis of cellulose.* Ten milligrams of chromatography paper Whatman No. 1 (Whatman, Springfield Mill, Maidstone, Great Britain), ground in a ball mill, indicated as W1, were incubated with 1.5 mg of lyophilized cellulase preparation (from *T. viride*) in 1.5 ml of 0.05 M citrate buffer, pH 4.8, at 40°C for 10, 45 and 90 min.

*Enzymatic hydrolysis of cellodextrins.* Cellopentaose (410  $\mu\text{g}$ ) was incubated with 48  $\mu\text{g}$  of lyophilized cellulases (*T. viride*) in 60  $\mu\text{l}$  of 0.05 M of citrate buffer, pH 4.8, at 40°C for 0.2, 0.45, 2.0 and 5.0 min.

---

\* These cellodextrins and the monomer will be indicated as G<sub>6</sub>, G<sub>5</sub>, G<sub>4</sub>, G<sub>3</sub>, G<sub>2</sub> and G<sub>1</sub> (glucose). Substances G<sub>2</sub>–G<sub>6</sub> are sometimes named cellooligosaccharides.



## RESULTS

*Effect of pH*

The separation of a mixture of celloextrins  $G_2$ – $G_6$  on TEAE-Spheron 1000 in the pH 7–9 region was studied at constant molarity of the borate buffer, 0.025  $M$ . The dependence of the retention volumes and of the resolution of neighbouring pairs of celloextrins on pH is shown in Fig. 1.

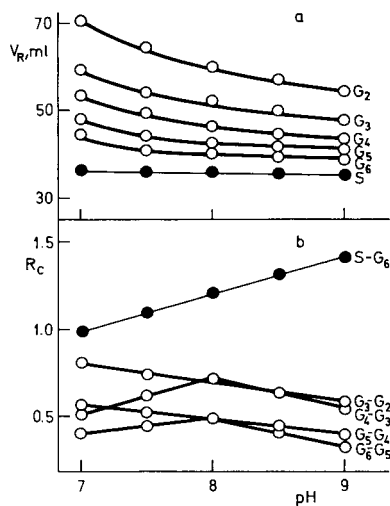


Fig. 1. Dependence of retention volumes,  $V_R$ , of celloextrins  $G_2$ – $G_6$  and saccharose (S) (a), and of resolution,  $R_c$  (b), on the pH values of 0.025  $M$  borate buffers during chromatography on TEAE-Spheron 1000 (2.0 mequiv./g, 13–18  $\mu m$ ). Column: 200  $\times$  8 mm I.D.; temperature 60°C. Flow-rate: 50 ml/h (flow of orcinol– $H_2SO_4$  through detector 1.93 ml/min plus 0.42 ml/min of effluent). The retention volumes are not corrected with respect to the volume of the detection system. The resolution values are corrected with respect to the spreading of the peaks in the detection system.

Saccharose (which is very weakly retained on the ion exchanger) was always added to the mixture of celloextrins. In the pH 7–9 region it was found that with increasing pH the retention volumes of all celloextrins are decreased.  $G_6$  is least strongly retained, and with decreasing number of glucose units the retention volumes of celloextrins increase.

The calculated values for the resolution of neighbouring pairs are dependent on pH. The pairs  $G_6$ – $G_5$ ,  $G_4$ – $G_3$  have optimum resolution at pH 8, while for  $G_5$ – $G_4$  and  $G_3$ – $G_2$  the resolution decreases with increasing pH. For further experiments the values pH 7.5 and 8 were selected.

From the calculation of the number of theoretical plates of a given column,  $n_c$ , it was found that the  $n_c$  values for  $G_6$ ,  $G_5$  do not vary greatly with pH, and those for  $G_4$ ,  $G_3$  and  $G_2$  slightly decrease with increasing pH.

*Ionic strength effect*

Chromatography of a mixture of  $G_2$ – $G_6$  was carried out at constant pH 7.5 on a TEAE-Spheron column in the borate form. After equilibration, elution was carried

out with water and borate buffers (0.005 *M*, 0.01 *M*, 0.017 *M*, 0.02 *M*, 0.25 *M* and 0.03 *M*). The dependence of the elution volumes,  $V_R$ , and the resolution,  $R_C$ , of cellodextrins on molarity is shown in Fig. 2.

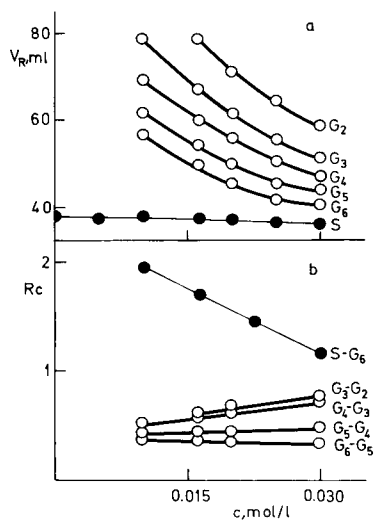


Fig. 2. Dependence of retention volumes of cellodextrins and saccharose (a) and of resolution (b) on the borate concentration in the elution buffer, pH 7.5, during chromatography on TEAE-Spheron 1000 (13–18  $\mu\text{m}$ , 2 mequiv./g). Conditions as in Fig. 1.

None of the cellodextrins could be eluted with water or with the 0.005 *M* borate buffer. Only saccharose was eluted. On chromatography with the 0.01 *M* buffer only  $G_2$  was retained, while higher cellodextrins were eluted with the indicated  $V_R$  values. With increasing molarity of the borate buffers, the elution volumes of all cellodextrins present were decreased.

In the buffer molarity range investigated it was found that for neighbouring pairs of cellodextrins the resolutions usually slightly increased with increasing borate concentration. From the values of the theoretical plates,  $n_c$ , it was found that for  $G_6$  and  $G_5$  the  $n_c$  values do not change with increasing molarity and for  $G_4$ ,  $G_3$  and  $G_2$  the  $n_c$  values increase.

For further experiments the concentration 0.025 *M* was selected.

#### *Elution of monosaccharides and cellodextrins*

The chromatography of cellodextrins was investigated in the presence of monosaccharides. It was evident that TEAE-Spheron 1000 is a suitable support for the separation of more complex mixtures of saccharides. Optimum conditions for the separation of  $G_2$ – $G_6$  and of mannose, arabinose, galactose, xylose and glucose by step-wise elution were as follows: elution with 0.025 *M* borate buffer of pH 7.5 on a column equilibrated with the same buffer, followed by 50 ml of 0.1 *M* borate buffer, pH 8.5, and 50 ml of 0.25 *M* borate buffer, pH 8.8. Elution of monosaccharides was only achieved when the 0.35 *M* borate buffer, pH 8.8, was applied. Glucose was eluted after 4 h.

The possibilities of substitution of step-wise elution by linear gradient elution with buffers of increasing pH and molarity are illustrated in Fig. 3. This figure shows a record of the chromatography of a mixture of monosaccharides and cello dextrans where isocratic elution of cello dextrans is followed by a steep linear gradient. Elution of glucose was achieved with 0.25 M buffer, pH 8.8, after 3.5 h. For the conditions see the caption to Fig. 1.

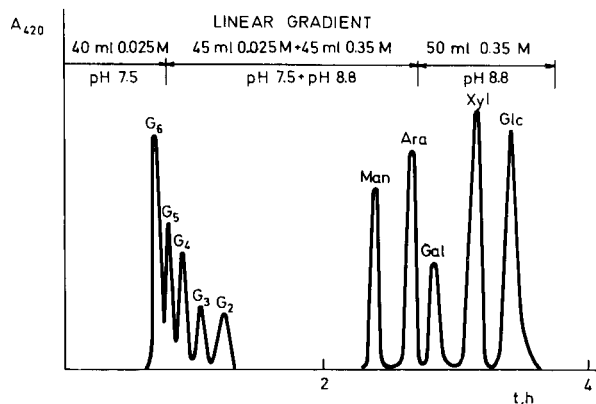


Fig. 3. Chromatography of a mixture of cello dextrans  $G_2$ – $G_6$  and five monosaccharides, arabinose (Ara), xylose (Xyl), galactose (Gal), mannose (Man) and glucose (Glc), on TEAE-Spheron 1000 (13–18  $\mu\text{m}$ , 2.0 mequiv./g). The column was equilibrated with 0.025 M borate buffer, pH 7.5. Elution was carried out first isocratically with 0.025 M borate buffer, pH 7.5, then a linear gradient was applied (45 ml of 0.025 M borate buffer, pH 7.5, plus 45 ml of 0.35 M borate buffer, pH 8.8). Chromatography was terminated by elution with 0.35 M borate buffer, pH 8.8. For other parameters see Fig. 1.

#### *Chromatography of enzymatic hydrolysates of cello dextrans*

The optimum conditions found for chromatography of cello dextrans may be used in the analysis of the effect of cellulolytic enzymes on individual cello dextrans. As an example, the hydrolysis of  $G_5$  with the cellulolytic system of the *T. viride* strain was selected. The reaction was carried out as mentioned in *Methods*. 30- $\mu\text{l}$  Aliquots were taken from the mixture and injected directly into the column (see Fig. 4).

#### *Chromatography of enzymatic hydrolysates of cellulose*

From the results of the chromatography of monosaccharides (Fig. 3) it follows that the strongly basic group of TEAE-Spheron enables the elution of glucose only by disturbance of the isocratic conditions through the introduction of a new buffer of 0.25 M and pH 8.8. To enable the isocratic elution of all hydrolysis products, the basicity of the functional group must be decreased. For the monitoring of the main products of the hydrolysis of cellulose,  $G_1$  and  $G_2$ , a suitable support from the series of DEAE-Spheron<sup>6</sup> was sought. DEAE-Spheron of capacity 0.6 mequiv./g and particle size 20–40  $\mu\text{m}$  was selected. With this support a 0.025 M buffer (pH 7.5) could be used which had already been found to be suitable in connection with TEAE-Spheron. The chromatography of the enzymatic hydrolysate is shown in Fig. 5.

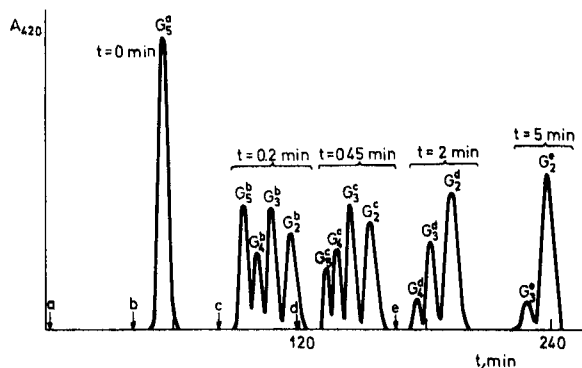


Fig. 4. Formation of lower cellobioses by action of the cellulolytic enzymes from *T. viride* on  $G_5$ . The column of TEAE-Spheron 1000 was equilibrated with 0.025 *M* borate buffer, pH 7.5, which was also used for isocratic elution. Conditions as in Fig. 1. The arrow and the letters a, b, c, d and e indicate the points of injection of the hydrolysates. a, Cellopentaose was not incubated with cellulases; b, time of incubation was 0.2 min; c, 0.45 min; d, 2 min; e, 5 min. The total time of chromatography was 78 min. The effluent persisted for 27 min in the detector. New samples were injected before the preceding analysis was terminated, approximately at 45-min intervals.

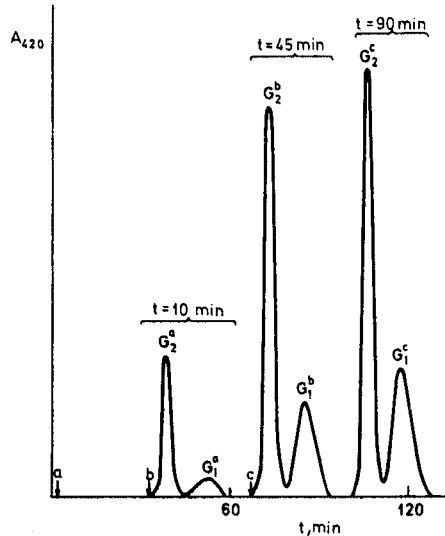


Fig. 5. Chromatography of the hydrolysate of the ground paper W1 with the cellulolytic enzymes of *T. viride* carried out on a column of DEAE-Spheron 300 (0.6 mequiv./g, 20–40  $\mu$ m), 250  $\times$  8 mm I.D., at 60°C; flow-rate 50 ml/h. The column was equilibrated and the elution carried out with 0.025 *M* borate buffer, pH 7.5. For the preparation of the hydrolysate see *Methods*. 100- $\mu$ l Samples hydrolysed for 10 min, 45 min and 90 min were injected. The total time of analysis was about 60 min, of which the eluent spent 27 min in the detector, and further samples were injected every 30 min. For the labelling of peaks see Fig. 4.

## DISCUSSION

Saccharides can be separated on ion exchangers<sup>9</sup> either using the partition chromatography principle, *i.e.*, elution with aqueous solutions of organic solvents,

mainly ethanol<sup>10</sup> of various concentrations or water<sup>11</sup>, or using ion-exchange chromatography with borate buffers of various pH and ionic strengths<sup>12</sup>. However, during the separation of some cellodextrins in the ethanol–water system precipitation may take place<sup>13</sup>. Moreover, the hydrolysates contain salts and proteins which also precipitate in aqueous–alcoholic solutions. The elimination of the precipitate affects the total content of cellodextrins in the sample. Chromatography of cellodextrins on cation exchangers with water as eluent is more advantageous than the use of organic solvents in that the sample is completely soluble in water, thus avoiding adjustment of the sample before chromatography<sup>14</sup>.

We therefore tested the possibility of chromatographing cellodextrins on a cation-exchange derivative of S-Spheron 1000 (particle size 13–18  $\mu\text{m}$ ) converted into its calcium form. Elution was carried out with deionized water at 85°C. Under these conditions individual saccharides could not be separated. The mixtures applied were eluted within the hold-up volume as a single peak. The previous separation of cellodextrins by this method<sup>1</sup> was carried out on supports of the xerogel type in which the sugar molecules must diffuse into the gel matrix. The hybrid support used by us has a macroreticular structure<sup>7</sup> created by very densely cross-linked xerogel microspheres into which sugar molecules cannot penetrate. The macropores are of the aerogel type and they are so large that the size exclusion effect cannot occur; this is probably the reason why the separation did not take place.

Therefore a suitable support was sought from the group of Spheron anion-exchange derivatives. On DEAE-Spheron higher oligosaccharides cannot be separated<sup>4</sup>. However, we used this type of anion exchanger to study the hydrolysis of cellulose with cellulases, during which glucose and cellobiose were well separated (Fig. 5). On a derivative of DEAE-Spheron 300, Type II (ref. 7), quaternized to 50% (*cf.*, ref. 5), higher cellodextrins G<sub>3</sub>–G<sub>6</sub> were poorly separated. On TEAE-Spheron 1000 (capacity 1.2 mequiv./g), a DEAE-derivative additionally fully quaternized with ethyl halide, G<sub>2</sub> and G<sub>3</sub> were well separated but the separation of G<sub>4</sub>–G<sub>6</sub> was imperfect. The best results were achieved on TEAE-Spheron 1000 (capacity 2 mequiv./g, particle size 13–18  $\mu\text{m}$ ) which even gave good separations of mixtures of saccharides more complex than those mentioned in Fig. 3. For this support the optimum conditions for elution were determined (Figs. 1 and 2) and they were exploited for monitoring the hydrolysis course of cellodextrins (Fig. 4).

Chromatography on a strongly basic quaternized support does not permit simultaneous elution of cellodextrins and glucose under isocratic conditions. Higher cellodextrins are very weakly retained on DEAE-derivatives and are therefore not separated, while glucose is retained sufficiently. On TEAE-derivatives, cellodextrins are well separated, while glucose is retarded excessively. Therefore, we tested the separation of G<sub>1</sub>–G<sub>6</sub> by means of a system of two columns (Fig. 6). Before the column with TEAE-Spheron (capacity 2 mequiv./g) another column was inserted, packed with DEAE-Spheron of lower capacity (0.6 mequiv./g) which should be selected optimally. On this column the group of cellodextrins were separated from glucose on isocratic elution. Their mutual separation was achieved on a second column with TEAE-Spheron using the same buffer. Switching between columns permitted consecutive detection of the separated cellodextrins and glucose after a single injection (Fig. 7).

The described method of chromatography of borate complexes of cellodextrins

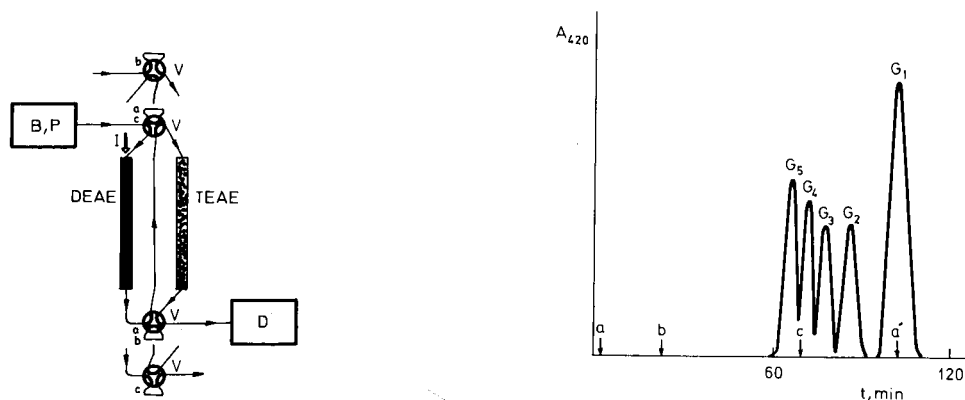


Fig. 6. Two-column ion-exchange system for simultaneous analysis of glucose, cellobiose and cellodextrins by isocratic elution. B, P = Buffer container and a laboratory piston-pump; V = six-port valve; a, b, c = individual positions of the valve; I = injector; DEAE, TEAE = ion-exchange columns of DEAE-Spheron 300 (250 × 8 mm), 20–40  $\mu\text{m}$ , 0.6 mequiv./g. and TEAE-Spheron 1000 (200 × 8 mm), 13–18  $\mu\text{m}$ , 2.0 mequiv./g.; D = detection system. A three-step operation cycle is employed (*cf.*, Fig. 7): after the introduction of the sample, valve position a connects the two columns for a short time (glucose is retained on the first, and cellodextrins pass into the second column). Position b excludes the first column and a separation of cellodextrins takes place in the second column. After detection of  $G_5$  ( $G_2$ – $G_4$  are already in the detector system) the second column is excluded by position c and the first column is simultaneously connected to the detector until glucose ( $G_1$ ) is eluted. Then the system is ready for a further cycle. Buffer: 0.025 M sodium borate, pH 7.5. Flow-rate: 50 ml/h. Temperature: 60°C.

Fig. 7. Chromatography of cellodextrins and glucose on the two-column system described in Fig. 6. Samples of 20  $\mu\text{g}$  of cellodextrins  $G_2$ – $G_6$  and 40  $\mu\text{g}$  of glucose ( $G_1$ ) were injected into a DEAE column. The letters a–c correspond to the three positions of the valve in Fig. 6. A further sample for analysis can be injected into this isocratic elution at the position a' (arrow).

on an automatic analyzer for sugars permits easy identification and quantification. The isocratic elution permits repetition of chromatography without equilibration. Thus, the anion-exchange derivatives of Spheron represent suitable supports not only for the separation of monosaccharides<sup>4</sup> and lower oligosaccharides<sup>5</sup> but also for cellodextrins.

#### REFERENCES

- 1 M. R. Ladisch, A. L. Huebner and G. T. Tsao, *J. Chromatogr.*, 147 (1978) 185.
- 2 E. Martinsson and O. Samuelson, *J. Chromatogr.*, 50 (1970) 429.
- 3 R. B. Kesler, *Anal. Chem.*, 39 (1967) 1416.
- 4 Z. Chytilová, O. Mikeš, J. Farkaš, P. Štrop and P. Vrátný, *J. Chromatogr.*, 153 (1978) 37.
- 5 P. Vrátný, O. Mikeš, J. Farkaš, P. Štrop, J. Čopíková and K. Nejeptinská, *J. Chromatogr.*, 180 (1979) 39.
- 6 O. Mikeš, P. Štrop, J. Zbrožek and J. Čoupek, *J. Chromatogr.*, 180 (1979) 17.
- 7 O. Mikeš, P. Štrop, J. Zbrožek and J. Čoupek, *J. Chromatogr.*, 119 (1976) 339.
- 8 G. L. Miller, J. Dean and R. Blum, *Arch. Biochem. Biophys.*, 91 (1960) 21.
- 9 P. Jandera and J. Churáček, *J. Chromatogr.*, 98 (1974) 55.
- 10 O. Samuelson and B. Swenson, *Acta Chem. Scand.*, 16 (1962) 2056.
- 11 R. M. Saunders, *Carbohydr. Res.*, 7 (1968) 76.
- 12 J. X. Khyrn and O. P. Zill, *J. Amer. Chem. Soc.*, 74 (1952) 2090.
- 13 J. Havlicek and O. Samuelson, *Anal. Chem.*, 47 (1975) 1854.
- 14 M. R. Ladisch and G. T. Tsao, *J. Chromatogr.*, 166 (1978) 85.

CHROM. 14,329

## APPLICATION OF DYE-LIGAND CHROMATOGRAPHY TO THE ISOLATION OF $\alpha$ -1-PROTEINASE INHIBITOR AND $\alpha$ -1-ACID GLYCOPROTEIN

G. BIRKENMEIER and G. KOPPERSCHLÄGER\*

*Institute of Physiological Chemistry, Karl-Marx-University Leipzig, DDR-7010 Leipzig (G.D.R.)*

(Received August 11th, 1981)

---

### SUMMARY

Various Cibacron blue F3G-A substituted Sephadex G-100 gels which differ in the density of the bound dye were investigated for their applicability in the affinity chromatography of human serum proteins. Protein adsorption was found to depend strongly on the density of the covalently attached dye and on the pH of the applied buffer.

A high degree of dye substitution of the gel caused binding of most of the serum proteins. Only a small number of proteins were found to appear in the breakthrough fraction. On this basis a simple and relatively mild procedure for the isolation of homogeneous  $\alpha$ -1-proteinase inhibitor and  $\alpha$ -1-acid glycoprotein from human serum was developed. Isolation of  $\alpha$ -1-acid glycoprotein succeeded in only a single step, whereas that of  $\alpha$ -1-proteinase inhibitor required two additional steps: a prior ammonium sulphate precipitation and a chromatographic step on DEAE-cellulose at pH 6.5.

---

### INTRODUCTION

Immobilized Cibacron blue F3G-A is frequently used as a powerful tool for the affinity chromatography of dehydrogenases and kinases<sup>1-3</sup>. The binding of these enzymes to dye matrix conjugates is regarded as a specific interaction of the dye with a typical structural element in these enzymes, designated as "dinucleotide fold"<sup>4</sup>. In addition to these groups of enzymes, other proteins apparently not having this fold in their molecules<sup>5,6</sup> have also been shown to bind to immobilized Cibacron blue F3G-A.

Travis and Pannell<sup>7</sup> originally reported the interaction of human serum albumin with this dye and developed an efficient procedure for the removal of albumin from other serum proteins. Since then, dye-ligand chromatography has been applied to the purification of various serum proteins<sup>8-10</sup>.

The strong interaction of human albumin with Cibacron blue F3G-A is apparently due to the binding of the dye to the bilirubin binding site of albumin<sup>11</sup>. Other plasma proteins have also been found to interact with Cibacron blue F3G-A. These

interactions depend strongly on the pH<sup>12</sup>, on the chemical properties of the matrix<sup>13</sup> and on the mode of covalent attachment of the dye to the insoluble support<sup>14</sup>.

This paper deals with the influence of the loading density of the gel and of pH on the binding of human serum proteins to immobilized Cibacron blue. By taking advantage of these interactions simple procedures for the isolation of pure  $\alpha$ -1-proteinase inhibitor and of  $\alpha$ -1-acid glycoprotein are presented.

## EXPERIMENTAL

### *Chemicals*

Cyanogum 41, agarose, Coomassie Brilliant Blue G-250 and DEAE-cellulose were purchased from Serva (Heidelberg, G.F.R.). Cibacron blue F3G-A was obtained from Ciba AG (Basle, Switzerland) and the chemicals for the immunological methods from Behringwerke (Marburg, G.F.R.). Bovine trypsin and cytochrome *c* were purchased from Boehringer (Mannheim, G.F.R.). Benzoylarginine-*p*-nitroanilide (BAPNA) was obtained from Ferak (Berlin, G.F.R.) and Sephadex G-100 from Pharmacia (Uppsala, Sweden). All other chemicals were of analytical-reagent grade. Human serum was a gift from the blood bank of the Medical Centre of the Karl-Marx-University (Leipzig, G.D.R.).

### *Coupling of Cibacron blue F3G-A to Sephadex G-100*

Covalent coupling of Cibacron blue F3G-A to Sephadex G-100 was effected by an ether link between the triazine ring and the polysaccharide matrix<sup>3</sup>. For preparation of gels with different degrees of substitution, different amounts of Cibacron blue F3G-A were applied in the range between 0.006 and 0.85 g per gram of dried Sephadex G-100. For maximal dye substitution the reaction temperature was kept constant at 80°C.

### *Determination of Cibacron blue substitution*

The determination of the amount of dye covalently bound to the matrix was carried out according to Chambers<sup>15</sup>. The gel was dried by washing with methanol and kept in a vacuum desiccator until the weight became constant.

### *Preparative column chromatography with Blue Sephadex*

The dye-Sephadex conjugate (Blue Sephadex) was equilibrated with 10 mM sodium phosphate solution (pH 5.8 or 6.8) in a column (50 × 5 cm) at 4°C. In the case of  $\alpha$ -1-proteinase inhibitor, solid ammonium sulphate was added to fresh human serum until 50% saturation was reached. The supernatant of the resulting precipitate was exhaustively dialysed against equilibration buffer. Then a small amount of precipitate was removed by centrifugation and the supernatant was applied to the column. For preparation of  $\alpha$ -1-acid glycoprotein the salt precipitation could be omitted. The flow-rate through the column was adjusted to 50 ml/h and fractions of 15 ml were collected. Unless mentioned otherwise, the pooled fractions were concentrated by employing an Amicon UM-10 membrane filter and dialysed against phosphate buffer (50 mM, pH 7.0) or against the equilibration buffer as applied in the subsequent chromatographic step.

For regeneration, the column containing the Cibacron blue-Sephadex con-



jugate was washed with 10 mM sodium hydroxide solution and finally with distilled water. The gel was stored at 4°C in 3 M ammonium sulphate solution containing 0.01 % of sodium azide.

#### *DEAE-cellulose chromatography*

After chromatography on Blue Sephadex the fractions containing the  $\alpha$ -1-proteinase inhibitor were applied to a column (20 × 1.5 cm) of DEAE-cellulose equilibrated with 5 mM sodium phosphate buffer (pH 6.5) containing 50 mM sodium chloride. The column was washed with two volumes of this buffer and then a linear gradient from 50 to 200 mM sodium chloride in 5 mM sodium phosphate (pH 6.5) was employed. The protein content of the effluent was monitored at 280 nm and the antitryptic activity was measured. The active fractions were pooled and concentrated. The preparation was either subjected to further tests or kept precipitated at 4°C.

#### *Electrophoresis*

Polyacrylamide gel electrophoresis was carried out in 8 × 0.5 cm tubes by using a linear gradient of acrylamide (3–15%)<sup>16</sup>. The electrophoretic runs were performed at 3 mA per tube and room temperature. For staining, the method of Diezel *et al.*<sup>17</sup> was applied.

Sodium dodecyl sulphate (SDS)–polyacrylamide gel electrophoresis was carried out in 7.0 % gels by application of the technique of Weber and Osborn<sup>18</sup>. For molecular weight determinations, cross-linked cytochrome *c* polymers served as a standard. The proteins were denatured in 1 % SDS solution containing 1 % of 2-mercaptoethanol at 100°C for 5 min and then loaded onto the gels. The runs were carried out for 4 h at 8 mA per tube.

#### *Assay of antitryptic activity*

The inhibitory power of the individual fractions on trypsin was measured according to Eriksson<sup>19</sup> by using crystallized, salt-free trypsin in 100 mM Tris–hydrochloric acid buffer (pH 7.8) containing 5 mM calcium chloride. After pre-incubation of 25  $\mu$ g of trypsin with the samples for 15 min at 25°C, the residual activity was measured by addition of BAPNA dissolved in dimethylformamide. The release of *p*-nitroaniline at 405 nm was monitored.

#### *Immunological methods*

Immunodiffusion was carried out according to Ouchterlony<sup>20</sup> in 100 mM sodium phosphate buffer (pH 7.5) and 1.5 % agarose. The purity of the antigen preparation was checked by immunoelectrophoresis<sup>21</sup>. The concentration of  $\alpha$ -1-acid glycoprotein was determined by the method of Mancini *et al.*<sup>22</sup> on M-Pärtigen plates using standard serum.

#### *Ultracentrifugation*

Sedimentation velocity experiments were performed with a Phywe Model U 60 L analytical ultracentrifuge by following the Schlieren pattern. The resulting apparent *s*-values obtained with five different protein concentrations were corrected to water and infinite dilution at 20°C.

The determination of protein was performed according to the method of Janatova *et al.*<sup>23</sup> using bovine serum albumin as standard.

## RESULTS

*Variation of the degree of dye substitution*

The influence of the degree of dye substitution of the matrix on the binding of serum proteins was investigated at pH 7.0 by employing three types of Blue Sephadex: low-substituted, medium-substituted and high-substituted gels.

With low-substituted gels the serum proteins are separated into two fractions: the breakthrough fraction and a fraction of retarded proteins which can be eluted by washing the column with 1 M sodium chloride solution (Fig. 1A).

Medium-substituted gel (Fig. 1B) shows a shift in protein distribution toward the retarded fractions, whereas high-substituted gels are capable of adsorbing most of the serum proteins (Fig. 1C). The electrophoretic analysis of the eluted fractions

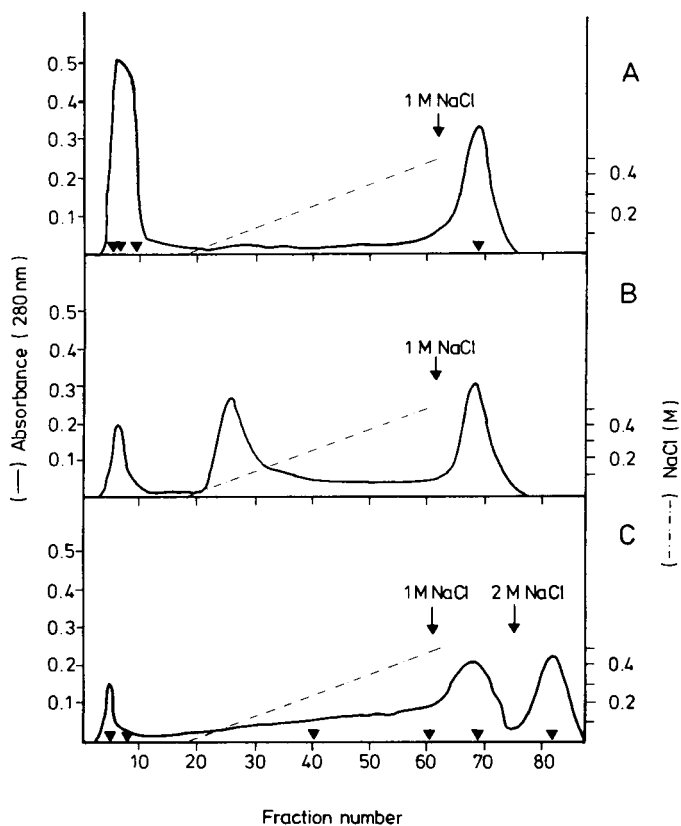


Fig. 1. Elution diagrams for human serum proteins chromatographed at pH 7.0 on Cibacron blue F3G-A-Sephadex G-100 gels with different degrees of dye substitution. (A) 4  $\mu\text{g}$  of dye per mg of Sephadex; (B) 73  $\mu\text{g}$  of dye per mg of Sephadex; (C) 214  $\mu\text{g}$  of dye per mg of Sephadex. A 2-ml volume of fresh human serum was dialysed against 10 mM sodium phosphate buffer (pH 7.0) and then applied to a column ( $40 \times 1.5$  cm) previously equilibrated with the same buffer. After removing the unbound protein fraction, elution was started by applying a gradient of 0–0.5 M sodium chloride in 10 mM sodium phosphate buffer (pH 7.0). Finally, the column was washed with 1 and 2 M sodium chloride solution. The flow-rate was 12 ml/h and 2-ml fractions were collected. The black triangles indicate the fractions subjected to polyacrylamide gel electrophoresis presented in Fig. 2.

showed that at low dye substitution only albumin is bound, whereas in the breakthrough fraction most of the other serum proteins appear. An asymmetric protein distribution in this fraction indicates weak interactions occurring between some protein components and the gel (Fig. 2A). With the high-substituted gels the breakthrough fraction contains only four proteins, which could be identified immunologically as  $\alpha$ -2-macroglobulin,  $\alpha$ -1-proteinase inhibitor,  $\alpha$ -1-acid glycoprotein and prealbumin (Figs. 1C and 2B).

Apparently,  $\alpha$ -1-acid glycoprotein does not exert any interaction with the immobilized Cibacron blue F3G-A. This protein is found in the leading edge of the wash-out fraction and so can be partially separated from the other serum proteins.

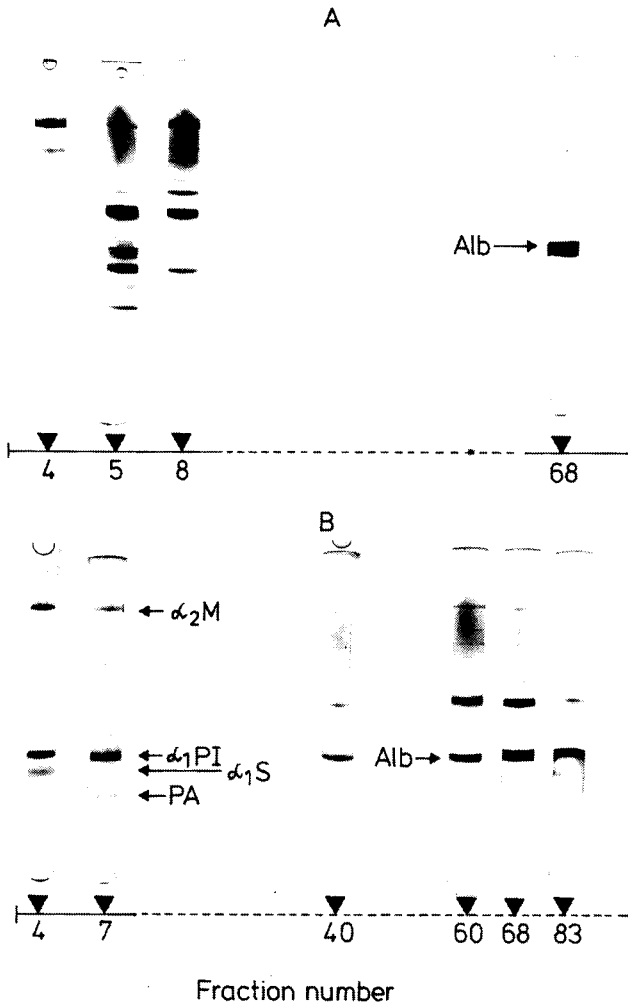


Fig. 2. Polyacrylamide gel electrophoresis of selected fractions from (A) Fig. 1A and (B) Fig. 1C. Each gel was loaded with 50–100  $\mu$ l of the respective eluate. The numbers correspond to the fraction numbers in Fig. 1A and C. Symbols: Alb = albumin;  $\alpha_2$ M =  $\alpha$ -2-macroglobulin;  $\alpha_1$ PI =  $\alpha$ -1-proteinase inhibitor;  $\alpha_1$ S =  $\alpha$ -1-acid glycoprotein; PA = prealbumin.

The subsequently eluted protein component was identified as  $\alpha$ -1-proteinase inhibitor. Because the electrophoretic mobility of this protein in alkaline polyacrylamide gel electrophoresis is similar to that of albumin, immunodiffusion tests using monospecific antisera against  $\alpha$ -1-proteinase inhibitor and albumin had to clarify whether this fraction is contaminated by albumin or not. Clear evidence of the absence of albumin from this fraction was obtained.

Attempts were made to fractionate the bound proteins, using a sodium chloride gradient from 0 to 0.5 *M*. However, all of the experiments were unsuccessful.

At pH 6.0 the affinity of serum proteins for the substituted gels increases considerably. With high-substituted gels, only  $\alpha$ -1-acid glycoprotein and a very small amount of  $\alpha$ -2-macroglobulin constitute the breakthrough fraction, whereas all of the other proteins are adsorbed, including  $\alpha$ -1-proteinase inhibitor and prealbumin (not shown). On the basis of these results simple methods for the purification of  $\alpha$ -1-proteinase inhibitor and  $\alpha$ -1-acid glycoprotein were developed.

#### Isolation of $\alpha$ -1-proteinase inhibitor

As mentioned above, high-substituted Sephadex G-100 binds at pH 7.0 all of the serum proteins except  $\alpha$ -1-proteinase inhibitor,  $\alpha$ -1-acid glycoprotein,  $\alpha$ -2-macroglobulin and prealbumin. When a Blue Sephadex column (loading density 170  $\mu$ g dye per milligram of dried gel) at pH 6.8 is charged with the supernatant resulting from ammonium sulphate precipitation of serum at 50% saturation, the breakthrough fraction differs from that of the whole serum. A typical example is shown in Fig. 3.

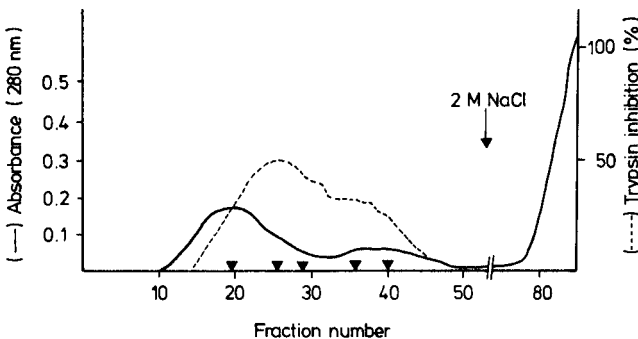


Fig. 3. Chromatography of human serum on Cibacron blue F3G-A-Sephadex G-100 at pH 6.8. A 30-ml volume of human serum was treated with ammonium sulphate at 50% saturation and then centrifuged. The supernatant was dialysed against 10 *mM* sodium phosphate buffer (pH 6.8) and charged on to a gel column (50  $\times$  5 cm) previously equilibrated with the same buffer. The unbound protein fraction was eluted with equilibration buffer, then the bound proteins were removed by applying 2 *M* sodium chloride solution. Samples 10–24 (I) and 25–50 (II) were pooled. The black triangles indicate the fractions subjected to polyacrylamide gel electrophoresis as presented in Fig. 4.

Some asymmetry in the diagram is observable, caused by slight retardation of the  $\alpha$ -1-proteinase inhibitor and prealbumin in comparison with the  $\alpha$ -1-acid glycoprotein.  $\alpha$ -2-Macroglobulin is lacking in the breakthrough fraction. The pattern of trypsin inhibition coincides with the protein bands of  $\alpha$ -1-proteinase inhibitor, as demonstrated in gel electrophoresis (Fig. 4).

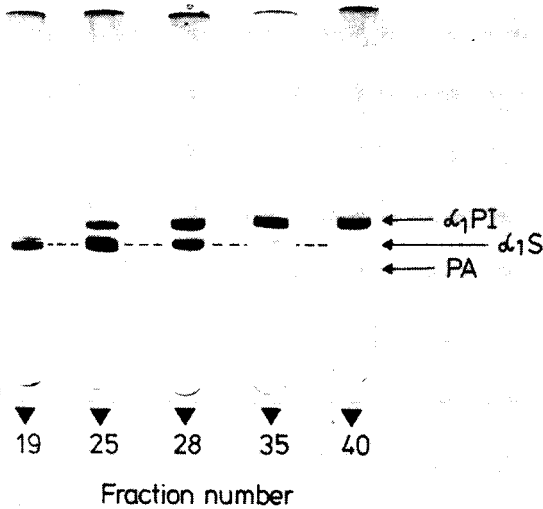


Fig. 4. Polyacrylamide gel electrophoresis of selected fractions from Fig. 3. Volumes of 50  $\mu$ l (fraction 19) and 100  $\mu$ l (fractions 25, 28, 35 and 40) of the samples were subjected to electrophoresis.

The partial separation of  $\alpha$ -1-proteinase inhibitor from  $\alpha$ -1-acid glycoprotein permits partition of the breakthrough fraction into two pools (I and II), one containing the major part of  $\alpha$ -1-acid glycoprotein (pool I) and the other that of  $\alpha$ -1-proteinase inhibitor (pool II).

The fractions collected in pool II were subjected to DEAE-cellulose chromatography at pH 6.5 according to Pannell *et al.*<sup>24</sup> (see Experimental). By this procedure a complete separation of  $\alpha$ -1-proteinase inhibitor from  $\alpha$ -1-acid glycoprotein and pre-albumin could be achieved. Polyacrylamide gel electrophoresis of the isolated  $\alpha$ -1-proteinase inhibitor yields in general a single band. Sometimes two bands moving closely together can be observed, and both were identified as  $\alpha$ -1-proteinase inhibitor (Fig. 5A). Apparently, this is due to the polymorphism of this protein, which can more distinctly be shown by isoelectric focusing. The homogeneity of the isolated  $\alpha$ -1-proteinase inhibitor can unequivocally be demonstrated by means of SDS-polyacrylamide gel electrophoresis in the presence of 2-mercaptoethanol (Fig. 5B) and immunoelectrophoresis (Fig. 6A). By SDS electrophoresis a single band is obtained. The comparison with the electrophoretic mobilities of cross-linked cytochrome *c* polymers permitted the molecular weight of the inhibitor to be calculated to be 52,500.

Immunoelectrophoresis yielded a single precipitation arc when tested against anti-whole human serum and monospecific anti-human  $\alpha$ -1-proteinase inhibitor. No precipitation was detected with antisera against human  $\alpha$ -1-acid glycoprotein, human serum albumin, human  $\alpha$ -1-lipoprotein and human Gc-globulin.

In the analytical ultracentrifugation in 50 mM sodium phosphate buffer (pH 7.0),  $\alpha$ -1-proteinase inhibitor showed a single symmetrical peak with a sedimentation coefficient of  $s_{20,w}^0 = 3.5$  S. This value is in close agreement with the sedimentation coefficient of 3.6 S published by Pannell *et al.*<sup>24</sup>.

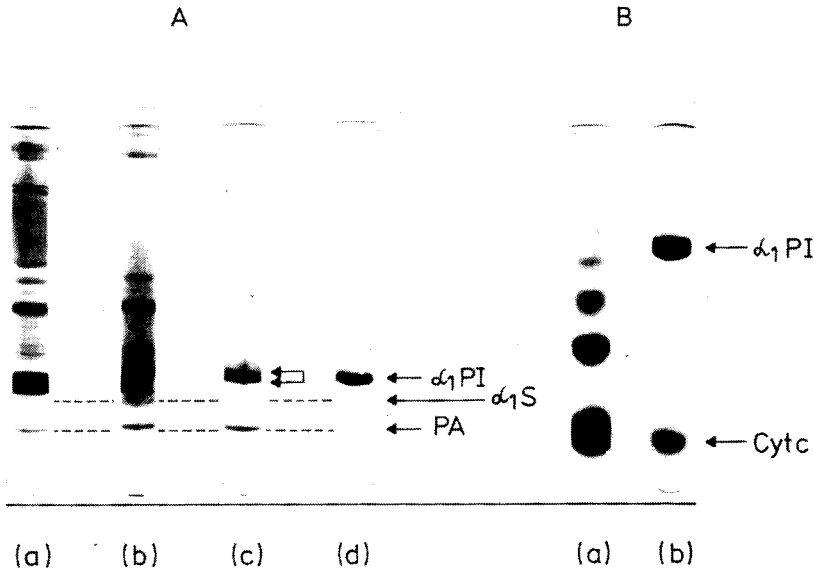


Fig. 5. (A) Polyacrylamide gel electrophoresis of samples containing  $\alpha$ -1-proteinase inhibitor. (a) Whole human serum (400  $\mu$ g); (b) supernatant after ammonium sulphate precipitation (300  $\mu$ g); (c)  $\alpha$ -1-proteinase inhibitor after ammonium sulphate precipitation and Blue Sephadex chromatography (40  $\mu$ g); (d)  $\alpha$ -1-proteinase inhibitor after ammonium sulphate precipitation, Blue Sephadex chromatography and DEAE-cellulose chromatography (30  $\mu$ g). The black arrows indicate the two bands of  $\alpha$ -1-proteinase inhibitor (for explanation see text). (B) SDS-electrophoresis of purified  $\alpha$ -1-proteinase inhibitor. (a) Cytochrome *c* (Cyt *c*) oligomers (40  $\mu$ g); (b)  $\alpha$ -1-proteinase inhibitor (30  $\mu$ g).

The yield of  $\alpha$ -1-proteinase inhibitor obtained by ammonium sulphate precipitation at 50% (first step), dye-ligand chromatography (second step) and DEAE-cellulose chromatography (third step) is about 30% relative to the total antitryptic activity of the serum. From 30 ml of serum 8.3 mg of purified human  $\alpha$ -1-proteinase inhibitor could be obtained.

#### Isolation of $\alpha$ -1-acid glycoprotein

When dialysed serum without prior ammonium sulphate precipitation is applied to a Cibacronblue Sephadex column (loading density 170  $\mu$ g of dye per milligram of dried gel) at pH 5.8 the only constituent of the breakthrough fraction is  $\alpha$ -1-acid glycoprotein (Fig. 7). After concentrating this fraction on an Amicon UM-10 membrane filter and dialysis against 50 mM sodium phosphate buffer of pH 7.0, 75–80% of the total serum  $\alpha$ -1-acid glycoprotein is recovered. Hence, 100 ml of human serum yield 40–45 mg of  $\alpha$ -1-acid glycoprotein from a total concentration of 55 mg per 100 ml.

In alkaline polyacrylamide gel electrophoresis (Fig. 8A) and SDS-polyacrylamide gel electrophoresis (Fig. 8B) the preparation shows a single protein band. By SDS electrophoresis a molecular weight of 42,500 was calculated.

Analytical ultracentrifugation of the  $\alpha$ -1-acid glycoprotein in 50 mM sodium phosphate buffer at pH 6.0 showed a single symmetrical peak having a sedimentation coefficient of  $s_{20,w}^0 = 3.27$  S.

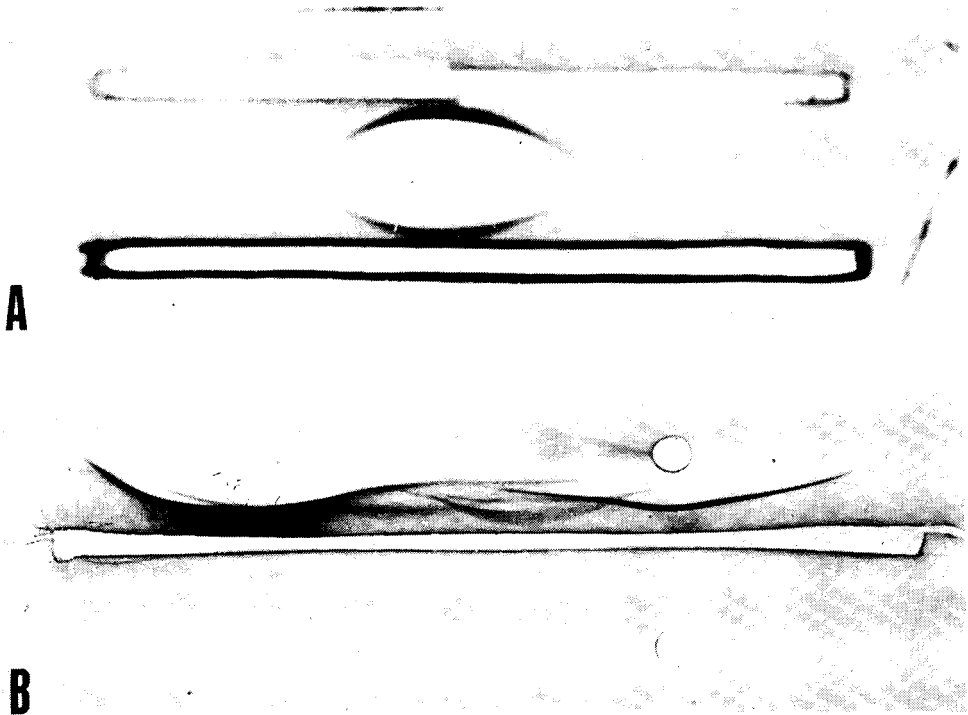


Fig. 6. Immunoelectrophoresis of (A)  $\alpha$ -1-proteinase inhibitor and (B)  $\alpha$ -1-acid glycoprotein. (A) Upper trough, monospecific rabbit anti-human  $\alpha$ -1-proteinase inhibitor; bottom trough, rabbit anti-human serum; well, purified  $\alpha$ -1-proteinase inhibitor. (B) Top well, normal human serum; bottom well, purified  $\alpha$ -1-acid glycoprotein; trough, anti-human serum fortified with monospecific anti-human  $\alpha$ -1-acid glycoprotein from rabbit.

Against anti-whole human serum fortified with monospecific anti-human  $\alpha$ -1-acid glycoprotein and monospecific anti-human  $\alpha$ -1-acid glycoprotein a single precipitation line was obtained (Fig. 6B).

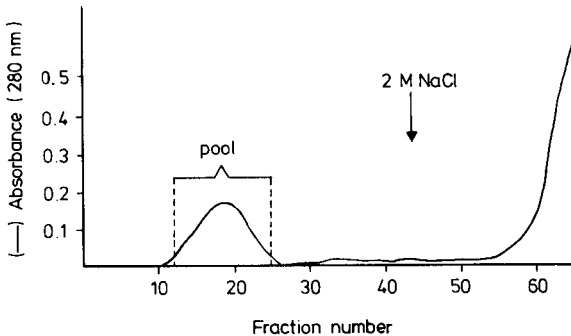


Fig. 7. Chromatography of human serum on Cibacron blue F3G-A-Sephadex G-100 at pH 5.8. A 50-ml volume of human serum was dialysed against 10 mM sodium phosphate buffer (pH 5.8) and applied to a gel column (50  $\times$  5 cm) equilibrated with the same buffer. After eluting the unbound protein fraction with 10 mM sodium phosphate buffer (pH 5.8), the bound proteins were removed with 2 M sodium chloride solution. The fractions indicated were pooled and concentrated.

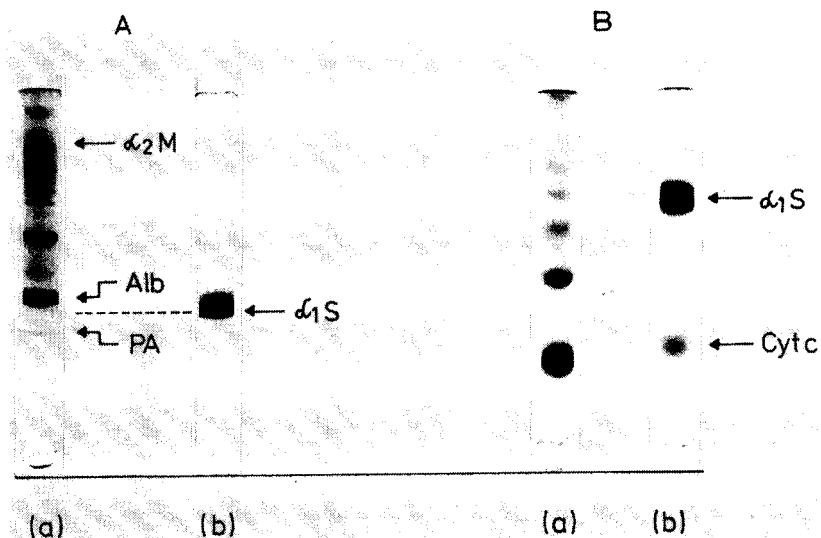


Fig. 8. (A) Polyacrylamide gel electrophoresis of purified  $\alpha$ -1-acid glycoprotein. (a) Human serum (400  $\mu$ g); (b) purified  $\alpha$ -1-acid glycoprotein (60  $\mu$ g). (B) SDS electrophoresis of purified  $\alpha$ -1-acid glycoprotein. (a) Cytochrome *c* oligomers (40  $\mu$ g); (b)  $\alpha$ -1-acid glycoprotein (30  $\mu$ g).

## DISCUSSION

Immobilized Cibacron blue F3G-A is capable of adsorbing a great number of serum proteins. In addition to albumin, lipoproteins<sup>11</sup>, blood coagulation factors<sup>25</sup>,  $\alpha$ -1-antichymotrypsin<sup>9</sup>, complement factors<sup>10</sup>, interferon<sup>14</sup> and other proteins have also been reported to bind to the immobilized dye. As shown in this paper, highly dye-substituted gels at appropriate ionic strength and pH of the buffer are capable of adsorbing almost all serum proteins.

In order to prepare gels, the covalent attachment of Cibacron blue F3G-A to the polysaccharide chain of Sephadex G-100 via an ether bridge was found to be superior to other coupling procedures<sup>26</sup>. The degree of substitution can easily be altered by changing the reaction temperature and the amount of the reacting dye per gram of Sephadex. The modified Sephadex G-100 is sufficiently stable also at high ligand concentrations. It exhibits good flow-rates in a column and can be used for large-scale chromatography.

There are many reports of the use of Sepharose gels for dye immobilization<sup>8,12,14</sup>. However, in contrast to the Sephadex used in our laboratory, the polysaccharide matrix of the Sepharose itself has a considerable non-specific binding capacity for proteins, especially at pH values below 7.0<sup>27</sup>.

Our results show that the nature and amount of the adsorbed serum proteins depend directly on the loading density of the Sephadex G-100 and are not seriously influenced by matrix-protein interactions.

The adsorption of the great variety of proteins to immobilized Cibacron blue F3G-A can hardly be explained on the basis of specific interactions as they have been postulated for several dehydrogenases<sup>4</sup> and kinases<sup>3</sup> or for albumin<sup>11</sup>. According to



theoretical considerations by Kopperschläger *et al.*<sup>28</sup>, the dye binding site is apparently an apolar region in the surface of the protein molecule surrounded by hydrophilic amino acid residues. All data indicate the involvement of hydrophobic and electrostatic forces in the dye-protein interaction. Their specificity depends primarily on hydrophobic forces, whereas their stability is governed by electrostatic forces. The nucleotide fold as present in dehydrogenases and in some of the kinases is only a special case in a dye binding site of a protein. Further, in a number of instances a second type of protein interaction can be recognized. This is based on the ability of the dye to act as weak cationic exchanger owing to its sulphonic acid groups. Consequently, below the isoelectric point almost all proteins should be able to bind to the dye.

These considerations are in line with the findings reported in this paper. Both lowering the pH and increasing the dye ligand concentration cause an increase in the binding strength and the binding capacity of the immobilized dye.

The significance of electrostatic interactions is stressed by the fact that  $\alpha$ -1-acid glycoprotein, having an isoelectric point of 2.8, does not show any affinity for the gel under the applied conditions. By taking advantage of these properties a rapid and efficient one-step purification procedure is possible. With respect to the yield and operating time the described method is superior to other techniques<sup>29</sup>. This procedure yields an immunochemically pure  $\alpha$ -1-glycoprotein preparation and can be applied to the isolation of this protein from small volumes of serum as obtained from individual humans. The high degree of purity was confirmed by several methods. The sedimentation coefficient of  $s_{20,w}^0 = 3.27$  S agrees well with the value of 3.19 S previously reported for human  $\alpha$ -1-acid glycoprotein<sup>29</sup>. The estimated molecular weight of 42,500 is close to the published value of 40,800<sup>29</sup>.

Various methods have been reported for the isolation of  $\alpha$ -1-proteinase inhibitor from plasma or serum. Albumin as the main contaminant of such preparations was removed by either concanavalin A<sup>30</sup>, zinc chelate<sup>31</sup> or Sepharose Blue Dextran<sup>24</sup>. In contrast to other reports in which immobilized Cibacron blue was also used for the purification of the  $\alpha$ -1-proteinase inhibitor, Blue Sephadex as applied in the work is able to retain not only albumin but also most other serum proteins. This contributes significantly to the high degree of purification.

In order to achieve an efficient purification on the  $\alpha$ -1-proteinase inhibitor, the ligand concentration on the gel should be between 170 and 250  $\mu$ g of dye per milligram of dry gel. The recovery of approximately 30% of the original inhibitory capacity by our procedure is comparable to that reported by Kurecki *et al.*<sup>31</sup>, but less than the best preparation (60%) described by Pannell *et al.*<sup>24</sup>. However, these two procedures take longer as they involve at least three chromatography steps.

#### ACKNOWLEDGEMENT

The authors are grateful to Professor E. Hofmann for many helpful discussions and critical reading of the manuscript.

## REFERENCES

- 1 R. L. Easterday and I. M. Easterday, in R. B. Dunlop (Editor), *Immobilized Biochemicals and Affinity Chromatography*, Plenum, New York, 1974, p. 123.
- 2 G. Kopperschläger, W. Diezel, R. Freyer, St. Liebe and E. Hofmann, *Eur. J. Biochem.*, 22 (1971) 40.
- 3 H.-J. Böhme, G. Kopperschläger, J. Schulz and E. Hofmann, *J. Chromatogr.*, 69 (1972) 209.
- 4 E. Stellwagen, R. Cass, S. T. Thompson and M. Woody, *Nature (London)*, 257 (1975) 716.
- 5 L. A. Haff and R. L. Easterday, in F. Eckstein and P. V. Sundaram (Editors), *Theory and Practice in Affinity Chromatography*, Academic Press, New York, 1978, p. 23.
- 6 R. S. Beissner, F. H. Quicho and F. B. Rudolph, *J. Mol. Biol.*, 134 (1979) 847.
- 7 J. Travis and R. Pannell, *Clin. Chim. Acta*, 49 (1973) 49.
- 8 G. D. Virca, J. Travis, P. K. Hall and R. C. Roberts, *Anal. Biochem.*, 89 (1974) 274.
- 9 J. Travis, D. Garner and J. Bowen, *Biochemistry*, 17 (1978) 5647.
- 10 A. P. Gee, T. Borsos and M. D. P. Boyle, *J. Immunol. Methods*, 30 (1978) 274.
- 11 R. J. Leatherbarrow and P. D. G. Dean, *Biochem. J.*, 189 (1980) 27.
- 12 S. Angal and P. D. G. Dean, *FEBS Lett.*, 96 (1978) 346.
- 13 S. Angal and P. D. G. Dean, *Biochem. J.*, 167 (1977) 301.
- 14 E. Bollin, K. Vastola, D. Oleszek and E. Sulkowski, *Prep. Biochem.*, 8 (1978) 259.
- 15 G. K. Chambers, *Anal. Biochem.*, 83 (1977) 551.
- 16 G. Kopperschläger, H. Storch and G. Birkenmeier, *Z. Med. Labor.-Diagn.*, 18 (1977) 300.
- 17 W. Diezel, G. Kopperschläger and E. Hofmann, *Anal. Biochem.*, 48 (1972) 617.
- 18 K. Weber and M. Osborn, *J. Biol. Chem.*, 244 (1969) 4406.
- 19 S. Eriksson, *Acta Med. Scand.*, 177, Suppl. 432 (1965) 1.
- 20 Ö. Ouchterlony, *Progr. Allergy*, 6 (1962) 30.
- 21 I. I. Scheidegger, *Int. Arch. Allergy Appl. Immunol.*, 7 (1955) 103.
- 22 G. Mancini, A. O. Carbonara and J. F. Heremans, *Immunochemistry*, 2 (1965) 235.
- 23 J. Janatova, J. K. Fuller and M. J. Hunter, *J. Biol. Chem.*, 243 (1968) 3612.
- 24 R. Pannell, D. Johnson and J. Travis, *Biochemistry*, 13 (1974) 5439.
- 25 A. C. W. Swart, B. H. M. Kop-Klaassen and H. C. Hemker, *Haemostasis*, 1 (1972/73) 237.
- 26 P. D. G. Dean and D. H. Watson, *J. Chromatogr.*, 165 (1979) 301.
- 27 S. Hjertén, *J. Chromatogr.*, 159 (1978) 47.
- 28 G. Kopperschläger, H.-J. Boehme and E. Hofmann, in A. Fiechter (Editor), *Advances in Biochemical Engineering*, Springer, Berlin, Heidelberg, New York, in press.
- 29 P. A. Charlwood, M. W. C. Hatton and E. Regoeczi, *Biochim. Biophys. Acta*, 453 (1976) 81.
- 30 P. Musiani and T. B. Tomasi, *Biochemistry*, 15 (1976) 798.
- 31 T. Kurecki, L. F. Kress and M. Laskowski, *Anal. Biochem.*, 99 (1979) 415.

CHROM. 14,267

## RADIOISOTOPE ASSAY FOR GLUTAMINE SYNTHETASE USING THIN-LAYER CHROMATOGRAPHY

SHAM L. PAHUJA and TED W. REID\*

*Yale University School of Medicine, Department of Ophthalmology and Visual Science, New Haven, CT (U.S.A.)*

(First received June 1st, 1981; revised manuscript received August 6th, 1981)

---

### SUMMARY

A simple radiochemical method for the determination of glutamine synthetase activity by thin-layer chromatography is described. The assay involves the separation of glutamine from glutamic acid on anion-exchange resin [Dowex 1 ( $\text{CH}_3\text{COO}^-$ )] coated plastic strips. The technique described is fast, reproducible and at least 50 times more sensitive than commonly used colorimetric methods. This method was used to determine the kinetic properties of glutamine synthetase and is applicable with either purified enzymes or crude tissue homogenates.  $K_M$  values for glutamic acid, ATP and ammonia determined by the present assay were similar to the values obtained by colorimetric methods.

---

### INTRODUCTION

The enzymatic conversion of glutamic acid to glutamine by glutamine synthetase [L-glutamate: ammonia ligase (ADP), E.C. 6.3.1.2.] occupies a central position in nitrogen metabolism. The presence of this enzyme has been determined in animal tissues, plants, and bacteria. Control and regulation of glutamine synthetase by hormones and various metabolites has been studied in cells grown in tissue culture and purified enzyme preparations<sup>1-7</sup>.

Assay methods generally used measure glutamine synthetase activity either by colorimetric<sup>8-10</sup>, or radiochemical methods based on the separation of glutamine from glutamic acid by column chromatography<sup>11-13</sup>. Major shortcomings associated with colorimetric techniques are: (1) they do not measure the physiological end products; (2) they lack sensitivity; (3) they are subject to interference by substances which can react with ammonium molybdate or ferric chloride. Radioisotopic methods on the other hand are very sensitive but are time consuming and tedious.

In this paper, we describe a simple, rapid, sensitive and specific assay which avoids the problems associated with the previous assays. The method involves detection and quantitation of glutamine formed from <sup>3</sup>H-labelled glutamic acid by thin-layer chromatography (TLC) on anion-exchange resin [Dowex 1 ( $\text{CH}_3\text{COO}^-$ )] coated plastic sheets. Glutamine and glutamic acid separate well due to the fact that glutamic

acid is strongly adsorbed while glutamine moves quite readily under the chromatographic conditions.

## MATERIALS AND METHODS

### *Materials*

Ionex SB-AC precoated plastic sheets were obtained from Brinkmann (Westbury, NY, U.S.A.). Prior to use,  $1.2 \times 9.0$  cm plastic strips were cut and equilibrated with 0.05% acetic acid for 30 min as recommended by Devenyi<sup>14</sup>. [3,4-<sup>3</sup>H]glutamic acid (40 Ci/mmol) was obtained from New England Nuclear (Boston, MA, U.S.A.). ATP, unlabelled glutamic acid and glutamine were obtained from Sigma (St. Louis, MO, U.S.A.). All other chemicals and reagents were obtained from the usual sources. Bovine retina was used as a source of glutamine synthetase. Retina was homogenized with 5 mM phosphate buffer (pH 7.1), 10 mM 2-mercaptoethanol, and 0.1 mM EDTA, and was centrifuged at 105,000 *g* for 30 min at 4°C. The supernatant was used as a source of crude enzyme preparation. Glutamine synthetase was purified from the crude extract by ammonium sulfate fractionation followed by conventional chromatographic techniques. The purified enzyme preparation was judged to be homogeneous on the basis of analytical gel electrophoretic techniques under various conditions and immunodiffusion analysis. Details of the enzyme purification and characterization will be published elsewhere<sup>15</sup>.

### *Analytical procedures*

The standard incubation mixture (total volume 50  $\mu$ l, pH 7.4) consisted of: 50 mM imidazole, 20 mM MgCl<sub>2</sub>, 10 mM ATP, 4 mM ammonium chloride, 10 mM [<sup>3</sup>H]glutamic acid (200–1000 cpm/nmole). The reaction was initiated by the addition of an appropriate amount of enzyme preparation. The reaction mixture was incubated at 37°C and stopped by rapid cooling in ice. Immediately after cooling, 5  $\mu$ l of the incubation mixture were spotted as a streak and dried at the origin 1 cm from the bottom of the strip. Ascending chromatography was carried out in ethyl acetate–pyridine–water (8:1:91) mixture till the solvent approached to within 1 cm of the top of the strip. Areas corresponding to glutamic acid and glutamine, as determined from the reference strips run under identical conditions, were cut and placed in scintillation vials. In cases where reference strips were not run, the strips were cut into 1-cm pieces and individual pieces were placed in separate vials. Amino acids were eluted from the resin by adding 2.5 ml of scintillation fluid (ACS) and 1 ml of 10% formic acid as recommended by Himoe and Rinne<sup>16</sup>. The unit of enzyme activity is expressed as the amount required to convert 1.0  $\mu$ mol of glutamic acid to product per min at 37°C.

Protein was determined by the method of Bradford<sup>17</sup> using bovine serum albumin as a standard.

## RESULTS

### *Separation of glutamic acid and glutamine*

Fig. 1 shows the separation of unlabelled glutamic acid and glutamine with ethyl acetate–pyridine–water mixture (8:1:91) obtained in 30 min. Glutamine moves near the solvent front, while glutamic acid remains near the origin. The contents of

the assay mixture do not significantly affect the separation of glutamic acid and glutamine. As shown in Fig. 2, glutamine formed from radiolabelled glutamic acid by glutamine synthetase was completely separated from the unreacted substrate. Table I shows the  $R_f$  values of glutamic acid and glutamine in various solvents. It is evident that as the concentration of acetic acid is increased, mobility of glutamic acid increases without any significant effect on mobility of glutamine.

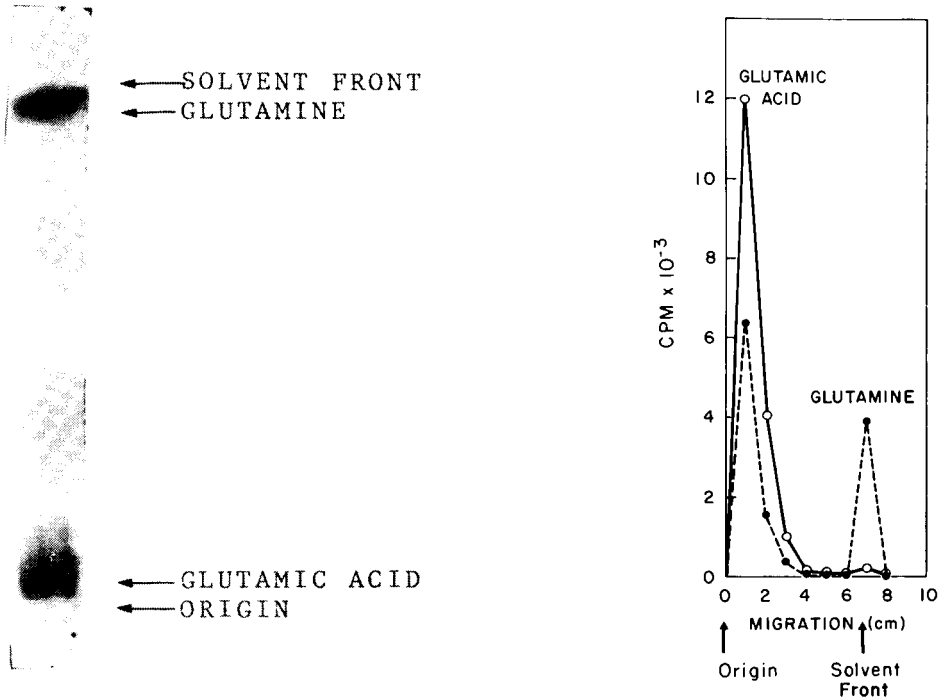


Fig. 1. Separation of glutamic acid and glutamine. A 2- $\mu$ l aliquot containing 4  $\mu$ g of glutamic acid and glutamine in imidazole buffer, pH 7.4 was spotted. After development, the strips were dried, sprayed with 0.2% ninhydrin in butanol-acetic acid (95:5) and spots visualized after brief exposure at 70°C.

Fig. 2. Separation of [<sup>3</sup>H]glutamine (●—●) formed from [<sup>3</sup>H]glutamic acid on Dowex 1-(acetate) coated plastic sheets. After development, the strips were dried, cut into 1-cm pieces and the radioactivity counted as described in the text. Assay mixture was incubated with 70  $\mu$ g of crude enzyme protein for 10 min at 37°C. ○—○, Migration of [<sup>3</sup>H]glutamic acid in the presence of assay mixture and enzyme after incubation at 0°C for 10 min. The composition of assay mixture was the same as described in Materials and methods.

*Relationship of glutamine synthesis with time and protein concentration*

Glutamine synthetase from bovine retina was used to test the linearity of the assay with time and protein concentration. Fig. 3A shows that the amount of glutamine synthesized is linear with respect to time for incubations up to 30 min. The amount of glutamine synthesized was also linear with respect to protein concentration of the crude retinal extract (Fig. 3B). The assay conditions are described under Materials and methods and in the legends to Fig. 3.

TABLE I

 $R_F$  VALUES OF GLUTAMIC ACID AND GLUTAMINE IN VARIOUS SOLVENTS

Solvent	$R_F$ (Glu)	$R_F$ (Gln)
1 Pyridine-acetic acid-water (0.5:0.2:99.3)	0.21	0.97
2 Pyridine-acetic acid-water (0.5:0.5:99)	0.46	0.97
3 Pyridine-acetic acid-water (0.5:1:98.5)	0.56	0.98
4 Acetic acid-water (0.2:99.8)	0.18	0.97
5 Acetic acid-water (0.5:99.5)	0.38	0.97
6 Acetic acid-water (1:99)	0.49	0.97
7 Methanol-acetic acid-water (10:0.2:89.8)	0.18	0.94
8 Ethyl acetate-acetic acid-ammonium hydroxide-water (5:0.1:0.1:94.8)	0.15	0.86
9 Ethyl acetate-pyridine-water (8:1:91)	0.04	0.98

*Requirements for glutamine synthesis*

In Table II, the requirements for glutamine synthetase reaction are illustrated. Essentially, no activity was obtained in the absence of ATP,  $Mg^{2+}$  or ammonia.

*Kinetic characteristics of retinal glutamine synthetase*

In order to test the usefulness of this simple procedure in kinetic studies, kinetic characteristics were determined for purified retinal glutamine synthetase. The enzyme shows Michaelis-Menten kinetics when one of the substrates is limiting. Double

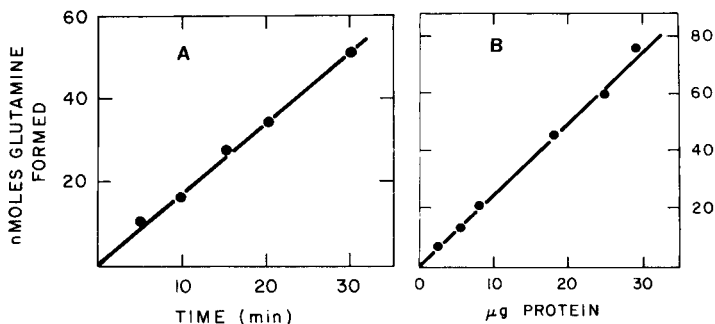


Fig. 3. Relationship of glutamine synthesis with incubation time and protein concentration. A. Effect of various incubation times on product formation using  $7.0 \mu g$  of crude enzyme. B. Effect of different protein concentrations on product formation during a 10 min incubation time. Each data point represents an average of three determinations. Other details were the same as described in Materials and methods.

TABLE II

## REQUIREMENTS FOR GLUTAMINE SYNTHETASE REACTION

The composition of complete system was same as described in Materials and methods.

Reaction conditions	Relative activity (%)
Complete	100
Minus ATP	2.9
Minus $MgCl_2$	2.9
Minus $NH_4Cl$	3.1

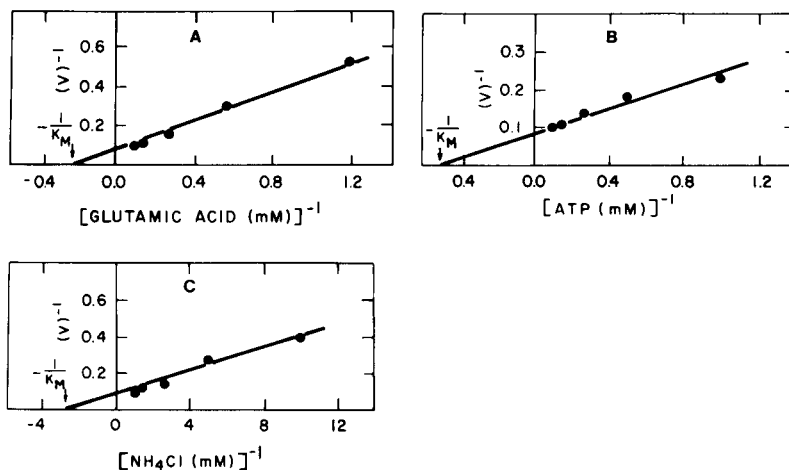


Fig. 4.  $K_M$  determination of glutamine synthetase for glutamic acid (A), ATP (B) and ammonia (C). In each case,  $0.92 \mu\text{g}$  of purified glutamine synthetase and a 10 min incubation time were used. Initial velocity is expressed as nmoles of product formed per min. For each determination, the concentration of all substrates except for the one used to determine the  $K_M$  was the same as described in Materials and methods for the standard assay.

reciprocal plots of velocity *versus* various concentration of glutamic acid, ATP and ammonium chloride are shown in Fig. 4. Michaelis constants ( $K_M$ ) for glutamic acid, ATP and ammonium chloride were found to be  $3.6 \text{ mM}$ ,  $1.9 \text{ mM}$  and  $0.34 \text{ mM}$ , respectively.  $K_M$  values for glutamic acid and ATP were  $3.4 \text{ mM}$  and  $2.1 \text{ mM}$  respectively, by the  $\gamma$ -hydroxyglutamate determination. The  $K_M$  value for ammonium chloride was found to be  $0.28 \text{ mM}$  by the inorganic phosphate determination. These values are in quite close agreement with the values obtained by the present assay.

## DISCUSSION

The separation of glutamic acid and glutamine is rapidly accomplished by thin-layer chromatography. Different solvent systems were tested as to their ability to separate glutamic acid from glutamine. The solvent system used in the present study had the advantages that both the components move as discrete, compact spots. Further, with this solvent system it is possible to separate  $\gamma$ -aminobutyric acid (GABA) from glutamine. The  $R_F$  value of GABA was found to be  $0.91 \pm 0.01$  from five separate runs in comparison to the  $R_F$  value of  $0.98 \pm 0.01$  for glutamine. This separation can be further increased by increasing development time with the solvent. The identity of glutamine as the only product formed under glutamine synthetase assay conditions has been determined by reversed-phase high-performance liquid chromatography (HPLC) and GABA formed in this reaction constitutes less than  $1\%$ <sup>18</sup>. Lack of GABA formation is not due to the absence of active glutamic acid decarboxylase (GAD) in the crude retinal homogenate, as the same retinal preparation is capable of GABA formation under the proper assay conditions. In every case only one product corresponding to either GABA or glutamine was observed depend-

ing upon the assay conditions<sup>18</sup>. The finding of no significant formation of GABA under the glutamine synthetase assay conditions is consistent with previous observations that the ATP and divalent cations used in glutamine synthetase assay are inhibitory for GAD reaction<sup>19-21</sup>.

The assay system described here appears to have many advantages over previously used methods. The assay is simple and allows for a rapid determination of multiple samples under controlled conditions. Previous attempts at separation of glutamine from glutamic acid by paper electrophoresis<sup>22</sup> or TLC<sup>23,24</sup> are not as simple to use and small differences in  $R_F$  values were seen for the glutamic acid and glutamine under these conditions. Bujard and Mauron<sup>24</sup> reported  $R_F$  values for glutamic acid and glutamine of 0.26 and 0.39, respectively. In the present assay,  $R_F$  values of 0.04 and 0.98 for glutamic acid and glutamine respectively allow for complete separation of the two compounds.

The measurement of glutamine synthetase by determination of inorganic phosphate<sup>8,9</sup> is subject to interference by substances such as ATP, ADP, AMP, pyrophosphate, proteins and low concentrations of detergents<sup>25-28</sup>. Assays which measure  $\gamma$ -glutamylhydroxamate formation<sup>9,10</sup>, are subject to interference by substances that can react with the ferric chloride reagent or glutamylhydroxamate. In addition, another major disadvantage with the hydroxamate method is that enzymes other than glutamine synthetase have been shown to catalyze the glutamate transferase reaction<sup>29</sup> and, hence, any changes in the activity in crude cellular extracts should be interpreted with caution.

Radioisotopic methods involving the use of Dowex 1 ( $\text{Cl}^-$ )<sup>11</sup>, alumina<sup>12</sup>, or Dowex 1 ( $\text{CH}_3\text{COO}^-$ ) followed by Amberlite CG-50 ( $\text{H}^+$ )<sup>13</sup> are tedious and time consuming. The elution of glutamic acid and glutamine is sensitive to various factors such as changes in pH, which would cause problems when changes in assay condition are required. Using the strip method we have not observed any changes in the mobility of glutamic acid and glutamine in varying pH of the assay mixture from 6.0 to 8.0.

The present assay is more sensitive than colorimetric methods, measures glutamine formation directly, and is simpler to use than ion exchange columns. With colorimetric methods, it is not possible to accurately determine less than: (1) 50 nmol of  $\gamma$ -glutamylhydroxamate ( $A_{535} = 0.08$ )<sup>30</sup> or  $5 \cdot 10^{-2}$  units enzyme activity; (2) 100 nmol of inorganic phosphate ( $A_{625} = 0.07$ )<sup>31</sup> or  $1 \cdot 10^{-1}$  units enzyme activity. Hence, these methods are not sensitive enough to determine low concentrations of enzyme as ordinarily found in cells in culture. Under the present conditions of assay, it is possible to detect the formation of 1 nmole of radiolabelled glutamine ( $1 \cdot 10^{-3}$  units enzyme activity) using [<sup>3</sup>H]glutamic acid (1000 cpm/nmol). Also, it is possible to make the method more sensitive by increasing the specific activity of the substrate. If it is necessary to add other compounds to the assay mixture which might affect the mobility of the product, reference strips can be run under the same conditions, or the strip can also be cut conveniently into 1-cm pieces and the position of glutamic acid and glutamine can be localized accurately. Also, internal standards can be added to the assay mixture and the strip stained with ninhydrin reagent to localize glutamic acid and glutamine before counting.

In summary, we feel that this assay offers several advantages. The procedure is simple, rapid, specific and sensitive and is applicable with a large number of samples. This assay technique is also useful for assaying GAD activity, and is being extended for the determination of glutaminase, aspartate synthetase, and asparaginase.



## ACKNOWLEDGEMENTS

We wish to thank Mary Bannon for her help in preparing this manuscript, Brian T. Mullins and Joseph Albert for their technical assistance. This work was supported by National Institutes of Health Grants EY-01656, EY-07000 and EY-00785 and unrestricted funds from Connecticut Lions Eye Research Foundation and Research to Prevent Blindness.

## REFERENCES

- 1 A. Ginsburg and E. R. Stadtman, in S. Prusiner and E. R. Stadtman (Editors), *Enzymes of Glutamine Metabolism*, Academic Press, New York, 1973, p. 9.
- 2 S. Tate and A. Meister, in S. Prusiner and E. R. Stadtman (Editors), *Enzymes of Glutamine Metabolism*, Academic Press, New York, 1973, p. 77.
- 3 D. C. Tiemeier and G. Milman, *J. Biol. Chem.*, 247 (1972) 5722.
- 4 T. W. Reid and P. Russell, *Trans. Ophthal. Soc.*, 94 (1974) 929.
- 5 R. J. Kulka and H. Cohen, *J. Biol. Chem.*, 248 (1973) 6738.
- 6 R. B. Crook, M. Louie, T. F. Deuel and G. M. Tomkins, *J. Biol. Chem.*, 253 (1978) 6125.
- 7 S. Seethalakshmi and N. Appajiroa, *Arch. Biochem. Biophys.*, 196 (1979) 588.
- 8 C. H. Fiske and Y. Subbarow, *J. Biol. Chem.*, 159 (1925) 21.
- 9 J. F. Speck, *J. Biol. Chem.*, 179 (1949) 1405.
- 10 F. Lippman and L. C. Tuttle, *J. Biol. Chem.*, 159 (1945) 2128.
- 11 S. Prusiner and L. Milner, *Anal. Biochem.*, 37 (1970) 429.
- 12 J. M. Ravel, J. S. Humphreys and W. Shive, *Arch. Biochem. Biophys.*, 111 (1965) 720.
- 13 M. R. Pishak and A. T. Phillips, *Anal. Biochem.*, 94 (1979) 82.
- 14 T. Devenyi, *Acta Biochem. Biophys. Acad. Sci., Hung.*, 5 (1970) 435.
- 15 S. L. Pahuja and T. W. Reid, *J. Neurochem.*, submitted for publication.
- 16 A. Himoe and R. W. Rinne, *Anal. Biochem.*, 88 (1978) 634.
- 17 M. Bradford, *Anal. Biochem.*, 72 (1976) 248.
- 18 S. L. Pahuja, J. Albert and T. W. Reid, *J. Chromatogr.*, 225 (1981) 37.
- 19 T. Tursky, *Eur. J. Biochem.*, 12 (1970) 544.
- 20 B. S. Vanderheiden, *Biochem. Med.*, 21 (1979) 22.
- 21 P. B. Molinoff and E. Kravitz, *J. Neurochem.*, 15 (1968) 391.
- 22 J. E. Vorhaben, L. Wong and J. W. Campbell, *Biochem. J.*, 135 (1973) 893.
- 23 P. Lund, *Biochem. J.*, 118 (1970) 35.
- 24 E. Bujard and J. Mauron, *J. Chromatogr.*, 21 (1966) 19.
- 25 R. Huxtable and R. Bressler, *Anal. Biochem.*, 54 (1973) 604.
- 26 M. J. Kushmerik, *Anal. Biochem.*, 46 (1972) 129.
- 27 J. J. Blum and K. W. Chambers, *Biochem. Biophys. Acta*, 18 (1955) 601.
- 28 Y. Tashima, *Anal. Biochem.*, 69 (1975) 410.
- 29 A. Meister, in P. D. Boyer, H. Lardy and K. Myrback (Editors), *Enzymes*, Vol. 6, Academic Press, New York, 2nd ed., 1962, p. 443.
- 30 D. C. Tiemeier and G. Milman, *J. Biol. Chem.*, 247 (1978) 2272.
- 31 L. F. Leloir and C. E. Cardini, *Methods Enzymol.*, 3 (1957) 840.

CHROM. 14,298

## FLUORODENSITOMETRIC DETERMINATION OF TRICHOHECENE MYCOTOXINS WITH NICOTINAMIDE AND 2-ACETILPYRIDINE ON A SILICA GEL LAYER

AKIRA SANO\*, YOSHIHIRO ASABE, SHOJI TAKITANI and YOSHIO UENO

*Faculty of Pharmaceutical Sciences, Science University of Tokyo, 12, Ichigaya-funagawara-machi, Shinjuku-ku, Tokyo 162 (Japan)*

(Received August 17th, 1981)

---

### SUMMARY

A fluorodensitometric method for the determination of trichothecene mycotoxins on silica gel thin-layer plates based on a fluorescence reaction of the epoxy group with nicotinamide and 2-acetylpyridine is described. The limits of detection for the five trichothecenes examined were 20–50 ng per spot with visual inspection under UV light (360 nm). Further, these trichothecenes could be determined fluorodensitometrically in the range from *ca.* 10–25 ng per spot to 1500 ng per spot with a coefficient of variation of about 10%.

---

### INTRODUCTION

Thin-layer chromatography (TLC) is one of the most useful methods for trichothecene mycotoxins with a characteristic 12,13-epoxytrichothec-9-ene nucleus, which are fungal metabolites produced by various species of *Fusarium*, *Myrothecium*, *Trichoderma*, *Cepharosporium*, etc., and are among the most interesting mycotoxins studied in the fields of foods and feeds. Sulphuric acid<sup>1–3</sup>, *p*-anisaldehyde<sup>1,4</sup>, aluminium chloride<sup>5</sup> and 4-(*p*-nitrobenzyl)pyridine<sup>6</sup> have been used as the detection reagents on thin-layer plates. However, these reagents, except for the last one, have a poor structural selectivity for the trichothecene nucleus.

We have previously investigated the analysis of trichothecene mycotoxins<sup>6–9</sup> and in the last paper<sup>6</sup> we reported a densitometric determination using 4-(*p*-nitrobenzyl)pyridine as the chromogenic reagent. Although our method is the most convenient and has the highest selectivity towards trichothecenes in comparison with other methods, it has some defects such as low colour stability and low sensitivity.

This work was aimed at establishing a fluorodensitometric method for determining these mycotoxins on thin-layer plates by making use of a fluorescence reaction of the 12,13-epoxy group in the trichothecene nucleus with nicotinamide and 2-acetylpyridine.

## EXPERIMENTAL

### *Chemicals*

The trichothecene mycotoxins used are listed in Table I. The stock standard solutions of the toxins were prepared at a concentration of 5  $\mu\text{g}/\mu\text{l}$  in chloroform, except for deoxynivalenol and nivalenol, which were dissolved in methanol.

Nicotinamide (Tokyo Kasei Co., Japan) was used as a 4% solution in acetone-ethanol (5:1). 2-Acetylpyridine (Nakarai Chemical Co., Japan; re-distilled under reduced pressure) was used as a 3% solution in *n*-hexane. Potassium hydroxide (Kanto Chemical Co., Japan) was used as a 2 *N* solution in 80% ethanol. Formic acid (98–100%; Nakarai Chemical Co.) was used as a 30% solution in diethyl ether.

Pre-coated silica gel 60 TLC plates (0.25 mm thickness) were purchased from E. Merck (Darmstadt, G.F.R.). All other chemicals were of analytical-reagent grade.

### *Apparatus*

A Shimadzu CS-910 dual-wavelength chromatoscanner (Shimadzu, Kyoto, Japan) equipped with an integrator was employed in the reflectance and linear scanning modes.

A 2- $\mu\text{l}$  volumetric micropipette (Microcaps; Drummond, Broomall, PA, U.S.A.), was used to apply the sample to the TLC plates, except for recovery examination in which a 5- $\mu\text{l}$  micropipette was used.

### *Thin-layer chromatography*

A 2- $\mu\text{l}$  volume of the sample solution was spotted at 2 cm from the lower edge of the plate and the plate was developed by the ascending technique until the front had reached a height of 10 cm using an appropriate solvent system. The solvent systems examined were chloroform-methanol (97:3, 95:5 and 7:1). The developed plate was dried in an air stream and was dipped in the nicotinamide solution\*. After evaporation of the solvent, the plate was heated in an oven for 15 min at 160°C in method I, which was used for the simultaneous analysis of both type A and B trichothecenes, or for 10 min at 140°C in method II, which was used only for type B trichothecenes, and then cooled to room temperature. The cooled plate was dipped in the 2-acetylpyridine solution and then sprayed with the potassium hydroxide solution. The plate was allowed to stand for 30 min at room temperature, then dipped in the formic acid solution. After evaporation of the solvent, the acidified plate was heated in an oven for 4 min at 100°C and then cooled to room temperature.

The trichothecene mycotoxins could be observed as light blue fluorescent spots on a very weak dark blue fluorescent background under UV light (360 nm).

### *Densitometry*

A CS-910 chromatoscanner was used under the following conditions: scanning speed, 20 mm/min; chart speed, 20 mm/min; wavelengths,  $\lambda_{\text{ex}} = 380$  nm,  $\lambda_{\text{em}} = 450$  nm (interference filter); and beam slit, 10  $\times$  0.5 mm. Scanning was also carried out in the direction of development.

---

\* Dipping was carried out in the direction of development.

## RESULTS AND DISCUSSION

By analogy with the fluorescence reaction of  $N^1$ -methylnicotinamide with an active methylene compound<sup>10</sup>, the fluorophore obtained by our method is assumed to be a stable naphthylidene derivative, which resulted from (1)  $N$ -alkylation of nicotinamide with the epoxy group and (2) subsequent condensation of  $N^1$ -alkyl-nicotinamide with 2-acetylpyridine in the presence of an alkali and followed by (3) treatment with an acid.

Trichothecene mycotoxins are classified into two groups (types A and B) according to the structural variations at the C-8 position of the trichothecene nucleus (see Table I). Various experimental conditions were examined, using T-2 toxin as a typical sample of type A and fusarenon-X as type B because the reactivity of type A trichothecenes in the reaction with nicotinamide differed distinctly from that of type B in our preliminary examinations.

*N-Alkylation reaction conditions*

Constant integrated values were obtained at concentrations above 1% for fusarenon-X in the examination of the influence of nicotinamide concentration on the  $N$ -alkylation reaction. On the other hand, the integrated values for T-2 toxin increased gradually within the 6% nicotinamide concentration range examined. Higher nicotinamide concentrations caused a higher fluorescent background, and also more polar solvent was necessary to dissolve the reagent, which resulted in diffusion of the spots. Hence a 4% acetone-ethanol (5:1) solution was chosen.

The relationship between fluorescence intensity and reaction time was studied at 140 and 160°C (Fig. 1). When the heating was carried out at 140°C, the reaction of T-2 toxin (type A trichothecenes) was incomplete after 30 min, but an approximately constant intensity was obtained after heating at 160°C for 10–30 min.

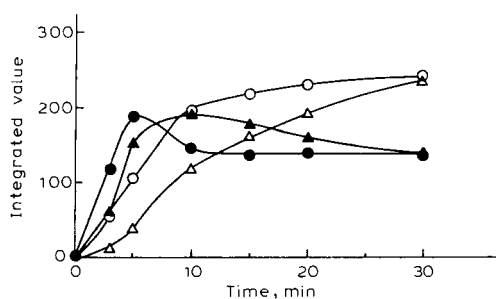


Fig. 1. Effect of reaction time and temperature on the  $N$ -alkylation reaction. Open symbols, T-2 (0.5  $\mu\text{g}$  per spot); closed symbols, F-X (1.0  $\mu\text{g}$  per spot).  $\Delta$ ,  $\blacktriangle$ , 140°C;  $\circ$ ,  $\bullet$ , 160°C. Abbreviations as in Table I.

On the other hand, with fusarenon-X (type B trichothecenes), an almost constant and maximal intensity was obtained after heating at 140°C for 10 min. Moreover, when the heating temperature was elevated to 160°C, the fluorescence intensity reached the maximal value after heating for 5 min and, after decreasing rapidly, the intensity reached a constant value (correspond to *ca.* 74% of the maximal intensity) after 10–30 min, whereas heating over 30 min resulted in a brown spot. As the maximal intensity after heating at 140°C for 10 min was *ca.* 1.4 times higher than

TABLE I  
STRUCTURES OF TRICHOPECENE MYCOTOXINS

Type A		Type B					
<i>Mycotoxin (abbreviation)</i>	<i>R</i> <sub>1</sub> <i>R</i> <sub>2</sub>	<i>R</i> <sub>3</sub> <i>R</i> <sub>5</sub>	<i>Mycotoxin (abbreviation)</i>	<i>R</i> <sub>1</sub>	<i>R</i> <sub>2</sub>	<i>R</i> <sub>3</sub>	<i>R</i> <sub>4</sub>
T-2 toxin (T-2)*	OH OCOCH <sub>3</sub>	OCOCH <sub>3</sub> OCOCH <sub>3</sub>	Fusarenon-X (F-X)***	OH	OCOCH <sub>3</sub>	OH	OH
Neosolaniol (NS)*	OH OCOCH <sub>3</sub>	OCOCH <sub>3</sub> OH	Nivalenol (Niv)§	OH	OH	OH	OH
Diacetoxyscirpenol (DAS)**	OH OCOCH <sub>3</sub>	OCOCH <sub>3</sub> H	Tetraacetylnivalenol (TAN)§	OCOCH <sub>3</sub>	OCOCH <sub>3</sub>	OCOCH <sub>3</sub>	OCOCH <sub>3</sub>
			Deoxynivalenol (DON)§§	OH	H	OH	OH

\* Cultured *Fusarium solani*.

\*\* Purchased from Makor Chemicals Ltd. (Israel).

\*\*\* Cultured *Fusarium nivale*.

§ Prepared from fusarenon-X.

§§ Supplied by T. Yoshizawa (Kagawa University, Japan).

the constant value at 160°C, heating at 140°C seemed optimal for the analysis of fusarenon-X.

Therefore, heating at 160°C for 15 min was selected in method I, which was used for simultaneous analysis of the both type A and B trichothecenes, and heating at 140°C for 10 min was also selected in method II, which was used exclusively for the analysis of type B trichothecenes.

As the best result was obtained when the subsequent reaction was done without heating, the plate was therefore cooled to room temperature before proceeding to the next step.

*Conditions of the condensation reaction of N<sup>1</sup>-alkylnicotinamide with 2-acetylpyridine*

Various active methylene compounds were examined as reagents in the condensation reaction. As shown in Table II, 2-acetylpyridine gave the highest fluorescence intensity; the intensities were twice and four times as great as that of acetophenone used as the reagent for T-2 toxin and fusarenon-X, respectively, whereas with common epoxy compounds such as glycidyl phenyl ether, the intensity obtained with 2-acetylpyridine was only 1.4 times as great as that of acetophenone<sup>11</sup>. Therefore, 2-acetylpyridine was chosen in the present method to increase the analytical sensitivity for mycotoxins. As almost constant fluorescence intensity was obtained at a concentration above 1% of 2-acetylpyridine for both type A and B trichothecenes, a 3% solution was used.

TABLE II

## EFFECT OF ACTIVE METHYLENES ON THE CONDENSATION REACTION

T-2 toxin, 0.5 µg per spot; fusarenon-X, 1.0 µg per spot. Results obtained by method I.

Compound*	Relative fluorescence intensity**		Compound*	Relative fluorescence intensity**	
	T-2	F-X		T-2	F-X
Acetone	0.3	0.9	<i>p</i> -Hydroxyacetophenone	0	0
Methyl ethyl ketone	0.9	2.4	<i>p</i> -Acetylacetophenone	41	16
Cyclopentanone	11	24	1-Acetylnaphthalene	2.7	3.4
Cyclohexanone	18	37	2-Acetylnaphthalene	6.0	3.7
1-Indanone	2.6	2.9	2-Acetylpyridine	100	100
$\alpha$ -Tetralone	4.3	5.6	3-Acetylpyridine	38	43
Acetophenone	57	24	4-Acetylpyridine	21	33
<i>p</i> -Chloroacetophenone	42	23	2-Acetylfuran	7.7	13
<i>p</i> -Bromoacetophenone	30	22	2-Acetylthiophene	5.1	11
<i>p</i> -Nitroacetophenone	0	0	3-Acetylidole***	0	0
<i>p</i> -Methylacetophenone	34	15			

\* Reagent concentration: 5%.

\*\* 2-Acetylpyridine arbitrarily taken as 100.

\*\*\* Saturated solution.

Potassium hydroxide was chosen as the alkali in the condensation reaction because it gave superior fluorescence intensity, signal-to-noise ratio and solubility in aqueous ethanol compared with other alkalis and organic bases. Although water or

an aqueous solvent is desirable for dissolving potassium hydroxide, it has an unfavourable effect on the silica gel layer. Therefore, an 80% ethanol solution was used in this step. Next, the effect of potassium hydroxide concentration on this reaction was studied; the formation of the fluorophore was affected by the alkali concentration, as shown in Fig. 2. The concentration used was 2 *N* because some destruction of the silica gel plate was observed when solutions of concentration higher than 3 *N* were used, although the maximal intensity was obtained with a 2.5 *N* solution.

For addition of the alkali solution, spraying was chosen in order to prevent peeling of the silica gel layer; in the other steps the reagent solutions were added to the silica gel plate by dipping.

The relationship between fluorescence intensity and the standing time after spraying with the potassium hydroxide solution was studied at room temperature. As a constant integrated value was obtained when the standing times were longer than 10 min for T-2 toxin and 20 min for fusarenon-X, a standing time of 30 min was therefore chosen.

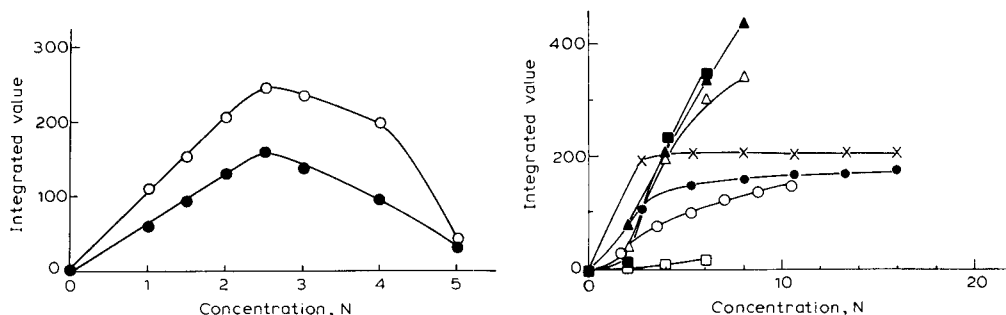


Fig. 2. Effect of potassium hydroxide concentration on the condensation reaction (method I). ○, T-2 (0.5 µg per spot); ●, F-X (1.0 µg per spot).

Fig. 3. Effect of acid species and their concentration on the acid treatment (method I). T-2 (0.5 µg per spot): ×, formic acid; ○, acetic acid; ▲, citric acid; △, malonic acid; ■, sulfuric acid; □, phosphoric acid. F-X (1.0 µg per spot): ●, formic acid.

#### Conditions of acid treatment

Various acids were examined (Fig. 3). Formic acid was chosen because it was superior in both stability and intensity of the resulting fluorescence and in solubility for non-polar solvent such as diethyl ether compared with the other acids examined, e.g., acetic, malonic, citric, sulphuric and phosphoric acids.

As almost constant intensities were obtained at concentrations above 10% (2.65 *N*) for T-2 toxin and 20% (5.3 *N*) for fusarenon-X, 30% (7.95 *N*) formic acid solution was used.

The heating step for the conversion of the reaction intermediate into the final product was studied; it was found that the reaction rate was slow at room temperature but the reaction was complete within a few minutes at 100°C. Therefore, heating at 100°C for 4 min was selected.

The fluorescences obtained by both methods I and II were stable at least for 4 h at room temperature.

Satisfactory results were obtained in the TLC of seven trichothecenes, as shown in Fig. 4.

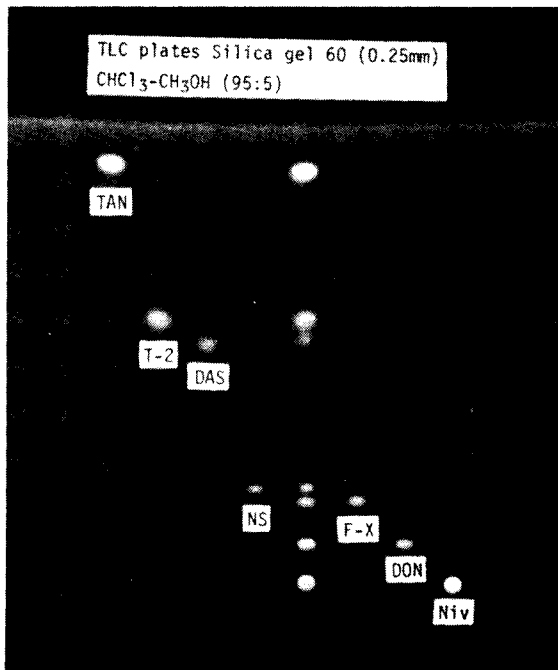


Fig. 4. Thin-layer chromatogram of trichothecene mycotoxins. Developing solvent: chloroform-methanol (95:5); method I.

#### *Limits of detection and calibration graphs*

The analytical data for T-2 toxin, diacetoxyscirpenol, fusarenon-X, deoxynivalenol and nivalenol obtained by the proposed methods are summarized in Table III; the limits of detection with visual inspection under UV light (360 nm) were 20–50 ng per spot, and the calibration graphs for these mycotoxins were straight lines in the concentration ranges given in Table III.

The coefficients of variation of the measurements were satisfactory in most instances.

#### *Detection of T-2 toxin, fusarenon-X, deoxynivalenol and nivalenol added to a corn sample*

The proposed method has a high selectivity for epoxy compounds but is seriously affected by other alkylating agents because the reactivity of trichothecenes in the N-alkylation reaction was considerably lower than that of common epoxy compounds. An attempt to apply our method directly to trichothecenes in agricultural samples was unsuccessful because several interfering materials prevented the detection of the spots. Hence, it is necessary to use some clean-up step prior to practical analyses.

The clean-up method of Kamimura *et al.*<sup>12</sup> was tested using a corn sample to which T-2 toxin, fusarenon-X, deoxynivalenol and nivalenol had been added. This method was effective for analysis by the integrated area method of T-2 toxin, fusarenon-X and nivalenol but not for deoxynivalenol, as shown in Figs. 5 and 6. Further,



TABLE III  
ANALYTICAL DATA FOR TRICHOPECENE MYCOTOXINS

Method	Developing solvent	Mycotoxin	R <sub>F</sub> value	Determination range* (ng per spot)	Coefficient of variation* (%)	Limit of detection (ng per spot)
I	CHCl <sub>3</sub> - CH <sub>3</sub> OH (97:3)	T-2 toxin	0.55	10-1500 (10-1250)	1.0 µg, 2.8 ( 7.4) 25 ng, 8.8 (12.5)	25
		Diacetoxyscirpenol	0.50	10-1500 (10-1000)	1.0 µg, 5.6 ( 3.9) 25 ng, 8.6 ( 9.3)	25
		Fusarenon-X	0.14	25-1500 (25-1250)	1.0 µg, 3.8 ( 5.8) 50 ng, 7.8 (13.0)	50
		Deoxynivalenol	0.08	25-1500 (25-1250)	1.0 µg, 4.4 ( 7.7) 50 ng, 9.0 (11.8)	50
		Nivalenol	0.02	25-1500 (25-1250)	1.0 µg, 5.2 ( 4.7) 50 ng, 7.3 ( 5.4)	50
II	CHCl <sub>3</sub> - CH <sub>3</sub> OH (7:1)	Fusarenon-X	0.64	20-1500 (20-1250)	1.0 µg, 5.4 ( 8.3) 50 ng, 8.8 (10.2)	25
		Deoxynivalenol	0.47	20-1500 (20-1250)	1.0 µg, 2.4 ( 4.7) 50 ng, 7.4 ( 7.3)	25
		Nivalenol	0.22	10-1500 (10-1250)	1.0 µg, 3.2 ( 9.7) 50 ng, 4.9 ( 3.3)	20

\* Values without parentheses, peak-area method; values in parentheses, peak-height method.

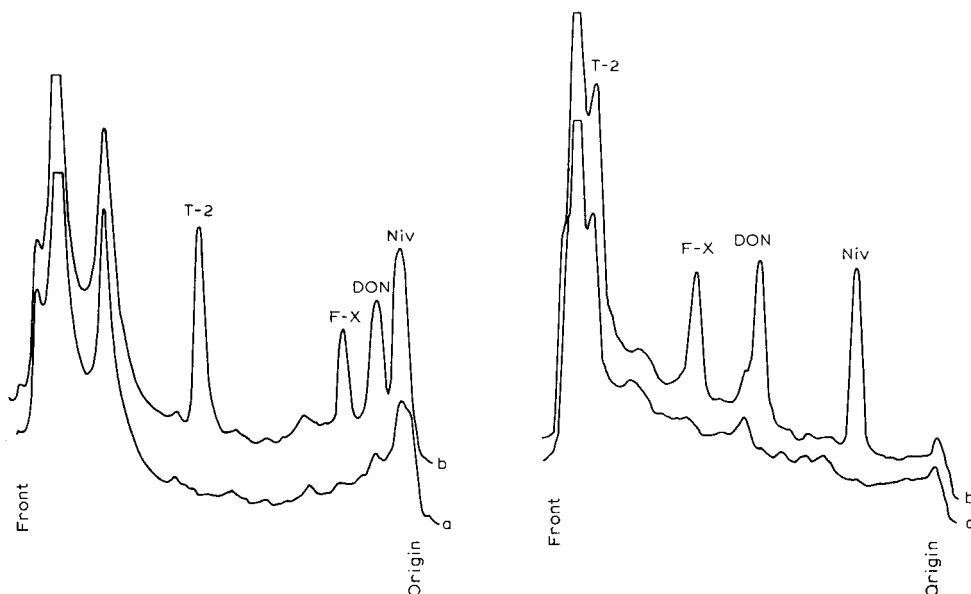


Fig. 5. Fluorodensitograms of extract from corn after fluorescent reaction (method I). (a) Corn; (b) corn + trichothecenes (corresponding to 0.5 ppm). Developing solvent: chloroform-methanol (97:3).

Fig. 6. Fluorodensitograms of extract from corn after fluorescent reaction (method II). (a) Corn; (b) corn + trichothecenes (corresponding to 0.5 ppm). Developing solvent: chloroform-methanol (7:1).

deoxynivalenol could be determined by the peak-height method; about 60–70% recoveries were obtained by the method II after development with chloroform-methanol (7:1) when 1 ppm of deoxynivalenol and nivalenol were added to an original corn sample.

As agricultural products are contaminated with various mycotoxins, further studies of clean-up procedures and the systematic analysis of these mycotoxins are required. Nevertheless, the present method seems to be useful for the analysis of trichothecene mycotoxins.

#### ACKNOWLEDGEMENT

The authors thank Dr. T. Yoshizawa for supplying the sample.

#### REFERENCES

- 1 N. Nakano, T. Kunimoto and K. Aibara, *Shokuhin Eiseigaku Zasshi*, 14 (1973) 56.
- 2 Y. Ueno, N. Sato, K. Ishii, K. Sakai, H. Tsunoda and M. Enomoto, *Appl. Microbiol.*, 25 (1973) 699.
- 3 Y. Naoi, E. Kazama, K. Saito, H. Ogawa, K. Shimura and Y. Kimura, *Ann. Rep. Tokyo Metr. Res. Lab. P. H.*, 25 (1974) 203.
- 4 P. M. Scott, J. W. Lawrence and W. van Walbeek, *Appl. Microbiol.*, 20 (1970) 839.
- 5 Y. Naoi, K. Saito, E. Kazama, H. Ogawa and Y. Kimura, *Ann. Rep. Tokyo Metr. Res. Lab. P. H.*, 23 (1971) 175.
- 6 S. Takitani, Y. Asabe, T. Kato, M. Suzuki and Y. Ueno, *J. Chromatogr.*, 172 (1979) 335.
- 7 T. Kato, Y. Asabe, M. Suzuki and S. Takitani, *Bunseki Kagaku (Jap. Anal.)*, 25 (1976) 659.
- 8 T. Kato, Y. Asabe, M. Suzuki and S. Takitani, *Bunseki Kagaku (Jap. Anal.)*, 26 (1977) 422.
- 9 T. Kato, Y. Asabe, M. Suzuki and S. Takitani, *Anal. Chim. Acta*, 106 (1979) 59.
- 10 J. W. Huff and W. A. Perlzweig, *J. Biol. Chem.*, 167 (1947) 157.
- 11 S. Takitani, A. Sano, Y. Asabe and M. Suzuki, *Anal. Chim. Acta*, in press.
- 12 H. Kamimura, M. Nishijima, K. Saito, S. Takahashi, A. Ibe, S. Ochiai and Y. Naoi, *Shokuhin Eiseigaku Zasshi*, 19 (1978) 443.

CHROM. 14,320

## Note

### Dissociation of sulphonic acids sorbed onto a non-polar stationary phase

BO F. NILSSON and OLOF SAMUELSON\*

*Department of Engineering Chemistry, Chalmers University of Technology, S-412 96 Göteborg (Sweden)*

(Received August 26th, 1981)

Non-polar stationary phases have increasingly become important for separation of anions in eluents containing quaternary ammonium ions with non-polar substituents, and of cations in the presence of hydrophobic anions such as alkyl sulphonates<sup>1,2</sup>. In some systems ion-pair formation may occur in the external solution and the term ion-pair chromatography is then justified. The quaternary ammonium salt and the sulphonate are enriched in the stationary phase which will behave as an anion exchanger or cation exchanger, respectively. The term "dynamic ion-exchange chromatography" has sometimes been used<sup>3</sup>, but since chromatography is itself a dynamic process the authors prefer the term "chromatography on sorbed ionic sites"<sup>4</sup>.

The free-acid form of a cation-exchange resin of the sulphonic acid type is virtually completely dissociated<sup>5</sup>. This has been demonstrated by studies of cation-exchange equilibria and reactions catalyzed by hydrogen ions. To determine whether hydrophobic electrolytes adsorbed on non-polar stationary phases are dissociated, we have studied the inversion of sucrose in aqueous solution by means of anthraquinone-2-monosulphonic acid (AMS) sorbed on a macroporous styrene-divinylbenzene resin, Hitachi gel 3011.

#### EXPERIMENTAL

The styrene-divinylbenzene resin (Hitachi 3011, Hitachi, Tokyo, Japan) had a particle size of  $12 \pm 5 \mu\text{m}$ . It was packed into a jacketed steel column ( $100 \times 5 \text{ mm}$ ) as described previously<sup>4</sup>. The breakthrough curves for AMS were calculated from absorbance measurements at 280 nm. The column was treated with 25% (w/w) ethanol to replace adsorbed AMS, and carefully washed with water before the curves were recorded. The inversion of sucrose was studied by passing aqueous solutions through this column.

The effluents were analyzed by partition chromatography in 75% ethanol on the sulphate form of an anion-exchange resin<sup>6</sup>. The temperature was 75°C. The calculations were based on determinations of glucose in the eluate. For experiments with large degrees of inversion, the decrease in sucrose concentration was in good agreement with that calculated from the formation of glucose.

## RESULTS AND DISCUSSION

The sorption of AMS onto the Hitachi gel was studied by recording the breakthrough curves at room temperature. As shown in Fig. 1, AMS was strongly retained by the resin. The breakthrough capacity calculated in bed volumes of the solution decreased by approximately 50% when the influent concentration was increased by a factor of ten. When the column was saturated with AMS ( $C/C_0 = 1$ ), the total amount of AMS in the column (calculated from the area between the breakthrough curve and the ordinate) was 5 mmol per litre of bed volume when the influent solution contained 0.1 mmol  $l^{-1}$ . At a ten-fold influent concentration the total amount of AMS was 23 mmol  $l^{-1}$ .

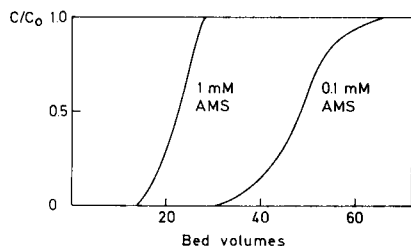


Fig. 1. Breakthrough curves recorded at room temperature for aqueous solutions of AMS containing 10 mmole of sucrose per litre. Nominal linear (empty tube) flow-rate: 5.0  $cm\ min^{-1}$ .

Evidently, the adsorption isotherm was non-linear within this concentration range. The increase in concentration resulted in a decrease in the distribution coefficient by approximately 55%. The ambiguity in the determination of the interstitial volume makes it impossible to calculate accurately the average concentration of AMS in the stationary phase, but it is reasonable to assume that this concentration was approximately 10 mmol  $l^{-1}$  at the lower concentration of AMS, and 50 mmol  $l^{-1}$  at the higher.

Inversion experiments were made on a column packed with Hitachi gel and conditioned with 0.1 mM AMS in 10 mM sucrose solution at 90°C. The inversion was approximately 3% at a nominal linear flow of 2.5  $cm\ min^{-1}$ . In a blank in which the same solution was heated in the absence of resin the inversion was less than 0.3%.

The concentration of AMS in the solution was then increased by a factor of ten. As shown in Fig. 2 this led to a markedly increased inversion of sucrose. The

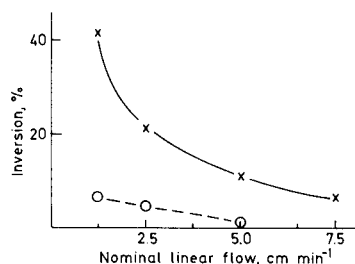


Fig. 2. Percentage inversion at 90°C of 10 mM sucrose solution as a function of the nominal linear flow-rate. The broken line refers to the inversion for blanks in 1 mM AMS without any resin present, recalculated on the assumption that the relative interstitial volume was 0.5 in the column packed with resin.

inversion was much higher than in blanks carried out in the absence of the Hitachi gel. Finally, blanks were made with the Hitachi gel without the presence of AMS. No formation of glucose was observed.

The results show that AMS adsorbed on a non-ionic stationary phase exerted a large catalytic effect on the inversion of sucrose. We conclude that the adsorbed sulphonic acid was dissociated and that the hydrogen ions present as counter ions in the stationary phase were responsible for the large inversion of sucrose. It is believed that in many other chromatographic systems with water as the predominant solvent, and with sulphonates or quaternary ammonium salts present in the eluent and enriched in the stationary phase, the ions in the stationary phase are dissociated. In such systems the term ion-pair chromatography may lead to misunderstanding. It is suggested that it is replaced by the term "chromatography on sorbed ionic sites". Additional arguments were given previously<sup>4</sup>.

#### REFERENCES

- 1 E. Tomlinson, T. M. Jefferies and C. M. Riley, *J. Chromatogr.*, 159 (1978) 315.
- 2 B. A. Bidlingmeyer, *J. Chromatogr. Sci.*, 18 (1980) 525.
- 3 C. P. Terweij-Groen, S. Heemstra and J. C. Kraak, *J. Chromatogr.*, 161 (1978) 69.
- 4 B. F. Nilsson and O. Samuelson, *J. Chromatogr.*, 212 (1981) 1.
- 5 O. Samuelson, *Studier rörande jonbytande fasta ämnen*, Esselte, Stockholm, 1944; reprinted as *Ingeniörsvetenskapsakademiens Handlingar*, No. 179 (1945).
- 6 L.-I. Larsson and O. Samuelson, *Acta Chem. Scand.*, 19 (1965) 1357.

## Note

### Gas chromatographic determination of methacrylamide and the other intermediates in reaction mixtures in the synthesis of methyl methacrylate from acetone cyanohydrin

J. BALÁK\*, M. POLIEVKA, L. UHLÁR and E. ČAVOJCOVÁ

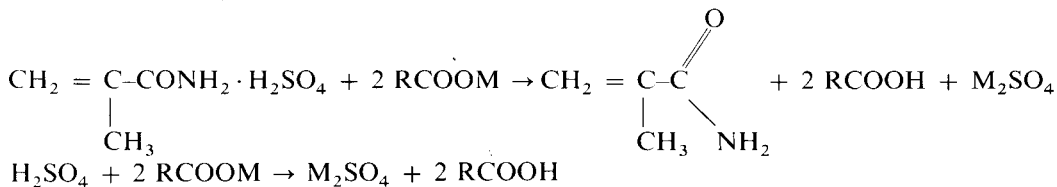
Research Institute for Petrochemistry, 97271, Nováky (Czechoslovakia)

(First received August 4th, 1981; revised manuscript received September 3rd, 1981)

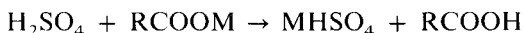
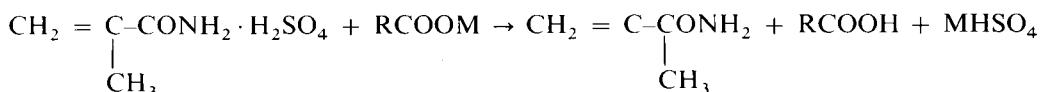
Previously described GC methods<sup>1–10</sup> for the determination of monomeric methyl methacrylate (MMA) can be applied only in the extraction and distillation stages of MMA technology. The main difficulty in the analysis of reaction mixtures is that they contain 20–40 wt.-% of sulphuric acid and methacrylamide bound as sulphate has to be freed. The problem with MMA production analyses has been solved by double-bond determinations<sup>11</sup> (determination of olefinic unsaturation by using potassium bromide–potassium bromate reagent), which is not a convenient method for the esterification stage where methacrylamide (MAA), methacrylic acid (MAK) and MMA are components of the mixture. Moreover, the determination is disturbed by oligomers that contain double bonds in their molecules.

For MMA determination a method based on hydrolysis of MAA and determination of the ammonia distilled off has been applied<sup>12</sup>. This method is relatively complex, slow and not always accurate.

The samples of reaction mixtures are pre-treated before GC determination with a reagent that binds sulphuric acid and at the same time liberates MAA. Subsequently, organic solvent is added, which dissolves the components to be determined and organic salts are separated out. Into the GC apparatus are injected only mixtures of organic compounds. Salts of alkali or alkaline earth metals with mono- and dicarboxylic acids (*e.g.*, potassium acetate or oxalate) can be used as reagents. Sulphuric acid displaces weaker acids and liberates the sulphate of the alkali or alkaline earth metal (M):

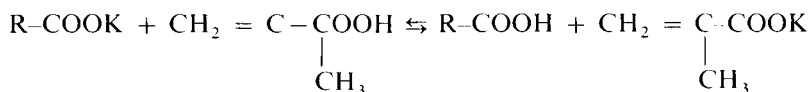


or



The most convenient solvent for the samples is dioxane, which is used in such an amount that gives concentrations of the components to be determined corresponding to the range of linearity of the detector. The inorganic salts are separated on the bottom of the vessel and the organic layer sampled for GC analysis. For the determination of MAA, MMA and methanol it is convenient to treat the samples of the reaction mixture with anhydrous potassium acetate.

In the determination of methacrylamidesulphate (MAAS), an aqueous solution of potassium acetate can be used. On the other hand, for methacrylic acid it is more convenient to treat the samples with an alkali metal salt of an acid with a lower  $pK_a$  value, e.g., potassium oxalate:



When the salt of an acid with a higher or similar  $pK_a$  value to that of MAK is used the system is equilibrated and the results are not reproducible.

This GC method has been patented<sup>13</sup>.

## EXPERIMENTAL AND RESULTS

### *Sample preparation*

To 0.3–0.35 g of reaction mixture were added 1 ml of distilled water (for MAA in MAAS) and 1 ml of the reagent (200 g of potassium acetate in 100 ml of water or 30 g potassium oxalate in 100 ml of water) and the solution was diluted with dioxane to give concentrations of the constituents to be determined corresponding to the range of linearity of the detector.

For samples from esterification that contain water, anhydrous reagents are used.

### *GC determination of MAA*

Analyses were carried out on a Chrom 41 apparatus equipped with a flame-ionization detector (FID) and a stainless-steel column (1.2 m × 3 mm I.D.) packed with 5% (w/w) of PEGA on Chezasorb support (0.1–0.5 mm). The following conditions were used: column temperature 160 C (isothermal); injector temperature, 250 C; carrier gas, nitrogen at a flow-rate of ca. 0.03 l/min; hydrogen flow-rate, 0.03 l/min; air flow-rate, 0.6 l/min; injection volume, 1 μl. For all analyses of reaction mixtures a small stainless-steel conical screen was inserted into the injection chamber, the dimensions being adapted to the length of the injection syringe needle. Dioxane and acetic acid eluted immediately and the retention times of MAK and MAA were 45 and 180 sec, respectively (Fig. 1); the standard deviation was 0.58% (w/w) and the relative standard deviation was 1.89%; the sensitivity of the amplifier was 1:1000.

### *GC determination of MAK*

The samples were treated as for the MAA determination and separately for MAA and MAK. The following conditions were used: column temperature, 130 C; injector temperature, 180 C; other conditions as given above. Dioxane and acetic

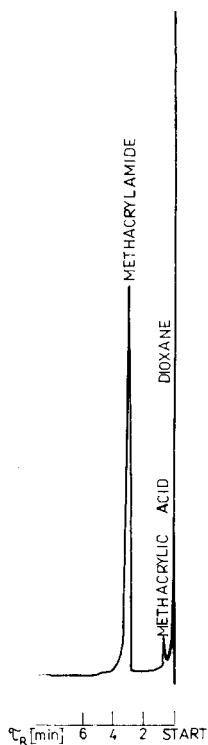


Fig. 1. GC determination of MAA.

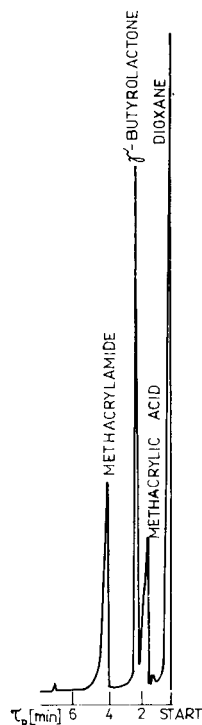


Fig. 2. GC determination of MAK.

acid eluted immediately and the retention times of MAK and MAA were 110 and 250 sec, respectively (Fig. 2); the standard deviation was 0.47% (w/w) and the relative standard deviation was 3.02%.

#### GC determination of MMA and methanol

Samples were treated as for MAA (see above). A CHROM 5 gas chromatograph with an FID was used; the column (3.7 m  $\times$  3 mm I.D.) was packed with 10% (w/w) of Carbowax 20M plus 1% (w/w) of sodium hydroxide on Chromaton NAW (0.2  $\times$  0.25 mm) support. The following conditions were used: column temperature, 100°C; injector temperature, 150°C (modification of injector as described above); carrier gas, nitrogen at a flow-rate of *ca.* 0.04 l/min; hydrogen flow-rate, 0.04 l/min; air flow-rate, 0.6 l/min; injection volume, 1  $\mu$ l. The retention times were as follows: methanol, 108 sec; MMA, 168 sec; impurity from dioxane, 144 sec; dioxane, 240 sec (Fig. 3). The standard deviations were 0.26% (w/w) for methanol and 0.658% (w/w) for MMA; the relative standard deviations were 3.78% and 2.22%, respectively.

For all analyses the method of direct calibration was employed.

#### CONCLUSION

A simple, rapid and accurate method for the determination of the main inter-



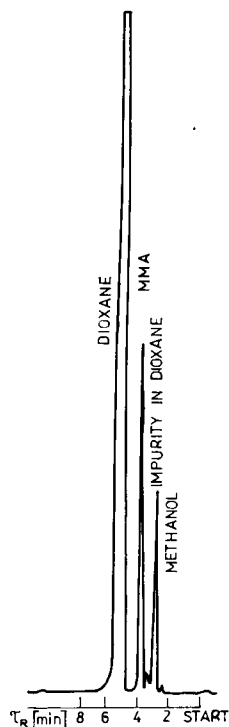


Fig. 3. GC determination of MMA and methanol.

mediate components in the synthesis of MMA from acetone cyanohydrin has been developed. The method involves pre-treatment of samples and makes possible the GC analysis of organic compounds in the presence of inorganic acids. The method can be employed directly in production plants for inter-stage control.

#### REFERENCES

- 1 J. Janák and M. Dobiašová, *Collect. Czech. Chem. Commun.*, 25 (1960) 1566.
- 2 C. E. R. Jones, *Gas Chromatogr. Proc. 3rd Symp., Edinburgh, 1960*, p. 401.
- 3 L. Szepesy and J. Simon, *Votr. Symp. Gas. Chromatogr., 4, Leuna, G.D.R., 1963*, p. 190; *C.A.*, 60 (1964) 1841a.
- 4 B. Kosek, *Chem. Prům.*, 15 (1965) 160.
- 5 V. J. Šnol and V. A. Averin, *Gas. Chromatogr. (Moscow)*, No. 2 (1964) 74; *C.A.*, 64 (1966) 15987.
- 6 R. W. Germaine and J. K. Haken, *J. Chromatogr.*, 43 (1969) 43.
- 7 G. Sassu and F. Zilio-Grandi, *Corsi Semin. Chim., 1969 (9)*, (1969) 133; *C.A.*, 72 (1970) 50486.
- 8 A. K. Demčenko and T. A. Utkina, *Avtom. Khim. Proizvod. (Moscow)*, No. 2 (1969) 105.
- 9 M. S. Kleščeva and I. T. Koržova, *Gazov. Khromatogr.* No. 10 (1969) 94.
- 10 J. Sokolowska and M. Hudzik, *Chem. Anal. (Warsaw)*, 20 (1975) 1047.
- 11 T. Takeuchi, *J. Chem. Soc. Jap., Ind. Chem. Sect.*, 65 (1962) 539; *Czech. Stand.*, No. 66 (1975).
- 12 T. Takeuchi, *J. Chem. Soc. Jap., Ind. Chem. Sect.*, 60 (1957) 1148.
- 13 M. Polievka, L. Uhlár, J. Balák, M. Jančík and E. Čavojeová, *Czech. Patent 204426* (1980).

## Note

### Outer-sphere ligand exchange chromatography of nucleotides and related compounds on a modified polysaccharide gel

D. CORRADINI\* and M. SINIBALDI

*C.N.R., Istituto di Cromatografia, Area della Ricerca di Roma, C.P. 10, 00016 Monterotondo Stazione (Italy)*

and

A. MESSINA

*Istituto di Chimica Analitica, Università di Roma, 00185 Rome (Italy)*

(Received August 31st, 1981)

In two recent papers concerning the study of new purification methods in biochemistry, Hubert and Porath<sup>1,2</sup> reported the fractionation of mono- and dinucleotides on a biscarboxymethylamino group-containing Sepharose gel loaded with a suitable metal. The dominant retention mechanism is considered to be an inner-sphere ligand exchange of the organic base moieties with the metal chelated on the support. On the other hand, a system with the support having a chemically bonded inert cationic complex has so far found less application in this field. In this instance outer-sphere complexing between the cationic complex and anionic sample species should control the retention mechanism. This approach was successfully exploited by Chow and Grushka<sup>3</sup> in the separation by high-performance liquid chromatography of nucleotides on a microparticulate siliceous support containing a  $\text{Co(en)}_3^{3+}$  moiety.

In this paper the preparation of a cross-linked dextran gel (Sephadex G-75) with amino-cobalt(III) complex groups is described. This phase is obtained by reaction of an  $\omega$ -aminobutyl-Sephadex derivative with  $[\text{Co}(\text{tetren})\text{Cl}]^{2+}$ . The separation of some mono- and dinucleotides on this support has been achieved.

## EXPERIMENTAL

Nucleotides and dinucleotides were obtained from Serva (Heidelberg, G.F.R.) and Sigma (St. Louis, MO, U.S.A.). All reagents were of analytical-reagent grade.

The  $\omega$ -amino polysaccharide derivative support was prepared according to the method described by Cuatrecasas<sup>4</sup> using 4.0 g (dry gel) of Sephadex G-75 (particle size 40–120  $\mu\text{m}$ ) (Pharmacia), cyanogen bromide (6.18 g) and diaminobutane (10 g) (Fluka, Buchs, Switzerland). Its nitrogen content was 0.44%. Chlorotetraethylenepentaminocobalt(III) tetrachlorozincate(II),  $[\text{Co}(\text{tetren})\text{Cl}]\text{ZnCl}_4$ , was synthesized as described by House and Garner<sup>5</sup>.

A 6-g amount of  $[\text{Co}(\text{tetren})\text{Cl}]\text{ZnCl}_4$  was dissolved in 200 ml of 1 N hydrochloric acid and the solution was percolated through two columns (19  $\times$  2.2 cm I.D.) packed with AG 1-X8 ( $\text{Cl}^-$ ) anion-exchange resin (100–200 mesh) (Bio-Rad Labs.,

Richmond, CA, U.S.A.) to make the eluate free from zinc as detected by flame atomic-absorption spectrophotometry on a Perkin-Elmer Model 372 instrument. The aminobutyl-Sephadex was added to the red-violet solution containing the cobalt(III) cation complex, adjusted to pH 7.0 with 1 *N* sodium hydroxide solution, then the mixture was stirred for 1 h at 80 °C. The suspension was filtered through a sintered-glass Buckner funnel and the resulting red-orange gel was washed with a large amount of distilled water. The nitrogen and cobalt contents were 0.97% and 0.44%, respectively.

Chromatography was performed at room temperature using a glass column (16 mm I.D.), a peristaltic pump and a Varian Aerograph Variscan LC continuously variable wavelength detector to monitor the column effluent at 254 nm.

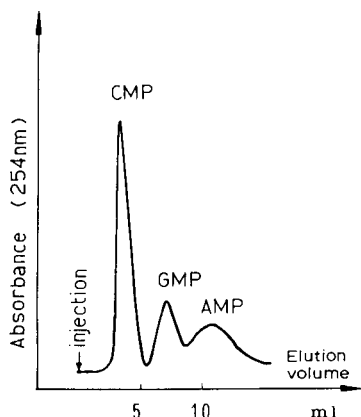


Fig. 1. Elution curve for the mononucleotides CMP, GMP and AMP. Column bed, 30 × 16 mm; buffer, Tris-0.01 *M* hydrochloric acid (pH 7.0)-0.01 *M* magnesium sulphate; flow-rate, 18 ml/h.

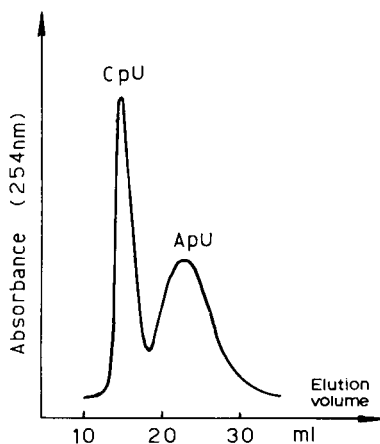


Fig. 2. Elution curve for the dinucleotides CpU and ApU. Column bed, 27 × 16 mm; buffer: Tris-0.01 *M* hydrochloric acid (pH 7.0)-0.003 *M* magnesium sulphate; flow-rate, 25 ml/h.

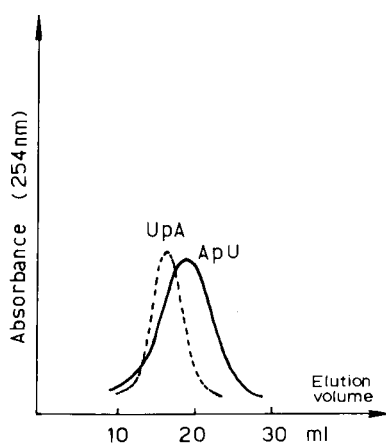


Fig. 3. Elution curve for the dinucleotides UpA and ApU eluted separately. Column bed and buffer as in Fig. 2; flow-rate, 24 ml/h.

## RESULTS

Figs. 1–3 show respectively the isocratic elution of three mononucleotides (CMP, GMP and AMP) and two pairs of dinucleotides (CpU–ApU and UpA–ApU). Separations were achieved for CMP, GMP and AMP (Fig. 1) and CpU–ApU (Fig. 2), but the UpA–ApU mixture could not be resolved (Fig. 3). On the  $\omega$ -aminopolysaccharide without the cobalt complex all of the above substances were strongly adsorbed and did not elute. It therefore seems that the separation effects obtained are due mainly to an outer-sphere complexing mechanism.

Further studies with this modified support are in progress in order to improve the separation of complex systems.

## REFERENCES

- 1 P. Hubert and J. Porath, *J. Chromatogr.*, 198 (1980) 247.
- 2 P. Hubert and J. Porath, *J. Chromatogr.*, 206 (1981) 164.
- 3 F. K. Chow and E. Grushka, *J. Chromatogr.*, 185 (1979) 361.
- 4 P. Cuatrecasas, *J. Biol. Chem.*, 245 (1970) 3059.
- 5 D. H. House and C. S. Garner, *Inorg. Chem.*, 5 (1966) 2097.

## Note

---

### Thin-layer and gas chromatographic separation of ferrocene oxathiolanes and dithiolanes

LEONARD OGIERMAN\*

*Institute of Plant Protection, 44153 Sosnowice (Poland)*

and

BRONISLAW CZECH

*Institute of Chemistry, Silesian University, 40006 Katowice (Poland)*

(Received August 19th, 1981)

Ferrocene derivatives are relatively stable organometallic compounds and have been analysed by means of thin-layer (TLC)<sup>1–3</sup>, gas-liquid (GLC)<sup>4,5</sup> and high-performance liquid chromatography (HPLC)<sup>6–8</sup>. Some methods for the separation of ferrocene compounds from reaction mixtures have been proposed<sup>1,2,6,8</sup>.

We have been investigating the application of chromatographic methods to the separation of oxygen- and sulphur-containing ferrocene derivatives<sup>3</sup>. In this paper we discuss the separation of selected ferrocene oxathiolanes and dithiolanes by means of TLC and GLC.

#### EXPERIMENTAL

##### *Preparation of ferrocene compounds*

Series of ferrocenyl dioxolanes, oxathiolanes and dithiolanes (see Table I) were prepared by reaction of formylferrocene and ferrocene ketones with 1,2-diols, 2-mercaptoethanol and 1,2-dimercaptoethane<sup>9</sup>. All of the derivatives were purified by column liquid chromatography. The glass column (40 × 3 cm I.D.) was filled with silica gel 60 (70–230 mesh) (E. Merck, Darmstadt, G.F.R.). The mobile phase was *n*-hexane–acetone (9:1).

##### *Partition thin-layer chromatography*

The sample substances were separated using pre-coated glass TLC plates covered with silanized silica gel 60-F<sub>254</sub> (E. Merck) and impregnated with 20% triethylene glycol in acetone. On these plates, 2 μl of a solution of the ferrocene derivatives in chloroform (5 mg/ml) were developed using *n*-hexane–carbon tetrachloride–benzene (12:1:1) as the mobile phase. The chromatograms were examined under UV light (254 nm).

##### *Gas-liquid chromatography*

A Perkin-Elmer 900 chromatograph with a flame-ionization detector was used, equipped with a glass column (6 ft. × 3 mm I.D.). The stationary phase was 3%

EGSP-Z on Gas-Chrom Q (100–120 mesh) (Applied Science Labs., State College, PA, U.S.A.). The operating conditions were as follows: detector temperature, 220°C; injection chamber temperature, 260°C; hydrogen flow-rate, 35 ml/min; air flow-rate, 180 ml/min; argon flow-rate, 40 ml/min. Isothermal analysis was performed at 220°C.

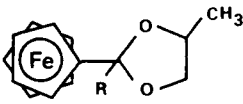

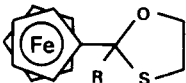
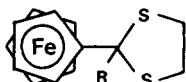
## RESULTS AND DISCUSSION

Results of the partition TLC separation of the ferrocene derivatives are given as  $R_F$  values in Table I. The conditions used (non-reversed phase) gave more satisfactory separations than adsorption TLC.

The results show that substitution of oxathiolane or dithiolane rings with methyl or phenyl groups in the 2-position increases the  $R_F$  values.

The qualitative separation achieved by TLC was confirmed by the results obtained by GLC. The results of isothermal separation on EGSP-Z as the stationary phase are given in Fig. 1 and Table II. The separations obtained are also given in the

TABLE I  
CHEMICAL CONSTITUTION AND  $R_F$  VALUES OF FERROCENE COMPOUNDS

Compound	Structural formula		$R_F$ value
	Formula	R	
<i>Dioxolanes:</i>			
2-Ferrocenyl-4-methyldioxolane-1,3		H	0.28
<i>Bisdithiolanes:</i>			
1,1'-Ferrocene-bis(dithiolane-1,3)		H	0.47
1,1'-Ferrocene-bis(2-methyldithiolane-1,3)		CH <sub>3</sub>	0.53
1,1'-Ferrocene-bis(2-phenyldithiolane-1,3)		C <sub>6</sub> H <sub>5</sub>	0.58
<i>Oxathiolanes:</i>			
2-Ferrocenyloxathiolane-1,3		H	0.56
2-Ferrocenyl-2-methyloxathiolane-1,3		CH <sub>3</sub>	0.61
2-Ferrocenyl-2-phenyloxathiolane-1,3		C <sub>6</sub> H <sub>5</sub>	0.67
<i>Dithiolanes:</i>			
2-Ferrocenyldithiolane-1,3		H	0.60
2-Ferrocenyl-2-methyldithiolane-1,3		CH <sub>3</sub>	0.65
2-Ferrocenyl-2-phenyldithiolane-1,3		C <sub>6</sub> H <sub>5</sub>	0.71

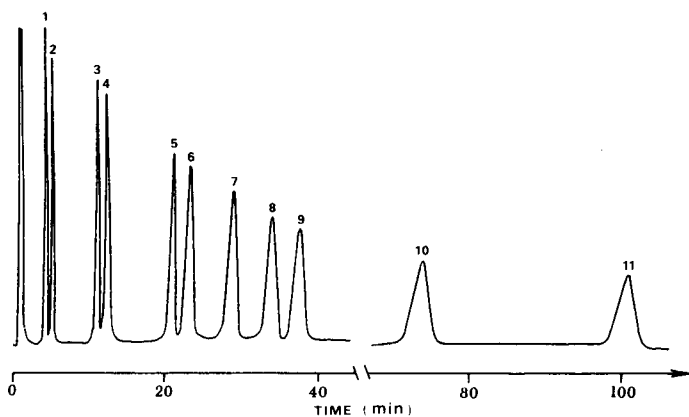


Fig. 1. Separation of a mixture of ferrocene oxathiolanes and dithiolanes using a 3% EGSP-Z column. Peaks: 1 = 2-ferrocenyl-4-methyldioxolane-1,3; 2 = internal standard (1,3-diphenylacetone); 3 = 2-ferrocenyloxathiolane-1,3; 4 = 2-ferrocenyl-2-methyloxathiolane-1,3; 5 = 2-ferrocenyldithiolane-1,3; 6 = 2-ferrocenyl-2-methyldithiolane-1,3; 7 = 2-ferrocenyl-2-phenyloxathiolane-1,3; 8 = 1,1'-ferrocene-bis(dithiolane-1,3); 9 = 1,1'-ferrocene-bis(2-methyldithiolane-1,3); 10 = 2-ferrocenyl-2-phenyldithiolane-1,3; 11 = 1,1'-ferrocene-bis(2-phenyldithiolane-1,3).

TABLE II

## GLC RETENTION VALUES OF FERROCENE DERIVATIVES

Compound separated	Retention value	
	$t_R$ (min)	$\alpha$
<i>Internal standard:</i>		
1,3-Diphenylacetone	4.8	1.00
<i>Dioxolane-1,3:</i>		
2-Ferrocenyl-4-methyldioxolane-1,3	4.0	0.84
<i>Bisdithiolanes:</i>		
1,1'-Ferrocene-bis(dithiolane-1,3)	33.5	7.05
1,1'-Ferrocene-bis(2-methyldithiolane-1,3)	37.0	7.78
1,1'-Ferrocene-bis(2-phenyldithiolane-1,3)	102.0	21.05
<i>Oxathiolanes:</i>		
2-Ferrocenyloxathiolane-1,3	10.5	2.21
2-Ferrocenyl-2-methyloxathiolane-1,3	12.0	2.52
2-Ferrocenyl-2-phenyloxathiolane-1,3	28.5	6.00
<i>Dithiolanes:</i>		
2-Ferrocenyldithiolane-1,3	20.5	4.31
2-Ferrocenyl-2-methyldithiolane-1,3	22.8	4.78
2-Ferrocenyl-2-phenyldithiolane-1,3	74.8	15.58

form of retention times ( $t_R$ ) and relative retention times ( $\alpha$ ), determined relative to the retention time of the internal standard, 1,3-diphenylacetone.

Application of the polar stationary phase EGSP-Z (McReynolds constant  $\Sigma AI = 2278$ ) permits the isothermal separation of the sample substances. Silicone stationary phases of the OV or SE type did not give efficient separations.

#### REFERENCES

- 1 K. Schlögl and H. Egger, *Monatsh. Chem.*, 94 (1963) 376.
- 2 R. E. Bozak and J. H. Fukuda, *J. Chromatogr.*, 26 (1967) 501.
- 3 L. Ogierman, B. Czech and A. Piórko, *J. Chromatogr.*, 198 (1980) 536.
- 4 O. E. Ayers, T. G. Smith, J. D. Burnett and B. W. Ponder, *Anal. Chem.*, 38 (1966) 1606.
- 5 C. Pomier and G. Guiochon, *Chromatographia*, 2 (1969) 346.
- 6 M. Shiga, M. Tsunashima, H. Kono, J. Motoyama and K. Hata, *Bull. Chem. Soc. Jap.*, 43 (1970) 841.
- 7 D. T. Haworth and T. Liu, *J. Chromatogr. Sci.*, 14 (1976) 519.
- 8 M. T. McKone, *J. Chem. Educ.*, 57 (1980) 380.
- 9 A. Ratajczak and B. Czech, *Rocz. Chem.*, 51 (1977) 1735.



CHROM. 14,217

## Book Review

---

*Pesticide analytical methodology* (ACS Symposium Series 136; ACS Meeting, Washington, DC, September 1979), edited by J. Harvey, Jr. and G. Zweig, American Chemical Society, Washington, DC, 1980, X + 406 pp., price US\$ 38.00, ISBN 0-8412-0581-7.

"Pesticide analytical methodology" has matured. There used to be a time when residue chemists significantly advanced the state of the art — not just of their own field but of organic trace analysis in general.

Now the emphasis has shifted. Government wants more numbers and less research, and the pesticide analyst is increasingly asked to acquire separation and detection capabilities developed in areas other than his own. A majority of the ACS Symposium papers is designed to lead him in this direction.

In a way, these particular chapters make for pleasant reading. Most of their material is, of course, neither new nor particularly germane to pesticide analysis, but it is usually well presented. Noteworthy in this context are articles on high-performance liquid chromatography (HPLC) column evaluation by DeStefano, RP-HPLC selectivity by Bakalyar, electrochemical detection in HPLC by Kissinger *et al.*, Fourier transform infrared spectroscopy by Lowry and Gray, and negative-ion mass spectrometry by Horning *et al.* I particularly liked the reasoned evaluation of immunoassay techniques by Hammock and Mumma.



Then, alas, there are a few well-done reviews that deal exclusively with pesticides. To me, the one by Seiber and co-workers felt like a fresh breeze in the field. It describes residue analysis of air, and anticipates future knowledge on atmospheric pathways and budgets — perhaps beyond the initial agricultural context. Excellent accounts are also provided by Cochrane on derivation and by Mallet on thin-layer chromatography–fluorimetry. Not to lose sight of the human aspect, Moseman and Oswald discuss pesticide exposure of the sublethal variety, while Tewari acquaints the reader with analysis after death.

Somewhat less lively are most of the other twenty chapters that fill this book. In general these combine and expand material from instrumental analysis courses, in-house reports, and research communications — in that order.

This is certainly in keeping with the times. Pesticide residue analysis, once an analytical endeavor *sui generis*, has merged with other areas of organic trace determination. Now government protocol decides which pollutant may pollute with priority. Analytically speaking, it makes little difference whether this happens to be a pesticide or not — thus general instrumental methodology is destined to assume ever-increasing importance. For its continuing education effort along these lines, and for its helpful reviews, one wishes this ACS booklet a place on the bookshelves of many a pesticide laboratory.

Halifax (Canada)

WALTER A. AUE

# Journal of chromatography news section

## EXHIBITION REPORT

### THE 14th EXHIBITION 'HET INSTRUMENT' IN AMSTERDAM

'Het Instrument 1981', better known internationally as the 'HET' exhibition, was held from September 23 to October 1, 1981, in the RAI Exhibition and Congress Centre in Amsterdam, The Netherlands. The 14th exhibition was organized, as over the past 25 years, by the Association of Dutch Instrument Dealers and Manufacturers 'Het Instrument'. Direct participation in the exhibition is possible only for Dutch instrument manufacturers and dealers, and for Dutch subsidiaries of foreign instrument industries, insofar as they are accepted as members of the Association 'Het Instrument'.

Although the Amsterdam instrument show is organized only every two years and is a local exhibition, it is gaining continually in international importance. Visitors come not only from the Netherlands, but also from Belgium, France, Germany, the Scandinavian countries, and from the United Kingdom.

The accent of the exhibition falls mainly on various types of laboratory instruments, although the importance of the show for people interested in instruments and components for use in process automation, and visitors looking for hospital and clinical equipment and apparatus, must not be underestimated. This year many instruments were displayed for the first time in the Netherlands and even in Europe, while a few made their world debut. The exhibition halls in the RAI Exhibition Centre have a gross surface area of about 70,000 m<sup>2</sup> while the total booth space is estimated at 28,000 m<sup>2</sup>. The number of exhibitors rose from 387 in 1979 to 448 this year.

Introduced at the 1981 Pittsburgh Conference and new to the European market was the FT-MS-1000 mass spectrometry system from the Nicolet Instrument Corp. The local Nicolet subsidiary organized a symposium around this Fourier Transform mass spectrometry system in a nearby hotel and invited the members of the Dutch Mass Spectrometry Discussion Group to attend. Professor Wilkins, one of the scientists who paved the road to FT-mass spectrometry for Nicolet, presented a paper during this symposium. The Nicolet system can easily be coupled with a gas chromatograph.

New in the mass spectrometry field was the label 'Finnigan' on the instruments from the MAT-plant in Bremen, G.F.R. The local representative, Gips Instrumenten BV, showed a Finnigan MAT Model 212 mass spectrometry system, connected to an SS 188 data system. Techmation, the Finnigan representative for products from Sunnyvale, CA, U.S.A., displayed their quadrupole GC-MS system 1020, complete with a data system based on a Data General Nova minicomputer.

Hewlett-Packard exposed the Model HP 5885A quadrupole GC-MS system, equipped with the most extended data system and suitable for electron impact and chemical ionization work. In the field of smaller systems, Hewlett-Packard showed a version of the HP 5995A, capable of chemical ionization work. The connected data system was based on the new 9826A desk-top computer.

Bruker Spectrospin BV showed (in addition to smaller and larger NMR-spectroscopy systems) the GC-MS 1001 from Bruker Franzen GmbH in Bremen, G.F.R., an instrument suitable for very fast GC-MS analysis, and designed for use in the life sciences.

Kratos' AEI division exposed a data system designed for use with the MS-80 mass spectrometer.

In the area of gas chromatography, the Spectra-Physics' SP-7100 gas chromatograph (designed by Delta Electronics) was shown for the first time in Europe. The SP-7100 system, introduced at the

1981 Pittsburgh Conference, offers a great variety of possibilities and is modular in design and construction. In addition, the SP-8100 HPLC system (also new to Europe) was displayed; it comprises the SP-8700 and SP-8400 units (introduced earlier) and a built-in auto-sampling system, which uses the well-known bar code for sample identification.

The new Dutch firm, Bester BV, showed the SiChromat gas chromatographs from Siemens AG, Karlsruhe, G.F.R., introduced in 1980. The SiChromats are advanced microprocessor-controlled gas chromatography systems, not very well known outside of Germany.

Packard-Becker, now more obviously acting as a United Technologies company, exhibited the new models 437 and 438. The Packard 437 gas chromatograph is a microcomputerized, extended version of the older Model 427, the model that started 'modern times' with Packard-Becker a few years ago. The 438 is the older 428 in a microprocessor-controlled version. Packard's new TCD detector did not make it to the exhibition; the new more sensitive component will soon be available for all Packard GC systems.

Philips Nederland BV showed (in the field of gas chromatography) Pye Unicam's top model 304 in combination with the new PU 4800 operating and data processing system. Up to four gas chromatographs can be connected to the system. The HPLC version was not exhibited but is currently available. The differences between the GC and LC systems lie in the software. New with Philips was the GC autosampler and head space analyzer.

Perkin-Elmer displayed components for 'high-speed liquid chromatography', including the LC-85 double-beam UV-VIS detector, and the LS-4 fluorescence detector. New in the field of fluorescence and phosphorescence spectrometry were the LS-5, a research type instrument, and the LS-3, a low cost routine type instrument. Perkin-Elmer also showed the SIGMA 115 Level 3 gas chromatograph, the ATD-50 automatic thermal desorption system, and the AS-100B programmable autosampler.

The Shimadzu dealers, Applikon and Pleuger, showed the gas chromatograph GC-7A and a complete HPLC system. Kontron also showed a complete HPLC system. Shimadzu's computing integrator Model C-R1A was present at several booths in a number of different colors. The same was true for the Spectra-Physics SP-4100 integrator.

Du Pont displayed their new multisolvent system, introduced during the 1981 Pittsburgh Conference; Salm & Kipp, the Dutch representatives of the German manufacturer, Knauer, showed a complete HPLC system. Beckman exposed a new line of HPLC instrumentation from the Beckman daughter, Altex.

Waters Associates BV, the Dutch subsidiary of Waters Associates, Inc., on their way to a distinct Millipore company with the appropriate logo, showed the most recent version of the WISP, the UV-VIS detector 441, the pumping system 45G, and the 720 System Controller.

Varian Benelux BV exhibited the HPLC top model 5060 and the new 6000 and 6500 gas chromatographs. The Model 6000 is in fact the microprocessor-controlled version of the famous Model 3700, extended with video tube presentation. The Model 6500 is an analytical unit that can be hooked up to the 6000 microprocessor electronics. Both models can be connected with the VISTA 401 data system.

Hewlett-Packard Nederland BV showed instruments from the 5880 family of gas chromatographs and the 1080 family of HPLC systems, in a number of cases connected with an HP-85 personal computer.

The latest novelties in ion chromatography were shown by Pleuger Nederland, dealer for the Dionex Corporation, and by Technation, a representative of Wescan. The development of the apparatus is rather slow in ion chromatography; development of stationary phases and ion-exchange resins in much faster, resulting in shorter analysis times.

Pleuger also showed a new microprocessor-controlled LC 7000 amino acid analyzer from Biotronik GmbH of Munich, G.F.R. Meyvis & Co, BV, exposed a complete HPLC system from Gilson Instruments, Inc., Middleton, WI, U.S.A., and the fluorescence detection version of the Rank Hilger Chromaspek amino acid analyzer.

The trend towards dedicated microprocessor-controlled systems, suitable for column switching techniques and equipped with video tube presentation was re-established by the 'HET' exhibition. In general, the manufacturers leaned toward automated systems, fitted with microprocessor control and built-in data processing. A new direction was that of self diagnosis and automated trouble shooting.

## PRESS CONFERENCE REPORT

### PHILIPS PRESS CONFERENCE AT BOEKELO, THE NETHERLANDS

On September 17–18, 1981, the international press in the field of laboratory instrumentation and apparatus were invited by the N.V. Philips' Gloeilampen Fabrieken. The Philips Science and Industry press officer, Stanley Lodder, and his staff succeeded in gathering together a remarkable number of press people from Europe and the United States in the quietly situated village of Boekelo in the eastern Netherlands, near the important Philips Science & Industry production plant in Almelo.

After an informal chat and a barbecue on the 17th, the guests gathered the next morning to hear the news from the various Philips and Pye Unicam specialists present in the Boekelo Hotel. A short and general introduction was given by Henk Bodt, president of the Philips Science and Industry Division, after which Pye Unicam's John Dolphin presented the new PU 4000 HPLC systems.

The PU 4000 series of HPLC systems consists of three members. The most versatile member is the PU 4002 system, equipped with a video tube unit and fully controlled by a microprocessor. Chromatograms and gradient profiles may be shown on the video screen. As many as 10 different methods can be stored. The methods can be complex combinations of gradient elution, column switching and flow programming. The results of various detectors can be presented, integrated and automatically compared with earlier results, stored in the memory of the system.

The second member of the family is the less complicated PU 4001, equipped with microprocessor-controlled gradient elution capabilities and column switching techniques. The top model, the 4001 is fitted with a spacious oven, offering space for 4 normal columns.

The simplest version of the PU 4000 family is the isocratic PU 4000 system, designed for routine applications, for example, quality control. The Pye Unicam PU 4000 family is fully modularly built, and the user may begin with a simple PU 4000 version and gradually expand to a system with analytical research capabilities.

In the gradient versions, the solvents are mixed on the low pressure side of the dual pumping system. The pumping speeds are controlled by the microprocessor electronics in such a way that the chosen mixing requirements are fulfilled. The systems of the Pye Unicam PU 4000 series can be equipped with UV-, electrochemical, RI and fluorescence detectors. The central video tube unit of the PU 4002 can be connected with two analytical units. This video unit is, in fact, the same unit used in the new Pye Unicam GC system. The differences lie in the software.

Such a system is complete only with an automatic sampling system. With the PU 4000 instrument, Pye Unicam offers an automatic sampler based on the PU 4700 GC sampling system and capable of performing 102 injections from normal or microsample vials. The PU 4001 and PU 4000 versions can be connected with the CDP 4 and CDP 1 computing integrators from the Pye Unicam program.

On the same occasion, Philips also introduced a new automated and computerized powder X-ray diffraction system and a library search program for the SP 3-080 infrared spectrophotometry data system.

Klaas H. Broer

## WORKSHOP COURSE

### ELEMENTS OF ANALYTICAL INSTRUMENT ELECTRONICS

This 'appreciation' course for novices, with practical work, will next be run during March 23–27, 1982, in Guildford, Great Britain. It includes aspects of chromatographic detectors and microprocessors.

For further information contact: Dr. E. Reid, Wolfson Bioanalytical Unit, Robens Institute, University of Surrey, Guildford GU2 5XH, Great Britain.

## MEETINGS

### 4th DANUBE SYMPOSIUM ON CHROMATOGRAPHY AND 7th INTERNATIONAL SYMPOSIUM "ADVANCES AND APPLICATION OF CHROMATOGRAPHY IN INDUSTRY"

The above symposium will be held in Bratislava, Czechoslovakia, on August 29–September 2, 1983. The scientific program will consist of plenary lectures and poster presentations covering the following topics: Advances in chromatography, Application of chromatographic methods in industry, Environmental analysis by chromatographic methods, and Biochemical and pharmaceutical application of chromatographic methods.

The official languages of the Symposium will be English and Russian.

Further information may be obtained from: Dr. Ján Remen, The Analytical Section of the Czechoslovak Scientific and Technical Society, Slovnaft, 823 00 Bratislava, Czechoslovakia.

### 3rd BIENNIAL SYMPOSIUM ON ADVANCES IN THIN-LAYER CHROMATOGRAPHY

The 3rd Biennial Symposium on Advances in Thin-Layer Chromatography will be held on December 6–8, 1982, at the Parsippany Hilton, Route 10, Parsippany, NJ, U.S.A.

Technical sessions topics will include, among others: HPTLC, RPTLC, automation of TLC, quantitative TLC, computer retrieval, and pharmaceutical, clinical and industrial applications.

The deadline for abstracts is July 1, 1982. For information and details concerning submission of abstracts of papers for presentation contact: Dr. Touchstone, Hospital of the University of Pennsylvania, Philadelphia, PA, U.S.A. Tel: (215) 662-2082.

## CALENDAR OF FORTHCOMING MEETINGS

- |  |  |
|--|--|
| March 8–12, 1982<br>Atlantic City, NJ, U.S.A.      | <b>1982 Pittsburgh Conference and Exhibition on Analytical Chemistry and Applied Spectroscopy</b><br>Contact: Mrs. Linda Briggs, Program Secretary, Pittsburgh Conference, Department J-057, 437 Donald Road, Pittsburgh, PA 15235, U.S.A.<br>(Further details published in Vol. 212, No. 2) |
| March 28–April 2, 1982<br>Las Vegas, NV, U.S.A.    | <b>183rd American Chemical Society National Meeting</b><br>Contact: A.T. Winstead, American Chemical Society, 1155 Sixteenth Street, NW, Washington, DC 20036, U.S.A.  |
| April 5–8, 1982<br>Las Vegas, NV, U.S.A.           | <b>17th International Symposium "Advances in Chromatography"</b><br>Contact: Prof. A. Zlatkis, Chemistry Department, University of Houston, Central Campus, 4800 Calhoun, Houston, TX 77004, U.S.A. Tel.: (713) 749-2623. (Complete program published in Vol. 219, No. 3.)                   |
| April 14–16, 1982<br>Amsterdam,<br>The Netherlands | <b>12th Annual Symposium on the Analytical Chemistry of Pollutants</b><br>Contact: Prof. Dr. Roland W. Frei, The Free University, De Boelelaan 108 1081 HV Amsterdam, The Netherlands. (Further details published in Vol. 206, No. 1)  |
| April 15–17, 1982<br>Tokyo, Japan                  | <b>18th International Symposium "Advances in Chromatography"</b><br>Contact: Prof. A. Zlatkis, Chemistry Department, University of Houston, Central Campus, 4800 Calhoun, Houston, TX 77004, U.S.A. Tel.: (713) 749-2623. (Complete program published in Vol. 234, No. 1.)                   |
| April 19–22, 1982<br>Barcelona, Spain              | <b>International Congress on Automation in Clinical Laboratory</b><br>Contact: Dr. R. Galimany, Sección de Automatización, Laboratorio de Analisis Clínicos, C.S. "Principes de Espana", Hospitalet de Llobregat, Barcelona, Spain.  |

MONTH		J	F	M	A	M	J	J	A	S	O	N	D
Journal of Chromatography		234/1 234/2 235/1 235/2	236/1 236/2	The publication schedule for further issues will be published later.									
Chromatographic Reviews													
Biomedical Applications		227/1	227/2										

### INFORMATION FOR AUTHORS

(Detailed *Instructions to Authors* were published in Vol. 209, No. 3, pp. 501–504. A free reprint can be obtained by application to the publisher)

**Types of Contributions.** The following types of papers are published in the *Journal of Chromatography* and the section on *Biomedical Applications*: Regular research papers (Full-length papers), Short communications and Notes. Short communications are preliminary announcements of important new developments and will, whenever possible, be published with maximum speed. Notes are usually descriptions of short investigations and reflect the same quality of research as Full-length papers, but should preferably not exceed four printed pages. For reviews, see page 2 of cover under Submission of Papers.

**Submission.** Every paper must be accompanied by a letter from the senior author, stating that he is submitting the paper for publication in the *Journal of Chromatography*. Please do not send a letter signed by the director of the institute or the professor unless he is one of the authors.

**Manuscripts.** Manuscripts should be typed in double spacing on consecutively numbered pages of uniform size. The manuscript should be preceded by a sheet of manuscript paper carrying the title of the paper and the name and full postal address of the person to whom the proofs are to be sent. Authors of papers in French or German are requested to supply an English translation of the title of the paper. As a rule, papers should be divided into sections, headed by a caption (e.g., Summary, Introduction, Experimental, Results, Discussion, etc.). All illustrations, photographs, tables, etc. should be on separate sheets.

**Introduction.** Every paper must have a concise introduction mentioning what has been done before on the topic described, and stating clearly what is new in the paper now submitted.

**Summary.** Full-length papers and Review articles should have a summary of 50–100 words which clearly and briefly indicates what is new, different and significant. In the case of French or German articles an additional summary in English, headed by an English translation of the title, should also be provided. (Short communications and Notes are published without a summary.)

**Illustrations.** The figures should be submitted in a form suitable for reproduction, drawn in Indian ink on drawing or tracing paper. Each illustration should have a legend, all the legends being typed (with double spacing) together on a *separate sheet*. If structures are given in the text, the original drawings should be supplied. Coloured illustrations are reproduced at the author's expense, the cost being determined by the number of pages and by the number of colours needed. The written permission of the author and publisher must be obtained for the use of any figure already published. Its source must be indicated in the legend.

**References.** References should be numbered in the order in which they are cited in the text, and listed in numerical sequence on a separate sheet at the end of the article. Please check a recent issue for the lay-out of the reference list. Abbreviations for the titles of journals should follow the system used by *Chemical Abstracts*. Articles not yet published should be given as "in press", "submitted for publication", "in preparation" or "personal communication".

**Proofs.** One set of proofs will be sent to the author to be carefully checked for printer's errors. Corrections must be restricted to instances in which the proof is at variance with the manuscript. "Extra corrections" will be inserted at the author's expense.

**Reprints.** Fifty reprints of Full-length papers, Short communications and Notes will be supplied free of charge. Additional reprints can be ordered by the authors. An order form containing price quotations will be sent to the authors together with the proofs of their article.

**News.** News releases of new products and developments, and information leaflets of meetings should be addressed to: The Editor of the News Section, *Journal of Chromatography*/*Journal of Chromatography, Biomedical Applications*, Elsevier Scientific Publishing Company, P.O. Box 330, 1000 AH Amsterdam, The Netherlands.

**Advertisements.** Advertisement rates are available from the publisher on request. The Editors of the journal accept no responsibility for the contents of the advertisements.

**FOUR  
NEW  
BOOKS**

## **Electron Capture – Theory and Practice in Chromatography**

*edited by A. ZLATKIS, Houston, TX, USA, and C. F. POOLE, Detroit, MI, USA*

JOURNAL OF CHROMATOGRAPHY LIBRARY – Volume 20

This comprehensive coverage of all aspects of the theory, design, operation and applications of the electron-capture detector in chromatography contains solutions to instrumental and technical problems which can arise during practice. It includes an extensive tabulation of all pertinent data concerning the use of this technique in gas and liquid chromatography. Each chapter has been prepared by experts in their fields and contains in-depth coverage of its topic.

**Sept. 1981 viii + 376 pages**

**Price: US \$76.50/Dfl. 180.00**

**ISBN 0-444-41954-3**

## **Affinity Chromatography and Related Techniques**

*edited by T. C. J. GRIBNAU, Oss, J. VISSER, Wageningen, and R. J. F. NIVARD, Nijmegen, The Netherlands*

ANALYTICAL CHEMISTRY SYMPOSIA SERIES – Volume 9

The 45 papers in this Proceedings volume cover the theoretical aspects of affinity chromatography, review the preparation and properties of polymeric matrices and methods for ligand immobilization, and illustrate the increasing importance of affinity techniques in industrial and biomedical/diagnostic applications. A wide variety of the applications of organic dyes are included, as well as information on the application of affinity techniques in high-performance liquid chromatography.

**Nov. 1981 xviii + 584 pages**

**Price: US \$83.00/Dfl. 195.00**

**ISBN 0-444-42031-2**

## **Drugs of Abuse**

*by L. FISHBEIN, Jefferson, AR, USA*

CHROMATOGRAPHY OF ENVIRONMENTAL HAZARDS 4

This is both a practical text and a literature reference source for chromatographic procedures used in the separation, detection and quantification of a spectrum of commonly abused drugs from biological, licit and illicit samples. These procedures are primarily useful in therapeutic monitoring, pharmacokinetic studies, emergency, clinical, forensic and toxicological analyses, and monitoring in drug abuse screening programs. It is the final volume in this series which also covers carcinogens, mutagens and teratogens, metals, gaseous and industrial pollutants, and pesticides.

**Oct. 1981 x + 490 pages**

**Price: US \$95.75/Dfl. 225.00**

**ISBN 0-444-42024-X**

## **Mass Spectrometry in Biochemistry, Medicine and Environmental Research, 7**

Proceedings of the 7th International Symposium on Mass Spectrometry in Biochemistry, Medicine and Environmental Research, Milan, Italy, 16-18 June 1980

*edited by A. FRIGERIO, Milan, Italy*

ANALYTICAL CHEMISTRY SYMPOSIA SERIES – Volume 7

The main topics covered in the 32 papers presented at this symposium are the applications of mass spectrometric techniques in drug metabolism, metabolism of other substances, the identification and/or quantitation of endogenous compounds, studies involving respiratory gases, and environmental studies. Advances in methodology are also included.

**Oct. 1981 x + 360 pages**

**Price: US \$72.50/Dfl. 170.00**

**ISBN 0-444-42029-0**



Order from your bookseller  
or directly from

ELSEVIER SCIENTIFIC  
PUBLISHING COMPANY  
P.O. Box 211,  
1000 AE Amsterdam,  
The Netherlands

ELSEVIER  
NORTH-HOLLAND INC.  
52 Vanderbilt Ave.,  
New York, NY 10017

Prepaid orders are supplied postfree.

The Dutch guilder price is definitive. US \$ prices  
are subject to exchange rate fluctuations.